

Stony Brook University



OFFICIAL COPY

The official electronic file of this thesis or dissertation is maintained by the University Libraries on behalf of The Graduate School at Stony Brook University.

© All Rights Reserved by Author.

**Ring Opening Metathesis Polymerization of
1-Substituted Cyclobutene Derivatives and Its Application to Antimicrobials:
From Homopolymers to Alternating Copolymers**

A Dissertation Presented

by

Airong Song

to

The Graduate School

in Partial Fulfillment of the

Requirements

for the Degree of

Doctor of Philosophy

in

Chemistry

Stony Brook University

May 2010

Copyright by

Airong Song

2010

Stony Brook University

The Graduate School

Airong Song

We, the dissertation committee for the above candidate for the
Doctor of Philosophy degree, hereby recommend
acceptance of this dissertation.

Nicole S. Sampson – Dissertation Advisor

Professor of Chemistry

Kathlyn A. Parker – Chairperson of Defense

Professor of Chemistry

Isaac Carrico– Third member of Defense

Assistant Professor of Chemistry

Stephen Walker – Outside Member of Defense

Associate Professor of Oral Biology and Pathology at Stony Brook University

This dissertation is accepted by the Graduate School

Lawrence Martin

Dean of the Graduate School

Abstract of the Dissertation

Ring Opening Metathesis Polymerization of
1-Substituted Cyclobutene Derivatives and Its Application to Antimicrobials:
From Homopolymers to Alternating Copolymers

By

Airong Song

In

Chemistry

Stony Brook University

2010

Ring opening metathesis polymerization (ROMP) is a chain-growth polymerization based on the ring opening of strained cyclic olefins providing a range of polymeric materials. Living ROMP of highly strained norbornene derivatives generates linear polymers with accurate molecular weight control and low polydispersities (PDIs). However, internally heterogeneous mixtures are obtained because the polymerization reactions lack complete stereochemical and regiochemical control. 1-Substituted cyclobutene amides undergo ruthenium-catalyzed ROMP to provide polymers with translationally invariant backbones (*E*-configuration) and excellent PDIs. To better understand the structural factors that control the regio- and stereochemistry of the ROMP reactions of 1-substituted cyclobutenes, several 1-substituted cyclobutenes with varied electron densities or steric interactions in the olefin bonds were prepared. 1-Cyclobutene

esters, 1-cyclobutene secondary amides, 1-cyclobutene tertiary amides or 1-cyclobutenylmethyl acetates, were subjected to ROMP. The stereo- and regiochemistry of the ROMP polymers were studied by 1D and 2D-NMR spectroscopy. NBO charge and energy difference calculations for intermediates and products were undertaken to explain the experimental results. Electrostatic interactions during formation of the initial π -complexes and steric interactions during metallocyclobutane formation determine the regio- and stereoisomers formed

ROM of 1-substituted cyclobutene ester by ruthenium catalysts generates kinetically trapped enoic ruthenium carbene that cannot undergo additional metathesis with 1-cyclobutene esters. However, the enoic ruthenium carbene can ring-open cyclohexene to generate a ruthenium alkylidene that will in turn react with a highly strained 1-cyclobutene ester to regenerate the enoic ruthenium carbene. As a result, alternating cyclobutene and cyclohexene units are incorporated into the propagating polymer chain. The precisely alternating pattern was confirmed by $^1\text{H-NMR}$ spectroscopy and stable isotope-labeling experiments. The alternating ring opening metathesis polymerization (AROMP) is tolerant to 4-substitution on the cyclohexene and various types of esters on the cyclobutene.

The amphipathic nature of antimicrobial peptides (AMPs) facilitates their disruption of bacterial membranes and bacterial death. A series of alternating amphiphilic copolymers (AMP mimics) containing different cationic groups and varying hydrophobicity were synthesized through AROMP of 1-cyclobutene ester and cyclohexene derivatives. Their antimicrobial activities were assayed and their selectivities were compared with random copolymers or homopolymers of similar charge. Their mechanisms of action were studied by cross-section transmission electron microscopy (TEM), dye leakage vesicle assays, membrane depolarization assays, and potassium release assays. It is concluded that mimics with a 8-10 Å spacing between cationic residues and ~ 4 repeating units exhibited the best antimicrobial activities and selectivities.

The amphiphilic polymers form vesicles in aqueous solution as demonstrated by TEM and dynamic light scattering (DLS). The pH and ionic strength dependence of vesicle formation was characterized by DLS. Polymer vesicles containing quarternary

ammonium groups are insensitive to changes in pH, whereas, for polymers containing primary ammonium groups, size change upon increasing pH change is a result of protonation and deprotonation of primary amine groups.

Table of Contents

List of Figures	ix
List of Schemes	xiv
List of Tables	xvi
List of Appendix Contents	xviii
List of Abbreviation	xxiv

Chapter 1 - Introduction

I. Ring-Opening Metathesis Polymerization (ROMP)	2
II. Antimicrobial Peptides (AMPs)	19
III. Specific Aims	24

Chapter 2 - Scope of the ROMP Reaction of 1-Substituted Cyclobutenes

I. Introduction	28
II. Results	31
III. Discussion	40
IV. Summary	58
V. Future Perspectives	59

Chapter 3 - Alternating Ring Opening Metathesis Polymerization

I. Introduction	61
-----------------	----

II. Results	65
III. Discussion	75
IV. Summary	89
V. Future Perspectives	90

Chapter 4 - Antibacterial Studies of Homo Polymers, Alternating Copolymers and Random Copolymers

I. Introduction	93
II. Results	100
III. Discussion	117
IV. Summary	127
V. Future Perspectives	127

Chapter 5 - Vesicle Formation of Homo Polymers, Alternating Copolymers and Random Copolymers

I. Introduction	130
II. Results	132
III. Discussion	132
IV. Summary	135
V. Future Perspectives	136

Chapter 6 - Experimental Methods

I. Synthesis and Preparation of Compounds	139
---	-----

II. Gaussian Computational Methods	167
III. Lipid Dye Leakage Assay	168
IV. Potassium Release Assay	168
V. Thin-section TEM	169
VI. Membrane Depolarization Assay and Cell Viability Assay	170
VII. MIC and Hemolysis Assay	170
VIII. Small Angle Neutron Scattering	170
Bibliography	171
Appendix	211

List of Figures

Figure		Page
1-1	Relative ring strain for select cyclic olefins (<i>kcal/mol</i>)	4
1-2	Timeline of milestones in the development of olefin metathesis catalysts	7
1-3	Functional group tolerance of various metal-based metathesis catalysts	8
1-4	Structures of Mo-based imido alkylidene catalysts	9
1-5	Stereospecific ROMP of 3-methyl-3-phenylcyclopropene	10
1-6	Synthesis of well-defined Ru alkylidene initiators 1-5	12
1-7	Typical structures of water-soluble Ru catalysts	14
1-8	Synthesis of cyclic polymers by ROMP	14
1-9	Synthesis of linear polymers containing the bioactive functional groups by ROMP and structures of some common monomers	15
1-10	Thermodynamics of monovalent and multivalent interactions	16
1-11	Representative binding mechanisms for multivalent ligands at an interface	17
1-12	Facially amphiphilic helical AMP magainin II, side view (left), top view (right)	21
1-13	Cell wall compositions of Gram-positive and Gram-negative bacteria	22
1-14	General structures of some common phospholipids	23
1-15	General mechanism of killing bacteria by AMPs	24
2-1	Cyclobutene monomers subjected to ROMP	31
2-2	Comparison of the ROMP rates of Group I monomers 6a-6e	35
2-3	ROM of Group II/III monomers 7a, 7b, 8a, 8b	36

2-4	ROMP of 9a and 9b	37
2-5	The structure of the 1-mer reaction products 13a and 14a of 8a and analysis of the ¹ H-NMR spectrum	38
2-6	(a) NBO charge populations of 1-substituted cyclobutene derivatives 6a , 7a , 8a and 9b , the corresponding ring-opened ruthenium carbenes of 6a and 9b , and ruthenium benzylidene. (b) AIM electron densities (atomic units) of olefin bonds in 1-substituted cyclobutene derivatives 6a and 8a calculated using AIMPAC package.	40
2-7	Structures of possible intermediates and ring opened products for ROMP of Group I and IV monomers	41
2-8	Relative free energy profiles of four possible different intermediates and four possible ring-opened products in the ROMP reactions of Group I monomer (a) and Group IV monomer (b)	42
2-9	¹ H-NMR spectra of the ROMP of monomer 6b in CD ₂ Cl ₂	44
2-10	¹ H-NMR spectra of ROM of monomer 7b in CD ₂ Cl ₂	45
2-11	¹ H-NMR spectra of the ROM of monomer 8a in CD ₂ Cl ₂	46
2-12	ROM regio- and stereochemistry of 8a and 8b	48
2-13	¹ H-NMR spectra of ROM of monomer 8a in CD ₂ Cl ₂	49
2-14	¹ H-NMR spectra of the ROMP of monomer 9a in CD ₂ Cl ₂	50
2-15	The structure of the 10-mer reaction product 18a for 9a and the analysis of the ¹ H-NMR spectrum	51
2-16	Six possible alkene configurations in the polymer backbone upon ROMP of Group IV monomers and their predicted proton chemical shifts	52
2-17	Cyclobutene ROMP reaction scheme	53
2-18	Relative free energy profiles for the ROMP reactions of Group I monomers (a) and Group IV monomers (b)	56
2-19	(a) Schematic presentation of how a second N-substituent blocks access	57

	of an incoming monomer to the ruthenium carbene; (b) Optimized structure of the new N,N-disubstituted carbonyl ruthenium carbene for monomer 7a	
2-20	Proposed relative free energy profiles for the coordination of 1-cyclobutene ester 8a (red curve) and cyclohexene (blue curve) to the enoic ruthenium carbene and the ROMP reactions of 1-cyclobutene amides 6a-6e (green curve)	58
2-21	Proposed 1-secondary amide substituted cycloalkene monomers	59
3-1	¹ H-NMR spectral changes with reaction time for AROMP of 8a and 18a using catalyst 5	76
3-2	¹ H-NMR spectra of alternating ROMP polymers (8a-20a) ₁₀ - (8a-20a) ₂₀₀	77
3-3	¹³ C-APT NMR spectrum of alternating ROMP polymer (8a-20a) ₂₀	78
3-4	¹ H- ¹ H gCOSY-NMR spectrum of alternating ROMP polymer (8a-20a) ₂₀	79
3-5	Alkene region of ¹ H-NMR spectra (CD ₂ Cl ₂) of polymers (8a-20a) ₂₀ and (8a-20a-D) ₂₀	80
3-6	Possible substructures generated in the copolymerization of 8a with cyclohexene-D ₁₀	82
3-7	¹ H-NMR spectrum of cyc-(8a-20a-D) ₂₀	83
3-8	Mechanism of formation of cyclic alternating copolymers	83
3-9	ESI-Mass spectrum of (8a-20a) ₃	84
3-10	Bimodal peak fitting of GPC trace of (8a-20a) ₂₀₀	85
3-11	Partial ¹ H-NMR spectra of alternating copolymers	86
3-12	¹ H-NMR spectrum of cyclic alternating copolymer prepared with 25	87
3-13	¹ H-NMR spectrum of alternating copolymer (8a-29a) ₁₀ prepared with 28 .	88

4-1	Structures of β -residues	95
4-2	Structures of antimicrobial foldamers	95
4-3	Structures of typical antimicrobial peptoids	96
4-4	Optimization of the antibacterial activity and selectivity of phenylene ethynylene oligomers	97
4-5	Optimization of the antibacterial activity and selectivity of arylamide oligomers	98
4-6	Structures of antimicrobial polyacrylates, polystyrenes and poly(4-vinylpyridine)s	99
4-7	Optimization of the antibacterial activity and selectivity of polynorbornenes	99
4-8	¹ H-NMR spectra of Intermediate-1 to Intermediate-7	105
4-9	Synthesis of Acopolymer-1 to Acopolymer-7	106
4-10	¹ H-NMR spectrum of Acopolymer-1	106
4-11	¹ H-NMR spectra of Intermediate-7 and Polymer-7	107
4-12	¹ H-NMR spectra of Intermediate-8 to Intermediate-10	109
4-13	¹ H- ¹ H gCOSY spectrum of Intermediate-10	110
4-14	¹ H-NMR spectra of Intermediate-11 and Intermediate-12	111
4-15	¹ H-NMR spectra of Intermediate-13 and Intermediate-14	114
4-16	Lipid vesicle dye leakage experiments	115
4-17	Relationship between cytoplasmic membrane depolarization, as assessed by the diSC ₃₅ assay, and cell viability, as measured by the counting of CFU at the same time as the membrane depolarization assay for <i>E. coli</i> (a) and <i>S. aureus</i> (b)	119
4-18	Potassium release assay	120
4-19	Thin-section TEM images of bacteria	122

4-20	MIC and HC ₅₀ data for amphiphilic polymers	123
4-21	Structure activity relationship for antimicrobial polymers	124
4-22	a) Percent potassium release vs MIC. b) Percent dye leakage from <i>E. coli</i> model membrane vesicles: POPE/POPG = 3/1, [lipid] = 4.5 μM, [polymer] = 4 μg/mL vs <i>E. coli</i> MIC. c) Percent dye leakage from <i>S. aureus</i> model membrane vesicles: [CL] = 4.5 μM, [polymer] = 4 μg/mL vs <i>S. aureus</i> MIC. d) Percent dye leakage from red blood cell model membrane vesicles: [DOPC] = 4.5 μM, [polymer] = 1 μg/mL vs HC50 data	126
4-23	Proposed model for the bactericidal mechanism of action of mimic polymers	128
5-1	Structures of vesicles and micelles	130
5-2	Alternating copolymers made from ATRP	131
5-3	pH-sensitive block copolymers	132
5-4	Hydrodynamic diameters (D _h) of Acopolymer-1 to Homopolymer-14	133
5-5	Hydrodynamic diameters (D _h) vs pH of polymer solutions	134
5-6	Hydrodynamic diameters (D _h) vs NaCl concentrations for Acopolymer-1	136
5-7	TEM images of Acopolymer-1 (a), Rcopolymer-10 (b), Homopolymer-12 (c) and Homopolymer-13 (d)	137
5-8	Proposed mechanism of vesicle size change due to change in NaCl concentration	137

List of Schemes

Scheme		Page
1-1	General mechanism for a typical ROMP reaction using Mo- or Ru-based catalysts	3
1-2	Illustration of typical secondary metathesis reactions in ROMP	5
1-3	Ziegler-Natta polymerization	7
2-1	Stereocenters of poly(NBE)s or poly(ONBE)s	28
2-2	Ring Opening Metathesis Polymerization of 6a	29
2-3	Two possible reaction pathways and their corresponding intermediates and products in the ruthenium-catalyzed ring-opening reactions of 1-cyclobutene derivatives	30
2-4	Synthesis of 1-substituted cyclobutenes	33
3-1	Representative structures of copolymers	61
3-2	Alternating copolymerization by ATRP or RAFT and some representative alternating copolymers	62
3-3	Proposed mechanism for ROIMP	63
3-4	AROMP of norbornene and cyclooctene	63
3-5	AROMP of norbornenes carrying nonprotected carboxy and amino groups	64
3-6	Proposed AROMP mechanism of 1-cyclobutene esters and cyclohexenes	64
3-7	Synthesis of 1-substituted cyclobutene esters 8c and 8d	65
3-8	Synthesis of cyclohexene derivatives	66
3-9	ROMP of cyclic olefins in THF	69

3-10	Synthesis of 1-methoxycyclopentene 29b and catalyst 28	73
3-11	Regioirregular addition of 1-methylcyclopentene to the enoic ruthenium carbene	89
3-12	Proposed methods to minimize backbiting	90
3-13	Proposed synthetic route of star polymers	91
4-1	Structures of antimicrobial Acopolymer-1 to Homopolymer-14	101
4-2	Synthesis of 1-substituted cyclobutene monomers	102
4-3	Synthesis of 4-substituted cyclohexene monomers	102
4-4	Synthesis of 5-substituted cyclooctene monomer	103

List of Tables

Table		Page
1-1	Summary of different metathesis catalyst systems	11
1-2	Comparison of different homogeneous well-defined Ru-based catalysts	12
1-3	Multivalent interactions at interfaces	18
1-4	Polymeric drug delivery systems	19
1-5	Amino acid sequences of some natural AMPs	21
2-1	ROMP results for Group I-IV monomers	34
3-1	AROMP polymers synthesized	67
3-2	Polymerization results	68
3-3	AROMP by catalyst 3	69
3-4	AROMP polymers synthesized	70
3-5	AROMP polymers synthesized	71
3-6	AROMP results	72
3-7	AROMP polymers synthesized	74
3-8	Polymerization results with catalyst 28	75
3-9	$^1\text{H-NMR}$ (500 MHz, CD_2Cl_2), $^{13}\text{C-NMR}$ (100 MHz, CD_2Cl_2), $^1\text{H-}^1\text{H}$ gCOSY (500 MHz, CD_2Cl_2), $^{13}\text{C-APT}$ (100 MHz, CD_2Cl_2), and $^1\text{H-}^{13}\text{C}$ gHMQC (500/125 MHz, CD_2Cl_2) data for compound (8a-20a) ₂₀ . Shaded rows correspond to the atoms in the repeating polymer unit	81
4-1	Representative SMAMPs	94
4-2	AROMP of 1-substituted cyclobutene esters with cyclohexenes	104
4-3	Polymerization results	105
4-4	Synthesis of Rcopolymer-8 to Rcopolymer-10	108

4-5	Polymerization results	110
4-6	Synthesis of Homopolymer-11 and Homopolymer-12	111
4-7	Synthesis of Homopolymer-13 and Homopolymer-14	112
4-8	Antibacterial and hemolytic activities of Acopolymer-1 to Homopolymer-14	113
4-9	Dye leakage percentages of Acopolymer-1 to Homopolymer-14 after 5 min	116
4-10	Potassium release percentages of Acopolymer-1 to Homopolymer-14 after 16 min	121
6-1	ROMP reactions monitored by $^1\text{H-NMR}$ spectroscopy	151

Appendix

Appendix		Page
A-1	Checklist for compounds	212
A-2	GPC traces of alternating copolymers	215
A-3	GPC traces of homopolymers	216
A-4	GPC traces of Intermediate-1 to Intermediate-7	217
A-5	GPC traces of Intermediate-8 to Intermediate-10	218
A-6	GPC traces of Intermediate-11 to Intermediate-14	219
A-7	ESI-Mass spectrum of cyclic alternating polymer with catalyst 25	220
A-8	ESI-Mass spectrum of (8a-20a)₁₀ with catalyst 5	221
A-9	¹ H-NMR spectrum of 6b	222
A-10	¹³ C-NMR spectrum of 6b	223
A-11	¹ H-NMR spectrum of 6c	224
A-12	¹³ C-NMR spectrum of 6c	225
A-13	¹ H-NMR spectrum of 6d	226
A-14	¹³ C-NMR spectrum of 6d	227
A-15	¹ H-NMR spectrum of 6e	228
A-16	¹³ C-NMR spectrum of 6e	229
A-17	¹ H-NMR spectrum of 7a	230
A-18	¹³ C-NMR spectrum of 7a	231
A-19	¹ H-NMR spectrum of 7b	232
A-20	¹³ C-NMR spectrum of 7b	233
A-21	¹ H-NMR spectrum of 8b	234

A-22	^{13}C -NMR spectrum of 8b	235
A-23	^1H -NMR spectrum of 8c	236
A-24	^{13}C -NMR spectrum of 8c	237
A-25	^1H -NMR spectrum of 8d	238
A-26	^{13}C -NMR spectrum of 8d	239
A-27	^1H -NMR spectrum of 8e	240
A-28	^{13}C -NMR spectrum of 8e	241
A-29	^1H -NMR spectrum of 8f	242
A-30	^{13}C -NMR spectrum of 8f	243
A-31	^1H -NMR spectrum of 8g	244
A-32	^{13}C -NMR spectrum of 8g	245
A-33	^1H -NMR spectrum of 9a	246
A-34	^{13}C -NMR spectrum of 9a	247
A-35	^1H -NMR spectrum of 20b	248
A-36	^{13}C -NMR spectrum of 20b	249
A-37	^1H -NMR spectrum of 20d	250
A-38	^{13}C -NMR spectrum of 20d	251
A-39	^1H -NMR spectrum of 20e	252
A-40	^{13}C -NMR spectrum of 20e	253
A-41	^1H -NMR spectrum of 20f	254
A-42	^{13}C -NMR spectrum of 20f	255
A-43	^1H -NMR spectrum of 20g	256
A-44	^1H -NMR spectrum of 20h	257

A-45	¹ H-NMR spectrum of 20k	258
A-46	¹³ C-NMR spectrum of 20k	259
A-47	¹ H-NMR spectrum of 20m	260
A-48	¹³ C-NMR spectrum of 20m	261
A-49	¹ H-NMR spectrum of 22	262
A-50	¹ H-NMR spectrum of 23	263
A-51	¹³ C-NMR spectrum of 23	264
A-52	¹ H-NMR spectrum of 29b	265
A-53	¹³ C-NMR spectrum of 29b	266
A-54	¹ H-NMR spectrum of 30	267
A-55	¹³ C-NMR spectrum of 30	268
A-56	¹ H-NMR spectrum of 31	269
A-57	¹ H-NMR spectrum of 33	270
A-58	¹³ C-NMR spectrum of 33	271
A-59	¹ H-NMR spectrum of 34	272
A-60	¹³ C-NMR spectrum of 34	273
A-61	¹ H-NMR spectrum of (6b) ₁₀	274
A-62	¹ H-NMR spectrum of (6c) ₁₀	275
A-63	¹ H-NMR spectrum of (6d) ₁₀	276
A-64	¹ H-NMR spectrum of (6e) ₁₀	277
A-65	¹ H-NMR spectrum of (9a) ₁₀	278
A-66	¹ H-NMR spectrum of (8a-20a) ₃	279
A-67	¹³ C-NMR spectrum of (8a-20a) ₃	280

A-68	¹ H-NMR spectrum of (8a-20a)₁₀	281
A-69	¹ H-NMR spectrum of (8a-20a)₂₀	282
A-70	¹³ C-NMR spectrum of (8a-20a)₂₀	283
A-71	¹³ C-APT-NMR spectrum of (8a-20a)₂₀	284
A-72	¹ H-gCOSY-NMR spectrum of (8a-20a)₂₀	285
A-73	¹ H- ¹³ C-HMQC-NMR spectrum of (8a-20a)₂₀	286
A-74	¹ H-NMR spectrum of (8a-20a)₅₀	287
A-75	¹ H-NMR spectrum of (8a-20a)₁₀₀	288
A-76	¹³ C-NMR spectrum of (8a-20a)₁₀₀	289
A-77	¹ H-NMR spectrum of (8a-20a)₂₀₀	290
A-78	¹ H-NMR spectrum of (8a-20d)₂₀	291
A-79	¹ H-NMR spectrum of (8a-20e)₂₀	292
A-80	¹ H-NMR spectrum of (8a-20i)₂₀	293
A-81	¹ H-NMR spectrum of (8a-20j)₂₀	294
A-82	¹ H-NMR spectrum of (8a-20a-D10)₂₀	295
A-83	¹ H-NMR spectrum of (8c-20a)₂₀	296
A-84	¹ H-NMR spectrum of (8d-20a)₁₀	297
A-85	¹ H-NMR spectrum of (8a)₁	298
A-86	¹³ C-NMR spectrum of (8a)₁	299
A-87	¹ H-NMR spectrum of cyc-(8a-20a-D10)₂₀	300
A-88	¹ H-NMR spectrum of (8a-20a-D10)₂₀-[25]	301
A-89	¹ H-NMR spectrum of (8a-29a-D10)₂₀-[28] (AROMP in CDCl₃)	302
A-90	¹ H-NMR spectrum of (8a-29a-D10)₂₀-[28] (AROMP in toluene-D₉)	303

A-91	¹ H-NMR spectrum of Intermediate-1	304
A-92	¹³ C-NMR spectrum of Intermediate-1	305
A-93	¹ H-NMR spectrum of Intermediate-2	306
A-94	¹ H-NMR spectrum of Intermediate-3	307
A-95	¹ H-NMR spectrum of Intermediate-4	308
A-96	¹ H-NMR spectrum of Intermediate-5	309
A-97	¹ H-NMR spectrum of Intermediate-6	310
A-98	¹ H-NMR spectrum of Intermediate-7	311
A-99	¹ H-NMR spectrum of Intermediate-8	312
A-100	¹ H-NMR spectrum of Intermediate-9	313
A-101	¹ H-NMR spectrum of Intermediate-10	314
A-102	¹ H-gCOSY-NMR spectrum of Intermediate-10	315
A-103	¹³ C-NMR spectrum of Intermediate-10	316
A-104	¹ H-NMR spectrum of Intermediate-11	317
A-105	¹ H-NMR spectrum of Intermediate-12	318
A-106	¹³ C-NMR spectrum of Intermediate-12	319
A-107	¹ H-NMR spectrum of Intermediate-13	320
A-108	¹ H-NMR spectrum of Intermediate-14	321
A-109	¹³ C-NMR spectrum of Intermediate-14	322
A-110	¹ H-NMR spectrum of Acopolymer-1	323
A-111	¹ H-NMR spectrum of Acopolymer-2	324
A-112	¹ H-NMR spectrum of Acopolymer-3	325
A-113	¹ H-NMR spectrum of Acopolymer-4	326

A-114	¹ H-NMR spectrum of Acopolymer-5	327
A-115	¹ H-NMR spectrum of Acopolymer-6	328
A-116	¹ H-NMR spectrum of Acopolymer-7	329
A-117	¹ H-NMR spectrum of Rcopolymer-8	330
A-118	¹ H-NMR spectrum of Rcopolymer-9	331
A-119	¹ H-NMR spectrum of Rcopolymer-10	332
A-120	¹ H-NMR spectrum of Homopolymer-11	333
A-121	¹ H-NMR spectrum of Homopolymer-12	334
A-122	¹ H-NMR spectrum of Homopolymer-13	335
A-123	¹ H-NMR spectrum of Homopolymer-14	336

List of Abbreviations

Ac	N-terminal acetyl
AMP	antimicrobial peptide
AN	acetonitrile
AROMP	alternating ring-opening metathesis polymerization
ATRP	atom transfer radical polymerization
BA	butyl acrylate
BOP-Cl	bis(2-oxo-3-oxazolidinyl)phosphinic chloride
CFU	colony forming unit
CL	cardiolipin
CM	cross metathesis
CONH ₂	C-terminal carboxyamine
CPP	cell penetrating peptide
D _h	hydrodynamic diameter
DIBAL-H	diisobutylaluminium hydride
DIEA	diisopropylethylamine
diSC ₃₅	3,3'-dipropylthiadicarbocyanine iodide
DLS	dynamic light scattering
DMAP	4-dimethylaminopyridine
ECP	effective core potential
EDC·HCl	1-(3-dimethylampropyl)-3-ethylcarbodiimide hydrochloride

Et ₂ O	diethylether
EtOAc	ethyl acetate
GPC	gel permeation chromatography
HRMS	high resolution mass spectroscopy
LPS	lipopolysaccharide
LTA	lipoteichoic acid
MA	methyl acrylate
MIC	minimum inhibitory concentration
NBE	norbornene
NBO	natural bond orbital
NHC	N-heterocyclic carbene
ONBE	oxanorbornene
ONBEDCI	oxanorbornene-dicarboximide
PBD	polybutadiene
PBFI-AM	potassium-binding benzofuran isophthalate-AM
PC	phosphatidylcholine
PCL	polycaprolactone
PDI	polydispersity index
PEO	polyethylene oxide
PFP	pentafluorophenol
PG	phosphatidylglycerol
PLA	polylactic acid
PMA	phosphomolybdic acid

PNB	polynorbornene
PPh ₃	triphenylphosphine
PPO	polypropylene oxide
PS	phosphatidylserine
RAFT	reversible addition-fragmentation chain transfer polymerization
RCM	ring closing metathesis
ROIMP	ring opening insertion metathesis polymerization
ROM	ring opening metathesis
ROMP	ring-opening metathesis polymerization
SANS	small angle neutron scattering
SAR	structure-activity relationship
SEM	scanning electron microscopy
SMAMP	synthetic mimics of AMP
TEA	triethylamine
TEM	transmission electron microscopy
TFA	trifluoroacetic acid
THF	tetrahydrofuran
TLC	analytical thin layer chromatography

Chapter 1

Introduction

I. Ring-Opening Metathesis Polymerization (ROMP)

I.1 Mechanism of ROMP

I.2 Development of ROMP Catalysts

I.3 Application of ROMP in Chemical Biology

II. Antimicrobial Peptides (AMPs)

II.1 Introduction of Antimicrobial Peptides and Cell Penetrating Peptides

II.2 Mechanism of AMPs to Inhibit Bacterial Growth

III. Specific Aims

I. Ring-Opening Metathesis Polymerization (ROMP)

Olefin metathesis reactions have been developed for almost 50 years since the discovery of Ziegler-Natta type olefin addition polymerization.¹⁻² They include ring closing metathesis (RCM),³⁻⁴ cross metathesis (CM)³ or ring-opening metathesis polymerization (ROMP).⁵⁻⁶ Recently, ROMP has received a lot of attention in either polymer chemistry or chemical biology for its controllable polymerization, functional group tolerance, and compatibility with other polymerization methods such as ATRP or RAFT.^{5,7-9}

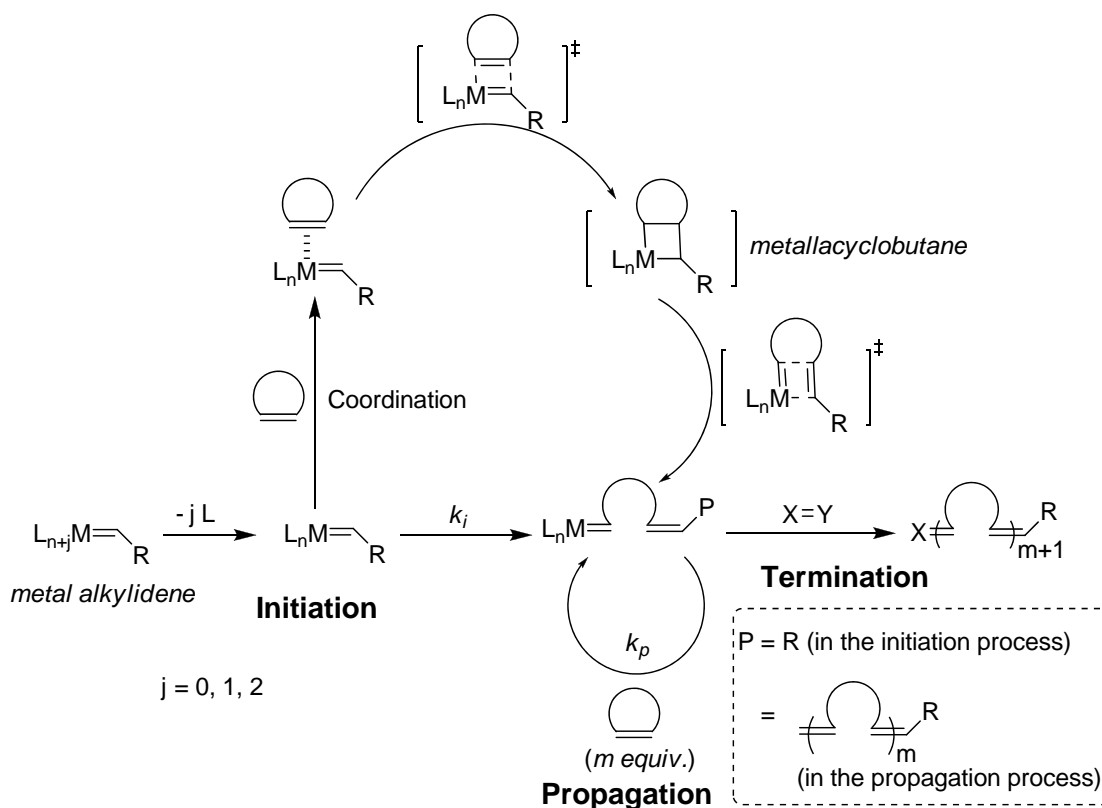
The development of the most popular ruthenium and molybdenum metathesis catalysts greatly facilitate the fast expansion of ROMP in different research fields.⁵ Theoretically, the most perfect catalysts must exhibit the best reactivity in either hydrophobic or hydrophilic solvents to provide linear polymers with controllable molecular weights and narrow polydispersity indexes (PDIs). The catalysts must be very stable when handled under air or moisture, and must be tolerant with most of the functional groups in ROMP monomers such as amides, esters, aldehydes and carboxylic acids.

Besides the great success in the catalyst design, the application of ROMP in either material sciences or chemical biology has received a lot of attention.^{5,7-9} Multiple functional group loading by ROMP provides an entry to study the protein receptor binding or cell imaging in biological systems, and to make drug delivery systems. Polymers with different morphologies such as linear, brush-type, star-shape and cross-linked polymers can be synthesized by ROMP alone or in combination with other polymerization methods.

I.1 Mechanism of ROMP

ROMP is a chain-growth polymerization based on the ring opening of strained cyclic olefins. Generally speaking, there are three steps in ROMP using Mo- or Ru-based catalysts: initiation, propagation and termination (Scheme 1-1).⁵ First the coordination of a cyclic olefin to an electron deficient metal alkylidene forms a metallacyclobutane

intermediate through [2+2] cycloaddition. This mechanism was proposed by Chauvin *et al.* in 1971.¹⁰⁻¹² The subsequent cycloreversion generates a ring-opened metal alkylidene, and this metal alkylidene is active enough to ring open additional cyclic olefins to propagate the chain. In the chain propagation process, theoretically, the metal alkylidene containing the propagating polymer chain should have a similar activity as the original metallocarbene initiator so that the propagation rate constant (k_p) stays the same during polymer chain growth.⁵ Depending on the coordination environment and the reaction conditions, the propagating metal center exists either in the metallocyclobutane form or in the metal alkylidene form.⁵ The chain propagation does not cease until all of the monomer is depleted, until thermodynamic equilibrium is reached (the ring-opening of cyclic olefins is reversible) or until a terminating reagent is added.⁵



Scheme 1-1. General mechanism for a typical ROMP reaction using Mo- or Ru-based catalysts.⁵

The driving force for ROMP is the release of cycloalkene ring strain (ΔH_p in Equation 1-1) that accompanies the ring-opening.^{5-6,13} To minimize the equilibrium monomer concentration ($[M]_e$), high ring-strain energy, high initial monomer concentration, and low reaction temperature are ideally required.¹³ However, to run the ROMP at low temperatures, the catalyst must have high activity and efficient initiation. The ring strain energy should be greater than 5 *kcal/mol* for ROMP to occur. This requirement suggests that ROMP is thermodynamically controlled.¹³⁻¹⁴ Therefore highly ring-strained cyclopropene, norbornene, cyclobutene and cyclooctene are common ROMP monomers (Figure 1-1).¹⁴

$$\ln[M]_e = \frac{\Delta H_p}{RT} - \frac{\Delta S^\theta}{T} \quad \text{(Equation 1-1)}^{13}$$

“Living Polymerization”, defined by Swarc in 1956,¹⁵ has become a valuable criterion to characterize the polymerization quality.¹⁶ Living ROMP must exhibit three features: 1) the initiation must be much faster than the chain propagation ($k_i \gg k_p$) and it must be complete; 2) there is a linear relationship between the number-averaged molecular weight of the polymer (M_n) and monomer conversion; 3) low PDIs (< 1.5).^{5,17} PDI is calculated according to the equation: $PDI = M_w/M_n$ (M_w is the weight-averaged molecular weight and M_n is the number-averaged molecular weight). To meet the first feature of the living ROMP, metal initiators with high activity and stability are strongly required. To get the better control of polymer molecular weights and lower PDIs, secondary metathesis reactions (chain transfer reactions) must be minimized ($k_p \gg k_s$, k_s is the secondary metathesis reaction rate constant).

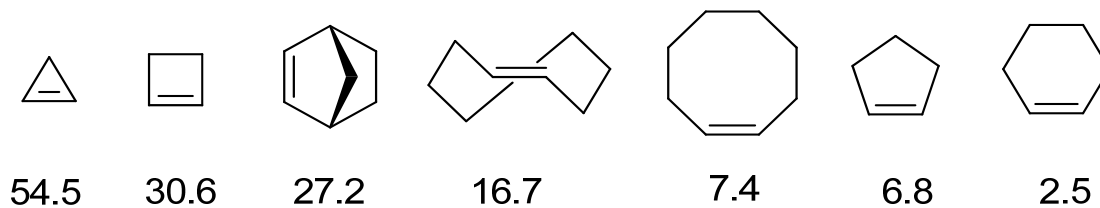
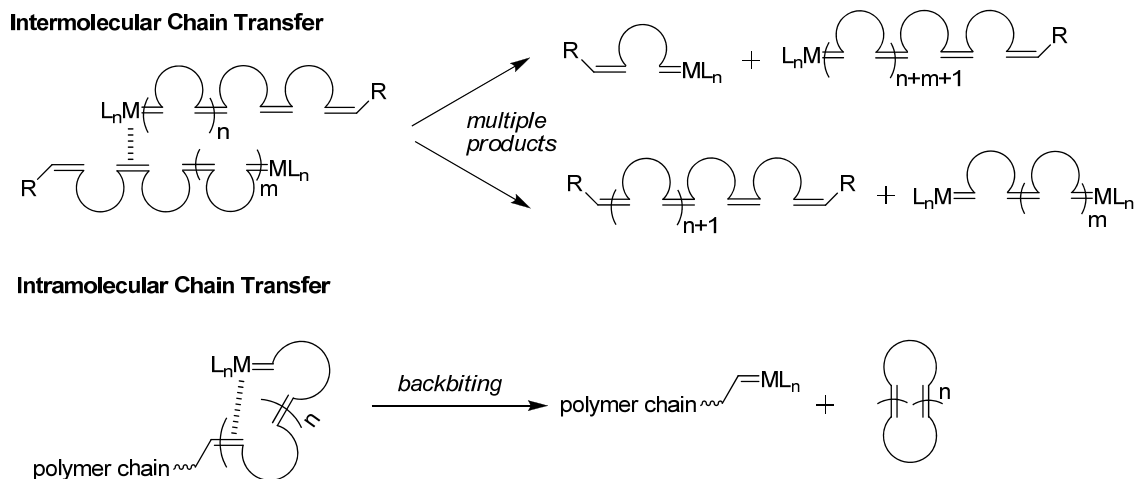


Figure 1-1. Relative ring strain for select cyclic olefins (*kcal/mol*).¹⁸

Secondary metathesis reactions include both intermolecular chain transfer and intramolecular chain transfer reactions (backbiting) (Scheme 1-2). The intermolecular chain transfer reaction represents the cross metathesis reaction between an active metal alkylidene containing the polymer chain and the olefin bond in another polymer chain. As a result, the PDI of the final polymer is increased due to the formation of multiple cross metathesis products, while M_n stays the same. Intramolecular chain transfer reaction means that an active metal alkylidene containing a polymer chain reacts with its own olefin bond along the polymer backbone to generate a cyclic species, and polymers with broad PDIs and lower M_n than the expected value are generated.



Scheme 1-2. Illustration of typical secondary metathesis reactions in ROMP.⁵

The most common reason for chain transfer in ROMP reactions is that the metal alkylidene is too active. Even though completely blocking the chain transfer reactions is challenging, there are several ways to minimize chain transfer by increasing the rate constant ratio k_p/k_s . First, choosing appropriate ROMP solvents may help to limit the secondary metathesis reaction. The addition of a small amount of tetrahydrofuran (THF) into the reaction or using THF as the only ROMP solvent limits secondary metathesis in the ROMP of monocyclic unhindered olefins. This suppression may be due to the coordination of THF to the active metal alkylidene.^{17,19} Second, the addition of external coordination reagents, such as PPh_3 or PPh_2H , limits secondary metathesis through

coordination to the metal alkylidene.^{17,20-21} Third, using hindered cyclic olefins, such as norbornene or 1-substituted cyclic olefins, limits chain transfer by sterically blocking the approach of a polymer chain to the polymer backbone.¹⁷ The reaction time can also affect chain transfer.¹⁷ Generally speaking, longer reaction times generate more chain transfer reaction products. Monomer concentration is also very important to control secondary metathesis. The critical monomer concentration $[M]_c$ has been defined as the initial monomer concentration threshold. Below this concentration, only linear and cyclic oligomers with low molecular weight are formed.^{17,22} Ring closing metathesis (intramolecular chain transfer in ROMP) is largely preferred in dilute solution. On the other hand, there is always a polymer solubility issue when high monomer concentrations are employed in ROMP. High molecular weight polymer chains become too viscous to be dissolved in organic solvents. Therefore, it is very hard to make ultrahigh molecular weight polymers at high monomer concentrations.

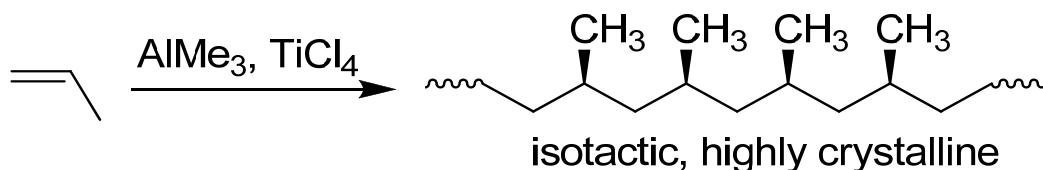
I.2 Development of ROMP Catalysts

In 2005, both Robert H. Grubbs and Richard R. Schrock were awarded the Nobel Prize in Chemistry for their advanced success in developing a series of Grubbs' catalysts and Schrock's catalysts for metathesis reactions.²³⁻²⁴ However, it took almost 35 years to produce the first well-defined efficient metal alkylidene metathesis initiator²⁵ after the discovery of Ziegler-Natta type olefin addition polymerizations in the 1950's. In this section, the history of metathesis catalyst development is reviewed. This review will illustrate how basic science can be applied to benefit the human world, and we also provide insight into the challenges in the design of the future catalysts and monomers.

I.2.1 From ill-defined to well-defined catalysts

From 1955 to the early 1980s, only ill-defined or heterogeneous catalyst systems were known. These catalysts were composed of transition metal salts, organic alkylating agents or solid depositing matrices (Figure 1-2).⁵ In 1955, Ziegler found that Ni salts, the contaminants in the oligomerization of ethylene, catalyzed the metathesis of ethylene to

generate butene instead of oligomers.²⁶ Later on, Ziegler and Natta produced a series of titanium salts in combination with trialkyl aluminum to successfully polymerize ethylene or propylene.²⁷⁻³² The polymer structure of poly(propylene) catalyzed by Ziegler-Natta catalyst was highly isotactic (Scheme 1-3). Their pioneering work brought in multibillion dollars' benefit to the industry, and also made them the Nobel Prize Laureates in Chemistry in 1963.



Scheme 1-3. Ziegler-Natta polymerization.

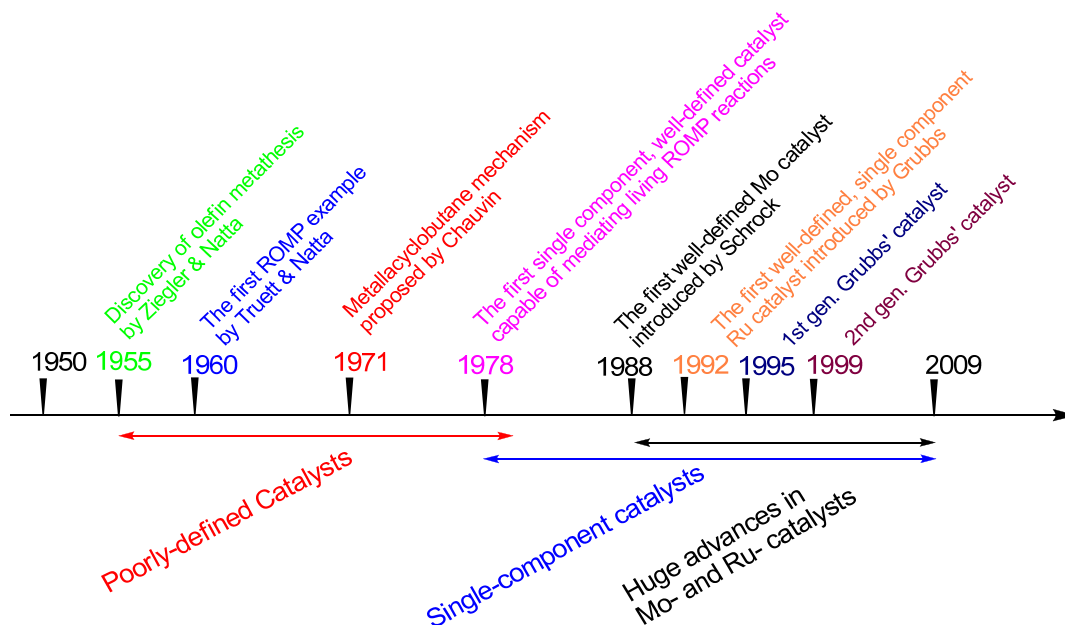


Figure 1-2. Timeline of milestones in the development of olefin metathesis catalysts.

Since then, a large amount of research has been undertaken to discover the mechanism of the olefin metathesis reaction and more efficient metathesis catalysts. A lot of mechanisms were proposed and studied based on the experimental results, and the

mechanism proposed by Chauvin was accepted by most chemists and was consistent with most of the experimental data.¹⁰ Lots of heterogeneous catalysts containing Ti, W, Mo and Re halides or oxides and some Lewis acids such as SiO₂, EtAlCl₂ or Bu₄Sn, were used in commercial applications of olefin metathesis due to their low cost and easy preparation.³³⁻³⁸

The first successful ROMP was achieved by Truetta and Natta independently at almost the same time in 1960.³³⁻³⁴ They found that norbornene could be polymerized by heterogeneous mixtures of Ti, W or Mo halides accompanied by strong Lewis acids to generate a polymer backbone containing repeating 1,3-dimethylidencyclopentane units. This first demonstration of the ring-opening polymerization of norbornene was followed up with much work on the ring-opening polymerization of cyclic olefins catalyzed by the homogeneous or heterogeneous catalyst systems. However, the big problems with these poorly-defined catalyst mixtures were the harsh reaction conditions required, and their poor functional group tolerance due to the use of strong Lewis acids (Table 1-1).⁶ After Chauvin proposed the metal alkylidene mechanism, special attention was paid to the analysis and application of well-defined metal-carbene compounds in ROMP. A series of single-component, well defined Ti-,³⁹⁻⁴⁴ Ta-⁴⁵⁻⁴⁹ or W-based⁵⁰⁻⁵⁶ catalysts were developed for ROMP of cyclic olefins (Table 1-1). A group of W-based imido alkylidene catalysts with the general formula (NAr)(OR')₂W=CHR were introduced by Schrock and became widely used.⁵⁷⁻⁵⁹ Even though their living ROMP succeeded with better initiation and higher activities under milder conditions than ever before, their further application was limited by the extremely poor functional group tolerance of the catalysts (Figure 1-3).

Ti/Ta	W	Mo	Ru
Acids	Acids	Acids	Olefins
Alcohols, Water	Alcohols, Water	Alcohols, Water	Acids
Aldehydes	Aldehydes	Aldehydes	Alcohols, Water
Ketones	Ketones	Olefins	Aldehydes
Esters, Amides	Olefins	Ketones	Ketones
Olefins	Esters, Amides	Esters, Amides	Esters, Amides

↑
Increasing Reactivity

Figure 1-3. Functional group tolerance of various metal-based metathesis catalysts.⁵⁻⁶

1.2.2 Mo-based metathesis catalysts

In 1988, the first single component, well-defined Mo catalysts able to mediate the living ROMP reaction were introduced by Schrock (Figure 1-4).^{25,60} These Mo catalysts exhibited much better functional group tolerance than previous catalysts. The high tolerance made them much easier to synthesize and purify, and more stable in storage or in reactions. It was discovered that **Mo-a** was compatible with ester, carbonate, ether, imide, cyano and halo functional groups in the living ROMP of norbornene derivatives, and it provided polymers with low PDIs (~ 1.1).⁶¹⁻⁶⁵

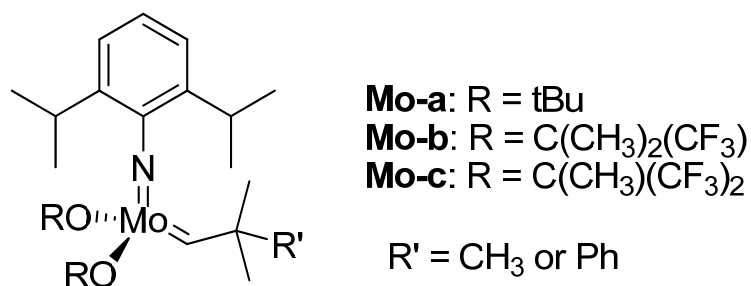


Figure 1-4. Structures of Mo-based imido alkylidene catalysts.

Notably, the Mo catalysts (**Mo-a** to **Mo-c**) showed much higher reactivities than other catalysts, and their high activity was due to the high oxidation state of Mo (four-coordinate 14-electron core). Another remarkable feature of these Mo catalysts is their tunable coordination environment around Mo, and that environment is closely related to their activity and stereoselectivity. The first living ROMP of 3,3-disubstituted cyclopentenes using Schrock's catalysts generated high molecular weight polymers with very low PDIs (<1.05).⁶⁶ Stereospecific ROMP of 3-methyl-3-phenylcyclopropene catalyzed by the biphenolate or binaphtholate coordinated Mo catalysts was also reported by Schrock (Figure 1-5). More than 99% tacticity could be achieved with high PDIs (>1.8) (Figure 1-5) using these catalysts.⁶⁷

The development of the well-defined, activity-tunable Mo-based metathesis catalysts stands as a very important milestone in the development of ROMP catalysts.

However, they are still more reactive with acids, alcohols or aldehydes than with olefins (Figure 1-5). This reactivity suggested that more functional group tolerant catalysts were needed for the further applications.

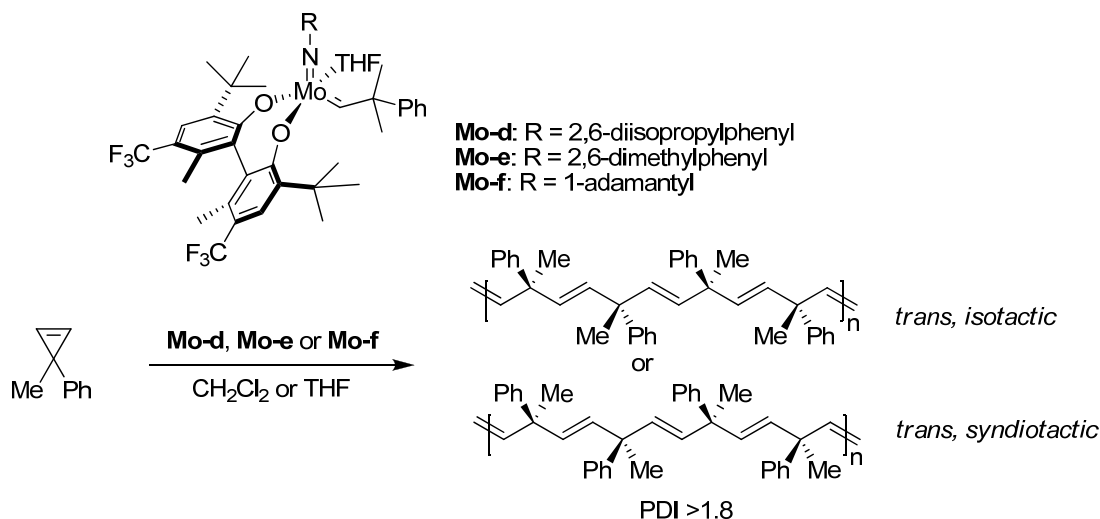


Figure 1-5. Stereospecific ROMP of 3-methyl-3-phenylcyclopropene.

1.2.3 Ru-based metathesis catalysts

Progress with the ruthenium-based catalysts was slow for almost 20 years at the beginning of metathesis catalyst development. Even though they were considered excellent candidates for ROMP due to their high oxidation state and low oxophilicity,⁶ the ROMP initiation time of some ruthenium salts, such as RuCl₃ (hydrate) was too long. However, there was growing evidence that the ROMP reactions were catalyzed by the ruthenium alkylidene species. This insight provided a clear direction for the design of active Ru catalysts.⁶⁸⁻⁷⁶

The first well-defined, single component Ru-based catalyst (PPh₃)₂Cl₂Ru=CHCH=CPh₂ **1** was successfully synthesized by Grubbs through the ring opening of 3,3-diphenylcyclopropene by RuCl₂(PPh₃)₂ in 1992 (Figure 1-6). This catalyst exhibited efficient activity for ROMP of norbornene or cyclobutene and high tolerance of water or ethanol.⁷⁷⁻⁷⁸ The catalyst (PCy₃)₂Cl₂Ru=CHCH=CPh₂ **2**,⁷⁹ containing a better

electron-donating ligand tricyclohexylphosphine (PCy₃), had much better ROMP activity and broader functional group tolerance than catalyst **1** (Table 1-2).⁷⁹ However, both catalyst **1** and **2** provided polymers with poor PDI (PDI > 2) in the ROMP of norbornene.⁷⁹

	Metal	Pros	Cons
Ill-defined catalysts	Ti, W, Mo, Re	low cost, simple preparation	harsh conditions, poor functional group tolerance
Well-defined catalysts	Ti	single-component, living ROMP	high reaction temperature, low activities and poor functional group tolerance
	Ta	single-component, living ROMP	bad control of PDIs, poor functional group tolerance
	W	single-component, living ROMP, high activities,	hard to handle, poor functional group tolerance
	Mo	single-component, living ROMP, high activities, tunable catalyst structures, good functional group tolerance	hard to handle
	Ru	single-component, living ROMP, high activities, tunable catalyst structures, best functional group tolerance	slower kinetics than Mo catalysts, hard to get ultra-high molecular weight polymers

Table 1-1. Summary of different metathesis catalyst systems.

The development of Grubbs' catalyst **3** (Figure 1-6) launched a huge amount of fascinating activities in metathesis reactions (RCM, CM or ROMP) due to its broad functional group tolerance.⁸⁰⁻⁹³ Although catalyst **3** (half-life > 1 week at 55 °C) is more thermally stable than most of the previous catalysts,⁹⁴ strictly inert conditions are required for storage and handling due to its easy decomposition. Mechanistic studies

suggested that chain propagation is catalyzed by the ruthenium carbene species containing only one phosphine ligand bound to Ru.^{84,95-99} However, catalyst **3** exhibited poor molecular weight control and high PDIs in polymerization of norbornene derivatives.

Catalyst	Ease of handling ^a	Rate of initiation ^b	Rate of polymerization ^b	Higher functional group tolerance ^c
1	++++	++	+	++
2	++++	++	++	+++
3	++	++++	+++	+++
4	+++	+++	++++	++++
5	+++++	++++	++++	+++++

Table 1-2. Comparison of different homogeneous well-defined Ru-based catalysts. ^a Less “+” represent more inert condition required. ^b More “+” represent faster initiation or polymerization rates. ^c More “+” represent better functional group tolerance. ^d More “+” represent better PDI control.

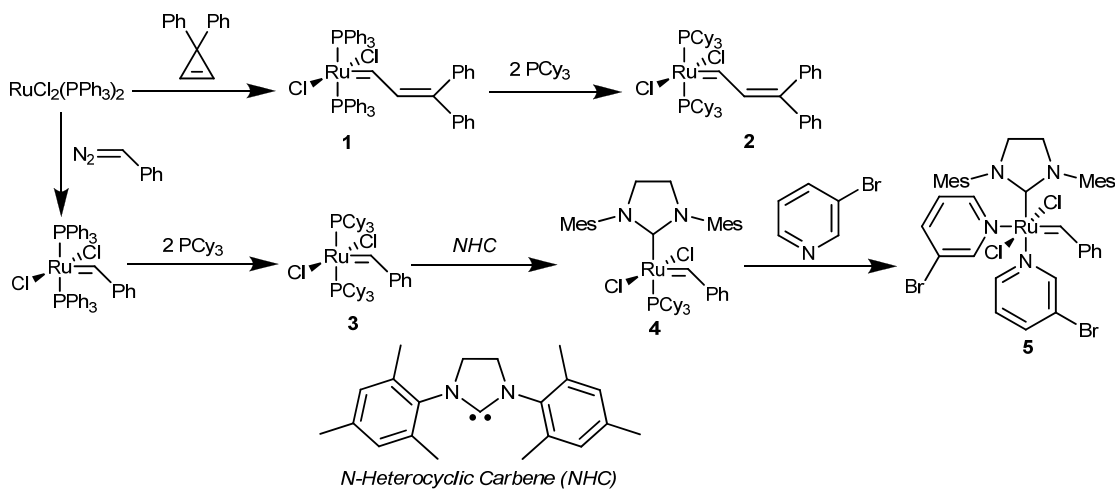


Figure 1-6. Synthesis of well-defined Ru alkylidene initiators **1-5**.

Grubbs' catalyst **4** was synthesized by replacing one PCy₃ group with the N-heterocyclic carbene (NHC).¹⁰⁰⁻¹⁰³ NHC can form a stronger bond with Ru and donate more electron density to the ruthenium alkylidene double bond.¹⁰⁴ As a result catalyst **4** had much better thermostability, ROMP activity, and functional group tolerance than catalyst **3**. However, the slower initiation rate and the competing secondary metathesis reactions limit the molecular weight control and raise the PDI of polymers in some cases.

Replacing the phosphine ligand in catalyst **4** with a weaker binding pyridine ligand to form Grubbs' catalyst **5** greatly improves the thermostability, ROMP activity, and initiation rate of the catalyst while keeping its excellent functional group tolerance intact.¹⁰⁵⁻¹⁰⁹ A lot of living ROMP reactions catalyzed by **5** generated linear polymers with accurate molecular weight control and low PDIs, and those polymers have been applied in a broad range of applications.^{5,9,17,110-111}

1.2.4 Challenges in the future development of Ru-based catalysts

One big challenge for the development of improved ruthenium catalysts is living ROMP in aqueous solution.⁵ Water-soluble polymers are especially required for biomedical applications. However, most of the common Ru catalysts are not soluble in water. Therefore, there is a high need for the development of water-soluble Ru catalysts that allow precise control of molecular weight and PDI. Several typical water-soluble Ru catalysts are illustrated in Figure 1-7.¹¹²⁻¹¹⁶ Although all these water-soluble Ru catalysts are metathesis active, living ROMP in water is very difficult to succeed without the presence of a strong acid (e.g. HCl) or a copper salt (e.g. CuSO₄) due to the rapid decomposition of the propagating species. There is still a long way to go to develop Ru catalysts with faster kinetics and better PDI control for aqueous ROMP reactions.⁵

Another challenge is the synthesis of polymer materials with special topologies.⁵ Bielawski and Grubbs developed a new class of catalysts (Figure 1-8)¹¹⁷⁻¹¹⁸ to polymerize cyclooctene or 1,5-cyclooctadiene generating cyclic polymers with high molecular weights (> 200 kDa) through the intramolecular backbiting. They also found that cyclic polymers exhibited higher melting and crystallization temperatures, and lower viscosities than linear polymers containing the same repeating units and molecular weights.¹¹⁷⁻¹¹⁸

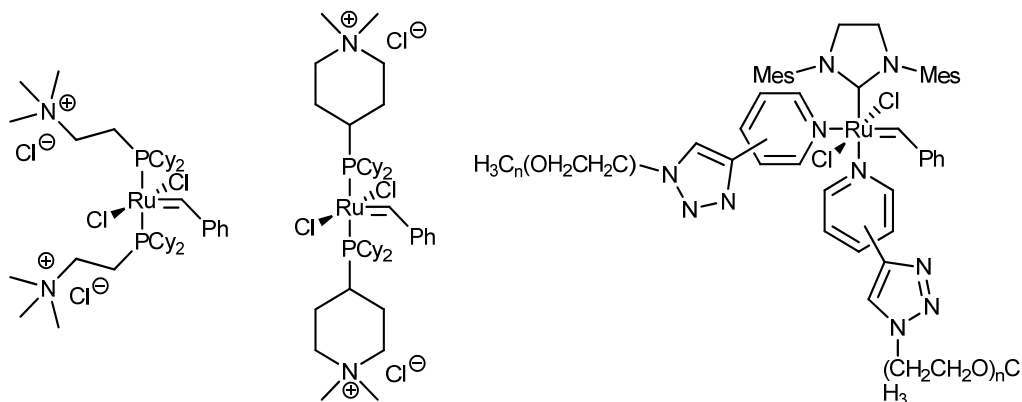


Figure 1-7. Typical structures of water-soluble Ru catalysts.

The challenge in the ROMP of trisubstituted or tetrasubstituted cyclic olefins is the steric hindrance that affects the binding of cyclic olefins to the ruthenium alkylidene. Sampson's group has developed the living ROMP of trisubstituted cyclobutene amides.¹¹¹ One of my projects was focused on further understanding the ROMP of other trisubstituted cyclobutene derivatives.

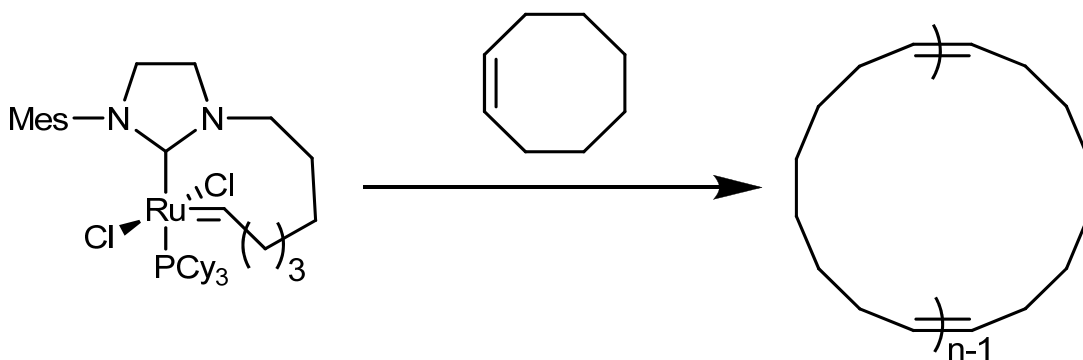


Figure 1-8. Synthesis of cyclic polymers by ROMP.

I.3 Application of ROMP in Chemical Biology

ROMP reactions catalyzed by the well-defined Ru-based initiators of cyclic olefins containing bioactive functional groups provide unsaturated linear polymer scaffolds with very low PDIs (Figure 1-9). These scaffolds have been applied in

biological and medicinal research with a fast-growing speed. Norbornene (NBE), oxanorbornene (ONBE) and oxanorbornene-dicarboximide (ONBEDCI) derivatives are the most popular ROMP monomers that have been applied in chemical biology (Figure 1-9).⁸

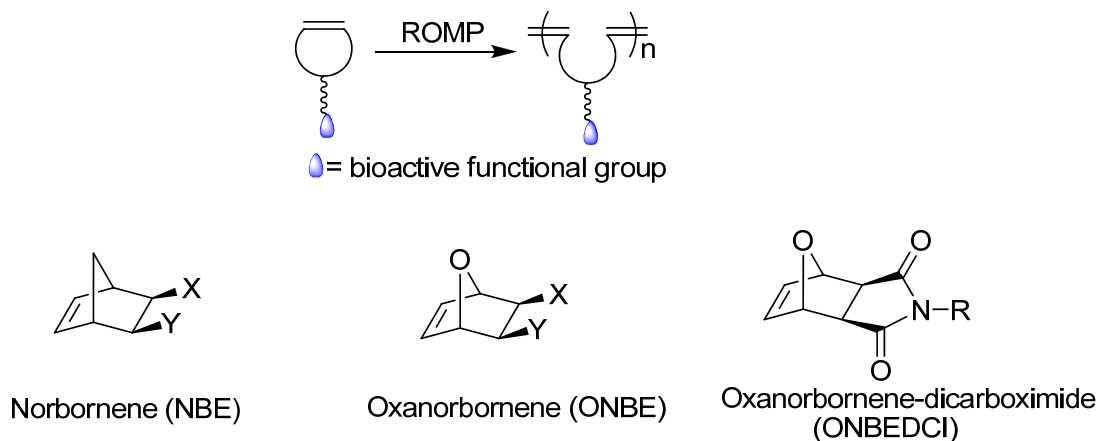


Figure 1-9. Synthesis of linear polymers containing the bioactive functional groups by ROMP and structures of some common monomers.

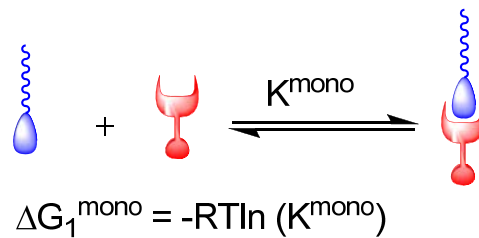
1.3.1 Multivalent binding in biological systems

A multivalent interaction represents the non-covalent association between multiple ligands and multiple receptors, and can exhibit much stronger binding than the monovalent interaction (Figure 1-10).¹¹⁹⁻¹²⁰ The cooperativity coefficient (α), defined in Figure 1-10, represents the degree of cooperativity in the multivalent interaction. Positive cooperativity (synergistic effect) is defined as $\alpha > 1$, while the noncooperative or additive multivalent interaction comes with $\alpha = 1$. Multivalent binding can include chelation, subsite binding, clustering and statistical rebinding (Figure 1-11).⁸⁻⁹

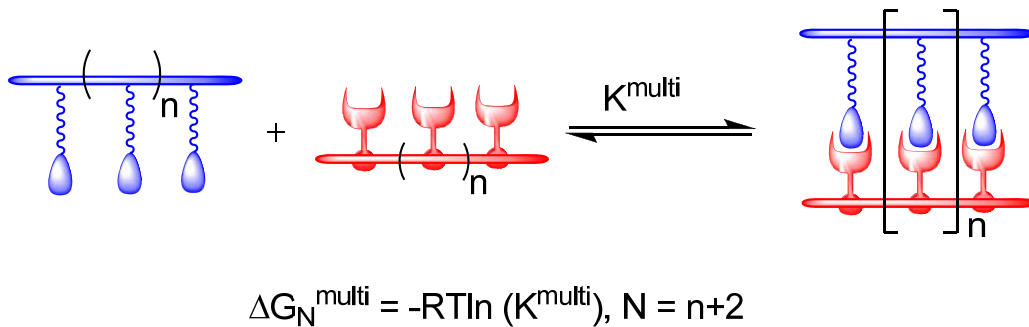
Kiessling and her coworkers pioneered making linear polymers containing multiple bioactive functional groups, e.g., carbohydrates, using Ru-catalyzed ROMP. These polymers were applied in the studies of the cell signal transduction and the *in vivo* immune response.^{9,121-124} Grubbs' group synthesized ROMP polymers containing the multiple GRGD or SRN peptides, and they found these polymers bound with cell surface

integrins synergistically.¹²⁵⁻¹²⁸ The binding mechanisms, receptor colocalization and interreceptor communication were analyzed through the ligand-receptor binding avidity assay by changing the polymer length or ligand density. These binding interactions are closely related to cell differentiation, cellular processes affecting migration or cell survival.^{9,122}

Monovalent interaction



Multivalent interaction



$$\alpha = \text{degree of cooperativity} = \Delta G_N^{\text{multi}} / (N \Delta G_1^{\text{mono}})$$

Figure 1-10. Thermodynamics of monovalent and multivalent interactions.

Sampson's group made a series of poly(NBE) homopolymers and triblock copolymers containing the ECD tripeptide motif to target the receptors in the mammalian egg membrane (Table 1-3).^{110,123,129-130} By comparing the binding affinities of polymers with varied polymer lengths and ECD densities, the bivalent binding mechanism was concluded and the existence of co-receptors in the egg membrane was suggested.

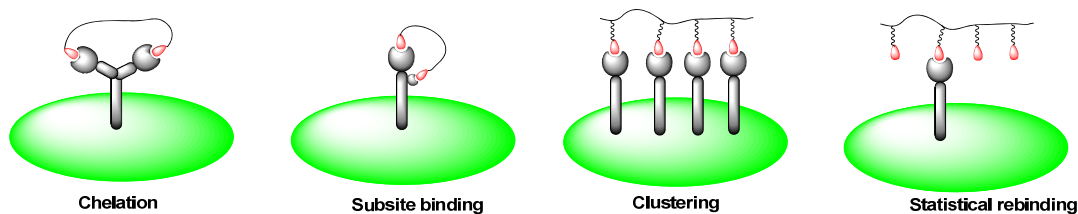


Figure 1-11. Representative binding mechanisms for multivalent ligands at an interface.

1.3.2 Polymeric drug delivery

ROMP has been applied in polymer drug delivery systems to make linear polymer carriers that bind the drug molecule through a covalent bond or noncovalent interaction such as hydrogen bonds, hydrophobic interactions or electrostatic interactions.⁸ It has been suggested that the polymeric drug delivery may overcome problems with small-molecule drugs, such as bad solubility in water, side effects, fast degradation or elimination *in vivo* or poor site-specificity.^{8,131}

There are several requirements for polymeric drug delivery systems: increased water solubility, biocompatibility or biodegradability, bioresponsive polymer-drug linker, adequate drug carrying capacity, and the ability to target.⁸ ROMP reactions catalyzed by the well-defined Ru initiators **3-5** provide homopolymers (drug motifs are connected with the side chains or with the main chains through the covalent bonds) and amphiphilic block copolymers (drug motifs are connected with the polymer carrier covalently or noncovalently during the micelle formation) with low PDIs and controllable polymer lengths (Table 1-4). Drug release is achieved through the enzymatic hydrolysis of ester bonds or the permeation of drug molecules out of the micelle wall.¹³²⁻¹³³

Site-targeting drug delivery can be easily accessed in the ROMP reactions through the incorporation of targeting motifs such as oligosaccharides, monoclonal antibodies or cell-penetrating peptides on the surface of the micelle, in one block of the block copolymers or in the terminus of the linear scaffold.¹³⁴⁻¹³⁷ However, the big challenges for ROMP-based polymer therapeutics are their broad mass distribution in the whole body and their slow degradation *in vivo*.¹³⁸⁻¹³⁹

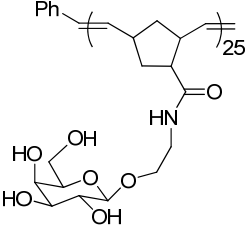
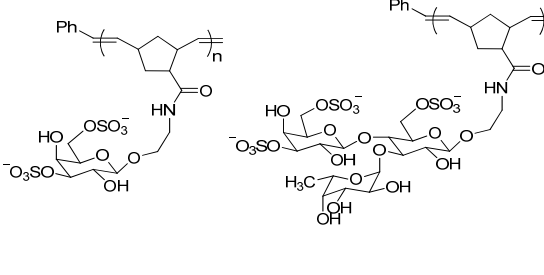
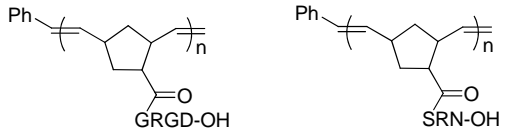
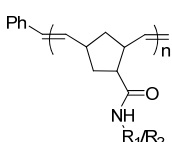
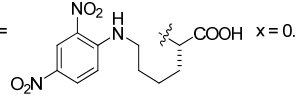
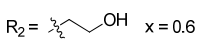
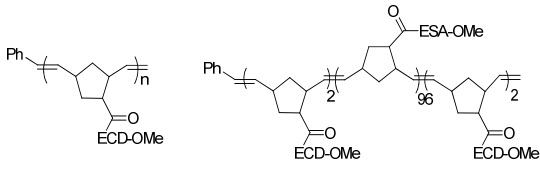
Interface	Receptor	Example polymers
Cell surface	Bacterial chemoreceptors ¹⁴⁰	
	L-Selectin ¹⁴¹⁻¹⁴⁵	
	Cell surface integrin ¹²⁵⁻¹²⁸	 <p>GRGD = Gly-Arg-Gly-Asp tetrapeptide SRN = Ser-Arg-Asn tripeptide</p>
	B cell antigen receptor ¹⁴⁶	 <p> $R_1 =$  $x = 0.4$ $R_2 =$  $x = 0.6$ </p>
Egg membrane	Egg membrane receptors for sperm binding and fusion ^{110,123,129-130}	 <p>ECD = Glu-Cys-Asp tripeptide ESA = Glu-Ser-Ala tripeptide</p>

Table 1-3. Multivalent interactions at interfaces.

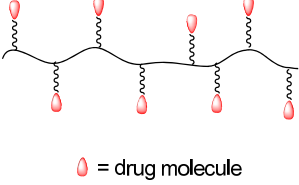
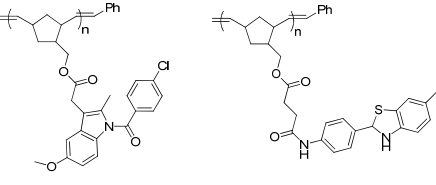
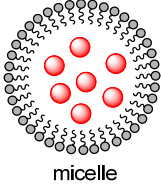
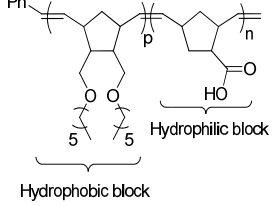
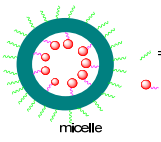
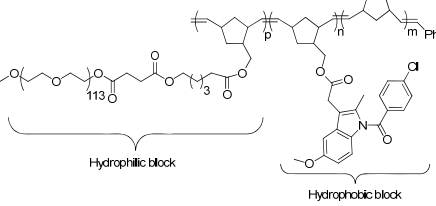
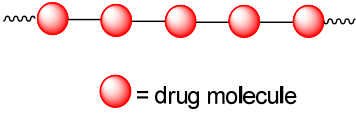
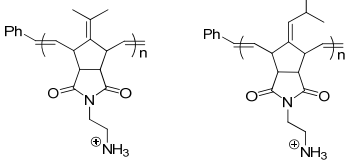
Drug delivery	Polymer carrier	Examples
	 <p style="text-align: center;">● = drug molecule</p>	
Therapeutic Polymer carrier ¹⁴⁷⁻¹⁵¹	 <p style="text-align: center;">● = drug molecule</p> <p style="text-align: center;">micelle</p>	 <p style="text-align: center;">Hydrophobic block</p> <p style="text-align: center;">Hydrophilic block</p>
	 <p style="text-align: center;">● = hydrophilic side chain</p> <p style="text-align: center;">● = drug-conjugated hydrophobic side chain</p> <p style="text-align: center;">micelle</p>	 <p style="text-align: center;">Hydrophilic block</p> <p style="text-align: center;">Hydrophobic block</p>
Main chain therapeutics ¹⁵²	 <p style="text-align: center;">● = drug molecule</p>	

Table 1-4. Polymeric drug delivery systems.

II. Antimicrobial Peptides (AMPs)

The fight against bacterial infection is one of the hottest fields in modern medicinal discovery. Since the 1940s, antibiotics terminate bacterial infections incredibly effectively, and in the process, a huge amount of human lives have been saved. Classic antibiotics work through several ways to inhibit bacterial infections, such as inhibiting bacterial cell wall formation or bacterial metabolism, interrupting protein synthesis, or interfering with DNA synthesis and/or cell membrane permeability. However, antibiotic resistance has become a very serious problem, because of widespread and inappropriate use of antibiotics, and is even challenging our most powerful antibiotics.¹⁵³⁻¹⁵⁴ Therefore, it is urgent to discover new classes of antibiotics to overcome bacterial drug resistance.

II.1 Introduction of Antimicrobial Peptides and Cell Penetrating Peptides

Arginine or lysine – rich antimicrobial peptides (AMPs) that are secreted from some microorganisms or mammalian animals have been studied a lot, since they exhibit excellent antibacterial activity against a broad spectrum of microbes and have very low host cytotoxicity.¹⁵⁵⁻¹⁵⁸ It was also discovered that these AMPs may not only act as antibiotics, but also as antivirals¹⁵⁹⁻¹⁶⁰ immunomodulators¹⁶¹ and antitumor drugs.¹⁶² These AMPs fold into different 3D structures, such as α -helix (Figure 1-12), β -sheet or a looped structure through the disulfide bond.^{154,163-164} The amino acid sequences of a series of common AMPs are listed in Table 1-5.^{157,163,165}

There are several common features for these AMPs. First they are short peptides (<10 kDa).¹⁶³ Second, they bear cationic charges along the peptide chain (Figure 1-12), no matter what 3D structures they have, and the net positive charges range from +2 to +9.¹⁶³ Third, the amphipathicity of α -helical peptides is presented through the alignment of hydrophilic amino acid residues along one side and hydrophobic residues along the opposite face (Figure 1-12), while the other AMP peptides show an unorganized polar and hydrophobic residue distribution.¹⁵⁷ Recently, several AMP databases have been established to further identify the structural features of both the discovered and potential AMPs to facilitate the peptide design for the structure-function relationship analysis (<http://aps.unmc.edu/AP/main.html>; www.bbcm.units.it/~tossi/pag1.htm).^{163,166}

II.2 Mechanism of AMPs to Inhibit Bacterial Growth

The cell wall of Gram-positive bacteria is composed of a cross-linked peptidoglycan polymer layer containing lipoteichoic acids (LTA) and an inner cytoplasmic membrane containing the phospholipid bilayers and some proteins (Figure 1-13).¹⁶³ The cell wall of Gram-negative bacteria consists of two membranes (outer membrane and inner membrane) and a central peptidoglycan layer between the above two membranes (Figure 1-13).¹⁶³ The outer membrane is rich in acidic lipids such as lipopolysaccharides (LPS).¹⁶³ In general, the microbial cell wall surface is highly

surrounded by the negative charges. Most bacterial plasma membranes contain a large amount of anionic phospholipids, such as phosphatidylglycerol (PG), phosphatidylserine (PS) and cardiolipin (CL).¹⁶³

AMP	Amino acid sequences	Mechanism
Cecropin A	KWKLFKKIEKVGQNIRDGIKAGPAVAVVGQATQIAKamide	Transmembrane pore formation: Carpet ¹⁶⁷⁻¹⁶⁸
Magainin II	GIGKFLHSAKKFGKAFVGEIMNS	Transmembrane pore formation: Toroidal pore ¹⁶⁹
Penetratin	RQIKWFQNRMRKWKK	Endocytosis, ¹⁷⁰ endosomal escape mediated by pH gradient or transmembrane potential ¹⁷¹⁻¹⁷²
Buforin II	TRSSRAGLQFPVGRVHRLLRK	Transmembrane pore formation, Bind nucleic acids ¹⁷³
Pep-1	AcKETWWETWWTEWSQPKKKRKV-cysteamine	Transmembrane pore formation, ¹⁷⁴ transmembrane potential w/o pores ¹⁷⁵
LAH4	KKALLALALHHLAHLALHLALALKKA-CONH ₂	Transmembrane pore formation ¹⁷⁶

Table 1-5. Amino acid sequences of some natural AMPs. Ac: N-terminal acetyl; CONH₂: C-terminal carboxyamine.

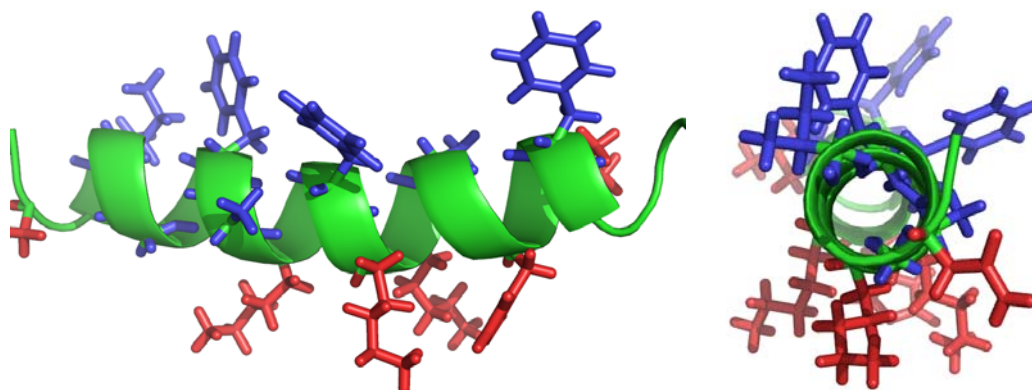


Figure 1-12. Facially amphiphilic helical AMP magainin II, side view (left), top view (right). Hydrophilic side chains are shown in red, and hydrophobic side chains in blue.¹⁵⁶

The facial lysines or arginines facilitate the attraction of AMPs to the bacterial cell wall through electrostatic interactions. No specific receptors were identified in the

bacterial cell walls or plasma membranes for the binding of AMPs,¹⁶³ and that suggests that the bacteria may only become resistant to AMPs through the whole lipid membrane deformation.

After the initial attachment of AMPs to the bacterial membranes, a lot of peptides accumulate on the bacterial membranes. As a result, the peptide concentration (C_l) on the bacterial membranes is much higher than that (C_w) in the aqueous phase.^{155,157,163} It has been suggested that the ratio between C_l and C_w is probably more than 10,000.¹⁵⁵ It was found that once C_l reached a specific value, referred to as the “threshold concentration”, the subsequent membrane disruption actions proceeded in a dramatically rapid way. This threshold concentration is described as the minimum inhibitory concentration (MIC).

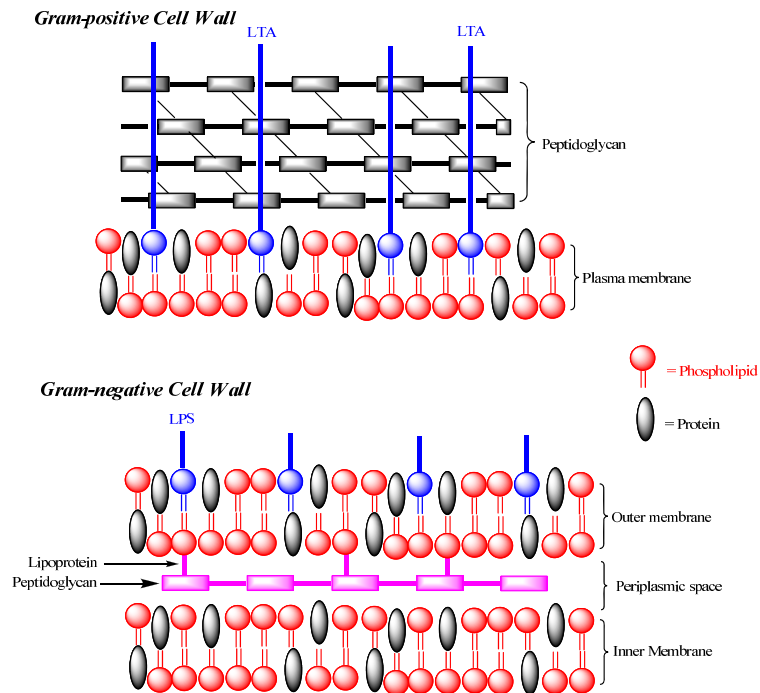


Figure 1-13. Cell wall compositions of Gram-positive and Gram-negative bacteria.

The regular amphiphilic structure of AMPs help them assemble on the lipid membrane, insert into the lipid layer and finally cause the bacterial membrane damage, such as forming pores or channels (Figure 1-15).^{155,157,163} Several mechanisms have been proposed to explain how AMPs could disrupt the bacterial membranes, including the

barrel-stave model, the carpet mode, the toroidal model and the distorted toroidal model.^{155,157} Different types of techniques have been applied to study the mechanisms of AMP activity, such as scanning and transmission electron microscopy (SEM and TEM),¹⁷⁷⁻¹⁷⁸ fluorescence labeling,^{169,179-183} ion channel formation monitoring,¹⁸⁴⁻¹⁸⁶ circular dichroism,¹⁸⁷⁻¹⁸⁸ solid-state NMR spectroscopy^{176,189-191} and neutron diffraction.¹⁹²⁻¹⁹⁵

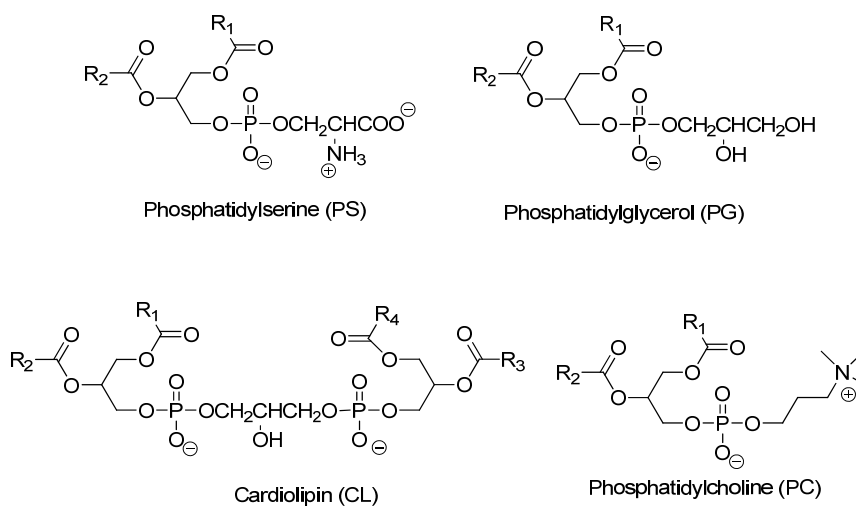


Figure 1-14. General structures of some common phospholipids.

The AMPs exhibit minimal toxicity towards mammalian cells. The low toxicity may be due to the different membrane composition of mammalian cells (Figure 1-15).^{155,157,163} Mammalian cell membranes are rich in the neutral phospholipids (such as PC, 45-55%) and cholesterol (10-20%),¹⁹⁶ so that they are more hydrophobic than the bacterial cell membranes. As a result, the electrostatic interaction between AMPs and mammalian cell membranes is much weaker than that between AMPs and bacterial cell membranes.

It was also discovered that some AMPs could penetrate through the bacterial plasma membrane and bind to intracellular targets, such as autolysins, phospholipases, DNA, and RNA molecules.^{155,157,197-203} The intracellular binding leads to cellular dysfunction or lysis, and finally cell death. These intracellular killing AMPs are rich in arginine rather than lysine, and they are also called cell penetrating peptides (CPPs).

Generally speaking, it is very hard for the bacteria to evolve AMP-resistance.¹⁵⁷ They would need to alter the net surface charges by changing the phospholipid bilayer composition or to change the membrane proteins. Regardless, some novel bacterial resistance to AMPs has been discovered.²⁰⁴⁻²⁰⁵ Therefore, a lot of research investigations are focused on the AMP studies for their potential application in the development of new antibiotics. In addition, the poor *in vivo* activity and the structural complexity of AMPs have led to the development of synthetic mimics of AMPs (SMAMPs).^{156,206}

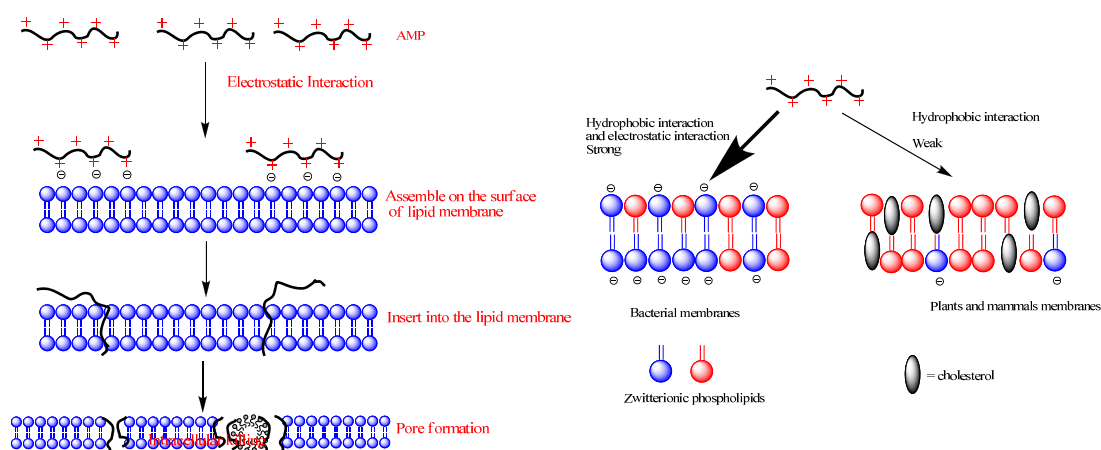


Figure 1-15. General mechanism of killing bacteria by AMPs.

III. Specific Aims

III.1 Scope of the ROMP Reaction of 1-Substituted Cyclobutenes

Linear polymers containing syndiotactic or isotactic functional groups are highly required in chemical biology applications to study structure-activity relationships (SAR). ROMP of NBE or OXNBE derivatives provides polymers containing lots of stereo- or regio- isomer centers, and these stereo- and regio-ambiguities may impair the analysis of their activity. Previously, Sampson's group reported 1-substituted cyclobutene amide underwent ruthenium-catalyzed ROMP to provide polymers with translationally invariant backbones (*E*-configuration) and excellent PDIs.¹¹¹ However, the source of the regio- and stereospecificity was not elucidated.

To better understand the regio- and stereochemistry of the ROMP reactions of 1-substituted cyclobutenes, several 1-substituted cyclobutenes with varied electron densities or steric interactions in the olefin bonds, such as 1-cyclobutene esters, 1-cyclobutene secondary amides, 1-cyclobutene tertiary amides or 1-cyclobutenylmethyl acetates, were synthesized and tested in ROMP. The stereo- and regiochemistry of the ROMP polymers were studied by 1D and 2D-NMR spectroscopy. NBO charge and energy difference calculations of intermediates and products were undertaken to explain the experimental results.

III.2 Alternating ROMP (AROMP) of Cyclobutenes and Cyclohexenes

Copolymers are employed in applications ranging from the biomedical to the electronic.²⁰⁷⁻²⁰⁸ Among the most commonly used are block copolymers that require phase separation of the two blocks for their function, e.g., drug delivery,²⁰⁹⁻²¹¹ or random copolymers that incorporate two functional moieties that communicate, e.g., organic light emitting diodes.²¹² Regularly alternating polymers allow optimal positioning of functional substituents. However, they are harder to access synthetically.

In the studies of 1-substituted cyclobutenes, it was found that ring-opening metathesis of 1-cyclobutenecarboxylate ester catalyzed by ruthenium catalyst **5** to generate the enoic ruthenium carbene occurred without polymerization. Grubbs' group²¹³⁻²¹⁴ had demonstrated that the enoic ruthenium carbene can ring-open unstrained cycloalkenes such as cyclohexene, cyclopentene²¹⁵ and cycloheptene.²¹⁵ These results suggested that alternating polymers of 1-cyclobutene ester and cyclohexene could be produced.

AROMP of 1-cyclobutene ester and cyclohexene was observed and confirmed by ¹H-NMR spectroscopy. The alternating structure of the polymers was characterized by NMR spectroscopy and stable isotope-labeling experiments. Lastly, the functional group tolerance of the AROMP methodology was tested.

III.3 Antimicrobial Studies of Cyclobutene Polymers: from ROMP to AROMP

Synthetic mimics of AMP (SMAMP) have been applied in the development of antibiotics and in the mechanism studies of AMPs. A variety of SMAMPs including β -peptides,²¹⁶⁻²²¹ peptoids,²²² arylamide oligomers,²²³⁻²²⁶ phenylene ethynylene oligomers,²²⁷⁻²²⁸ polyacrylates²²⁹⁻²³³ and polynorbornenes,²³⁴⁻²³⁸ have been synthesized and tested as antibiotics.

In our group, a series of alternating amphiphilic copolymers containing different amine groups and amphiphilicity were synthesized through AROMP of 1-cyclobutene ester and cyclohexene. Their antimicrobial activities were assayed and their selectivities were compared with random copolymers or homopolymers. Their mechanisms in inhibiting the bacterial growth were studied by thin-section transmission electron microscopy (TEM), dye leakage vesicle assays, membrane depolarization assays and potassium release assays.

Chapter 2

Scope of the ROMP Reaction of 1-Substituted Cyclobutenes

I. Introduction

II. Results

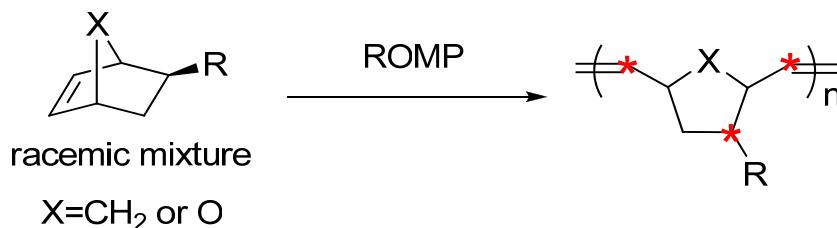
III. Discussion

IV. Summary

V. Future Perspectives

I. Introduction

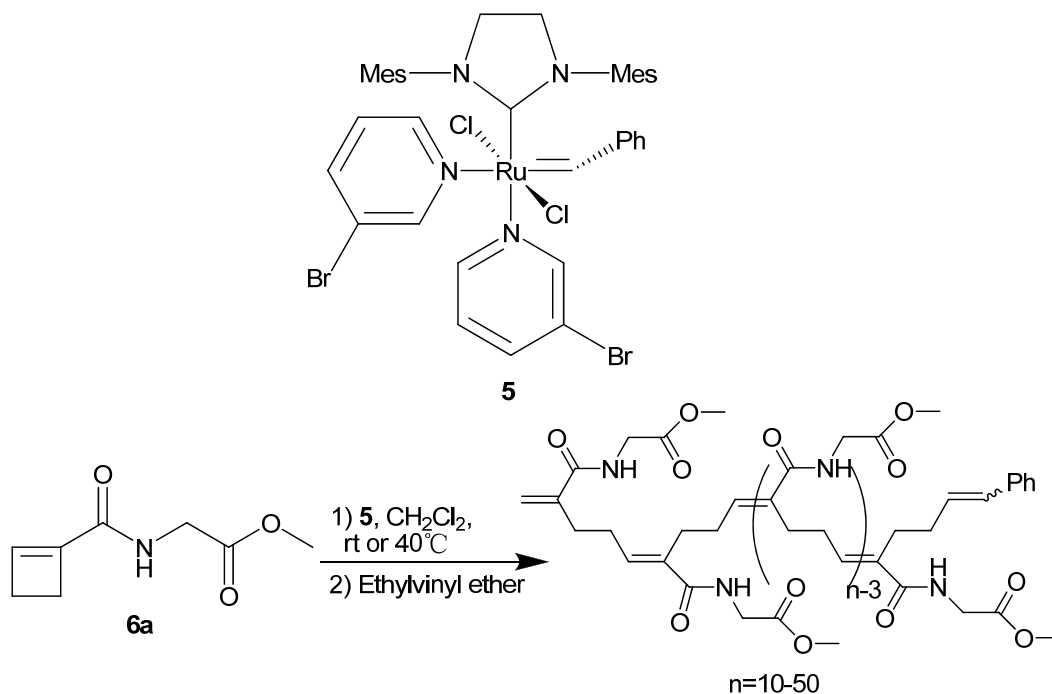
A variety of strained monomers undergo ring opening metathesis polymerization (ROMP) to provide a range of polymer materials.²³⁹⁻²⁴⁴ Development of N-heterocyclic carbene-substituted ruthenium catalysts with pyridyl ligands (3rd generation Grubbs' catalysts), e.g., **5**, provided entry into living ROMP reactions. The fast initiation rate ($k_i \gg k_p$) (Scheme 1), high thermal stability, and excellent functional group tolerance of **5** enabled a multitude of applications to be pursued.^{5-6,105-106,108-109,125,245} Norbornene (NBE), oxanorbornene (ONBE), and oxanorbornene-dicarboximide (ONBEDCI) derivatives are the most popular ROMP monomers due to their high ring strain, easy preparation, and the facility with which functional groups are attached.⁸ Living ROMP of these monomers generates linear polymers with accurate molecular weight control and low polydispersities (PDIs). However, internally heterogeneous mixtures are obtained because the polymerization reactions lack complete stereochemical and regiochemical control (Scheme 2-1).^{125,243,246} The synthesis of linear polymers with stereoregular backbones by ROMP should allow the development of improved "structure-property" relationships for the optimization of electrical, physical and biomedical properties.^{63,247-249}



Scheme 2-1. Stereocenters of poly(NBE)s or poly(ONBE)s. (Red stars represent the stereocenters)

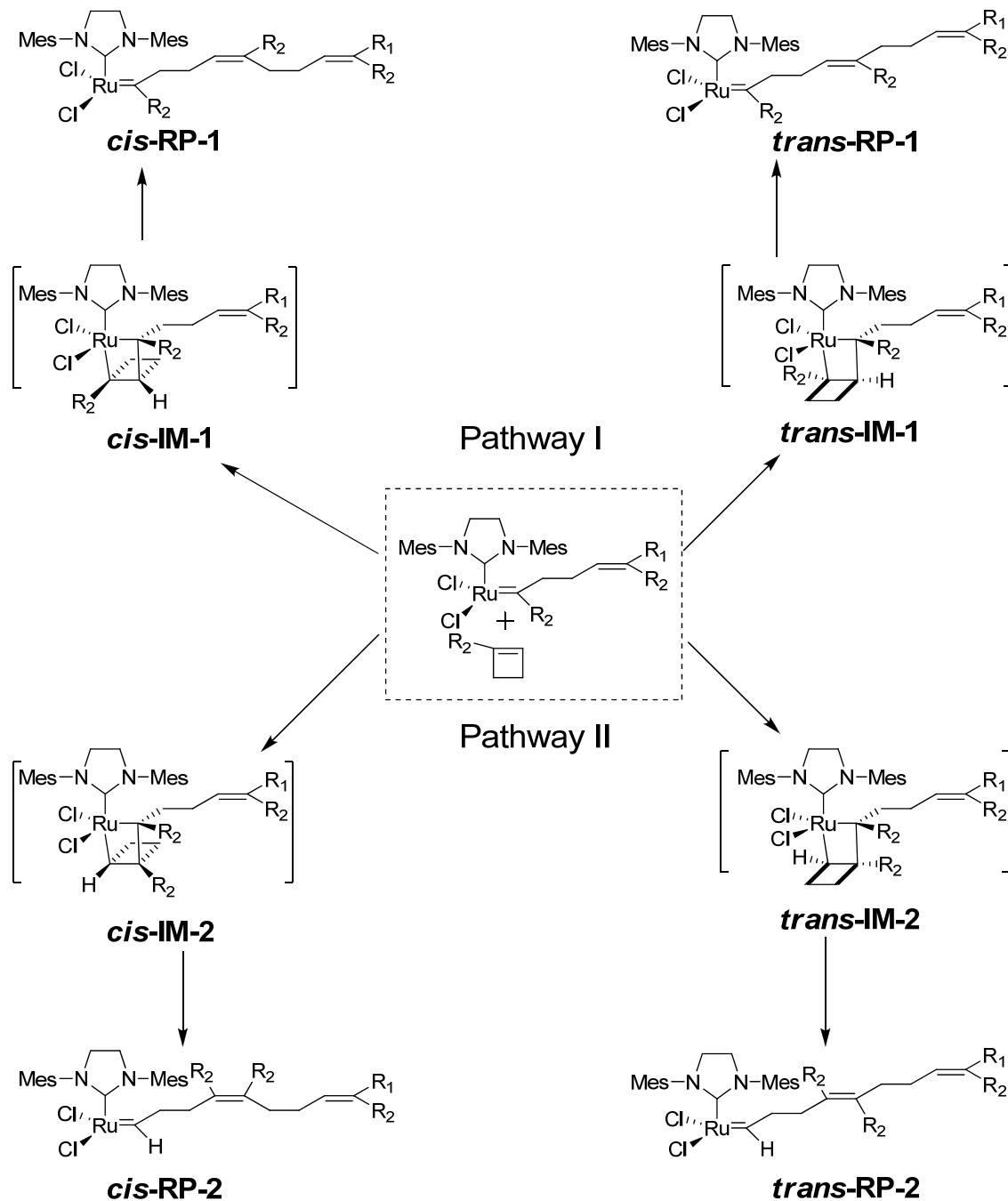
To overcome the stereochemical ambiguities, the Sampson group developed the living ROMP reaction of 1-substituted cyclobutene monomer **6a** catalyzed by the Ru initiator **5** (Scheme 2-2). As a result, a polymer backbone with both high regio- and stereoregularity is produced.¹¹¹ The synthesized polymer length ranged from 10-mers to

50-mers with low PDIs (1.3-1.5) and accurate molecular weight control.¹¹¹ This regio- and stereoselective ROMP provides an entry to synthesize linear polymers containing tactic bioactive functional groups that can be applied in the biomedical studies.



Scheme 2-2. Ring Opening Metathesis Polymerization of **6a**.

The stereo- and regiochemistry of ROMP of 1-substituted cyclobutenes is summarized in Scheme 2-2. When 1-substituted cyclobutene coordinates to the ruthenium center of the catalyst, there are two Ru-cyclobutane intermediates that may be formed (*cis* or *trans-IM-1* and *cis* or *trans-IM-2*, Scheme 2-2). In Pathway I, the Ru-cyclobutane ring is formed with a 1,3-relationship between two substituents. Whereas in Pathway II, there is a 1,2-relationship between the two substituents. As a result, four different ring-opened ruthenium carbenes (*cis* or *trans-RP-1* and *cis* or *trans-RP-2*, Scheme 2-2) can be generated. The selectivity for the intermediate and the product carbenes determines the regiochemistry and stereochemistry of polymer formation. Carbene **RP-1** can be clearly distinguished from **RP-2** by different ruthenium carbene proton peaks in their ¹H-NMR spectra.



Scheme 2-3. Two possible reaction pathways and their corresponding intermediates and products in the ruthenium-catalyzed ring-opening reactions of 1-cyclobutene derivatives. R_2 is the substituent at the 1 position of the cyclobutene catalyzed by the ruthenium catalyst.

In the ROMP reactions of monomer **6a**, only Pathway I and the formation of **RP-1** were observed, and a polymer backbone containing translationally invariant amino acid

side chains is generated. However, the sources of the regio- and stereocontrol were not elucidated clearly.¹¹¹ Herein, we investigate the scope of ROMP of 1-substituted cyclobutenes that are readily synthesized in two steps. We determined the kinetic and thermodynamic influence of secondary amide substitution, esters, tertiary amides and carbinol esters (Figure 1). We found that ROMP of a variety of secondary amides of cyclobutene-1-carboxylic acid (Group I) provides polymers with translationally invariant backbones (*E*-configuration) and excellent PDIs whereas ROMP of the 1-cyclobutene-1-methanol esters (Group IV) is neither regio- nor stereoselective. In contrast, both 1-cyclobutenecarboxylic acid esters (Group III) and 1-cyclobutenecarboxylic acid tertiary amides (Group II) undergo only a single ring-opening metathesis cycle (ROM) without polymerization. We present the kinetic data for these polymerizations, the computed energies of key reaction intermediates and products, and the correlation between these energies and the observed reactivities.

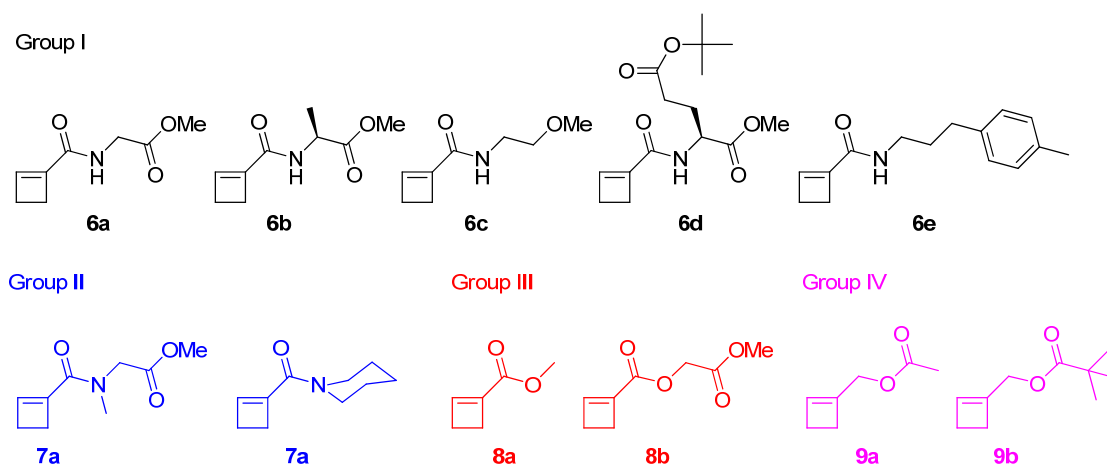


Figure 2-1. Cyclobutene monomers subjected to ROMP (Group I, secondary amides; Group II, tertiary amides; Group III, esters; Group IV, carbinol esters.).

II. Results

II.1 Synthesis of 1-Substituted Cyclobutenes

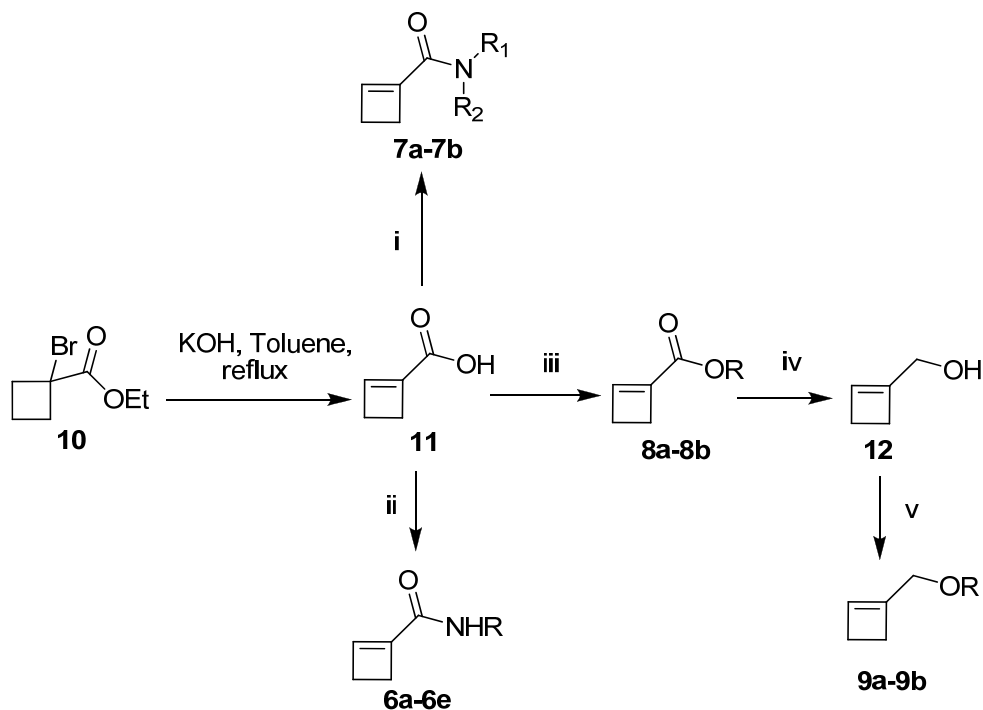
Four groups of 1-substituted cyclobutene derivatives were synthesized (Scheme 2-4). The elimination and hydrolysis of commercially available ethyl-1-bromocyclobutane carboxylate **10** generated 1-cyclobutenecarboxylic acid **11**. The synthesis of Group I monomer **6a-6e** was performed in dichloromethane (CH₂Cl₂) with 1-(3-dimethylamopropyl)-3-ethylcarbodiimide hydrochloride (EDC·HCl), and *N,N*-diisopropylethylamine (DIEA) at room temperature (rt). The coupling reagents for the synthesis of monomer **7a** and **7b** are EDC·HCl/4-dimethylaminopyridine (DMAP)/DIEA/CH₂Cl₂ and bis(2-oxo-3-oxazolidinyl)phosphinic chloride (BOP-Cl)/piperidine/DIEA/CH₂Cl₂, respectively. (Methoxycarbonyl)methyl 1-cyclobutenecarboxylate **8b** was synthesized through the coupling of **11** and BrCH₂CO₂Me in the presence of KI and DIEA in CH₂Cl₂. Methyl 1-cyclobutenecarboxylate **8a** was prepared using *N,N'*-diisopropyl-*O*-methylisourea as the coupling reagent in diethylether (Et₂O) at rt.²⁵⁰⁻²⁵¹ The reduction of **8a** with diisobutylaluminium hydride (DIBAL-H) provided 1-cyclobutenemethanol **12**. 1-Cyclobutenemethanol **12** was coupled with acetyl chloride or pivaloyl chloride in CH₂Cl₂ in the presence of DMAP/DIEA to generate monomers **9a** and **9b**, respectively. Synthesized compounds were purified by silica flash column chromatography and characterized by ¹H- and ¹³C-NMR spectroscopy and ESI mass spectroscopy.

II.2 ROMP/ROM of Group I-IV Monomers

ROMP of Group I-IV monomers was monitored by ¹H-NMR spectroscopy (Table 2-1). Monomer (10 equiv.) and catalyst **5** (1 equiv.) were mixed in CD₂Cl₂ at rt with [5] = 0.01 M. Changes in the NMR spectra as a function of reaction time were recorded to monitor the regio- and stereochemistry of the polymer formed. The corresponding molar ratios between the monomer proton peaks and the polymer proton peaks were used to calculate the percentage of consumed monomer.

The kinetic curves for ROMP of Group I-IV monomers are plotted in Figures 2-2, 2-3 and 2-4. The reaction time *t*₅₀ for 50% consumption of monomer was calculated from the kinetic curves (Table 2-1). ROMP of Group IV monomers exhibits the fastest kinetics (Figure 2-4), while only 10% monomer consumption could be achieved at equilibrium for

Group II/III monomers (Figure 2-3). Group I monomers show intermediate ROMP rates (Figure 2-2).

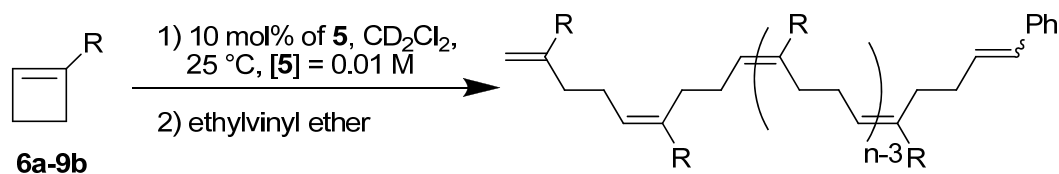


Scheme 2-4. Synthesis of 1-substituted cyclobutenes. (i) **7a**: EDC·HCl, DMAP, DIEA, CH₂Cl₂, rt; **7b**: BOP-Cl, piperidine, DIEA, CH₂Cl₂, rt. (ii) EDC·HCl, DIEA, CH₂Cl₂, rt. (iii) **8a**: N,N'-diisopropyl-O-methylisourea, Et₂O, rt; **8b**: BrCH₂CO₂CH₃, KI, DIEA, rt. (iv) DIBAL-H, Et₂O, -78 °C. (v) Pivaloyl chloride or acetyl chloride, DIEA, DMAP, CH₂Cl₂, 0 °C to rt.

For ROMP of Group I monomers, it took 3-6 h to consume 90% of the monomer. For ROMP of Group IV monomers, it took 1.5 h to consume 98% of the monomer. However, for ROMP of Group II and III monomers, it took 2-3 h to reach thermodynamic equilibrium with only 10% of the monomer consumed, and the 10% conversion yield suggests that only ROM reactions took place for these monomers without further ring-opening polymerization.

To further confirm the ROM reactions of Group II monomers, both monomer **7a** and **7b** were allowed to react with catalyst **5** ([**5**] = 0.1 M) in CD₂Cl₂ in a 1:1 molar ratio. The ROM reactions were monitored by ¹H-NMR spectroscopy (Table 2-1). It took 20-30

h to reach thermodynamic equilibrium with 72-78% of the monomer consumed. The kinetics of the ROM reactions are quite slow.



Group	Monomer	n	% Conv. ^a	Rxn Time /h	t_{50} /min ^b	M_n (theo)	M_n^d	M_w^e	PDI
I	6a	10	93	3	3	1796	1835	2220	1.21
I	6b	10	97	6	3	1936	1820	2522	1.39
I	6c	10	85	3	4	1656	1349	1653	1.23
I	6d	10	94	4	3	3077	3483	4796	1.38
I	6e	10	96	6	3	2397	2222	3047	1.37
II	7a	10	10	2	∞	n/a	n/a	n/a	n/a
II	7b	10	10	2	∞	n/a	n/a	n/a	n/a
III	8a	10	10	3	∞^f	n/a	n/a	n/a	n/a
III	8a^c	1	78	21	87	n/a	n/a	n/a	n/a
III	8b	10	10	3	∞	n/a	n/a	n/a	n/a
III	8b^c	1	72	31	333	n/a	n/a	n/a	n/a
IV	9a	10	98	1.5	<2	1366	2057	2740	1.33
IV	9b	10	99	1.5	<2	1786	2067	2726	1.33

Table 2-1. ROMP results for Group I-IV monomers. General reaction conditions: CD_2Cl_2 , 25 °C, $[\text{monomer}] = 0.1 \text{ M}$, $[\mathbf{5}] = 0.01 \text{ M}$. ^aDetermined by $^1\text{H-NMR}$ spectroscopy. ^bReaction time for 50% consumption of monomer. ^c $[\mathbf{5}] = 0.1 \text{ M}$. ^dNumber-average molecular weight by GPC using polystyrene standards. ^eWeight-average molecular weight by GPC using polystyrene standards. ^fThe reaction stops after 10% consumption of monomer.

ROM of monomer **8a** was also performed on a larger scale in CH_2Cl_2 at rt with $[\mathbf{5}] = 0.067 \text{ M}$. The final one-mer products **13a** and **14b** were purified by flash column

chromatography, and were characterized by $^1\text{H-NMR}$ (Figure 2-5), $^{13}\text{C-NMR}$ spectroscopy and LC-MS (APCI) spectroscopy.

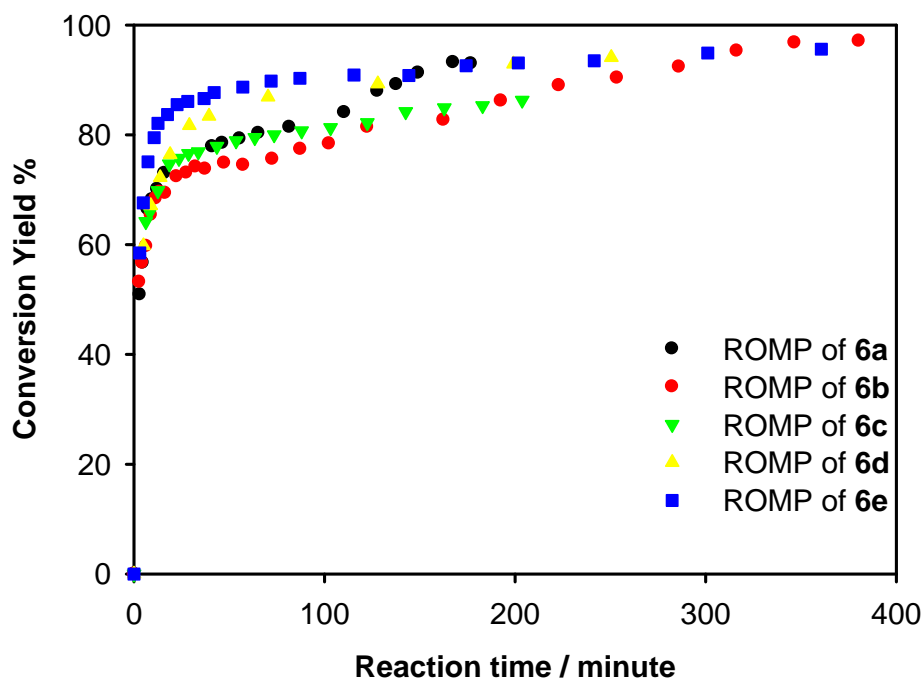
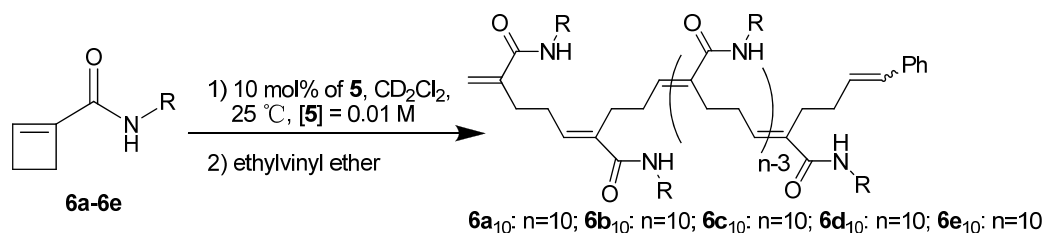


Figure 2-2. Comparison of the ROMP rates of Group I monomers **6a-6e**. Conversion yield represents the percent of monomer consumed. All the data were collected by comparing the integration of the monomer proton peaks and the proton peaks in the propagating polymer chains.

The molecular weights and PDIs of polymers **6a**₁₀, **6b**₁₀, **6c**₁₀, **6d**₁₀, **6e**₁₀, **9a**₁₀ and **9b**₁₀ were characterized by gel permeation chromatography (GPC) with polystyrene standards (Table 1). The polymer traces were monitored by UV spectroscopy with tetrahydrofuran (THF) as the running effluent. The number-average molecular weight M_n ,

weight-averaged molecular weight M_w and PDI are calculated with the following equations:

$$M_n = \frac{\sum_i N_i M_i}{\sum_i N_i}; M_w = \frac{\sum_i N_i M_i^2}{\sum_i N_i M_i}; PDI = M_w / M_n.$$

M_i is the molecular weight of an individual macromolecule, and N_i represents the number of molecules of molecular weight M_i . All the measured M_n values are very close to the theoretical values, and the PDIs are around 1.2-1.3.

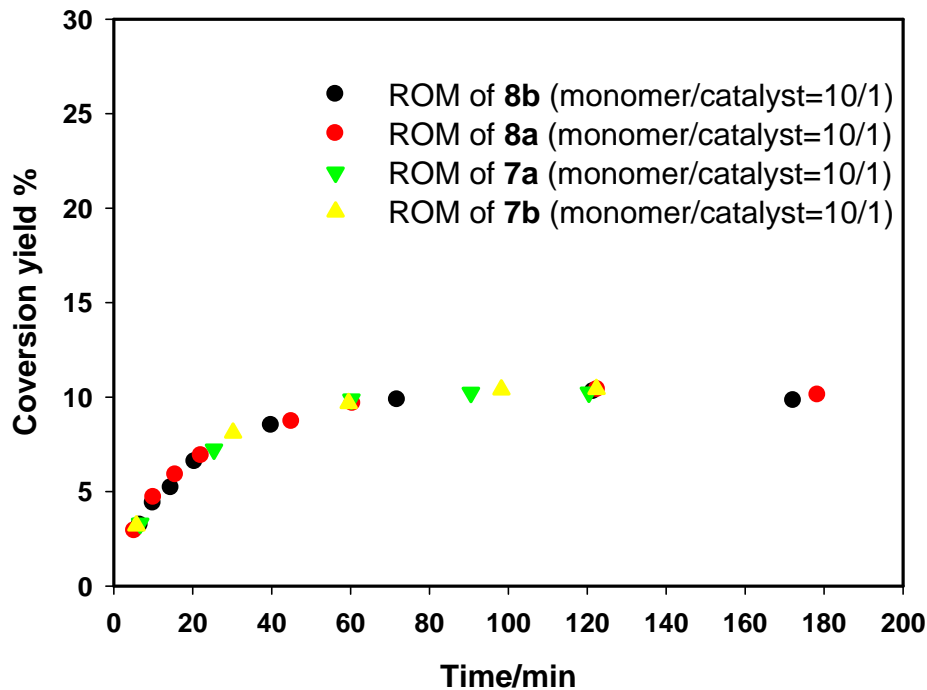
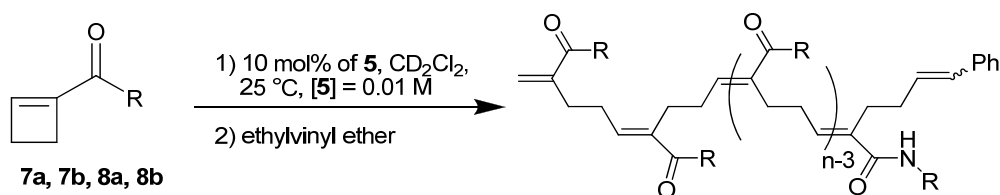


Figure 2-3. ROM of Group II/III monomers **7a**, **7b**, **8a**, **8b**. Conversion yield represents the percent of monomer consumed. All the data were collected by comparing the integration of the monomer proton peaks and the proton peaks in the propagating polymer chains.

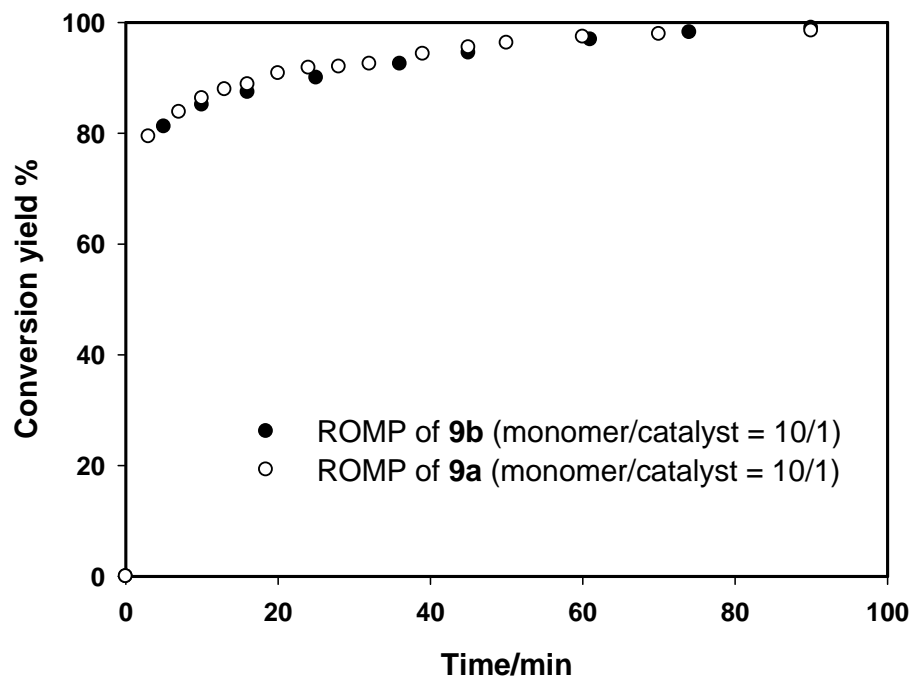
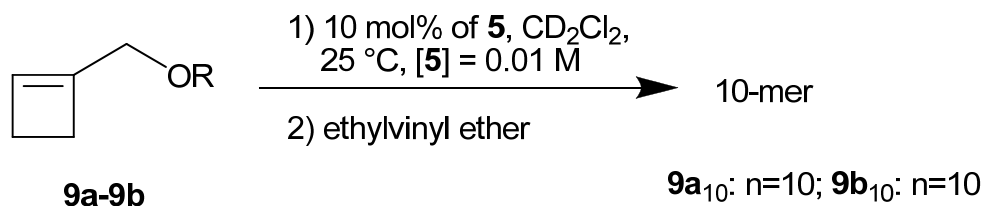


Figure 2-4. ROMP of **9a** and **9b**. Conversion yield represents the percent of monomer consumed. All the data were collected by comparing the integration of the monomer proton peaks and the proton peaks in the propagating polymer chains.

II. 3 NBO Charge Calculation and Geometry Optimization of ROMP Intermediates and Products

Based on our observations that group I amides polymerize, whereas the group III enoic carbenes do not undergo further reaction with cyclobutene esters, we hypothesized that electronic effects play an important role in determining the reactivity of the ruthenium carbene center. In addition, to the rate of reaction, we reasoned that the regiochemistry of 1-substituted cyclobutene addition to the ruthenium carbene would

depend on the distribution of charge in both the ruthenium alkene and the cyclobutene olefin. Therefore we calculated the natural bond orbital charge populations for the cyclobutene monomers and their respective propagating carbenes.

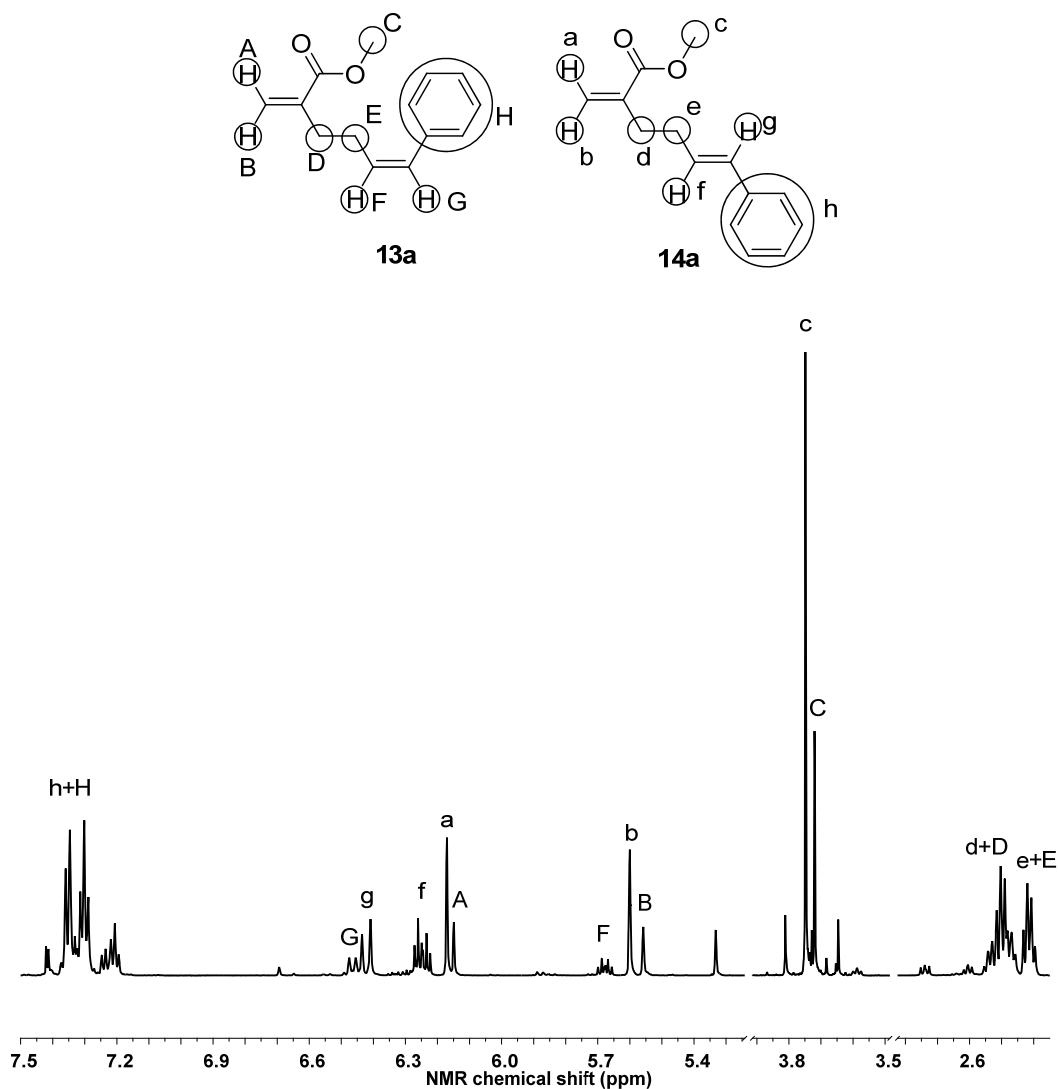


Figure 2-5. The structure of the 1-mer reaction products **13a** and **14a** of **8a** and analysis of the ¹H-NMR spectrum.

To optimize the geometries of the cyclobutene monomers (**6a**, **7a**, **8a** and **9b**), we used B3LYP/6-31G* which is frequently employed for simple organic compounds²⁵²⁻²⁵⁵ because it provides accurate structural predictions with economical calculations. The corresponding ring-opened ruthenium carbenes and ruthenium benzylidenes were

optimized with B3LYP/LANL2DZ. We modeled the substituents on the Group I and IV ruthenium carbenes as single ring-opened monomers ($\text{CH}_2\text{CH}_2\text{CH}=\text{CHPh}$) to limit the number of atoms included in the calculations and thereby facilitate the calculations. The B3LYP/LANL2DZ method was chosen because it has been used extensively for the geometry optimization of ruthenium carbenes. The LANL2DZ basis set has superior properties with respect to effective core potentials (ECPs) and polarization functions on the ruthenium,^{97,256-268} and calculated results agreed very well with the experimental data, e.g., X-ray crystal structures,²⁶⁵⁻²⁶⁶ IR and NMR spectra,²⁵⁶ thermal parameters,^{258,262,268} or metathesis reactivities. The natural bond orbital (NBO) charge populations for the olefins were calculated by Hartree-Fock with the 6-31G++* basis set (for cyclobutene monomers) and the LANL2DZ basis set (for ruthenium carbenes) in Gaussian 03W (Figure 2-6a). The AIM (atoms in molecule) electron density analysis was performed using the AIMPAC package (Figure 2-6b).

ROMP of all Group I monomers is stereospecific providing *E*-trisubstituted olefinic bonds. However, ROMP of Group IV monomers generates stereoirregular polymers. Therefore, we compared the thermodynamic stabilities of the four possible metallocyclobutane intermediates (**I**) and four possible ring-opened ruthenium carbene products (**RP**) in the ROMP of 1-cyclobutene derivatives (Scheme 2-3) using *ab initio* calculations. To simplify the computation, the polymer chain and the 1-carbonyl amide group, were modeled as a methyl group and a CONHCH_3 substituent, respectively (Figure 2-7). The geometry optimizations were performed with B3LYP/LANL2DZ using Gaussian 03W. To prevent ring opening and to find the local minimum of the intermediate structures only one bond in the metallocyclobutane ring was optimized while the other three bond lengths were kept constant, and the partial optimization was rotated to optimize the other three bonds, until the optimized structure changed little in energy ($\Delta E < 6.3 \times 10^{-4}$ kcal/mol). Vibrational frequency calculations using B3LYP/LANL2DZ were performed for all model compounds, and there were no imaginary vibrational frequencies indicating that local minima had been found for each structure. Free energies computed for structures (Figure 2-8) in solvent (CH_2Cl_2) include the electronic energy plus the solvation free energy from the conductor-like polarizable

continuum model (CPCM) based on the United Atom Kohn-Sham (UAKS) radii to build cavities using Gaussian 03W.

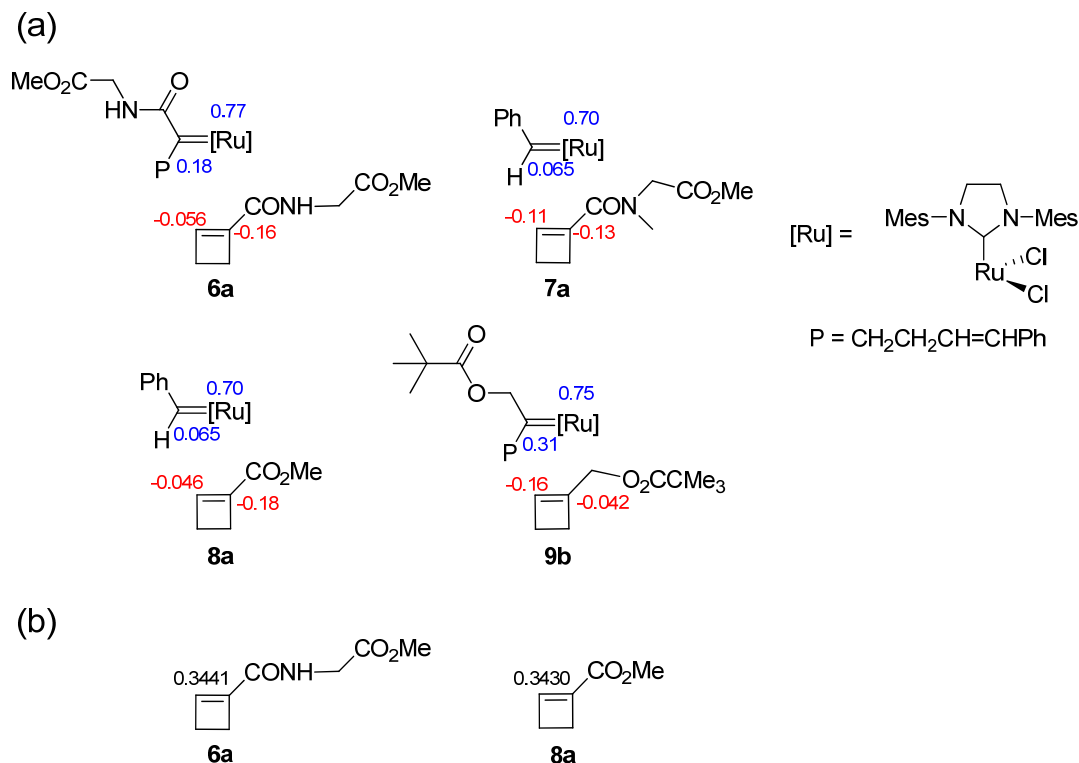


Figure 2-6. (a) NBO charge populations of 1-substituted cyclobutene derivatives **6a**, **7a**, **8a** and **9b**, the corresponding ring-opened ruthenium carbenes of **6a** and **9b**, and ruthenium benzylidene. Hartree-Fock calculations were performed with the 6-311G+++ basis set (for cyclobutene monomers) and the LANL2DZ basis set (for ruthenium carbenes) using Gaussian 03W. (b) AIM electron densities (atomic units) of olefin bonds in 1-substituted cyclobutene derivatives **6a** and **8a** calculated using AIMPAC package.

III. Discussion

III.1 ROMP of Group I Monomers

The ROMP kinetics of monomers **6a-6e** were measured by monitoring the ROMP reactions in CD_2Cl_2 at 25 °C by $^1\text{H-NMR}$ (Figure 2-2). We postulated that coordination of γ -ester or γ -ether oxygens to the ruthenium center might enhance the rate of

polymerization by stabilizing the metathesis transition states.²⁶⁹ Therefore, we investigated the rates of polymerization of **6a**, **6b**, and **6d** which contain γ -esters, as well as **6c** which has a γ -ether substituent. We compared their rates of polymerization to the rate of monomer **6e**, in which a phenyl group is substituted for the oxygen coordinating moieties. The rates of consumption of monomers **6a-6e** are very similar (t_{50} entries, Table 2-1, Figure 2-2). We concluded that coordination of an oxo γ -substituent is not required for efficient polymerization. However, we note that the polymerization rates of **6** are approximately 4 times slower than ROMP of 3-substituted cyclobutenes, which are less sterically hindered at the face of the alkene.²⁷⁰

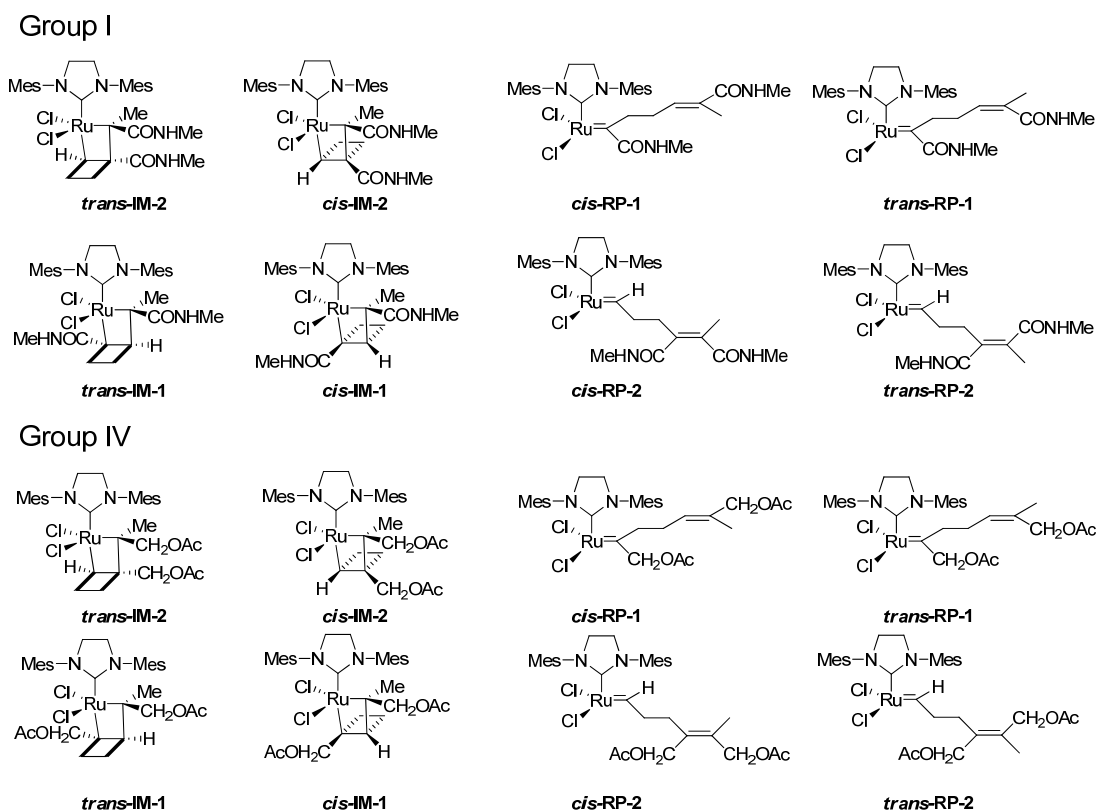


Figure 2-7. Structures of possible intermediates and ring opened products for ROMP of Group I and IV monomers. To simplify the computation, the polymer chain and the 1-carbonyl amide group, were modeled as a methyl group and a CONHCH₃ substituent, respectively.

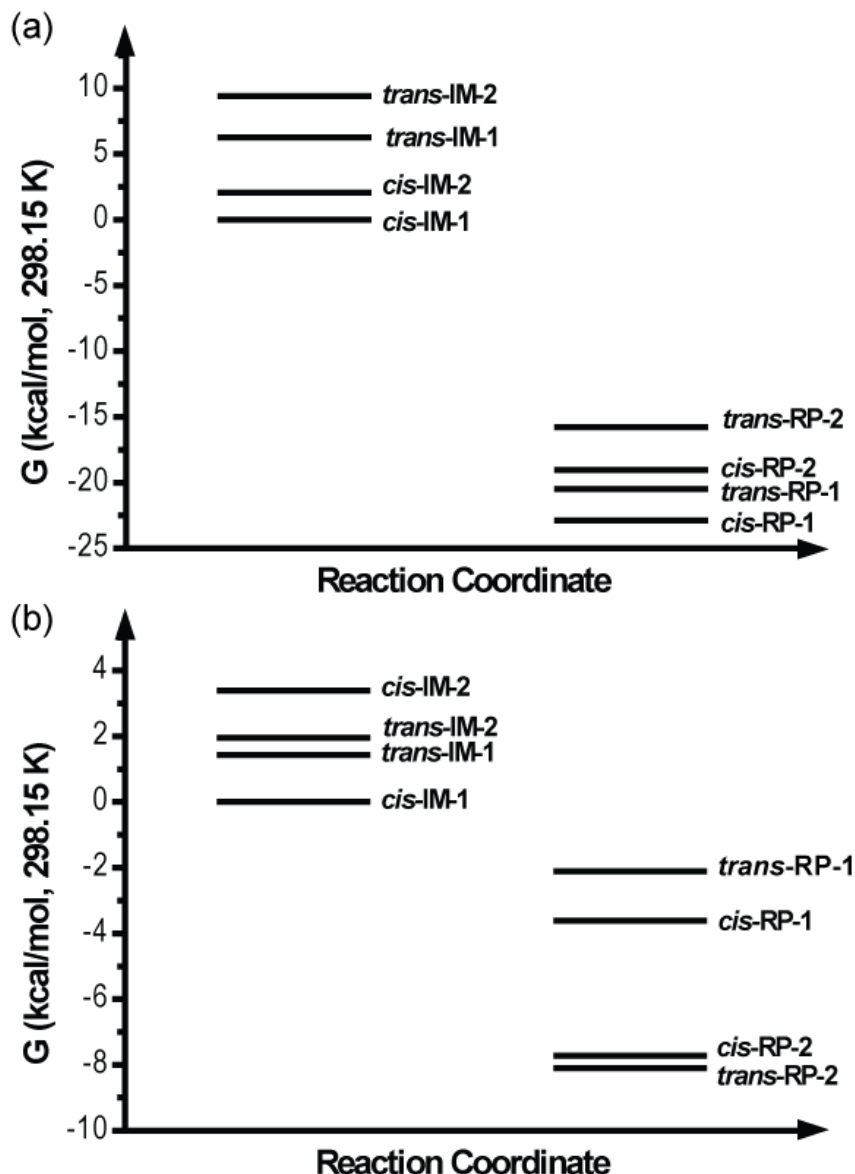


Figure 2-8. Relative free energy profiles of four possible different intermediates and four possible ring-opened products in the ROMP reactions of Group I monomer (a) and Group IV monomer (b). Structures were optimized with B3LYP/LANL2DZ in the Gaussian 03W program. Free energies computed for structures in solvent (CH_2Cl_2) include the electronic energy plus the solvation free energy from the CPCM solvation model based on the UAKS radii using Gaussian 03W.

The $^1\text{H-NMR}$ spectra of the ROMP reaction of monomer **6b** illustrate the kinetics of the reaction and the assignment of stereochemistry (Figure 2-9). As a function of time, the integration of the proton peaks a, b and c in monomer **6b** decreased as the integration of the proton peaks d and e (attributed to protons on the chain of the ring-opened

ruthenium carbene) increased. In the $^1\text{H-NMR}$ spectra, a single broad proton peak at 6.2 ppm appeared during the course of the reaction indicating the formation of an internal trisubstituted olefin with *E*-configuration. There was no peak at 18.0-19.1 ppm indicating that the ruthenium alkylidene ($[\text{Ru}]=\text{CHPh}$ or $[\text{Ru}]=\text{CH-CH}_2\text{R}$) proton signal is absent, and that an enamide ruthenium carbene is formed. These spectroscopic results are consistent with polymerization through ruthenium carbene **RP-1** in Pathway I (Scheme 2-3). The $^1\text{H-NMR}$ spectra of the polymers show that the 10-mers are formed with high regioselectivity and stereoselectivity. The trisubstituted olefins have only the *E*-configuration.

III.2 ROM of Group II Monomers

Next we tested the reactivity of tertiary amides **7a** and **7b**. Reaction of Group II monomers **7a** and **7b** with 10 mol% catalyst **5** results in the ring-opening metathesis (ROM) of approximately 10 mol% of the monomer. However, no polymerization was observed; only ring-opened monomer was formed (Table 2-1, Figure 2-10). The ring-opening reaction took 2 hours to reach completion.

ROM of **7a** and **7b** exhibits the same regioselectivity as Group I monomers, and only resonances consistent with Pathway I were observed in the $^1\text{H-NMR}$ spectra (Figure 2-10). Although Group I amides with γ -branching (i.e., **6b** and **6d**) undergo ROMP, we observed that Group III monomers with β -branches only yield ring-opened monomer. We hypothesize that the increased steric bulk around the ruthenium resulting from formation of ruthenium carbene **RP-1** hinders the binding of subsequent monomers to the enamide carbene.

III.23 ROM of Group III Monomers

Attempts to effect ROMP of Group III monomers **8a** and **8b** with 10 mol% of catalyst **5** resulted in the ring opening metathesis (ROM) of approximately 10 mol% of the monomer with no polymerization (Table 2-1, Figure 2-3). The reaction of monomer **8a** is shown in Figure 2-11. The peak at 19.1 ppm corresponding to the carbene proton on

the catalyst **5** disappears over time and no new carbene proton peak appears. At the same time, the styrenyl peaks from the ring-opened monomer appear (peak b-e, Figure 2-11). Therefore, **RP-1** is formed preferentially to **RP-2**. The remaining 9 equiv. of monomer do not react. We concluded that enoic ruthenium carbene **RP-1** is sufficiently deactivated that it cannot undergo metathesis with an unsaturated ester.

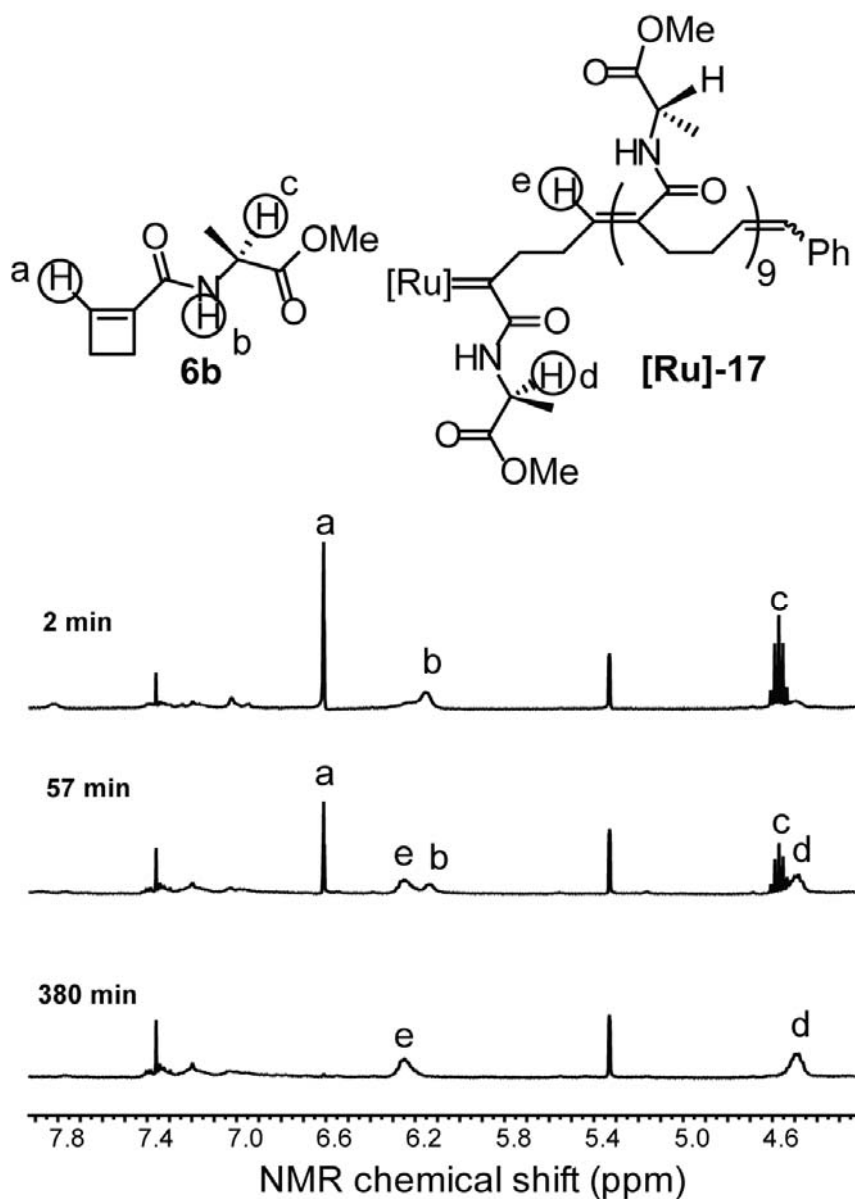


Figure 2-9. $^1\text{H-NMR}$ spectra of the ROMP of monomer **6b** in CD_2Cl_2 . ($[\mathbf{6b}] = 0.1 \text{ M}$, $[\mathbf{5}] = 0.01 \text{ M}$, $25 \text{ }^\circ\text{C}$) Reaction times are 2 min, 57 min and 380 min, respectively.

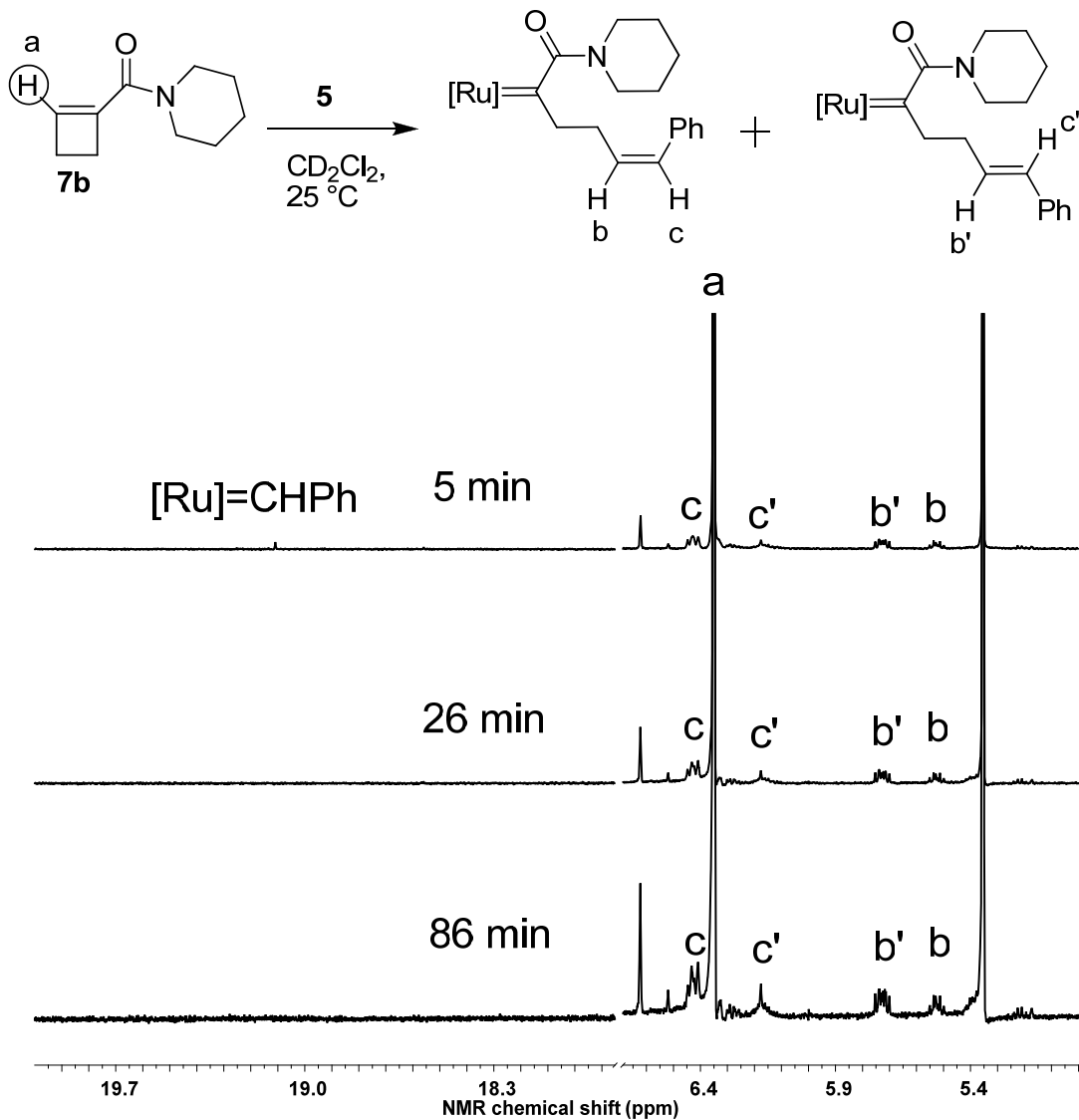


Figure 2-10. $^1\text{H-NMR}$ spectra of ROM of monomer **7b** in CD_2Cl_2 . [**7b**] = 0.1 M, [**5**] = 0.01 M, 25°C .

Next, we examined the reaction of **8a** and **8b** using a 1:1 molar ratio of monomer and catalyst to determine the kinetics of reaction and to analyze the structures of the products in greater detail (Figure 2-12 and 2-13). Again, the NMR spectra were monitored as a function of time. The ring-opening rates of **8a** and **8b** were so slow that the reaction took more than 20 h to reach 75% consumption of monomer. The slow reaction rates suggested that an ester further reduces the reactivity of the cyclobutene olefin relative to the amide-substituted cyclobutenes. In contrast to the Group II

secondary amides, these esters have no β - or γ -branching and are more analogous in structure to Group I amides. These comparisons suggested that the failure of ester monomers **8a** and **8b** to polymerize is the result of an electronic factor rather than steric congestion at the catalytic center.

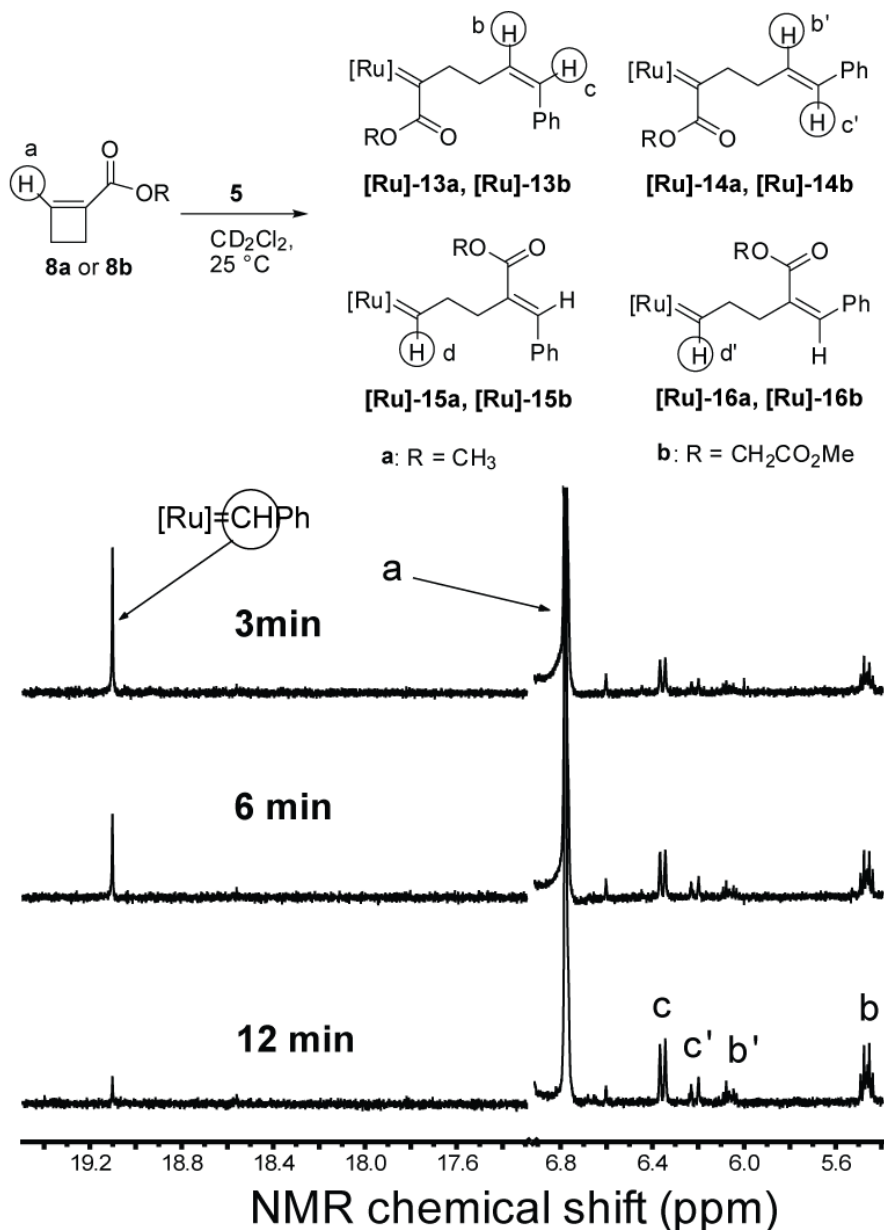


Figure 2-11. ^1H -NMR spectra of the ROM of monomer **8a** in CD_2Cl_2 ([**8a**] = 0.1 M, [**5**] = 0.01 M, 25°C). Reaction times are 3 min, 6 min and 12 min, respectively. Resonance corresponding to H (d) and H (d') are predicted to occur at 18.5 ppm. These resonances are not observed.

There are four possible ROM products that may be formed from monomer **8a** or **8b** (Figure 2-11 and 2-12). As described above, ROM of 1-substituted esters was regioregular. The primary products **[Ru]-13a** and **[Ru]-14a** are formed as a 1/2 mixture of *Z/E* styrenyl olefins (Figure 2-12a) through Pathway I (Scheme 2-3). At 75% consumption of monomer, the combined yield of **[Ru]-15a** and **[Ru]-16a** (via Pathway II) was no more than 3% (based on integration of the ruthenium alkylidene proton at 18.5 ppm in the ¹H-NMR spectrum, Figure 2-13). It is reasonable to assume that **[Ru]-15a** and **[Ru]-16a** initiate ROM with monomer **8a**; the resulting carbenes would be enoic and stable to further reaction prior to quenching. The quenched reaction products were purified and characterized by ¹H-NMR spectroscopy (Figure 2-5) and LC-MS (APCI) spectroscopy to establish their structures. The time course (Figure 2-12) revealed that these species are formed in the initial reaction and are not secondary products from cross metatheses.

High ROM regiospecificity was observed with monomer **8b**. The ROM products of **8b** formed by the formation of the enoic carbene (Pathway I, Scheme 2-3) are a mixture of *Z* and *E* styrene olefins (**[Ru]-13b** and **[Ru]-14b**) with a *Z/E* ratio around 2/3 (Figure 2-12b). At 75% conversion of monomer, the combined yield of **[Ru]-15b** and **[Ru]-16b** generated through formation of the alkylidene carbene (Pathway II, Scheme 2-3) is less than 4%. Thus, Pathway I (Scheme 2-3) to form the enoic carbene is the energetically favorable pathway.

III.4 ROMP and ROM of Group IV Monomers

Metathesis reactions with 1 equivalent of catalyst **5** and 10 equivalents of monomer **9a** or **9b** were monitored by ¹H-NMR spectroscopy at room temperature for 1.5 hours (Table 2-1, Figure 2-4). Greater than 98% of the monomers was consumed in 1 hour and the *t*₅₀ values are at least 5 times smaller than the *t*₅₀ values for Group I, II or III monomers. That is, the Group IV monomers undergo metathesis much faster than Group I monomers. Moreover, the ruthenium carbene formed upon initial ring opening is sufficiently reactive that it polymerizes with remaining monomer.

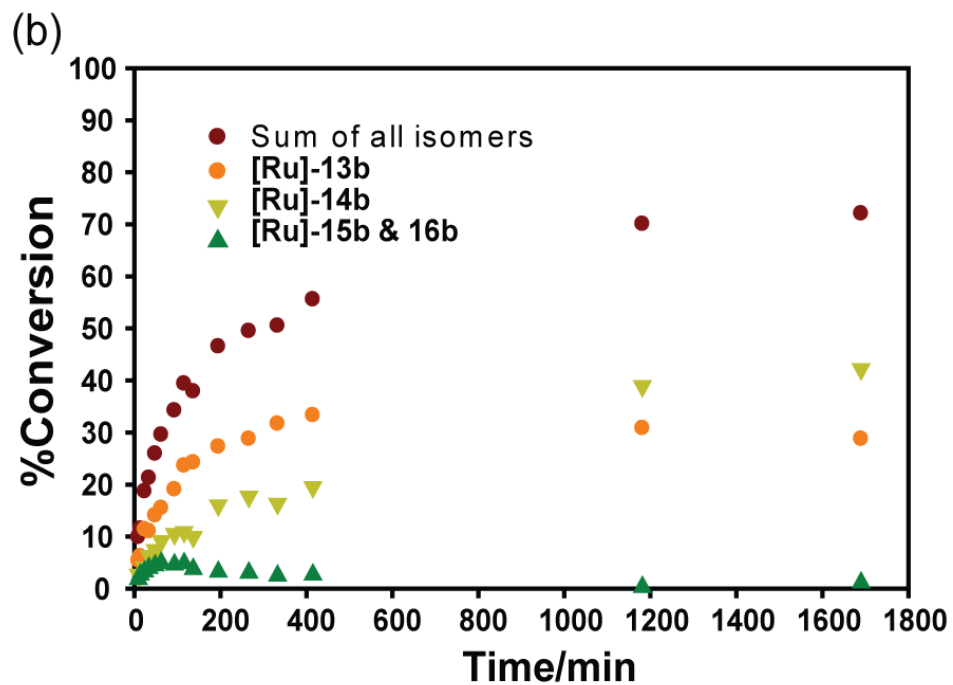
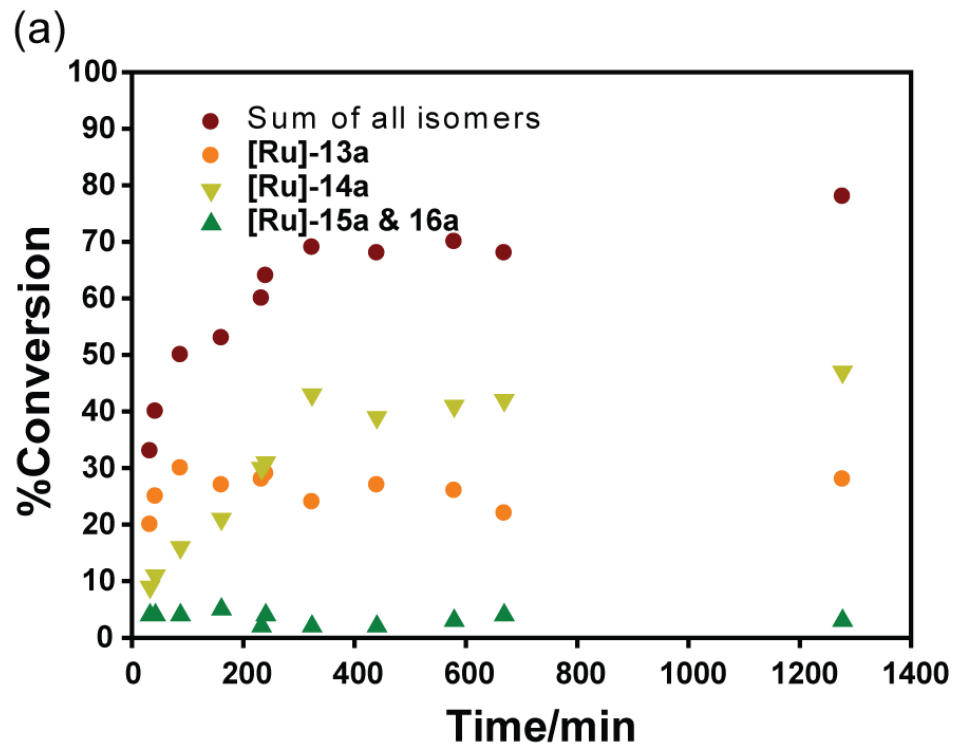


Figure 2-12. ROM regio- and stereochemistry of **8a** and **8b**. [**8a**] or [**8b**] = 0.1 M, [**5**] = 0.1 M, 25 °C.

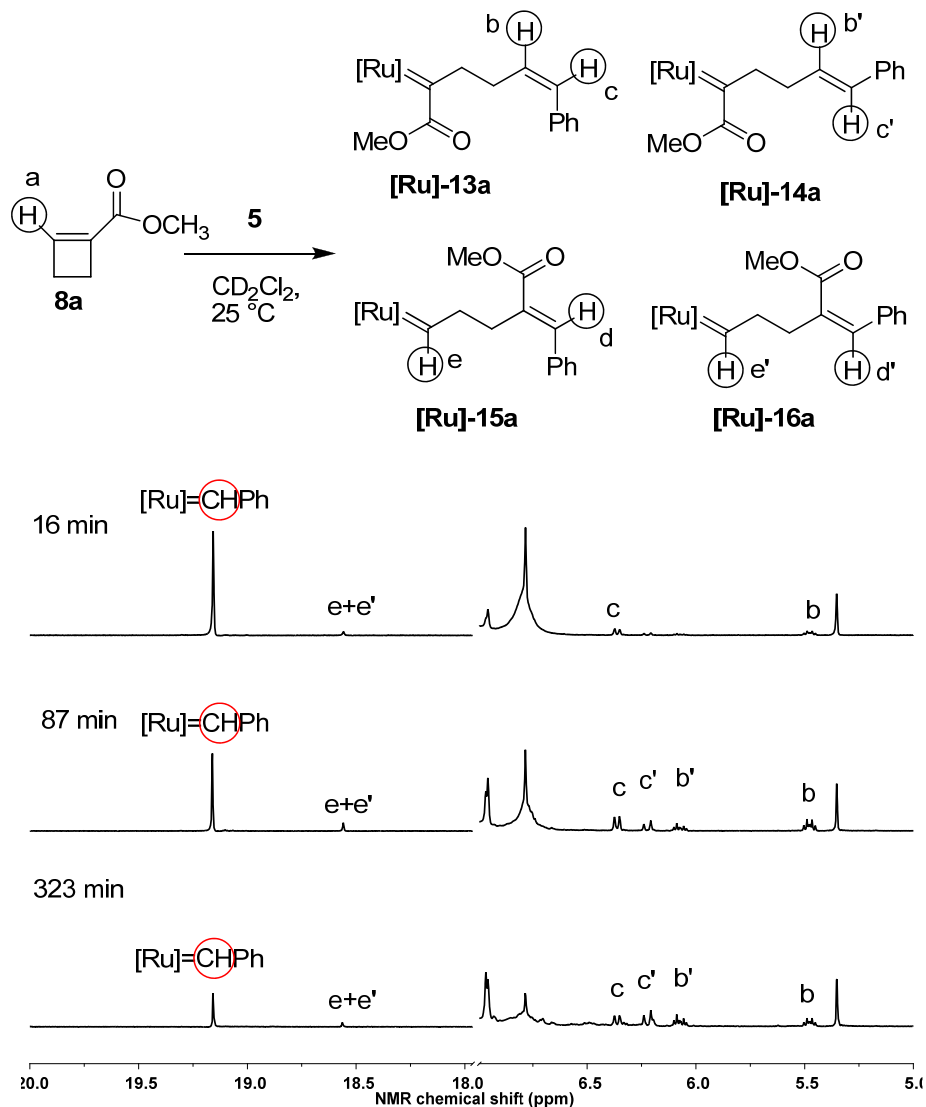


Figure 2-13. $^1\text{H-NMR}$ spectra of ROM of monomer **8a** in CD_2Cl_2 . $[\mathbf{8a}] = 0.1 \text{ M}$, $[\mathbf{5}] = 0.1 \text{ M}$, 25°C .

In the $^1\text{H-NMR}$ spectrum of the **[Ru]-18a** polymer, the methylene protons adjacent to the ester oxygen are observed as three broad signals centered at 4.64, 4.57 and 4.46 ppm of approximately equal intensity (Figure 2-14, peak d and Figure 2-15, peaks f, g and h). The assignment of the resonances was corroborated by $^{13}\text{C-NMR}$, $^{13}\text{C-APT}$, gCOSY and gHMQC spectroscopy of the purified 10-mer products **18a** and **18b**.²⁷¹ If the polymerization were regioselective, the polymer backbone would only contain configurations I and II that result from head-to-tail polymerization, or configurations

III/IV and V/VI, that result from tail-to-tail and head-to-head polymerization, respectively (Figure 2-16). The presence of three major methylene resonances in the 4.4-4.7 ppm region of the spectra indicates that both head-to-tail and head-to-head dyads are present. Therefore, the polymerization is not regioselective.

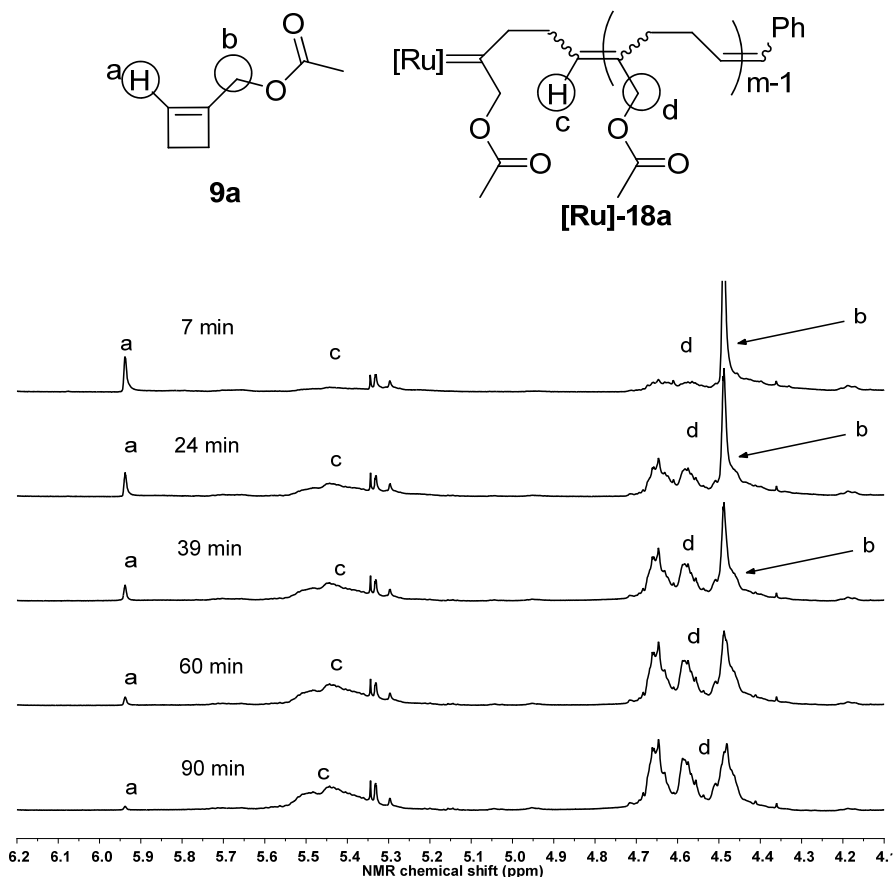


Figure 2-14. ^1H -NMR spectra of the ROMP of monomer **9a** in CD_2Cl_2 . $[\mathbf{9a}] = 0.1 \text{ M}$, $[\mathbf{5}] = 0.01 \text{ M}$, $25 \text{ }^\circ\text{C}$.

Moreover, the formation of three methylene resonances separated by approximately 0.1 ppm indicates that the polymerization is not stereoselective. The calculated chemical shifts for the *cis* and *trans* isomers differ by 0.1 ppm in both the trisubstituted (I/II) and tetrasubstituted (V/VI) olefins. The observed chemical shifts are consistent with the presence of at least one *cis/trans* pair, although the absolute values of the chemical shifts are not precisely the same as the calculated values and it is not possible without synthesis of model compounds to assign which stereoisomers are

obtained. Furthermore, the $^1\text{H-NMR}$ spectrum of the **[Ru]-18a** polymer exhibits multiple broad resonances for the olefinic protons in the polymer backbone at 5.35–5.62 ppm (Figure 2-14, peak c), indicating that the polymer backbone is composed of different types of olefins (Figure 2-16). The presence of at least two olefin resonances indicates that the structure of the polymer is not translationally invariant.

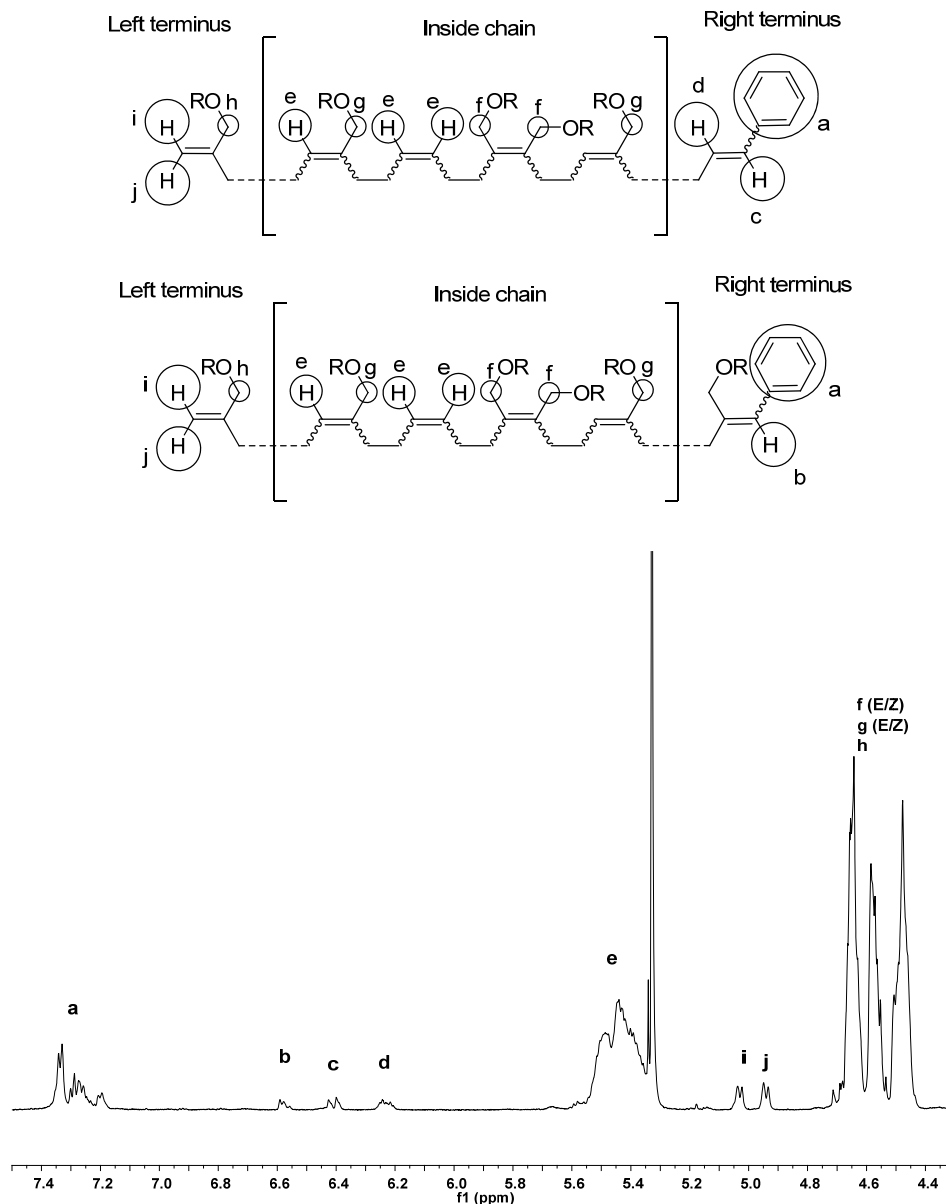


Figure 2-15. The structure of the 10-mer reaction product **18a** for **9a** and the analysis of the $^1\text{H-NMR}$ spectrum. The numbers indicate the protons in the structure. E, Z: *E*-configuration and *Z*-configuration in the olefins of the structure.

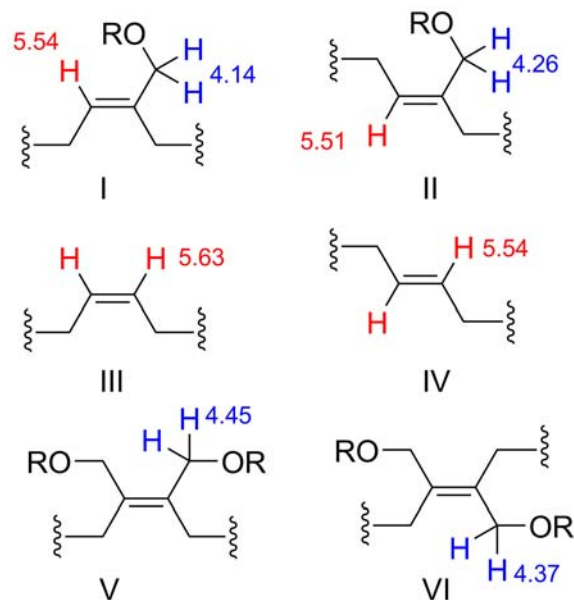


Figure 2-16. Six possible alkene configurations in the polymer backbone upon ROMP of Group IV monomers and their predicted proton chemical shifts. Calculated with B3LYP/6-31G(d) using Gaussian 03W.

III.5 NBO Charge Calculations

We calculated the natural bond orbital charge populations for the cyclobutene monomers and their respective propagating carbenes. For the ester and amide cyclobutene monomers, the calculations showed that the electron density is higher on C-1 than on C-2 as expected for olefins bearing conjugated electron withdrawing groups. In contrast to the carbonyl substituents, the C-1 carbinol substituent (monomer **9b**) is electron donating, making C-1 more electropositive than C-2. In the ruthenium carbenes, the metal atom is more electropositive than the adjacent carbon atom.

III.6 ROMP Regioselectivity and Stereoselectivity Analysis by Metallocyclobutane Intermediate and Ring-opened Product Computation

The rate of formation of the 14-electron ruthenium complex upon dissociation of bromopyridine from **5** is the same regardless of cyclobutene structure and will not contribute to the regio or stereoselectivities. Therefore, two kinetic steps after dissociation were considered: (a) formation of the metallocyclobutane intermediate, and

(b) formation of ring-opened product. We calculated the natural bond orbital charge populations for the cyclobutene monomers and their respective propagating carbenes, as well as the activation energies of the reaction products (**RP**) to understand the regioselectivity of π -complex (π -**SM**) formation (Figure 2-17). We calculated the energies of the reaction intermediates (**IM**) and products (**RP**) to predict the relative activation energies for metallocyclobutane formation and subsequent ring opening.

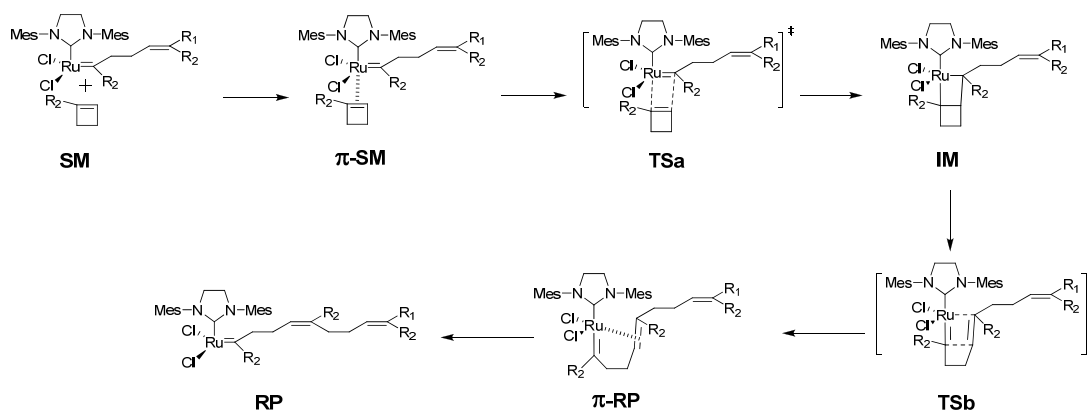


Figure 2-17. Cyclobutene ROMP reaction scheme. **SM**: starting material; π -**SM**: π -complex of starting material; **TS**: transition state; **IM**: intermediate; π -**RP**: π -complex of reaction product; **RP**: reaction product.

The relative energies of the cyclobutene π -complexes depend on the energies of the 14 electron carbene species. Because the active carbene species of the cyclobutene π -complex is the same as the reaction product carbene (**RP**), these energies were used to order the relative free energies of the four regio- and stereo-isomers. In addition, we assumed that additional contributions to the relative energies of the cyclobutene π -complexes would primarily be determined by the charge distribution of the cyclobutenes rather than steric effects between the coordinating cyclobutene and the carbene due to the long distance between the cyclobutene and Ru in the π -complex. Lastly, we assumed that the stabilization energy between free 14-electron ruthenium carbene and π -stabilized 16-electron ruthenium carbene to be about 14 kcal/mol less than the 18 kcal/mol calculated by Zhao and coworkers for ethylene²⁷² and measured by Chen and coworkers for norbornene.²⁷³ In the case of Group I monomers, alignment of the cyclobutene and the

electron-deficient Ru to pair C-1 and the Ru to form the π -complex (π -**SM**) is favored by both the carbene stability (Figure 2-17) and the electronic factors (Figure 2-6a). In the case of Group IV monomers, both electronic factors (Figure 2-6a) and the relative stability of the carbenes (Figure 2-17) favor a cycloaddition in which C-2 becomes bonded to the ruthenium.

We estimated the strain energy of 1-substituted cyclobutene to be ~ 26 kcal/mol based on the calculations of Goddard and coworkers.²⁷⁴ In addition, using the differences in energies calculated for the metallocyclobutane reaction intermediates and the 14-electron ruthenium carbene reaction products, we constructed approximate thermodynamic profiles along the reaction coordinates of Group I and Group IV monomer (Figure 2-18).

In the case of 1-substituted cyclobutene amides, the *cis*-pathway I starting (**SM**), intermediate (**IM**) and product (**RP**) complexes are always the lowest energy isomers. By extension, the transition states are expected to be the lowest energy transition states and the corresponding activation energies for their formation the most favorable. Therefore, *cis*-**RP-1** is obtained with high selectivity (>99%) for Group I and by extension Group II and III monomers.¹¹¹

In the case of Group IV monomers, the relative starting complex (π -**SM**) and intermediate (**IM**) energies are similar to those observed by Chen for norbornene.²⁷³ Likewise by the Hammond postulate, we surmise that **TSb** is not rate limiting. If we consider the partitioning of metallocyclobutane intermediate forward to ring-opened product versus backward to the coordinated cyclobutene, the forward reaction is favored due to the release of ring strain upon formation of π -**RP** and π -**SM** is not in equilibrium with **IM**. Thus, the activation energies for formation of **TSa** from π -**SM** determine the regio and stereoselectivities. NBO charge calculations suggest that *trans*- π -**SM-2** and *cis*- π -**SM-2** are lower in energy than the π -**SM-1** regioisomers. However, upon formation of the metallocyclobutane intermediate steric interactions destabilize **IM-2** relative to **IM-1** counteracting electronic effects. As these steric interactions develop in the transition state, the difference in **TSa** energies is much smaller than in either ground state. The consequence is that the activation energies for formation of *trans* and *cis*-**TSa-1** are smaller than for formation of *trans* and *cis*-**TSa-2**. Despite the higher ground state

energies of *trans* and *cis-π-SM-1*, they react at a faster rate. Thus, poor regio- and stereoselectivity are observed. Overall, the estimated activation energies for Group IV monomers are smaller than for Group I monomers, consistent with the increased rates of propagation observed for Group IV monomers (Table 2-1).

III.7 Geometry of Group II ROM Intermediate

Kinetic studies with Group II monomers **7a** and **7b** revealed that only ROM reactions occurred. We hypothesized that the second N-substituent may block the approach and binding of an incoming monomer at the ruthenium carbene center. To test our hypothesis, geometry optimization of the N,N-disubstituted carbonyl ruthenium carbene formed from monomer **7a** was performed with B3LYP/LANL2DZ using Gaussian 03W (Figure 2-19). In the optimized structure of the ruthenium carbene (Figure 2-19), the N-methyl group blocks the face of the metal carbene to which the incoming cyclobutene must bind. Therefore, we conclude that severe steric crowding is responsible for a lack of propagation after the initial ring opening occurs.

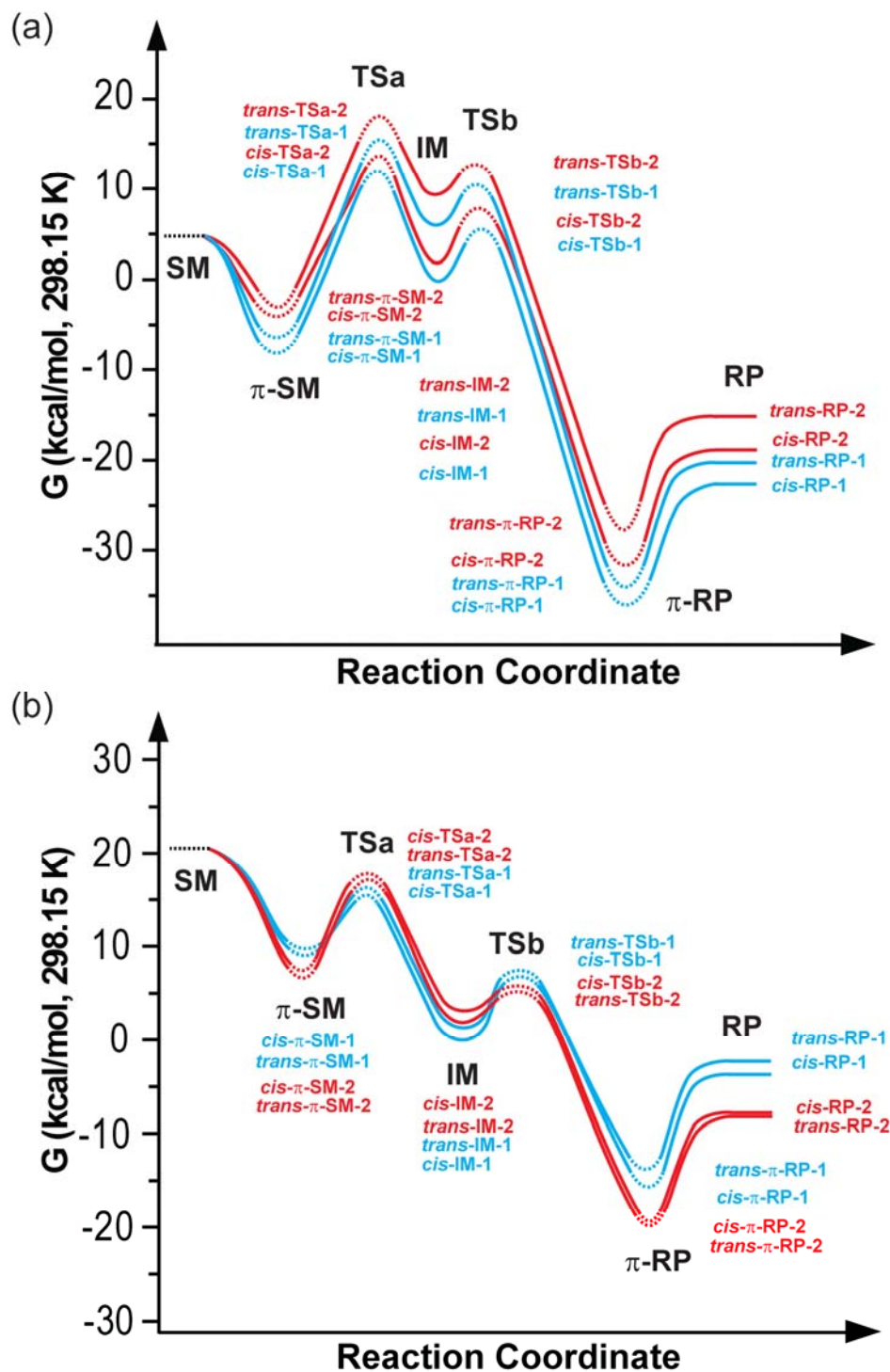


Figure 2-18. Relative free energy profiles for the ROMP reactions of Group I monomers (a) and Group IV monomers (b). Structures were optimized with B3LYP/LANL2DZ in the Gaussian 03W program. Free energies computed for structures in solvent (CH_2Cl_2) at 298.15 K include the electronic energy plus the solvation free energy from the CPCM solvation model based on the UAKS radii using Gaussian 03W.

III.8 Inability of Group III monomers to form homopolymer

Our initial hypothesis for the lack of polymerization of enoic carbene was that the electron withdrawing nature of the ester deactivated the cyclobutene olefin to further metathesis reaction. However, the NBO calculations followed by AIM electron density analysis reveal that the charge density on the ester-substituted cyclobutene is not significantly different than the charge density on the amide-substituted cyclobutene, which does undergo ROMP (Figure 2-6a and 2-6b). *Ab initio* calculations for the enoic carbene reaction product of **8a** revealed that the ester oxygen forms a chelate at the open coordination site of the 14-electron ruthenium center. This chelation stabilizes the ester approximately 7 kcal/mol relative to the enamide carbene. This type of ester coordination was previously observed in the calculations of Fomine and coworkers that investigated the reactivity of the enoic carbene.²⁶⁸ In our system, the chelated enoic carbene is kinetically trapped from further reaction with the sterically hindered 1-substituted cyclobutene ester, **8**. However, ring-opening metathesis with the relatively more electron-rich olefin of cyclohexene²⁷⁵ is still feasible due to the lower activation energy of this reaction (Figure 2-20).

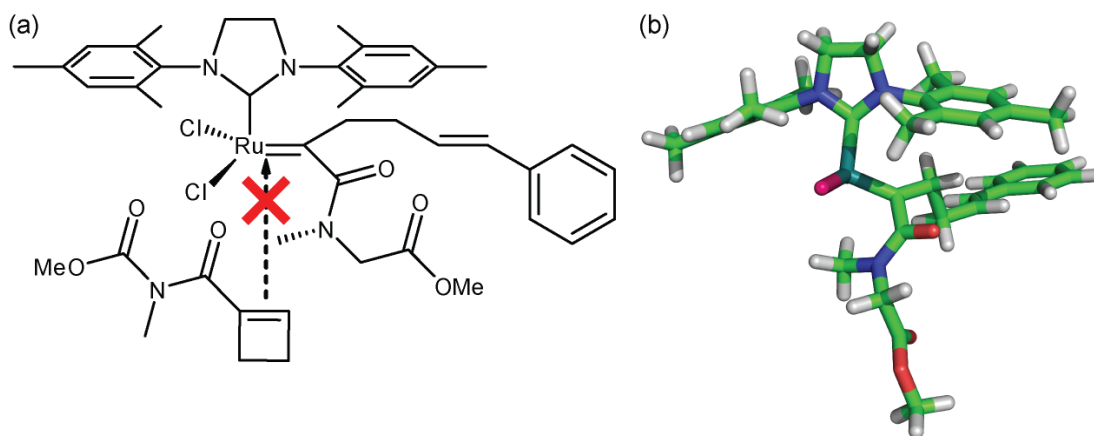


Figure 2-19. (a) Schematic presentation of how a second N-substituent blocks access of an incoming monomer to the ruthenium carbene; (b) Optimized structure of the new N,N-disubstituted carbonyl ruthenium carbene for monomer **7a**. Color Key: Ru (cyan), Cl (pink), C (green), N (blue), O (red), H (white). (Optimization method: B3LYP/LANL2DZ with Gaussian 03W)

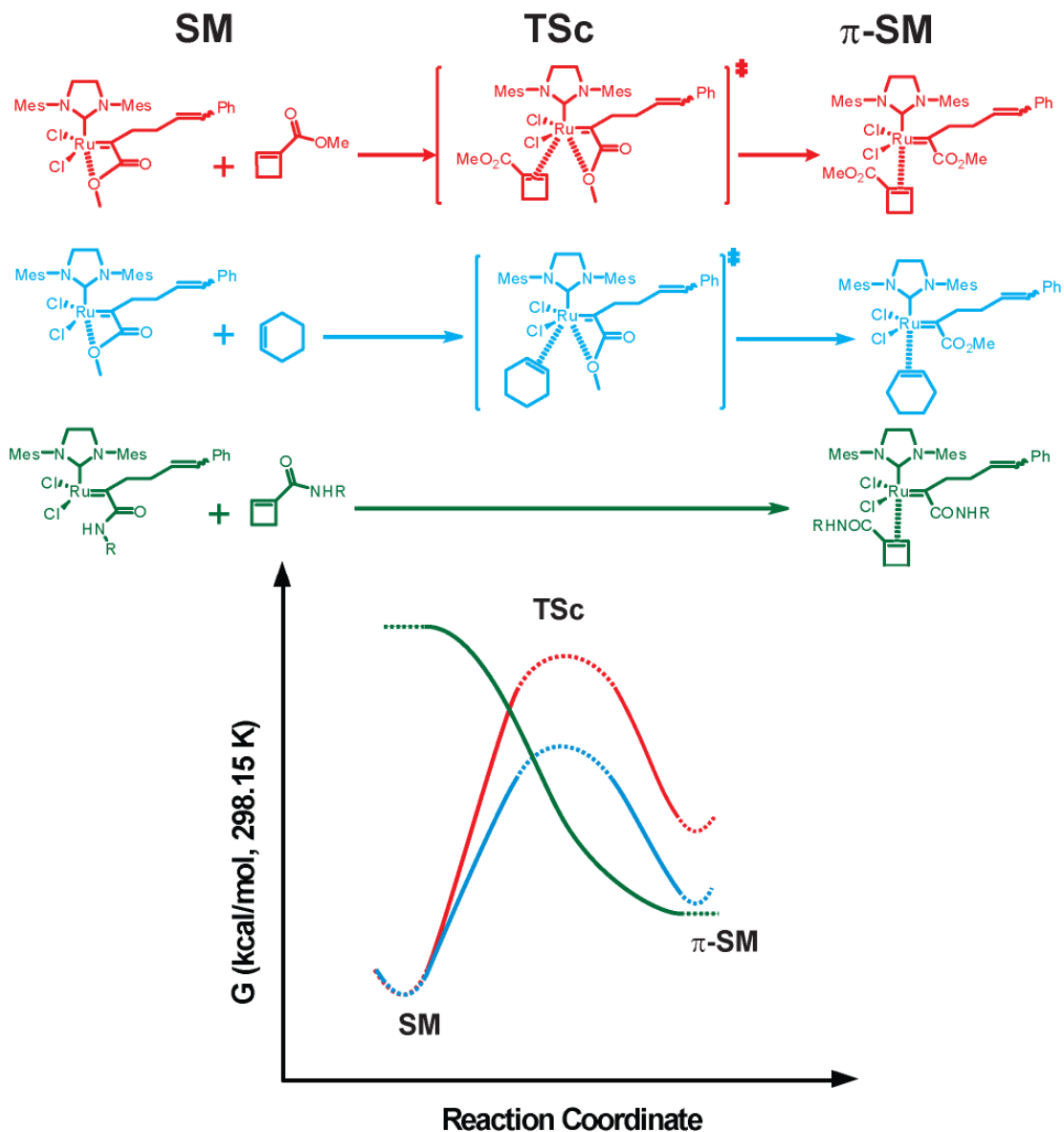


Figure 2-20. Proposed relative free energy profiles for the coordination of 1-cyclobutene ester **8a** (red curve) and cyclohexene (blue curve) to the enoic ruthenium carbene and the ROMP reactions of 1-cyclobutene amides **6a-6e** (green curve).

IV. Summary

In summary, we have found that cyclobutenes undergo stereo- and regioselective ring opening metathesis when substituted with an electron withdrawing carbonyl at the 1-position. Regioselective addition to the catalyst carbene is consistent with both the calculated charge distribution for the carbene and the cyclobutene, and the minimum

number of steric interactions. In the case of more electron-rich 1-substituents, the inverse rank order of energies between the intermediates and the π -complexed starting materials strongly suggests that the corresponding activation energies to reach the transition states may be close enough in magnitude to make ROMP of Group IV monomers neither regio- nor stereoselective.

When an enoic carbene is formed from Group II monomers, the formation of a ruthenium chelate with the ester oxygen traps the enoic carbene in a stabilized state that reduces the reactivity of these esters with 1-substituted cyclobutene esters, e.g., in homopolymerizations. However, the stabilized enoic carbene can still undergo metathesis with an electron rich alkene, e.g., cyclohexene. This reactivity opens an avenue for preparing alternating polymers with unique functionality.²⁷⁵ Steric crowding also prevents propagation as was observed for tertiary amide substituents (Figure 2-19). In conclusion, secondary amide substituted cyclobutenes comprise the optimal level of reactivity and stereo- and regio- control to provide translationally invariant polymers.

V. Future Perspectives

In the future, ROMP of some other 1-secondary amide substituted cycloalkenes, e.g., 1-cyclopropene amides or 1-cyclooctene amides, can be employed to provide translationally invariant polymers (Figure 2-21). Cyclopropene has the highest ring strain (54.5 kcal/mol) among all the cyclic olefins.¹⁸ As a result, 1-cyclopropene amides can exhibit much higher ROMP activity than 1-cyclobutene amides. However, it is very hard to synthesize stable cyclopropene derivatives. Cyclooctene has much smaller ring strain (8.4 kcal/mol).¹⁸ Therefore, it is proposed that the ROMP activity of 1-cyclooctene amides may be lower than that of 1-cyclobutene amides.

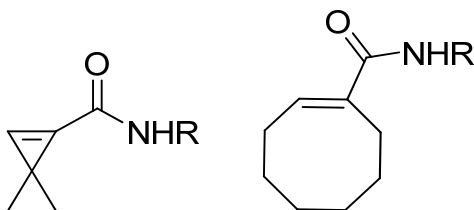


Figure 2-21. Proposed 1-secondary amide substituted cycloalkene monomers.

Chapter 3

Alternating Ring Opening Metathesis Polymerization*

I. Introduction

II. Results

III. Discussion

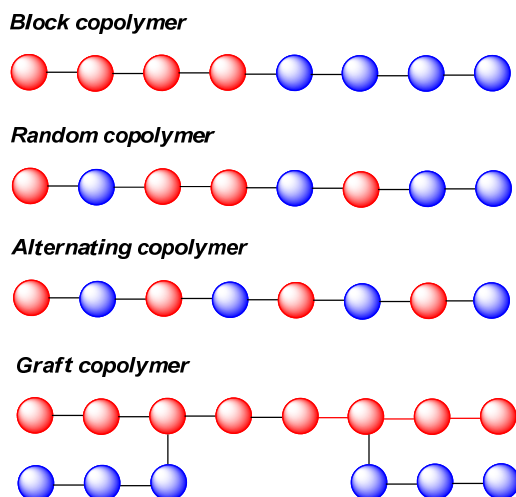
IV. Summary

V. Future Perspectives

*Much of the work described in this chapter has been described in *J. Am. Chem. Soc.*, **2009**, 131, 3444-3445.

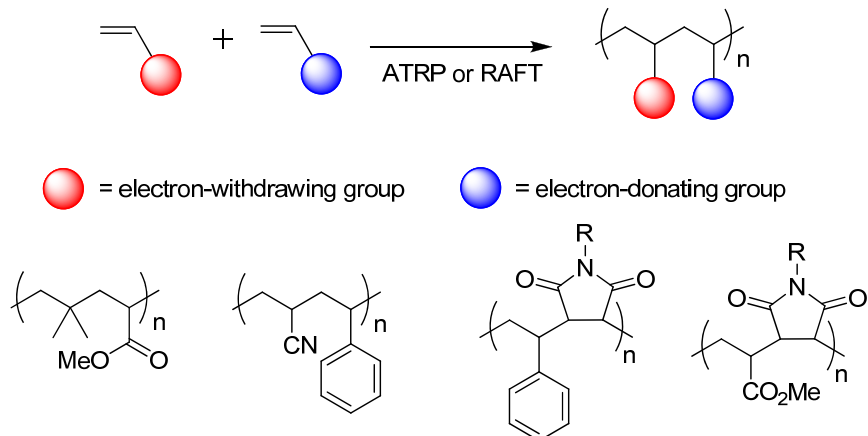
I. Introduction

Copolymers are employed in applications ranging from the biomedical to the electronic.^{151,207-208,276-277} There are several types of copolymers: block copolymers, random copolymers, alternating copolymers and graft copolymers (Scheme 3-1). Among the most commonly used are block copolymers that require phase separation of the two blocks for their function, e.g., drug delivery,²⁰⁹⁻²¹¹ and random copolymers in which two functional moieties communicate, e.g., organic light emitting diodes.²¹² Regularly alternating polymers allow optimal positioning of functional substituents and are useful in a variety of applications.



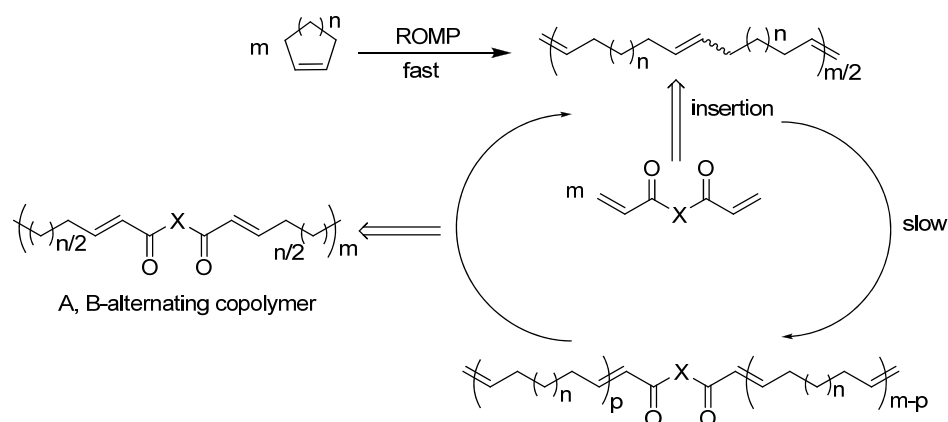
Scheme 3-1. Representative structures of copolymers.

Alternating polymers are generally synthesized by radical polymerization reactions such as atom transfer radical polymerization (ATRP) or reversible addition-fragmentation chain transfer polymerization (RAFT) with kinetic control of the order of monomer incorporation.²⁷⁸⁻²⁸⁰ Alternating copolymers of isobutene with methyl acrylate (MA), butyl acrylate (BA), and acetonitrile (AN) have been synthesized by ATRP using $\text{CuBr}(\text{bpy})_3$ as the catalyst and 1-phenylethyl bromide as the initiator at 50 °C (Scheme 3-2). These alternating copolymerization reactions exhibited accurate molecular weight control and relatively high PDIs (~ 1.5).²⁸¹



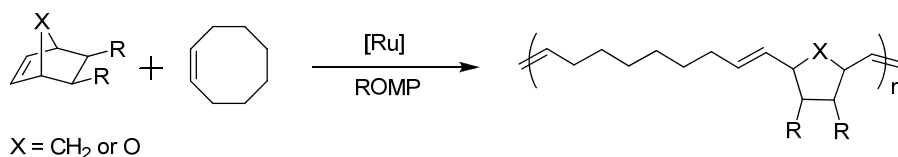
Scheme 3-2. Alternating copolymerization by ATRP or RAFT and some representative alternating copolymers.

However, there are isolated examples of the synthesis of alternating copolymers by ring opening metathesis polymerization (ROMP). Early on, it was reported that the ROMP of racemic 1-methylbicyclo[2.2.1]hept-2-ene with ReCl_5 gave polymer in which the two enantiomers alternate.²⁸² More recently, several reports of alternating polymers as the products of ROMP have appeared. Grubbs' group developed a ring opening insertion metathesis (ROIMP) approach to copolymerize cycloalkenes and diacrylates using ruthenium catalyst **4** (Scheme 3-3).²⁸³ The linear polymers containing more than 90% alternation were generated based on the ¹H-NMR spectroscopic analysis, and the alternation is controlled by equilibration. However, ROIMP exhibited relatively high PDIs (1.4-2.1) and poor molecular weight control. Some groups copolymerize norbornenes with cyclooctenes or cyclopentenes using ruthenium-based catalysts (Scheme 3-4), and the alternation relies on the pairing of a bulky but strained monomer (norbornene) with an unhindered and only slightly strained monomer (cyclooctene or cyclopentene). In all cases except one,²⁸⁴ a significant excess of one of the monomers is required for high levels of alternation (> 90%).²⁸⁵⁻²⁹⁰ F. Sanda et al. copolymerized norbornenes carrying nonprotected carboxy and amino groups to generate alternating copolymers based on acid-base interactions (Scheme 3-5).²⁹¹



Scheme 3-3. Proposed mechanism for ROIMP.

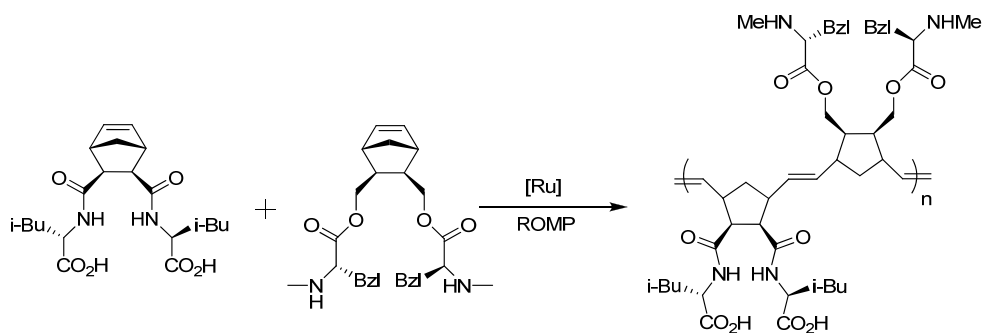
Our laboratory recently developed cyclobutene 1-carboxamides as monomers that undergo ruthenium-catalyzed ring-opening metathesis to yield translationally invariant polymers.¹¹¹ During the course of extending the ROMP to cyclobutenecarboxylic acid derivatives, we observed that cyclobutene methyl ester **8a** underwent ring-opening



Scheme 3-4. AROMP of norbornene and cyclooctene.

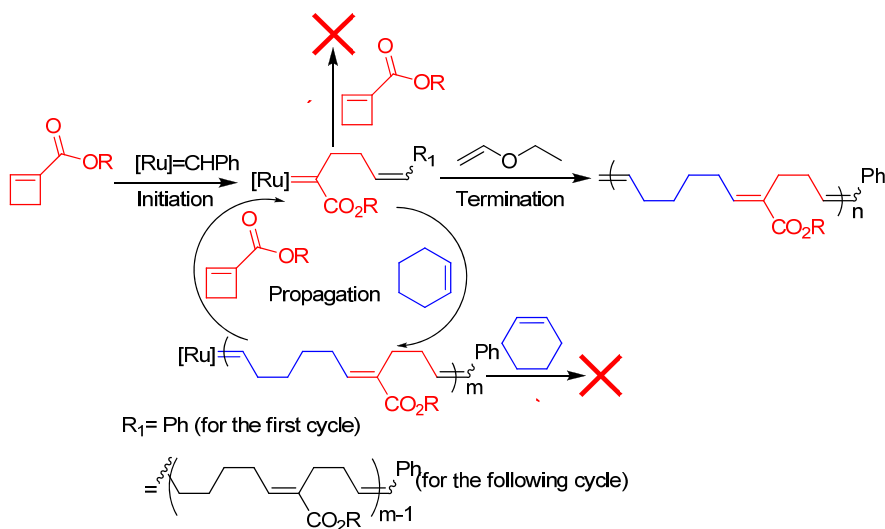
metathesis without polymerization to afford, with 10 mole % of catalyst, approximately 10% of the α -methylene ester **13a** & **14a**. As in the ring-opening metathesis of 1-substituted cyclobutene amides,¹¹¹ this reaction is regioselective. However with ester **8a**, the key enoic ruthenium carbene **[Ru]-13a** and **[Ru]-14a** does not react with additional substrate; rather, it survives to react with the quenching agent, providing ester **13a** & **14a**.

Cyclohexene is a ring-opening metathesis inactive substrate with ruthenium catalysts due to its low ring strain energy.³⁸ However, it undergoes ring opening cross metathesis with acrylates.²¹³⁻²¹⁴ It was suggested from *ab initio* transition state calculation that the coordination of the carbonyl group to the ruthenium center can greatly stabilize



Scheme 3-5. AROMP of norbornenes carrying nonprotected carboxy and amino groups.

the transition state in the ring opening of cyclohexene.²⁶⁸ On the basis of this result and the observation noted above, we postulated that ester **8a** and cyclohexene, subjected together to an active ruthenium catalyst, would undergo AROMP (Scheme 3-6).



Scheme 3-6. Proposed AROMP mechanism of 1-cyclobutene esters and cyclohexenes.

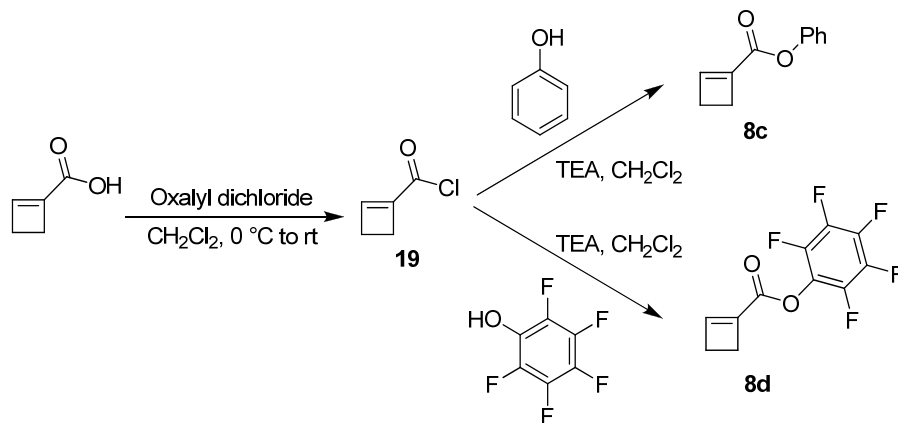
ROM of 1-substituted cyclobutene ester by ruthenium catalysts generates a kinetically trapped enic ruthenium carbene, and that carbene cannot ring-open additional 1-cyclobutene esters. Instead the enic ruthenium carbene can ring-open cyclohexene to generate an electron-rich ruthenium alkylidene, and that ruthenium alkylidene can only react with a 1-cyclobutene ester monomer due to the high ring strain of cyclobutene to

make the enoic ruthenium carbene again. As a result, alternating cyclobutene and cyclohexene units can be present in the propagating polymer chain.

II. Results

II.1 Synthesis of Cyclobutene and Cyclohexene Monomers

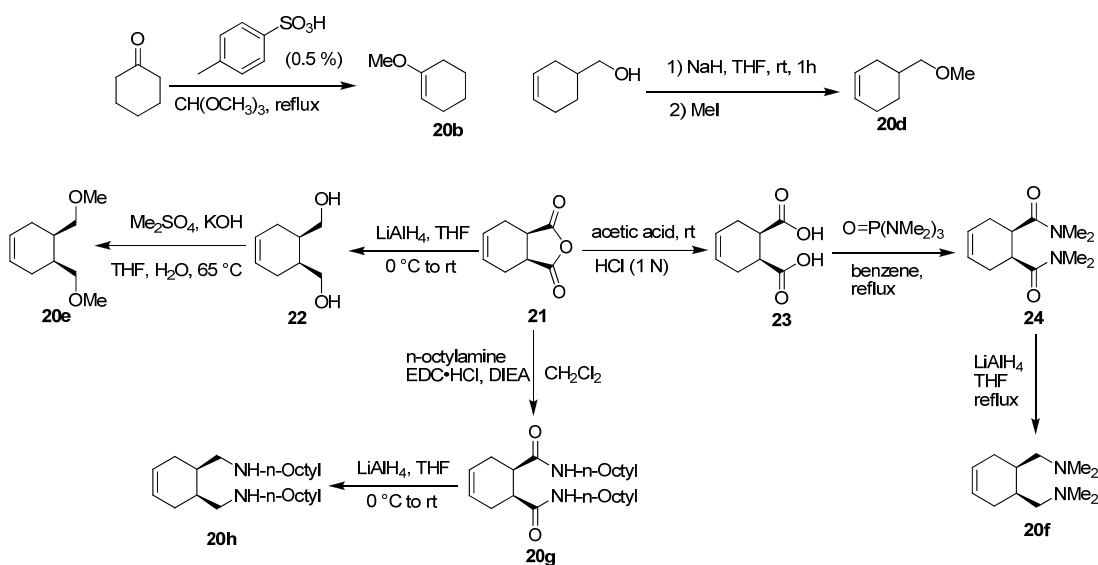
Two 1-substituted cyclobutene ester monomers were synthesized through their respective acyl chlorides (Scheme 3-7). 1-Cyclobutene carbonyl chloride **19** was prepared by reaction of 1-cyclobutenecarboxylic acid with oxalyl dichloride. The coupling of **19** with phenol or pentafluorophenol (PFP) in the presence of trimethylamine (TEA) generated esters **8c** or **8d**, respectively.



Scheme 3-7. Synthesis of 1-substituted cyclobutene esters **8c** and **8d**.

A variety of cyclohexene derivatives were synthesized (Scheme 3-8). 1-Methoxycyclohexene **20b** was made by heating cyclohexanone and trimethyl orthoformate to reflux in the presence of 0.5% *p*-toluene sulfonic acid.²⁹²⁻²⁹³ 4-(Methoxymethyl)cyclohexene **20d** was synthesized through the methylation of 3-cyclohexene-1-methanol using NaH/MeI in THF. The reduction of **21** with LiAlH_4 yielded diol **22**. Diol **22** was allowed to react with dimethylsulfate under basic solutions to generate cyclohexene monomer **20e**.²⁹⁴ n-Octylamine was coupled with **21** using 1-

ethyl-3-(3-dimethylaminopropyl)carbodiimide hydrochloride (EDC·HCl) and diisopropylethylamine (DIEA) in CH₂Cl₂ to generate diamide **20g**, which was reduced with LiAlH₄ to form diamine **20h**. Cyclohexene **21** was hydrolyzed in acetic acid and HCl (1 N) solution to generate diacid **23**. Diacid **23** was coupled with O=P(NMe₂)₃ to make diamide **24** upon heating to reflux in benzene. Diamine **20f** was synthesized through reduction of **24** with LiAlH₄.



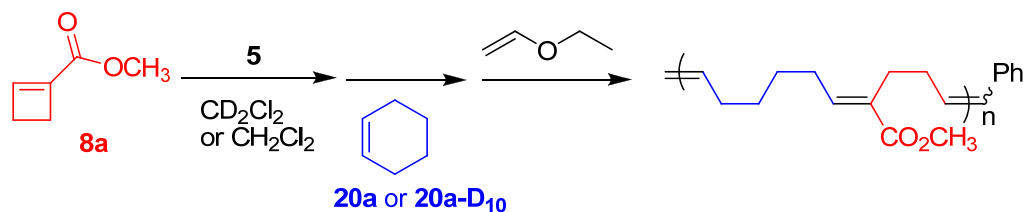
Scheme 3-8. Synthesis of cyclohexene derivatives.

II.2 AROMP of Cyclobutene **8a** and Cyclohexene **20a** or **20a-D₁₀** with Catalyst **5**

First, we tested with ¹H-NMR spectroscopy if cyclohexene alone could be polymerized with the ruthenium catalyst **5** in CD₂Cl₂. In 6 h, no monomer was consumed confirming that cyclohexene is ROMP inactive.

In order to test our premise that 1-cyclobutene ester and cyclohexene may be polymerized alternately with the ruthenium catalyst **5** (Scheme 3-6), we examined the fate of a mixture of cyclobutene ester **8a** and cyclohexene **20a** in the presence of catalyst **5**. First, cyclobutene ester **8a** and catalyst **5** were mixed in CD₂Cl₂ or CH₂Cl₂ to allow complete initiation of the catalyst. Then, an excess of cyclohexene **20a** or deuterated

cyclohexene **20a-D₁₀** was added to the above solution to propagate polymerization. The polymerization was terminated upon addition of ethylvinyl ether. We observed polymerization with 74-98% conversion of monomer (Table 3-1). Taken together with the regioselective ROM (but not ROMP) of ester **8a** and the lack of reactivity of cyclohexene, this result strongly suggested that AROMP had occurred.



A	B	[Ru] (M)	[A]:[B]:[Ru]	Rxn time (h)	Prod.	% Conv ^a
none	20a	0.01	0:40:1	6	NP ^b	0
8a	20a	0.05	3:6:1	6	(8a-20a)₃	74 ^c
8a	20a	0.01	10:20:1	3	(8a-20a)₁₀	98
8a	20a	0.01	20:40:1	3	(8a-20a)₂₀	98
8a	20a	0.01	50:100:1	3	(8a-20a)₅₀	98
8a	20a	0.01	100:200:1	3	(8a-20a)₁₀₀	97
8a	20a	0.01	200:400:1	1.5	(8a-20a)₁₀₀	50
8a	20a	0.01	300:600:1	4	(8a-20a)₁₀₀	34
8a	20a	0.005	200:400:1	6	(8a-20a)₂₀₀	73
8a	20a	0.01	200:400:1	6	(8a-20a)₂₀₀	75
8a	20a	0.01	20:24:1	3	(8a-20a-D₁₀)₂₀	97
8a	20a-D₁₀	0.01	20:40:1	3	(8a-20a-D₁₀)₂₀	97
8a	20a-D₁₀	0.01	20:160:1	3	(8a-20a-D₁₀)₂₀	97

Table 3-1. AROMP polymers synthesized. All ROMP reactions were performed in CD₂Cl₂ and monitored by ¹H-NMR spectroscopy at rt. ^aPercent conversion determined by integration of ¹H-NMR spectra unless specified otherwise. ^bNo polymerization. ^cReaction was performed in CH₂Cl₂ and the isolated yield was determined after flash column chromatography purification.

The molecular weights and PDIs of the above alternating copolymers were characterized by GPC using polystyrene standards (Table 3-2). The polymers had very

broad molecular weight ranges and high PDIs (> 2). The poor molecular weight and PDI control was due to the existence of a large amount of secondary metathesis reactions.

A	B	[Ru]/ M	[A]:[B]:[Ru]	%Conv ^a	Calcd <i>M_n</i>	PSS <i>M_n</i>	PSS <i>M_w</i>	PDI ^b
8a	20a	0.01	10:20:1	98	2044	376	962	2.6
8a	20a	0.01	20:40:1	98	3984	668	1816	2.7
8a	20a	0.01	50:100:1	98	9804	652	2634	4.0
8a	20a	0.01	100:200:1	97	19504	1869	10872	5.8
8a	20a	0.01	200:400:1	50	19504	3201	18106	5.7
8a	20a	0.005	300:600:1	34	19504	1892	7181	3.8
8a	20a	0.01	200:400:1	74	29010	7749	18501	2.4

Table 3-2. Polymerization results. ^aConversion yield of monomer. ^bMolecular weight and PDI were determined by GPC using polystyrene standards.

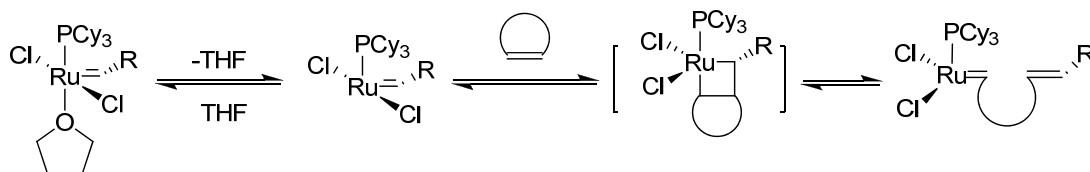
II.3 AROMP of Cyclobutene **8a** and Cyclohexene **20a** with Other Catalysts

The AROMP of cyclobutene **8a** and cyclohexene **20a** was performed using catalyst **3** (Table 3-3). It was reported that the addition of triphenylphosphine (PPh₃)^{17,21} and the use of THF as the reaction solvent^{17,21,245} could greatly help limit secondary metathesis reactions due to their coordination to the ruthenium carbene. Therefore, we copolymerized **8a** and **20a** in CD₂Cl₂ or THF-D₈ with or without the addition of PPh₃ using catalyst **3** to see if we could limit or even prevent chain transfer reactions (Table 3-3). The addition of PPh₃ inhibited AROMP of cyclobutene and cyclohexene no matter which solvent was used. The AROMP deactivation of PPh₃ may be due to the stronger coordination of PPh₃ to the ruthenium carbene than the other monomers. Without the addition of PPh₃, only 43% monomer was consumed in 4 h in CD₂Cl₂ at 39 °C, and only 16% conversion of monomer was obtained in THF-D₈ in 4 h at 50 °C. It has been previously reported that the ROMP reactions in THF exhibited slower kinetics relative to

[A]:[B]:[PPh ₃]:[Ru]	Rxn Conditions	% conv ^a	Calcd. M _n	PSS M _n	PSS M _w	PDI ^b
50:100:0:1	CD ₂ Cl ₂ , rt-39°C, 4 h	43	3984	1584	4530	2.9
20:40:20:1	CD ₂ Cl ₂ , rt-39°C, 4 h	0	n/a ^c	n/a	n/a	n/a
50:100:0:1	THF-D ₈ , rt-50°C, 4 h	16	n/a	n/a	n/a	n/a
20:40:20:1	THF-D ₈ , rt-50°C, 4 h	0	n/a	n/a	n/a	n/a

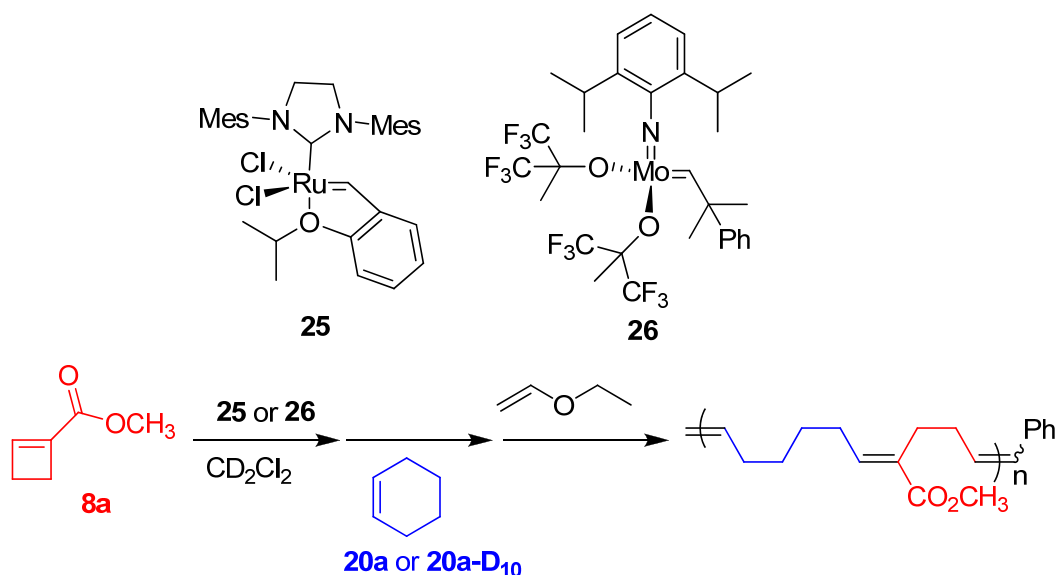
Table 3-3. AROMP by catalyst **3**. All ROMP reactions were monitored by ¹H-NMR spectroscopy at rt. ^aPercent conversion determined by integration of ¹H-NMR spectra unless specified otherwise. ^bMolecular weight and PDI were determined by GPC using polystyrene standards. ^cNot applicable.

benzene or CH₂Cl₂.^{245,295} THF may coordinate to the ruthenium metal center suppressing metathesis activity (Scheme 3-9). As a result, less monomer was consumed during AROMP in THF-D₈ than in CD₂Cl₂.



Scheme 3-9. ROMP of cyclic olefins in THF.

AROMP of cyclobutene **8a** with cyclohexene **20a** was also tested using catalyst **25** (Table 3-4). It took 9h to reach 89% monomer conversion at 39 °C in the 20-mer



A	B	Catalyst	[Cat] (M)	[A]:[B]:[Ru]	Rxn time (h)	% conv ^a
8a	20a-D ₁₀	25	0.01	20:40:1	9	89
8a	20a	26	0.01	50:100:1	3	NP ^b

Table 3-4. AROMP polymers synthesized. All ROMP reactions were performed in CD₂Cl₂ and monitored by ¹H-NMR spectroscopy at rt. ^aPercent conversion determined by integration of ¹H-NMR spectra unless specified otherwise. ^bNo polymerization.

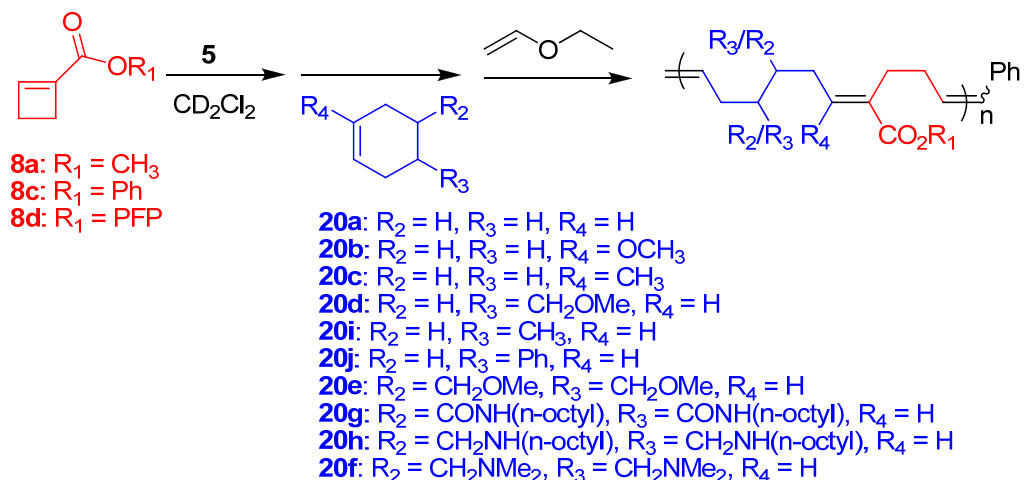
reaction. The slower AROMP kinetics with catalyst **25** is due to the much slower initiation rate of catalyst **25** than other Grubbs' catalysts **3-5**.²⁹⁶

Schrock's catalyst **26** was also tested in AROMP of 1-cyclobutene ester and cyclohexene (Table 3-4). In the 50-mer reaction, no polymerization was observed at all based on the ¹H-NMR spectroscopic analysis. It is possible that catalyst **26** was poisoned by the ester group of cyclobutene **8a** due to the lower functional group tolerance of Mo-based catalysts (Figure 1-3).

II.4 AROMP of Other Cyclobutene and Cyclohexene Derivatives by Catalyst 5

One important property of alternating copolymers is their presentation of alternating functional groups that are bioactive or useful in energy transfer. To investigate

the functional group tolerance of AROMP, a variety of functional groups in either the cyclobutene or cyclohexene unit were evaluated (Table 3-5).



A	B	[Ru] (M)	[A]:[B]:[Ru]	Rxn time (h)	Prod.	% conv ^a
8a	20b	0.01	10:20:1	3	n/a ^b	NP ^c
8a	20c	0.01	10:20:1	3	n/a	NP
8a	20d	0.01	20:40:1	4	(8a-20d) ₂₀	95
8a	20i	0.01	20:40:1	4	(8a-20i) ₂₀	95
8a	20j	0.01	20:40:1	6	(8a-20j) ₂₀	90
8a	20e	0.01	20:40:1	6	(8a-20e) ₂₀	90
8a	20g	0.01	10:20:1	6	n/a	NP
8a	20h	0.01	20:40:1	5	n/a	NP
8a	20f	0.01	20:40:1	5	n/a	NP
8c	20a	0.01	20:40:1	4	(8c-20a) ₂₀	96
8d	20a	0.01	10:20:1	5	(8d-20a) ₁₀	95

Table 3-5. AROMP polymers synthesized. All ROMP reactions were performed in CD₂Cl₂ and monitored by ¹H-NMR spectroscopy at rt. ^aPercent conversion determined by integration of ¹H-NMR spectra unless specified otherwise. ^bNot applicable. ^cNo polymerization.

Both 1-methylcyclohexene **20c** and 1-methoxy-cyclohexene **20b**, when subjected to AROMP with **8a**, did not generate any polymer (Table 3-5). That could be due to the hindered 1-substituents of cyclohexene when coordinating to the ruthenium carbene. However, substitution remote from the cyclohexene alkene was tolerated. Both 4-

substituted cyclohexenes **20d** and **20i** underwent AROMP with **8a** to generate the corresponding alternating polymers (Table 3-5), and around 95% monomer consumption was achieved in 4 h. However, it took 6 h to reach 90% monomer consumption for AROMP of 4-phenylcyclohexene **20j** and cyclobutene **8a**. The slower AROMP rate is presumably due to steric hindrance by the phenyl substituent in AROMP. In AROMP of 4,5-(dimethoxymethyl)cyclohexene **20e** and **8a**, 90% conversion was achieved in 6 h. However, for the other 4,5-disubstituted cyclohexenes **20g** (diamide), **20h** (diamine) and **20f** (diamine), no polymerization was observed in AROMP with cyclobutene **8a** (Table 3-5), and their inactivity in AROMP may be caused by the large steric hindrance from two substituents.

Next, we investigated the effect of substituents on the reactivity of the cyclobutene. We found, for example, that AROMP of **20a** and phenyl ester **8c** or PFP ester **8d** proceeded with high conversion (>95%) at room temperature in 4-5 hours to yield **(8c-20a)₂₀** and **(8d-20a)₁₀** respectively (Table 3-5). This type of product is viewed as a precursor to polymers with a variety of side chains because of the electrophilicity of phenyl or PFP esters. The alternating copolymers in Table 3-6 were characterized by GPC, and they exhibit broad PDIs (> 2) and much lower molecular weights than expected. Therefore, backbiting occurs within these monomers as well.

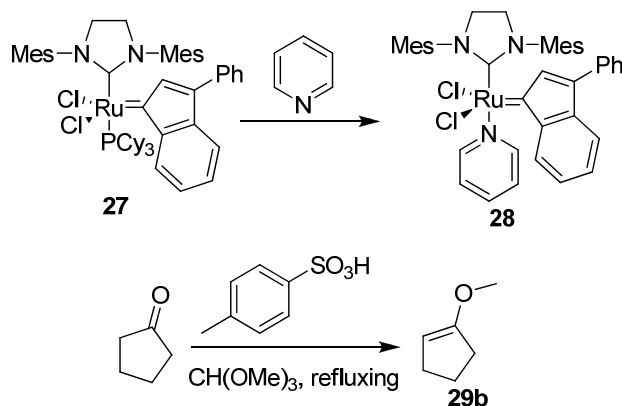
Polymer	Calcd M_n	PSS M_n	PSS M_w	PDI ^a
(8a-20d)₂₀	4870	1506	3719	2.5
(8a-20i)₂₀	4270	1345	3228	2.4
(8a-20j)₂₀	5511	1679	4365	2.6
(8a-20e)₂₀	5752	1583	3799	2.4
(8c-20a)₂₀	5224	1572	3302	2.1
(8d-20a)₁₀	3567	1203	3489	2.9

Table 3-6. AROMP results. ^aMolecular weight and PDI were determined by GPC using polystyrene standards.

II.5 AROMP of Cyclobutene and 1-Cyclopentene Derivatives by Ruthenium Catalysts

One major reason that there are so many chain transfer reactions in AROMP of cyclobutene and cyclohexene is the existence of a large amount of disubstituted olefin bonds in the polymer chain. Although 1-substituted cyclopentene has greater ring strain than cyclohexene, we hypothesized that its AROMP rate would be similar to cyclohexene due to the steric hindrance by 1-substituents in the cyclopentene. AROMP of cyclobutene **8a** and 1-substituted cyclopentene was performed using catalyst **5** or catalyst **28** to minimize the chain transfer by increasing the percentage of trisubstituted olefin bonds in the propagating polymer chain (Table 3-7).

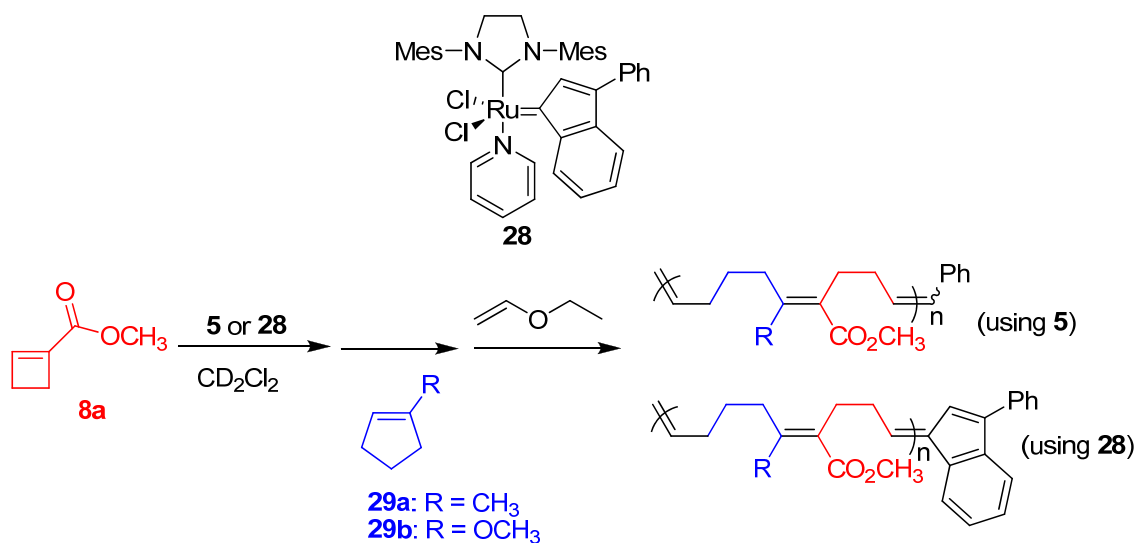
Nolan's catalyst **28** was synthesized by substituting the phosphine group (PCy₃) in catalyst **27** with a pyridine group according to the literature (Scheme 3-10).²⁹⁷⁻²⁹⁸ 1-Methoxycyclopentene **29b** was synthesized by trapping the enol of cyclopentanone with trimethyl orthoformate in 5% *p*-toluene sulfonic acid (Scheme 3-10).²⁹²⁻²⁹³



Scheme 3-10. Synthesis of 1-methoxycyclopentene **29b** and catalyst **28**.

AROMP of cyclobutene **8a** and 1-methylcyclopentene **29a** was performed using catalyst **28** under different reaction conditions (Table 3-7). In CDCl₃, it took 5 h to reach 50% conversion for AROMP of **8a** and **29a** at 50 °C. In toluene-D₈ AROMP of **8a** and **29a** at 80 °C proceeded to 50% conversion in 2 h. However, no matter what reaction

temperature was used, only polymers with a lower M_n than expected were generated (Table 3-8). The poor molecular weight control indicates that the chain transfer was not



A	B	Cat.	Rxn Conditions	[A]:[B]:[Ru]	Prod.	% conv ^a
8a	29a	28	CDCl ₃ , 50 °C, [Ru] = 0.01M, 5 h	20:40:1	(8a-29a)₁₀	50
8a	29a	28	Toluene-D ₈ , 80 °C, [Ru] = 0.01M, 2 h	20:40:1	(8a-29a)₁₀	50
8a	29b	5	CDCl ₃ , 50 °C, [Ru] = 0.01M, 4 h	40:80:1	NP ^b	NP
8a	29b	28	CDCl ₃ , 50 °C, [Ru] = 0.01M, 4 h	40:80:1	NP	NP

Table 3-7. AROMP polymers synthesized. ^aPercent conversion determined by integration of ¹H-NMR spectra unless specified otherwise. ^bNo polymerization.

suppressed.

AROMP of cyclobutene **8a** and 1-methoxycyclopentene **29b** was performed using catalyst **5** or catalyst **28** in CDCl₃ at 50 °C (Table 3-7). No polymerization was observed for either catalyst within 4 h. We hypothesize that the ruthenium carbene is deactivated by strong coordination of the methoxy group in **29b** to the ruthenium metal center.

A	B	[Ru]/ M	[A]:[B]:[Ru]	%Conv ^a	Calcd M_n^b	PSS M_n	PSS M_w	PD I^c
8a	29a	0.01	20:40:1	50	2044	1101	2522	2.3
8a	29a	0.01	20:40:1	50	3014	508	1393	2.7

Table 3-8. Polymerization results with catalyst **28**. ^aConversion yield of monomer. ^bCalculated based on the conversion yielded. ^cMolecular weight and PDI were determined by GPC using polystyrene standards.

III. Discussion

III.1 AROMP of Cyclobutene and Cyclohexene Using Catalyst 5

III.1.1 AROMP of **8a** and **20a** Using Catalyst 5

AROMP of **8a** and **20a** using catalyst **5** (from 10-mer to 200-mer) was monitored by ¹H-NMR spectroscopy (Table 3-1). The NMR spectral changes as a function of reaction time for the 100-mer reaction are plotted to illustrate the formation of AB dyad (Figure 3-1). The proton peak integrals for the disubstituted (4.40 ppm) and trisubstituted (5.75 ppm) olefin bonds increased simultaneously.

¹H-NMR spectroscopic analysis (Figure 3-2) of each of the polymers ((**8a-20a**)₁₀ - (**8a-20a**)₂₀₀) revealed the phenyl protons and two sets of vinyl protons. The ratio of the signal for the protons on the disubstituted, non-conjugated olefin ($\delta=5.4$ ppm) to the signal for the protons on the trisubstituted, conjugated olefin ($\delta=6.8$ ppm) was approximately 2:1. This result is consistent with polymer structure (**8a-20a**)_n which contains nearly equal numbers of repeating units A and B generated from monomers **8a** and **20a** respectively.

To further confirm the alternating structure, (**8a-20a**)₂₀ was characterized by ¹³C-NMR, ¹³C-APT NMR (Figure 3-3), ¹H-¹H gCOSY (Figure 3-4) and ¹H-¹³C gHMQC spectroscopy. The correlated NMR chemical shifts are summarized in Table 3-9. ¹H-¹H gCOSY spectroscopy of (**8a-20a**)₂₀ clearly showed internal connectivity between repeating units A and B (Figure 3-4), further establishing the alternating nature of the polymer backbone.

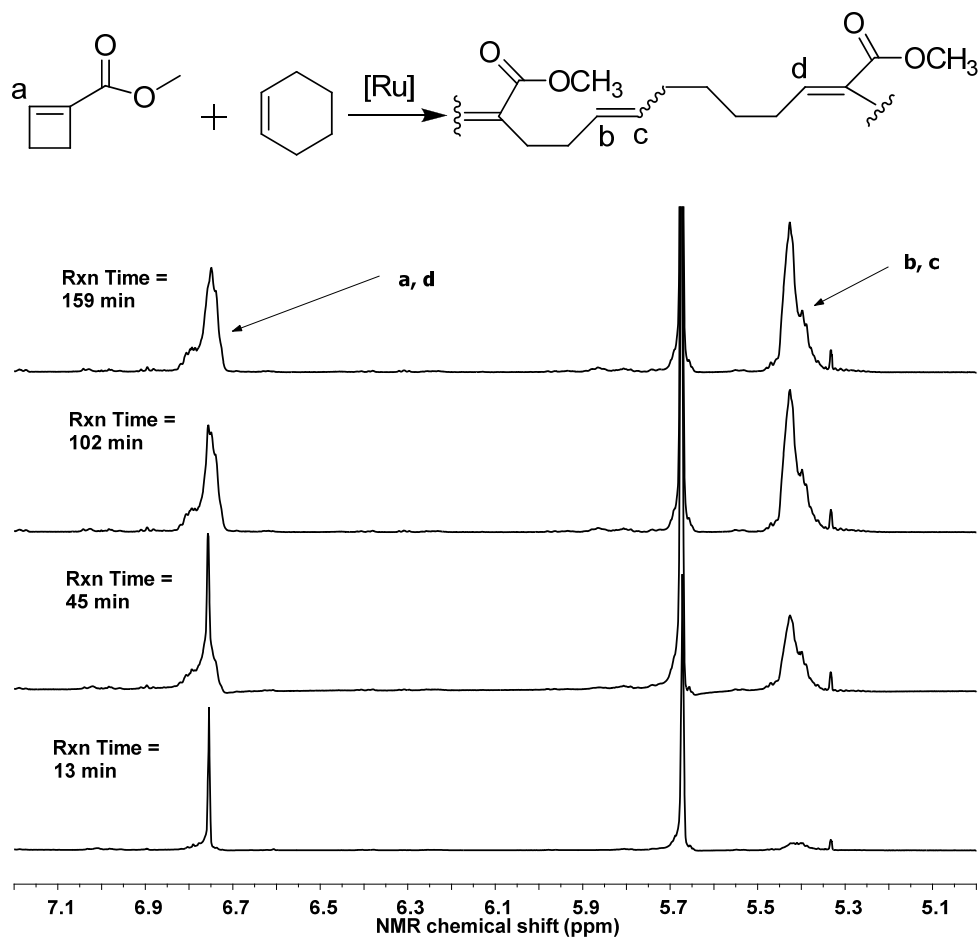


Figure 3-1. $^1\text{H-NMR}$ spectral changes with reaction time for AROMP of **8a** and **18a** using catalyst **5**. [**8a**]:[**18a**]:[**5**] = 100: 200:1, 97% conversion yield, CD_2Cl_2 , rt.

In order to ascertain with greater accuracy the extent of alternation in the sequence of monomer units, we undertook an isotopic labeling experiment. Cyclohexene- D_{10} , **20a-D₁₀**, and cyclobutene **8a** were subjected to AROMP (Table 3-1), the $^1\text{H-NMR}$ spectra of the crude polymers acquired, and the intensities of the olefinic peaks integrated against the phenyl end group (Figure 3-5).

As expected, for a deuterated alternating AB copolymer (**8a-20a-D₁₀**)₂₀, the relative intensity of the signal at $\delta = 5.4$ ppm was reduced to half of that in the spectrum of polymer (**8a-20a**)₂₀ (Figure 3-6A). This halved intensity is consistent with the absence of BB repeat in the polymer (Figure 3-6B). Moreover, the intensity of the signal at $\delta = 6.8$ ppm in the spectrum of (**8a-20a-D₁₀**)₂₀ was reduced to 9% of its relative intensity in

the spectrum of the undeuterated polymer ((**8a-20a**)₂₀), showing that only 9% of the dyads are of type AA (Figure 3-6B).

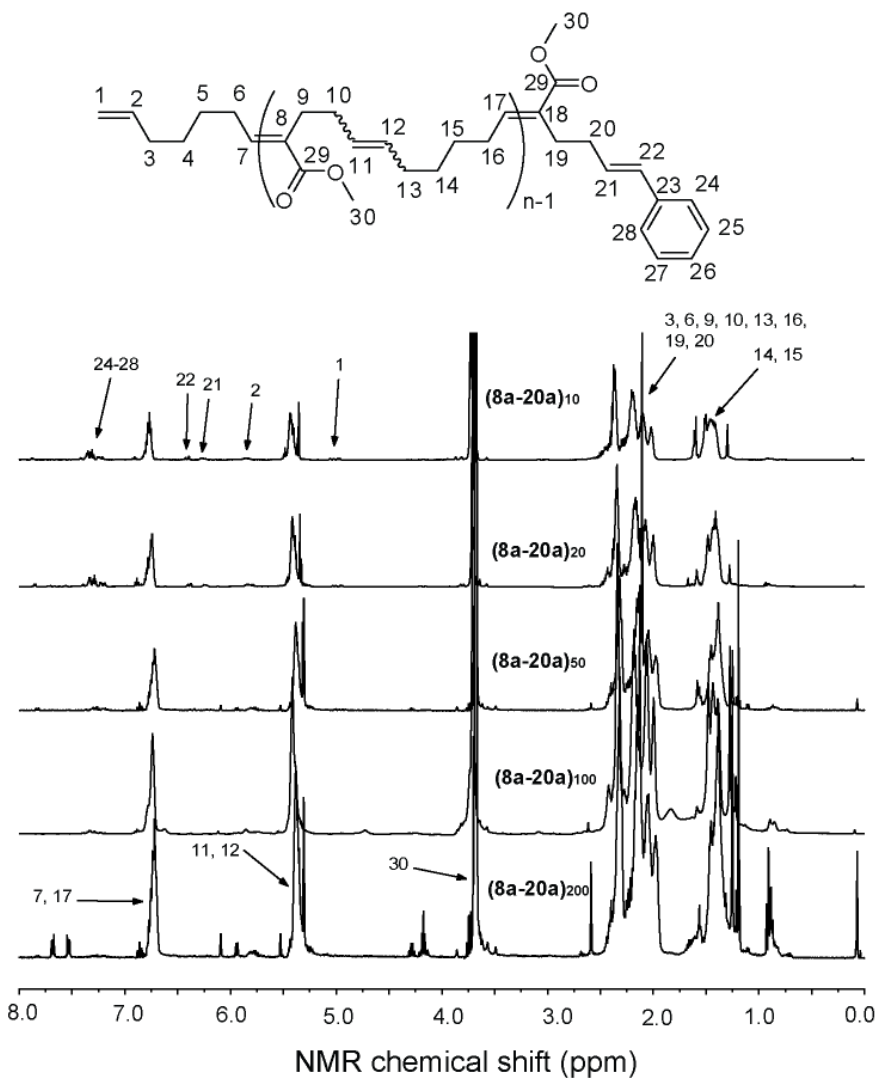


Figure 3-2. ¹H-NMR spectra of alternating ROMP polymers (**8a-20a**)₁₀ - (**8a-20a**)₂₀₀.

We observed that the fraction of AA dyad was constant regardless of the original A:B feed ratio (from 20:24 to 20:160) in the AROMP reaction (Table 3-1). Therefore, the polymer chain grows with alternation by a mechanism that does not depend on monomer concentration.

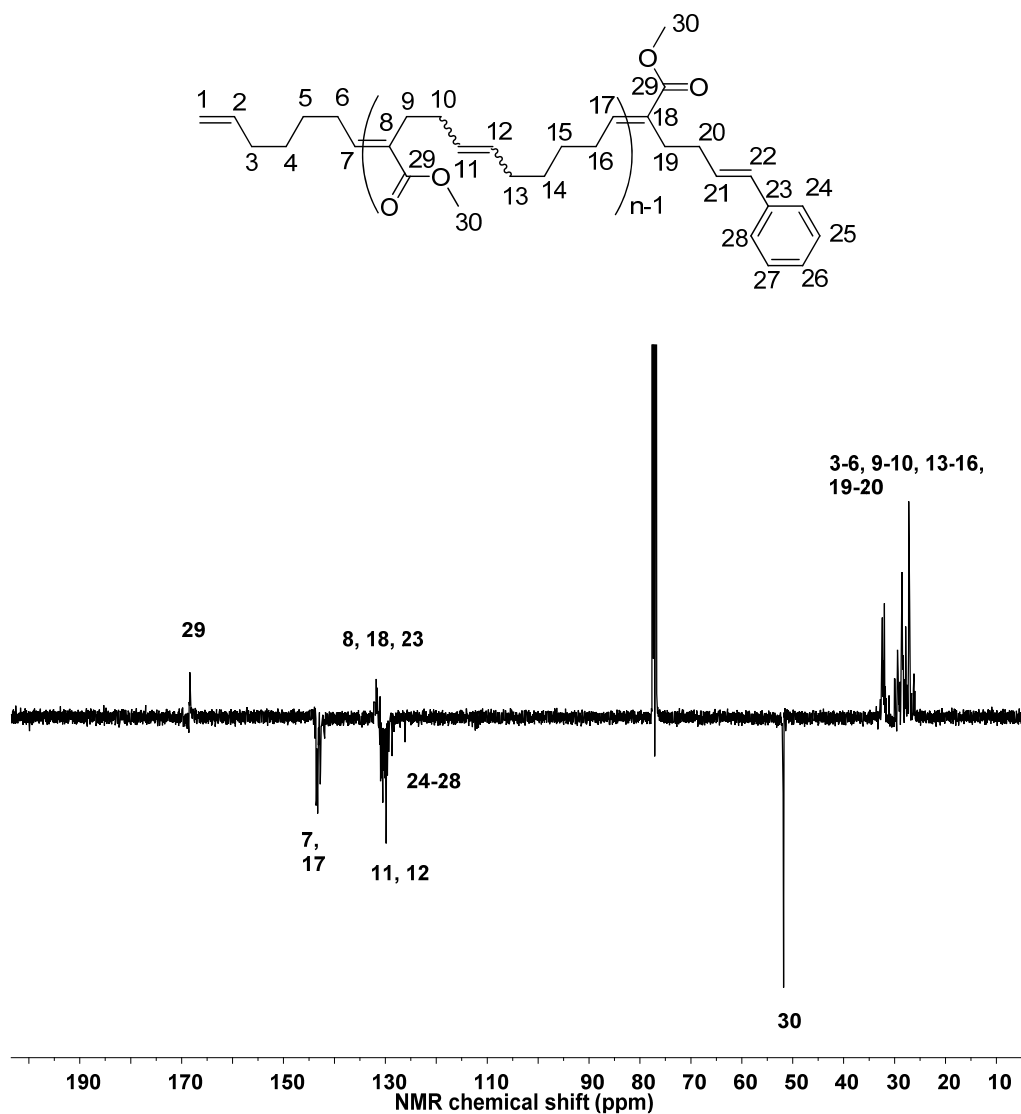


Figure 3-3. ^{13}C -APT NMR spectrum of alternating ROMP polymer $(8a-20a)_{20}$.

The concentration-independent population of the AA dyad and the absence of BB dyad suggested that the AA dyads result from intramolecular backbiting of the enoic ruthenium carbene on the disubstituted alkene (Figure 3-8).²⁹⁹⁻³⁰⁰ Partial separation of the components of the polymer ($(8a-20a-D_{10})_{20}$) by flash chromatography gave a fraction ($\text{cyc-}(8a-20a-D_{10})_{20}$) that contained the AA substructure (as indicated by a clean triplet at 6.8 ppm) but not the phenyl end group (Figure 3-7). Isolation of this material supports a model in which the AA repeat is generated at the backbiting junction during the

cyclization step (Figure 3-8). The existence of cyclic products was further confirmed by the ESI-Mass spectral analysis of $(\mathbf{8a-20a})_3$ (Figure 3-9). Most of the mass peaks of $(\mathbf{8a-20a})_3$ were assigned to cyclic polymers containing only cyclobutene and cyclohexene units. The backbiting most likely took place at the disubstituted olefin bonds rather than the trisubstituted olefin bonds as the latter are sterically blocked.

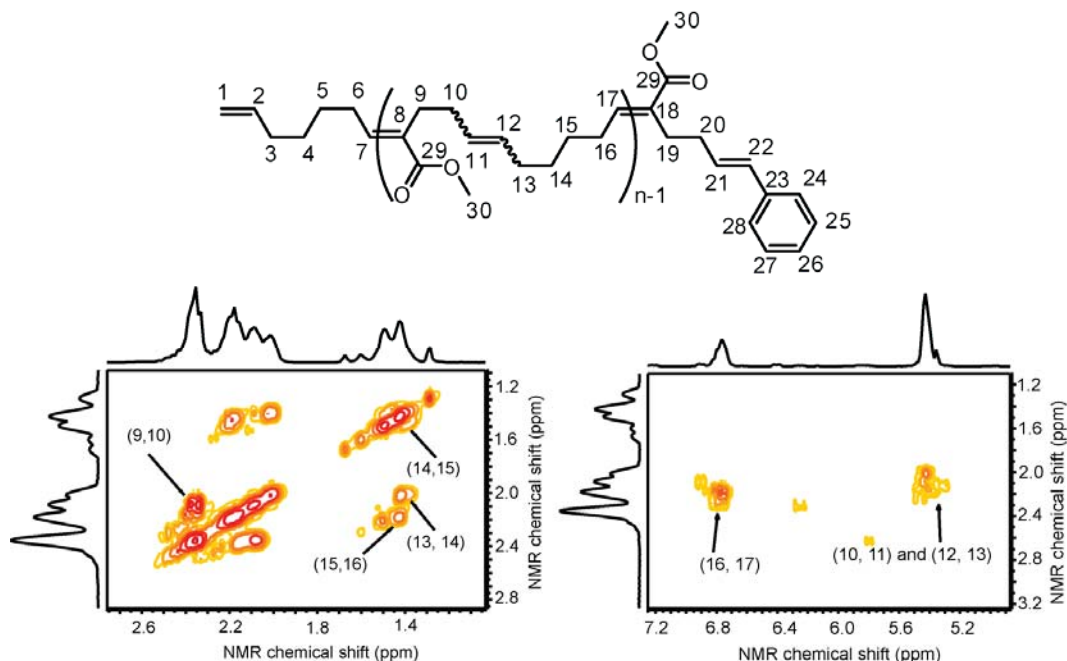


Figure 3-4. ^1H - ^1H gCOSY-NMR spectrum of alternating ROMP polymer $(\mathbf{8a-20a})_{20}$.

We found that the M_w 's of all the alternating copolymers (Table 3-2) were shorter than expected and the PDIs were large (>2). Polymer $(\mathbf{8a-20a})_{200}$ had a bimodal molecular weight distribution in which the higher molecular weight peak corresponded to the desired polymer with a PDI of 1.2 (Figure 3-10). These data are consistent with backbiting to form cyclic polymer during chain growth.

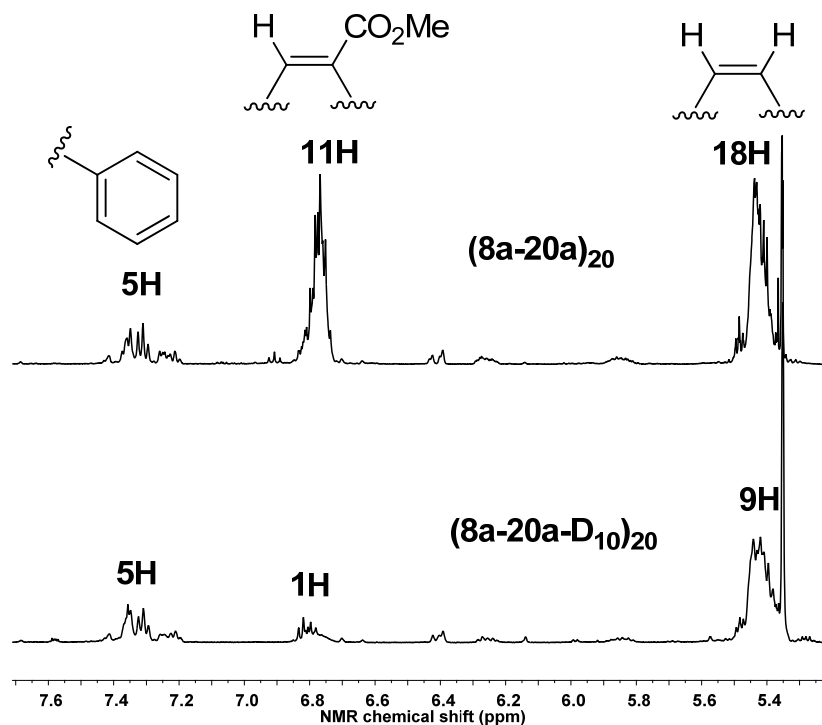


Figure 3-5. Alkene region of ¹H-NMR spectra (CD₂Cl₂) of polymers **(8a-20a)₂₀** and **(8a-20a-D₁₀)₂₀**. Proton integrations and assignments are indicated above the peaks.

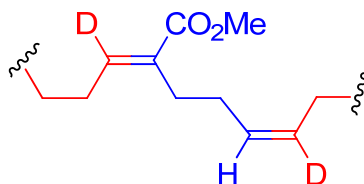
III.1.2 AROMP of Cyclobutene and Cyclohexene Derivatives Using Catalyst **5**

In order to explore the breadth of AROMP applications possible, we examined the effects of varying the structures of the monomers (Table 3-5 and Table 3-6). Cyclobutene esters (**8c** and **8d**) were successfully copolymerized with cyclohexene using catalyst **5** to prepare alternating copolymers with 95-96% conversion. 1-Substituted cyclohexenes (**20b** and **20c**) did not polymerize with cyclobutene **8a** due to the steric hindrance by 1-substituents, while AROMP of 4-substituted cyclohexenes (**20d**, **20i** and **20j**) and cyclobutene **8a** exhibited a slower reaction rate than that of cyclohexene **20a** and cyclobutene **8a** (Table 3-5). The reduced rate is most likely due to steric effects. The regiochemistry of metathesis could not be determined in the polymerization of **20d**, **20i** or **20j**, and is most likely random. 4-Substituted cyclohexenes are attractive monomers for AROMP because they are readily available through Diels-Alder chemistry.

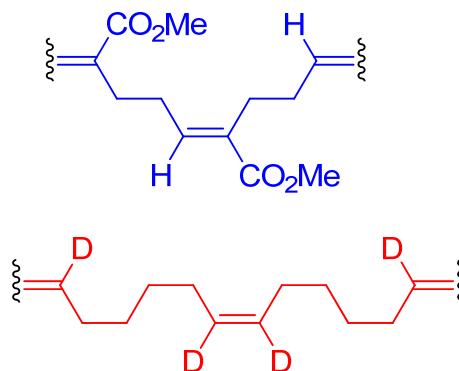
No.	δ_H (J in Hz)	δ_C	1H - 1H gCOSY	^{13}C -APT
1	4.97 d (15) 5.04 d (17)			
2	5.79 b	129.5-132.5		CH
3	2.04-2.50 b	26.7-32.5		CH ₂
4	1.42 b	29.2-29.9		CH ₂
5	1.42 b	29.2-29.9		CH ₂
6	2.04-2.50 b	26.7-32.5		CH ₂
7	6.74 b	142.7-143.7		CH
8		131.8		q
9	2.04-2.50 b	26.7-32.5		CH ₂
10	2.04-2.50 b	26.7-32.5	11	CH ₂
11	5.40 m	129.5-131.1	10	CH
12	5.40 m	129.9-131.0	13	CH
13	2.04-2.50 b	26.7-32.5	12, 14, 16	CH ₂
14	1.42 b	29.2-29.9	13, 15	CH ₂
15	1.42 b	29.2-29.9	14, 16	CH ₂
16	2.04-2.50 b	26.7-32.5	13, 15, 17	CH ₂
17	6.74 b	142.7-143.7	16	CH
18		131.8		q
19	2.04-2.50 b	26.7-32.5		CH ₂
20	2.04-2.50 b	26.7-32.5		CH ₂
21	6.24 b	129.7		CH
22	6.39 d (16)	129.7		CH
23		131.9		q
24-28	7.19-7.33 m	128.3-129.7		CH
29		168.2		q
30	3.70 s	51.8		CH ₃

Table 3-9. 1H -NMR (500 MHz, CD₂Cl₂), ^{13}C -NMR (100 MHz, CD₂Cl₂), 1H - 1H gCOSY (500 MHz, CD₂Cl₂), ^{13}C -APT (100 MHz, CD₂Cl₂), and 1H - ^{13}C gHMQC (500/125 MHz, CD₂Cl₂) data for compound (**8a-20a**)₂₀. Shaded rows correspond to the atoms in the repeating polymer unit.

A. Substructure in alternating AB copolymer



B. Substructures in AB block copolymer



Red carbons are perdeuterated. Blue carbons bear hydrogen.

Figure 3-6. Possible substructures generated in the copolymerization of **8a** with cyclohexene- D_{10} .

For the 4,5-disubstituted cyclohexenes (**20e-20h**), only 4,5-(dimethoxymethyl)cyclohexene **20e** polymerized with cyclobutene **8a**. The AROMP was slower than reaction of **8a** with cyclohexene **20a** or monosubstituted cyclohexene **20d** (Table 3-5). The slower rate may be due to the stronger steric or coordination interaction from 4,5-disubstituents in cyclohexene **20e**.

Partial $^1\text{H-NMR}$ spectra of the above polymers were plotted to illustrate the formation of disubstituted and trisubstituted olefin bonds (Figure 3-11). The disubstituted olefin proton signals are observed at 5.4 ppm for all the alternating copolymers. For polymers (**8a-20d**)₂₀, (**8a-20e**)₂₀, (**8a-20i**)₂₀ and (**8a-20j**)₂₀, the trisubstituted olefin proton signals are observed at 6.8 ppm. For polymers (**8c-20a**)₂₀ and (**8d-20a**)₁₀, the chemical shift of the trisubstituted olefin protons is around 7.1-7.2 ppm. The downfield shift is caused by the electron withdrawing nature of the phenyl or PFP group.

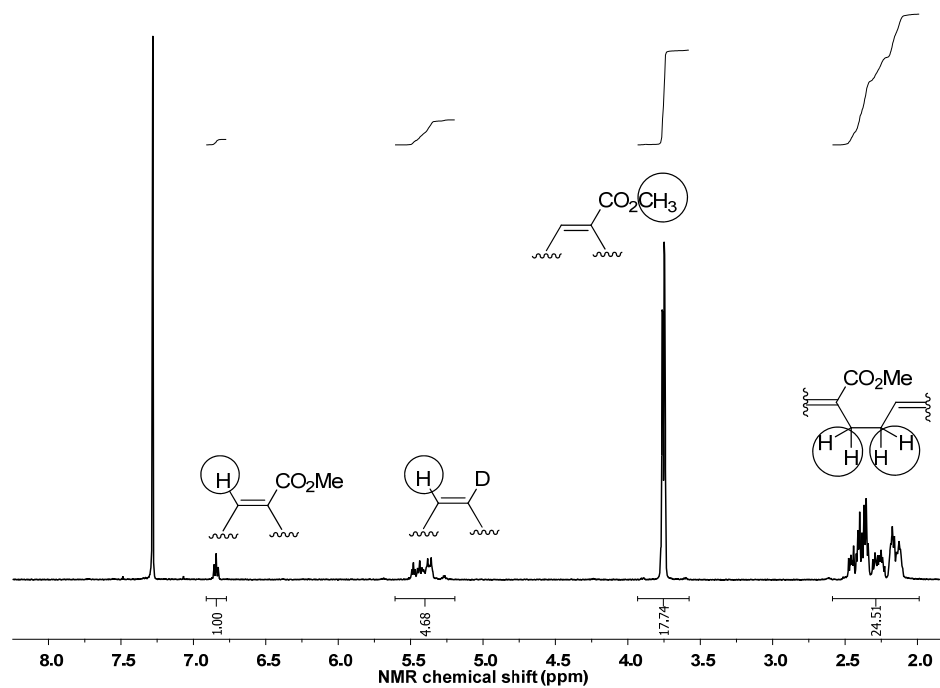


Figure 3-7. ^1H -NMR spectrum of cyc-(8a-20a-D₁₀)₂₀.

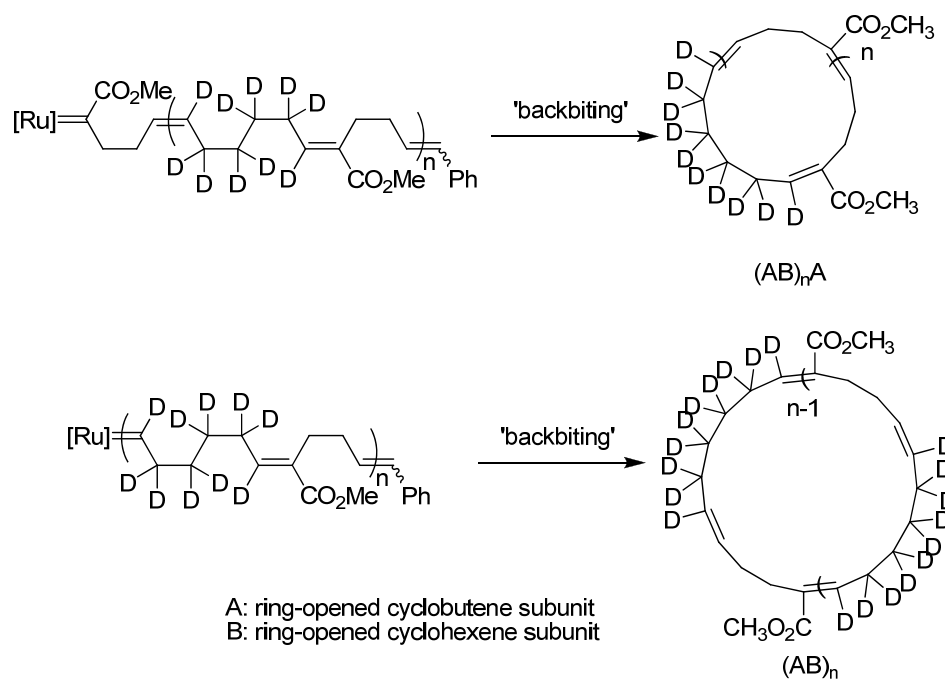


Figure 3-8. Mechanism of formation of cyclic alternating copolymers.

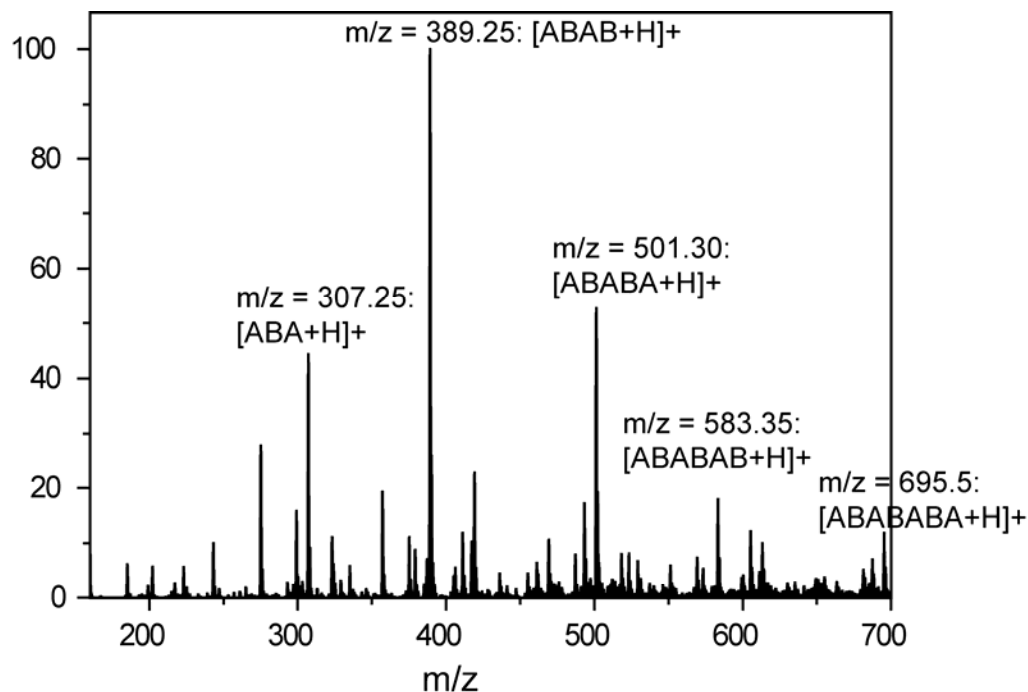


Figure 3-9. ESI-Mass spectrum of **(8a-20a)₃**. A and B represent the cyclobutene and cyclohexene units, respectively.

All the above alternating copolymers exhibit lower molecular weights than expected and large PDIs (>2). These properties are caused by backbiting in the AROMP reactions (Figure 3-8).

III.2 AROMP of Cyclobutene and Cyclohexene Using Other Catalysts

It has been reported that addition of triphenylphosphine (PPh₃)²¹ and the use of THF as a reaction solvent^{17,21,245} together with catalyst **3** can greatly limit secondary metathesis reactions. AROMP of **8a** and cyclohexene **20a** at room temperature using catalyst **3** in CD₂Cl₂ exhibited much slower reaction rate than when catalyst **5** was used (Table 3-3). This result is consistent with the lower reactivity and slower initiation of catalyst **3** in ROMP. Therefore, the above solution was heated up to 39 °C to increase the reaction rate. However, it still took 4 h to reach 45% conversion, and the molecular weight of the resulting polymer was much smaller than expected. The smaller M_n and the

large PDI suggest that backbiting was not prevented. AROMP of **8a** and cyclohexene **20a** using catalyst **3** in THF-D₈ at 39 °C was also tested (Table 3-3). Only 16% monomer consumption was achieved in 4 h. The much slower ROMP rate may be due to the coordination of THF to the ruthenium carbene. The addition of PPh₃ (equimolar to cyclobutene ester) inhibited AROMP of **8a** and **20a** in both CD₂Cl₂ and THF-D₈ (Table 3-3).

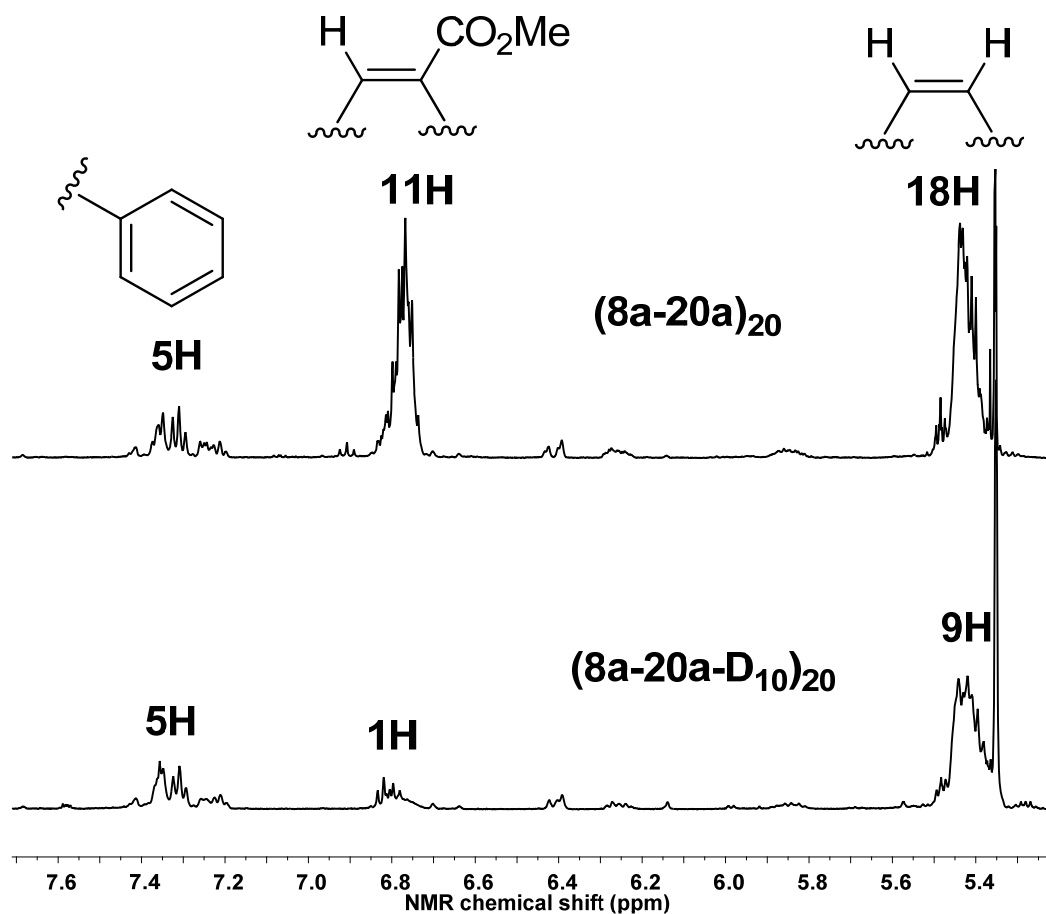


Figure 3-10. Bimodal peak fitting of GPC trace of $(8a-20a)_{200}$. $[8a]:[20a]:[5] = 200:400:1$, 73% conversion yield, CD₂Cl₂, rt

AROMP of **8a** and cyclohexene **20a-D₁₀** at room temperature using catalyst **25** in CD₂Cl₂ was performed (Table 3-4), and it took 9 h to reach 89% conversion. The slower reaction rate is also consistent with the slower initiation of catalyst **25**.²⁹⁶ One interesting

result from this AROMP is that only cyclic alternating copolymer was generated, and its $^1\text{H-NMR}$ spectrum is shown in Figure 3-12.

AROMP of **8a** and cyclohexene **20a** using Schrock's catalyst **26** in CD_2Cl_2 was also tested (Table 3-4). Cyclobutene **8a** and catalyst **26** were mixed in CD_2Cl_2 at room temperature. No initiation was observed even after the reaction temperature was increased from rt to $39\text{ }^\circ\text{C}$ within 1 h. Cyclohexene **20a** was added to the above solution, and no polymerization was observed in 3 h at $39\text{ }^\circ\text{C}$.

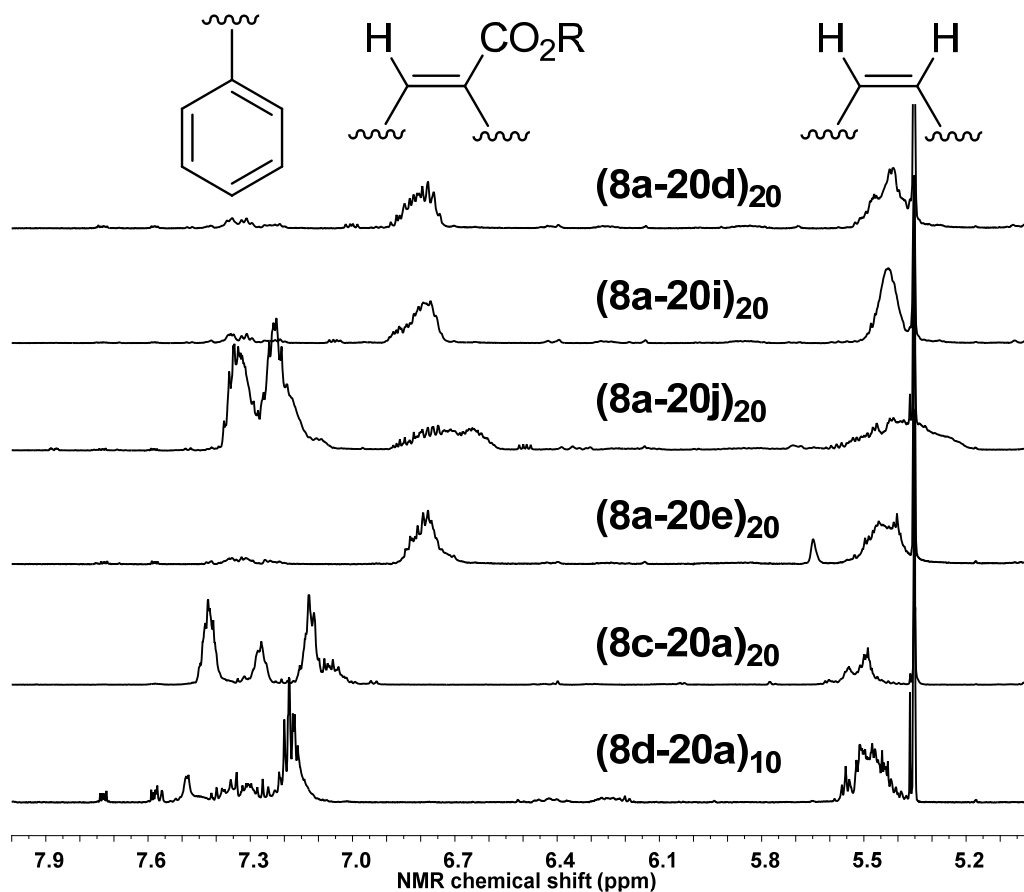


Figure 3-11. Partial $^1\text{H-NMR}$ spectra of alternating copolymers.

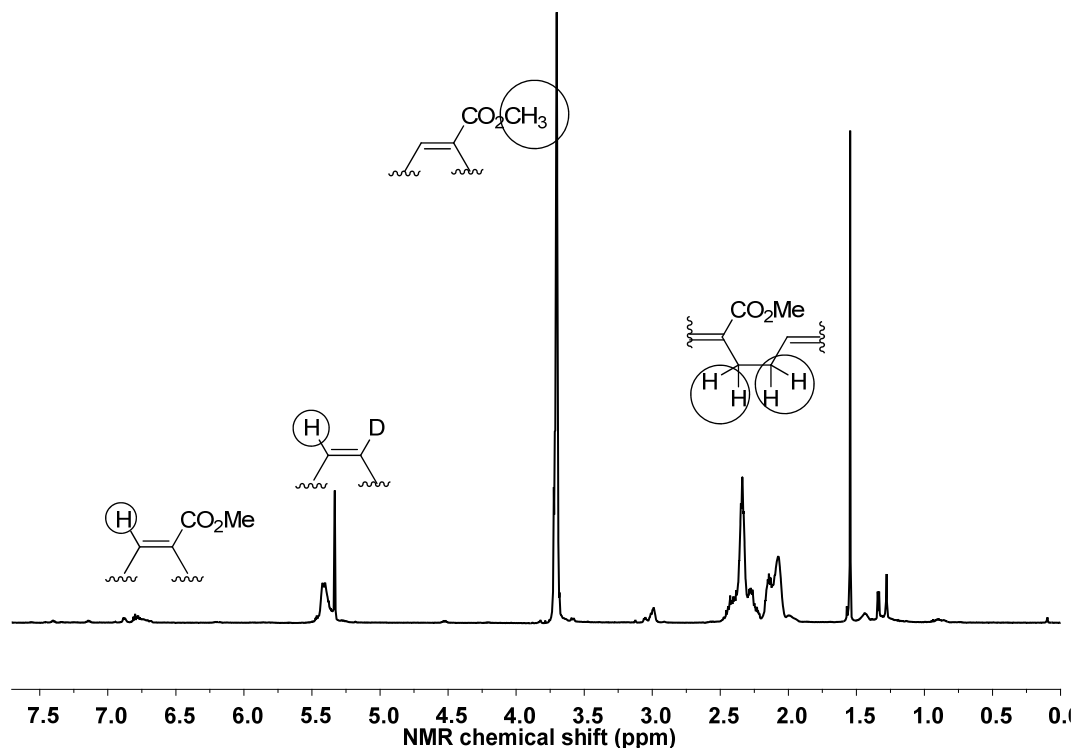


Figure 3-12. ^1H -NMR spectrum of cyclic alternating copolymer prepared with **25**. $[\mathbf{8a}]:[\mathbf{20a-D}_{10}]:[\mathbf{25}] = 20: 40:1$, 89% conversion yield, CD_2Cl_2 , rt.

III.3 AROMP of Cyclobutene and Cyclopentene

As we discussed earlier, the backbiting most likely takes place on the disubstituted olefin bonds during AROMP of cyclobutene ester and cyclohexene. One efficient way to minimize the intramolecular chain transfer is to minimize the amount of disubstituted olefin bonds in the polymer chain. Therefore, 1-substituted cyclopentenes and disubstituted ruthenium alkylidene **28** were applied in AROMP with 1-cyclobutene ester. It was expected that only trisubstituted olefin bonds would be generated in the terminus or the middle of polymer backbone (Table 3-7).

However, AROMP of 1-methylcyclopentene **29a** and cyclobutene **8a** using catalyst **28** proceeded with 50% conversion in 2-5 h at 50 °C or 80 °C (Table 3-7). The ^1H -NMR spectrum of polymer $(\mathbf{8a-29a})_{10}$ is shown in Figure 3-13. There are multiple

broad peaks at 5.0-5.4 ppm, and they are assigned to dialkyl substituted olefin protons and trialkyl substituted olefin protons (Figure 3-13). The fact that the molecular weights characterized by GPC are smaller than the expected values (Table 3-7) confirms that backbiting is still happening. Backbiting is dependent on the presence of disubstituted olefin bonds, whose existence was confirmed by the $^1\text{H-NMR}$ spectrum of polymer (**8a-29a**)₁₀. All the above results suggest that the regioirregular binding of 1-methylcyclopentene to the enoic ruthenium carbene is responsible for the generation of disubstituted alkenes and the subsequent backbiting (Scheme 3-11).

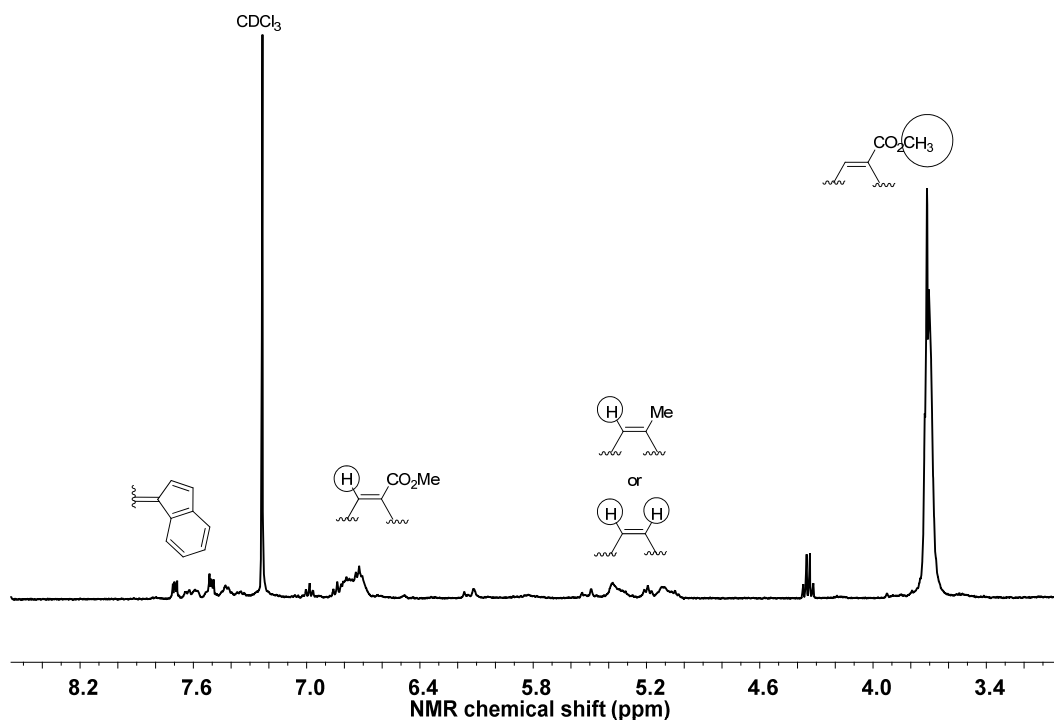
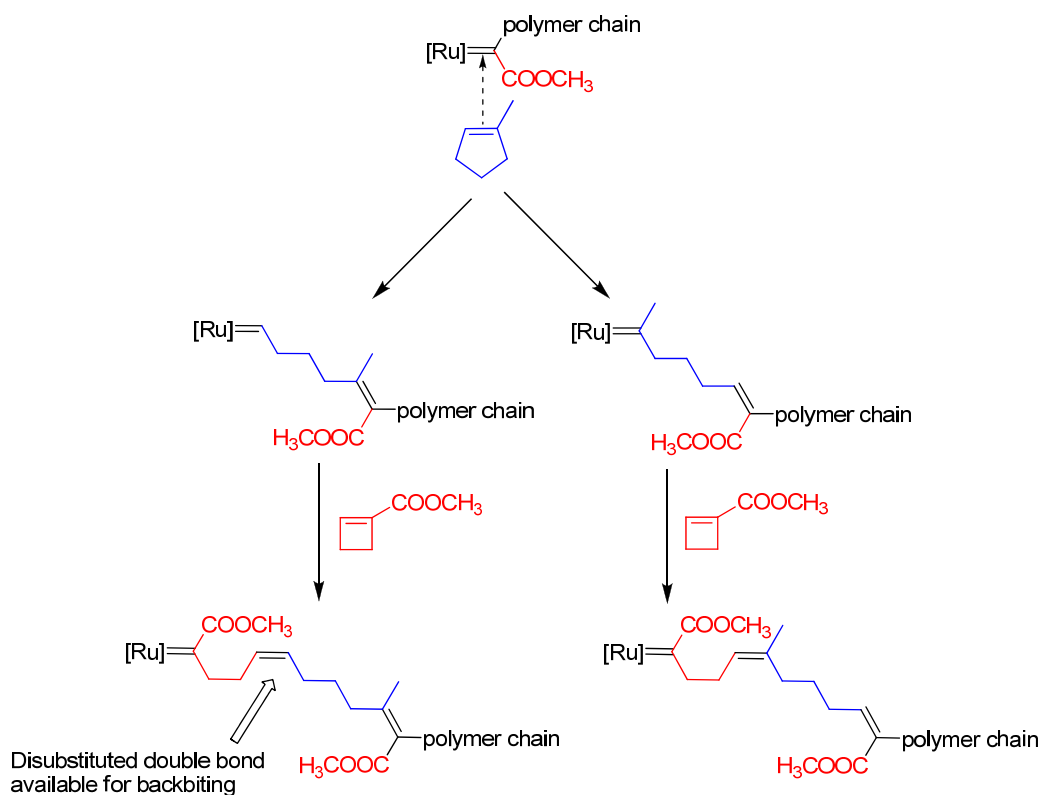


Figure 3-13. $^1\text{H-NMR}$ spectrum of alternating copolymer (**8a-29a**)₁₀ prepared with **28**. [**8a**]:[**29a**]:[**28**] = 20: 40:1, 50% conversion yield, CDCl_3 , 50 °C.

AROMP of 1-methoxycyclopentene **29b** and cyclobutene **8a** using catalyst **5** or **28** did not succeed. No polymerization was observed, and it may be due to the strong coordination of the enol ether group to the ruthenium carbene or the steric hindrance of the 1-methoxy group.

IV. Summary

In conclusion, we have demonstrated that synthetically accessible, select monomer pairs undergo AROMP with the reactive precatalyst **5** to form $(AB)_n$ heteropolymers with an alternating backbone and alternating functionality. The regiocontrol of heteropolymer formation derives from the inability of the cyclobutene ester and cyclohexene monomers to undergo homopolymerization in combination with the favorable kinetics of cross polymerization.



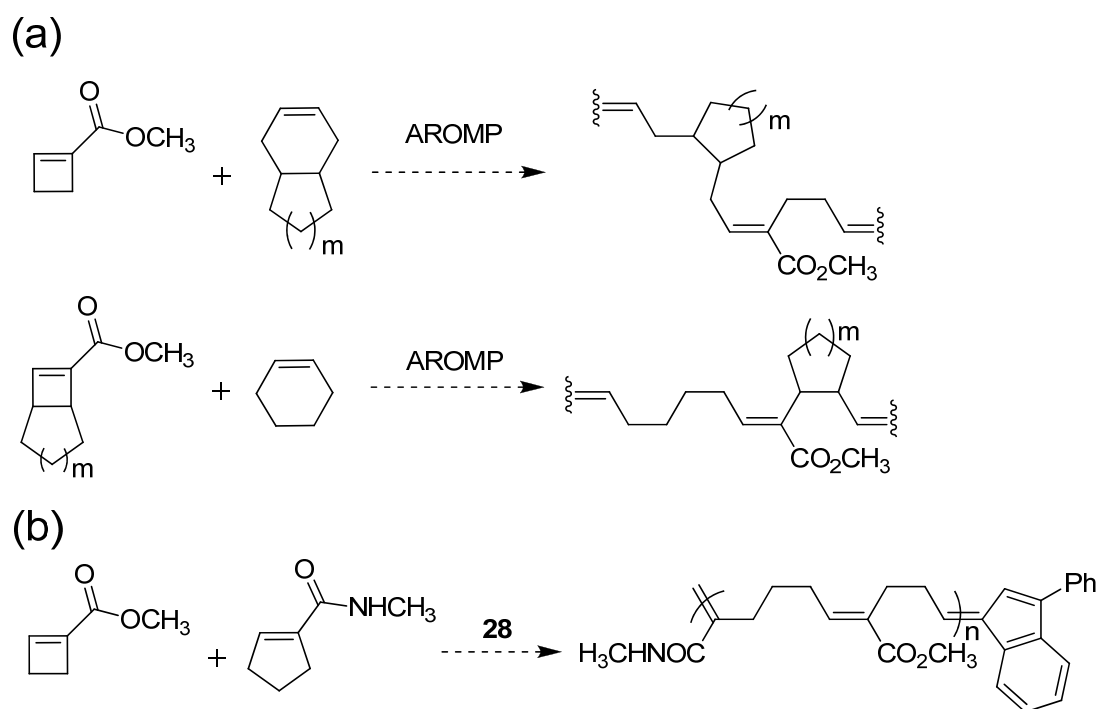
Scheme 3-11. Regioirregular addition of 1-methylcyclopentene to the enoic ruthenium carbene

A large amount of intramolecular chain transfer (backbiting) exists in AROMP, and cannot be limited easily. Some efforts have been tested to prevent backbiting, such as changing catalysts or solvent, adding PPh₃, or using trisubstituted cycloalkene monomers. However, little progress was achieved. There is still a large amount of work required to

minimize backbiting and to obtain linear alternating copolymers with high molecular weights and narrow PDIs.

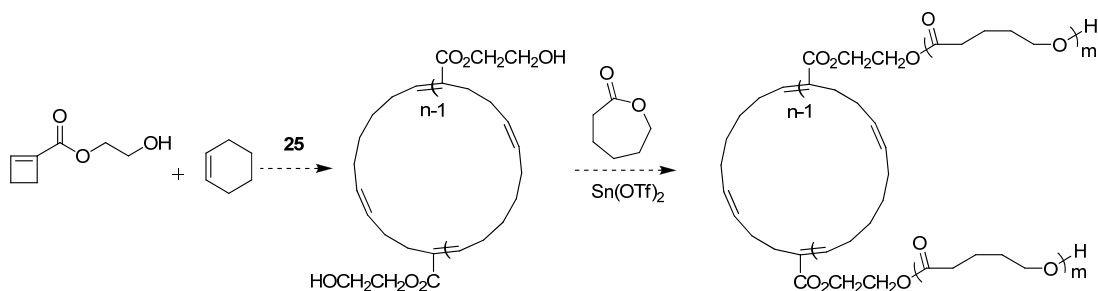
V. Future Perspectives

To get rid of backbiting, several methods can be used in the future, such as increasing the steric hindrance in the polymer backbone (Scheme 3-12a), or minimizing the amount of disubstituted olefin bonds using 1-secondary amide substituted cyclopentenes (Scheme 3-12b). Increasing the steric hindrance in the propagating polymer chain is a very efficient method to minimize chain transfer reactions.¹⁷ It is proposed that ring-opening of 1-cyclopentene secondary amide may be regioregular by following Pathway I just as the regioregular ring-opening of 1-cyclobutene amides. As a result, AROMP of 1-cyclobutene ester and 1-cyclopentene secondary amide using catalyst **28** can provide a polymer chain containing only trisubstituted olefins.



Scheme 3-12. Proposed methods to minimize backbiting.

AROMP of 1-cyclobutene ester and cyclohexene with catalyst **25** provides entirely cyclic alternating polymers. The functionalization of the side chains in the cyclic polymers with hydroxy groups can trigger ring opening polymerization (ROP) of cyclic esters³⁰¹⁻³⁰⁵ to provide star polymers (Scheme 3-13).



Scheme 3-13. Proposed synthetic route of star polymers.

Chapter 4

Antibacterial Studies of Homo Polymers, Alternating Copolymers, and Random Copolymers*

I. Introduction

II. Results

III. Discussion

IV. Summary

V. Future Perspectives

*All the MIC and HC₅₀ data are provided by Dr. Stephen Walker.

I. Introduction

Antibiotic resistance is endemic in both community and hospital-acquired infections.³⁰⁶ Moreover, some infections are resistant to all available antibiotics and new therapeutics are required to reduce morbidity and mortality.³⁰⁷ One attractive avenue for new antibiotic development is the use of “host-defense” antimicrobial peptides. Antimicrobial peptides are produced by eukaryotes as part of the organisms’ innate immune response against bacterial infection.¹⁵⁷⁻¹⁵⁸ They range in length from about 12 to 80 amino acid residues. These peptides adopt a variety of active conformations, that include α -helices and disulfide-stabilized β -sheets, e.g., maigainin and defensin, respectively.^{163,308} The most important part of their structure appears to be an amphipathic topology in which cationic residues, containing for example, ammonium and guanidinium moieties, are segregated from hydrophobic side-chains.¹⁵⁶

The amphipathic nature of the antimicrobial peptides facilitates their binding and insertion into lipid bilayers. Ultimately treatment with the peptides leads to disruption of the bacterial cytoplasmic membrane^{157,163,309-311} and bacterial death. Development of bacterial resistance to these peptides is infrequent because the mechanism of action depends on creating pores or channels through the lipid membrane and the lipid is not easily altered. However, many antimicrobial peptides cause cell death by additional mechanisms including membrane depolarization,^{163,312} and binding to cytoplasmic receptors, such as DNA or RNA,¹⁵⁵ and bacteria can evolve resistance to these toxicity mechanisms, although more slowly.²⁰⁴⁻²⁰⁵

Mimicry of antimicrobial peptides is an attractive approach to the development of synthetic antibiotic compounds that may be used as coatings or as pharmaceuticals. Synthetic mimics may overcome the poor *in vivo* activities and limited tissue distributions observed with antimicrobial peptides.^{156,223} A lot of macromolecules such as β -amino acid peptides,^{158,313-323} polynorbornes,^{152,234,236-238,324} polymethacrylates,²³²⁻²³³ polystyrenes,³²⁵⁻³²⁶ poly(4-vinylpyridine)s,³²⁷⁻³³¹ poly(propylene imine) dendrimers,³³²⁻³³³ peptoids,^{222,334-336} phenylene-ethylene oligomers^{206,227-228,337-339} and aromatic arylamide oligomers^{206,223-224,226,340} have been used as scaffolds. These scaffolds all enable mimicry of the amphiphilic antimicrobial peptides. Their efficacies correlate with

the spacing between cationic residues and the type of backbone (Table 4-1). In addition, mimics with more rigid backbones and fewer repeating units exhibited the best antibacterial activities and minimal cytotoxicities toward host cells.

SMAMP	Spacer distance (Å) ^a	# of monomer units ^b	Antimicrobial activity ^{b,c}	Selectivity ^{b,c}
β -Peptides ^{158,313-323}	> 4.9	10-30	++++	+++
Peptoids ^{222,334-336}	10.8	12	++++	+++
Arylamide oligomers ^{206,223-224,226,340}	9.6	2	+++++	+++++
Phenylene ethylene oligomers ^{206,227-228,337-339}	12.0	2	+++++	+++++
Polymethacrylates ²³²⁻²³³	2.5	32-46	++++	++
Polynorbornenes ^{152,234,236-238,324}	5.8	~40	++++	++++
Polystyrenes ³²⁵⁻³²⁶	2.5	~18	+++	++
Poly(4-vinylpyridine)s ³²⁷⁻³³¹	2.5	200~600	++	++
Poly(propylene imine) dendrimers ³³²⁻³³³	n/a ^d	4-64 ^e	++++	n/a

Table 4-1. Representative SMAMPs. ^aCalculated between two neighboring monomer units containing basic groups. ^bBased on the most optimized SAR results. ^cMore + represent better activity or selectivity. ^dNot applicable. ^e# of quarternary ammonium groups

β -Peptides (also called foldamers) that are highly resistant to proteases³⁴¹ represent an analogous structure as α -peptides. Both α - and β -peptides can form intramolecular hydrogen bonds through amide groups. As a result, different types of helices can be formed by β -peptides, e.g., 10-helices, 12-helices and 14-helices.^{216,219,221,316,319,342} Gellman's group has developed a series of amphiphilic

foldamers based on different β -residues (Figure 4-1), such as β^3 -residue, β^2 -residue, ACPC/APC residue, and ACHC/DCHC residue.^{3,6,8} In antimicrobial studies of these foldamers, they found that oligomers (10 - 15 residues) with an appropriate amphiphilicity exhibited great selectivity in killing bacteria or mammalian cells (Figure 4-2). Antimicrobial foldamers containing heterogeneous α - and β -amino acids were also prepared through two different strategies: alternating connection (**Fold-3**, Figure 4-2) and random connection (**Fold-4**, Figure 4-2) of α - and β -amino acids.²¹⁹ The advantages of heterogeneous backbones over homogeneous backbones are their ability to conform many new molecular shapes based on variations in the stoichiometries and patterns of the subunit combinations and improved prospects for side chain diversification.

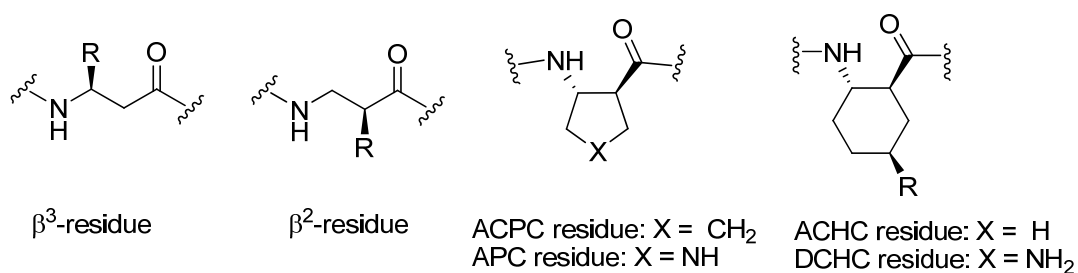


Figure 4-1. Structures of β -residues.

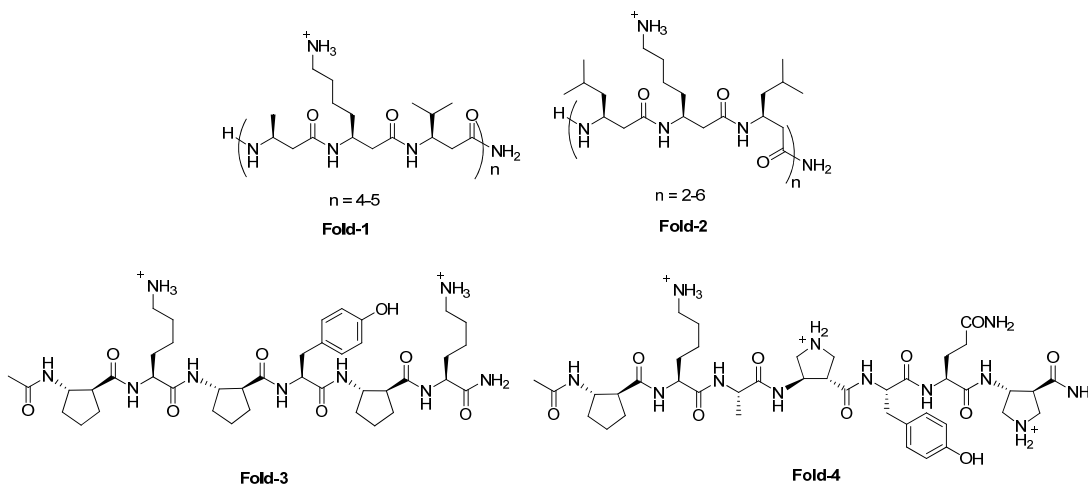


Figure 4-2. Structures of antimicrobial foldamers.

Peptoids are another group of peptidomimetic oligomers that can also adopt a stable helical structure^{223,316,319,343-344} and are resistant to proteolysis.³⁴⁵ The structural difference between α -peptides and peptoids is that there is a side chain appendage at the amide nitrogen in peptoids. Peptoids containing certain bulky side chains at the amide nitrogen exhibit remarkable antibacterial activity and selectivity (Figure 4-3).^{222,343-344}

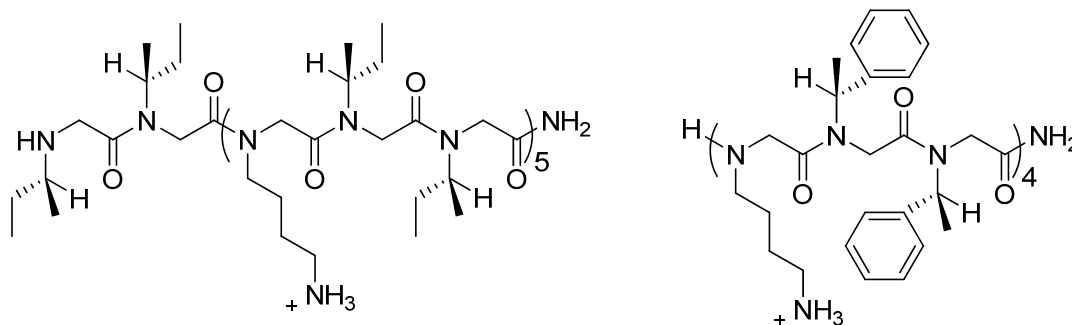


Figure 4-3. Structures of typical antimicrobial peptoids.

Tew's group developed a group of phenylene-ethylene oligomers with excellent antimicrobial activity and selectivity (Figure 4-4).^{227-228,339} Aromatic monomer **PE-1** exhibited low antibacterial activity, while increased activity was observed for phenylene-ethylene oligomer **PE-2**. Oligomer **PE-3** that combines a phenylene-ethylene scaffold and **PE-1** motifs showed outstanding activity and selectivity against a large panel of pathogenic and potential biowarfare bacteria.

Aromatic arylamide oligomers with different hydrophobic and hydrophilic side chains were employed in the antimicrobial studies (Figure 4-5).^{223-226,340,346} Oligomer **AA-1** containing three benzene rings showed reasonable antibacterial activity but low selectivity. In **AA-1**, basic groups are attached to the backbone through a thioether bond, and the backbone is rigidified through the intramolecular NH-thioether hydrogen bonding. Further backbone rigidification through the intramolecular NH-ether (**AA-2**) or NH-pyrimidine (**AA-3**) hydrogen bonding resulted in improved activity and selectivity. The replacement of *t*-butyl groups with trifluoromethyl groups and the terminus attachment of

guanidine groups via amide bonds in **AA-3** led to greatly optimized potency and safety in **AA-4** for killing bacteria.²⁰⁶

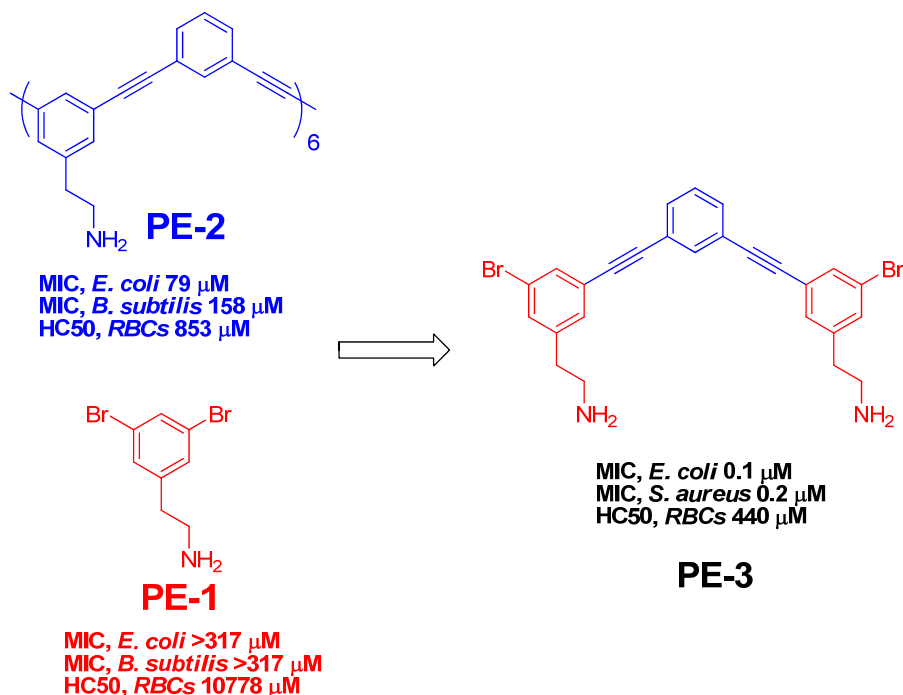


Figure 4-4. Optimization of the antibacterial activity and selectivity of phenylene ethynylene oligomers.

The use of polymers generated in one-pot reactions is attractive due to the ease with which antimicrobials may be produced in large scale processes. Whereas the folding of small polypeptides and aryl oligomers into regular structures is fairly well understood, the prediction of secondary structure of hydrocarbon-based polymers is much less advanced. In addition, the regio- and stereochemistry of a polymer may not always be well controlled. One possible reason for the lower efficacy of polymers may be the imprecision with which cationic groups are positioned within the structure of the polymer.

Antimicrobial polymers have been developed based on four different backbones: polystyrenes, poly(4-vinylpyridine)s, polynorbornenes and polymethacrylates (Figure 4-6 and Figure 4-7).^{152,232-234,236-238,324-331} The amphiphilicity of antimicrobial polyacrylates can be tuned by changing the stoichiometries and patterns of hydrophobic and

hydrophilic blocks (Figure 4-6). Generally speaking, polyacrylates exhibited high antibacterial and hemolytic activity, while low antimicrobial activity and selectivity was observed for polystyrenes and poly(4-vinylpyridine)s. In contrast, polynorbornenes showed high activity and tunable selectivity (Figure 4-7). **PN-1** was moderately active and quite nonhemolytic, while **PN-2** was much more active and hemolytic than **PN-1**.¹⁵² Block copolymerization of **PN-1** and **PN-2** segments yielded **PN-3** with greatly improved antibacterial activity and selectivity.¹⁵²

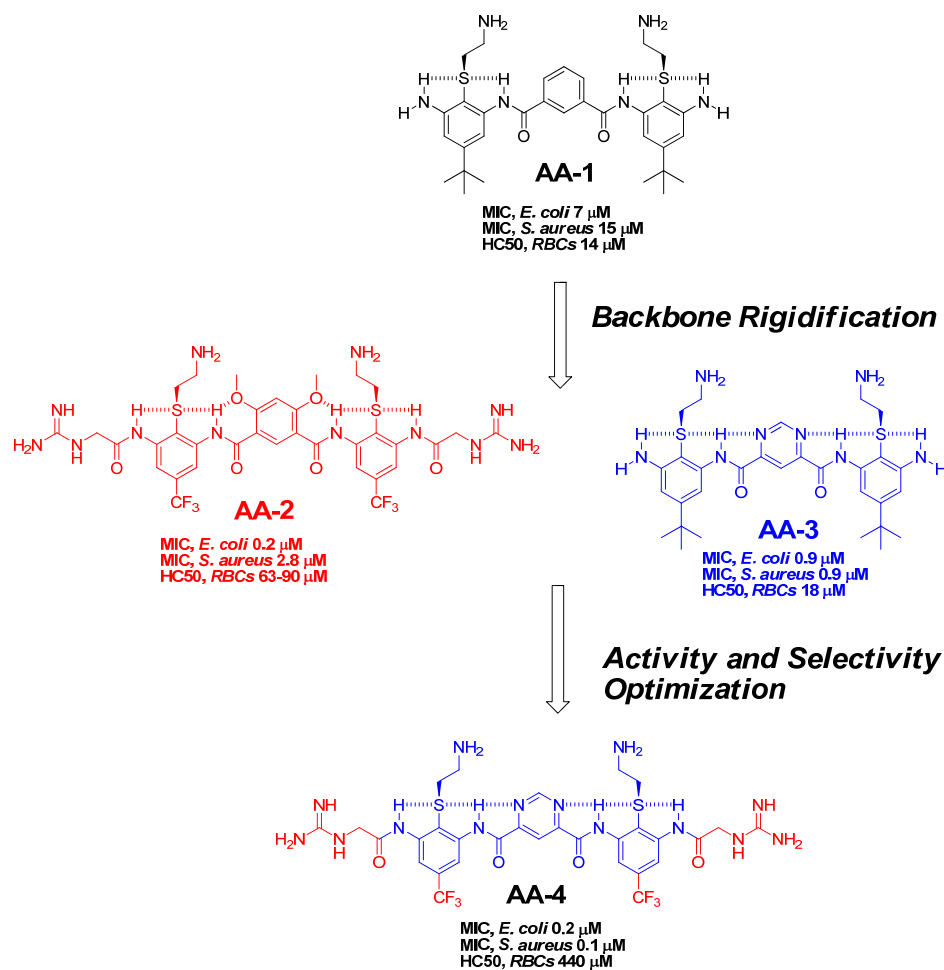


Figure 4-5. Optimization of the antibacterial activity and selectivity of arylamide oligomers.

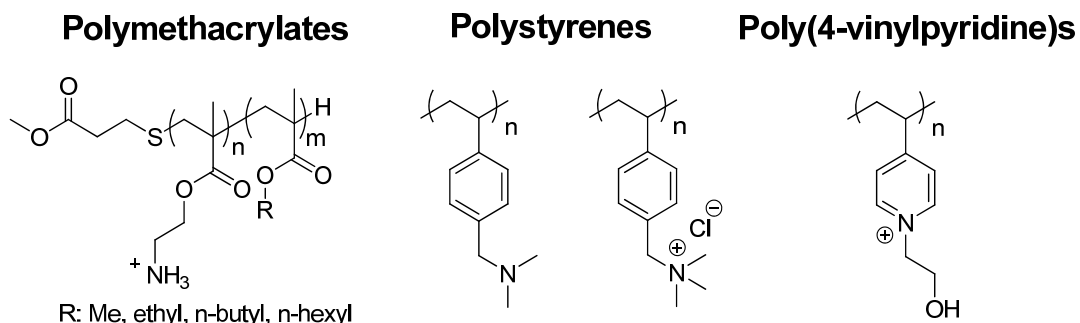


Figure 4-6. Structures of antimicrobial polyacrylates, polystyrenes and poly(4-vinylpyridine)s.

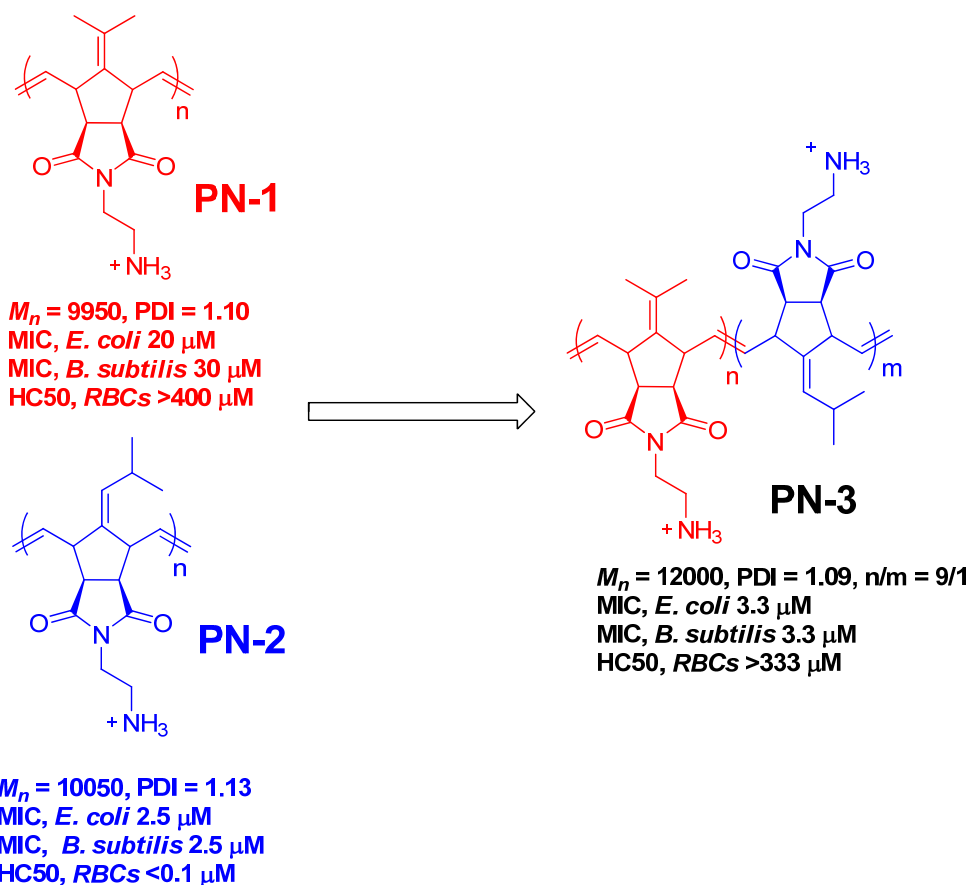


Figure 4-7. Optimization of the antibacterial activity and selectivity of polynorbornenes.

We previously reported an alternating ring opening metathesis polymerization (AROMP) method to incorporate alternating cyclobutene and cyclohexene units into a polymer backbone.²⁷⁵ We reasoned that this methodology could be used to synthesize polymers with regularly alternating hydrophobic and hydrophilic groups. Furthermore, the hydrophilicity of the polymers could be tuned by modifying the substituents on the cyclobutene or cyclohexene monomers. The alternating copolymer method allows introduction of a larger spacing between cationic groups while maintaining a regular structure in the backbone.

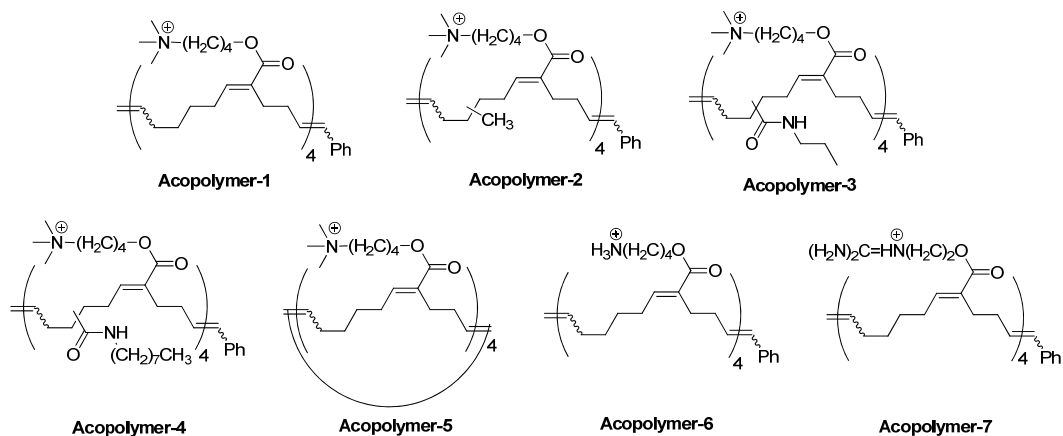
Here we report, the synthesis of a series of alternating copolymers containing different cationic groups and spacers of varying hydrophobicity (Figure 1). The antimicrobial activities of these polymers were screened against six species of bacteria including both Gram-positive and Gram-negative strains. The alternating polymers showed good *in vitro* antimicrobial activity against all strains. Moreover, the polymers had low host cell cytotoxicities as measured by erythrocyte lysis. The alternating polymers cause membrane depolarization, lysis, and leakage of cellular contents as has been observed with other amphiphilic mimics. In comparison to random copolymers of similar size and functionality, we found that the regularly alternating polymers were more effective antimicrobial agents.

II. Results

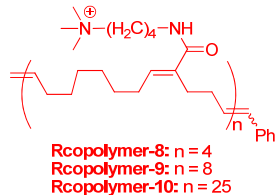
II.1 Synthesis of ROMP/AROMP Monomers

Cyclobutene monomers (**8e-8g**) were synthesized through their respective acyl chlorides (Scheme 4-2). 1-Cyclobutenecarboxylic chloride **19** was prepared by reacting 1-cyclobutenecarboxylic acid with oxalyl dichloride. The coupling of **19** with different alcohols in the presence of trimethylamine (TEA) generated esters **8e**, **8f** or **8g**, respectively. 4-Chlorobutylamine was coupled with 1-cyclobutenecarboxylic acid using 1-(3-dimethylamopropyl)-3-ethylcarbodiimide hydrochloride (EDC·HCl) and pyridine to generate 1-substituted cyclobutene amide **30**.

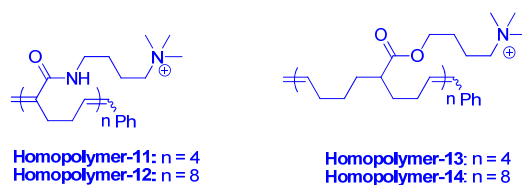
Alternating Copolymers



Random Copolymers

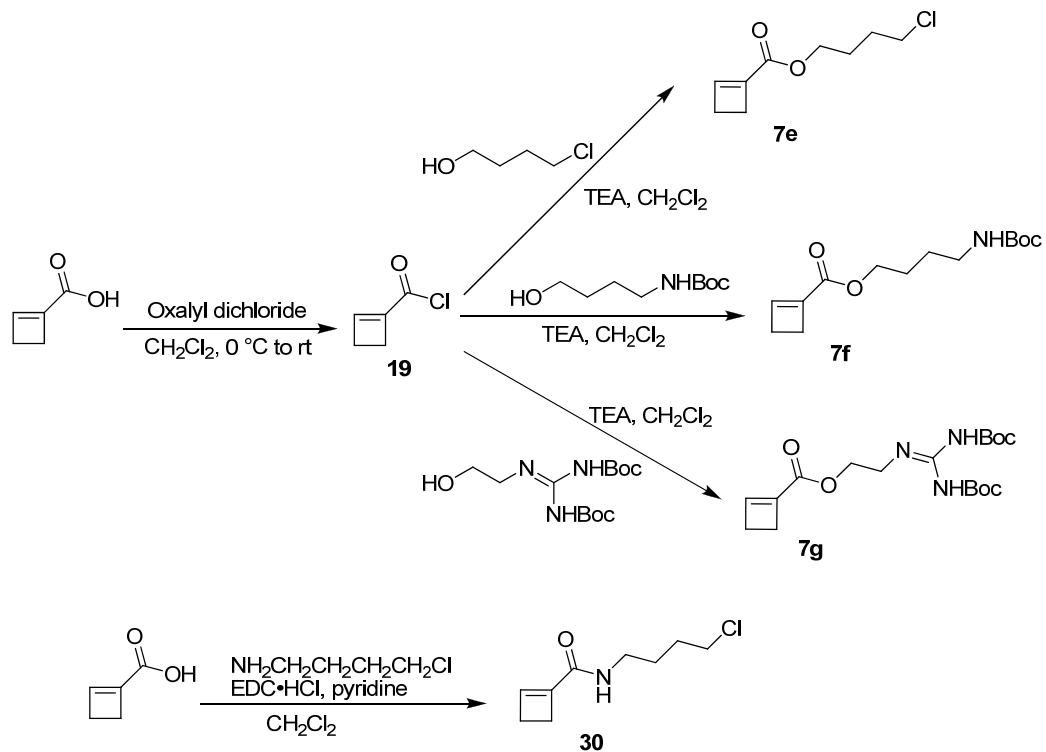


Homopolymers

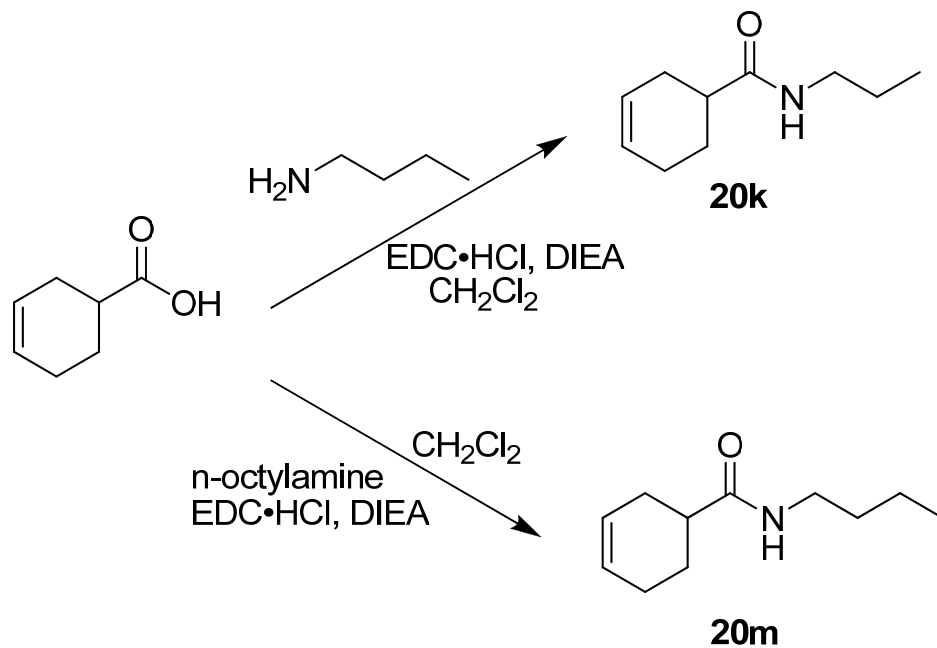


Scheme 4-1. Structures of antimicrobial **Acopolymer-1** to **Homopolymer-14**.

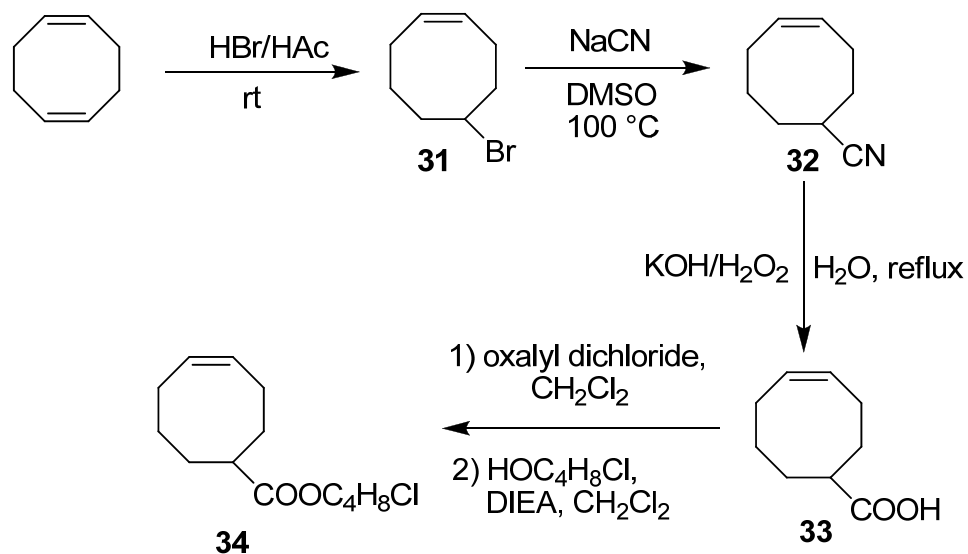
Cyclohexene monomers (**20k** and **20m**) were prepared via coupling of 3-cyclohexenecarboxylic acid with n-propyl amine or n-octylamine in the presence of EDC·HCl/DIEA (Scheme 4-3). Hydrobromination of 1,5-cyclooctadiene was achieved through a reaction with HBr/acetic acid to generate 5-bromocyclooctene **31** (Scheme 4-4).³⁴⁷ The bromide group in **31** was substituted with a cyanide group to form 5-cyanocyclooctene **32**.³⁴⁸ Compound **32** was hydrolyzed in a basic solution to generate 4-cyclooctenecarboxylic acid **33**. 5-Substituted cyclooctene ester **34** was made by reaction of its corresponding acyl chloride with 4-chlorobutanol in the presence of DIEA (Scheme 4-4).³⁴⁸



Scheme 4-2. Synthesis of 1-substituted cyclobutene monomers.



Scheme 4-3. Synthesis of 4-substituted cyclohexene monomers.



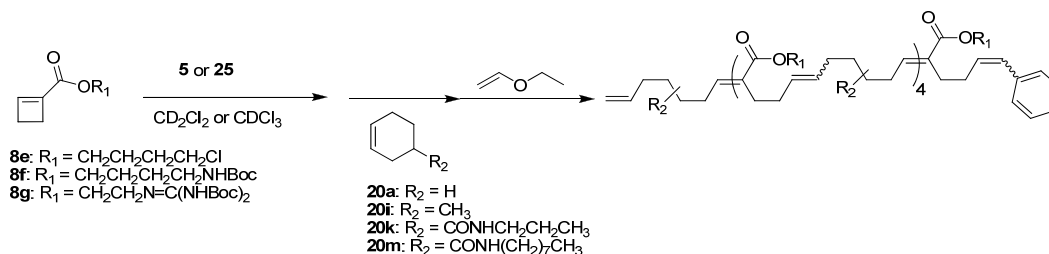
Scheme 4-4. Synthesis of 5-substituted cyclooctene monomer.

II.2 AROMP of 1-Substituted Cyclobutene Esters and Cyclohexenes

Alternating copolymers **Intermediate-1** to **Intermediate-7** were prepared according to the AROMP methodology described in Chapter 3,²⁷⁵ with high monomer conversion yields (90-96%). AROMP of 1-substituted cyclobutene ester **8e** and cyclohexene **20a** was performed using catalyst **5** in CD_2Cl_2 at rt to reach 90% conversion in 5 h (Table 4-2). AROMP of 1-substituted cyclobutene ester **8e** and cyclohexene **20a** was also performed using catalyst **25** in CDCl_3 at 50 °C to obtain 92% conversion in 4 h (Table 4-2). It took 2-5 h for AROMP of 1-substituted cyclobutene ester **8e** and 4-substituted cyclohexenes **20i**, **20k** or **20m** using catalyst **5** in CDCl_3 at 50 °C to achieve 92-96% conversion (Table 4-2). And 95-97% conversion was achieved for AROMP of 1-substituted esters **8f** or **8g** and cyclohexene **20a** in CDCl_3 at 50 °C (Table 4-2).

Their alternating structures were confirmed based on the fact that the proton integration ratios between peaks at 6.8 ppm and 5.4 ppm are around 1:2 in $^1\text{H-NMR}$ spectra of **Intermediate-1** to **Intermediate-7** (Figure 4-8). In Chapter 3, we demonstrated that AROMP catalyzed by catalyst **25** provides a cyclic alternating copolymer. Therefore, AROMP of cyclobutene **8e** and cyclohexene **20a** generated cyclic

alternating polymer **Intermediate-5**, and its cyclic structure was confirmed by the disappearance of a terminus phenyl proton peak in the $^1\text{H-NMR}$ spectrum (Figure 4-8).



A	B	Cat.	[Ru] (M)	[A]:[B]:[Ru]	Rxn time (h)	Prod.	% conv ^a
8e	20a	5	0.01	25:50:1	5	Intermediate-1	90 ^b
8e	20i	5	0.01	25:50:1	2	Intermediate-2	92 ^c
8e	20k	5	0.01	25:50:1	3	Intermediate-3	92 ^c
8e	20m	5	0.01	25:50:1	5	Intermediate-4	96 ^c
8e	20a	25	0.01	25:50:1	4	Intermediate-5	92 ^c
8f	20a	5	0.01	25:50:1	2	Intermediate-6	97 ^c
8g	20a	5	0.01	25:50:1	2	Intermediate-7	95 ^c

Table 4-2. AROMP of 1-substituted cyclobutene esters with cyclohexenes. All AROMP reactions were monitored by $^1\text{H-NMR}$ spectroscopy. ^aPercent conversion determined by integration of $^1\text{H-NMR}$ spectra unless specified otherwise. ^bReaction was performed in CD_2Cl_2 at rt. ^cReaction was performed in CDCl_3 at 50 °C. The monomer feed ratio was 25:1, and the final degree of polymerization (DP) was around 4.

The molecular weights and PDIs of the above polymers were characterized by GPC using polystyrene standards (Table 4-3). Due to the existence of backbiting in AROMP, all of the polymers exhibited lower molecular weights than expected and broad PDIs (1.3-2.4).²⁷⁵

Substitution of the chlorides with trimethylamine provided amphiphilic polymers **Acopolymer-1** to **Acopolymer-5** (Figure 4-9). The degree of substitution was measured via $^1\text{H-NMR}$ spectrum analysis and found to be greater than 99% (Figure 4-10). **Acopolymer-6** and **Acopolymer-7** were prepared from **Intermediate-6** and **Intermediate-7**, respectively, by quantitative deprotection of the Boc groups using trifluoroacetic acid (TFA) (Figure 4-9 and Figure 4-11).

Polymer	Calcd. M_n^a	PSS M_n	PSS M_w	PDI ^b
Intermediate-1	6874	2154	3945	1.8
Intermediate-2	7225	1265	3012	2.4
Intermediate-3	9002	1436	2323	1.6
Intermediate-4	10755	1443	2298	1.6
Intermediate-5	6874	1327	2812	2.1
Intermediate-6	8891	2141	2885	1.3
Intermediate-7	11744	2235	3591	1.6

Table 4-3. Polymerization results. ^aCalculated M_n was calculated based on conversion yields of monomers. ^bMolecular weight and PDI were determined by GPC using polystyrene standards.

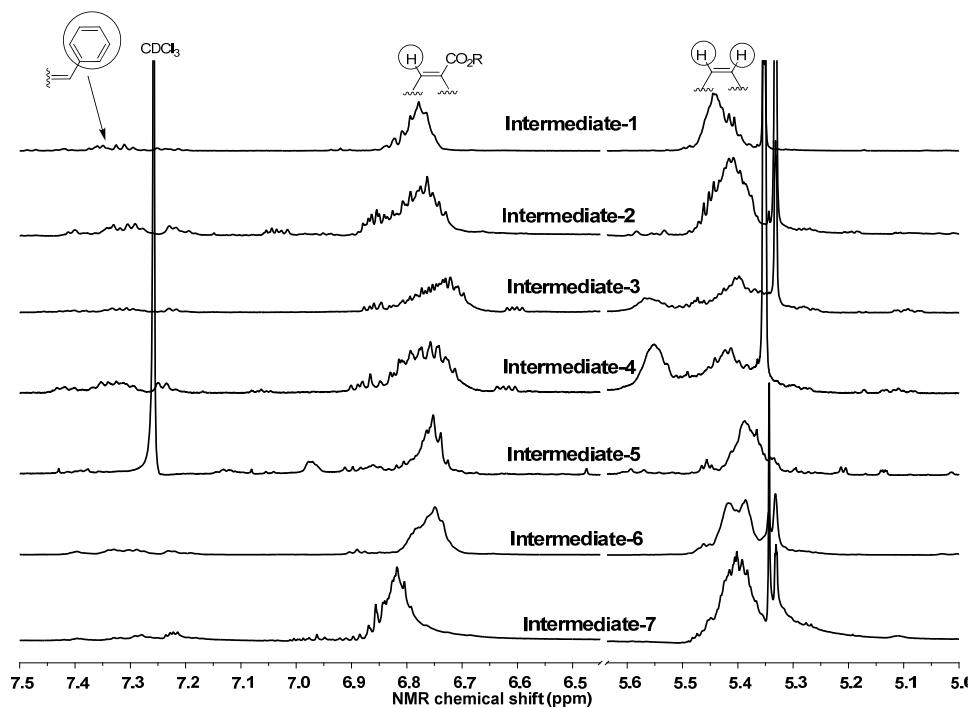


Figure 4-8. ¹H-NMR spectra of **Intermediate-1** to **Intermediate-7**.

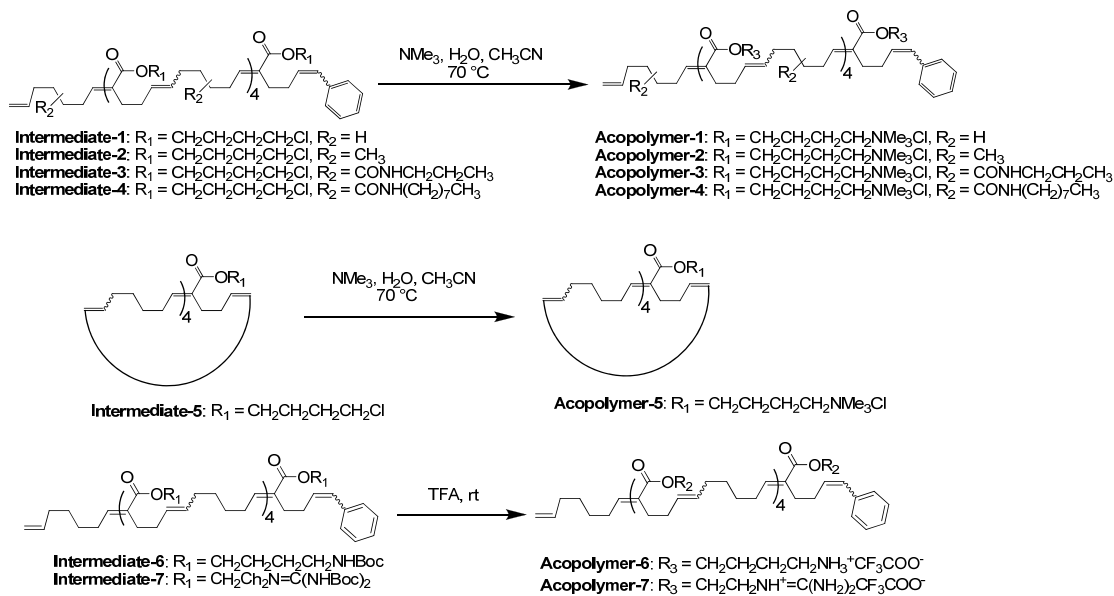


Figure 4-9. Synthesis of Acopolymer-1 to Acopolymer-7.

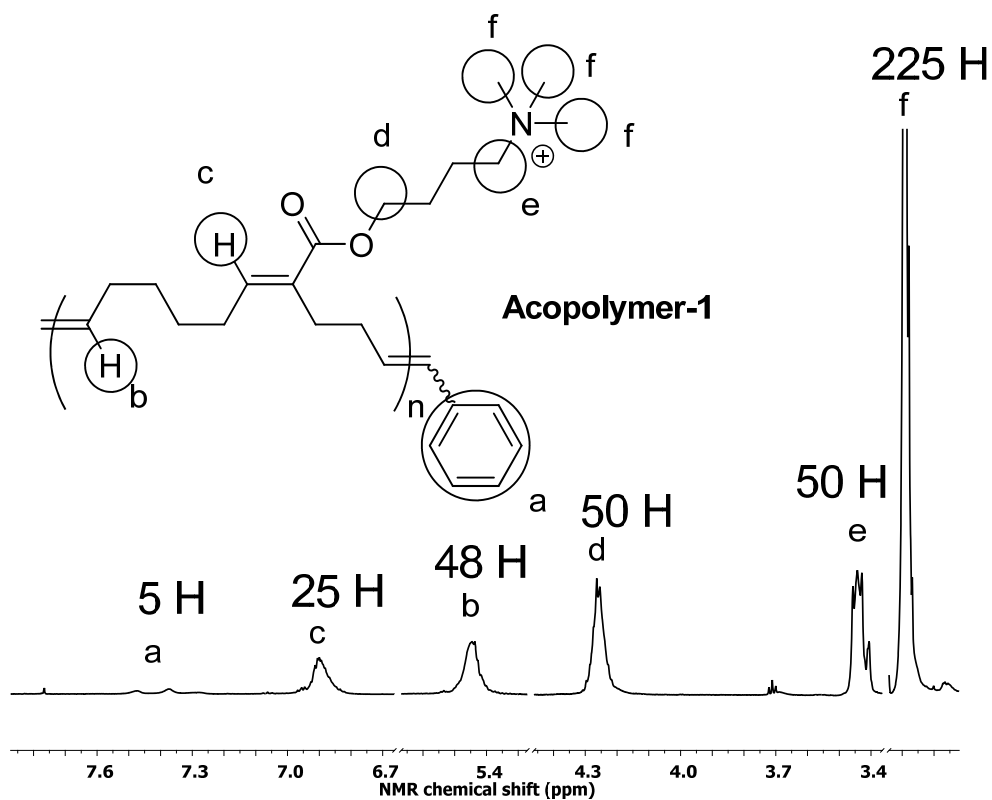


Figure 4-10. ^1H -NMR spectrum of Acopolymer-1.

II.3 ROMP of 1-Substituted Cyclobutene Amides and Cyclooctene

Both 1-cyclobutene amide¹¹¹ and *cis*-cyclooctene³⁴⁹ undergo efficient homopolymerization using catalyst **5**. We expected that ROMP of an equimolar mixture of 1-cyclobutene amide and *cis*-cyclooctene using catalyst **5** would provide random copolymers containing a mixture of poly(1-cyclobutene amide), *AA*, and poly(*cis*-cyclooctene), *BB*, blocks and alternating, *AB*, structures. We subjected 1-cyclobutene amide **30** and cyclooctene to ROMP in CD₂Cl₂ at rt using catalyst **5** (Table 4-4). **Intermediate-8** through **Intermediate-10** were obtained with greater than 99% conversion. Random copolymerization showed excellent molecular weight control, but bad PDI control (1.4-2.5) (Table 4-4). Cationic polymers **Rcopolymer-8** to **Rcopolymer-10** were synthesized via the substitution of the chlorides with trimethylamine (Table 4-4).

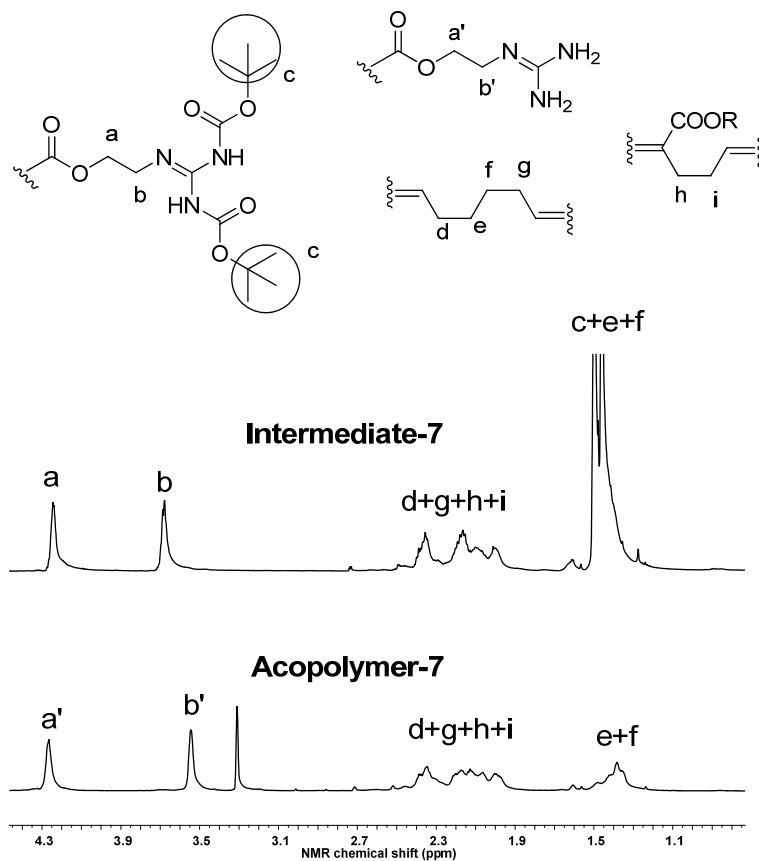
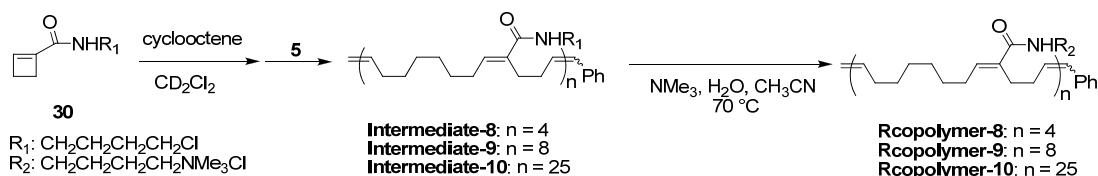


Figure 4-11. ¹H-NMR spectra of **Intermediate-7** and **Polymer-7**.

The random nature of the polymer backbones of **Intermediate-8** to **Intermediate-10** was confirmed by $^1\text{H-NMR}$ spectroscopy (Figure 4-12) and $^1\text{H-}^1\text{H}$ gCOSY spectroscopy (Figure 4-13). In the $^1\text{H-}^1\text{H}$ gCOSY spectrum of **Intermediate-10**, several couplings between a trisubstituted olefin proton and its adjacent CH_2 protons, or between a disubstituted olefin proton and its neighboring CH_2 protons corresponding to the *AA*, *BB* and *AB* repeats were observed. The multiple couplings confirm the random polymer backbone structure of **Intermediate-10**.



A	B	Cat.	[Ru] (M)	[A]:[B]:[Ru]	Rxn time (h)	Prod.	% conv ^a
30	35	5	0.01	4:4:1	2	Intermediate-8	>99
30	35	5	0.01	8:8:1	2	Intermediate-9	>99
30	35	5	0.01	25:25:1	2	Intermediate-10	>99

Table 4-4. Synthesis of **Rcopolymer-8** to **Rcopolymer-10**. All ROMP reactions were performed in CD_2Cl_2 and monitored by $^1\text{H-NMR}$ spectroscopy at rt. ^aPercent conversion determined by integration of $^1\text{H-NMR}$ spectra unless specified otherwise.

II.4 ROMP of 1-Substituted Cyclobutene Amides

Previously, we demonstrated that ROMP of 1-substituted cyclobutene amides yields homopolymers with translationally invariant backbones.¹¹¹ Homopolymers **Intermediate-11** and **Intermediate-12** were synthesized through ROMP of 1-substituted cyclobutene amide **30** using catalyst **5** in CD_2Cl_2 at rt with greater than 90% conversion (Table 4-6). The stereoregular and regioregular polymer backbones of **Intermediate-11** and **Intermediate-12** were confirmed by $^1\text{H-NMR}$ analysis (Figure 4-14). Molecular weights of polymers **Intermediate-11** and **Intermediate-12** characterized by GPC are close to the expected values. **Homopolymer-11** and **Homopolymer-12** were prepared through substitution of the chlorides with trimethylamine.

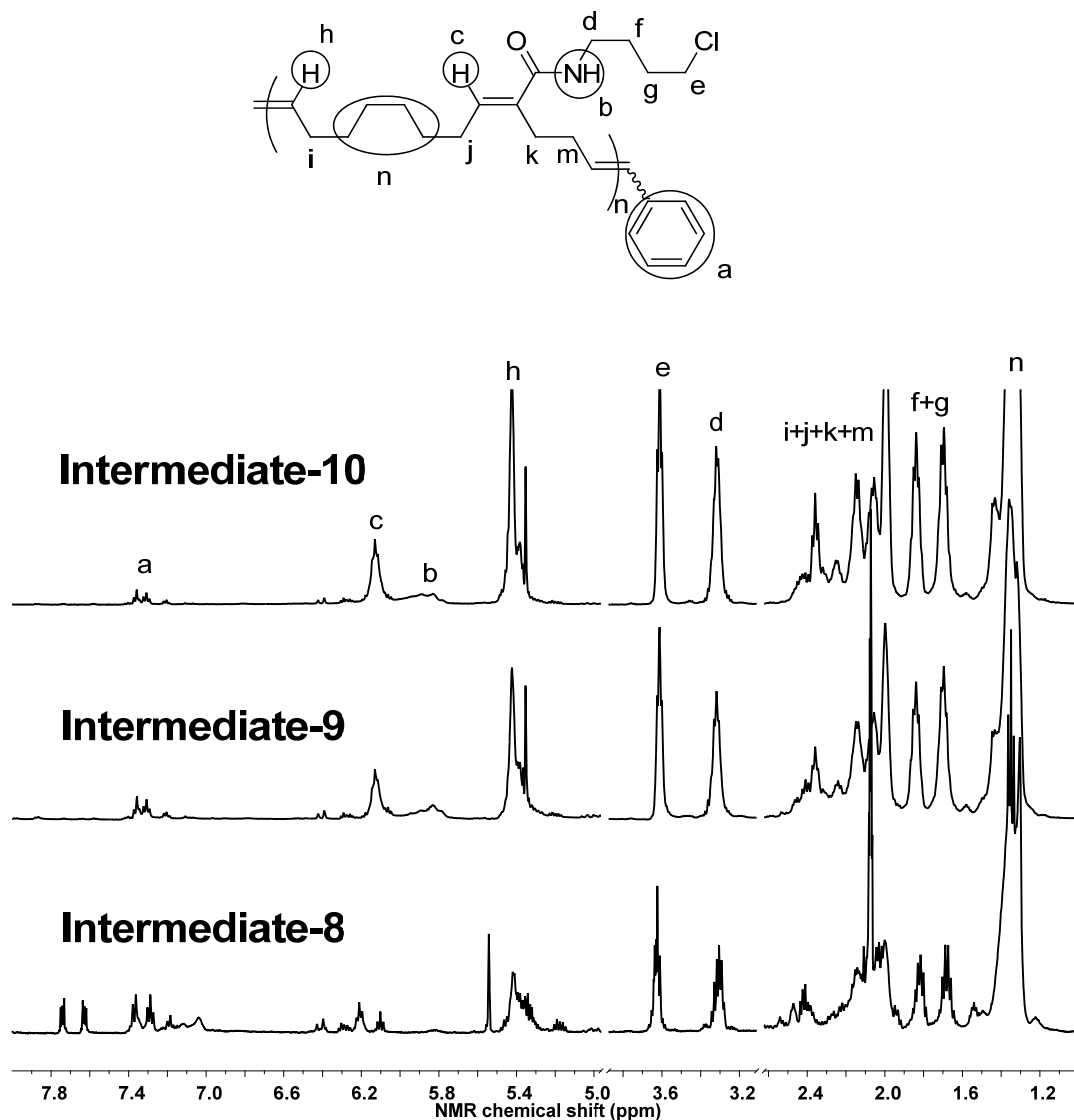


Figure 4-12. ¹H-NMR spectra of **Intermediate-8** to **Intermediate-10**.

II.5 ROMP of 5-Substituted Cyclooctene Esters

ROMP of 5-substituted cyclooctene **34** was performed in CD₂Cl₂ at rt using catalyst **5** to generate polymers **Intermediate-13** and **Intermediate-14**. Within 4 h, more than 99% conversion was achieved (Table 4-7). The structures of **Intermediate-13** and **Intermediate-14** were confirmed by ¹H-NMR analysis (Figure 4-15). Polymers **Intermediate-13** and **Intermediate-14** exhibited reasonable molecular weight and PDI

control (Table 4-7). The substitution of the chlorides in **Intermediate-13** and **Intermediate-14** with trimethylamine yielded **Homopolymer-13** and **Homopolymer-14**.

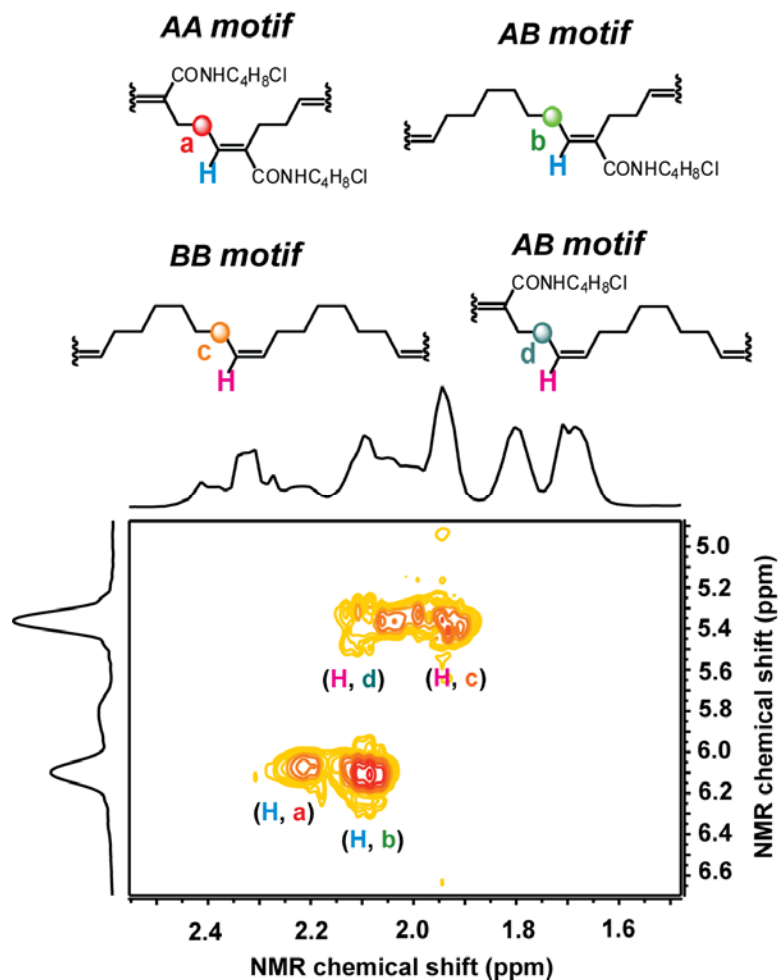
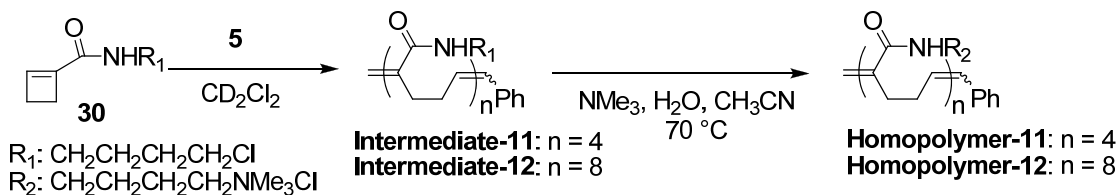


Figure 4-13. ^1H - ^1H gCOSY spectrum of **Intermediate-10**.

Polymer	Calcd. M_n^a	PSS M_n	PSS M_w	PDI ^b
Intermediate-8	1295	830	1183	1.4
Intermediate-9	2495	2800	7042	2.5
Intermediate-10	7575	9363	20004	2.1

Table 4-5. Polymerization results. ^aCalculated M_n was calculated based on conversion yields of monomers. ^bMolecular weight and PDI were determined by GPC using polystyrene standards.



[Ru] (M)	[A]:[Ru]	Rxn time (h)	Prod.	% conv ^a	Calcd. M_n^b	PSS M_n^c	PDI
0.01	4:1	4	Intermediate-11	93	855	589	3.5
0.01	8:1	3	Intermediate-12	92	1606	2052	1.3

Table 4-6. Synthesis of **Homopolymer-11** and **Homopolymer-12**. All ROMP reactions were performed in CD_2Cl_2 and monitored by $^1\text{H-NMR}$ spectroscopy. ^aPercent conversion determined by integration of $^1\text{H-NMR}$ spectra unless specified otherwise. ^bCalculated M_n was calculated based on conversion yields of monomers. ^cMolecular weight and PDI were determined by GPC using polystyrene standards.

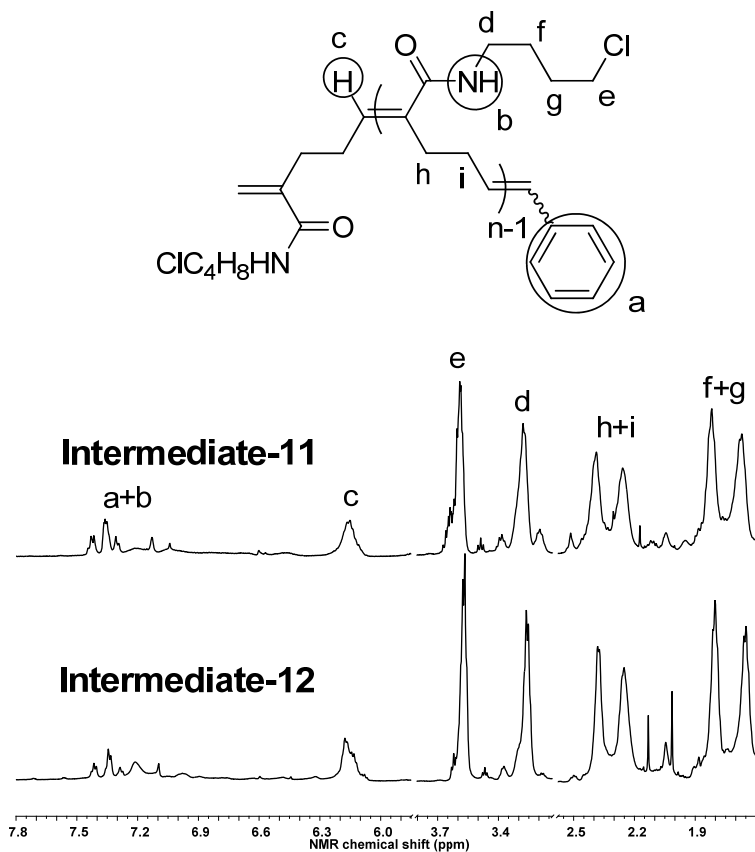
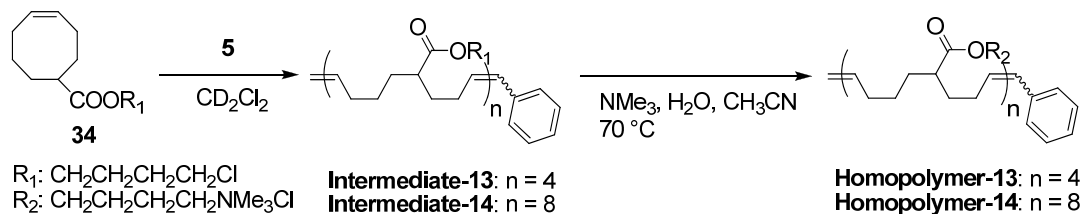


Figure 4-14. $^1\text{H-NMR}$ spectra of **Intermediate-11** and **Intermediate-12**.



[Ru] (M)	[A]:[Ru]	Rxn time (h)	Prod.	% conv ^a	Calcd. M_n^b	PSS M_n^c	PDI
0.01	4:1	1	Intermediate-13	99	1083	1265	1.33
0.01	8:1	1	Intermediate-14	99	2062	2256	1.23

Table 4-7. Synthesis of **Homopolymer-13** and **Homopolymer-14**. All ROMP reactions were performed in CD_2Cl_2 and monitored by $^1\text{H-NMR}$ spectroscopy. ^aPercent conversion determined by integration of $^1\text{H-NMR}$ spectra unless specified otherwise. ^bCalculated M_n was calculated based on conversion yields of monomers. ^cMolecular weight and PDI were determined by GPC using polystyrene standards.

II.6 Antimicrobial Activity and Selectivity

The antimicrobial activities of all the amphiphilic polymers (**Acopolymer-1** to **Homopolymer-14**) were measured against six different bacteria, *Pseudomonas aeruginosa* (*P. aeruginosa*), *Escherichia coli* (*E. coli*), *Bacillus cereus* (*B. cereus*), *Staphylococcus aureus* (*S. aureus*), *Enterococcus faecalis* (*E. faecalis*), and *Enterococcus faecium* (*E. faecium*) (Table 4-8). The minimal inhibitory concentrations (MIC) required to completely inhibit bacterial growth after 18 h at 37 °C were determined. As a measure of host cell cytotoxicity, hemolysis of sheep red blood cells was performed by measuring the polymer concentrations at which 50% lysis occurred. The antimicrobial selectivity is defined as the ratio of the HC_{50} values over the corresponding MIC value.

Polymer	MIC ($\mu\text{g/mL}$)						HC ₅₀ ($\mu\text{g/mL}$)
	<i>P.</i>	<i>E. coli</i>	<i>B. cereus</i>	<i>S. aureus</i>	<i>E. faecalis</i>	<i>E. faecium</i>	
	<i>aeruginosa</i>	ATCC	ATCC	ATCC	ATCC	ATCC	
	ATCC27853	25922	10987	25923	19433	19434	
Acopolymer-1	160	40	12	6	10	10	256
Acopolymer-2	>256	160	40	12	24	24	768
Acopolymer-3	>256	>256	64	32	128	64	>1024
Acopolymer-4	>256	256	24	24	24	24	192
Acopolymer-5	256	64	40	12	20	20	1024
Acopolymer-6	192	64	96	48	64	32	1024
Acopolymer-7	32	12	12	6	12	12	512
Rcopolymer-8	>256	>256	32	16	16	16	512
Rcopolymer-9	>256	256	32	16	16	16	>1024
Rcopolymer-10	>256	>256	48	24	24	24	>1024
Homopolymer-11	>512	>512	>512	384	>512	>512	>2048
Homopolymer-12	>512	>512	320	288	320	320	>2048
Homopolymer-13	128	32	12	8	8	8	379
Homopolymer-14	>256	64	16	8	8	8	443

Table 4-8. Antibacterial and hemolytic activities of **Acopolymer-1** to **Homopolymer-14**. All the MIC and HC₅₀ data were characterized by Dr. Stephen Walker. The data shown are the average of triplicate measurements for each of two independent samples.

II.7 Lipid Vesicle Dye Leakage Experiments

In dye leakage experiments, POPE/POPG (3/1), cardiolipin (CL) and DOPC vesicles were applied to mimic *E. coli*, *S. aureus* and human red blood cell lipid membranes (Figure 4-16). The mixture of lipid and calcein dye in phosphate buffer was stirred for 1 h, followed by five freeze-thaw cycles and extrusion through a polycarbonate membrane (Whatman, pore size 100 nm). Lipid vesicles containing calcein dye were separated from extracellular calcein dye via gel filtration (Sephadex G-25 resin). The vesicle size was characterized by dynamic light scattering to be around 100 nm. The vesicle solution was placed in a fluorescence cuvette, and background signals were monitored by fluorescence for 1 min at 37 °C. Then a specific amount of polymer

aqueous solution was added to the above vesicle solution, and the subsequent fluorescence change was recorded for 5 min. Triton X-100 (20%) was added to the above solution to maximize dye leakage. Dye leakage percentage was calculated using the equation: %dye leakage = $100[(I_t - I_0)/(I_\infty - I_0)]$, where I_0 is the fluorescence intensity before the addition of samples, I_t is the fluorescence intensity after addition of samples, and I_∞ is the fluorescence intensity after addition of Triton X-100 (20%). The dye leakage percentage at 5 min for each polymer is listed in Table 4-9.

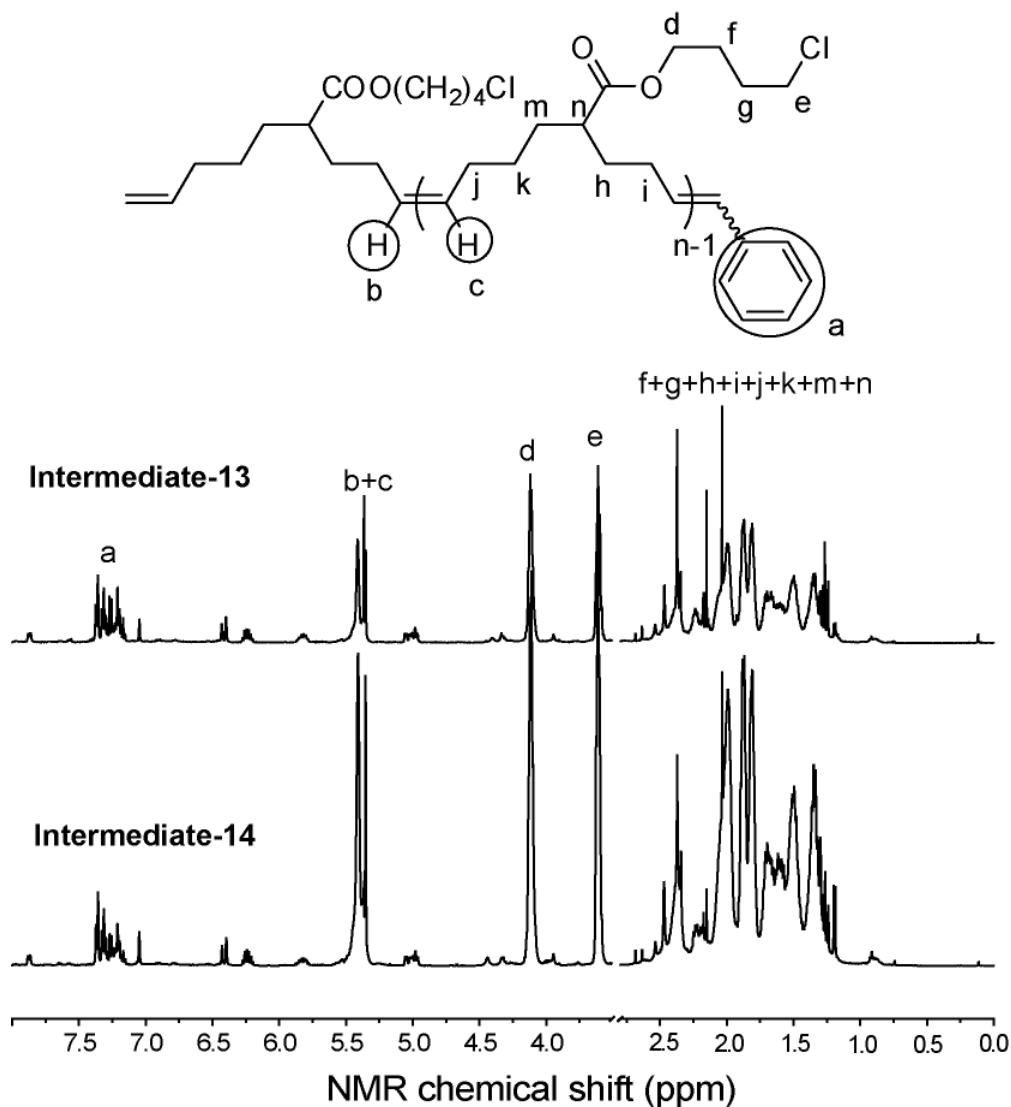


Figure 4-15. ¹H-NMR spectra of **Intermediate-13** and **Intermediate-14**.

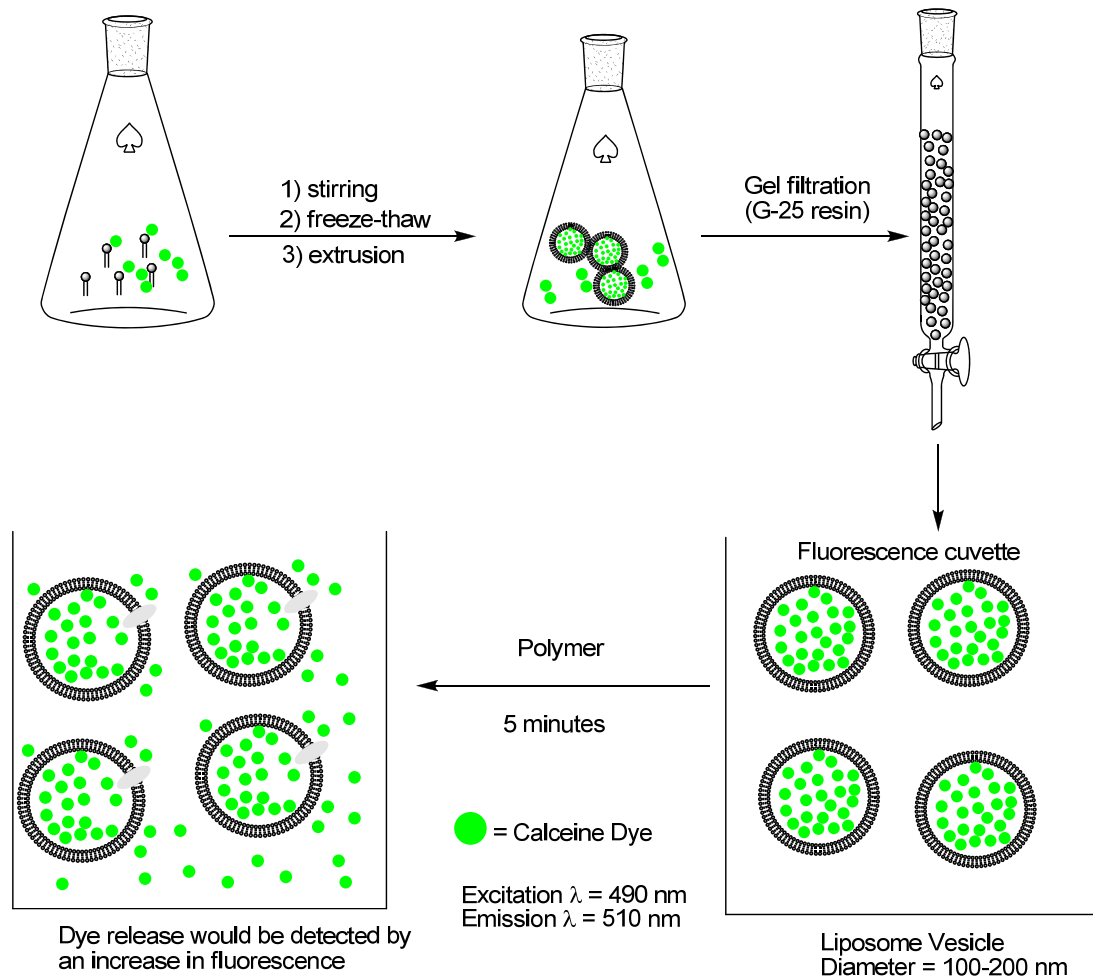


Figure 4-16. Lipid vesicle dye leakage experiments.

II.8 Membrane Depolarization Assay

Normally a potential gradient ($\Delta\psi$) of around 140 mV at neutral pH is present across the bacterial membrane. Disruption of the cytoplasmic membrane can depolarize the membrane potential gradient and contribute to bacterial death.^{156,350-353} We assessed whether the bacterial plasma membranes were depolarized by mimic polymers using a membrane potential sensitive dye diSC₃5 (3,3'-dipropylthiadicarbocyanine iodide). DiSC₃5 intercalates into the cytoplasmic membrane of energized cells under the effect of $\Delta\psi$, and its fluorescence is quenched. Upon disruption of the potential, diSC₃5 is displaced into the buffer solution, and an increase in fluorescence is observed.

Coincident with the membrane depolarization assay, we measured cell viability by counting remaining colony forming units (CFU) to assess the relationship between disruption of membrane potential and loss of survival. The membrane depolarization assay and cell viability assay results for valinomycin (positive control), **Acopolymer-1**, **Rcopolymer-8**, **Homopolymer-11** and **Homopolymer-13** are plotted in Figure 4-17.

Polymer	%Dye leakage ([vesicle] = 4.5 μ M) ^a		
	POPE/POPG (3/1) ([Polymer] = 4 μ g/mL)	Cardiolipin ([Polymer] = 4 μ g/mL)	DOPC ([Polymer] = 1 μ g/mL)
Acopolymer-1	76 \pm 5	65 \pm 2	83 \pm 3
Acopolymer-2	62 \pm 2	75 \pm 1	37 \pm 3
Acopolymer-3	37 \pm 3	20 \pm 1	9 \pm 9
Acopolymer-4	71 \pm 3	37 \pm 2	50 \pm 1
Acopolymer-5	82 \pm 1	49 \pm 1	37 \pm 4
Acopolymer-6	85 \pm 4	45 \pm 1	58 \pm 4
Acopolymer-7	98 \pm 1	69 \pm 4	85 \pm 4
Rcopolymer-8	23 \pm 7	50 \pm 1	28 \pm 2
Rcopolymer-9	47 \pm 1	34 \pm 3	41 \pm 2
Rcopolymer-10	50 \pm 1	49 \pm 1	50 \pm 4
Homopolymer-11	19 \pm 1	13 \pm 2	2 \pm 1
Homopolymer-12	22 \pm 9	11 \pm 1	2 \pm 1
Homopolymer-13	92 \pm 5	59 \pm 2	77 \pm 6
Homopolymer-14	80 \pm 2	51 \pm 1	65 \pm 7

Table 4-9. Dye leakage percentages of **Acopolymer-1** to **Homopolymer-14** after 5 min. ^aDye release percentage was calculated relative to the fluorescence increase after adding Triton X-100. The data shown are the average of triplicate measurements for each of two independent samples.

II.9 Potassium Release Assay

Potassium release triggered by mimic polymers was investigated using K⁺-sensitive fluorophore PBFI-AM (potassium-binding benzofuran isophthalate-AM) (Figure 4-18). A stable fluorescence signal was achieved after adding PBFI-AM to the bacterial suspension. The addition of SMAMP polymers to the bacterial suspension generated potassium efflux in bacteria, and the released potassium ions bound to PBFI-AM yielding an immediate increase in fluorescence. The fluorescence increase for each mimic polymer was recorded for 16 min (Table 4-10), and the potassium release percentage was calculated according to the equation: %potassium leakage = 100[($I_t - I_0$)/($I_{max} - I_{min}$)], where I_0 is the fluorescence intensity before addition of sample, I_t is the fluorescence intensity after addition of sample, I_{min} is the fluorescence intensity before addition of valinomycin (positive control), and I_{max} is the fluorescence intensity 16 min after the addition of valinomycin.

II.10 Thin-section Transmission Electron Microscopy (TEM) of Bacteria

To visualize if and how our SMAMP polymers disrupted bacterial membranes, thin-section TEM imaging of bacteria was undertaken. After treatment with or without **Acopolymer-1** (1×MIC or 10×MIC concentration), bacteria (*E. coli* or *S. aureus*) were imaged by TEM, and the photograph comparison is shown in Figure 4-19.

III. Discussion

III.1 Structure-Activity Relationship Analysis

First, we compared the efficacy of cationic groups. Both **Acopolymer-1** and **Acopolymer-7** exhibited the best antimicrobial activities against all six different bacteria and were most effective against *Staphylococcus* and *Enterococcus*. **Acopolymer-6** was less effective than either. In a neutral buffer solution, the primary amine groups in **Acopolymer-6** are not completely protonated, whereas **Acopolymer-1** and **Acopolymer-**

6 are entirely positively charged at physiologic pH. Thus, these polymers behave like many other antibacterial peptide mimics and positive charges enable attachment to anionic bacterial membranes. The selectivities of **Acopolymer-1** and **Acopolymer-7** for bacteria were as high as 40-80 in the case of *S. aureus* (Figure 4-20a). However, they showed little to no selectivity for *Pseudomonas* which has a low permeability outer membrane compared to other bacteria, in addition to active efflux pumps which eliminate molecules that reach the cell membrane.³⁵⁴ We chose the trimethyl ammonium moiety for use in additional analogs because it was straightforward to prepare and was stable.

We adjusted the amphiphilicity of the alternating polymers by attaching increasingly hydrophobic groups, i.e., methyl, n-propyl carboxamide or n-octyl carboxamide, at the 4-carbon of the cyclohexene monomers (**Acopolymer-2**, **-3**, and **-4**). However, increasing the hydrophobicity from **Acopolymer-1** to **Acopolymer-4** did not increase the antimicrobial activity (Figure 4-20b). Rather the more hydrophobic polymers had lower antibacterial activities than that of **Acopolymer-1**. Interestingly, increasing hydrophobicity did not increase erythrocyte lysis as has been observed with other mimics.³⁵⁵ These results suggest that **Acopolymer-1** may present the best hydrophobic/hydrophilic balance at the microstructural level to effectively kill bacteria.³⁵⁵

Backbiting reactions that occur during the AROMP reaction of cyclobutene and cyclohexenes result in the formation of cyclic copolymers in addition to the desired linear copolymers and the mixtures are difficult to separate even by gel permeation chromatography. Therefore, we developed a method for preparing entirely cyclic alternating polymer, **Acopolymer-5** from the same monomers employed in the synthesis of **Acopolymer-1**. **Acopolymer-5** exhibited much lower antimicrobial activities than **Acopolymer-1** indicating that linear polymers are more efficient antimicrobial polymers than their cyclic counterparts.

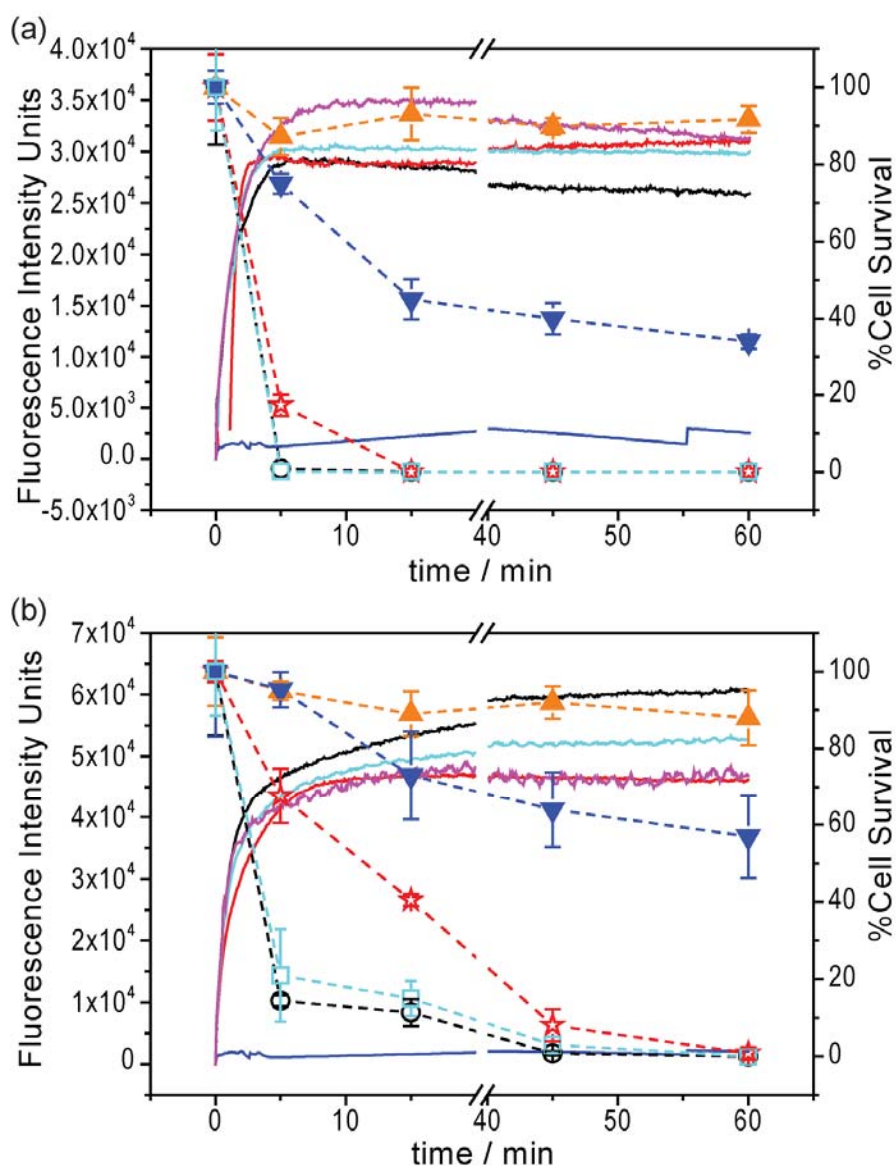


Figure 4-17. Relationship between cytoplasmic membrane depolarization, as assessed by the diSC₃₅ assay, and cell viability, as measured by the counting of CFU at the same time as the membrane depolarization assay for *E. coli* (a) and *S. aureus* (b). Solid curves represent data obtained from the diSC₃₅ assay, and dashed curves represent data from the cell viability assay. ○, **Acopolymer-1** (16 μg/mL for *E. coli*; 4 μg/mL for *S. aureus*); ★, **Rcopolymer-8** (16 μg/mL for *E. coli*; 4 μg/mL for *S. aureus*); ▼, **Homopolymer-11** (16 μg/mL for *E. coli*; 4 μg/mL for *S. aureus*); □, **Homopolymer-13** (16 μg/mL for *E. coli*; 4 μg/mL for *S. aureus*); ▲, Control (no polymer was added). The pink solid line represents data obtained from the diSC₃₅ assay for valinomycin (10 μg/mL). The data shown are the average of triplicate measurements for each of two independent samples.

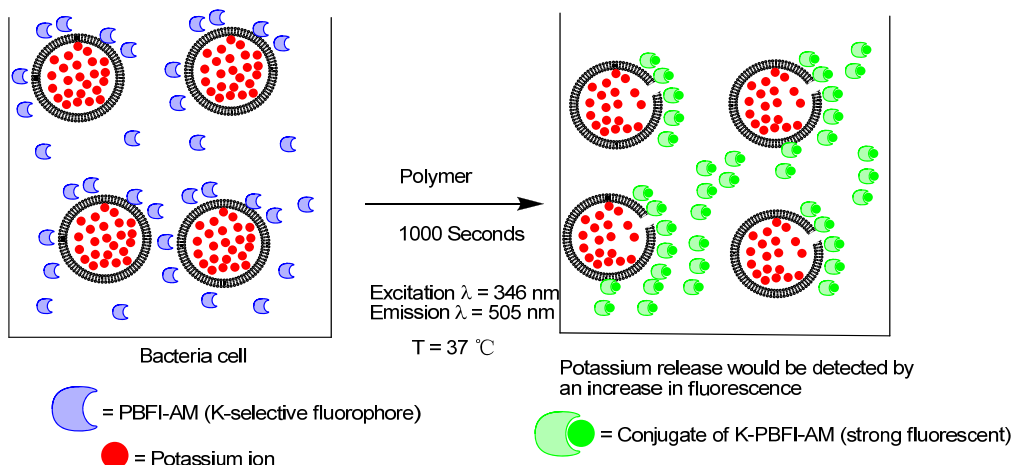


Figure 4-18. Potassium release assay.

Next, we tested whether the antimicrobial activities of **Acopolymer-1** was due to the precise spatial separation of the quaternary ammonium groups or to the global hydrophobic/hydrophilic balance of the polymer. Random copolymers (**Rcopolymer-8**, **-9**, and **-10**) contained unevenly distributed positive charges due to the random addition of cyclobutene amide and cyclooctene amide to the growing polymer chain. The antibacterial activities of the random copolymers were 2- to 4-fold lower than alternating copolymers **Acopolymer-1** and **Acopolymer-7** (Figure 4-20c). These results strongly suggest that the excellent antimicrobial activity of alternating copolymers is due to the localized alternating structures. This requirement for alternating structure at the monomer level is consistent with the high antibacterial efficiencies observed with aryl oligomers.^{226,355}

To further explore the correlation between spacer distance and antibacterial activity two types of homopolymers were prepared. **Homopolymers-11** and **-12** were prepared by ROMP of cyclobutene amide to provide a cation spacing of $\sim 4\text{\AA}$. **Homopolymers-13** and **-14** were prepared by ROMP of cyclooctene in which the cation spacing is $\sim 8.4\text{\AA}$. The activities of these homopolymers were compared to that of **Acopolymer-1** which has an approximately 10.2\AA cation spacer distance. Neither **Homopolymer-11** nor **-12** had any antimicrobial activity (Figure 4-20d). **Homopolymers-13** and **-14** exhibited antimicrobial activities and selectivities comparable to but slightly lower than **Acopolymer-1**. Therefore, the distance between

cations required for antibacterial activity is greater than 4Å and a range of 8 to 10 Å appears optimal. This spacing requirement is consistent with the cation spacing (> 5 Å) in AMPs.

Polymer	%Potassium release ^a	
	<i>E. coli</i>	<i>S. aureus</i>
Acopolymer-1	47 ± 5	77 ± 6
Acopolymer-2	21 ± 16	37 ± 7
Acopolymer-3	18 ± 10	19 ± 2
Acopolymer-4	36 ± 7	33 ± 5
Acopolymer-5	35 ± 7	70 ± 10
Acopolymer-6	49 ± 19	73 ± 17
Acopolymer-7	41 ± 17	42 ± 4
Rcopolymer-8	27 ± 14	18 ± 5
Rcopolymer-9	21 ± 7	24 ± 5
Rcopolymer-10	19 ± 9	30 ± 17
Homopolymer-11	8 ± 1	7 ± 1
Homopolymer-12	8 ± 2	10 ± 3
Homopolymer-13	55 ± 8	69 ± 13
Homopolymer-14	40 ± 10	65 ± 5

Table 4-10. Potassium release percentages of **Acopolymer-1** to **Homopolymer-14** after 16 min. ^aPotassium release percentage was calculated relative to the fluorescence increase after adding valinomycin. The data shown are the average of triplicate measurements for each of two independent samples.

Increasing the average number of cationic charges from 4 to 8 did not improve efficacy, for example, **Homopolymers-13** and **-14** had identical activities (Figure 4-20d). Moreover, the charge density may not be higher than every 8 Å. **Homopolymer-12**

presents 4 cations separated by 8 Å, analogous to the spacing in **Acopolymer-1** and **Homopolymer-13** (Figure 4-21). However, **Homopolymer-12** has twice the charge density of **Acopolymer-1** or **Homopolymer-13** with an average net total of 8 cations. Therefore, the charge density may not be higher than every 8 Å, and the spacer between cations cannot be charged. Gellman and coworkers have observed an analogous effect of charge density with random β-peptide copolymers.³²² In their work, a high feed ratio of cationic β-peptide compared to hydrophobic β-peptide results in regions of closely spaced (~ 5 Å) ammonium groups. It is suggested that inhibition of bacterial growth or hemolysis by AMP mimics require a certain amount of lipophilicity.³²² **Homopolymers-11** and **-12** may contain too low lipophilicity to kill bacteria effectively as compared to **Homopolymers-13** and **-14**.

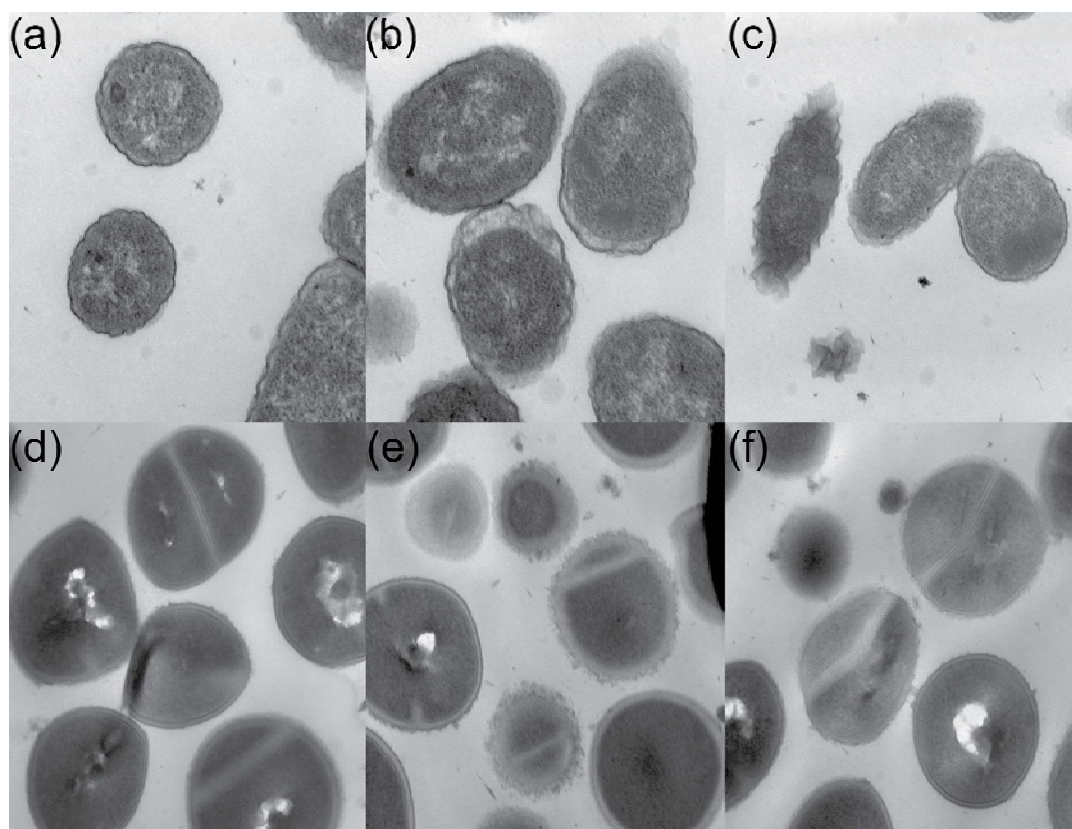


Figure 4-19. Thin-section TEM images of bacteria. **a:** *E. coli* without treating with **Acopolymer-1**; **b:** *E. coli* treated with 1×MIC of **Acopolymer-1**; **c:** *E. coli* treated with 10×MIC of **Acopolymer-1**; **d:** *S. aureus* without treating with **Acopolymer-1**; **e:** *S. aureus* treated with 1×MIC of **Acopolymer-1**; **f:** *S. aureus* treated with 10×MIC of **Acopolymer-1**

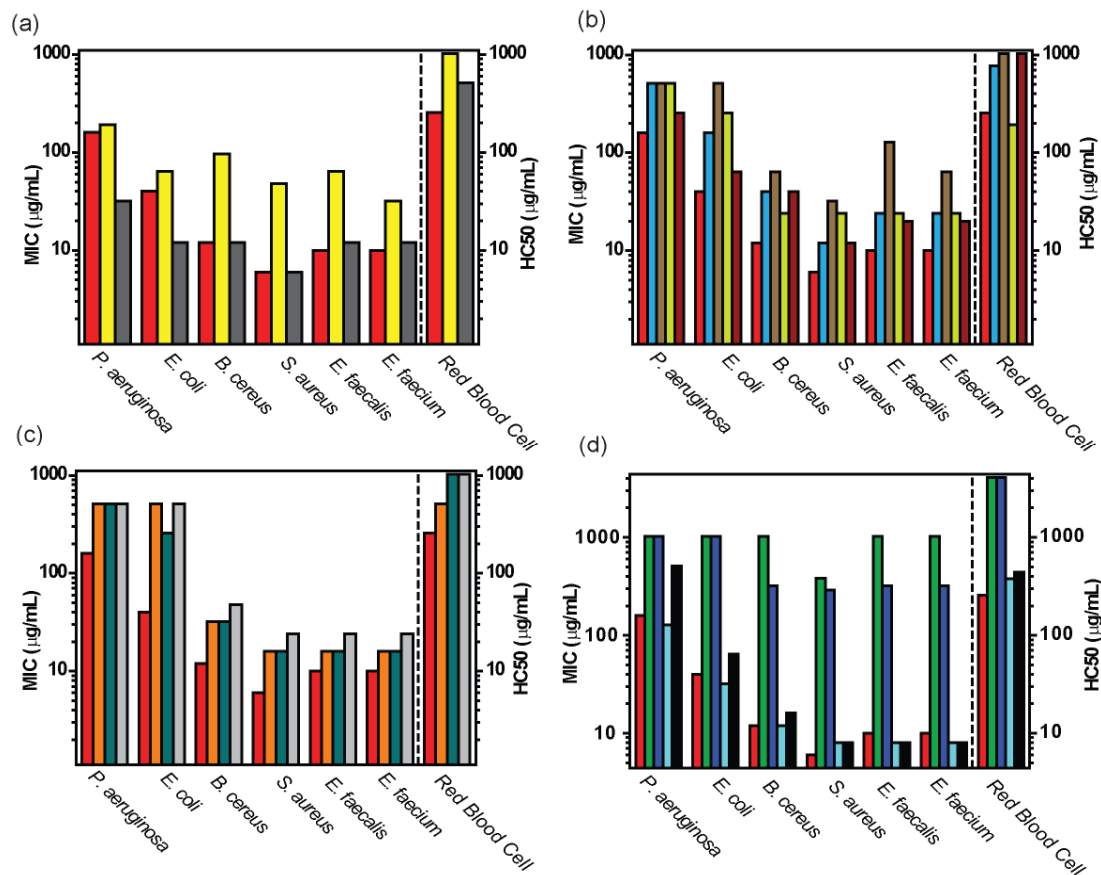


Figure 4-20. MIC and HC₅₀ data for amphiphilic polymers. a) Alternating copolymers with different cationic groups: **■**, **Acopolymer-1**; **■**, **Acopolymer-6**; **■**, **Acopolymer-7**. b) Alternating copolymers with varying hydrophobic spacers: **■**, **Acopolymer-2**; **■**, **Acopolymer-3**; **■**, **Acopolymer-4**; **■**, **Acopolymer-5**. c) **Acopolymer-1** compared to random copolymers: **■**, **Rcopolymer-8**; **■**, **Rcopolymer-9**; **■**, **Rcopolymer-10**. d) **Acopolymer-1** vs homopolymers: **■**, **Homopolymer-11**; **■**, **Homopolymer-12**; **■**, **Homopolymer-13**; **■**, **Homopolymer-14**. The MIC data are the average of triplicate measurements with two independent preparations of each polymer.

III.2 Mechanism of Polymer Action

To further establish the relationship between structure and antimicrobial properties, we selected **Acopolymer-1**, **Rcopolymer-8**, **Homocopolymer-11** and **Homocopolymer-13** for further study. On average, each of these polymers has 4 cations presented along their respective polymer backbones. Therefore, study of their mechanisms of action reports on the influence of spacing and backbone.

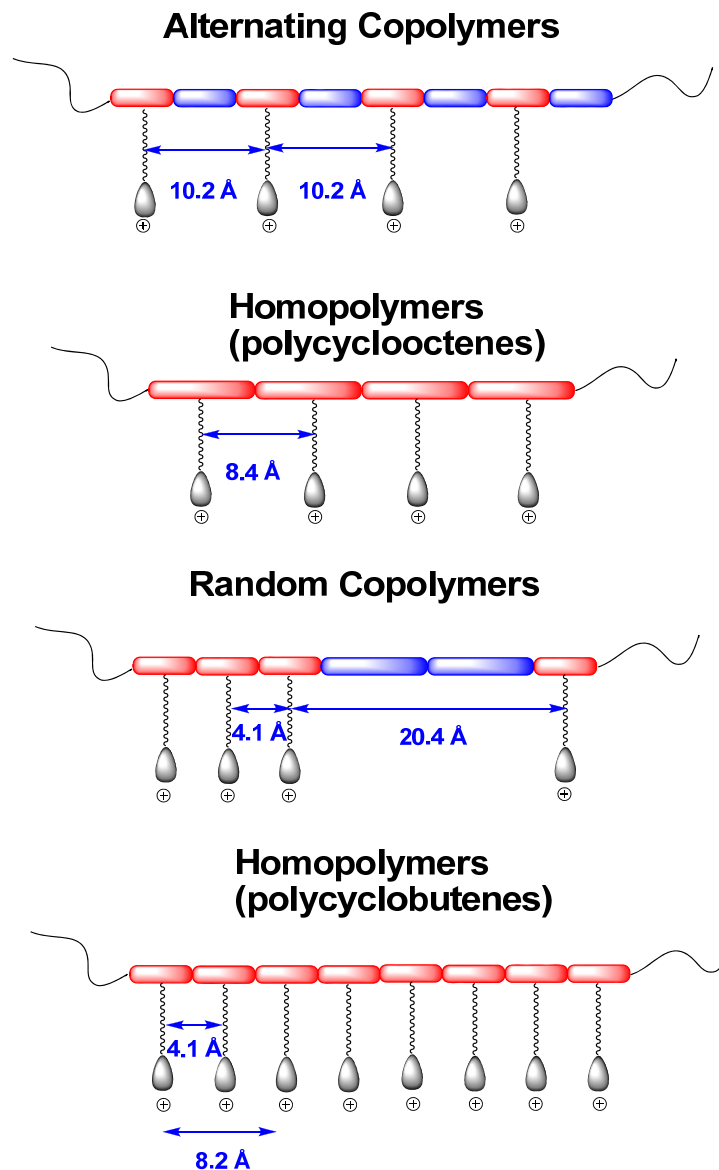


Figure 4-21. Structure activity relationship for antimicrobial polymers. Polymers containing longer spacing exhibit better antimicrobial activities.

Maximal release of diSC₃₅ after the addition of **Acopolymer-1**, **Rcopolymer-8**, and **Homopolymer-13** to both *E. coli* and *S. aureus* was observed within 10 min. This timescale is similar to rate of depolarization induced by the antibiotic valinomycin (Figure 4-17). After 15 min, *E. coli* cells treated with **Acopolymer-1**, **Rcopolymer-8**, or **Homopolymer-13** were no longer viable (Figure 4-17a). Cell viability decreases in

parallel with membrane depolarization for *E. coli* suggesting that cell killing is closely correlated with membrane potential disruption.

Loss of *S. aureus* survival upon addition of **Acopolymer-1**, **Rcopolymer-8**, and **Homopolymer-13** was slower than observed for *E. coli*. After 15 minutes, cell viability was only reduced to 11%, 41% and 15% for **Acopolymer-1**, **Rcopolymer-8**, and **Homopolymer-13** respectively. The incomplete decrease in cell viability for *S. aureus* demonstrates that membrane depolarization caused by **Acopolymer-1** and **Rcopolymer-8** is not sufficient to cause cell death, and other slower mechanisms, e.g., pore formation or intracellular binding, may work together to trigger cell death. **Acopolymer-1** killed *S. aureus* more rapidly than **Rcopolymer-8** (Figure 4-17b), and the faster killing kinetics of **Acopolymer-1** correlate with its lower MIC.

Over the course of one hour, very little membrane depolarization occurred upon addition of **Homopolymer-11**, as expected based on its high MIC (Figure 4-17). Furthermore, approximately 40-70% of bacteria survived after 15 min. The data suggest that cell killing by **Homopolymer-11** is very slow.

Next, we examined whether membrane disruption by the polymers is specific for the types of lipids present in *E. coli* and *S. aureus* versus in red blood cell membranes. We prepared lipid vesicles composed of POPE/POPG (3/1), cardiolipin (CL) and DOPC vesicles that encapsulated calcein dye. Percent dye leakage was measured relative to total lysis that was induced with 20% Triton X-100 (Figure 4-22a-c, Table 4-9). A comparison of the level of lysis reveals that **Acopolymer-1**, **Rcopolymer-8**, and **Homopolymer-13** are not specific for the negatively charged POPE/POPG and cardiolipin vesicles over the neutral DOPC vesicles. Vesicles are a simplistic model of bacterial plasma membranes as they lack structural components and associated proteins that appear to be important for specificity. Therefore the function of these polymers requires more than a simple electrostatic interaction with the bacterial plasma membrane. The low levels of vesicle lysis observed with **Homopolymer-11** support the idea that a 8-10 Å cationic spacing and a certain amount of lipophilicity is critical for plasma membrane disruption.

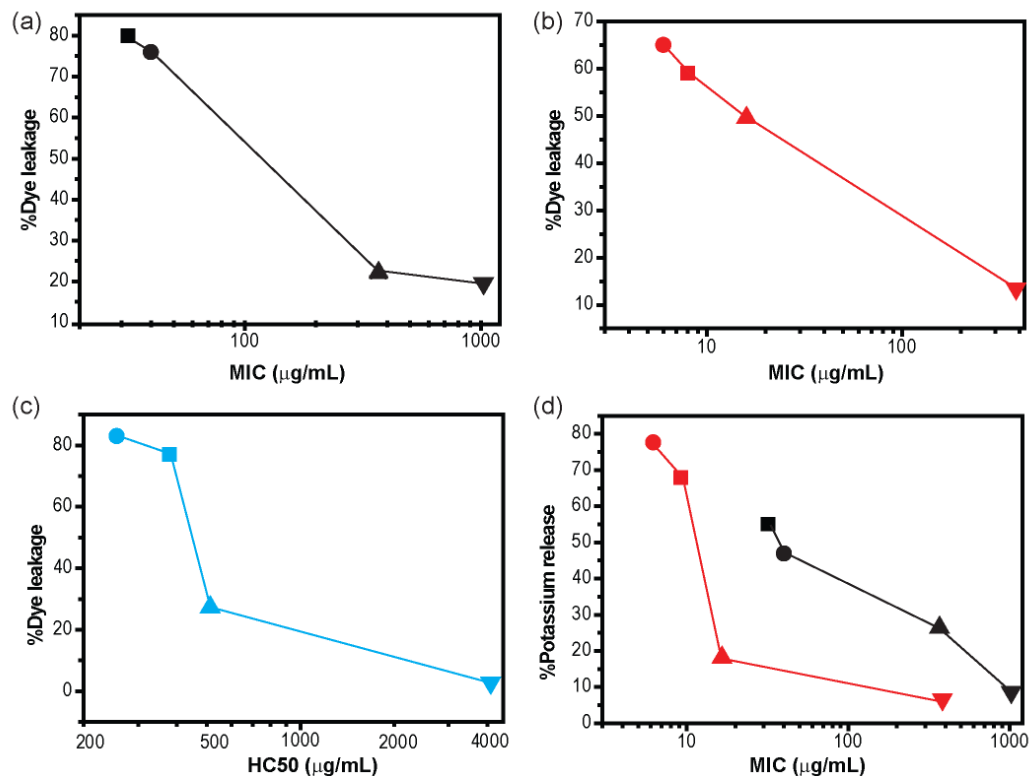


Figure 4-22. a) Percent dye leakage from *E. coli* model membrane vesicles: POPE/POPG = 3/1, [lipid] = 4.5 μM , [polymer] = 4 $\mu\text{g/mL}$ vs *E. coli* MIC. b) Percent dye leakage from *S. aureus* model membrane vesicles: [CL] = 4.5 μM , [polymer] = 4 $\mu\text{g/mL}$ vs *S. aureus* MIC. c) Percent dye leakage from red blood cell model membrane vesicles: [DOPC] = 4.5 μM , [polymer] = 1 $\mu\text{g/mL}$ vs HC50 data. d) Percent potassium release vs MIC. Black symbols are for *E. coli* (MIC); red symbols are for *S. aureus* (MIC); blue symbols are for red blood cells (HC50). \circ , **Acopolymer-1**. \triangle , **Rcopolymer-8**. ∇ , **Homopolymer-11**. \square , **Homopolymer-13**. The data shown are the average of triplicate measurements for each of two independent samples.

Release of potassium from the bacterial cell occurs upon disruption of the membrane potential.^{331,356} We investigated the levels of postassium release incurred by our polymers using potassium ion sensitive fluorophore, potassium-binding benzofuran isophthalate-AM (PBFI-AM). Percent potassium release was measured 16 minutes after the addition of polymer and reported relative to valinomycin (100%) (Figure 4-22d, Table 4-10). **Acopolymer-1** and **Homopolymer-13** were the most effective at causing a

high (> 50%) level of potassium release consistent with their lower MICs. Thus, the ability to disrupt membrane potential correlates with potassium release.

To determine to what extent **Acopolymer-1** disrupts bacterial lipid membranes, thin-section TEM was employed (Figure 4-19). The cell surface of *E. coli* and *S. aureus* bacteria treated with **Acopolymer-1** (1×MIC or 10×MIC) exhibited severely damaged cell surfaces containing membrane blebs (Figure 6b, c, e and f) as compared to untreated bacteria (Figure 4-19a and d). Similar levels of membrane disruption are observed with antimicrobial peptide-treated bacteria.³⁵⁷⁻³⁵⁹

IV. Summary

We conclude that an ordered microstructure is required for optimal antimicrobial activity even in the context of a polymer backbone with irregular conformation. Moreover, the spacer distance between neighboring ammonium groups must be greater than 4 Å and preferably 8-10 Å. The longer spacer distance may improve the attachment of the polymers to the bacterial membrane. Random copolymers do not have a uniform spacer distance, but local regions within the polymer backbone may achieve optimal cation spacing. Therefore, random copolymers exhibit moderate antimicrobial activities compared to regularly spaced copolymers.

Like antimicrobial peptides and other mimics, the polymers prepared in this work caused rapid membrane depolarization and potassium release, followed by cell death. Ultimately the bacterial membrane is disrupted, but it is not clear whether the membrane lysis is the cause or the effect of bacterial cell death (Figure 4-23). Loss of viability occurs rapidly suggesting that these antimicrobial polymers can be used as contact microbiocides.^{328,331} Future work will explore whether the **Acopolymer-1** can be used in a surface active format.

V. Future Perspectives

One future project will explore the antimicrobial activity of linear alternating polymers. It is suggested that linear alternating polymer in **Acopolymer-1** exhibit much

higher antimicrobial activity than its cyclic counterparts. If we can develop a new AROMP method to stop backbiting, linear alternating polymers with different DPs can be synthesized, and the relationship between MIC and DP can be investigated.

The SAR analysis of polycyclooctene mimics in antimicrobial studies can be further investigated. The antimicrobial activities of polycyclooctenes containing different cationic groups, e.g., primary ammonium groups or guanidine groups, can be compared. The amphiphilicity of polycyclooctenes can be adjusted by attaching varying hydrophobic groups to the 6-position of cyclooctene.

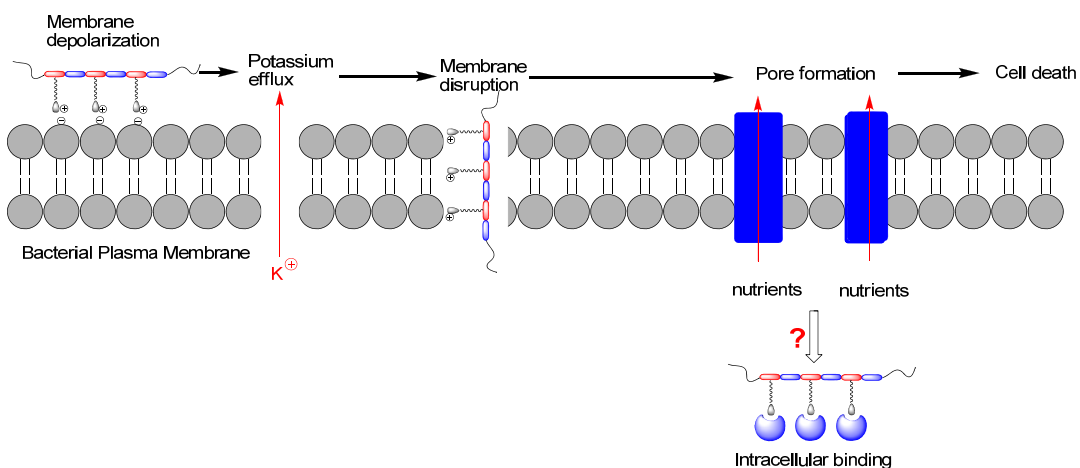


Figure 4-23. Proposed model for the bactericidal mechanism of action of mimic polymers.

Chapter 5

Vesicle Formation of Homo Polymers, Alternating Copolymers, and Random Copolymers

I. Introduction

II. Results

III. Discussion

IV. Summary

V. Future Perspectives

I. Introduction

It is very common for amphiphilic polymers to form micelles/vesicles in aqueous solution.³⁶⁰⁻³⁷⁵ In vesicles, the hydrophilic chains are exposed inside and outside the hydrophobic membrane in aqueous solution, whereas polymer micelles contain only one layer of membrane (Figure 5-1). Compared to liposomes, polymer vesicles exhibit better properties, e.g., higher toughness, better stability or tailorable membrane properties.³⁷⁵ Therefore, polymer vesicles have been routinely applied in encapsulation, nanoreactors or stimuli-responsive drug delivery.^{361,363-364}

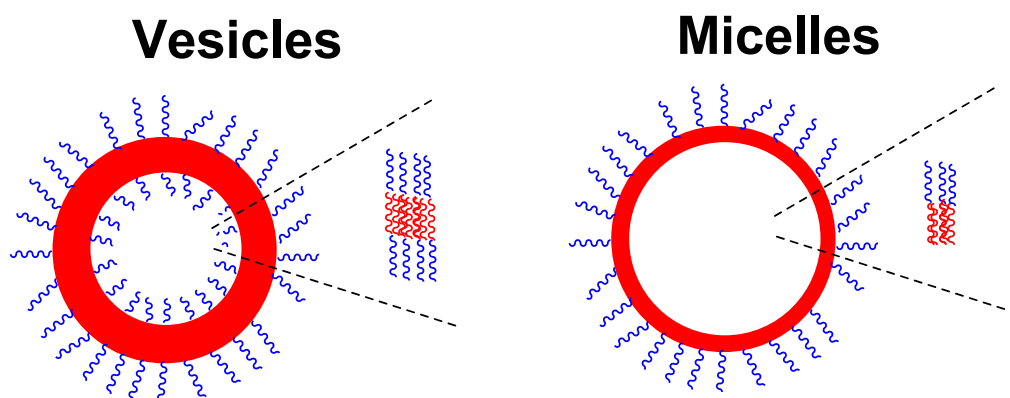


Figure 5-1. Structures of vesicles and micelles.

Polymer micelles or vesicles have been prepared from various amphiphilic block copolymers, such as polyethylene oxide (PEO),³⁷⁶⁻³⁷⁹ polybutadiene (PBD),³⁸⁰⁻³⁸³ polylactic acid (PLA),³⁸⁴⁻³⁸⁸ polystyrene,³⁸⁹⁻³⁹² polypropylene oxide (PPO),³⁹³⁻³⁹⁵ polycaprolactone (PCL)^{384-388,396} and polynorbornene (PNB).³⁹⁷ There are several factors controlling the self-assembly morphology of block copolymers: the hydrophobic/hydrophilic balance, polymer concentration, polymer length, organic solvent properties, salt concentration,³⁹⁸ solution pH and temperature.^{363,399} Besides control of morphology, block copolymers with designed functionality have been applied to adjust vesicle membrane fluidity, permeability, thickness and stimuli responses.^{363,399}

To the best of our knowledge, only one example has been reported discussing micelle/vesicle formation of amphiphilic alternating copolymers, which were made by atom transfer radical polymerization (ATRP) (Figure 5-2).³⁶⁴ Wu et al. reported that alternating polymers containing hydrophobic maleate esters and hydrophilic hydroxy vinyl ethers self-assembled to form vesicles (2-15 nm).³⁶⁴ They also characterized the encapsulation and release properties of these alternating polymer vesicles.³⁶⁴

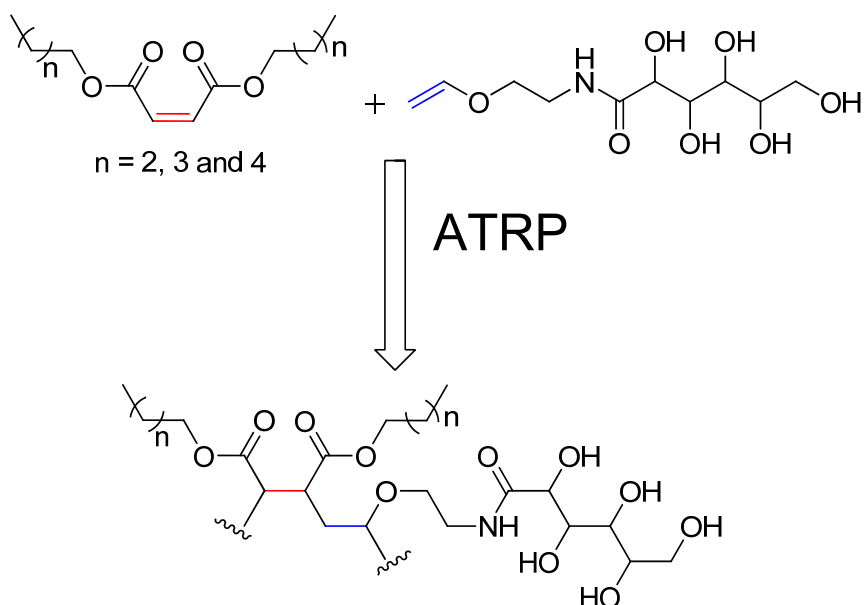


Figure 5-2. Alternating copolymers made from ATRP.

Stimuli-responsive polymer vesicles have been developed based on vesicle membranes. Stimuli include hydrolysis, oxidation, reduction, pH, temperature and light.^{361,363} The Armes' group found that the size of PMPC-b-PDPA polymer vesicles varied with pH change (Figure 5-3).^{363,400} At low pH (2 - 5.5) vesicle formation was not observed, whereas, at pH > 6 vesicles (hydrodynamic diameter $D_h = 140$ nm) were observed by both TEM and dynamic light scattering (DLS).

In our group, we synthesized a series of amphiphilic homopolymers, alternating copolymers, and random copolymers (**Acopolymer-1** to **Homopolymer-14**). We observed that these polymers self-assemble to form vesicles in aqueous solution. Using DLS, we monitored their change in size as a function of pH or salt concentration. Wall

thickness of the vesicle was studied by synchrotron small angle neutron scattering (SANS).

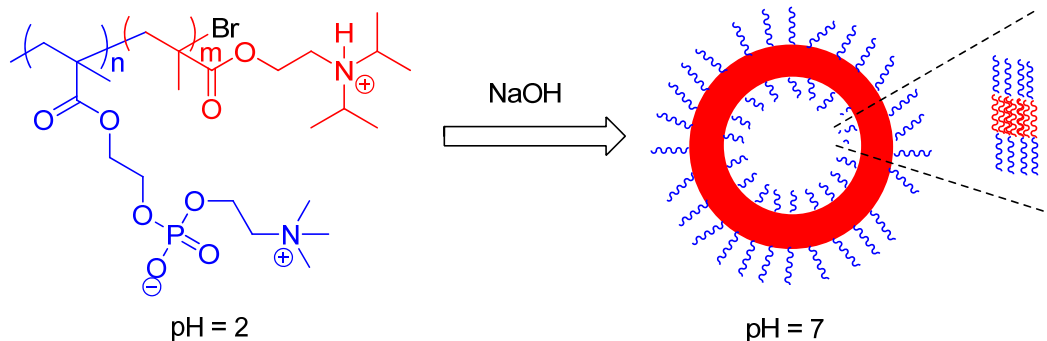


Figure 5-3. pH-sensitive block copolymers.

II. Results

One interesting phenomenon observed from these cationic polymers is that they self-assembled to form vesicles in aqueous solution. Their hydrodynamic diameters in aqueous solutions were characterized by DLS, and are shown in Figure 5-4. Changes in D_h of the vesicles as a function of pH and NaCl concentration are plotted in Figure 5-5 and Figure 5-6, respectively. Shapes of these vesicles were imaged by TEM (Figure 5-7). Wall thickness of the **Acopolymer-1** vesicle was characterized by SANS.

III. Discussion

We observed by DLS and TEM that all our amphiphilic polymers (**Acopolymer-1** to **Homopolymer-14**) self-assembled to form vesicles in aqueous solution (Figure 5-4 and Figure 5-7). Large vesicles ($D_h = 300-500$ nm) were formed from alternating copolymers (**Acopolymer-1** to **Acopolymer-7**), while much smaller vesicles ($D_h = 10-130$ nm) were generated from random copolymers and homopolymers (**Rcopolymer-8** to **Homopolymer-14**). This suggests that the larger vesicles formed from alternating copolymers is related to their alternating structures. Using SANS, the wall thickness of

the **Acopolymer-1** vesicle is around 37 nm in water (SANS data were characterized by Dr. Shuo Qian at Oak Ridge National Lab).

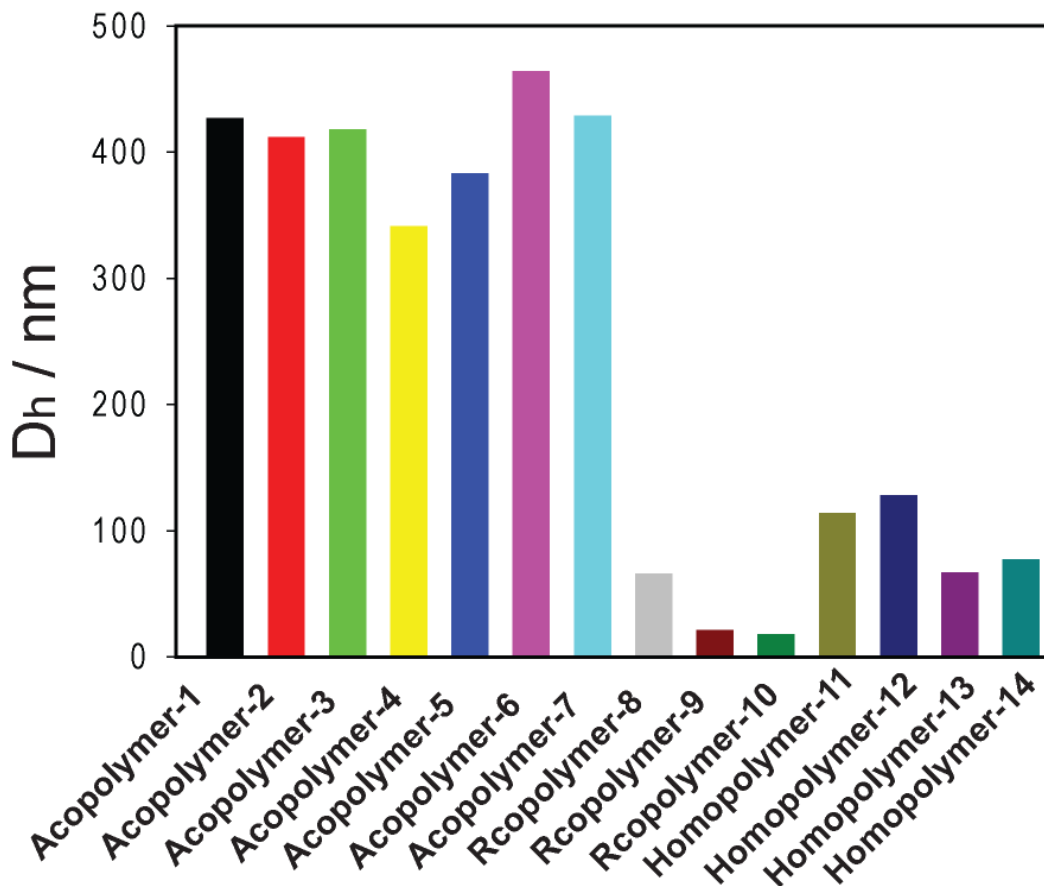


Figure 5-4. Hydrodynamic diameters (D_h) of **Acopymer-1** to **Homopolymer-14**. [Polymer] = 0.1 mg/mL, pH = 7.0, [sodium phosphate] = 10 mM.

Changes in vesicle size as a function of pH were investigated for polymers containing quarternary ammonium groups or primary ammonium groups (Figure 5-5). Two protocols were applied to make vesicle solutions in buffer solutions: 1) dry polymers were resuspended in the buffer solution; 2) a stock polymer solution (2 mg/mL) in water was prepared first, followed by dilution into buffer solution ($[\text{PO}_4^{3-}] = 10 \text{ mM}$). Both of these two protocols yielded the same results. For polymers containing quarternary ammonium groups (**Acopymer-1** and **Homopolymer-12**), the hydrodynamic diameters (D_h) of their vesicles remained constant in the phosphate buffer

solution (pH = 2-11). However, for polymers containing primary ammonium groups (**Acopolymer-6** and **Acopolymer-7**), at low pH (2-5), smaller (< 50 nm) or no vesicles were observed, and at high pH (6-11), their vesicle size increased dramatically from 50 to 900 nm. The vesicle size change due to pH change for **Acopolymer-6** and **Acopolymer-7** is explained as a protonation-deprotonation process.⁴⁰⁰⁻⁴⁰¹ When the pH is below 6, **Acopolymer-6** and **Acopolymer-7** are protonated and become water-soluble. In contrast, in neutral and basic solutions, the amine groups on **Acopolymer-6** and **Acopolymer-7** become hydrophobic due to the deprotonation, and as a result, larger vesicles are formed. Although **Acopolymer-1** and **Homopolymer-12** contain positively charged quarternary ammonium groups, they form stable vesicles probably due to the shielding of positive charges by tetrasubstituted alkyl groups.⁴⁰²

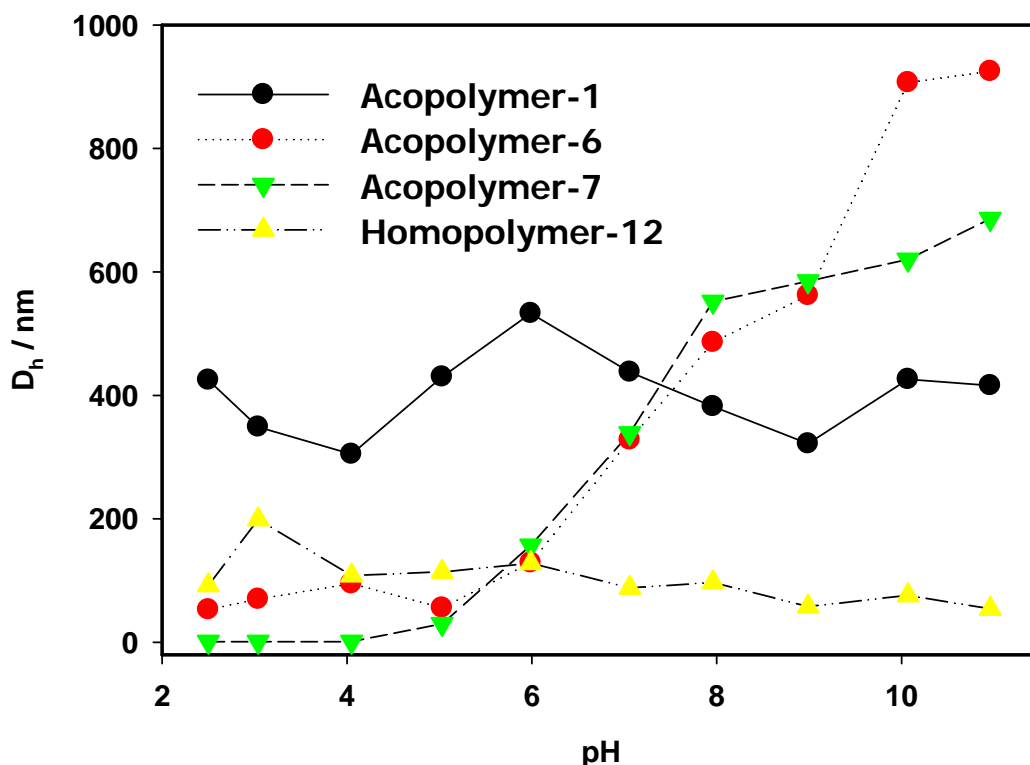


Figure 5-5. Hydrodynamic diameters (D_h) vs pH of polymer solutions. [Polymer] = 0.1 mg/mL, [sodium phosphate] = 10 mM.

The vesicle size change in water versus increasing NaCl concentration for **Acopolymer-1** was characterized by DLS (Figure 5-6). Two protocols were used to prepare vesicles: 1) dry **Acopolymer-1** was dissolved in water containing increasing NaCl concentrations; 2) a concentrated **Acopolymer-1** stock solution in water was diluted into solutions of increasing NaCl concentrations. In the first protocol, the vesicle was formed after the addition of aqueous solutions, and an increase in vesicle size was observed with increasing ionic strength ($[\text{NaCl}] = 0\text{-}1\text{M}$). Increasing ionic strength caused the increase of the vesicle aggregation number by screening the electrostatic repulsions between chains, and larger vesicle sizes were observed. For the second protocol, at low NaCl concentrations (0-200 mM), vesicle diameters decreased 7-8 fold with increasing ionic strength. This may be because the addition of a small amount of salt after vesicle formation will shrink the vesicle via shielding the electrostatic repulsions in the charged corona (Figure 5-8).⁴⁰³ In water, at high NaCl concentrations (400-1000 mM), a rapid vesicle size increase was observed with increasing ionic strength. The vesicle size increase at high ionic strength could be due to the increase in polymer aggregation number resulting from the stronger shielding of electrostatic repulsions among corona chains (Figure 5-8). The above vesicle size change due to salt concentration change suggests that polymer vesicles are nonequilibrium structures.

IV. Summary

Vesicle formation from amphiphilic polymers was observed by TEM and DLS. The pH-sensitivity of these cationic polymers was characterized by DLS. Polymers containing quarternary ammonium groups are resistant to pH changes. However, polymers containing primary ammonium groups are sensitive to pH, and their size change with pH change are consistent with protonation and deprotonation of primary amine groups. By DLS, it was observed that vesicle size varied with ionic strength of the polymer solution.

V. Future Perspectives

Cryo-TEM of these amphiphilic polymer vesicles can be employed to visualize the wall thickness of vesicles. The application of our polymer vesicles in drug delivery can be explored. For example, drug molecules can be mixed together with **Acopolymer-6** at low pH first. The pH of the solution can be slowly adjusted to 7, and higher drug encapsulation can be achieved along with formation of vesicles as compared to the drug encapsulation by mixing drug molecules and polymer vesicles at pH = 7.⁴⁰⁰

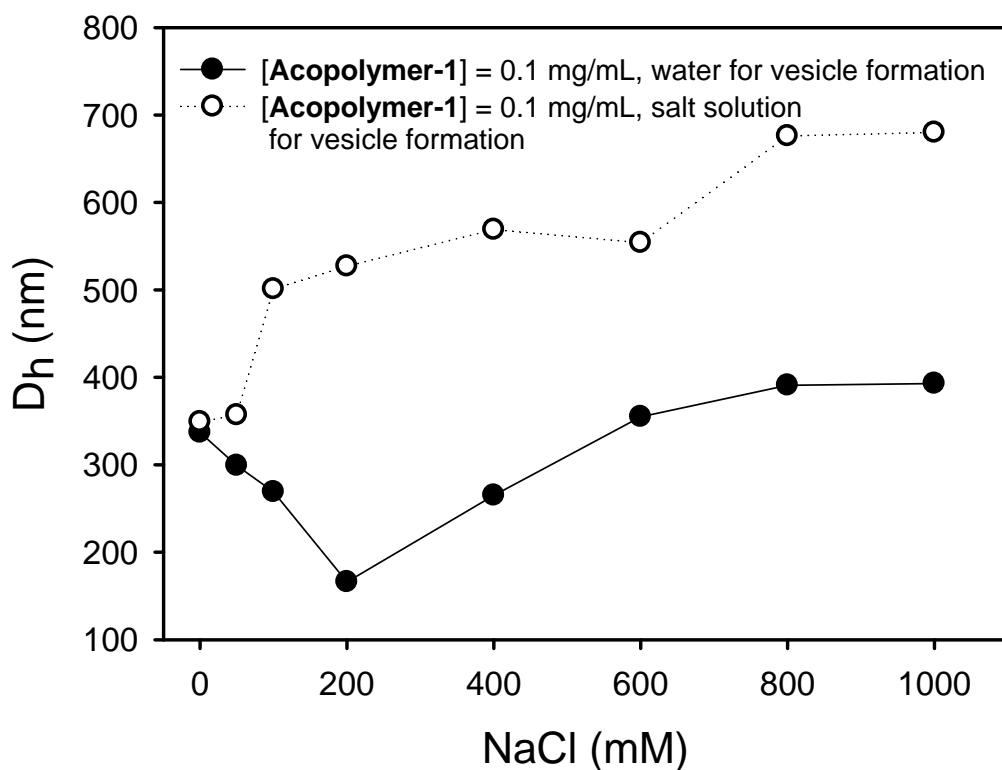


Figure 5-6. Hydrodynamic diameters (D_h) vs NaCl concentrations for **Acopolymer-1**.

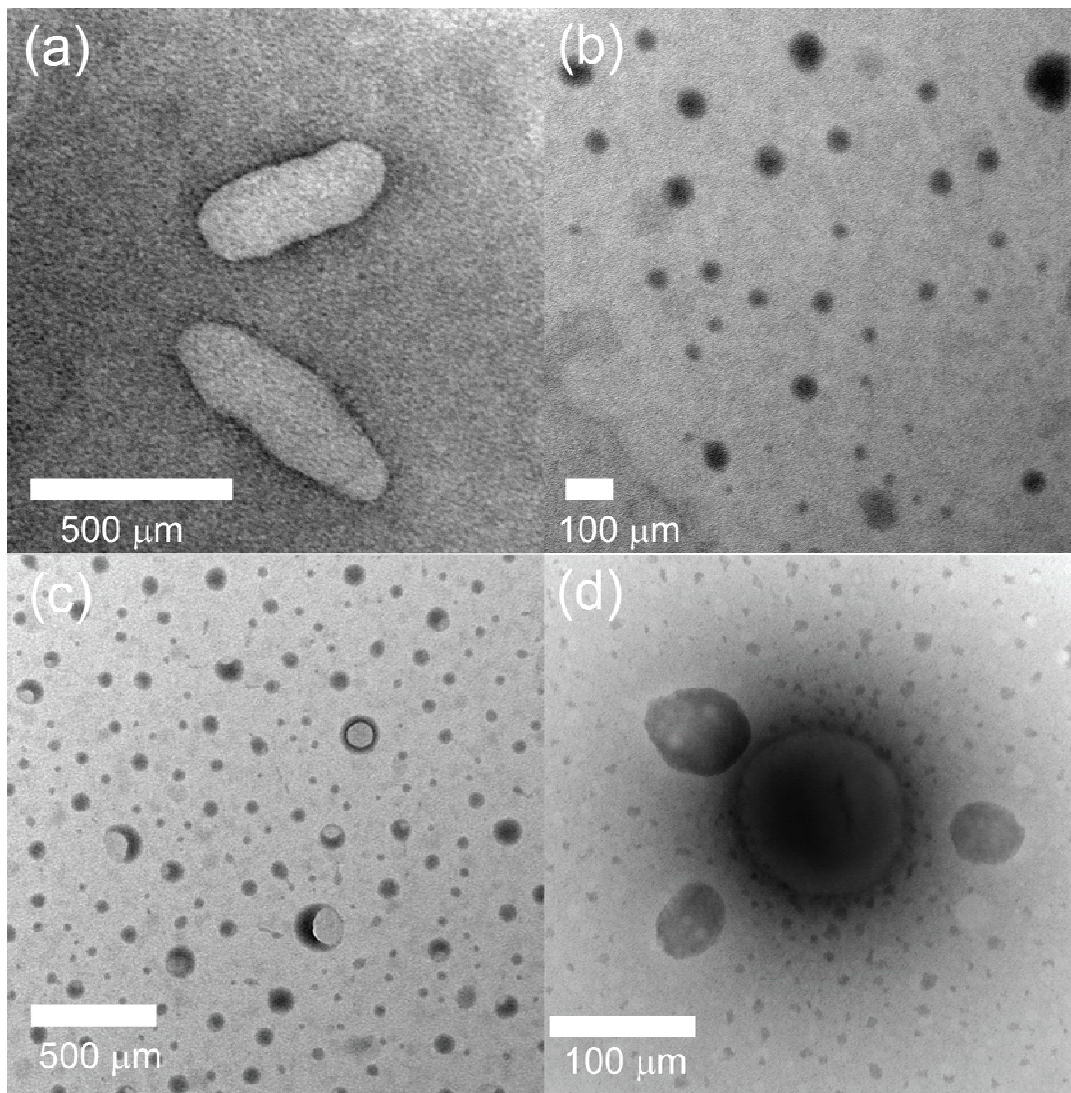


Figure 5-7. TEM images of **Acopolymer-1** (a), **Rcopolymer-10** (b), **Homopolymer-12** (c) and **Homopolymer-13** (d).

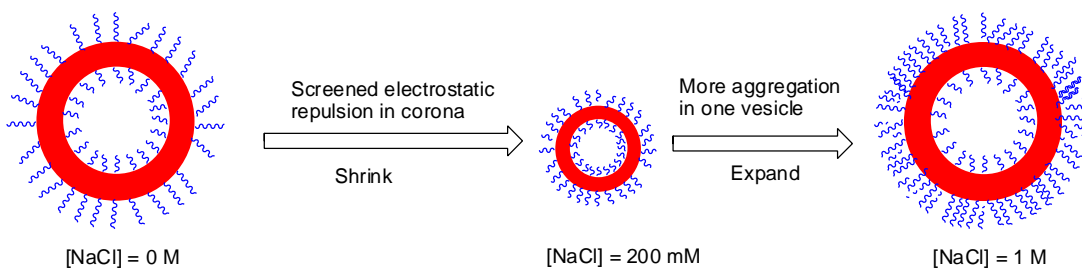


Figure 5-8. Proposed mechanism of vesicle size change due to change in NaCl concentration.

Chapter 6

Experimental Methods

I. Synthesis and Preparation of Compounds

II. Gaussian Computational Methods

III. Lipid Dye Leakage Assay

IV. Potassium Release Assay

V. Thin-section TEM

VI. Membrane Depolarization Assay and Cell Viability Assay

VII. MIC and Hemolysis Assay

VIII. Small Angle Neutron Scattering

I. Synthesis and Preparation of Compounds

Materials and General Procedures: Amino acids and coupling agents used were purchased from Advanced Chem Tech. (Louisville, KY) or PerSeptive Biosystems (Framingham, MA). Solvents and chemical reagents were obtained from Fisher Scientific, Inc. (Springfield, NJ) or Sigma-Aldrich (Milwaukee, WI). Second generation Grubbs' catalyst [(H₂IMes)(PCy₃)Cl₂Ru=CHPh] and ethyl 1-bromocyclobutanecarboxylate were purchased from Aldrich (Cat # 569747 and 197297). (H₂IMes)(3-Brpyr)₂Cl₂Ru=CHPh **5** was prepared according to the literature.¹⁰⁶ Pyridine-Nolan's catalyst **28** was prepared according to the literature.²⁹⁷⁻²⁹⁸ CH₂Cl₂, benzene, Et₂O, THF and CH₃OH were dried in a GlassContour solvent pushstill system; Pentane was used without further purification. All reactions were carried out under an Ar atmosphere in oven-dried glassware unless otherwise specified. 1-Cyclobutenecarboxylic acid was synthesized according to the literature.^{111,404} Analytical thin layer chromatography (TLC) was performed on precoated silica gel plates (60F254), flash chromatography on silica gel-60 (230–400 mesh) and Combi-Flash chromatography on RediSep normal phase silica columns (silica gel-60, 230–400 mesh). TLC spots were detected by UV light and by staining with phosphomolybdic acid (PMA). Inova400, Inova500 and Inova600 MHz NMR Instruments were used to perform NMR analysis, and spectra were recorded in CDCl₃ or CD₂Cl₂ unless otherwise noted. ¹H-NMR spectra are reported as chemical shift in parts per million (multiplicity, coupling constant in Hz, integration). ¹H-NMR data are assumed to be first order. Copies of NMR spectra are available in the appendix. The usual workup for ester or amide coupling reactions was three washes of the CH₂Cl₂ solution with 5% NaHCO₃, followed by three washes with 1 N HCl and drying of the CH₂Cl₂ over Na₂SO₄. After evaporation of solvent, the final product was purified by flash silica chromatography or Combi-Flash chromatography instrument (Teledyne Isco company). LC-MS spectra were acquired on a Waters ACQUITY Ultra Performance Liquid Chromatography system with an SQD detector using 10 cm×2.1 mm ACQUITY™ BEH C18 (particle size = 1.7 μm) column (Waters Corp, Milford, USA) with elution by a linear gradient of 20-100% *B* at 0.5 mL/min, where *A* = water and *B* = methanol. TEM images were acquired on FEI BioTwinG² transmission electron

microscope. High resolution mass spectra were obtained on Thermo Fisher Scientific LTQ Orbitrap XL ETD.

PDI (Polydispersity Index) determination. The polymers (before flash column chromatography purification) were dissolved in THF (0.5 mg/mL). An aliquot (100 μ L) of the polymer solution was injected and analyzed by gel permeation chromatography using a Phenogel column (300 x 7.80 mm, 5 μ m, linear mixed bed, 0-40k MW range). Elution was performed at 0.7 mL/min with THF and detection at 220 nm and 254 nm at 30 °C. Narrowly dispersed polystyrene standards from Aldrich were used as molecular weight calibrants. The number average and weighted average molecular weights were calculated from the chromatogram.

ESI-Mass analysis. The compounds were dissolved in CH₂Cl₂ (0.1 mg/mL). ESI-MS spectra were acquired on an Agilent 1100LC (API-ES)/MSD-VL instrument. Flow injection analysis with positive mode was applied, and the running solvent system is H₂O:CH₃CN:0.1%HCO₂H.

1.1 Synthesis of Monomers

Cyclobut-1-enecarboxylic Acid, 11. The acid (45% yield) was prepared according to the literature.^{111,404} ¹H-NMR (400 MHz) δ 10.23 (bs, 1H), 6.94 (t, J=1.2 Hz, 1H), 2.76 (t, J=3.2 Hz, 2H), 2.51 (td, J=3.2 Hz, 1.2 Hz, 2H). ¹³C-NMR (100 MHz, CDCl₃) δ 162.7, 146.5, 138.8, 51.2, 29.3, 27.3.

CB-Gly-OMe, 6a. The amide (42% yield) was prepared as previously described¹¹¹. ¹H-NMR (400 MHz) δ 6.66 (s, 1H), 6.04 (s, 1H), 4.10 (d, J=5.2 Hz, 2H), 3.77 (s, 3H), 2.73 (m, 2H), 2.47 (m, 2H). ¹³C-NMR (400 MHz, CDCl₃) δ 170.6, 162.7, 141.5, 140.9, 52.5, 40.9, 28.6, 26.5.

CB-Ala-OMe, 6b. H-Ala-OMe·HCl (0.61 mmol, 77 mg), 1-cyclobutenecarboxylic acid (0.51 mmol, 50 mg) and 1-ethyl-3-(3-dimethylaminopropyl) carbodiimide

hydrochloride (EDC·HCl) (0.61 mmol, 117 mg) were dissolved in 2 mL CH₂Cl₂. Diisopropylethyl amine (DIEA) (1.0 mmol, 181 μL) was added at 0 °C, and the reaction was stirred for 12 h at rt. The usual workup and chromatography (EtOAc:CH₂Cl₂/2:8) yielded amide **6b** (43 mg, 33%) as a white powder. ¹H-NMR (400 MHz) δ 6.65 (s, 1H), 6.11 (s, 1H), 4.66 (m, 1H), 3.76 (s, 3H), 2.72 (m, 2H), 2.47 (m, 2H), 1.44 (d, J=7.2, 3H). ¹³C-NMR (100 MHz, CDCl₃) δ 173.9, 162.3, 141.8, 141.2, 52.9, 48.2, 29.1, 26.8, 18.7. HRMS (ESI) calcd. for C₉H₁₄NO₃ [M+H]⁺ 184.0974, found 184.0973.

CB-CONHCH₂CH₂OMe, 6c. H₂CH₂CH₂OCH₃ (0.61 mmol, 46 mg), 1-cyclobutenecarboxylic acid (0.51 mmol, 50 mg) and EDC·HCl (0.61 mmol, 117 mg) were dissolved in 2 mL CH₂Cl₂. DIEA (1.0 mmol, 181 μL) was added at 0 °C, and the reaction was stirred for 12 h at rt. The usual workup and chromatography (EtOAc:CH₂Cl₂/3:7) yielded **6c** (29 mg, 44%) as a white powder. ¹H-NMR (400 MHz) δ 6.60 (s, 1H), 5.92 (s, 1H), 3.50 (m, 4H), 3.36 (s, 3H), 2.69 (m, 2H), 2.45 (m, 2H). ¹³C-NMR (100 MHz, CDCl₃) δ 162.9, 141.6, 140.6, 71.4, 59.0, 38.9, 28.7, 26.3. HRMS (ESI) calcd. for C₈H₁₄NO₂ [M+H]⁺ 156.1025, found 156.1028.

CB-Glu(OtBu)-OMe, 6d. H-Glu(OtBu)-OMe·HCl (0.61 mmol, 155 mg), 1-cyclobutenecarboxylic acid (0.51 mmol, 50 mg) and EDC·HCl (0.61 mmol, 117 mg) were dissolved in 2 mL CH₂Cl₂. DIEA (1.0 mmol, 181 μL) was added at 0 °C, and the reaction was stirred for 4 h at rt. The usual workup and chromatography (EtOAc:CH₂Cl₂/3:7) yielded **6d** (64 mg, 42%) as a white powder. ¹H-NMR (500 MHz) δ 6.67 (s, 1H), 6.44 (d, J=7 Hz, 1H), 4.65 (m, 1H), 3.78 (s, 3H), 2.74 (t, J=3.0 Hz, 2H), 2.48 (d, J=2.5 Hz, 2H), 2.34 (m, 2H), 2.17 (m, 1H), 2.03 (m, 1H), 1.46 (s, 9H). ¹³C-NMR (100 MHz, CD₂Cl₂) δ 172.8, 163.7, 142.3, 140.8, 81.1, 52.2, 51.7, 31.7, 28.5, 27.6, 26.5, 26.3. HRMS (ESI) calcd. for C₁₅H₂₄NO₅ [M+H]⁺ 298.1654, found 298.1663.

CB-CONHCH₂CH₂CH₂Ph(*p*-CH₃), 6e. NH₂CH₂CH₂CH₂Ph(*p*-CH₃) (0.61 mmol, 91 mg), 1-cyclobutenecarboxylic acid (0.51 mmol, 50 mg) and EDC·HCl (0.61 mmol, 117 mg) were dissolved in 2 mL CH₂Cl₂. DIEA (1.0 mmol, 181 μL) was added at 0 °C, and the reaction was stirred for 4 h at rt. The usual workup and chromatography

(acetone:CH₂Cl₂/1:9) yielded **6e** (29 mg, 25%) as a white powder. ¹H-NMR (400 MHz) δ 7.10 (d, J=1.2 Hz, 4H), 6.49 (s, 1H), 3.29 (m, 2H), 2.61-2.64 (m, 4H), 2.43 (m, 2H), 2.31 (s, 3H), 1.82 (m, 2H). ¹³C-NMR (100 MHz, CD₂Cl₂) δ 162.5, 142.1, 139.6, 138.8, 135.7, 129.4, 129.2, 128.5, 38.9, 33.1, 31.5, 29.9, 28.6, 26.2, 20.9. HRMS (ESI) calcd. for C₁₅H₂₀NO [M+H]⁺ 230.1545, found 230.1543.

CB-CON(Me)CH₂CO₂Me, 7a. NH(CH₃)CH₂CO₂CH₃·HCl (0.61 mmol, 85 mg), 1-cyclobutenecarboxylic acid (0.51 mmol, 50 mg), DMAP (0.10 mmol, 13 mg) and EDC·HCl (0.61 mmol, 117 mg) were dissolved in 2 mL CH₂Cl₂. DIEA (1.0 mmol, 181 μL) was added at 0 °C, and the reaction was stirred for 16 h at rt. The usual workup and chromatography (EtOAc:CH₂Cl₂/1:9) yielded **7a** (12 mg, 13%) as a white powder. ¹H-NMR (400 MHz) δ 6.53 (s, 1H), 6.33 (s, 0.47H), 4.22-4.11 (m, 2H+0.94 H), 3.77 (s, 0.94H), 3.74 (s, 2H), 3.22 (s, 3H), 3.03 (s, 1.41H), 2.85 (t, J=3.2 Hz, 2H), 2.78 (t, J=3.2 Hz, 0.94H), 2.48 (t, J=3.2 Hz, 2H), 2.45 (t, J=3.2 Hz, 0.94H). ¹³C-NMR (100 MHz, CDCl₃) δ 170.0, 169.9, 164.5, 164.1, 142.9, 141.1, 140.8, 52.3, 49.9, 37.1, 35.2, 31.6, 27.4. HRMS (ESI) calcd. for C₉H₁₄NO₃ [M+H]⁺ 184.0974, found 184.0975.

CB-CO-piperidine, 7b. Bis(2-oxo-3-oxazolidinyl)phosphinic chloride (BOP-Cl) (0.83 mmol, 211 mg) and 1-cyclobutenecarboxylic acid (0.75 mmol, 74 mg) were dissolved in 3 mL CH₂Cl₂. DIEA (0.75 mmol, 134 μL) was added at 0 °C, and the reaction was stirred for 2 h at rt. Piperidine (0.91 mmol, 77 mg) and diisopropylethyl amine (DIEA) (0.75 mmol, 134 μL) were added into the solution, which was kept stirring for another 20 h. The usual workup and chromatography (acetone:CH₂Cl₂/1:9) yielded **7b** (76 mg, 61%) as a white powder. ¹H-NMR (500 MHz) δ 6.40 (s, 1H), 3.62 (t, J=2.5 Hz, 4H), 2.85 (t, J=2.5 Hz, 2H), 2.49 (t, J=2.5 Hz, 2H), 1.69-1.58 (m, 6H). ¹³C-NMR (100 MHz, CDCl₃) δ 162.9, 141.5, 139.8, 47.0, 43.0, 32.0, 27.4, 24.8. HRMS (ESI) calcd. for C₁₀H₁₆NO [M+H]⁺ 166.1232, found 166.1233.

CB-CO₂Me, 8a. The methyl ester (50% yield) was prepared according to the literature.²⁵⁰⁻²⁵¹ ¹H-NMR (400 MHz) δ 6.74 (s, 1H), 3.68 (s, 3H), 2.69 (m, 2H), 2.46 (m,

2H). ^{13}C -NMR (100 MHz) δ 162.7, 146.5, 138.8, 51.2, 29.3, 27.3. HRMS (EI) calcd. for $\text{C}_6\text{H}_8\text{O}_2$ $[\text{M}]^+$ 112.05243, found 112.05228.

CB-CO₂CH₂CO₂Me, 8b. 1-cyclobutenecarboxylic acid (0.51 mmol, 50 mg) and $\text{BrCH}_2\text{CO}_2\text{CH}_3$ were dissolved in 2 mL dry CH_2Cl_2 . KI (0.10 mmol, 17 mg) and DIEA (0.61 mmol, 108 μL) were added into the solution at 0 °C. The reaction was stirred overnight at rt. The usual workup and chromatography ($\text{EtOAc}:\text{CH}_2\text{Cl}_2/5:95$) yielded **8b** (46 mg, 53%) as a sticky oil. ^1H -NMR (500 MHz) δ 6.92 (s, 1H), 4.69 (s, 2H), 3.79 (s, 3H), 2.80 (m, 2H), 2.53 (m, 2H). ^{13}C -NMR (100 MHz, CD_2Cl_2) δ 168.4, 161.1, 148.4, 137.8, 60.3, 52.2, 29.2, 27.6. HRMS (ESI) calcd. for $\text{C}_8\text{H}_{10}\text{O}_4\text{Na}$ $[\text{M}+\text{Na}]^+$ 193.0477, found 193.0485.

1-Cyclobutenecarboxylic chloride. 1-Cyclobutenecarboxylic acid (1.02 mmol, 100 mg) was dissolved in 1.5 mL dry CH_2Cl_2 . The solution was cooled to 0 °C and oxalyl dichloride (4.08 mmol, 345 μL) was added. The temperature of the solution was raised to rt, and the mixture was allowed to react for 1 h. The solvent was evaporated to generate 1-cyclobutenecarboxylic chloride as a viscous oil that was used immediately without further purification.

CB-CO₂Ph, 8c. Phenol (0.51 mmol, 48 mg) and triethylamine (1.02 mmol, 142 μL) were dissolved in 0.5 mL dry CH_2Cl_2 , and the solution was stirred at 0 °C for 45 min before being added to a vial containing the 1-cyclobutenecarboxylic chloride. The reaction mixture was stirred for 16 h at rt. The reaction was quenched with 1 N HCl, and was extracted with CH_2Cl_2 (30 mL). The CH_2Cl_2 solution was washed with 5 % NaHCO_3 (2 \times 10 mL), dried over Na_2SO_4 , concentrated by rotary evaporation, and then purified by flash column chromatography (100% CH_2Cl_2) to yield **8c** as a colorless oil (42 mg, 47%). ^1H -NMR (100 MHz) δ 7.42 (m, 2H), 7.28 (m, 1H), 7.14 (m, 2H), 7.02 (s, 1H), 2.88 (t, $J=3.0$ Hz, 2H), 2.60 (m, 2H). ^{13}C -NMR (100 MHz) δ 160.5, 150.8, 149.2, 138.3, 129.6, 125.9, 121.8, 29.5, 27.7. HRMS (EI) calcd. for $\text{C}_{11}\text{H}_{10}\text{O}_2$ $[\text{M}]^+$ 174.0679, found 174.0681.

CB-CO₂PFP, 8d. 2,3,4,5,6-Pentafluorophenol (0.51 mmol, 94 mg) and triethylamine (1.02 mmol, 142 μ L) were dissolved in 0.5 mL dry CH₂Cl₂, and the solution was kept stirring at 0 °C for 45 min before being added to a vial containing 1-cyclobutenecarboxylic chloride. And then the reaction was stirred overnight at rt. The reaction was quenched with 1 N HCl, and was extracted with 30 ml CH₂Cl₂. The CH₂Cl₂ solution was washed with 5 % NaHCO₃ twice, and dried over Na₂SO₄, concentrated by rotary evaporation, and then purified by flash column chromatography (100% CH₂Cl₂) to yield **8d** (59 mg, 44%) as a colorless oil. ¹H-NMR (500 MHz, CDCl₃) δ 7.12 (s, 1H), 2.86 (m, 2H), 2.60 (m, 2H). ¹³C-NMR (125 MHz, CDCl₃) δ 156.7, 152.6, 142.1, 140.3, 138.8, 138.3, 135.2, 53.3, 30.6, 29.2. HRMS (ESI) calcd. for C₁₁H₆O₂F₅ [M+H]⁺ 265.0293, found 265.0288.

CB-CO₂C₄H₈Cl, 8e. 4-Chlorobutanol (1.36 mmol, 148 mg) and triethylamine (2.72 mmol, 379 μ L) were dissolved in 1.0 mL dry CH₂Cl₂, and the solution was stirred at 0 °C for 45 min before being added to a vial containing 1-cyclobutenecarboxylic chloride. The reaction mixture was stirred for 16 h at rt. The CH₂Cl₂ solution was concentrated by rotary evaporation, and then purified by flash column chromatography (60% CH₂Cl₂/pentane) to yield **8e** as a colorless oil (98 mg, 38%). ¹H-NMR (500 MHz, CDCl₃) δ 6.73 (s, 1H), 4.11 (t, J=6.0 Hz, 2H), 3.54 (t, J=6.0 Hz, 2H), 2.68 (t, J=6.0 Hz, 2H), 2.43 (m, 2H), 1.81 (m, 4H). ¹³C NMR (100 MHz, CDCl₃) δ 162.27, 146.69, 138.71, 63.31, 44.58, 29.31, 29.20, 27.20, 26.20. HRMS (ESI) calcd. for C₉H₁₄ClO₂ [M+H]⁺ 189.0677, found 189.0674.

CB-CO₂C₄H₈NHBoc, 8f. *t*-Butyl 4-hydroxybutylcarbamate (1.22 mmol, 232 mg) and pyridine (2.04 mmol, 164 μ L) were dissolved in 1.0 mL dry CH₂Cl₂, and the solution was stirred at 0 °C for 45 min before being added to a vial containing 1-cyclobutenecarboxylic chloride. The reaction mixture was stirred for 16 h at rt. The CH₂Cl₂ solution was concentrated by rotary evaporation, and then purified by flash column chromatography (acetone:CH₂Cl₂/5:95) to yield **8f** as a colorless oil (170 mg, 62%). ¹H NMR (400 MHz, CDCl₃) δ 8.56 (s, 2H), 6.78 (s, 1H), 4.20 (t, J= 8Hz, 2H), 3.67 (m, 2H), 2.69 (m, 2H), 2.42 (m, 2H), 1.44 (m, 2H). ¹³C NMR (100 MHz, CDCl₃) δ

163.60, 161.92, 153.27, 147.52, 138.36, 83.38, 83.31, 79.54, 79.49, 77.54, 77.22, 76.90, 53.58, 39.75, 39.45, 37.33, 31.03, 29.21, 28.41. HRMS (ESI) calcd. for C₁₄H₂₄NO₄ [M+H]⁺ 270.1705, found 270.1693.

CB-CO₂C₂H₄N=C(NHBoc)₂, 8g. HOC₂H₄N=C(NHBoc)₂ (0.51 mmol, 155 mg) and pyridine (2.04 mmol, 164 μL) were dissolved in 1.0 mL dry CH₂Cl₂, and the solution was stirred at 0 °C for 45 min before being added to a vial containing 1-cyclobutenecarboxylic chloride. The reaction mixture was stirred for 16 h at rt. The CH₂Cl₂ solution was concentrated by rotary evaporation, and then purified by flash column chromatography (acetone:CH₂Cl₂/1:9) to yield **8g** as a colorless oil (90 mg, 46%). ¹H NMR (600 MHz, CDCl₃) δ 6.76 (s, 1H), 4.13 (t, J= 6 Hz, 2H), 3.15 (m, 2H), 2.71 (m, 2H), 2.46 (m, 2H), 1.68 (m, 2H), 1.55 (m, 2H), 1.43 (s, 9H). ¹³C NMR (100 MHz, CDCl₃) δ 162.31, 156.19, 146.68, 138.93, 64.16, 53.72, 40.46, 31.10, 29.32, 28.60, 27.27, 26.22. HRMS (ESI) calcd. for C₁₈H₃₀N₃O₆ [M+H]⁺ 384.2129, found 384.2128.

CB-CH₂OH, 12. 1-Cyclobutenemethanol, **12** was obtained by synthetic procedures previously described in the literature²⁵¹ with major modifications using DIBAL-H. Dry Et₂O (4.6 mL) was added to a solution of **7a** (302 mg, 2.70 mmol) in dry CH₂Cl₂ (1.8 mL) and the solution was cooled to -78 °C. DIBAL-H (1.2 mL, 6.74 mmol) was added dropwise to the solution. After stirring at -78 °C for 4 h, the reaction mixture was poured slowly into a mixture of Et₂O (18.0 mL) and saturated aqueous potassium sodium tartrate (70 mL). The mixture was stirred until both layers turned clear (30 min), and the Et₂O layer was separated. Additional Et₂O (18 mL × 2) was added to the separated aqueous solution to extract the product. The combined Et₂O extracts were dried over anhydrous Na₂SO₄. The solvent was carefully evaporated under reduced pressure (10 mm Hg) and the residue was further purified by vacuum distillation (25 °C, 0.01 mm Hg) using a Kugelrohr apparatus (92.4 mg, 45% yield). ¹H-NMR (400 MHz, CDCl₃) δ 5.93 (m, 1H), 4.09 (m, 2H), 2.52 (m, 2H), 2.42 (m, 2H), 1.37 (t, J=6.0 z, 1H); ¹³C-NMR (100 MHz, CDCl₃) δ 148.7, 128.8, 61.6, 29.6, 27.1.

CB-CH₂OAc, 9a. 3,3-Dimethylaminopyridine (DMAP) (29.1 mg, 0.238 mmol) and DIEA (1.18 mL, 7.14 mmol) were added to a solution of **12** (200 mg, 2.38 mmol) in dry CH₂Cl₂ (5.0 mL) and cooled to 0 °C. Acetyl chloride (339 μL, 4.76 mmol) was added dropwise to the solution at 0 °C. The reaction mixture was stirred at rt for 2 h. After the reaction was complete, iced H₂O (25 mL) was added slowly to the reaction mixture. The mixture was extracted with CH₂Cl₂ (50 mL × 2) and the combined organic extracts were washed with 1N aq HCl (25 mL × 2), 5% aq NaHCO₃ (25 mL) and 10% aq NaCl (25 mL). The organic layer was dried over anhydrous Na₂SO₄ and the solvent was evaporated under reduced pressure. The residue was purified by silica column chromatography with CH₂Cl₂ to afford **9a** (258 mg, 86%). The purified fractions were concentrated and diluted with dry CH₂Cl₂ and the solution was stored at -20 °C. ¹H-NMR (600 MHz, CDCl₃) δ 5.86 (s, 1H), 4.42 (s, 2H), 2.44 (b, 2H), 2.34 (b, 2H), 2.00 (s, 3H); ¹³C-NMR (100 MHz, CDCl₃) δ 170.71, 143.61, 131.53, 62.06, 30.05, 27.23, 20.76. HRMS (ESI) calcd. for C₇H₁₁O₂ [M+H]⁺ 127.0754, found 127.0752.

1-Methoxycyclohexene, 20b. Cyclohexanone (0.19 mol, 20 mL) and *p*-toluenesulfonic acid (0.97 mmol, 184 mg) were mixed together, and cooled to -20 °C. Trimethoxymethane (0.21 mol, 23 ml) was added to the solution. The reaction was allowed to react for 24 h at rt. The solution was distilled at 139 °C to yield **20b** (13 g, 61%) as a colorless liquid. ¹H-NMR (500 MHz, CDCl₃) δ 4.55 (t, J=3.5 Hz, 1H), 3.42 (s, 3 H), 2.00 (m, 4H), 1.62 (m, 2H), 1.50 (m, 2H). ¹³C-NMR (125 MHz, CDCl₃) δ 157.9, 95.5, 56.1, 30.3, 26.0, 25.5, 25.4. LC-MS (APCI): Peak time=1.59 min, m/z calcd for C₇H₁₃O [M+H]⁺ 113.09, found 113.08.

4-(Methoxymethyl)cyclohexene, 20d. 3-Cyclohexene-1-methanol (8.92 mmol, 1.00 g) and NaH (17.8 mmol, 428 mg) were mixed in THF (30 mL) at rt, and the THF solution was stirred for 1 h at rt. MeI (17.8 mmol, 1.10 mL) was added slowly into the above THF solution. After stirring for 16 h at rt, the solution was diluted with water (30 mL), and then was extracted with diethyl ether (30 mL × 2). The organic layer was dried over Na₂SO₄, was concentrated by rotary evaporation, and then was distilled to generate the final product **20d** as a colorless liquid (460 mg, 41%). ¹H-NMR (500 MHz) δ 5.68 (m,

2H), 3.36 (s, 3H), 3.28 (dd, J=6.5 Hz, J=4 Hz), 2.06-2.14 (m, 3H), 1.92 (m, 1H), 1.83 (m, 1H), 1.75 (m, 1H), 1.29 (m, 1H). ¹³C-NMR (100 MHz) δ 127.2, 126.1, 78.0, 58.9, 34.0, 28.6, 25.8, 24.7. LC-MS (APCI): peak time = 1.59 min, M/z calcd for C₈H₁₅O [M+H]⁺ 127.11, found 127.10.

4,5-Bis(methoxymethyl)cyclohexene, 20e. Cyclohexene **21** (19.7 mmol, 3.0 g) was dissolved in dry THF (25 mL), and the solution was cooled to 0 °C. The THF solution (25 mL) of LiAlH₄ (99 mmol, 3.8 g) was added dropwise to the above solution at 0 °C. After stirring at 0 °C for 4 h, the reaction mixture was poured slowly into the saturated aqueous Na₂SO₄ (70 mL). The mixture was stirred until all white solid precipitated. The solution was filtered, and extracted with EtOAc (60 mL × 3). The combined EtOAc extracts were dried over anhydrous Na₂SO₄, and concentrated to yield 4-Cyclohexene-1,2-diyl dimethanol **22** as a colorless oil. ¹H NMR (600 MHz, CDCl₃) δ 5.60 (s, 2H), 3.74 (m, 2H), 3.60 (m, 2H), 2.48 (s, 2H), 2.17-2.01 (m, 6H). Cyclohexene **22** (2.8 mmol, 398 mg) and KOH (19.8 mmol, 1.1 g) were dissolved in THF/H₂O (4 mL, v/v = 3/1). Me₂SO₄ (13.9 mmol, 1.8 g) was added to the above solution dropwise. The solution was heated at 65 °C for 8 h. The mixture was filtered, and the supernatant was diluted in H₂O (10 mL). The aqueous solution was extracted with Et₂O (30 mL × 3). The combined Et₂O extracts were dried over anhydrous Na₂SO₄, concentrated and purified by silica column chromatography with (acetone:CH₂Cl₂/5:95) to afford **20e** (166 mg, 35% yield). ¹H NMR (600 MHz, CDCl₃) δ 5.58 (s, 2H), 3.35-3.24 (m, 10H), 2.12-1.89 (m, 6H). ¹³C-NMR (100 MHz, CDCl₃) δ 125.6, 73.9, 58.6, 34.6, 27.4.

4-Cyclohexene-1,2-dicarboxylic acid, 23. The acid (99% yield) was prepared according to the literature.⁴⁰⁵ ¹H NMR (400 MHz, CD₃OD) δ 5.64 (s, 2H), 4.94 (s, 2H), 3.00 (m, 2H), 2.52-2.34 (m, 4H). ¹³C NMR (100 MHz, CD₂Cl₂) δ 176.8, 126.0, 40.2, 26.5.

1,1'-(4-Cyclohexene-1,2-diyl)bis(N,N-dimethylmethanamine), 20f. The amine (75% yield) was prepared according to the literature.⁴⁰⁵ ¹H NMR (600 MHz, CDCl₃) δ 5.53 (s, 2H), 2.17-1.82 (m, 18H). ¹³C NMR (100 MHz, CDCl₃) δ 126.2, 60.6, 33.1, 28.3.

*N*¹, *N*²-**dioctyl-4-cyclohexene-1,2-dicarboxamide, 20g**. n-Octylamine (5.8 mmol, 748 mg), cyclohexene **21** (2.6 mmol, 400 mg) and EDC·HCl (5.8 mmol, 1.1 g) were dissolved in dry CH₂Cl₂ (7 mL). DIEA (5.8 mmol, 1.0 L) was added at 0 °C, and the reaction was stirred for 12 h at rt. The usual workup and chromatography (acetone: CH₂Cl₂/1:9) yielded **20g** (833 mg, 81%) as a white powder. ¹H-NMR (600 MHz, CDCl₃) δ 5.51 (s, 2H), 2.46 (m, 4H), 2.00-1.81 (m, 6H), 1.37-1.19 (m, 24H), 0.78 (t, J = 0.6 Hz, 6H).

N,N'-(**4-cyclohexene-1,2-diylbis(methylene)**)**dioctan-1-amine, 20h**. The amine (95% yield) was prepared according to the similar procedure described in the literature.⁴⁰⁵ ¹H NMR (600 MHz, CDCl₃) δ 5.75-5.63 (m, 2H), 3.34-2.91 (m, 4H), 2.57-2.47 (m, 4H), 2.35-1.78 (m, 6H), 1.50-1.29 (m, 24H), 0.90 (t, J = 0.6 Hz, 6H).

N-propyl 3-cyclohexenecarboxamide, 20k. 3-Cyclohexenecarboxylic acid (0.71 mmol, 90 mg), NH₂CH₂CH₂CH₃ (0.86 mmol, 70 μL) and EDC·HCl (0.86 mmol, 164 mg) were dissolved in CH₂Cl₂ (3mL). DIEA (1.43 mmol, 252 μL) was added at 0 °C, and the reaction was stirred for 16 h at rt. The usual workup and chromatography (acetone/CH₂Cl₂/10:90) yielded N-propylcyclohex-3-enecarboxamide **20k** as a white powder (65 mg, 55%). ¹H NMR (400 MHz, CDCl₃) δ 5.64 (m, 3H), 3.17 (dd, J= 8 Hz, J=8 Hz, 2H), 2.30-1.93 (m, 5H), 1.87-1.81 (m, 1H), 1.72-1.59 (m, 1H), 1.43 (m, 2H), 0.87 (t, J= 8 Hz, 3H). ¹³C NMR (100 MHz, CDCl₃) δ 175.93, 126.94, 125.61, 41.52, 41.22, 28.35, 25.97, 24.80, 23.07, 11.49. HRMS (ESI) calcd. for C₁₀H₁₈NO [M+H]⁺ 168.1383, found 168.1379.

N-octyl 3-cyclohexenecarboxamide, 20m. 3-Cyclohexenecarboxylic acid (1.11 mmol, 140 mg), NH₂-octyl (1.33 mmol, 220 μL) and EDC·HCl (1.33 mmol, 255 mg) were dissolved in CH₂Cl₂ (3mL). DIEA (2.22 mmol, 393 μL) was added at 0 °C, and the reaction was stirred for 16 h at rt. The usual workup and chromatography (acetone/CH₂Cl₂/10:90) yielded N-octylcyclohex-3-enecarboxamide **20m** as a white

powder (215 mg, 82%). ^1H NMR (400 MHz, CDCl_3) δ 5.77 (s, 1H), 5.63 (s, 2H), 3.18 (dd, $J=8$ Hz, $J=8$ Hz, 2H), 2.33-2.00 (m, 5H), 1.86-1.82 (s, 1H), 1.70-1.60 (m, 1H), 1.43 (m, 2H), 1.22 (m, 10H), 0.82 (t, $J=8$ Hz, 3H). ^{13}C NMR (100 MHz, CDCl_3) δ 175.89, 126.88, 125.59, 41.46, 39.56, 31.91, 29.81, 29.39, 29.33, 28.32, 27.05, 25.93, 24.79, 22.75, 14.19. HRMS (ESI) calcd. for $\text{C}_{15}\text{H}_{28}\text{NO}$ $[\text{M}+\text{H}]^+$ 238.2165, found 238.2160.

1-Methoxycyclopentene, 29b. Cyclopentanone (0.23 mol, 20 mL) and *p*-toluenesulfonic acid (2.3 mmol, 430 mg) were mixed together, and cooled to -20 °C. Trimethoxymethane (0.27 mol, 30 ml) was added to the solution. The temperature was raised to rt, and the reaction was allowed to react for 24 h. Then the solution was kept refluxing for 3 h. The solution was distilled at 110 °C to yield **29b** (13 g, 58%) as a colorless liquid. ^1H -NMR (500 MHz, CDCl_3) δ 4.45 (m, 1H), 3.59 (s, 3H), 2.31 (m, 4H), 1.85 (m, 2H). ^{13}C -NMR (125 MHz, CDCl_3) δ 161.2, 94.0, 56.9, 32.0, 29.1, 21.6.

CB-CONHC₄H₈Cl, 30. $\text{H}_2\text{NCH}_2\text{CH}_2\text{CH}_2\text{CH}_2\text{OH}$ (2.24 mmol, 200 mg) was dissolved in benzene (2 mL). SOCl_2 (500 μL) was added slowly into the solution to get white precipitate. The solution was stirred at rt for 2h. The precipitate was filtered, washed with benzene and dried under vacuum to generate $\text{H}_2\text{NCH}_2\text{CH}_2\text{CH}_2\text{CH}_2\text{Cl}\cdot\text{HCl}$ (320 mg, 99%). $\text{H}_2\text{NCH}_2\text{CH}_2\text{CH}_2\text{CH}_2\text{Cl}\cdot\text{HCl}$ (2.24 mmol, 320 mg), 1-cyclobutenecarboxylic acid (1.12 mmol, 110 mg) and $\text{EDC}\cdot\text{HCl}$ (1.35 mmol, 258 mg) were dissolved in CH_2Cl_2 (10 mL). Pyridine (4.49 mmol, 362 μL) was added at 0 °C, and the reaction was stirred for 16 h at rt. The workup (washed with 1N HCl twice, and then washed with brine twice) and chromatography (acetone: CH_2Cl_2 /10:90) yielded **30** as a viscous oil (98 mg, 47%). ^1H NMR (400 MHz, CDCl_3) δ 6.56 (s, 1H), 5.79 (s, 1H), 3.52 (t, $J=8$ Hz, 2H), 3.28 (m, 2H), 2.63 (m, 2H), 2.41 (m, 2H), 1.75 (m, 2H), 1.65 (m, 2H). ^{13}C NMR (100 MHz, CDCl_3) δ 162.98, 141.55, 140.46, 44.75, 38.40, 29.96, 28.63, 27.22, 26.29. HRMS (ESI) calcd. for $\text{C}_9\text{H}_{15}\text{ClNO}$ $[\text{M}+\text{H}]^+$ 188.0837, found 188.0835.

(Z)-5-Bromocyclooctene, 31. The compound (75% yield) was prepared according to the literature.⁴⁰⁶ ^1H NMR (500 MHz, CDCl_3) δ 5.65 (m, 2H), 4.33 (m, 1H), 2.47-1.54 (m, 11H).

(Z)-4-Cyclooctenecarboxylic acid, 33. **(Z)-4-Cyclooctenecarboxylic acid 33** (60% yield) was prepared according to the literature.³⁴⁸ ¹H NMR (500 MHz, CDCl₃) δ 11.67 (s, 1H), 5.69 (m, 2H), 2.51-1.41 (m, 11H). ¹³C NMR (125 MHz, CDCl₃) δ 184.6, 130.8, 129.5, 43.4, 31.6, 29.4, 27.9, 26.2, 24.2.

(Z)-4-Chlorobutyl 4-cyclooctenecarboxylate, 34. 4-Cyclooctenecarboxylic acid (1.04 mmol, 160 mg) was dissolved in 6 mL dry CH₂Cl₂. The solution was cooled to 0 °C and oxalyl dichloride (4.16 mmol, 356 μL) was added. The temperature of the solution was raised to rt, and the mixture was allowed to react for 1 h. The solvent was evaporated to generate a viscous oil. 4-chlorobutanol (1.04 mmol, 113 mg) and triethylamine (2.07 mmol, 287 μL) were dissolved in 6 mL dry CH₂Cl₂, and the solution was stirred at 0 °C for 45 min before being added to a vial containing 4-cyclooctenecarboxylic chloride. The reaction mixture was stirred for 16 h at rt. The CH₂Cl₂ solution was concentrated by rotary evaporation, and then purified by flash column chromatography (CH₂Cl₂) to yield **34** as a colorless oil (200 mg, 79%). ¹H NMR (500 MHz, CDCl₃) δ 5.64 (m, 2H), 4.03 (m, 2H), 3.51 (t, J = 15 Hz, 2H), 2.43-1.36 (m, 15H). ¹³C NMR (125 MHz, CDCl₃) δ 177.5, 130.4, 129.6, 63.6, 44.6, 43.5, 31.6, 29.4, 27.8, 25.9, 24.0. HRMS (ESI) calcd. for C₁₃H₂₂ClO₂ [M+H]⁺ 245.1303, found 245.1298.

I.2 NMR Tube ROMP/ROM/AROMP Reactions

General Procedure for NMR Tube ROMP Reactions. An NMR tube was evacuated for 15 min, and then was purged with Ar for another 15 min. Under an Ar atmosphere, a solution of monomer in CD₂Cl₂ (300 μL) was added to the NMR tube. A solution of precatalyst (H₂IMes)(3-Br-Py)₂(Cl)₂Ru=CHPh in CD₂Cl₂ (300 μL) was added to the NMR tube. The stoichiometries of the reactions are indicated in Table 6-1. After complete mixing of the solution, the NMR tube was placed into the 400 MHz, 500 MHz or 600 MHz NMR spectrometer, and the reaction was monitored for several hours at 25 °C until almost all of the monomer had been consumed. Then the reaction was quenched with ethylvinyl ether (50 μL), and was monitored for an additional 1 h.

Polymer	Monomer (0.06 mmol)	Catalyst 5
6a ₁₀	6a	0.006 mmol
6b ₁₀	6b	0.006 mmol
6c ₁₀	6c	0.006 mmol
6d ₁₀	6d	0.006 mmol
6e ₁₀	6e	0.006 mmol
n/a	7a	0.006 mmol
n/a	7b	0.006 mmol
n/a	8a	0.006 mmol
8b ₁	8b	0.06 mmol
n/a	8b	0.006 mmol
9a ₁₀	9a	0.006 mmol
9b ₁₀	9b	0.006 mmol

Table 6-1. ROMP reactions monitored by ¹H-NMR spectroscopy.

ROM of 8a: 13a and 14a. A solution of **8a** (40.0 mg, 0.357 mmol) in dry CH₂Cl₂ (4 mL) was added to a solution of precatalyst **5** (474 mg, 0.536 mmol) in dry CH₂Cl₂ (4 mL) at rt. The solution was stirred at rt for 20 h and ethylvinyl ether (5 mL, 52.2 mmol) was added to the reaction mixture. After 60 min, the solvent was evaporated and the residue was purified by silica column chromatography with CH₂Cl₂. The purified fractions were evaporated to afford the product **13a** and **14a** (42.1 mg, 55% yield) with *E/Z*molar ratio 2.3/1. ¹H-NMR (600 MHz, CD₂Cl₂) 1-mer **13a** *Z*-isomer δ 7.36-7.19 (m, 5H), 6.47 (d, J=12.6 Hz, 1H), 6.15 (s, 1H), 5.68 (dt, J=11.4, 7.8 Hz, 1H), 5.60 (s, 1H), 3.72 (s, 3H), 2.50 (m, 2H), 2.43 (m, 2H). 1-mer **14a** *E*-isomer δ 7.36-7.19 (m, 5H), 6.42 (d, J=16.2 Hz, 1H), 6.25 (dt, J=22.8, 6.0 Hz, 1H), 6.17 (s, 1H), 5.60 (s, 1H), 3.75 (s, 3H), 2.50 (m, 2H), 2.43 (m, 2H). ¹³C-NMR (100 MHz, CD₂Cl₂) 1-mer **13a** *Z*-isomer δ 167.9, 140.6, 138.1, 132.1, 130.8, 130.0, 129.3, 128.6, 127.2, 125.5, 52.2, 32.6, 28.0. 1-mer **14a**

E-isomer δ 168.0, 140.7, 138.1, 131.0, 130.3, 129.0, 128.7, 127.5, 126.5, 52.2, 32.4, 32.3. LC-MS (APCI): Peak time=2.18 min, m/z calcd for $C_{14}H_{16}O_2$ $[M+H]^+$ 217.12, found 217.21, m/z calcd for $C_{14}H_{15}NaO_2$ $[M+Na]^+$ 239.10, found 239.26, m/z calcd for $C_{13}H_{13}O$ $[M-CH_3O]^+$ 185.10, found 185.14, m/z calcd for $C_{12}H_{13}$ $[M-CO_2CH_3]^+$ 157.11, found 157.15.

ROMP of 9a: 9a₁₀. A solution of **9a** (7.6 mg, 0.06 mmol) in dry CD_2Cl_2 (300 μ L) was added to a solution of precatalyst **5** (5.3 mg, 0.006 mmol) in dry CD_2Cl_2 (300 μ L) at rt. The reaction was monitored by NMR spectroscopy at rt for 1.5 h and ethylvinyl ether (300 μ L, 3.13 mmol) was added to the reaction mixture. After 30 min, the solvent was evaporated and the residue was purified by silica column chromatography with 2% MeOH/ CH_2Cl_2 . The purified fractions were evaporated to afford the product **9a₁₀** (6 mg, 73% yield). 1H -NMR (600 MHz, CD_2Cl_2) δ 7.34-7.20 (m, 5H), 6.58 (m, 0.4H), 6.42(m, 0.6H), 6.24 (m, 0.6H), 5.43 (m, 10H), 5.03 (m, 1H), 4.94 (m, 1H), 4.66-4.48 (, 20H), 2.35-1.92 (m, 70H).

Intermediate-11 and Homopolymer-11. Cyclobutene **30** (0.048 mmol) and **5** (0.012 mmol) were mixed in CD_2Cl_2 (1.2 mL) in an NMR tube. The reaction was maintained for 4 h to reach 93% completion before the addition of ethylvinyl ether (300 μ L). After 30 min, the solvent was evaporated and the residue was purified by silica column chromatography with 2% MeOH/ CH_2Cl_2 . The purified fractions were evaporated to afford the product **Intermediate-11** (7.7 mg, 75% yield). 1H -NMR (500 MHz, CD_2Cl_2) δ 7.43-7.04 (m, 9H), 6.35 (b, 4H), 3.59 (b, 8H), 3.28 (b, 8H), 2.39-1.51 (m, 32H). **Intermediate-11** and trimethylamine aqueous solution (45% wt, 1 mL) were mixed in acetonitrile (2 mL). The solution was heated to 70°C for 4 h. The crude solution was evaporated to remove solvent to provide **Homopolymer-11** as a brown powder. 1H NMR (600 MHz, D_2O) δ 7.51-7.19 (m, 5H), 6.17 (b, 4H), 3.42 (b, 8H), 3.31 (b, 8H), 3.18 (b, 36H), 2.42-2.26 (m, 16H), 1.87-1.63 (m, 16H).

Intermediate-12 and Homopolymer-12. Cyclobutene **30** (0.096 mmol) and **5** (0.012 mmol) were mixed in CD_2Cl_2 (1.2 mL) in an NMR tube. The reaction was

maintained for 4 h to reach 92% completion before the addition of ethylvinyl ether (300 μL). After 30 min, the solvent was evaporated and the residue was purified by silica column chromatography with 2% MeOH/ CH_2Cl_2 . The purified fractions were evaporated to afford the product **Intermediate-12** (14 mg, 74% yield). $^1\text{H-NMR}$ (600 MHz, CD_2Cl_2) δ 7.42-6.98 (m, 13H), 6.18 (b, 8H), 3.58 (b, 16H) 3.25 (b, 16H), 2.38-1.65 (m, 128H). $^{13}\text{C-NMR}$ (125 MHz, CDCl_3) δ 170.8, 136.1, 134.7, 134.4, 130.3, 129.0, 128.8, 128.3, 44.9, 39.4, 30.1, 27.9, 27.2, 26.8. **Intermediate-12** and trimethylamine aqueous solution (45% wt, 1 mL) were mixed in acetonitrile (2 mL). The solution was heated to 70°C for 4 h. The crude solution was evaporated to remove solvent to provide **Homopolymer-12** as a brown powder. $^1\text{H NMR}$ (600 MHz, D_2O) δ 7.51-7.20 (m, 5H), 6.18 (b, 8H), 3.42 (b, 16H), 3.31 (b, 16H), 3.19 (b, 72H), 2.43-2.18 (m, 32H), 1.87-1.64 (m, 32H).

Intermediate-13 and Homopolymer-13. Cyclooctene **34** (0.048 mmol) and **5** (0.012 mmol) were mixed in CD_2Cl_2 (1.2 mL) in an NMR tube. The reaction was maintained for 4 h to reach 93% completion before the addition of ethylvinyl ether (300 μL). After 30 min, the solvent was evaporated and the residue was purified by silica column chromatography with 5% acetone/ CH_2Cl_2 . The purified fractions were evaporated to afford the product **Intermediate-13** (9.9 mg, 76% yield). $^1\text{H NMR}$ (500 MHz, CD_2Cl_2) δ 7.36-7.20 (m, 5H), 6.43 (m, 1H), 6.23 (m, 1H), 5.81 (m, 1H), 5.41 (b, 8H), 5.03 (m, 1H), 4.12 (m, 8H), 3.61 (m, 8H), 2.37-1.27 (m, 60H). **Intermediate-13** and trimethylamine aqueous solution (45% wt, 1 mL) were mixed in acetonitrile (2 mL). The solution was heated to 70°C for 4 h. The crude solution was evaporated to remove solvent to provide **Homopolymer-13** as a brown powder. $^1\text{H NMR}$ (600 MHz, D_2O) δ 7.37 (b, 5H), 6.41 (b, 1H), 6.26 (b, 1H), 5.88 (b, 1H), 5.45 (b, 8H), 5.06 (b, 1H), 4.21 (b, 8H), 3.42 (b, 8H), 3.18 (b, 36H), 2.54-1.38 (m, 60H).

Intermediate-14 and Homopolymer-14. Cyclobutene **34** (0.096 mmol) and **5** (0.012 mmol) were mixed in CD_2Cl_2 (1.2 mL) in an NMR tube. The reaction was maintained for 4 h to reach 92% completion before the addition of ethylvinyl ether (300 μL). After 30 min, the solvent was evaporated and the residue was purified by silica column chromatography with 2% MeOH/ CH_2Cl_2 . The purified fractions were evaporated

to afford the product **Intermediate-14** (19.5 mg, 78% yield). ^1H NMR (500 MHz, CD_2Cl_2) δ 7.36-7.15 (m, 5H), 6.43 (m, 1H), 6.24 (m, 1H), 5.81 (m, 1H), 5.41 (b, 16H), 5.02 (m, 1H), 4.11 (m, 16H), 3.60 (m, 16H), 2.37-1.26 (m, 120H). ^{13}C NMR (125 MHz, CDCl_3) δ 176.4, 130.8, 130.4, 129.9, 129.4, 129.0, 126.2, 63.7, 45.4, 33.0, 32.2, 30.8, 29.6, 26.7. **Intermediate-14** and trimethylamine aqueous solution (45% wt, 1 mL) were mixed in acetonitrile (2 mL). The solution was heated to 70°C for 4 h. The crude solution was evaporated to remove solvent to provide **Homopolymer-14** as a brown powder. ^1H NMR (600 MHz, D_2O) δ 7.39 (b, 5H), 6.41 (b, 1H), 6.27 (b, 1H), 5.90 (b, 1H), 5.47 (b, 16H), 5.07 (b, 1H), 4.23 (b, 16H), 3.41 (b, 16H), 3.18 (b, 72H), 2.47-1.40 (m, 120H).

General Procedure for NMR Tube AROMP Reactions. The NMR tube was evacuated under high vacuum for 15 min, and then was purged with Ar gas for another 15 min. Under an Ar atmosphere, a solution of monomer **A** (1-cyclobutenecarboxylate ester) in CD_2Cl_2 (300 μL) was added to the NMR tube. Then a solution of ruthenium precatalyst in CD_2Cl_2 (300 μL) was added to the NMR tube. After complete mixing of the solution, the NMR tube was spun for 4-30 min at 25 °C in the NMR spectrometer (400, 500 or 600 MHz) until the precatalyst had reacted. Then monomer **B** (cyclohexene or cyclopentene derivatives) in CD_2Cl_2 (300 μL) was added to the NMR tube. After all of monomer **A** was converted, the reaction was quenched with ethylvinyl ether (50 μL) and was stirred for 1 h.

(8a-20a)₁₀. Cyclobutene **8a** (0.06 mmol), cyclohexene **20a** (0.12 mmol) and **5** (0.006 mmol) were mixed in CD_2Cl_2 (600 μL) in an NMR tube. The reaction was maintained for 3 h to reach 98% completion. $M_n^{\text{calc}} = 2044$. $M_n^{\text{GPC}} = 376$. $M_w^{\text{GPC}} = 962$. PDI = 2.6.

(8a-20a)₂₀. Cyclobutene **8a** (0.12 mmol), cyclohexene **20a** (0.24 mmol) and **5** (0.006 mmol) were mixed in CD_2Cl_2 (600 μL) in an NMR tube. The reaction was maintained for 3 h to reach 98% completion. $M_n^{\text{calc}} = 3984$. $M_n^{\text{GPC}} = 668$. $M_w^{\text{GPC}} = 1816$. PDI = 2.7.

(8a-20a)₂₀[3]. Cyclobutene **8a** (0.12 mmol), cyclohexene **20a** (0.24 mmol), PPh₃ (0.12 mmol) and **3** (0.006 mmol) were mixed in CD₂Cl₂ (600 μL) in an NMR tube at 39 °C. The reaction was maintained for 4 h to reach 0% completion.

Cyclobutene **8a** (0.12 mmol), cyclohexene **20a** (0.24 mmol), PPh₃ (0.12 mmol) and **3** (0.006 mmol) were mixed in THF-D₈ (600 μL) in an NMR tube at 50 °C. The reaction was maintained for 4 h to reach 0% completion.

(8a-20a)₅₀. Cyclobutene **8a** (0.30 mmol), cyclohexene **20a** (0.60 mmol) and **5** (0.006 mmol) were mixed in CD₂Cl₂ (600 μL) in an NMR tube. The reaction was maintained for 3 h to reach 98% completion. $M_n^{\text{calc}} = 9804$. $M_n^{\text{GPC}} = 652$. $M_w^{\text{GPC}} = 2634$. PDI = 4.0.

(8a-20a)₅₀[3]. Cyclobutene **8a** (0.30 mmol), cyclohexene **20a** (0.60 mmol) and **3** (0.006 mmol) were mixed in CD₂Cl₂ (600 μL) in an NMR tube at 39 °C. The reaction was maintained for 4 h to reach 43% completion. $M_n^{\text{calc}} = 3984$. $M_n^{\text{GPC}} = 1584$. $M_w^{\text{GPC}} = 4530$. PDI = 2.9.

Cyclobutene **8a** (0.30 mmol), cyclohexene **20a** (0.60 mmol) and **3** (0.006 mmol) were mixed in THF-D₈ (600 μL) in an NMR tube at 50 °C. The reaction was maintained for 4 h to reach 16% completion.

(8a-20a)₅₀[26]. Cyclobutene **8a** (0.30 mmol), cyclohexene **20a** (0.60 mmol) and **26** (0.006 mmol) were mixed in CD₂Cl₂ (600 μL) in an NMR tube at rt. The reaction was maintained for 3 h to reach 0% completion.

(8a-20a)₁₀₀. Cyclobutene **8a** (0.60 mmol), cyclohexene **20a** (1.20 mmol) and **5** (0.006 mmol) were mixed in CD₂Cl₂ (600 μL) in an NMR tube. The reaction was maintained for 3 h to reach 97% completion. The crude solution was evaporated to remove solvent, and the residue was purified by flash column chromatography (acetone:CH₂Cl₂/3:97) to provide polymer **(8a-20a)₁₀₀** (72 mg, 62 %). According to GPC chromatographic analysis, the copolymer had a bimodal molecular weight distribution. $M_n^{\text{calc}} = 19504$. $M_n^{\text{GPC}} = 1869$. $M_w^{\text{GPC}} = 10872$. PDI = 5.8.

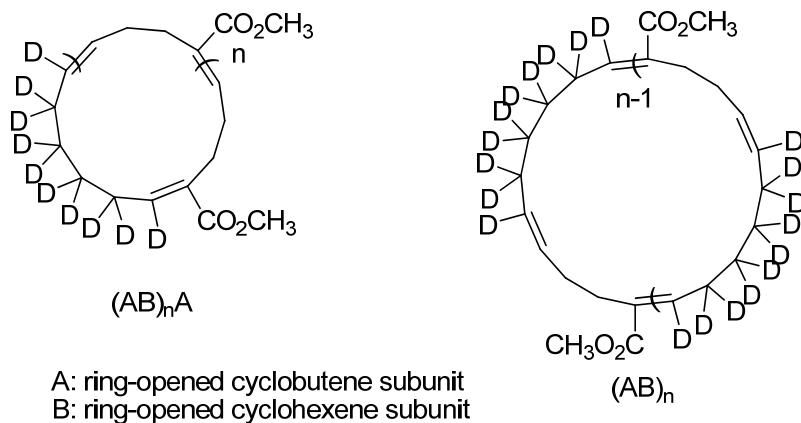
Cyclobutene **8a** (0.60 mmol), cyclohexene **20a** (1.20 mmol) and **5** (0.003 mmol) were mixed in CD₂Cl₂ (600 μL) in an NMR tube. The reaction was maintained for 1.5 h to reach 50% completion. DP = 50. According to GPC chromatographic analysis, the copolymer had a bimodal molecular weight distribution. $M_n^{\text{calc}} = 29010$. The overall GPC result: $M_n^{\text{GPC}} = 3201$, $M_w^{\text{GPC}} = 20106$, PDI = 5.7. Peak **A**: $M_n^{\text{GPC}} = 25088$, $M_w^{\text{GPC}} = 28697$, PDI = 1.1. Peak **B**: $M_n^{\text{GPC}} = 1383$, $M_w^{\text{GPC}} = 2143$, PDI = 1.5.

Cyclobutene **8a** (1.20 mmol), cyclohexene **20a** (2.40 mmol) and **5** (0.006 mmol) were mixed in CD₂Cl₂ (600 μL) in an NMR tube. The reaction was maintained for 4 h to reach 34% completion. $M_n^{\text{calc}} = 19504$. $M_n^{\text{GPC}} = 1892$. $M_w^{\text{GPC}} = 7181$. PDI = 3.8.

(8a-20a)₂₀₀. Cyclobutene **8a** (1.20 mmol), cyclohexene **20a** (2.40 mmol) and **5** (0.006 mmol) were mixed in CD₂Cl₂ (600 μL) in an NMR tube. The reaction was maintained for 6 h to reach 74% completion. The crude solution was evaporated to remove solvents, and was purified by flash column chromatography (acetone:CH₂Cl₂/3:97) to generate polymer **(8a-20a)₂₀₀** (96 mg, 41 %). DP = 74. According to GPC chromatographic analysis, the copolymer had a bimodal molecular weight distribution (Figure S6). $M_n^{\text{calc}} = 29010$. The overall GPC result: $M_n^{\text{GPC}} = 7749$, $M_w^{\text{GPC}} = 18501$, PDI = 2.4. The individual peaks were fitted by using OriginPro 7.5 (OriginLab Corp.), and the molecular weight and PDI data of each peak were calculated. Peak **A**: $M_n^{\text{GPC}} = 17703$, $M_w^{\text{GPC}} = 20388$, PDI = 1.2. Peak **B**: $M_n^{\text{GPC}} = 1038$, $M_w^{\text{GPC}} = 3539$, PDI = 3.4.

(8a-20a-D₁₀)₂₀-[25]. Cyclobutene **8a** (0.12 mmol), cyclohexene **20a-D₁₀** (0.24 mmol) and **25** (0.006 mmol) were mixed in CD₂Cl₂ (600 μL) in an NMR tube at rt. The reaction was maintained for 9 h to reach 89% completion. The crude solution was evaporated to remove solvent, and the residue was purified by flash column chromatography (acetone:CH₂Cl₂/3:97) to provide polymer **(8a-20a-D₁₀)₂₀-[25]** (11 mg, 44%). ¹H-NMR (500 MHz, CD₂Cl₂) δ 6.79 (m, 2H), 5.40 (s, 18H), 3.71 (s, 60H), 2.34-2.07 (m, 80H).

(8a-20a-D₁₀)₂₀ (24 equiv. of 20a-D₁₀). Cyclobutene **8a** (0.12 mmol), cyclohexene **20a-D₁₀** (0.144 mmol) and **5** (0.006 mmol) were mixed in CD₂Cl₂ (600 μL) in an NMR tube. The reaction was maintained for 3 h to reach 97% completion. The solvent was evaporated, and the residue was purified by flash column chromatography (acetone:CH₂Cl₂/4:96) to provide polymer **(8a-20a-D₁₀)₂₀** as a sticky oil (17.4 mg, 71%). ¹H (500 MHz, CD₂Cl₂) δ 7.41-7.21(m, 5H), 6.78 (t, J=2.5 Hz, 2H), 6.39(m, 1H), 6.27(m, 1H), 5.43 (m, 20H), 5.06-5.02 (d, J=2.0 Hz, 1H), 4.98-4.97(d, J=0.5 Hz, 1H), 3.72 (s, 60H), 2.36-2.09 (m, 80H). polymer **(8a-20a-D₁₀)₂₀** was further purified by flash chromatography (acetone:CH₂Cl₂/4:96) to provide cyclic polymer **cyc-(8a-20a-D₁₀)₂₀** as a sticky oil (3.3 mg). Polymer **cyc-(8a-20a-D₁₀)₂₀** was characterized by ¹H-NMR spectroscopy and its structures were shown below. ¹H-NMR (500 MHz, CDCl₃) δ 6.84 (t, J=1.0 Hz, 1H) 5.48-5.36 (m, 5H), 3.75 (m, 18H), 2.47-2.12 (m, 24H).



(8a-20a-D₁₀)₂₀ (40 equiv. of 20a-D₁₀). Cyclobutene **8a** (0.12 mmol), cyclohexene **20a-D₁₀** (0.24 mmol) and **5** (0.006 mmol) were mixed in CD₂Cl₂ (600 μL) in an NMR tube. The reaction was maintained for 3 h to reach 97% completion.

(8a-20a-D₁₀)₂₀ (160 equiv. of 20a-D₁₀). Cyclobutene **8a** (0.12 mmol), cyclohexene **20a-D₁₀** (0.96 mmol) and **5** (0.006 mmol) were mixed in CD₂Cl₂ (600 μL) in an NMR tube. The reaction was maintained for 3 h to reach 97% completion.

(8c-20a)₂₀. Cyclobutene **8c** (0.12 mmol), cyclohexene **20a** (0.24 mmol) and **5** (0.006 mmol) were mixed in CD₂Cl₂ (600 μL) in an NMR tube. The reaction was maintained for 4 h to reach 96% completion. The solvent was removed from the crude mixture in vacuo and the residue was purified by flash column chromatography (100% CH₂Cl₂) to provide polymer **(8c-20a)₂₀** (16 mg, 55%). ¹H (500 MHz, CD₂Cl₂) δ 7.44-6.95 (m, 125H), 6.40 (m, 0.5H+0.5H), 6.31 (b, 0.5H), 6.03 (b, 1H), 5.78 (b, 0.5H), 5.60-5.40 (b, m, 38H), 5.03 (m, 2H), 2.66-2.10 (b, m, 160H), 1.73-1.42 (b, m, 80H). $M_n^{\text{calc}} = 5224$. $M_n^{\text{GPC}} = 1572$. $M_w^{\text{GPC}} = 3302$. PDI = 2.1.

(8d-20a)₁₀. Cyclobutene **8d** (0.06 mmol), cyclohexene **20a** (0.12 mmol) and **5** (0.006 mmol) were mixed in CD₂Cl₂ (600 μL) in an NMR tube. The reaction was maintained for 13 h to reach 95% completion. The solvent was removed from the crude mixture in vacuo and the residue was purified by flash column chromatography (100% CH₂Cl₂) to generate polymer **(8d-20a)₁₀** (13 mg, 61%). ¹H (500 MHz, CD₂Cl₂) δ 7.26-7.40 (m, 5H), 7.25-7.16 (m, 10H), 6.42 (m, 1H), 6.27 (m, 2H), 5.47 (m, 18 H), 4.90 (2H), 2.75-2.09 (m, 80H), 1.75-1.38 (m, 40H).

(8a-20b)₁₀. Cyclobutene **8a** (0.06 mmol), cyclohexene **20b** (0.12 mmol) and **5** (0.006 mmol) were mixed in CD₂Cl₂ (600 μL) in an NMR tube. The reaction was maintained for 3 h, and no monomer conversion was observed.

(8a-20c)₁₀. Cyclobutene **8a** (0.06 mmol), cyclohexene **20c** (0.12 mmol) and **5** (0.006 mmol) were mixed in CD₂Cl₂ (600 μL) in an NMR tube. The reaction was maintained for 3 h, and no monomer conversion was observed.

(8a-20d)₂₀. Cyclobutene **8a** (0.12 mmol), cyclohexene **20d** (0.24 mmol) and **5** (0.006 mmol) were mixed in CD₂Cl₂ (600 μL) in an NMR tube. The reaction was maintained for 4 h to reach 95% completion. The solvent was removed from the crude mixture in vacuo and the residue was purified by flash column chromatography (100% CH₂Cl₂) to generate polymer **(8a-20d)₂₀** (15 mg, 59 %). ¹H (500 MHz, CD₂Cl₂) δ 7.41-7.21 (m, 5H), 6.83 (m, 20H), 6.42 (m, 1H), 6.27 (m, 1H), 5.83 (m, 1H), 5.42 (m, 38H),

5.02 (m, 2H), 3.72 (bs, 60H), 3.34-3.17 (m, 100H), 2.47-2.06 (m, 160H), 1.78-1.24 (m, 60H). DP = 95. $M_n^{\text{calc}} = 4264$. $M_n^{\text{GPC}} = 1506$. $M_w^{\text{GPC}} = 3719$. PDI = 2.5.

(8a-20e)₂₀. Cyclobutene **8a** (0.12 mmol), cyclohexene **20e** (0.24 mmol) and **5** (0.006 mmol) were mixed in CD₂Cl₂ (600 μL) in an NMR tube. The reaction was maintained for 6 h to reach 90% completion.

(8a-20f)₂₀. Cyclobutene **8a** (0.12 mmol), cyclohexene **20f** (0.24 mmol) and **5** (0.006 mmol) were mixed in CD₂Cl₂ (600 μL) in an NMR tube. The reaction was maintained for 5 h, and no monomer conversion was observed.

(8a-20g)₁₀. Cyclobutene **8a** (0.06 mmol), cyclohexene **20g** (0.12 mmol) and **5** (0.006 mmol) were mixed in CD₂Cl₂ (600 μL) in an NMR tube. The reaction was maintained for 6 h, and no monomer conversion was observed.

(8a-20h)₂₀. Cyclobutene **8a** (0.12 mmol), cyclohexene **20h** (0.24 mmol) and **5** (0.006 mmol) were mixed in CD₂Cl₂ (600 μL) in an NMR tube. The reaction was maintained for 5 h, and no monomer conversion was observed.

(8a-20i)₂₀. Cyclobutene **8a** (0.12 mmol), cyclohexene **20i** (0.24 mmol) and **5** (0.006 mmol) were mixed in CD₂Cl₂ (600 μL) in an NMR tube. The reaction was maintained for 4 h to reach 95% completion.

(8a-20j)₂₀. Cyclobutene **8a** (0.12 mmol), cyclohexene **20j** (0.24 mmol) and **5** (0.006 mmol) were mixed in CD₂Cl₂ (600 μL) in an NMR tube. The reaction was maintained for 6 h to reach 90% completion.

(8a-29a)₂₀-[28]. Cyclobutene **8a** (0.12 mmol), cyclopentene **29a** (0.24 mmol) and **28** (0.006 mmol) were mixed in CDCl₃ (600 μL) in an NMR tube at 50 °C. The reaction was maintained for 5 h to reach 50% completion.

Cyclobutene **8a** (0.12 mmol), cyclopentene **29a** (0.24 mmol) and **28** (0.006 mmol) were mixed in toluene-D₈ (600 μL) in an NMR tube at 80 °C. The reaction was maintained for 5 h to reach 50% completion.

(8a-29b)₄₀-[5]. Cyclobutene **8a** (0.24 mmol), cyclopentene **29b** (0.48 mmol) and **5** (0.006 mmol) were mixed in CDCl₃ (600 μL) in an NMR tube at 50 °C. The reaction was maintained for 4 h, and no monomer conversion was observed.

(8a-29b)₄₀-[28]. Cyclobutene **8a** (0.24 mmol), cyclopentene **29b** (0.48 mmol) and **28** (0.006 mmol) were mixed in CDCl₃ (600 μL) in an NMR tube at 50 °C. The reaction was maintained for 4 h, and no monomer conversion was observed.

(20a)₂₀. Cyclohexene **20a** (0.12 mmol) and **5** (0.006 mmol) were mixed in CD₂Cl₂ (600 μL) in an NMR tube. No ROMP or ROM was observed.

Intermediate-1 and Acopolymer-1. Cyclobutene **8e** (0.15 mmol), cyclohexene **20a** (0.30 mmol) and **5** (0.006 mmol) were mixed in CD₂Cl₂ (600 μL) in an NMR tube. The reaction was maintained for 5 h at rt to reach 90% completion. The crude solution was evaporated to remove solvent, and the residue was purified by flash column chromatography (acetone:CH₂Cl₂/5:95) to provide **Intermediate-1** (21 mg, 51%). ¹H NMR (500 MHz, CD₂Cl₂) δ 7.40-7.21 (m, 5H), 6.78 (b, 25H), 6.43 (m, 1H), 6.27 (m, 1H), 5.85(m, 1H), 5.44 (b, 42H), 4.17 (b, 50H), 3.63 (b, 50H), 2.44-2.02 (m, 188H), 1.88 (m, 100H), 1.52-1.44 (b, 88H). ¹³C NMR (125 MHz, CDCl₃) δ 168.0, 143.3, 131.9, 131.0, 130.9, 130.7, 130.5, 130.4, 130.1, 129.9, 129.7, 129.3, 128.7, 128.5, 125.5, 63.7, 44.8, 32.6, 32.4, 31.9, 29.6, 29.4, 29.2, 29.1, 29.0, 28.8-27.3, 26.4. **Intermediate-1** and trimethylamine aqueous solution (45% wt, 1 mL) were mixed in acetonitrile (2 mL). The solution was heated to 70 °C for 4 h. The crude solution was evaporated to remove solvent to provide **Acopolymer-1** as a brown powder. ¹H NMR (600 MHz, D₂O) δ 7.50-7.27 (m, 5H), 6.91 (b, 25H), 6.39 (b, 1H), 6.28 (b, 1H), 5.89 (b, 1H), 5.45 (b, 44H), 4.25 (b, 50H), 3.44 (b, 50H), 3.19 (s, 225H), 2.40-2.04 (m, 188H), 1.94 (m, 50H), 1.84 (m, 50H), 1.47 (m, 88H).

Intermediate-2 and Acopolymer-2. Cyclobutene **8e** (0.15 mmol), cyclohexene **20i** (0.30 mmol) and **5** (0.006 mmol) were mixed in CDCl₃ (600 μL) in an NMR tube. The reaction was maintained for 3 h at 50°C to reach 94% completion. The crude solution was evaporated to remove solvent, and the residue was purified by flash column chromatography (acetone:CH₂Cl₂/10:90) to provide **Intermediate-2** (35 mg, 81%). ¹H NMR (600 MHz, CD₂Cl₂) δ 7.38-7.21 (m, 5H), 6.75 (b, 25H), 6.39 (b, 1H), 6.22 (b, 1H), 5.81 (b, 1H), 5.42 (b, 34H), 4.14 (b, 50H), 3.61 (b, 50H), 2.36-2.01 (m, 172H), 1.84 (m, 100H), 1.57-1.36 (m, 108H). **Intermediate-2** and trimethylamine aqueous solution (45% wt, 1 mL) were mixed in acetonitrile (2 mL). The solution was heated to 70°C for 4 h. The crude solution was evaporated to remove solvent to provide **Acopolymer-2** as a brown powder. ¹H NMR (600 MHz, D₂O) δ 7.36-7.15 (m, 5H), 6.75 (b, 17H), 5.27 (b, 13H), 4.08 (b, 34H), 3.26 (b, 34H), 3.02 (b, 153H), 2.40-1.97 (m, 124H), 1.76-1.66 (b, 68H), 1.37-1.08 (m, 84H).

Intermediate-3 and Acopolymer-3. Cyclobutene **8e** (0.15 mmol), cyclohexene **20k** (0.30 mmol) and **5** (0.006 mmol) were mixed in CDCl₃ (600 μL) in an NMR tube. The reaction was maintained for 3 h at 50°C to reach 92% completion. The crude solution was evaporated to remove solvent, and the residue was purified by flash column chromatography (acetone:CH₂Cl₂/10:90) to provide **Intermediate-3** (28 mg, 53%). ¹H NMR (600 MHz, CD₂Cl₂) δ 7.43-7.21 (m, 5H), 6.73 (s, 31H), 6.36 (b, 1H), 6.21 (b, 1H), 5.83 (b, 1H), 5.56-5.40 (b, 44H), 4.15 (b, 62H), 3.60 (b, 62H), 3.17 (b, 46H), 2.44-2.08 (m, 216H), 1.85-1.82 (m, 124H), 1.61-1.51 (m, 115H), 0.92 (m, 69H). **Intermediate-3** and trimethylamine aqueous solution (45% wt, 1 mL) were mixed in acetonitrile (2 mL). The solution was heated to 70°C for 4 h. The crude solution was evaporated to remove solvent, diluted with water and washed by Et₂O to provide **Acopolymer-3** as a brown powder. ¹H NMR (600 MHz, D₂O) δ 7.53-7.31 (m, 5H), 6.86 (m, 30H), 5.47 (b, 48H), 4.28 (b, 60H), 3.41 (b, 60H), 3.17 (b, 270H), 2.57-2.18 (m, 220H), 1.93-1.56 (m, 195H), 0.94 (b, 75H).

Intermediate-4 and Acopolymer-4. Cyclobutene **8e** (0.15 mmol), cyclohexene **20m** (0.30 mmol) and **5** (0.006 mmol) were mixed in CDCl₃ (600 μL) in an NMR tube. The reaction was maintained for 5 h at 50°C to reach 96% completion. The crude solution was evaporated to remove solvent, and the residue was purified by flash column chromatography (acetone:CH₂Cl₂/10:90) to provide **Intermediate-4** (39 mg, 61%). ¹H NMR (500 MHz, CD₂Cl₂) δ 7.41-7.23 (m, 5H), 6.76 (b, 22H), 6.42 (b, 1H), 6.23 (b, 1H), 5.94 (b, 1H), 5.41 (b, 38H), 4.17 (b, 44H), 3.61 (b, 44H), 3.22 (40H), 2.53-2.11 (m, 168H), 1.86 (m, 88H), 1.62-1.50 (m, 60H), 1.32 (m, 240H), 0.91 (m, 60H). **Intermediate-4** and trimethylamine aqueous solution (45% wt, 1 mL) were mixed in acetonitrile (2 mL). The solution was heated to 70°C for 4 h. The crude solution was evaporated to remove solvent, diluted with water and washed by Et₂O to provide **Acopolymer-4** as a brown powder. ¹H-NMR (600 MHz, D₂O) δ 7.46-7.30 (m, 5H), 6.88 (b, 25H), 5.48 (b, 48H), 4.26 (b, 50H), 3.42 (b, 50H), 3.18 (b, 225H), 2.40-1.31 (m, 650H).

Intermediate-5 and Acopolymer-5. Cyclobutene **8e** (0.15 mmol), cyclohexene **20a** (0.30 mmol) and **23** (0.006 mmol) were mixed in CD₂Cl₂ (600 μL) in an NMR tube. The reaction was maintained for 5 h at rt to reach 90% completion. The crude solution was evaporated to remove solvent, and the residue was purified by flash column chromatography (acetone:CH₂Cl₂/5:95) to provide **Intermediate-5** (16 mg, 39%). ¹H NMR (600 MHz, CDCl₃) δ 6.75 (b, 25H), 5.39 (b, 30H), 4.16 (b, 50H), 3.57 (b, 50H), 2.48-1.98 (164H), 1.85 (b, 100H), 1.49-1.37 (b, 64H). **Intermediate-5** and trimethylamine aqueous solution (45% wt, 1 mL) were mixed in acetonitrile (2 mL). The solution was heated to 70°C for 4 h. The crude solution was evaporated to remove solvent to provide **Acopolymer-5** as a brown powder. ¹H NMR (600 MHz, D₂O) δ 6.89 (b, 25H), 5.42 (b, 30H), 4.28 (s, 50H), 3.42 (s, 50H), 3.19 (b, 225H), 2.42-1.26 (m, 328H).

Intermediate-6 and Acopolymer-6. Cyclobutene **8f** (0.15 mmol), cyclohexene **20a** (0.30 mmol) and **5** (0.006 mmol) were mixed in CDCl₃ (600 μL) in an NMR tube. The reaction was maintained for 80 min at 50°C to reach 97% completion. The crude solution was evaporated to remove solvent, and the residue was purified by flash column

chromatography (acetone:CH₂Cl₂/10:90) to provide **Intermediate-6** (26 mg, 49%). ¹H NMR (600 MHz, CD₂Cl₂) δ 7.40-7.20 (m, 5H), 6.75 (b, 25H), 6.36 (m, 1H), 6.22 (b, 1H), 5.79 (b, 1H), 5.39 (b, 38H), 4.67 (b, 25H), 4.12 (b, 50H), 3.13 (b, 50H), 2.44-2.02 (m, 180H), 1.69-1.28 (m, 405H). **Intermediate-6** and trifluoroacetic acid (TFA) (2 mL) were mixed in CH₂Cl₂ (2 mL). The solution was stirred at rt for 2 h. The crude solution was purged by Ar gas flow to remove solvent to provide **Acopolymer-6** as a brown powder. ¹H NMR (600 MHz, D₂O) δ 7.34-7.06 (m, 5H), 6.70 (b, 18H), 5.24 (b, 22H), 4.04 (m, 36H), 2.94 (b, 36H), 2.34-1.84 (m, 120H), 1.66-1.09 (m, 282H).

Intermediate-7 and Acopolymer-7. Cyclobutene **8g** (0.15 mmol), cyclohexene **20a** (0.30 mmol) and **5** (0.006 mmol) were mixed in CDCl₃ (600 μL) in an NMR tube. The reaction was maintained for 80 min at 50 °C to reach 97% completion. The crude solution was evaporated to remove solvent, and the residue was purified by flash column chromatography (acetone:CH₂Cl₂/10:90) to provide **Intermediate-7** (51 mg, 73%). ¹H-NMR (500 MHz, CD₂Cl₂) δ 8.59 (b, 50H), 7.56-7.21 (m, 5H), 6.84 (b, 25H), 5.41 (b, 48H), 4.28 (m, 50H), 3.68 (m, 50H), 2.49-1.61 (m, 300H), 1.49 (b, 450H). **Intermediate-7** and TFA (2 mL) were mixed in CH₂Cl₂ (2 mL). The solution was stirred at rt for 2 h. The crude solution was purged by Ar gas flow to remove solvent to provide **Acopolymer-7** as a brown powder. ¹H-NMR (600 MHz, D₂O) δ 7.38-7.18 (m, 5H), 6.85 (b, 25H), 5.35 (b, 48H), 4.27 (b, 50H), 3.55 (b, 50H), 2.35-2.00 (m, 200H), 1.38 (m, 100H).

General Procedure for NMR Tube Random ROMP Reactions. The NMR tube was evacuated under high vacuum for 15 min, and then was purged with Ar gas for another 15 min. Under an Ar atmosphere, a solution of monomer **A** (1-cyclobutenecarboxylate amide) and monomer **B** (cyclooctene) in CD₂Cl₂ (300 μL) was added to the NMR tube. Then a solution of ruthenium precatalyst in CD₂Cl₂ (300 μL) was added to the NMR tube, and the NMR tube was placed into the 400 MHz, 500 MHz or 600 MHz NMR spectrometer, and the reaction was monitored for several hours at 25 °C until almost all of the monomer had been consumed. After all the monomers were

converted, the reaction was quenched with ethylvinyl ether (50 μ L) and was stirred for 1 h.

Intermediate-8 and Rcopolymer-8. Cyclobutene **30** (0.048 mmol) and cyclooctene (0.048 mmol) were mixed in CD_2Cl_2 (1.2 mL). Then catalyst **5** (0.012 mmol) was added to the solution. The reaction was maintained for 1 h at rt to reach >99% completion. The crude solution was evaporated to remove solvent, and was purified by flash column chromatography (acetone: CH_2Cl_2 /5:95) to provide **Intermediate-8** (10 mg, 66%). ^1H NMR (500 MHz, acetone- D_6) δ 7.38-7.18 (m, 5H), 6.30-6.09 (m, 4H), 5.42 (b, 10H), 3.62 (b, 8H), 3.32 (b, 8H), 2.54-1.66 (m, 52H), 1.33 (m, 40H). **Intermediate-8** and trimethylamine aqueous solution (45% wt, 1 mL) were mixed in acetonitrile (2 mL). The solution was heated to 70°C for 4 h. The crude solution was evaporated to remove solvent to provide **Rcopolymer-8** as a brown powder. ^1H NMR (600 MHz, D_2O) δ 7.35-6.96 (m, 11H), 6.29-6.09 (m, 6H), 5.24 (b, 16H), 3.25-3.16 (m, 24H), 3.00 (b, 54H), 2.36-1.45 (m, 84H), 1.19 (b, 72H).

Intermediate-9 and Rcopolymer-9. Cyclobutene **30** (0.064 mmol) and cyclooctene (0.064 mmol) were mixed in CD_2Cl_2 (0.8 mL). Then catalyst **5** (0.008 mmol) was added to the solution. The reaction was maintained for 1 h at rt to reach >99% completion. The crude solution was evaporated to remove solvent, and was purified by flash column chromatography (acetone: CH_2Cl_2 /5:95) to provide **Intermediate-9** (14 mg, 74%). ^1H NMR (500 MHz, CD_2Cl_2) δ 7.37-7.19 (m, 5H), 6.12 (b, 11H), 5.85 (b, 11H), 5.42 (b, 28H), 3.60 (b, 22H), 3.31 (b, 22H), 2.41-1.70 (m, 148H), 1.35 (b, 120H). **Intermediate-9** and trimethylamine aqueous solution (45% wt, 1 mL) were mixed in acetonitrile (2 mL). The solution was heated to 70°C for 4 h. The crude solution was evaporated to remove solvent to provide **Rcopolymer-9** as a brown powder. ^1H NMR (600 MHz, D_2O) δ 7.28-6.98 (m, 5H), 6.21 (b, 9H), 5.25 (b, 24H), 3.24 (m, 36H), 3.00 (b, 81H), 2.33-1.20 (m, 228H).

Intermediate-10 and Rcopolymer-10. Cyclobutene **30** (0.20 mmol) and cyclooctene (0.20 mmol) were mixed in CD_2Cl_2 (0.8 mL). Then catalyst **5** (0.008 mmol) was added to the solution. The reaction was maintained for 1 h at rt to reach >99%

completion. The crude solution was evaporated to remove solvent, and was purified by flash column chromatography (acetone:CH₂Cl₂/5:95) to provide **Intermediate-10** (40 mg, 68%). ¹H NMR (500 MHz, CD₂Cl₂) δ 7.39-7.22 (m, 5H), 6.13 (b, 25H), 5.42 (b, 62H), 3.61 (b,50H), 3.32 (b, 50H), 2.44-1.71 (m, 328H), 1.35 (b, 256H). ¹³C NMR (125 MHz, CDCl₃) δ 170.1, 136.6, 135.4, 131.6, 130.5, 130.3, 129.2, 126.1, 44.8, 39.0, 32.8, 32.2, 30.1, 29.2, 27.3. **Intermediate-10** and trimethylamine aqueous solution (45% wt, 1 mL) were mixed in acetonitrile (2 mL). The solution was heated to 70°C for 4 h. The crude solution was evaporated to remove solvent to provide **Rcopolymer-10** as a brown powder. ¹H NMR (600 MHz, D₂O) δ 7.20-7.01 (m, 5H), 6.23 (b, 25H), 5.28 (b, 60H), 3.28 (m, 100H), 3.02 (b, 225H), 2.43-1.50 (m, 324H) 1.21 (b, 248H).

1.3 Preparative Scale ROMP/ROM/AROMP

8a₁: 13a and 14a. A solution of **8a** (40.0 mg, 0.357 mmol) in dry CH₂Cl₂ (4 mL) was added to a solution of precatalyst **5** (474 mg, 0.536 mmol) in dry CH₂Cl₂ (4 mL) at rt. The solution was stirred at rt for 20 h and ethylvinyl ether (5 mL, 52.2 mmol) was added to the reaction mixture. After 60 min, the solvent was evaporated and the residue was purified by silica column chromatography with CH₂Cl₂. The purified fractions were evaporated to afford the products **13a** (*Z*) and **14a** (*E*) (42.1 mg, 55%) in a 1:2.3 molar ratio. ¹H-NMR (600 MHz, CD₂Cl₂) 1-mer **13a** *Z*-isomer δ 7.36-7.19 (m, 5H), 6.47 (d, J=12.6 Hz, 1H), 6.15 (s, 1H), 5.68 (dt, J=11.4, 7.8 Hz, 1H), 5.60 (s,1H), 3.72 (s, 3H), 2.50 (m, 2H), 2.43 (m, 2H). 1-mer **14a** *E*-isomer δ 7.36-7.19 (m, 5H), 6.42 (d, J=16.2 Hz, 1H), 6.25 (dt, J=22.8, 6.0 Hz, 1H), 6.17 (s, 1H), 5.60 (s, 1H), 3.75 (s, 3H), 2.50 (m, 2H), 2.43 (m, 2H). ¹³C-NMR (100 MHz, CD₂Cl₂) 1-mer **13a** *Z*-isomer δ 167.9, 140.6, 138.1, 132.1, 130.8, 130.0, 129.3, 128.6, 127.2, 125.5, 52.2, 32.6, 28.0. 1-mer **14a** *E*-isomer δ 168.0, 140.7, 138.1, 131.0, 130.3, 129.0, 128.7, 127.5, 126.5, 52.2, 32.4, 32.3. LC-MS (APCI): peak time=2.18 min, M/Z calcd for C₁₄H₁₆O₂ [M+H]⁺ 217.12, found 217.21.

(8a-20a)₃. Cyclobutene **8a** (0.28 mmol, 31 mg) and **5** (0.093 mmol, 82 mg) were mixed in CH₂Cl₂ (2 mL) and stirred for 3 h at rt. Then cyclohexene **20a** (0.56 mmol, 56 μL) was added to the solution, which was stirred for 3 h. The reaction was quenched with

ethylvinyl ether (500 μL) and was stirred for 1 h. The solvent was evaporated, and the residue was purified by flash column chromatography (acetone: CH_2Cl_2 /4:96) to provide polymer (**8a-20a**)₃ as a sticky oil (47 mg, 74 %). ¹H-NMR (125 MHz, CD_2Cl_2) δ 7.35-7.21 (m, 5H), 6.80 (m, 6H), 6.42 (d, J=16 Hz, 1H), 6.26 (m, 1H), 5.84 (b, 1H), 5.44 (b, 4 H), 5.04 (d, J=17 Hz, 1H), 4.97 (d, J=15 Hz, 1H), 3.73 (b, 9H), 2.61-2.04 (b, 24H), 1.54 (b, 12H). ¹³C (125 MHz, CD_2Cl_2) δ 170.70 (m), 146.00-145.08 (m), 134.30-132.03 (m), 131.10, 130.77, 129.51, 128.53, 127.51, 126.91, 54.00, 36.20-34.11 (m), 32.34-28.48 (m).

(**8a-20a**)₁₀. Cyclobutene **8a** (0.23 mmol, 26 mg) and **5** (0.024 mmol, 21 mg) were mixed in CH_2Cl_2 (2.3 mL) and stirred for 25 min at rt. Then cyclohexene **20a** (0.47 mmol, 47 μL) was added to the solution, which was stirred for 4 h. The reaction was quenched with ethylvinyl ether (350 μL), and was stirred for 1 h. The solvent was evaporated, and the residue was purified by flash column chromatography (acetone: CH_2Cl_2 /1:99) to provide polymer (**8a-20a**)₁₀ as a sticky oil (32 mg, 71 %). ¹H-NMR (500 MHz, CD_2Cl_2) 7.41-7.21 (m, 5H), 6.77 (b, 10H), 6.41 (d, J=15.5 Hz, 1H), 6.26 (d, J=16.0 Hz, 1H), 5.84 (b, 1H), 5.49 (b, 18H), 5.04 (d, J=17.0 Hz, 1H), 4.97 (d, J= 10.0 Hz, 1H), 3.72 (s, 30H), 2.56- 2.02 (b, m, 80H), 1.46 (b, 40H). The broad signal centered at 7.29 ppm was assigned to the phenyl group. All the internal trisubstituted olefinic protons exhibited a broad signal centered at 6.78 ppm, which confirmed all the internal trisubstituted olefin bonds carried the *E*-configuration. All the internal disubstituted olefinic protons also showed a broad signal centered at 5.39 ppm. The peaks at 5.87 ppm and 5.02 ppm correspond to the terminal vinyl protons, while the peaks at 6.42 ppm and 6.30 ppm could be assigned to the two styrenyl olefinic protons with *E*-configuration. The relative intensities of all these signals were (5: 11: 18: 1: 1: 2: 1) (7.29, 6.78, 5.39, 6.42, 6.30, 5.02, 5.89 ppm), which clearly indicated that polymer (**8a-20a**)₁₀ contained nearly equal amounts of repeating units A and B generated from monomers **8a** and **20a**, respectively.

(**8a-20a**)₂₀. Cyclobutene **8a** (0.47 mmol, 53 mg) and **5** (0.024 mmol, 21 mg) were mixed in CH_2Cl_2 (2 mL) and stirred for 25 min at rt. Then cyclohexene **20a** (0.94 mmol, 95 μL) was added to the solution, and the solution was stirred for 5 h thereafter. The reaction was quenched with ethylvinyl ether (350 μL), and was stirred for 1 h. The

solvent was evaporated, and the residue was purified by flash column chromatography (acetone:CH₂Cl₂/4:96) to provide polymer (**8a-20a**)₂₀ as a sticky oil (67 mg, 74%). Polymer (**8a-20a**)₂₀ was characterized by ¹H-NMR, ¹³C-NMR, gHMQC, ¹H-¹H gCOSY and ¹³C-APT spectroscopy (Table 3-9).

II. Gaussian Computational Methods

All the structure optimizations were performed using the hybrid DFT method at the B3LYP level, a combination of Becke's three-parameter hybrid exchange function (B3)⁴⁰⁷⁻⁴⁰⁸ with the Lee-Yang-Parr correlation function⁴⁰⁹ as implemented in Gaussian 03W. The basis sets for the optimization of monomers and their corresponding ring-opened ruthenium carbenes were 6-31G* and LANL2DZ, respectively. The predicted chemical shifts were calculated using B3LYP and the /6-31G(d) basis set. The NBO charge calculations were performed using Hartree-Fock with the 6-31G+++ basis set (for cyclobutene monomers) and the LANL2DZ basis set (for ruthenium carbenes). The AIM (atoms in molecule) electron density analysis was performed using the AIMPAC package.⁴¹⁰

The initial ruthenium-carbene structure was obtained from the crystal structure of (H₂IMes)(Pyridine)₂Cl₂Ru=CHPh,¹⁰⁵ and was modified with GaussianView 3.0. The optimization of the ruthenium-carbenes was performed using the B3LYP/LANL2DZ method. The structures of the metallacyclobutane intermediates were optimized using B3LYP/LANL2DZ in the following way: only one bond in the metallocyclobutane ring was optimized while the other three bond lengths were kept constant, and the partial optimization was continued optimizing each bond in turn until the optimized structure changed little in energy ($\Delta E < 6.3 \times 10^{-4}$ kcal/mol). Vibrational frequency calculations using B3LYP/LANL2DZ were performed for all model compounds, and there were no imaginary vibrations present in any of the final structures. Free energies computed for structures in solvent (CH₂Cl₂) include the electronic energy plus the solvation free energy from the CPCM solvation model based on the UAKS radii using Gaussian 03W.

III. Lipid Dye Leakage Assay

Lipid Vesicle Preparation.^{324,411} Two stock buffer solutions were used: buffer A (20 mM calcein, 10 mM Na₂HPO₄, pH = 7.0) and buffer B (10 mM Na₂HPO₄, 90 mM NaCl, pH = 7.0). Appropriate amounts of lipid (DOPC 25 mg, POPE/POPG 20 mg/15.6 mg, 1, 1', 2, 2'-tetraoleoyl cardiolipin (sodium salt) (CL) 47.8 mg) were dissolved in buffer A (1 mL) separately, followed by one hour stirring. The solution was subjected to five freeze-thaw cycles, and was extruded five times through a polycarbonate membrane (Whatman, pore size 100 nm). The external calcein was removed by gel filtration (Sephadex G-25 resin) with the use of buffer B. After gel filtration, the solution was typically diluted 7-fold to yield a final lipid concentration of around 4.5 mM in buffer B. The above vesicle solution (100 μ L) was diluted in buffer B (9.9 mL) to make the stock vesicle solution (45 μ M).

Dye Leakage Experiments of Lipid Vesicles.^{324,411} The stock vesicle solution (100 μ L) and buffer B (900 μ L) were mixed in a fluorimeter cuvette. The fluorescence signal was allowed to stabilize ($\lambda_{\text{excitation}} = 490$ nm, $\lambda_{\text{emission}} = 510$ nm) for 100 s at 37 °C before addition of polymer solution (1 μ g/mL or 4 μ g/mL). The change in fluorescence over 5 min was recorded followed by the addition of 20% Triton X-100 (50 μ L) to determine the maximum fluorescence of the dye. The dye leakage percentage was calculated according to the equation:

$$\text{dye leakage percentage} = 100[(I_t - I_0)/(I_\infty - I_0)]$$

Where I_0 is the fluorescence intensity before the addition of samples, and I_∞ is the fluorescence intensity after the addition of 20% Triton X-100.

IV. Potassium Release Assay

Potassium ion release assays were performed by following the method of Silverman et al.⁴¹² *E. coli* (ATCC 25922) and *S. aureus* (ATCC 25923) were grown to the logarithmic phase in MHBc (OD₆₀₀ = 1.0). The bacterial suspension was washed twice with 10 mM HEPES (pH 7.2) and 0.5% glucose, and was resuspended in the same

amount of 10 mM HEPES (pH 7.2) and 0.5% glucose. The bacterial suspension (2 ml) was placed in a fluorimeter cuvette containing a stir bar. The fluorescence of the bacterial suspension was allowed to stabilize for 60 s at 37 °C ($\lambda_{\text{excitation}} = 346 \text{ nm}$, $\lambda_{\text{emission}} = 505 \text{ nm}$) before the addition of PBFI-AM (potassium indicator, 1 μM). Data were collected for an additional 2 min to establish a baseline signal before the addition of polymers (32 $\mu\text{g}/\text{mL}$). The fluorescence signals were collected for each sample over 1000 s. For the control sample, valinomycin (10 $\mu\text{g}/\text{mL}$) was added to the sample solution and stirred for 1000 s, followed by the addition of KCl (1 mM) to demonstrate continued indicator responsiveness. Data were normalized relative to the fluorescent signal change in 1000 s after the addition of valinomycin according to the equation:

$$\text{Potassium release percentage} = 100[(I_t - I_0)/(I_\infty - I_0)]$$

Where I_0 is I_t before the addition of polymers, I_t is the fluorescence intensity before the addition of valinomycin, and I_∞ is the fluorescence intensity at 1000 s after the addition of valinomycin.

V. Thin-section TEM

Both *E. coli* (ATCC 25922) and *S. aureus* (ATCC 25923) were grown to the logarithmic phase in MHBc (OD600 = 1.0). The bacterial suspension was washed with PBS buffer (pH 7.0) twice, and was resuspended in the same amount of PBS buffer (pH 7.0). An aqueous solution of **Acopolymer-1** was added to the bacterial suspension, and the mixture was incubated at 37 °C for 30 min. The bacterial suspension was washed with PBS buffer (pH 7.0), and was resuspended in the same amount of 2.5% glutaraldehyde in sodium cacodylate buffer (pH 7.0). After fixation, samples were then placed in 2% osmium tetroxide in PBS buffer (pH 7.0), dehydrated in a graded series of ethyl alcohol and embedded in Epon resin. Ultrathin sections of 80 nm were cut with a Reichert-Jung Ultracut E ultramicrotome and placed on formvar coated slot copper grids. Sections were then counterstained with uranyl acetate and lead citrate and viewed with a FEI Tecnai12 BioTwinG² electron microscope. Digital images were acquired with an AMT XR-60 CCD Digital Camera system.

VI. Membrane Depolarization Assay and Cell Viability Assay

Both *E. coli* (ATCC 25922) and *S. aureus* (ATCC 25923) were grown to the logarithmic phase in MHBc (OD600 = 0.05). The bacterial suspension was washed with HEPES buffer (5 mM, pH 7.4) twice, and was resuspended in the same amount of HEPES buffer (5 mM, pH 7.4). A final concentration of 0.2 mM EDTA (pH 7.4) was added to the bacterial suspension. The bacterial suspension (2 mL) was transferred to a fluorescence cuvette, and diSC₃₅ was added at a final concentration of 0.4 μM. The fluorescence was allowed to quench for 20-30 min before the addition of 100 mM KCl. The fluorescence was allowed to stabilize for 60 s before the addition of valinomycin, **Acopolymer-1**, **Rcopolymer-8**, **Homopolymer-11** or **Homopolymer-13**. The fluorescence change thereafter was recorded for 1 h.

The residual cell viability in the membrane depolarization assay was assessed. At regular intervals (0, 5, 15, 45 and 60 min) an aliquot of the bacterial suspension was plated on MH agar plates and incubated at 37 °C for 24 h (*E. coli*) or 48 h (*S. aureus*), and residual colony forming units (CFU) were determined.

VII. MIC and Hemolysis Assay

MIC assays were conducted using a standardized assay.⁴¹³ Hemolysis assays were conducted using 0.1 M phosphate buffer (pH = 7.4) as described by Murthy et al (1999)⁴¹⁴ except washed sheep RBC were used.

VIII. Small Angle Neutron Scattering (SANS)

The SANS experiments were performed at room temperature with a 30 m SANS instrument installed at High Flux Isotope Reactor (HFIR) in Oak Ridge National Laboratory (ORNL), Tennessee, USA. The incident neutron beam was monochromatized to be 4.75Å. The SANS experiment was performed according to the literature.⁴¹⁵ $D = (12 \cdot R_g^2)^{1/2}$, where R_g is the radius of gyration, calculated from the slope of Guinier plot (I^2 vs q^2), and D is the thickness of the vesicle membrane.

Bibliography

1. Ziegler, K.; Holzkamp, E.; Breil, H.; Martin, H. "Das mulheimer normaldruck-polyathylen-verfahren.," *Angew. Chem.* **1955**, *67*, 541-547.
2. Natta, G.; Pino, P.; Corrdini, P.; Danusso, F.; Mantica, E.; Mazzanto, G. "Crystallizing high polymers of α -olefins.," *J. Am. Chem. Soc.* **1955**, *77*, 1708-1710.
3. Jorgensen, M.; Hadwiger, P.; Madsen, R.; Stutz, A. E.; Wrodnigg, T. M. "Olefin metathesis in carbohydrate chemistry," *Curr. Org. Chem.* **2000**, *4*, 565-588.
4. Maier, M. E. "Synthesis of medium-sized rings by the ring-closing metathesis reaction," *Angew. Chem. Int. Ed.* **2000**, *39*, 2073-2077.
5. Bielawski, C. W.; Grubbs, R. H. "Living ring-opening metathesis polymerization," *Prog. Polym. Sci.* **2007**, *32*, 1-29.
6. Trnka, T. M.; Grubbs, R. H. "The development of $L_2X_2Ru=CHR$ olefin metathesis catalysts: An organometallic success story," *Acc. Chem. Res.* **2001**, *34*, 18-29.
7. Binder, J. B.; Raines, R. T. "Olefin metathesis for chemical biology," *Curr. Opin. Chem. Biol.* **2008**, *12*, 767-773.
8. Smith, D.; Pentzer, E. B.; Nguyen, S. T. "Bioactive and therapeutic ROMP polymers," *Poly. Rev.* **2007**, *47*, 419-459.
9. Kiessling, L. L.; Gestwicki, J. E.; Strong, L. E. "Synthetic multivalent ligands as probes of signal transduction," *Angew. Chem. Int. Ed.* **2006**, *45*, 2348-2368.
10. Herisson, J. L.; Chauvin, Y. "Catalysis of olefin transformations by tungsten complexes. II. Telomerization of cyclic olefins in the presence of acyclic olefins.," *Makromol. Chem.* **1971**, *141*, 161-167.
11. Grubbs, R. H.; Carr, D. D.; Hoppin, C.; Burk, P. L. "Consideration of mechanism of metal-catalyzed olefin metathesis reaction," *J. Am. Chem. Soc.* **1976**, *98*, 3478-3483.
12. Grubbs, R. H.; Burk, P. L.; Carr, D. D. "Consideration of mechanism of olefin metathesis reaction," *J. Am. Chem. Soc.* **1975**, *97*, 3265-3267.

13. Hejl, A.; Scherman, O. A.; Grubbs, R. H. "Ring-opening metathesis polymerization of functionalized low-strain monomers with ruthenium-based catalysts," *Macromolecules* **2005**, *38*, 7214-7218.
14. Benson, S. W.; Cruicksh, F. R.; Golden, D. M.; Haugen, G. R.; Oneal, H. E.; Rodgers, A. S.; Shaw, R.; Walsh, R. "Additivity rules for estimation of thermochemical properties," *Chem. Rev.* **1969**, *69*, 279-324.
15. Szwarc, M. "Living polymers," *Nature* **1956**, *178*, 1168-1169.
16. Darling, T. R.; Davis, T. P.; Fryd, M.; Gridnev, A. A.; Haddleton, D. M.; Ittel, S. D.; Matheson, R. R.; Moad, G.; Rizzardo, E. "Living polymerization: Rationale for uniform terminology," *J. Polym. Sci. Pol. Chem.* **2000**, *38*, 1706-1708.
17. Walker, R.; Conrad, R. M.; Grubbs, R. H. "The living ROMP of trans-cyclooctene," *Macromolecules* **2009**, *42*, 599-605.
18. Schleyer, P. V.; Williams, J. E.; Blanchard, K. R. "Evaluation of strain in hydrocarbons - strain in adamantane and its origin," *J. Am. Chem. Soc.* **1970**, *92*, 2377-2386.
19. Myers, S. B.; Register, R. A. "Crystalline-crystalline diblock copolymers of linear polyethylene and hydrogenated polynorbornene," *Macromolecules* **2008**, *41*, 6773-6779.
20. Wu, Z.; Wheeler, D. R.; Grubbs, R. H. "Living ring-opening metathesis polymerization of cyclobutene - the thermodynamic effect of a reversibly binding ligand," *J. Am. Chem. Soc.* **1992**, *114*, 146-151.
21. Bielawski, C. W.; Benitez, D.; Morita, T.; Grubbs, R. H. "Synthesis of end-functionalized poly(norbornene)s via ring-opening metathesis polymerization," *Macromolecules* **2001**, *34*, 8610-8618.
22. Chen, Z. R.; Claverie, J. P.; Grubbs, R. H.; Kornfield, J. A. "Modeling ring-chain equilibria in ring-opening polymerization of cycloolefins," *Macromolecules* **1995**, *28*, 2147-2154.
23. Schrock, R. R. "Multiple metal-carbon bonds for catalytic metathesis reactions (Nobel lecture)," *Angew. Chem. Int. Ed.* **2006**, *45*, 3748-3759.
24. Grubbs, R. H. "Olefin-metathesis catalysts for the preparation of molecules and materials (Nobel lecture)," *Angew. Chem. Int. Ed.* **2006**, *45*, 3760-3765.

25. Schrock, R. R.; Murdzek, J. S.; Bazan, G. C.; Robbins, J.; Dimare, M.; Oregan, M. "Synthesis of molybdenum imido alkylidene complexes and some reactions involving acyclic olefins," *J. Am. Chem. Soc.* **1990**, *112*, 3875-3886.
26. Ziegler K, H. E., Breil H, Martin H. "Das mulheimer normaldruck-polyathylen-verfahren.," *Angew. Chem.* **1955**, *67*, 541-547.
27. Natta G, P. P., Corrdini P, Danusso F, Mantica E, Mazzanto G, et al. "Crystallizing high polymers of α -olefins.," *J. Am. Chem. Soc.* **1955**, *77*, 1708-1710.
28. Natta, G. "Stereospezifische katalysen und isotaktische polymere.," *Angew. Chem.* **1956**, *68*, 393-403.
29. Ziegler, K. "Folgen und werdegang einer erfindung Nobel-Vortrag am 12.," *Angew. Chem.* **1963**, *76*, 545-553.
30. Natta, G. "Von der stereospezifischen polymerisation zur asymmetrischen autokatalytischen Synthese von makromolekulen Nobel-Vortrag am 12.," *Angew. Chem.* **1963**, *76*, 553-566.
31. Mckinney, R. J. "Ziegler-Natta catalysis - an alternative mechanism involving metallacycles," *J. Chem. Soc. Chem. Comm.* **1980**, 490-492.
32. Wilke, G. "Fifty years of Ziegler catalysts: Consequences and development of an invention," *Angew. Chem. Int. Ed.* **2003**, *42*, 5000-5008.
33. Truett, W. L.; Johnson, D. R.; Robinson, I. M.; Montague, B. A. "Polynorbornene by coordination polymerization," *J. Am. Chem. Soc.* **1960**, *82*, 2337-2340.
34. Calderon, N.; Ofstead, E. A.; Ward, J. P.; Judy, W. A.; Scott, K. W. "Olefin metathesis .I. acyclic vinylenic hydrocarbons," *J. Am. Chem. Soc.* **1968**, *90*, 4133-4140.
35. Eleuterio, H. S. "Olefin metathesis - chance favors those minds that are best prepared," *J. Mol. Catal.* **1991**, *65*, 55-61.
36. Calderon, N.; Ofstead, E. A.; Judy, W. A. "Mechanistic aspects of olefin metathesis," *Angew. Chem. Int. Ed.* **1976**, *15*, 401-409.
37. Calderon, N.; Ofstead, E. A.; Judy, W. A. "Ring-opening polymerization of unsaturated alicyclic compounds," *J. Polym. Sci. A1* **1967**, *5*, 2209-2217.

38. Ivin, K. J.; Mol, J. C. "Olefin metathesis and metathesis polymerization," Academic Press: London, **1997**.
39. Tebbe, F. N.; Parshall, G. W.; Reddy, G. S. "Olefin homologation with titanium methylene-compounds," *J. Am. Chem. Soc.* **1978**, *100*, 3611-3613.
40. Tebbe, F. N.; Parshall, G. W.; Ovenall, D. W. "Titanium-catalyzed olefin metathesis," *J. Am. Chem. Soc.* **1979**, *101*, 5074-5075.
41. Klabunde, U.; Tebbe, F. N.; Parshall, G. W.; Harlow, R. L. "Methylene exchange-reactions catalyzed by alkylidene derivatives of titanium and phosphorus," *J. Mol. Catal.* **1980**, *8*, 37-51.
42. Howard, T. R.; Lee, J. B.; Grubbs, R. H. "Titanium metallocarbene-metallacyclobutane reactions - stepwise metathesis," *J. Am. Chem. Soc.* **1980**, *102*, 6876-6878.
43. Grubbs, R. H.; Tumas, W. "Polymer synthesis and organotransition metal chemistry," *Science* **1989**, *243*, 907-915.
44. Straus, D. A.; Grubbs, R. H. "Titanacyclobutanes - substitution pattern and stability," *Organometallics* **1982**, *1*, 1658-1661.
45. Schrock, R. R.; Fellmann, J. D. "Multiple metal-carbon bonds .8. Preparation, characterization, and mechanism of formation of tantalum and niobium neopentylidene complexes, $M(\text{CH}_2\text{CMe}_3)_3(\text{CHCMe}_3)$," *J. Am. Chem. Soc.* **1978**, *100*, 3359-3370.
46. Rupprecht, G. A.; Messerle, L. W.; Fellmann, J. D.; Schrock, R. R. "Multiple metal-carbon bonds .15. Octahedral alkylidene complexes of niobium and tantalum by ligand-promoted alpha-abstraction," *J. Am. Chem. Soc.* **1980**, *102*, 6236-6244.
47. Wallace, K. C.; Dewan, J. C.; Schrock, R. R. "Multiple metal-carbon bonds .44. Isolation and characterization of the 1st simple tantalacyclobutane complexes," *Organometallics* **1986**, *5*, 2162-2164.
48. Wallace, K. C.; Schrock, R. R. "Ring-opening polymerization of norbornene by a tantalum catalyst - a living polymerization," *Macromolecules* **1987**, *20*, 448-450.
49. Wallace, K. C.; Liu, A. H.; Dewan, J. C.; Schrock, R. R. "Preparation and reactions of tantalum alkylidene complexes containing bulky phenoxide or

- thiolate ligands - controlling ring-opening metathesis polymerization activity and mechanism through choice of anionic ligand," *J. Am. Chem. Soc.* **1988**, *110*, 4964-4977.
50. Rocklage, S. M.; Fellmann, J. D.; Rupprecht, G. A.; Messerle, L. W.; Schrock, R. R. "Multiple metal-carbon bonds .19. How niobium and tantalum complexes of the type-M(CHCMe₃)(Pr₃)₂Cl₃ can be modified to give olefin metathesis catalysts," *J. Am. Chem. Soc.* **1981**, *103*, 1440-1447.
 51. Kress, J.; Wesolek, M.; Osborn, J. A. "Tungsten(IV) carbenes for the metathesis of olefins - direct observation and identification of the chain carrying carbene complexes in a highly-active catalyst system," *J. Chem. Soc. Chem. Comm.* **1982**, 514-516.
 52. Kress, J.; Osborn, J. A. "Tungsten carbene complexes in olefin metathesis - a cationic and chiral active species," *J. Am. Chem. Soc.* **1983**, *105*, 6346-6347.
 53. Kress, J.; Osborn, J. A. "Stereochemically nonrigid tungsten alkylidene complexes - barriers to rotation about the tungsten to carbon double-bond," *J. Am. Chem. Soc.* **1987**, *109*, 3953-3960.
 54. Ivin, K. J.; Kress, J.; Osborn, J. A. "Kinetics of initiation and propagation of the metathesis polymerization of the exo Diels-Alder adduct of cyclopentadiene and maleic-anhydride initiated by the tungsten carbene complex W[C(CH₂)₃CH₂](OCH₂CMe₃)₂Br₂," *J. Mol. Catal.* **1988**, *46*, 351-358.
 55. Kress, J.; Osborn, J. A.; Greene, R. M. E.; Ivin, K. J.; Rooney, J. J. "The detection of living propagating tungsten carbene complexes in the ring-opening polymerization of bicycloalkenes," *J. Chem. Soc. Chem. Comm.* **1985**, 874-876.
 56. Ivin, K. J. K., J.; Osborn, J.A. "Proton NMR study of the kinetics of metathesis polymerization of 5- and 5, 6-methoxycarbonyl derivatives of bicyclo[2.2.1]hept-2-ene, initiated by cyclopentylidenedibromobis(neopentyloxy)tungsten," *Makromol. Chem.* **1992**, *193*, 1685-1707.
 57. Schrock, R. R.; Depue, R. T.; Feldman, J.; Schaverien, C. J.; Dewan, J. C.; Liu, A. H. "Preparation and reactivity of several alkylidene complexes of the type W(CHR')(N-2,6-C₆H₃-i-Pr₂)(OR)₂ and related tungstacyclobutane complexes -

- controlling metathesis activity through the choice of alkoxide ligand," *J. Am. Chem. Soc.* **1988**, *110*, 1423-1435.
58. Schrock, R. R. "Living ring-opening metathesis polymerization catalyzed by well-characterized transition-metal alkylidene complexes," *Acc. Chem. Res.* **1990**, *23*, 158-165.
59. Schrock, R. R.; Feldman, J.; Cannizzo, L. F.; Grubbs, R. H. "Ring-opening polymerization of norbornene by a living tungsten alkylidene complex," *Macromolecules* **1987**, *20*, 1169-1172.
60. Schrock, R. R.; Krouse, S. A.; Knoll, K.; Feldman, J.; Murdzek, J. S.; Yang, D. C. "Controlled ring-opening metathesis polymerization by molybdenum and tungsten alkylidene complexes," *J. Mol. Catal.* **1988**, *46*, 243-253.
61. Bazan, G. C.; Khosravi, E.; Schrock, R. R.; Feast, W. J.; Gibson, V. C.; Oregan, M. B.; Thomas, J. K.; Davis, W. M. "Living ring-opening metathesis polymerization of 2,3-difunctionalized norbornadienes by Mo(CH-t-Bu)(N-2,6-C₆H₃-Iso-Pr₂)(O-t-Bu)₂," *J. Am. Chem. Soc.* **1990**, *112*, 8378-8387.
62. Bazan, G. C.; Oskam, J. H.; Cho, H. N.; Park, L. Y.; Schrock, R. R. "Living ring-opening metathesis polymerization of 2,3-difunctionalized 7-oxanorbornenes and 7-oxanorbornadienes by Mo(CHCMe₂R)(N-2,6-C₆H₃-Iso-Pr₂)(O-Tert-Bu)₂ and Mo(CHCMe₂R)(N-2,6-C₆H₃-Iso-Pr₂)(OCMe₂CF₃)₂," *J. Am. Chem. Soc.* **1991**, *113*, 6899-6907.
63. Bazan, G. C.; Schrock, R. R.; Cho, H. N.; Gibson, V. C. "Polymerization of functionalized norbornenes employing Mo(CH-t-Bu)(NAr)(O-t-Bu)₂ as the initiator," *Macromolecules* **1991**, *24*, 4495-4502.
64. Khosravi, E.; Al-Hajaji, A. A. "Ring opening metathesis polymerisation of n-alkyl norbornene dicarboxyimides using well-defined initiators," *Polymer* **1998**, *39*, 5619-5625.
65. Khosravi, E.; Feast, W. J.; Al-Hajaji, A. A.; Leejarkpai, T. "ROMP of N-alkyl norbornene dicarboxyimides: from classical to well-defined initiators, an overview," *J. Mol. Catal. A-Chem.* **2000**, *160*, 1-11.
66. Singh, R.; Czekelius, C.; Schrock, R. R. "Living ring-opening metathesis polymerization of cyclopropenes," *Macromolecules* **2006**, *39*, 1316-1317.

67. Singh, R.; Schrock, R. R. "Stereospecific ring-opening metathesis polymerization of 3-methyl-3-phenylcyclopropene by molybdenum alkylidene initiators," *Macromolecules* **2008**, *41*, 2990-2993.
68. Porri, L.; Diversi, P.; Lucherini, A.; Rossi, R. "Catalysts derived from ruthenium and iridium for ring-opening polymerization of cycloolefins," *Makromol. Chem.* **1975**, *176*, 3121-3125.
69. Porri, L.; Rossi, R.; Diversi, P.; Lucherini, A. "Ring-opening polymerization of cycloolefins with catalysts derived from ruthenium and iridium," *Makromol. Chem.* **1974**, *175*, 3097-3115.
70. Novak, B. M.; Grubbs, R. H. "Catalytic organometallic chemistry in water - the aqueous ring-opening metathesis polymerization of 7-oxanorbornene derivatives," *J. Am. Chem. Soc.* **1988**, *110*, 7542-7543.
71. Hillmyer, M. A.; Lepetit, C.; Mcgrath, D. V.; Novak, B. M.; Grubbs, R. H. "Aqueous ring-opening metathesis polymerization of carboximide-functionalized 7-oxanorbornenes," *Macromolecules* **1992**, *25*, 3345-3350.
72. Lu, S. Y.; Amass, J. M.; Majid, N.; Glennon, D.; Byerley, A.; Heatley, F.; Quayle, P.; Booth, C. "Aqueous ring-opening metathesis polymerization of 7-oxanorbornene derivatives with oxygen-containing functionalities," *Macromol. Chem. Phys.* **1994**, *195*, 1273-1288.
73. Lu, S. Y.; Quayle, P.; Booth, C.; Yeates, S. G.; Padget, J. C. "Aqueous dispersions by ring-opening metathesis polymerization of exo,exo-2,3-bis(methoxymethyl)-7-oxanorbornene," *Polym. Int.* **1993**, *32*, 1-4.
74. Lu, S. Y.; Quayle, P.; Heatley, F.; Booth, C.; Yeates, S. G.; Padget, J. C. "Aqueous ring-opening metathesis polymerization and copolymerization of 2,3-dicarboxylic acid anhydride, 2,3-bis(methoxymethyl) and 2,3-dicarboxylic acid mono-methyl ester derivatives of 7-oxanorbornene," *Eur. Polym. J.* **1993**, *29*, 269-279.
75. Zenkl, E.; Stelzer, F. "The aqueous ring-opening metathesis polymerization of 7-oxa-norbornene-2,3-dicarboxylic acid dimethyl ester and norbornene with Ru catalysts," *J. Mol. Catal.* **1992**, *76*, 1-14.

76. Lu, S. Y.; Quayle, P.; Heatley, F.; Booth, C.; Yeates, S. G.; Padget, J. C. "Aqueous ring-opening metathesis polymerization of exo,exo-2,3-bis(methoxymethyl)-7-oxanorbornene catalyzed by Ruthenium trichloride," *Macromolecules* **1992**, *25*, 2692-2697.
77. Nguyen, S. T.; Johnson, L. K.; Grubbs, R. H.; Ziller, J. W. "Ring-opening metathesis polymerization (ROMP) of norbornene by a Group-VIII carbene complex in protic media," *J. Am. Chem. Soc.* **1992**, *114*, 3974-3975.
78. Wu, Z.; Benedicto, A. D.; Grubbs, R. H. "Living ring-opening metathesis polymerization of bicyclo[3.2.0]heptene catalyzed by a ruthenium alkylidene complex," *Macromolecules* **1993**, *26*, 4975-4977.
79. Nguyen, S. T.; Grubbs, R. H.; Ziller, J. W. "Syntheses and activities of new single-component, ruthenium-based olefin metathesis catalysts," *J. Am. Chem. Soc.* **1993**, *115*, 9858-9859.
80. Schwab, P.; France, M. B.; Ziller, J. W.; Grubbs, R. H. "A series of well-defined metathesis catalysts - synthesis of $[\text{RuCl}_2(=\text{CHR}')(\text{PR}_3)_2]$ and its reactions," *Angew. Chem. Int. Ed.* **1995**, *34*, 2039-2041.
81. Schwab, P.; Grubbs, R. H.; Ziller, J. W. "Synthesis and applications of $\text{RuCl}_2(=\text{CHR}')(\text{PR}_3)_2$: the influence of the alkylidene moiety on metathesis activity," *J. Am. Chem. Soc.* **1996**, *118*, 100-110.
82. Lynn, D. M.; Kanaoka, S.; Grubbs, R. H. "Living ring-opening metathesis polymerization in aqueous media catalyzed by well-defined ruthenium carbene complexes," *J. Am. Chem. Soc.* **1996**, *118*, 784-790.
83. Weck, M.; Schwab, P.; Grubbs, R. H. "Synthesis of ABA triblock copolymers of norbornenes and 7-oxanorbornenes via living ring-opening metathesis polymerization using well-defined, bimetallic ruthenium catalysts," *Macromolecules* **1996**, *29*, 1789-1793.
84. Maughon, B. R.; Grubbs, R. H. "Ruthenium alkylidene initiated living ring-opening metathesis polymerization (ROMP) of 3-substituted cyclobutenes," *Macromolecules* **1997**, *30*, 3459-3469.

85. Weck, M.; Mohr, B.; Maughon, B. R.; Grubbs, R. H. "Synthesis of discotic columnar side-chain liquid crystalline polymers by ring-opening metathesis polymerization (ROMP)," *Macromolecules* **1997**, *30*, 6430-6437.
86. Morehead, A.; Grubbs, R. "Formation of bridged bicycloalkenes via ring closing metathesis," *Chem. Commun.* **1998**, 275-276.
87. Zuercher, W. J.; Scholl, M.; Grubbs, R. H. "Ruthenium-catalyzed polycyclization reactions," *J. Org. Chem.* **1998**, *63*, 4291-4298.
88. Scholl, M.; Grubbs, R. H. "Total synthesis of (-)- and (+/-)-frontalin via ring-closing metathesis," *Tetrahedron Lett.* **1999**, *40*, 1425-1428.
89. Nicolaou, K. C.; Vourloumis, D.; Winssinger, N.; Baran, P. S. "The art and science of total synthesis at the dawn of the twenty-first century," *Angew. Chem. Int. Ed.* **2000**, *39*, 44-122.
90. Nicolaou, K. C.; He, Y.; Vourloumis, D.; Vallberg, H.; Roschangar, F.; Sarabia, F.; Ninkovic, S.; Yang, Z.; Trujillo, J. I. "The olefin metathesis approach to epothilone A and its analogues," *J. Am. Chem. Soc.* **1997**, *119*, 7960-7973.
91. Meng, D. F.; Su, D. S.; Balog, A.; Bertinato, P.; Sorensen, E. J.; Danishefsky, S. J.; Zheng, Y. H.; Chou, T. C.; He, L. F.; Horwitz, S. B. "Remote effects in macrolide formation through ring-forming olefin metathesis: An application to the synthesis of fully active epothilone congeners," *J. Am. Chem. Soc.* **1997**, *119*, 2733-2734.
92. Blackwell, H. E.; Grubbs, R. H. "Highly efficient synthesis of covalently cross-linked peptide helices by ring-closing metathesis," *Angew. Chem. Int. Ed.* **1998**, *37*, 3281-3284.
93. Miller, S. J.; Grubbs, R. H. "Synthesis of conformationally restricted amino-acids and peptides employing olefin metathesis," *J. Am. Chem. Soc.* **1995**, *117*, 5855-5856.
94. Ulman, M.; Grubbs, R. H. "Ruthenium carbene-based olefin metathesis initiators: Catalyst decomposition and longevity," *J. Org. Chem.* **1999**, *64*, 7202-7207.
95. Dias, E. L.; Nguyen, S. T.; Grubbs, R. H. "Well-defined ruthenium olefin metathesis catalysts: Mechanism and activity," *J. Am. Chem. Soc.* **1997**, *119*, 3887-3897.

96. Tallarico, J. A.; Bonitatebus, P. J.; Snapper, M. L. "Ring-opening metathesis. A ruthenium catalyst caught in the act," *J. Am. Chem. Soc.* **1997**, *119*, 7157-7158.
97. Adlhart, C.; Hinderling, C.; Baumann, H.; Chen, P. "Mechanistic studies of olefin metathesis by ruthenium carbene complexes using electrospray ionization tandem mass spectrometry," *J. Am. Chem. Soc.* **2000**, *122*, 8204-8214.
98. Hinderling, C.; Adlhart, C.; Chen, P. "Olefin metathesis of a ruthenium carbene complex by electrospray ionization in the gas phase," *Angew. Chem. Int. Ed.* **1998**, *37*, 2685-2689.
99. Aagaard, O. M.; Meier, R. J.; Buda, F. "Ruthenium-catalyzed olefin metathesis: A quantum molecular dynamics study," *J. Am. Chem. Soc.* **1998**, *120*, 7174-7182.
100. Herrmann, W. A.; Kocher, C. "N-heterocyclic carbenes," *Angew. Chem. Int. Ed.* **1997**, *36*, 2162-2187.
101. Weskamp, T.; Schattenmann, W. C.; Spiegler, M.; Herrmann, W. A. "A novel class of ruthenium catalysts for olefin metathesis," *Angew. Chem. Int. Ed.* **1998**, *37*, 2490-2493.
102. Arduengo, A. J. "Looking for stable carbenes: The difficulty in starting anew," *Acc. Chem. Res.* **1999**, *32*, 913-921.
103. Bourissou, D.; Guerret, O.; Gabbai, F. P.; Bertrand, G. "Stable carbenes," *Chem. Rev.* **2000**, *100*, 39-91.
104. Scholl, M.; Ding, S.; Lee, C. W.; Grubbs, R. H. "Synthesis and activity of a new generation of ruthenium-based olefin metathesis catalysts coordinated with 1,3-dimesityl-4,5-dihydroimidazol-2-ylidene ligands," *Org. Lett.* **1999**, *1*, 953-956.
105. Sanford, M. S.; Love, J. A.; Grubbs, R. H. "A versatile precursor for the synthesis of new ruthenium olefin metathesis catalysts," *Organometallics* **2001**, *20*, 5314-5318.
106. Love, J. A.; Morgan, J. P.; Trnka, T. M.; Grubbs, R. H. "A practical and highly active ruthenium-based catalyst that effects the cross metathesis of acrylonitrile," *Angew. Chem. Int. Ed.* **2002**, *41*, 4035-4037.
107. Love, J. A.; Sanford, M. S.; Day, M. W.; Grubbs, R. H. "Synthesis, structure, and activity of enhanced initiators for olefin metathesis," *J. Am. Chem. Soc.* **2003**, *125*, 10103-10109.

108. Slugovc, C.; Demel, S.; Stelzer, F. "Ring opening metathesis polymerisation in donor solvents," *Chem. Commun.* **2002**, 2572-2573.
109. Frenzel, U.; Weskamp, T.; Kohl, F. J.; Schattenman, W. C.; Nuyken, O.; Herrmann, W. A. "N-Heterocyclic carbenes: application of ruthenium-alkylidene complexes in ring-opening metathesis polymerization," *J. Organomet. Chem.* **1999**, 586, 263-265.
110. Baessler, K. A.; Lee, Y.; Roberts, K. S.; Facompre, N.; Sampson, N. S. "Multivalent fertilinbeta oligopeptides: the dependence of fertilization inhibition on length and density," *Chem. Biol.* **2006**, 13, 251-259.
111. Lee, J. C.; Parker, K. A.; Sampson, N. S. "Amino acid-bearing ROMP polymers with a stereoregular backbone," *J. Am. Chem. Soc.* **2006**, 128, 4578-4579.
112. Mohr, B.; Lynn, D. M.; Grubbs, R. H. "Synthesis of water-soluble, aliphatic phosphines and their application to well-defined ruthenium olefin metathesis catalysts," *Organometallics* **1996**, 15, 4317-4325.
113. Kirkland, T. A.; Lynn, D. M.; Grubbs, R. H. "Ring-closing metathesis in methanol and water," *J. Org. Chem.* **1998**, 63, 9904-9909.
114. Lynn, D. M.; Mohr, B.; Grubbs, R. H.; Henling, L. M.; Day, M. W. "Water-soluble ruthenium alkylidenes: Synthesis, characterization, and application to olefin metathesis in protic solvents," *J. Am. Chem. Soc.* **2000**, 122, 6601-6609.
115. Lynn, D. M.; Grubbs, R. H. "Novel reactivity of ruthenium alkylidenes in protic solvents: Degenerate alkylidene proton exchange," *J. Am. Chem. Soc.* **2001**, 123, 3187-3193.
116. Samanta, D.; Kratz, K.; Zhang, X.; Emrick, T. "A synthesis of PEG- and phosphorylcholine-substituted pyridines to afford water-soluble ruthenium benzylidene metathesis catalysts," *Macromolecules* **2008**, 41, 530-532.
117. Bielawski, C. W.; Benitez, D.; Grubbs, R. H. "An "endless" route to cyclic polymers," *Science* **2002**, 297, 2041-2044.
118. Bielawski, C. W.; Benitez, D.; Grubbs, R. H. "Synthesis of cyclic polybutadiene via ring-opening metathesis polymerization: The importance of removing trace linear contaminants," *J. Am. Chem. Soc.* **2003**, 125, 8424-8425.

119. Choi, S.-K. "Synthetic multivalent molecules: concepts and biomedical applications;" 1st ed.; Wiley-Interscience, **2004**.
120. Mammen, M.; Choi, S. K.; Whitesides, G. M. "Polyvalent interactions in biological systems: Implications for design and use of multivalent ligands and inhibitors," *Angew. Chem. Int. Ed.* **1998**, *37*, 2755-2794.
121. Mortell, K. H.; Gingras, M.; Kiessling, L. L. "Synthesis of cell agglutination inhibitors by aqueous ring-opening metathesis polymerization," *J. Am. Chem. Soc.* **1994**, *116*, 12053-12054.
122. Kiessling, L. L.; Gestwicki, J. E.; Strong, L. E. "Synthetic multivalent ligands in the exploration of cell-surface interactions," *Curr. Opin. Chem. Biol.* **2000**, *4*, 696-703.
123. Lee, Y.; Sampson, N. S. "Romping the cellular landscape: linear scaffolds for molecular recognition," *Curr. Opin. Struct. Biol.* **2006**, *16*, 544-550.
124. Puffer, E. B.; Pontrello, J. K.; Hollenbeck, J. J.; Kink, J. A.; Kiessling, L. L. "Activating B cell signaling with defined multivalent ligands," *ACS Chem. Biol.* **2007**, *2*, 252-62.
125. Maynard, H. D.; Okada, S. Y.; Grubbs, R. H. "Synthesis of norbornenyl polymers with bioactive oligopeptides by ring-opening metathesis polymerization," *Macromolecules* **2000**, *33*, 6239-6248.
126. Ruoslahti, E.; Pierschbacher, M. D. "New perspectives in cell-adhesion - RGD and integrins," *Science* **1987**, *238*, 491-497.
127. Aota, S.; Nomizu, M.; Yamada, K. M. "The short amino-acid-sequence Pro-His-Ser-Arg-Asn in human fibronectin enhances cell-adhesive function," *J. Biol. Chem.* **1994**, *269*, 24756-24761.
128. Pierschbacher, M. D.; Polarek, J. W.; Craig, W. S.; Tschopp, J. F.; Sipes, N. J.; Harper, J. R. "Manipulation of cellular interactions with biomaterials toward a therapeutic outcome - a perspective," *J. Cell Biochem.* **1994**, *56*, 150-154.
129. Lee, Y.; Sampson, N. S. "Polymeric ADAM protein mimics interrogate mammalian sperm-egg binding," *ChemBioChem.* **2009**, *10*, 929-937.
130. Baessler, K. A.; Lee, Y.; Sampson, N. S. " β 1 integrin is an adhesion protein for sperm binding to eggs," *ACS Chem. Biol.* **2009**, *4*, 357-366.

131. Singla, A. K.; Garg, A.; Aggarwal, D. "Paclitaxel and its formulations," *Int. J. Pharm.* **2002**, *235*, 179-192.
132. Helmlinger, G.; Schell, A.; Dellian, M.; Forbes, N. S.; Jain, R. K. "Acid production in glycolysis-impaired tumors provides new insights into tumor metabolism," *Clin. Cancer Res.* **2002**, *8*, 1284-1291.
133. Marshall, T. H.; Akgun, A. "Specificity of porcine elastase and alpha-chymotrypsin - Effect of fatty acid chain length in a homologous series of nitrophenyl esters," *J. Biol. Chem.* **1971**, *246*, 6019-6023.
134. Lundberg, P.; Langel, U. "A brief introduction to cell-penetrating peptides," *J. Mol. Recogn.* **2003**, *16*, 227-233.
135. Lu, Y. J.; Low, P. S. "Folate-mediated delivery of macromolecular anticancer therapeutic agents," *Adv. Drug Deliver. Rev.* **2002**, *54*, 675-693.
136. Gabius, H. J.; Siebert, H. C.; Andre, S.; Jimenez-Barbero, J.; Rudiger, H. "Chemical biology of the sugar code," *ChemBioChem.* **2004**, *5*, 741-764.
137. Jaracz, S.; Chen, J.; Kuznetsova, L. V.; Ojima, L. "Recent advances in tumor-targeting anticancer drug conjugates," *Bioorg. Med. Chem.* **2005**, *13*, 5043-5054.
138. Seymour, L. W.; Duncan, R.; Strohalm, J.; Kopecek, J. "Effect of molecular weight (Mw) of N-(2-hydroxypropyl)methacrylamide copolymers on body distribution and rate of excretion after subcutaneous, intraperitoneal, and intravenous administration to rats," *J. Biomed. Mater. Res.* **1987**, *21*, 1341-1358.
139. Godwin, A.; Hartenstein, M.; Muller, A. H.; Brocchini, S. "Narrow molecular weight distribution precursors for polymer-drug conjugates," *Angew. Chem. Int. Ed.* **2001**, *40*, 594-597.
140. Stock, J.; Levit, N. "Signal transduction: Hair brains in bacterial chemotaxis," *Curr. Biol.* **2000**, *10*, 11-14.
141. Simanek, E. E.; McGarvey, G. J.; Jablonowski, J. A.; Wong, C. H. "Selectin-carbohydrate interactions: From natural ligands to designed mimics," *Chem. Rev.* **1998**, *98*, 833-862.
142. Thoma, G.; Duthaler, R. O.; Magnani, J. L.; Patton, J. T. "Nanomolar E-selectin inhibitors: 700-fold potentiation of affinity by multivalent ligand presentation," *J. Am. Chem. Soc.* **2001**, *123*, 10113-10114.

143. Thoma, G.; Patton, J. T.; Magnani, J. L.; Ernst, B.; Ohrlein, R.; Duthaler, R. O. "Versatile functionalization of polylysine: Synthesis, characterization, and use of neoglycoconjugates," *J. Am. Chem. Soc.* **1999**, *121*, 5919-5929.
144. Manning, D. D.; Hu, X.; Beck, P.; Kiessling, L. L. "Synthesis of sulfated neoglycopolymers: Selective P-selectin inhibitors," *J. Am. Chem. Soc.* **1997**, *119*, 3161-3162.
145. Sanders, W. J.; Gordon, E. J.; Dwir, O.; Beck, P. J.; Alon, R.; Kiessling, L. L. "Inhibition of L-selectin-mediated leukocyte rolling by synthetic glycoprotein mimics," *J. Biol. Chem.* **1999**, *274*, 5271-5278.
146. Puffer, E. B.; Pontrello, J. K.; Hollenbeck, J. J.; Kink, J. A.; Kiessling, L. L. "Activating B cell signaling with defined multivalent ligands," *ACS Chem. Biol.* **2007**, *2*, 252-262.
147. Watson, K. J.; Anderson, D. R.; Nguyen, S. T. "Toward polymeric anticancer drug cocktails from ring-opening metathesis polymerization," *Macromolecules* **2001**, *34*, 3507-3509.
148. Beyer, U.; Roth, T.; Schumacher, P.; Maier, G.; Unold, A.; Frahm, A. W.; Fiebig, H. H.; Unger, C.; Kratz, F. "Synthesis and in vitro efficacy of transferrin conjugates of the anticancer drug chlorambucil," *J. Med. Chem.* **1998**, *41*, 2701-2708.
149. Mcelwain, T. J.; Toy, J.; Smith, E.; Peckham, M. J.; Austin, D. E. "Combination of chlorambucil, vinblastine, procarbazine and prednisolone for treatment of Hodgkins-disease," *Brit. J. Cancer* **1977**, *36*, 276-280.
150. Quemener, D.; Heroguez, V.; Gnanou, Y. "Synthesis of acid-sensitive latices by ring-opening metathesis polymerization," *J. Polym. Sci. Pol. Chem.* **2005**, *43*, 217-229.
151. Carrillo, A.; Kane, R. S. "Block copolymer nanoparticles of controlled sizes via ring-opening metathesis polymerization," *J. Polym. Sci. Pol. Chem.* **2004**, *42*, 3352-3359.
152. Ilker, M. F.; Nusslein, K.; Tew, G. N.; Coughlin, E. B. "Tuning the hemolytic and antibacterial activities of amphiphilic polynorbornene derivatives," *J. Am. Chem. Soc.* **2004**, *126*, 15870-15875.

153. prevention, C. f. d. c. a. "<http://www.cdc.gov/getsmart/>," *Centers for disease control and prevention* **2010**.
154. Hancock, R. E. "Peptide antibiotics," *Lancet* **1997**, *349*, 418-422.
155. Melo, M. N.; Ferre, R.; Castanho, M. A. "Antimicrobial peptides: linking partition, activity and high membrane-bound concentrations," *Nat. Rev. Microbiol.* **2009**, *7*, 245-250.
156. Som, A.; Vemparala, S.; Ivanov, I.; Tew, G. N. "Synthetic mimics of antimicrobial peptides," *Biopolymers* **2008**, *90*, 83-93.
157. Brogden, K. A. "Antimicrobial peptides: pore formers or metabolic inhibitors in bacteria?," *Nat. Rev. Microbiol.* **2005**, *3*, 238-250.
158. Zasloff, M. "Antimicrobial peptides of multicellular organisms," *Nature* **2002**, *415*, 389-395.
159. Albiol Matanic, V. C.; Castilla, V. "Antiviral activity of antimicrobial cationic peptides against Junin virus and herpes simplex virus," *Int. J. Antimicrob. Agents* **2004**, *23*, 382-389.
160. Robinson, W. E., Jr.; McDougall, B.; Tran, D.; Selsted, M. E. "Anti-HIV-1 activity of indolicidin, an antimicrobial peptide from neutrophils," *J. Leukoc. Biol.* **1998**, *63*, 94-100.
161. Bowdish, D. M.; Davidson, D. J.; Hancock, R. E. "A re-evaluation of the role of host defence peptides in mammalian immunity," *Curr. Protein Pept Sci.* **2005**, *6*, 35-51.
162. Hoskin, D. W.; Ramamoorthy, A. "Studies on anticancer activities of antimicrobial peptides," *Biochim. Biophys. Acta* **2008**, *1778*, 357-375.
163. Yount, N. Y.; Bayer, A. S.; Xiong, Y. Q.; Yeaman, M. R. "Advances in antimicrobial peptide immunobiology," *Biopolymers* **2006**, *84*, 435-458.
164. Yeaman, M. R.; Yount, N. Y. "Mechanisms of antimicrobial peptide action and resistance," *Pharmacol. Rev.* **2003**, *55*, 27-55.
165. Radis-Baptista, G.; Kerkis, A.; Prieto-Silva, A. R.; Hayashi, M. A. F.; Kerkis, I.; Yamane, T. "Membrane-translocating peptides and toxins: from nature to bedside," *J. Braz. Chem. Soc.* **2008**, *19*, 211-225.

166. Wang, Z.; Wang, G. "APD: the antimicrobial peptide database," *Nucleic Acids Res.* **2004**, *32*, 590-592.
167. Gazit, E.; Boman, A.; Boman, H. G.; Shai, Y. "Interaction of the mammalian antibacterial peptide cecropin P1 with phospholipid vesicles," *Biochemistry* **1995**, *34*, 11479-11488.
168. Shai, Y. "Molecular recognition between membrane-spanning polypeptides," *Trends Biochem. Sci.* **1995**, *20*, 460-464.
169. Matsuzaki, K.; Murase, O.; Miyajima, K. "Kinetics of pore formation by an antimicrobial peptide, magainin 2, in phospholipid bilayers," *Biochemistry* **1995**, *34*, 12553-12559.
170. Thoren, P. E. G.; Persson, D.; Isakson, P.; Goksor, M.; Onfelt, A.; Norden, B. "Uptake of analogs of penetratin, Tat(48-60) and oligoarginine in live cells," *Biochem. Biophys. Res. Commun.* **2003**, *307*, 100-107.
171. Magzoub, M.; Pramanik, A.; Graslund, A. "Modeling the endosomal escape of cell-penetrating peptides: Transmembrane pH gradient driven translocation across phospholipid bilayers," *Biochemistry* **2005**, *44*, 14890-14897.
172. Fischer, R.; Kohler, K.; Fotin-Mleczek, M.; Brock, R. "A stepwise dissection of the intracellular fate of cationic cell-penetrating peptides," *J. Biol. Chem.* **2004**, *279*, 12625-12635.
173. Kobayashi, S.; Chikushi, A.; Tougu, S.; Imura, Y.; Nishida, M.; Yano, Y.; Matsuzaki, K. "Membrane translocation mechanism of the antimicrobial peptide buforin 2," *Biochemistry* **2004**, *43*, 15610-15616.
174. Deshayes, S.; Heitz, A.; Morris, M. C.; Charnet, P.; Divita, G.; Heitz, F. "Insight into the mechanism of internalization of the cell-penetrating carrier peptide Pep-1 through conformational analysis," *Biochemistry* **2004**, *43*, 1449-1457.
175. Henriques, S. T.; Castanho, M. A. R. B. "Consequences of nonlytic membrane perturbation to the translocation of the cell penetrating peptide pep-1 in lipidic vesicles," *Biochemistry* **2004**, *43*, 9716-9724.
176. Bechinger, B. "The structure, dynamics and orientation of antimicrobial peptides in membranes by multidimensional solid-state NMR spectroscopy," *Biochim. Biophys. Acta* **1999**, *1462*, 157-183.

177. Kalfa, V. C.; Jia, H. P.; Kunkle, R. A.; McCray, P. B.; Tack, B. F.; Brogden, K. A. "Congeners of SMAP29 kill ovine pathogens and induce ultrastructural damage in bacterial cells," *Antimicrob. Agents Chemother.* **2001**, *45*, 3256-3261.
178. Park, C. B.; Yi, K. S.; Matsuzaki, K.; Kim, M. S.; Kim, S. C. "Structure-activity analysis of buforin II, a histone H2A-derived antimicrobial peptide: The proline hinge is responsible for the cell-penetrating ability of buforin II," *Proc. Natl. Acad. Sci.* **2000**, *97*, 8245-8250.
179. Ladokhin, A. S.; Selsted, M. E.; White, S. H. "Sizing membrane pores in lipid vesicles by leakage of co-encapsulated markers: Pore formation by melittin," *Biophys. J.* **1997**, *72*, 1762-1766.
180. Matsuzaki, K.; Yoneyama, S.; Miyajima, K. "Pore formation and translocation of melittin," *Biophys. J.* **1997**, *73*, 831-838.
181. Kang, J. H.; Shin, S. Y.; Jang, S. Y.; Lee, M. K.; Hahm, K. S. "Release of aqueous contents from phospholipid vesicles induced by Cecropin A (1-8)-Magainin II (1-12) hybrid and its analogues," *J. Pept. Res.* **1998**, *52*, 45-50.
182. Hristova, K.; Selsted, M. E.; White, S. H. "Critical role of lipid composition in membrane permeabilization by rabbit neutrophil defensins," *J. Biol. Chem.* **1997**, *272*, 24224-24233.
183. Zhao, H.; Mattila, J. P.; Holopainen, J. M.; Kinnunen, P. K. "Comparison of the membrane association of two antimicrobial peptides, magainin 2 and indolicidin," *Biophys. J.* **2001**, *81*, 2979-2991.
184. Christensen, B.; Fink, J.; Merrifield, R. B.; Mauzerall, D. "Channel-forming properties of cecropins and related model compounds incorporated into planar lipid membranes," *Proc. Natl. Acad. Sci.* **1988**, *85*, 5072-5076.
185. Lockey, T. D.; Ourth, D. D. "Formation of pores in Escherichia coli cell membranes by a cecropin isolated from hemolymph of *Heliothis virescens* larvae," *Eur. J. Biochem.* **1996**, *236*, 263-271.
186. Kagan, B. L.; Selsted, M. E.; Ganz, T.; Lehrer, R. I. "Antimicrobial defensin peptides form voltage-dependent ion-permeable channels in planar lipid bilayer membranes," *Proc. Natl. Acad. Sci.* **1990**, *87*, 210-214.

187. Lee, M. T.; Chen, F. Y.; Huang, H. W. "Energetics of pore formation induced by membrane active peptides," *Biochemistry* **2004**, *43*, 3590-3599.
188. Wu, Y.; Huang, H. W.; Olah, G. A. "Method of oriented circular dichroism," *Biophys. J.* **1990**, *57*, 797-806.
189. Bechinger, B.; Zasloff, M.; Opella, S. J. "Structure and orientation of the antibiotic peptide magainin in membranes by solid-state nuclear magnetic resonance spectroscopy," *Protein Sci.* **1993**, *2*, 2077-2084.
190. Yamaguchi, S.; Hong, T.; Waring, A.; Lehrer, R. I.; Hong, M. "Solid-state NMR investigations of peptide-lipid interaction and orientation of a beta-sheet antimicrobial peptide, protegrin," *Biochemistry* **2002**, *41*, 9852-9862.
191. Yamaguchi, S.; Huster, D.; Waring, A.; Lehrer, R. I.; Kearney, W.; Tack, B. F.; Hong, M. "Orientation and dynamics of an antimicrobial peptide in the lipid bilayer by solid-state NMR spectroscopy," *Biophys. J.* **2001**, *81*, 2203-2214.
192. Spaar, A.; Munster, C.; Salditt, T. "Conformation of peptides in lipid membranes studied by X-ray grazing incidence scattering," *Biophys. J.* **2004**, *87*, 396-407.
193. Ludtke, S. J.; He, K.; Heller, W. T.; Harroun, T. A.; Yang, L.; Huang, H. W. "Membrane pores induced by magainin," *Biochemistry* **1996**, *35*, 13723-13728.
194. Yang, L.; Harroun, T. A.; Heller, W. T.; Weiss, T. M.; Huang, H. W. "Neutron off-plane scattering of aligned membranes. I. Method Of measurement," *Biophys. J.* **1998**, *75*, 641-645.
195. Yang, L.; Weiss, T. M.; Harroun, T. A.; Heller, W. T.; Huang, H. W. "Supramolecular structures of peptide assemblies in membranes by neutron off-plane scattering: method of analysis," *Biophys. J.* **1999**, *77*, 2648-2656.
196. Virtanen, J. A.; Cheng, K. H.; Somerharju, P. "Phospholipid composition of the mammalian red cell membrane can be rationalized by a superlattice model," *Proc. Natl. Acad. Sci.* **1998**, *95*, 4964-4969.
197. Futaki, S.; Suzuki, T.; Ohashi, W.; Yagami, T.; Tanaka, S.; Ueda, K.; Sugiura, Y. "Arginine-rich peptides - An abundant source of membrane-permeable peptides having potential as carriers for intracellular protein delivery," *J. Biol. Chem.* **2001**, *276*, 5836-5840.

198. Zhao, H. X.; Kinnunen, P. K. J. "Modulation of the activity of secretory phospholipase A(2) by antimicrobial peptides," *Antimicrob. Agents Chemother.* **2003**, *47*, 965-971.
199. Scheller, A.; Oehlke, J.; Wiesner, B.; Dathe, M.; Krause, E.; Beyermann, M.; Melzig, M.; Bienert, M. "Structural requirements for cellular uptake of alpha-helical amphipathic peptides," *J. Pept. Sci.* **1999**, *5*, 185-194.
200. Richard, J. P.; Melikov, K.; Vives, E.; Ramos, C.; Verbeure, B.; Gait, M. J.; Chernomordik, L. V.; Lebleu, B. "Cell-penetrating peptides - A reevaluation of the mechanism of cellular uptake," *J. Biol. Chem.* **2003**, *278*, 585-590.
201. Wadia, J. S.; Stan, R. V.; Dowdy, S. F. "Transducible TAT-HA fusogenic peptide enhances escape of TAT-fusion proteins after lipid raft macropinocytosis," *Nat. Med.* **2004**, *10*, 310-315.
202. Casteels, P.; Ampe, C.; Jacobs, F.; Tempst, P. "Functional and chemical characterization of hymenoptaecin, an antibacterial polypeptide that is infection-inducible in the honeybee (*Apis-Mellifera*)," *J. Biol. Chem.* **1993**, *268*, 7044-7054.
203. Shi, J. H.; Ross, C. R.; Chengappa, M. M.; Sylte, M. J.; McVey, D. S.; Blecha, F. "Antibacterial activity of a synthetic peptide (PR-26) derived from PR-39, a proline-arginine-rich neutrophil antimicrobial peptide," *Antimicrob. Agents Chemother.* **1996**, *40*, 115-121.
204. Perron, G. G.; Zasloff, M.; Bell, G. "Experimental evolution of resistance to an antimicrobial peptide," *Proc. Biol. Sci.* **2006**, *273*, 251-256.
205. Buckling, A.; Brockhurst, M. "Microbiology: RAMP resistance," *Nature* **2005**, *438*, 170-171.
206. Tew, G. N.; Scott, R. W.; Klein, M. L.; Degrado, W. F. "De Novo design of antimicrobial polymers, foldamers, and small molecules: from discovery to practical applications," *Acc. Chem. Res.* **2010**, *43*, 30-39.
207. Klok, H. A.; Lecommandoux, S. "Supramolecular materials via block copolymer self-assembly," *Adv. Mater.* **2001**, *13*, 1217-1229.
208. Grayson, S. M.; Frechet, J. M. J. "Convergent dendrons and dendrimers: from synthesis to applications," *Chem. Rev.* **2001**, *101*, 3819-3867.

209. Murphy, J. J.; Furusho, H.; Paton, R. M.; Nomura, K. "Precise synthesis of poly(macromonomer)s containing sugars by repetitive ROMP and their attachments to poly(ethylene glycol): Synthesis, TEM analysis and their properties as amphiphilic block fragments," *Chem-Eur. J.* **2007**, *13*, 8985-8997.
210. Kumar, R.; Chen, M. H.; Parmar, V. S.; Samuelson, L. A.; Kumar, J.; Nicolosi, R.; Yoganathan, S.; Watterson, A. C. "Supramolecular assemblies based on copolymers of PEG600 and functionalized aromatic diesters for drug delivery applications," *J. Am. Chem. Soc.* **2004**, *126*, 10640-10644.
211. Bronich, T. K.; Keifer, P. A.; Shlyakhtenko, L. S.; Kabanov, A. V. "Polymer micelle with cross-linked ionic core," *J. Am. Chem. Soc.* **2005**, *127*, 8236-8237.
212. Furuta, P. T.; Deng, L.; Garon, S.; Thompson, M. E.; Frechet, J. M. J. "Platinum-functionalized random copolymers for use in solution-processible, efficient, near-white organic light-emitting diodes," *J. Am. Chem. Soc.* **2004**, *126*, 15388-15389.
213. Choi, T. L.; Lee, C. W.; Chatterjee, A. K.; Grubbs, R. H. "Olefin metathesis involving ruthenium enoic carbene complexes," *J. Am. Chem. Soc.* **2001**, *123*, 10417-10418.
214. Ulman, M.; Belderrain, T. R.; Grubbs, R. H. "A series of ruthenium(II) ester-carbene complexes as olefin metathesis initiators: metathesis of acrylates," *Tetrahedron Lett.* **2000**, *41*, 4689-4693.
215. Randl, S.; Connon, S. J.; Blechert, S. "Ring opening-cross metathesis of unstrained cycloalkenes," *Chem. Commun.* **2001**, 1796-1797.
216. Gellman, S. H. "Foldamers: A manifesto," *Acc. Chem. Res.* **1998**, *31*, 173-180.
217. Hill, D. J.; Mio, M. J.; Prince, R. B.; Hughes, T. S.; Moore, J. S. "A field guide to foldamers," *Chem. Rev.* **2001**, *101*, 3893-4011.
218. Seebach, D.; Beck, A. K.; Bierbaum, D. J. "The world of beta- and gamma-peptides comprised of homologated proteinogenic amino acids and other components," *Chem. Biodivers.* **2004**, *1*, 1111-1239.
219. Horne, W. S.; Gellman, S. H. "Foldamers with heterogeneous backbones," *Acc. Chem. Res.* **2008**, *41*, 1399-1408.
220. Seebach, D.; Hook, D. F.; Glattli, A. "Helices and other secondary structures of beta- and gamma-peptides," *Biopolymers* **2006**, *84*, 23-37.

221. Cheng, R. P.; Gellman, S. H.; DeGrado, W. F. "Beta-peptides: From structure to function," *Chem. Rev.* **2001**, *101*, 3219-3232.
222. Patch, J. A.; Barron, A. E. "Helical peptoid mimics of magainin-2 amide," *J. Am. Chem. Soc.* **2003**, *125*, 12092-12093.
223. Tew, G. N.; Liu, D. H.; Chen, B.; Doerksen, R. J.; Kaplan, J.; Carroll, P. J.; Klein, M. L.; DeGrado, W. F. "De novo design of biomimetic antimicrobial polymers," *Proc. Natl. Acad. Sci.* **2002**, *99*, 5110-5114.
224. Liu, D. H.; Choi, S.; Chen, B.; Doerksen, R. J.; Clements, D. J.; Winkler, J. D.; Klein, M. L.; DeGrado, W. F. "Nontoxic membrane-active antimicrobial arylamide oligomers," *Angew. Chem. Int. Ed.* **2004**, *43*, 1158-1162.
225. Pophristic, V.; Vemparala, S.; Ivanov, I.; Liu, Z. W.; Klein, M. L.; DeGrado, W. F. "Controlling the shape and flexibility of arylamides: A combined ab initio, ab initio molecular dynamics, and classical molecular dynamics study," *J. Phys. Chem. B* **2006**, *110*, 3517-3526.
226. Choi, S.; Isaacs, A.; Clements, D.; Liu, D. H.; Kim, H.; Scott, R. W.; Winkler, J. D.; DeGrado, W. F. "De novo design and in vivo activity of conformationally restrained antimicrobial arylamide foldamers," *Proc. Natl. Acad. Sci.* **2009**, *106*, 6968-6973.
227. Rennie, J.; Arnt, L.; Tang, H. Z.; Nusslein, K.; Tew, G. N. "Simple oligomers as antimicrobial peptide mimics," *J. Ind. Microbiol. Biot.* **2005**, *32*, 296-300.
228. Arnt, L.; Nusslein, K.; Tew, G. N. "Nonhemolytic abiogenic polymers as antimicrobial peptide mimics," *J. Polym. Sci. Pol. Chem.* **2004**, *42*, 3860-3864.
229. Tashiro, T. "Antibacterial and bacterium adsorbing macromolecules," *Macromol. Mater. Eng.* **2001**, *286*, 63-87.
230. Worley, S. D.; Sun, G. "Biocidal polymers," *Trends Polym. Sci.* **1996**, *4*, 364-370.
231. Kenawy, E. R.; Mahmoud, Y. A. G. "Biologically active polymers, 6 - Synthesis and antimicrobial activity of some linear copolymers with quaternary ammonium and phosphonium groups," *Macromol. Biosci.* **2003**, *3*, 107-116.
232. Kuroda, K.; DeGrado, W. F. "Amphiphilic polymethacrylate derivatives as antimicrobial agents," *J. Am. Chem. Soc.* **2005**, *127*, 4128-4129.

233. Kuroda, K.; Caputo, G. A.; DeGrado, W. F. "The role of hydrophobicity in the antimicrobial and hemolytic activities of polymethacrylate derivatives," *Chem-Eur. J.* **2009**, *15*, 1123-1133.
234. Lienkamp, K.; Madkour, A. E.; Musante, A.; Nelson, C. F.; Nusslein, K.; Tew, G. N. "Antimicrobial polymers prepared by ROMP with unprecedented selectivity: A molecular construction kit approach," *J. Am. Chem. Soc.* **2008**, *130*, 9836-9843.
235. Colak, S.; Nelson, C. F.; Nusslein, K.; Tew, G. N. "Hydrophilic modifications of an amphiphilic polynorbornene and the effects on its hemolytic and antibacterial activity," *Biomacromolecules* **2009**, *10*, 353-359.
236. Lienkamp, K.; Tew, G. N. "Synthetic Mimics of Antimicrobial Peptides-A Versatile Ring-Opening Metathesis Polymerization Based Platform for the Synthesis of Selective Antibacterial and Cell-Penetrating Polymers," *Chem-Eur. J.* **2009**, *15*, 11784-11800.
237. Lienkamp, K.; Kumar, K. N.; Som, A.; Nusslein, K.; Tew, G. N. "'Doubly selective' antimicrobial polymers: How do they differentiate between bacteria?," *Chem-Eur. J.* **2009**, *15*, 11710-11714.
238. Lienkamp, K.; Madkour, A. E.; Kumar, K. N.; Nusslein, K.; Tew, G. N. "Antimicrobial polymers prepared by ring-opening metathesis polymerization: manipulating antimicrobial properties by organic counterion and charge density variation," *Chem-Eur. J.* **2009**, *15*, 11715-11722.
239. Lynn, D. M.; Mohr, B.; Grubbs, R. H. "Living ring-opening metathesis polymerization in water," *J. Am. Chem. Soc.* **1998**, *120*, 1627-1628.
240. Royappa, A. T.; Saunders, R. S.; Rubner, M. F.; Cohen, R. E. "Langmuir-Blodgett films of conducting diblock copolymers," *Langmuir* **1998**, *14*, 6207-6214.
241. Gordon, E. J.; Gestwicki, J. E.; Strong, L. E.; Kiessling, L. L. "Synthesis of end-labeled multivalent ligands for exploring cell-surface-receptor-ligand interactions," *Chem. Biol.* **2000**, *7*, 9-16.
242. Cairo, C. W.; Gestwicki, J. E.; Kanai, M.; Kiessling, L. L. "Control of multivalent interactions by binding epitope density," *J. Am. Chem. Soc.* **2002**, *124*, 1615-1619.

243. Baessler, K. A.; Lee, Y.; Roberts, K. S.; Facompre, N.; Sampson, N. S. "Multivalent fertilin beta oligopeptides: The dependence of fertilization inhibition on length and density," *Chem. Biol.* **2006**, *13*, 251-259.
244. Komiya, Z.; Pugh, C.; Schrock, R. R. "Synthesis of side-chain liquid-crystal polymers by living ring-opening metathesis polymerization .2. Influence of molecular-weight, polydispersity, and flexible spacer length (N = 9-12) on the thermotropic behavior of the resulting polymers," *Macromolecules* **1992**, *25*, 6586-6592.
245. Sanford, M. S.; Love, J. A.; Grubbs, R. H. "Mechanism and activity of ruthenium olefin metathesis catalysts," *J. Am. Chem. Soc.* **2001**, *123*, 6543-6554.
246. Amir-Ebrahimi, V.; Corry, D. A.; Hamilton, J. G.; Thompson, J. M.; Rooney, J. J. "Characteristics of RuCl₂(CHPh)(PCy₃)₂ as a catalyst for ring-opening metathesis polymerization," *Macromolecules* **2000**, *33*, 717-724.
247. Scherman, O. A.; Kim, H. M.; Grubbs, R. H. "Synthesis of well-defined poly((vinyl alcohol)(2)-alt-methylene) via ring-opening metathesis polymerization," *Macromolecules* **2002**, *35*, 5366-5371.
248. Scherman, O. A.; Walker, R.; Grubbs, R. H. "Synthesis and characterization of stereoregular ethylene-vinyl alcohol copolymers made by ring-opening metathesis polymerization," *Macromolecules* **2005**, *38*, 9009-9014.
249. Feast, W. J.; Gibson, V. C.; Marshall, E. L. "A Remarkable Ancillary Ligand Effect in Living Ring-Opening Metathesis Polymerization," *J. Chem. Soc. Chem. Comm.* **1992**, 1157-1158.
250. Mathias, L. J. "Esterification and Alkylation Reactions Employing Isooureas," *Synthesis-Stuttgart* **1979**, 561-576.
251. Griffin, R. J.; Arris, C. E.; Bleasdale, C.; Boyle, F. T.; Calvert, A. H.; Curtin, N. J.; Dalby, C.; Kanugula, S.; Lembicz, N. K.; Newell, D. R.; Pegg, A. E.; Golding, B. T. "Resistance-modifying agents. 8. Inhibition of O-6-alkylguanine-DNA alkyltransferase by O-6-alkenyl-, O-6-cycloalkenyl-, and O-6-(2-oxoalkyl)guanines and potentiation of temozolomide cytotoxicity in vitro by O-6-(1-cyclopentenylmethyl)guanine," *J. Med. Chem.* **2000**, *43*, 4071-4083.

252. Fujitsuka, M.; Cho, D. W.; Tojo, S.; Yamashiro, S.; Shinmyozu, T.; Majima, T. "Transannular distance dependence of stabilization energy of the intramolecular dimer radical cation of cyclophanes," *J. Phys. Chem. A* **2006**, *110*, 5735-5739.
253. Aleman, C.; Casanovas, J. "Theoretical investigation on the rotational isomerism of calix[4]arenes: Influence of the hydroxyl \rightarrow methoxy replacement," *J. Phys. Chem. A* **2005**, *109*, 8049-8054.
254. Keating, A. E.; GarciaGaribay, M. A.; Houk, K. N. "Origins of stereoselective carbene 1,2-shifts and cycloadditions of 1,2-dichloroethylidene: A theoretical model based on CBS-Q and B3LYP calculations," *J. Am. Chem. Soc.* **1997**, *119*, 10805-10809.
255. Shambayati, S.; Blake, J. F.; Wierschke, S. G.; Jorgensen, W. L.; Schreiber, S. L. "Structure and basicity of silyl ethers - a crystallographic and abinitio inquiry into the nature of silicon oxygen interactions," *J. Am. Chem. Soc.* **1990**, *112*, 697-703.
256. Cabeza, J. A.; del Rio, I.; Miguel, D.; Perez-Carreno, E.; Sanchez-Vega, M. G. "Activation of two C-H bonds of NHCN-methyl groups on triosmium and triruthenium carbonyl clusters," *Dalton Trans.* **2008**, 1937-1942.
257. Fomine, S.; Ortega, J. V.; Tlenkopatchev, M. A. "Metathesis of halogenated olefins - A computational study of ruthenium alkylidene mediated reaction pathways," *J. Mol. Catal. A-Chem.* **2007**, *263*, 121-127.
258. Hofmann, P.; Volland, M. A. O.; Hansen, S. M.; Eisentrager, F.; Gross, J. H.; Stengel, K. "Isolation and characterization of a monomeric, solvent coordinated ruthenium(II)carbene cation relevant to olefin metathesis," *J. Organomet. Chem.* **2000**, *606*, 88-92.
259. Hoffmann, M.; Marciniak, B. "Quantum chemical study of the mechanism of ethylene elimination in silylative coupling of olefins," *J. Mol. Model.* **2007**, *13*, 477-483.
260. Cornejo, A.; Fraile, J. M.; Garcia, J. I.; Gil, M. J.; Martinez-Merino, V.; Mayoral, J. A.; Salvatella, L. "Asymmetric versus C_2 -symmetric ligands: origin of the enantioselectivity in ruthenium--pybox-catalyzed cyclopropanation reactions," *Angew. Chem. Int. Ed.* **2005**, *44*, 458-461.

261. Fomine, S.; Tlenkopatchev, M. A. "Metathesis of fluorinated olefins by ruthenium alkylidene catalysts. Fluorine substituent effects on a Ru-carbene (alkylidene) complex stability: A computational study," *Appl. Catal. A-Gen.* **2009**, *355*, 148-155.
262. Wang, D.; Wurst, K.; Knolle, W.; Decker, U.; Prager, L.; Naumov, S.; Buchmeiser, M. R. "Cationic Ru-II complexes with N-heterocyclic carbene ligands for UV-Induced ring-opening metathesis polymerization," *Angew. Chem. Int. Ed.* **2008**, *47*, 3267-3270.
263. Buchmeiser, M. R.; Wang, D. R.; Zhang, Y.; Naumov, S.; Wurst, K. "Novel ruthenium(II) N-heterocyclic carbene complexes as catalyst precursors for the ring-opening metathesis polymerization (ROMP) of enantiomerically pure monomers: X-ray structures, reactivity, and quantum chemical considerations," *Eur. J. Inorg. Chem.* **2007**, 3988-4000.
264. Straub, B. F. "Ligand influence on metathesis activity of ruthenium carbene catalysts: A DFT study," *Adv. Synth. Catal.* **2007**, *349*, 204-214.
265. Chou, H. H.; Lin, Y. C.; Huang, S. L.; Liu, Y. H.; Wang, Y. "Reactions of ruthenium acetylidene and vinylidene complexes containing a 2-pyridyl group," *Organometallics* **2008**, *27*, 5212-5220.
266. Cantat, T.; Demange, M.; Mezailles, N.; Ricard, L.; Jean, Y.; Le Floch, P. "A bis(thiophosphinoyl)methylene ruthenium carbene complex: Synthesis, X-ray crystal structure, and DFT calculations of its thermally promoted reverse alpha-hydride migration process," *Organometallics* **2005**, *24*, 4838-4841.
267. Occhipinti, G.; Bjorsvik, H. R.; Jensen, V. R. "Quantitative structure-activity relationships of ruthenium catalysts for olefin metathesis," *J. Am. Chem. Soc.* **2006**, *128*, 6952-6964.
268. Fomine, S.; Tlenkopatchev, M. A. "Ring-opening of cyclohexene via metathesis by ruthenium carbene complexes. A computational study," *Organometallics* **2007**, *26*, 4491-4497.
269. Giudici, R. E.; Hoveyda, A. H. "Directed catalytic asymmetric olefin metathesis. Selectivity control by enoate and ynoate groups in Ru-catalyzed asymmetric ring-opening/cross-metathesis," *J. Am. Chem. Soc.* **2007**, *129*, 3824-3825.

270. Lapinte, V.; de Fremont, P.; Montembault, V. R.; Fontaine, L. "Ring opening metathesis polymerization (ROMP) of *cis*- and *trans*-3,4-bis(acetyloxymethyl)cyclobut-1-enes and synthesis of block copolymers," *Macromol. Chem. Phys.* **2004**, *205*, 1238-1245.
271. Lee, J. "Probing ligand-receptor interactions in mammalian fertilization using ring opening metathesis polymerization," PhD thesis, Stony Brook University, **2006**.
272. Zhao, Y.; Truhlar, D. G. "Attractive noncovalent interactions in the mechanism of Grubbs second-generation Ru catalysts for olefin metathesis," *Org. Lett.* **2007**, *9*, 1967-1970.
273. Torker, S.; Merki, D.; Chen, P. "Gas-phase thermochemistry of ruthenium carbene metathesis catalysts," *J. Am. Chem. Soc.* **2008**, *130*, 4808-4814.
274. Khoury, P. R.; Goddard, J. D.; Tam, W. "Ring strain energies: substituted rings, norbornanes, norbornenes and norbornadienes," *Tetrahedron* **2004**, *60*, 8103-8112.
275. Song, A.; Parker, K. A.; Sampson, N. S. "Synthesis of copolymers by alternating ROMP (AROMP)," *J. Am. Chem. Soc.* **2009**, *131*, 3444-3445.
276. Rosler, A.; Vandermeulen, G. W. M.; Klok, H. A. "Advanced drug delivery devices via self-assembly of amphiphilic block copolymers," *Adv. Drug Deliver. Rev.* **2001**, *53*, 95-108.
277. Cho, I. "New ring-opening polymerizations for copolymers having controlled microstructures," *Prog. Polym. Sci.* **2000**, *25*, 1043-1087.
278. Braunecker, W. A.; Matyjaszewski, K. "Controlled/living radical polymerization: Features, developments, and perspectives," *Prog. Polym. Sci.* **2007**, *32*, 93-146.
279. Maki, Y.; Mori, H.; Endo, T. "Synthesis of well-defined alternating copolymers by RAFT copolymerization of N-Vinylnaphthalimide," *Macromolecules* **2008**, *41*, 8397-8404.
280. Matyjaszewski, K.; Xia, J. "Atom transfer radical polymerization," *Chem. Rev.* **2001**, *101*, 2921-90.
281. Gaynor, S. G.; Matyjaszewski, K. "How to make polymer chains of various shapes, compositions, and functionalities by atom transfer radical polymerization," *ACS Symp. Series* **1998**, *685*, 396-417.

282. Hamilton, J. G.; Ivin, K. J.; Rooney, J. J.; Waring, L. C. "Alternating copolymerization of enantiomers of 1-methylbicyclo[2.2.1]-hept-2-ene by a metathesis catalyst," *J. Chem. Soc. Chem. Comm.* **1983**, 159-161.
283. Choi, T. L.; Rutenberg, I. M.; Grubbs, R. H. "Synthesis of A,B-alternating copolymers by ring-opening-insertion-metathesis polymerization," *Angew. Chem. Int. Ed.* **2002**, *41*, 3839-3841.
284. Ilker, M. F.; Coughlin, E. B. "Alternating copolymerizations of polar and nonpolar cyclic olefins by ring-opening metathesis polymerization," *Macromolecules* **2002**, *35*, 54-58.
285. Bornand, M.; Torker, S.; Chen, P. "Mechanistically designed dual-site catalysts for the alternating ROMP of norbornene and cyclooctene," *Organometallics* **2007**, *26*, 3585-3596.
286. Bornand, M.; Chen, P. "Mechanism-based design of a ROMP catalyst for sequence-selective copolymerization," *Angew. Chem. Int. Ed.* **2005**, *44*, 7909-11.
287. Vehlow, K.; Wang, D.; Buchmeiser, M. R.; Blechert, S. "Alternating copolymerizations using a Grubbs-type initiator with an unsymmetrical, chiral N-heterocyclic carbene ligand," *Angew. Chem. Int. Ed.* **2008**, *47*, 2615-8.
288. Amir-Ebrahimi, V.; Rooney, J. J. "Remarkable alternating effect in metathesis copolymerization of norbornene and cyclopentene using modified Grubbs ruthenium initiators," *J. Mol. Catal. A-Chem.* **2004**, *208*, 115-121.
289. AlSamak, B.; Carvill, A. G.; Hamilton, J. G.; Rooney, J. J.; Thompson, J. M. "Alternating ring-opening metathesis copolymerization of bicyclo[2.2.1]hept-2-ene and cyclopentene," *Chem. Commun.* **1997**, 2057-2058.
290. Lichtenheldt, M.; Wang, D. R.; Vehlow, K.; Reinhardt, I.; Kuhnel, C.; Decker, U.; Blechert, S.; Buchmeiser, M. R. "Alternating ring-opening metathesis copolymerization by Grubbs-type initiators with unsymmetrical N-heterocyclic carbenes," *Chem-Eur. J.* **2009**, *15*, 9451-9457.
291. Sutthasupa, S.; Shiotsuki, M.; Masuda, T.; Sanda, F. "Alternating ring-opening metathesis copolymerization of amino acid derived norbornene monomers carrying nonprotected carboxy and amino groups based on acid-base interaction," *J. Am. Chem. Soc.* **2009**, *131*, 10546-10551.

292. Hashiyama, T.; Morikawa, K.; Sharpless, K. B. "Alpha-hydroxy ketones in high enantiomeric purity from asymmetric dihydroxylation of enol ethers," *J. Org. Chem.* **1992**, *57*, 5067-5068.
293. Wohl, R. A. "Convenient one-step procedure for synthesis of cyclic enol ethers - preparation of 1-methoxy-1-cycloalkenes," *Synthesis-Stuttgart* **1974**, 38-40.
294. Achet, D.; Rocrelle, D.; Murengezi, I.; Delmas, M.; Gaset, A. "Reactions in slightly hydrated solid liquid heterogeneous media - the methylation reaction with dimethylsulfoxide," *Synthesis-Stuttgart* **1986**, 642-643.
295. Klavetter, F. L.; Grubbs, R. H. "Polycyclooctatetraene (polyacetylene) - synthesis and properties," *J. Am. Chem. Soc.* **1988**, *110*, 7807-7813.
296. Kingsbury, J. S.; Harrity, J. P. A.; Bonitatebus, P. J.; Hoveyda, A. H. "A recyclable Ru-based metathesis catalyst," *J. Am. Chem. Soc.* **1999**, *121*, 791-799.
297. Monsaert, S.; Drozdak, R.; Dragutan, V.; Dragutan, I.; Verpoort, F. "Indenylidene-ruthenium complexes bearing saturated N-heterocyclic carbenes: Synthesis and catalytic investigation in olefin metathesis reactions," *Eur. J. Inorg. Chem.* **2008**, 432-440.
298. Monsaert, S.; De Canck, E.; Drozdak, R.; Van Der Voort, P.; Verpoort, F.; Martins, J. C.; Hendrickx, P. M. S. "Indenylidene complexes of ruthenium bearing NHC ligands - structure elucidation and performance as catalysts for olefin metathesis," *Eur. J. Org. Chem.* **2009**, 655-665.
299. Thorn-Csanyi, E.; Ruhland, K. "Quantitative description of the metathesis polymerization depolymerization equilibrium in the 1,4-polybutadiene system, 1 - Influence of feed concentration and temperature," *Macromol. Chem. Phys.* **1999**, *200*, 1662-1671.
300. Kamau, S. D.; Hodge, P.; Hall, A. J.; Dad, S.; Ben-Haida, A. "Cyclo-depolymerization of olefin-containing polymers to give macrocyclic oligomers by metathesis and the entropically-driven ROMP of the olefin-containing macrocyclic esters," *Polymer* **2007**, *48*, 6808-6822.
301. Forrest, M. L.; Yanez, J. A.; Remsberg, C. M.; Ohgami, Y.; Kwon, G. S.; Davies, N. M. "Paclitaxel prodrugs with sustained release and high solubility in poly(ethylene glycol)-b-poly(epsilon-caprolactone) micelle nanocarriers:

- Pharmacokinetic disposition, tolerability, and cytotoxicity," *Pharm. Res.* **2008**, *25*, 194-206.
302. Heald, C. R.; Stolnik, S.; Kujawinski, K. S.; De Matteis, C.; Garnett, M. C.; Illum, L.; Davis, S. S.; Purkiss, S. C.; Barlow, R. J.; Gellert, P. R. "Poly(lactic acid)-poly(ethylene oxide) (PLA-PEG) nanoparticles: NMR studies of the central solidlike PLA core and the liquid PEG corona," *Langmuir* **2002**, *18*, 3669-3675.
303. Letchford, K.; Liggins, R.; Wasan, K. M.; Burt, H. "In vitro human plasma distribution of nanoparticulate paclitaxel is dependent on the physicochemical properties of poly(ethylene glycol)-block-poly(caprolactone) nanoparticles," *Eur. J. Pharm. Biopharm.* **2009**, *71*, 196-206.
304. Palma, S.; Manzo, R. H.; Allemandi, D.; Fratoni, L.; Lo Nostro, P. "Solubilization of hydrophobic drugs in octanoyl-6-O-ascorbic acid micellar dispersions," *J. Pharm. Sci.* **2002**, *91*, 1810-1816.
305. Zhang, X. F.; Li, Y. X.; Chen, X. S.; Wang, X. H.; Xu, X. Y.; Liang, Q. Z.; Hu, J. L.; Jing, X. B. "Synthesis and characterization of the paclitaxel/MPEG-PLA block copolymer conjugate," *Biomaterials* **2005**, *26*, 2121-2128.
306. Opar, A. "Bad bugs need more drugs," *Nat. Rev. Drug. Discov.* **2007**, *6*, 943-944.
307. Boucher, H. W.; Talbot, G. H.; Bradley, J. S.; Edwards, J. E.; Gilbert, D.; Rice, L. B.; Scheld, M.; Spellberg, B.; Bartlett, J. "Bad bugs, no drugs: no ESKAPE! An update from the Infectious Diseases Society of America," *Clin. Infect. Dis.* **2009**, *48*, 1-12.
308. Radis-Baptista, G.; Kerkis, A.; Prieto-Silva, A. R.; Hayashi, M. A. F.; Kerkis, I.; Yamane, T. "Membrane-translocating peptides and toxins: from nature to bedside," *J. Braz. Chem. Soc.*, **2008**, *19*, 211-225.
309. Akira, S.; Uematsu, S.; Takeuchi, O. "Pathogen recognition and innate immunity," *Cell* **2006**, *124*, 783-801.
310. Breukink, E.; van Heusden, H. E.; Vollmerhaus, P. J.; Swiezewska, E.; Brunner, L.; Walker, S.; Heck, A. J. R.; de Kruijff, B. "Lipid II is an intrinsic component of the pore induced by nisin in bacterial membranes," *J. Biol. Chem.* **2003**, *278*, 19898-19903.

311. Beckloff, N.; Laube, D.; Castro, T.; Furgang, D.; Park, S.; Perlin, D.; Clements, D.; Tang, H.; Scott, R. W.; Tew, G. N.; Diamond, G. "Activity of an antimicrobial peptide mimetic against planktonic and biofilm cultures of oral pathogens," *Antimicrob. Agents Chemother.* **2007**, *51*, 4125-4132.
312. Juvvadi, P.; Vunnam, S.; Merrifield, R. B. "Synthetic melittin, its enantio, retro, and retroenantio isomers, and selected chimeric analogs: Their antibacterial, hemolytic, and lipid bilayer action," *J. Am. Chem. Soc.* **1996**, *118*, 8989-8997.
313. Zasloff, M. "Magainins, a Class of Antimicrobial Peptides from *Xenopus* Skin - Isolation, Characterization of 2 Active Forms, and Partial Cdna Sequence of a Precursor," *P. Natl. Acad. Sci.* **1987**, *84*, 5449-5453.
314. Castro, M. S.; Cilli, E. M.; Fontes, W. "Combinatorial synthesis and directed evolution applied to the production of alpha-helix forming antimicrobial peptides analogues," *Curr. Protein. Pept. Sc.* **2006**, *7*, 473-478.
315. Chen, Y. X.; Mant, C. T.; Farmer, S. W.; Hancock, R. E. W.; Vasil, M. L.; Hodges, R. S. "Rational design of alpha-helical antimicrobial peptides with enhanced activities and specificity/therapeutic index," *J. Biol. Chem.* **2005**, *280*, 12316-12329.
316. Hamuro, Y.; Schneider, J. P.; DeGrado, W. F. "De novo design of antibacterial beta-peptides," *J. Am. Chem. Soc.* **1999**, *121*, 12200-12201.
317. Won, H. S.; Jung, S. J.; Kim, H. E.; Seo, M. D.; Lee, B. J. "Systematic peptide engineering and structural characterization to search for the shortest antimicrobial peptide analogue of gaegurin 5," *J. Biol. Chem.* **2004**, *279*, 14784-14791.
318. Porter, E. A.; Wang, X.; Lee, H. S.; Weisblum, B.; Gellman, S. H. "Non-haemolytic beta-amino-acid oligomers (vol 404, pg 565, 2000)," *Nature* **2000**, *405*, 298-298.
319. Liu, D. H.; DeGrado, W. F. "De novo design, synthesis, and characterization of antimicrobial beta-peptides," *J. Am. Chem. Soc.* **2001**, *123*, 7553-7559.
320. Epanand, R. F.; Raguse, T. L.; Gellman, S. H.; Epanand, R. M. "Antimicrobial 14-helical beta-peptides: Potent bilayer disrupting agents," *Biochemistry* **2004**, *43*, 9527-9535.

321. Salick, D. A.; Kretsinger, J. K.; Pochan, D. J.; Schneider, J. P. "Inherent antibacterial activity of a peptide-based beta-hairpin hydrogel," *J. Am. Chem. Soc.* **2007**, *129*, 14793-14799.
322. Mowery, B. P.; Lindner, A. H.; Weisblum, B.; Stahl, S. S.; Gellman, S. H. "Structure-activity relationships among random Nylon-3 copolymers that mimic antibacterial host-defense peptides," *J. Am. Chem. Soc.* **2009**, *131*, 9735-9745.
323. Schmitt, M. A.; Weisblum, B.; Gellman, S. H. "Interplay among folding, sequence, and lipophilicity in the antibacterial and hemolytic activities of alpha/beta-peptides," *J. Am. Chem. Soc.* **2007**, *129*, 417-428.
324. Al-Badri, Z. M.; Som, A.; Lyon, S.; Nelson, C. F.; Nusslein, K.; Tew, G. N. "Investigating the effect of increasing charge density on the hemolytic activity of synthetic antimicrobial polymers," *Biomacromolecules* **2008**, *9*, 2805-2810.
325. Gelman, M. A.; Weisblum, B.; Lynn, D. M.; Gellman, S. H. "Biocidal activity of polystyrenes that are cationic by virtue of protonation," *Org. Lett.* **2004**, *6*, 557-560.
326. Endo, Y.; Tani, T.; Kodama, M. "Antimicrobial activity of tertiary amine covalently bonded to a polystyrene fiber," *Appl. Environ. Microb.* **1987**, *53*, 2050-2055.
327. Sharma, S. K.; Chauhan, G. S.; Gupta, R.; Ahn, J. H. "Tuning anti-microbial activity of poly(4-vinyl 2-hydroxyethyl pyridinium) chloride by anion exchange reactions," *J. Mater. Sci. Mater. Med.* **2009**, 3932-3939.
328. Sambhy, V.; MacBride, M. M.; Peterson, B. R.; Sen, A. "Silver bromide nanoparticle/polymer composites: dual action tunable antimicrobial materials," *J. Am. Chem. Soc.* **2006**, *128*, 9798-9808.
329. Li, G. J.; Shen, J. R. "A study of pyridinium-type functional polymers. IV. Behavioral features of the antibacterial activity of insoluble pyridinium-type polymers," *J. Appl. Polym. Sci.* **2000**, *78*, 676-684.
330. Li, G. J.; Shen, J. R.; Zhu, Y. L. "Study of pyridinium-type functional polymers. II. Antibacterial activity of soluble pyridinium-type polymers," *J. Appl. Polym. Sci.* **1998**, *67*, 1761-1768.

331. Allison, B. C.; Applegate, B. M.; Youngblood, J. P. "Hemocompatibility of hydrophilic antimicrobial copolymers of alkylated 4-vinylpyridine," *Biomacromolecules* **2007**, *8*, 2995-2999.
332. Chen, C. Z.; Beck-Tan, N. C.; Dhurjati, P.; van Dyk, T. K.; LaRossa, R. A.; Cooper, S. L. "Quaternary ammonium functionalized poly(propylene imine) dendrimers as effective antimicrobials: structure-activity studies," *Biomacromolecules* **2000**, *1*, 473-480.
333. Chen, C. Z.; Tan, N. C. B.; Cooper, S. L. "Incorporation of dimethyldodecylammonium chloride functionalities onto poly(propylene imine) dendrimers significantly enhances their antibacterial properties," *Chem. Commun.* **1999**, 1585-1586.
334. Brouwer, C. P. J. M.; Bogaards, S. J. P.; Wulferink, M.; Velders, M. P.; Welling, M. M. "Synthetic peptides derived from human antimicrobial peptide ubiquicidin accumulate at sites of infections and eradicate (multi-drug resistant) *Staphylococcus aureus* in mice," *Peptides* **2006**, *27*, 2585-2591.
335. Haynie, S. L.; Crum, G. A.; Doele, B. A. "Antimicrobial Activities of Amphiphilic Peptides Covalently Bonded to a Water-Insoluble Resin," *Antimicrob. Agents Chemother.* **1995**, *39*, 301-307.
336. Chongsiriwatana, N. P.; Patch, J. A.; Czyzewski, A. M.; Dohm, M. T.; Ivankin, A.; Gidalevitz, D.; Zuckermann, R. N.; Barron, A. E. "Peptoids that mimic the structure, function, and mechanism of helical antimicrobial peptides," *P. Natl. Acad. Sci.* **2008**, *105*, 2794-2799.
337. Arnt, L.; Tew, G. N. "New poly(phenyleneethynylene)s with cationic, facially amphiphilic structures," *J. Am. Chem. Soc.* **2002**, *124*, 7664-7665.
338. Arnt, L.; Tew, G. N. "Cationic facially amphiphilic poly(phenylene ethynylene)s studied at the air-water interface," *Langmuir* **2003**, *19*, 2404-2408.
339. Yang, L. H.; Gordon, V. D.; Mishra, A.; Sorn, A.; Purdy, K. R.; Davis, M. A.; Tew, G. N.; Wong, G. C. L. "Synthetic antimicrobial, oligomers induce a composition-dependent topological transition in membranes," *J. Am. Chem. Soc.* **2007**, *129*, 12141-12147.

340. Tang, H. Z.; Doerksen, R. J.; Tew, G. N. "Synthesis of urea oligomers and their antibacterial activity," *Chem. Commun.* **2005**, 1537-1539.
341. Hintermann, T.; Seebach, D. "The biological stability of beta-peptides: No interactions between alpha- and beta-peptidic structures," *Chimia* **1997**, *51*, 244-247.
342. Arvidsson, P. I.; Ryder, N. S.; Weiss, H. M.; Hook, D. F.; Escalante, J.; Seebach, D. "Exploring the antibacterial and hemolytic activity of shorter- and longer-chain beta- alpha,beta-, and gamma-peptides, and of beta-peptides from beta(2)-3-aza- and beta(3)-2-methylidene-amino acids bearing proteinogenic side chains - A survey," *Chem. Biodivers.* **2005**, *2*, 401-420.
343. Wu, C. W.; Sanborn, T. J.; Huang, K.; Zuckermann, R. N.; Barron, A. E. "Peptoid oligomers with alpha-chiral, aromatic side chains: Sequence requirements for the formation of stable peptoid helices," *J. Am. Chem. Soc.* **2001**, *123*, 6778-6784.
344. Sanborn, T. J.; Wu, C. W.; Zuckerman, R. N.; Barron, A. E. "Extreme stability of helices formed by water-soluble poly-N-substituted glycines (polypeptoids) with alpha-chiral side chains," *Biopolymers* **2002**, *63*, 12-20.
345. Miller, S. M.; Simon, R. J.; Ng, S.; Zuckermann, R. N.; Kerr, J. M.; Moos, W. H. "Comparison of the proteolytic susceptibilities of homologous L-amino-acid, D-amino-acid, and N-substituted glycine peptide and peptoid oligomers," *Drug Develop. Res.* **1995**, *35*, 20-32.
346. Tang, H.; Doerksen, R. J.; Jones, T. V.; Klein, M. L.; Tew, G. N. "Biomimetic facially amphiphilic antibacterial oligomers with conformationally stiff backbones," *Chem. Biol.* **2006**, *13*, 427-435.
347. Ashby, E. C.; Coleman, D. "Evidence for single electron-transfer in the reactions of lithium dimethylcuprate with alkyl-halides," *J. Org. Chem.* **1987**, *52*, 4554-4565.
348. Bloodworth, A. J.; Melvin, T.; Mitchell, J. C. "Mechanistic aspects of oxygen-transfer by *gem*-dialkylperoxonium ions," *J. Org. Chem.* **1988**, *53*, 1078-1082.
349. Grubbs, R. H. "Handbook of Metathesis;" Wiley-VCH: Weinheim, Germany, **2003**; Vol. 3.

350. Zhang, L. J.; Scott, M. G.; Yan, H.; Mayer, L. D.; Hancock, R. E. W. "Interaction of polyphemusin I and structural analogs with bacterial membranes, lipopolysaccharide, and lipid monolayers," *Biochemistry* **2000**, *39*, 14504-14514.
351. Anderson, R. C.; Hancock, R. E. W.; Yu, P. L. "Antimicrobial activity and bacterial-membrane interaction of ovine-derived cathelicidins," *Antimicrob. Agents Chemother.* **2004**, *48*, 673-676.
352. Silvestro, L.; Weiser, J. N.; Axelsen, P. H. "Antibacterial and antimembrane activities of cecropin A in Escherichia coli," *Antimicrob. Agents Chemother.* **2000**, *44*, 602-607.
353. Zhang, L. J.; Dhillon, P.; Yan, H.; Farmer, S.; Hancock, R. E. W. "Interactions of bacterial cationic peptide antibiotics with outer and cytoplasmic membranes of Pseudomonas aeruginosa," *Antimicrob. Agents Chemother.* **2000**, *44*, 3317-3321.
354. Hancock, R. E. W. "Resistance mechanisms in Pseudomonas aeruginosa and other nonfermentative Gram-negative bacteria," *Clin. Infect. Dis.* **1998**, *27*, S93-S99.
355. Gabriel, G. J.; Maegerlein, J. A.; Nelson, C. F.; Dabkowski, J. M.; Eren, T.; Nusslein, K.; Tew, G. N. "Comparison of facially amphiphilic versus segregated monomers in the design of antibacterial copolymers," *Chem-Eur. J.* **2009**, *15*, 433-439.
356. Herranz, C.; Cintas, L. M.; Hernandez, P. E.; Moll, G. N.; Driessen, A. J. M. "Enterocin P causes potassium ion efflux from Enterococcus faecium T136 cells," *Antimicrob. Agents Chemother.* **2001**, *45*, 901-904.
357. Fjell, C. D.; Jenssen, H.; Hilpert, K.; Cheung, W. A.; Pante, N.; Hancock, R. E.; Cherkasov, A. "Identification of novel antibacterial peptides by chemoinformatics and machine learning," *J. Med. Chem.* **2009**, *52*, 2006-2015.
358. Sawyer, J. G.; Martin, N. L.; Hancock, R. E. "Interaction of macrophage cationic proteins with the outer membrane of Pseudomonas aeruginosa," *Infect. Immun.* **1988**, *56*, 693-698.
359. Malina, A.; Shai, Y. "Conjugation of fatty acids with different lengths modulates the antibacterial and antifungal activity of a cationic biologically inactive peptide," *Biochem. J.* **2005**, *390*, 695-702.

360. Sun, G.; Fang, H. F.; Cheng, C.; Lu, P.; Zhang, K.; Walker, A. V.; Taylor, J. S. A.; Wooley, K. L. "Benzaldehyde-functionalized polymer vesicles," *ACS Nano* **2009**, *3*, 673-681.
361. Li, M. H.; Keller, P. "Stimuli-responsive polymer vesicles," *Soft Matter* **2009**, *5*, 927-937.
362. He, J.; Tong, X.; Tremblay, L.; Zhao, Y. "Corona-cross-linked polymer vesicles displaying a large and reversible temperature-responsive volume transition," *Macromolecules* **2009**, *42*, 7267-7270.
363. Du, J. Z.; O'Reilly, R. K. "Advances and challenges in smart and functional polymer vesicles," *Soft Matter* **2009**, *5*, 3544-3561.
364. Wu, D.; Abezgauz, L.; Danino, D.; Ho, C. C.; Co, C. C. "Alternating polymer vesicles," *Soft Matter* **2008**, *4*, 1066-1071.
365. Zhou, Y. F.; Yan, D. Y.; Dong, W. Y.; Tian, Y. "Temperature-responsive phase transition of polymer vesicles: Real-time morphology observation and molecular mechanism," *J. Phys. Chem. B* **2007**, *111*, 1262-1270.
366. Wittemann, A.; Azzam, T.; Eisenberg, A. "Biocompatible polymer vesicles from biamphiphilic triblock copolymers and their interaction with bovine serum albumin," *Langmuir* **2007**, *23*, 2224-2230.
367. Morishima, Y. "Thermally responsive polymer vesicles," *Angew. Chem. Int. Ed.* **2007**, *46*, 1370-1372.
368. Qin, S. H.; Geng, Y.; Discher, D. E.; Yang, S. "Temperature-controlled assembly and release from polymer vesicles of poly(ethylene oxide)-block-poly(N-isopropylacrylamide)," *Adv. Mater.* **2006**, *18*, 2905-2909.
369. Yang, J.; Levy, D.; Deng, W.; Keller, P.; Li, M. H. "Polymer vesicles formed by amphiphilic diblock copolymers containing a thermotropic liquid crystalline polymer block," *Chem. Commun.* **2005**, 4345-4347.
370. Kita-Tokarczyk, K.; Grumelard, J.; Haefele, T.; Meier, W. "Block copolymer vesicles - using concepts from polymer chemistry to mimic biomembranes," *Polymer* **2005**, *46*, 3540-3563.

371. Choi, H. J.; Brooks, E.; Montemagno, C. D. "Synthesis and characterization of nanoscale biomimetic polymer vesicles and polymer membranes for bioelectronic applications," *Nanotechnology* **2005**, *16*, 143-149.
372. Zhou, Y. F.; Yan, D. Y. "Supramolecular self-assembly of giant polymer vesicles with controlled sizes," *Angew. Chem. Int. Ed.* **2004**, *43*, 4896-4899.
373. Antunes, F. E.; Marques, E. F.; Gomes, R.; Thuresson, K.; Lindman, B.; Miguel, M. G. "Network formation of cationic vesicles and oppositely charged polyelectrolytes. Effect of polymer charge density and hydrophobic modification," *Langmuir* **2004**, *20*, 4647-4656.
374. Ge, L. Q.; Mohwald, H.; Li, J. B. "Polymer-stabilized phospholipid vesicles formed on polyelectrolyte multilayer capsules," *Biochem. Biophys. Res. Commun.* **2003**, *303*, 653-659.
375. Discher, D. E.; Eisenberg, A. "Polymer vesicles," *Science* **2002**, *297*, 967-973.
376. Yuan, Z. W.; Hao, J. C.; Hoffmann, H. "A promising system of mixed single- and double-short-tailed PEO ether phosphate esters: Phase behavior and vesicle formation," *J. Colloid. Interface Sci.* **2006**, *302*, 673-681.
377. Smarsly, B.; Xomeritakis, G.; Yu, K.; Liu, N. G.; Fan, H. Y.; Assink, R. A.; Drewien, C. A.; Ruland, W.; Brinker, C. J. "Microstructural characterization of polystyrene-block-poly(ethylene oxide)-templated silica films with cubic-ordered spherical mesopores," *Langmuir* **2003**, *19*, 7295-7301.
378. Yu, K.; Hurd, A. J.; Eisenberg, A.; Brinker, C. J. "Syntheses of silica/polystyrene-block-poly(ethylene oxide) films with regular and reverse mesostructures of large characteristic length scales by solvent evaporation-induced self-assembly," *Langmuir* **2001**, *17*, 7961-7965.
379. Cox, J. K.; Yu, K.; Constantine, B.; Eisenberg, A.; Lennox, R. B. "Polystyrene-poly(ethylene oxide) diblock copolymers form well-defined surface aggregates at the air/water interface," *Langmuir* **1999**, *15*, 7714-7718.
380. Dan, N.; Shimoni, K.; Pata, V.; Danino, D. "Effect of mixing on the morphology of cylindrical micelles," *Langmuir* **2006**, *22*, 9860-9865.
381. Dimova, R.; Seifert, U.; Pouligny, B.; Forster, S.; Dobereiner, H. G. "Hyperviscous diblock copolymer vesicles," *Eur. Phys. J. E* **2002**, *7*, 241-250.

382. Discher, B. M.; Bermudez, H.; Hammer, D. A.; Discher, D. E.; Won, Y. Y.; Bates, F. S. "Cross-linked polymersome membranes: Vesicles with broadly adjustable properties," *J. Phys. Chem. B* **2002**, *106*, 2848-2854.
383. Maskos, M.; Harris, J. R. "Double-shell vesicles, strings of vesicles and filaments found in crosslinked micellar solutions of poly(1,2-butadiene)-block-poly(ethylene oxide) diblock copolymers," *Macromol. Rapid Comm.* **2001**, *22*, 271-273.
384. Ahmed, F.; Discher, D. E. "Self-porating polymersomes of PEG-PLA and PEG-PCL: hydrolysis-triggered controlled release vesicles," *J. Control. Release* **2004**, *96*, 37-53.
385. Katz, J. S.; Levine, D. H.; Davis, K. P.; Bates, F. S.; Hammer, D. A.; Burdick, J. A. "Membrane stabilization of biodegradable polymersomes," *Langmuir* **2009**, *25*, 4429-4434.
386. Meng, F. H.; Engbers, G. H. M.; Feijen, J. "Biodegradable polymersomes as a basis for artificial cells: encapsulation, release and targeting," *J. Control. Release* **2005**, *101*, 187-198.
387. Meng, F. H.; Hiemstra, C.; Engbers, G. H. M.; Feijen, J. "Biodegradable polymersomes," *Macromolecules* **2003**, *36*, 3004-3006.
388. Najafi, F.; Sarbolouki, M. N. "Biodegradable micelles/polymersomes from fumaric/sebacic acids and poly(ethylene glycol)," *Biomaterials* **2003**, *24*, 1175-1182.
389. Luo, L. B.; Eisenberg, A. "Thermodynamic size control of block copolymer vesicles in solution," *Langmuir* **2001**, *17*, 6804-6811.
390. Luo, L. B.; Eisenberg, A. "Thermodynamic stabilization mechanism of block copolymer vesicles," *J. Am. Chem. Soc.* **2001**, *123*, 1012-1013.
391. Shen, H. W.; Eisenberg, A. "Morphological phase diagram for a ternary system of block copolymer PS₃₁₀-b-PAA₅₂/dioxane/H₂O," *J. Phys. Chem. B* **1999**, *103*, 9473-9487.
392. Shen, H. W.; Eisenberg, A. "Block length dependence of morphological phase diagrams of the ternary system of PS-b-PAA/dioxane/H₂O," *Macromolecules* **2000**, *33*, 2561-2572.

393. Schillen, K.; Bryskhe, K.; Mel'nikova, Y. S. "Vesicles formed from a poly(ethylene oxide)-poly(propylene oxide)-poly(ethylene oxide) triblock copolymer in dilute aqueous solution," *Macromolecules* **1999**, *32*, 6885-6888.
394. Zipfel, J.; Berghausen, J.; Schmidt, G.; Lindner, P.; Alexandridis, P.; Tsianou, M.; Richtering, W. "Shear induced structures in lamellar phases of amphiphilic block copolymers," *Phys. Chem. Chem. Phys.* **1999**, *1*, 3905-3910.
395. Zipfel, J.; Lindner, P.; Tsianou, M.; Alexandridis, P.; Richtering, W. "Shear-induced formation of multilamellar vesicles ("onions") in block copolymers," *Langmuir* **1999**, *15*, 2599-2602.
396. Ghoroghchian, P. P.; Li, G. Z.; Levine, D. H.; Davis, K. P.; Bates, F. S.; Hammer, D. A.; Therien, M. J. "Bioresorbable vesicles formed through spontaneous self-assembly of amphiphilic poly(ethylene oxide)-block-polycaprolactone," *Macromolecules* **2006**, *39*, 1673-1675.
397. Sutthasupa, S.; Sanda, F.; Masuda, T. "Copolymerization of amino acid functionalized norbornene monomers. Synthesis of amphiphilic block copolymers forming reverse micelles," *Macromolecules* **2008**, *41*, 305-311.
398. Claessens, M. M. A. E.; van Oort, B. F.; Leermakers, F. A. M.; Hoekstra, F. A.; Stuart, M. A. C. "Charged lipid vesicles: Effects of salts on bending rigidity, stability, and size," *Biophys. J.* **2004**, *87*, 3882-3893.
399. Soo, P. L.; Eisenberg, A. "Preparation of block copolymer vesicles in solution," *J. Polym. Sci. Pol. Phys.* **2004**, *42*, 923-938.
400. Du, J. Z.; Tang, Y. P.; Lewis, A. L.; Armes, S. P. "pH-sensitive vesicles based on a biocompatible zwitterionic diblock copolymer," *J. Am. Chem. Soc.* **2005**, *127*, 17982-17983.
401. Borchert, U.; Lipprandt, U.; Bilanz, M.; Kimpfler, A.; Rank, A.; Peschka-Suss, R.; Schubert, R.; Lindner, P.; Forster, S. "pH-induced release from P2VP-PEO block copolymer vesicles," *Langmuir* **2006**, *22*, 5843-5847.
402. Paul, G. K.; Indi, S. S.; Ramakrishnan, S. "Synthesis and vesicular polymerization of novel counter-ion polymerizable/crosslinkable surfactants," *J. Polym. Sci. Pol. Chem.* **2004**, *42*, 5271-5283.

403. Lee, A. S.; Butun, V.; Vamvakaki, M.; Armes, S. P.; Pople, J. A.; Gast, A. P. "Structure of pH-dependent block copolymer micelles: Charge and ionic strength dependence," *Macromolecules* **2002**, *35*, 8540-8551.
404. Campbell, A.; Rydon, H. N. "The Synthesis of Caryophyllenic Acid," *J. Chem. Soc.* **1953**, 3002-3008.
405. Gay, M.; Montana, A. M.; Moreno, V.; Font-Bardia, M.; Solans, X. "Synthesis and structure of an unexpected platinum π complex formed from substituted 1,4-diamino ligands through an elimination process," *Chem-Eur. J.* **2005**, *11*, 2130-2134.
406. Ashby, E. C.; Pham, T. N. "The use of 5-halocyclooctenes as a radical probe - reactions with lithium aluminum-hydride," *J. Org. Chem.* **1986**, *51*, 3598-3602.
407. Becke, A. D. "Density-functional thermochemistry .4. A new dynamical correlation functional and implications for exact-exchange mixing," *J. Chem. Phys.* **1996**, *104*, 1040-1046.
408. Becke, A. D. "Density-Functional Thermochemistry .3. The Role of Exact Exchange," *J. Chem. Phys.* **1993**, *98*, 5648-5652.
409. Lee, C. T.; Yang, W. T.; Parr, R. G. "Development of the Colle-Salvetti Correlation-Energy Formula into a Functional of the Electron-Density," *Phys. Rev. B* **1988**, *37*, 785-789.
410. "<http://www.chemistry.mcmaster.ca/aimpac/>," *AIMPAC download site* **2010**, Chemistry Department, McMaster University.
411. Mason, A. J.; Moussaoui, W.; Abdelrahman, T.; Boukhari, A.; Bertani, P.; Marquette, A.; Shooshtarizadeh, P.; Moulay, G.; Boehm, N.; Guerold, B.; Sawers, R. J.; Kichler, A.; Metz-Boutigue, M. H.; Candolfi, E.; Prevost, G.; Bechinger, B. "Structural determinants of antimicrobial and antiplasmodial activity and selectivity in histidine-rich amphipathic cationic peptides," *J. Biol. Chem.* **2009**, *284*, 119-133.
412. Silverman, J. A.; Perlmutter, N. G.; Shapiro, H. M. "Correlation of daptomycin bactericidal activity and membrane depolarization in *Staphylococcus aureus*," *Antimicrob. Agents Chemother.* **2003**, *47*, 2538-2544.

413. *Methods for Dilution Antimicrobial Susceptibility Tests for Bacteria That Grow Aerobically, 6th ed., Approved Standard M7-A6*; CLSI, Ed.; Clinical and Laboratory Standards Institute, Wayne, PA, 2006.
414. Murthy, N.; Robichaud, J. R.; Tirrell, D. A.; Stayton, P. S.; Hoffman, A. S. "The design and synthesis of polymers for eukaryotic membrane disruption," *J. Control. Release* **1999**, *61*, 137-143.
415. Kiselev, M. A.; Zemlyanaya, E. V.; Aswal, V. K.; Neubert, R. H. H. "What can we learn about the lipid vesicle structure from the small-angle neutron scattering experiment?," *Eur. Biophys. J.* **2006**, *35*, 477-493.

Appendix

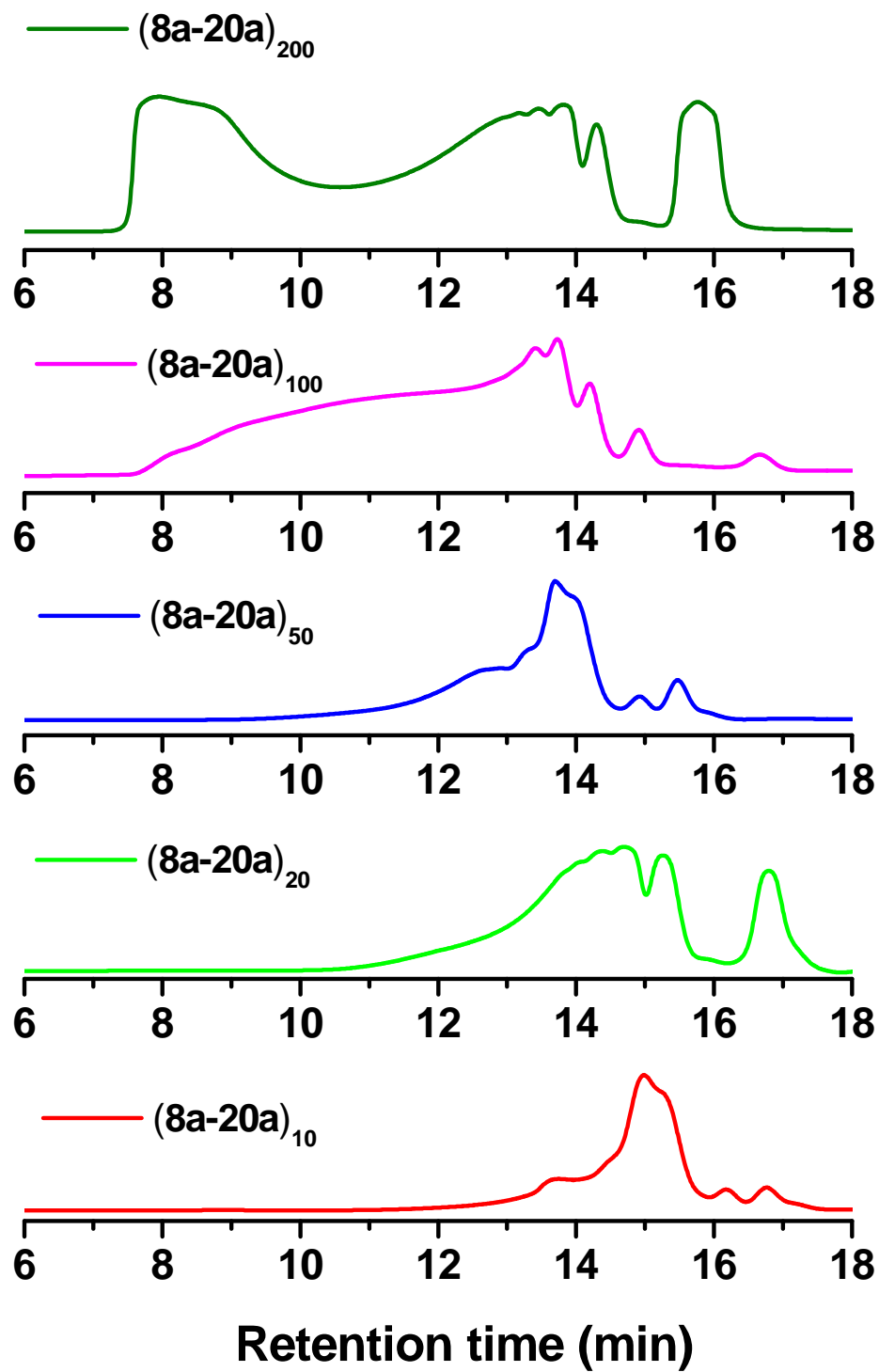
A-1: Checklist for compounds

Compound	Ref.	¹ H-NMR	¹³ C-NMR	Other
11	111, 404	O	O	
6a	111	O	O	
6b		O	O	HRMS (ESI)
6v		O	O	HRMS (ESI)
6d		O	O	HRMS (ESI)
6e		O	O	HRMS (ESI)
8a		O	O	HRMS (ESI)
7b		O	O	HRMS (ESI)
8a	250, 251	O	O	HRMS (ESI)
8b		O	O	HRMS (ESI)
8c		O	O	HRMS (ESI)
8d		O	O	HRMS (ESI)
8e		O	O	HRMS (ESI)
8f		O	O	HRMS (ESI)
8g		O	O	HRMS (ESI)
12		O	O	
9a		O	O	HRMS (ESI)
20b		O	O	LC-MS (APCI)
20d		O	O	LC-MS (APCI)
20e		O	O	
23	405	O	O	
20f	405	O	O	
20g		O		
20h	405	O		
20k		O	O	HRMS (ESI)
20m		O	O	HRMS (ESI)
29b		O	O	
30		O	O	HRMS (ESI)
31	406	O		

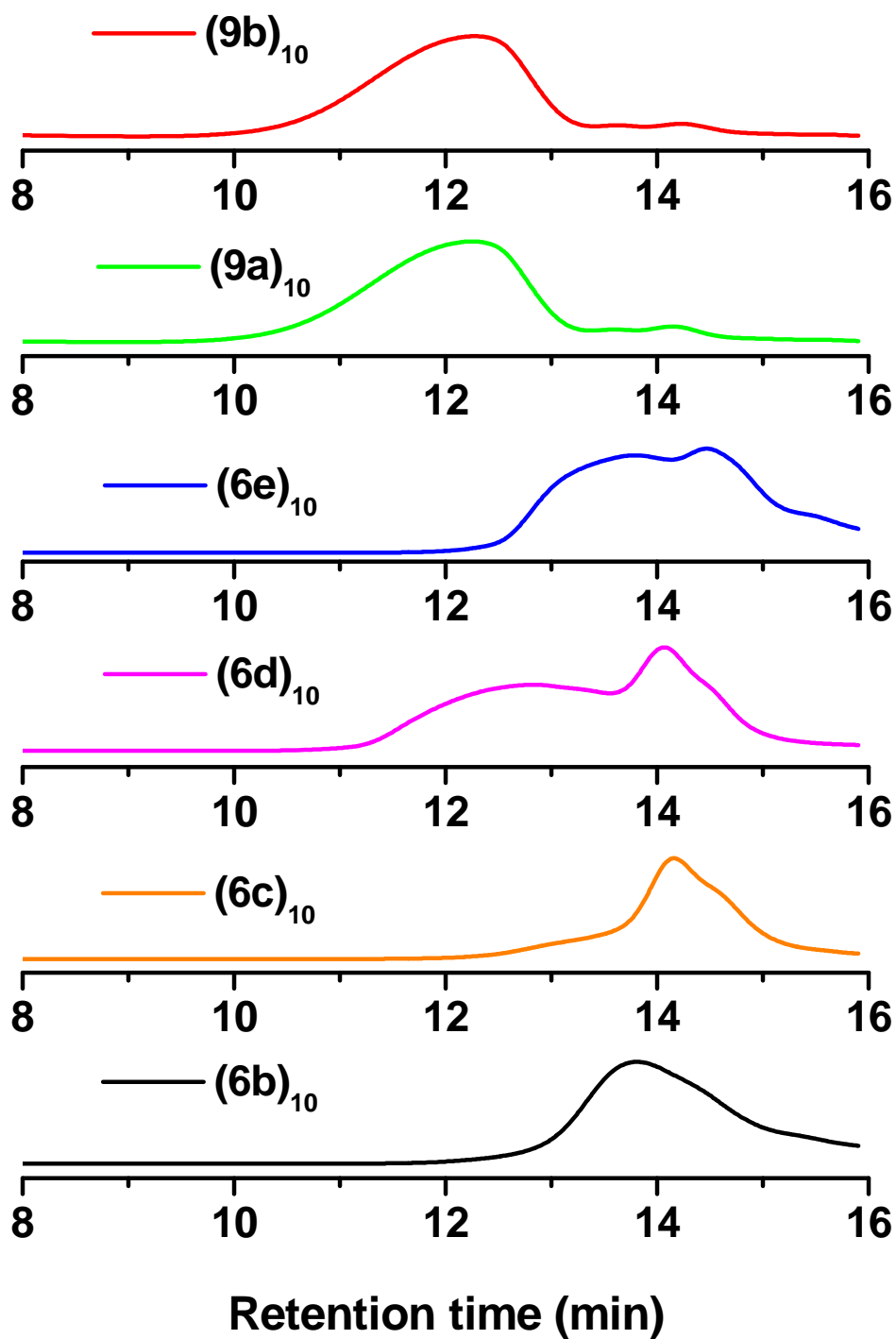
Compound	Ref.	¹ H-NMR	¹³ C-NMR	Other
33	348	O	O	
34		O	O	HRMS (ESI)
6a₁₀		O		
6b₁₀		O		
6c₁₀		O		
6d₁₀		O		
6e₁₀		O		
8a₁		O	O	
9a₁₀		O		
(8a-20a)₃		O	O	
(8a-20a)₁₀		O		
(8a-20a)₂₀		O	O	gCOSY, gHMQC, ¹³ C-APT
(8a-20a)₅₀		O		
(8a-20a)₁₀₀		O	O	
(8a-20a)₂₀₀		O		
(8a-20a-D₁₀)₂₀		O		
(8a-20a-D₁₀)₂₀-[25]		O		
cyc-(8a-20a-D₁₀)₂₀		O		
(8c-20a)₂₀		O		
(8d-20a)₁₀		O		
(8a-20d)₂₀		O		
(8a-29a)₂₀-[28]		O		
Intermediate-1		O	O	
Intermediate-2		O		
Intermediate-3		O		
Intermediate-4		O		
Intermediate-5		O		
Intermediate-6		O		
Intermediate-7		O		

Compound	Ref.	¹ H-NMR	¹³ C-NMR	Other
Intermediate-8		O		
Intermediate-9		O		
Intermediate-10		O	O	gCOSY
Intermediate-11		O		
Intermediate-12		O	O	
Intermediate-13		O		
Intermediate-14		O	O	
Acopolymer-1		O		
Acopolymer-2		O		
Acopolymer-3		O		
Acopolymer-4		O		
Acopolymer-5		O		
Acopolymer-6		O		
Acopolymer-7		O		
Rcopolymer-8		O		
Rcopolymer-9		O		
Rcopolymer-10		O		
Homopolymer-11		O		
Homopolymer-12		O		
Homopolymer-13		O		
Homopolymer-14		O		

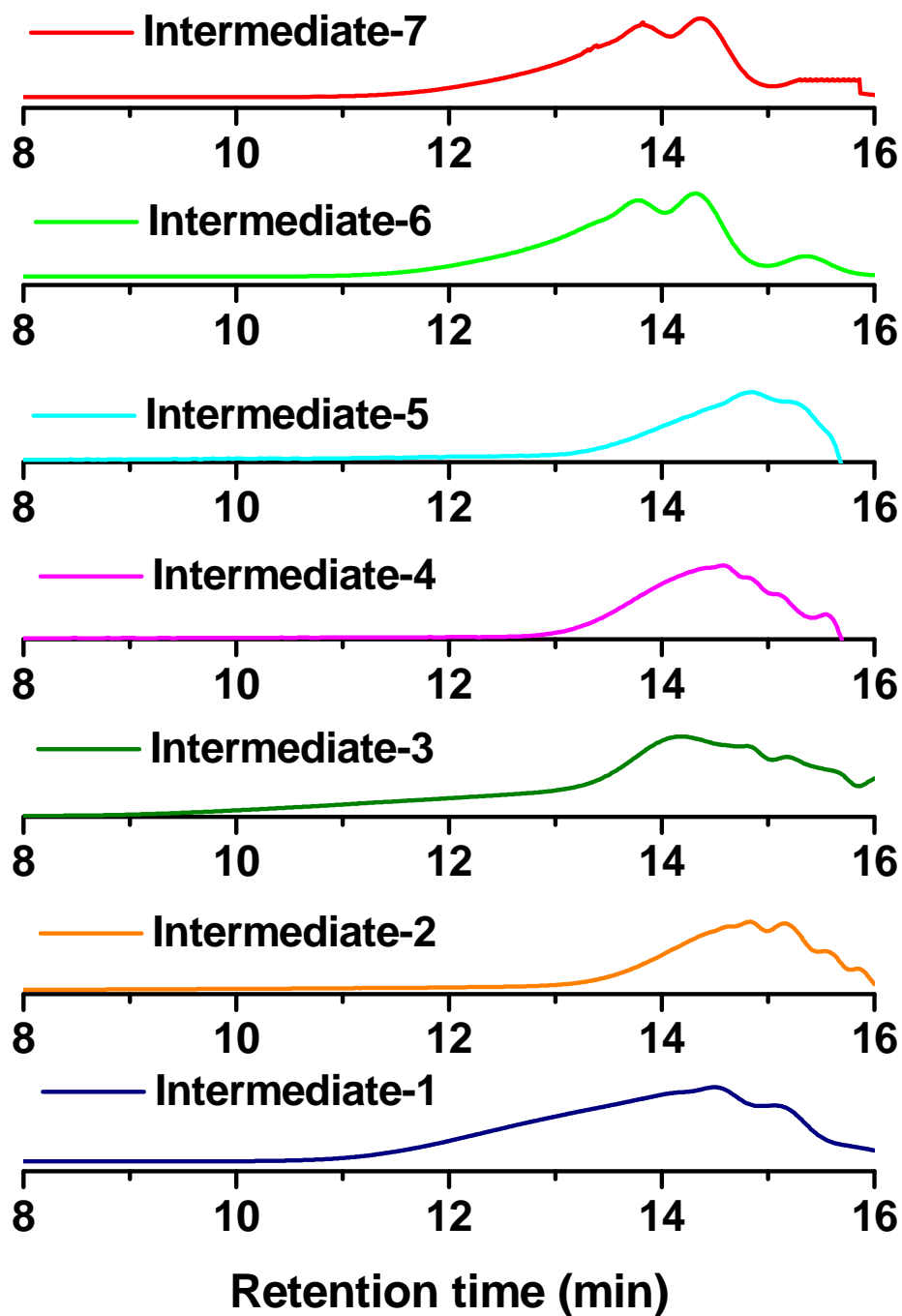
A-2: GPC traces of alternating copolymers



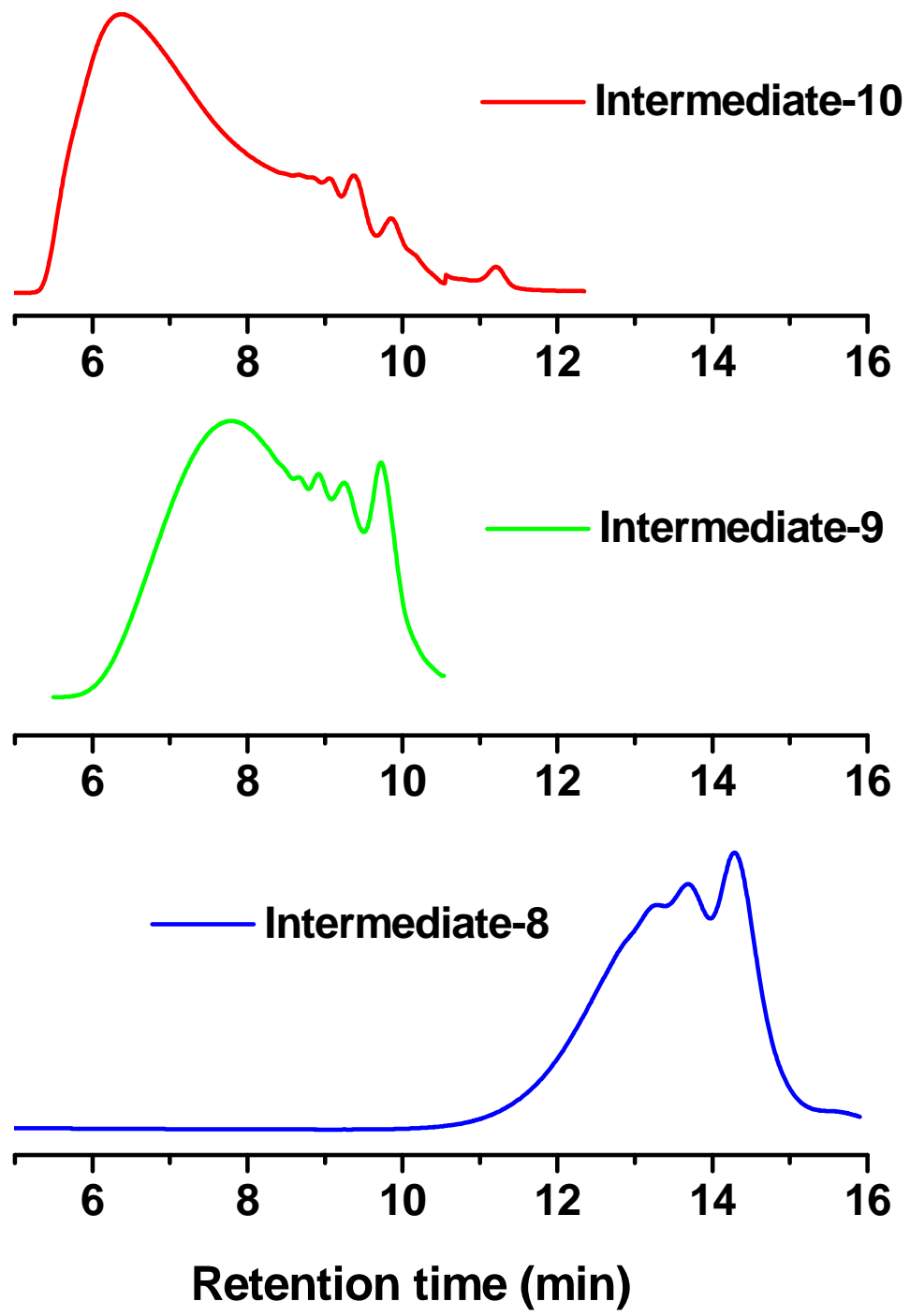
A-3: GPC traces of homopolymers



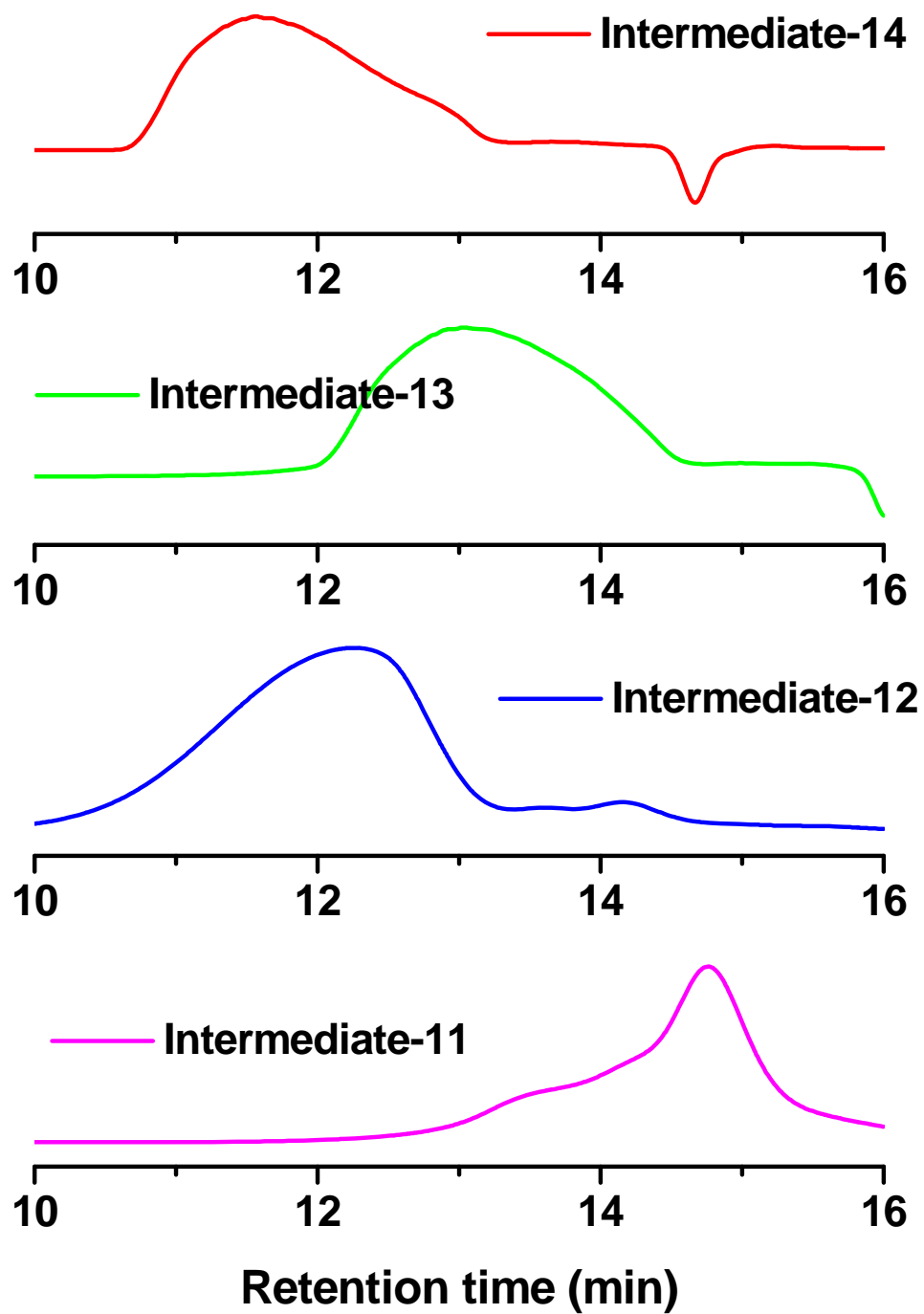
A-4: GPC traces of Intermediate-1 to Intermediate-7



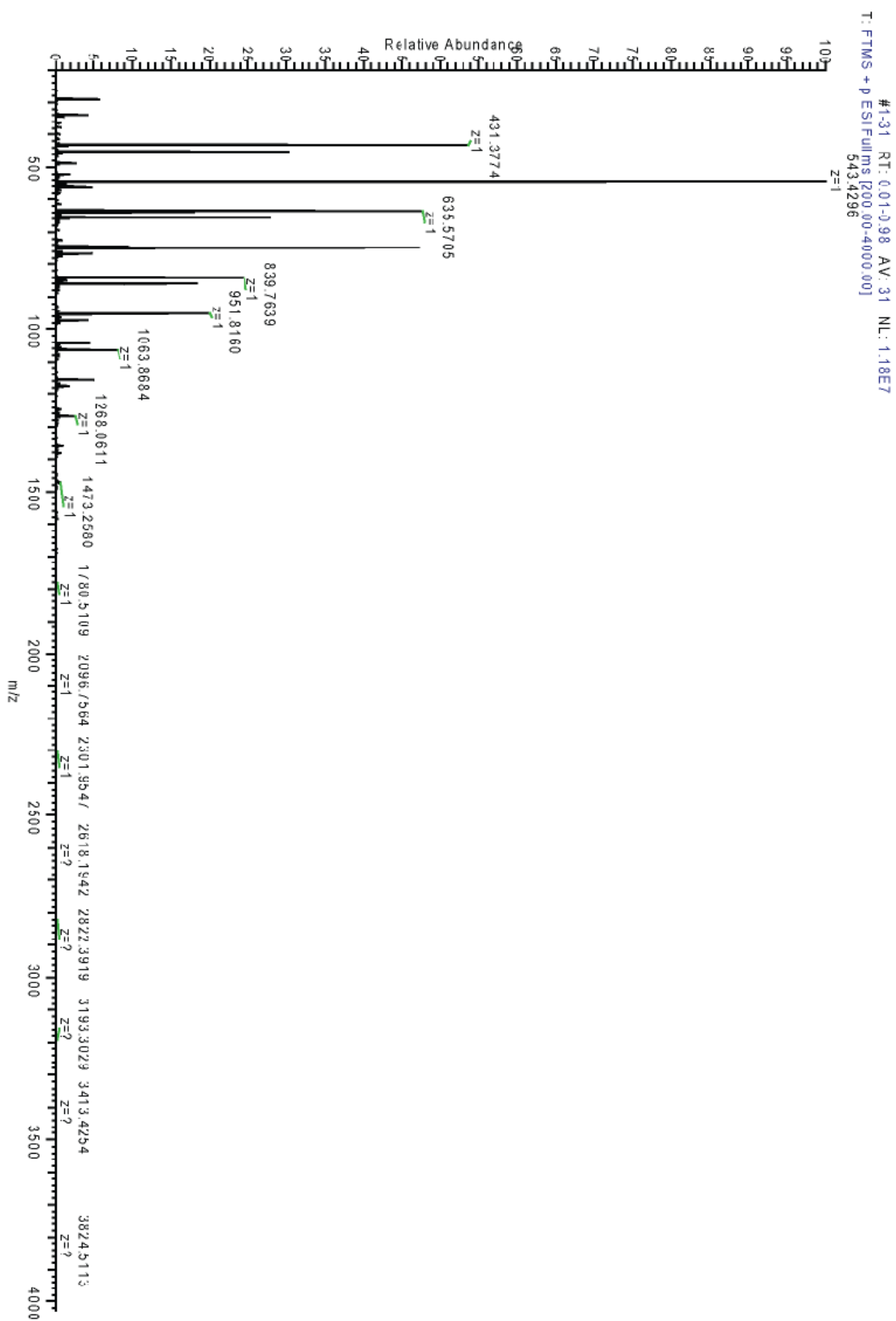
A-5: GPC traces of Intermediate-8 to Intermediate-10



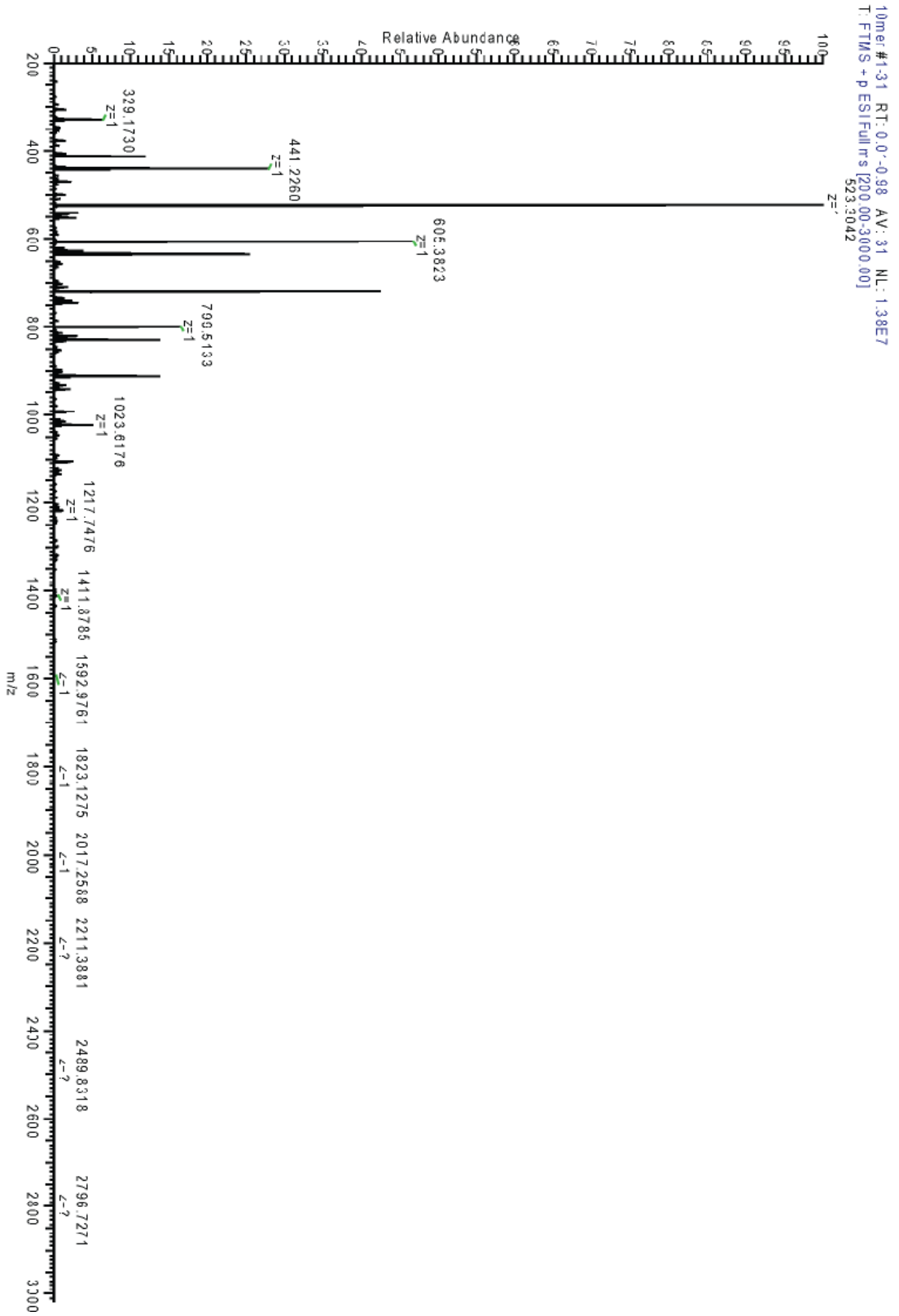
A-6: GPC traces of Homopolymer-11 to Homopolymer-14

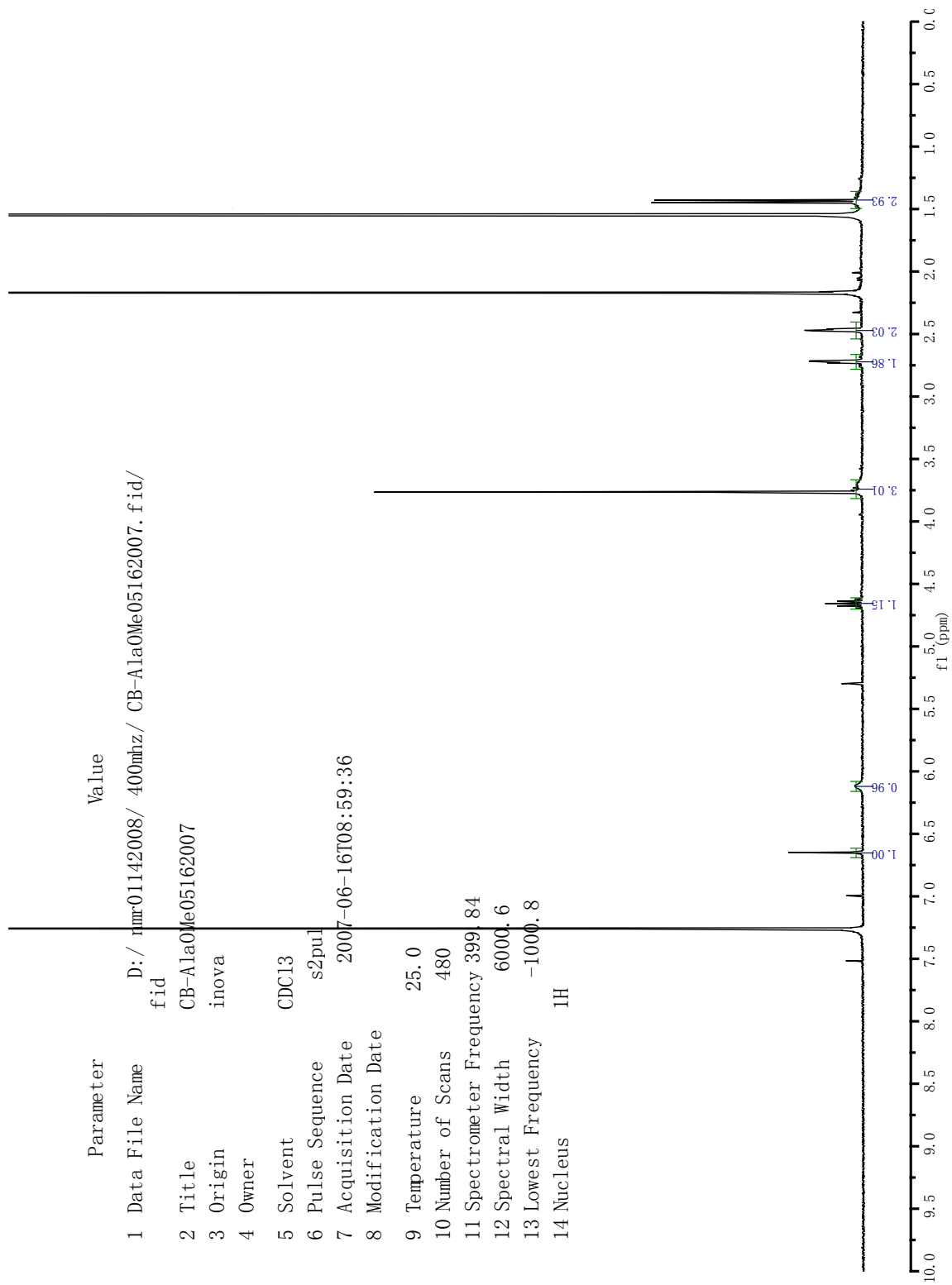


A-7: ESI-Mass spectrum of cyclic alternating polymer with catalyst 25

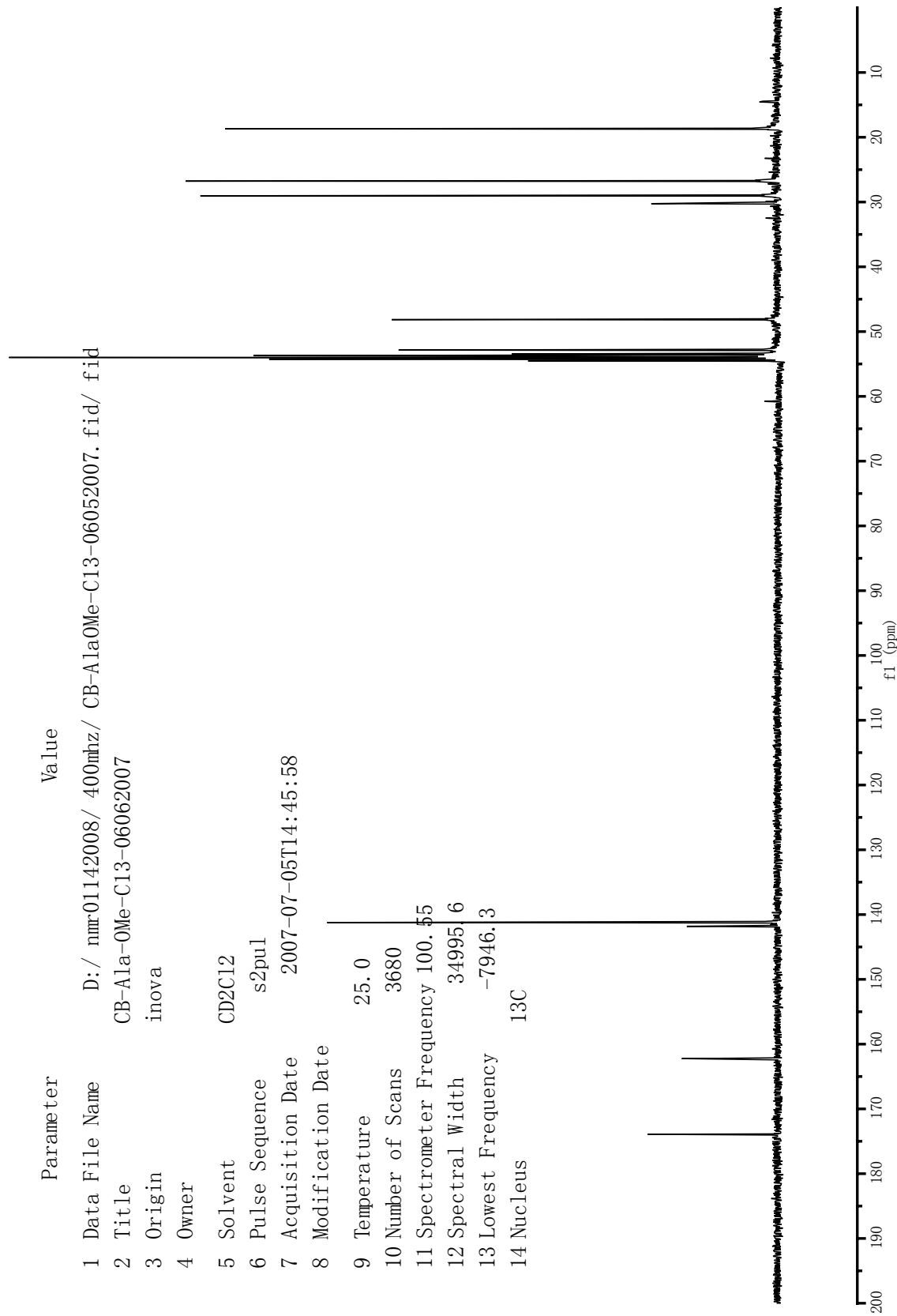


A-8: ESI-Mass spectrum of (8a-20a)₁₀ with catalyst 5





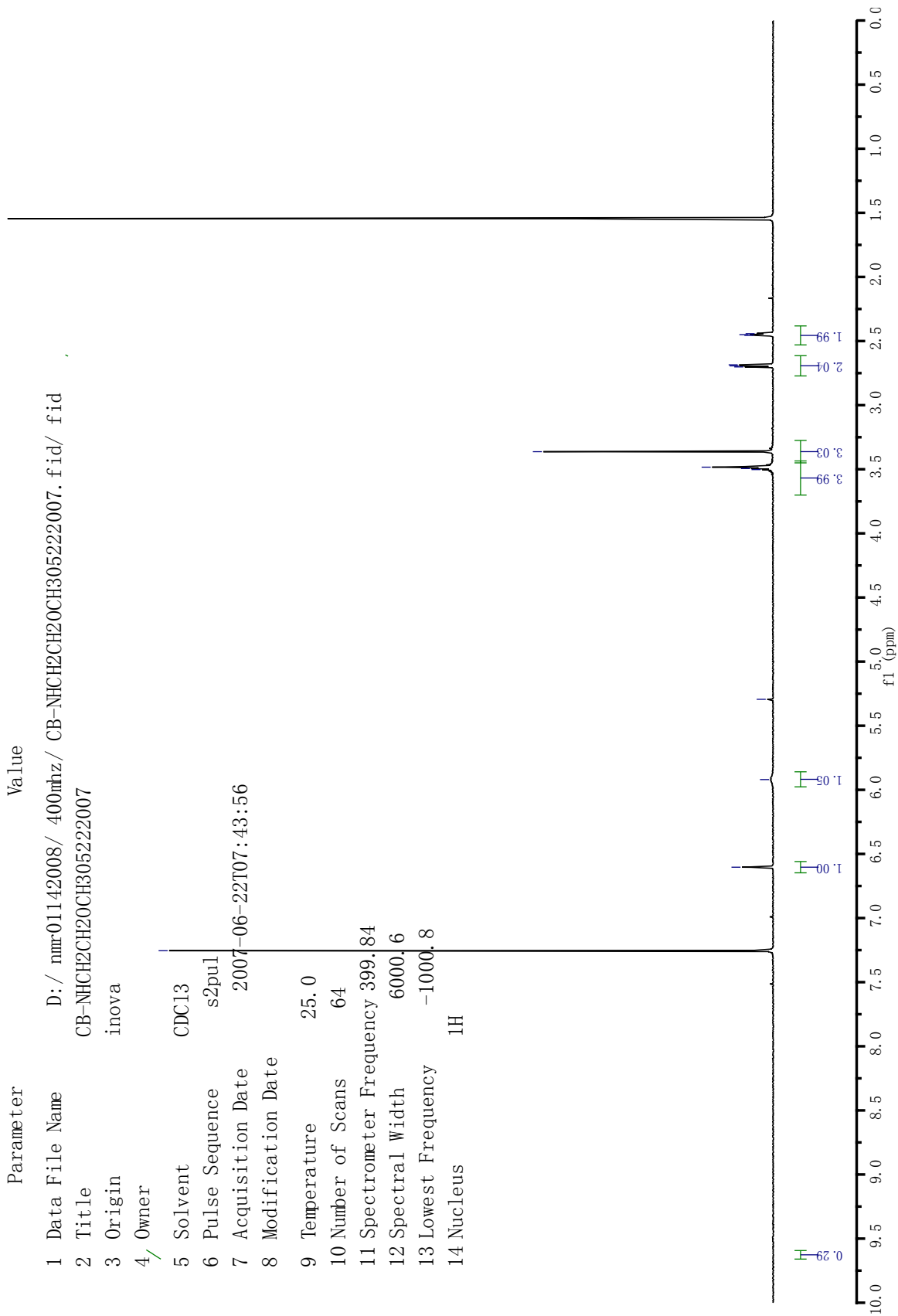
A-9: ¹H-NMR spectrum of 6b



A-10: ¹³C-NMR spectrum of 6b

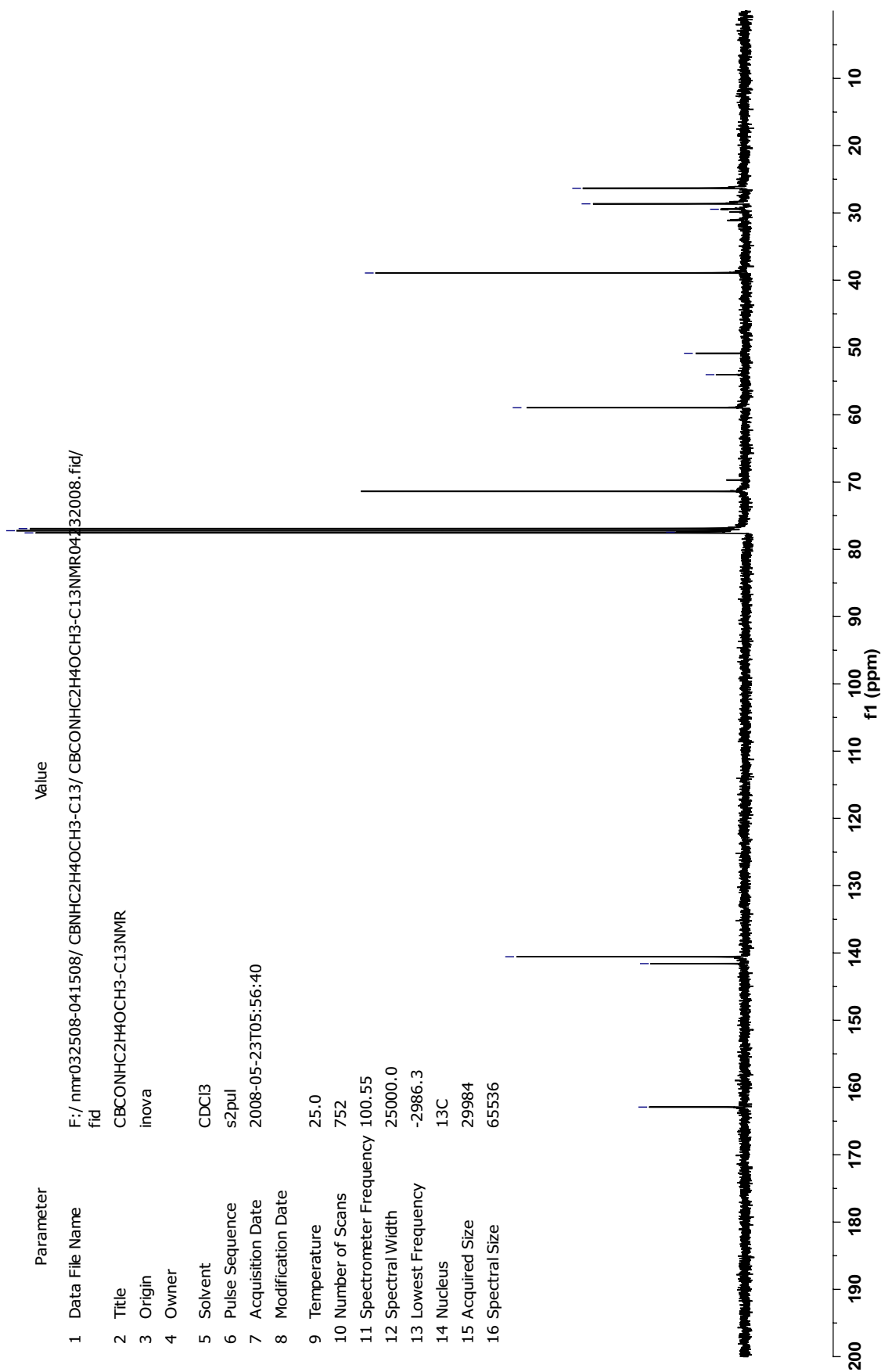
Parameter Value

1 Data File Name D:/nmr01142008/400mhz/CB-NHC₂H₂CH₂CH₃05222007.fid/ fid
2 Title CB-NHC₂H₂CH₂CH₃05222007
3 Origin inova
4/ Owner
5 Solvent CDCl₃
6 Pulse Sequence s2pu1
7 Acquisition Date 2007-06-22T07:43:56
8 Modification Date
9 Temperature 25.0
10 Number of Scans 64
11 Spectrometer Frequency 399.84
12 Spectral Width 6000.6
13 Lowest Frequency -1000.8
14 Nucleus ¹H



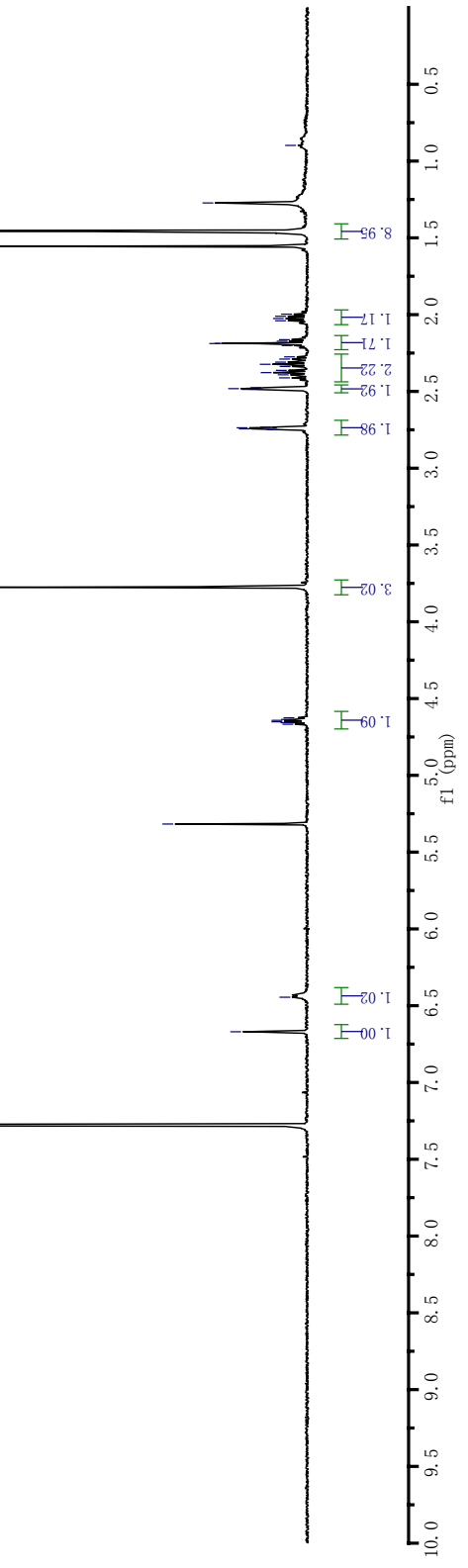
A-11: ¹H-NMR spectrum of 6c

Parameter	Value
1 Data File Name	F:/nmr032508-041508/CBNHC2H4OCH3-C13/CBCONHC2H4OCH3-C13NMR04132008.fid/
2 Title	CBCONHC2H4OCH3-C13NMR
3 Origin	inova
4 Owner	
5 Solvent	CDCl3
6 Pulse Sequence	s2pul
7 Acquisition Date	2008-05-23T05:56:40
8 Modification Date	
9 Temperature	25.0
10 Number of Scans	752
11 Spectrometer Frequency	100.55
12 Spectral Width	25000.0
13 Lowest Frequency	-2986.3
14 Nucleus	13C
15 Acquired Size	29984
16 Spectral Size	65536



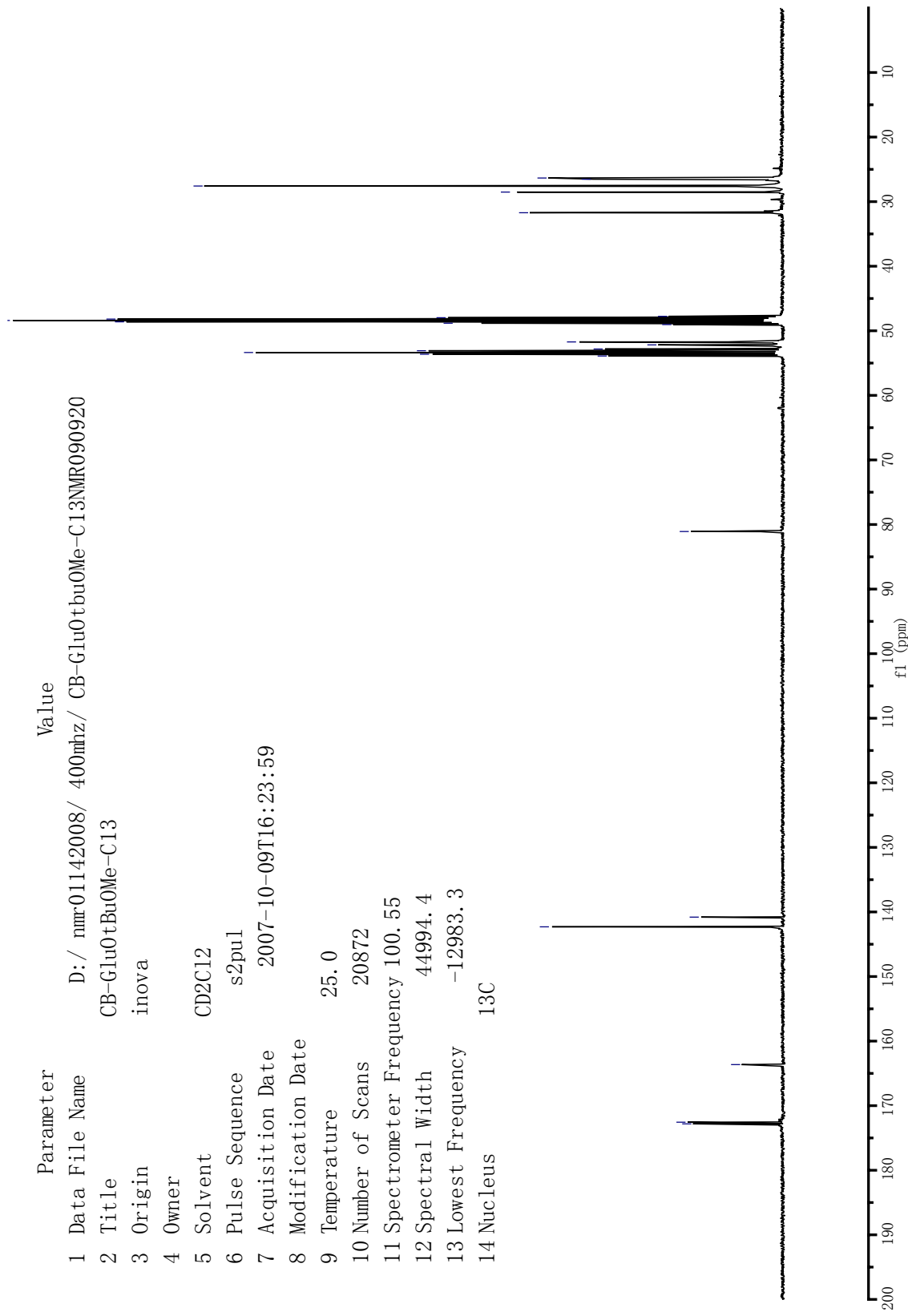
A-12: ¹³C-NMR spectrum of 6c

Parameter	Value
1 Data File Name	D:/ nmr01142008/ 500mhz/ CB-Glu0tBu0Me06282007. fid/
2 Title	fid
3 Origin	CB-Glu0tBu0Me06282007
4 Owner	inova
5 Solvent	CDCl3
6 Pulse Sequence	s2pul
7 Acquisition Date	2007-07-28T11:30:09
8 Modification Date	
9 Temperature	25.0
10 Number of Scans	20
11 Spectrometer Frequency	499.90
12 Spectral Width	7998.4
13 Lowest Frequency	-999.9
14 Nucleus	1H



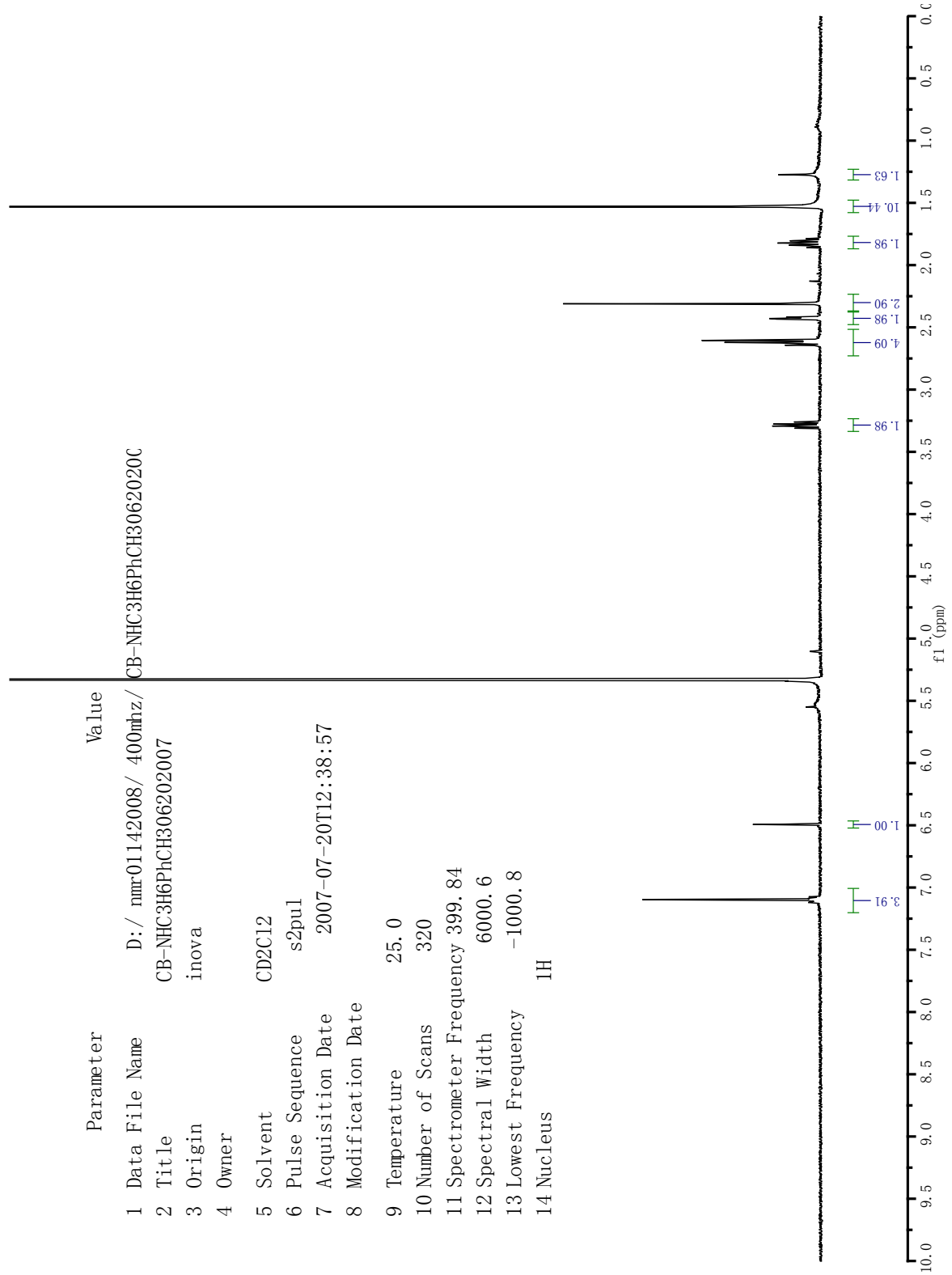
A-13: ¹H-NMR spectrum of 6d

Parameter	Value
1 Data File Name	D:/ nmr01142008/ 400mhz/ CB-Glu0tbuOMe-C13NMR090920
2 Title	CB-Glu0tbuOMe-C13
3 Origin	inova
4 Owner	
5 Solvent	CD2Cl2
6 Pulse Sequence	s2pul
7 Acquisition Date	2007-10-09T16:23:59
8 Modification Date	
9 Temperature	25.0
10 Number of Scans	20872
11 Spectrometer Frequency	100.55
12 Spectral Width	44994.4
13 Lowest Frequency	-12983.3
14 Nucleus	¹³ C



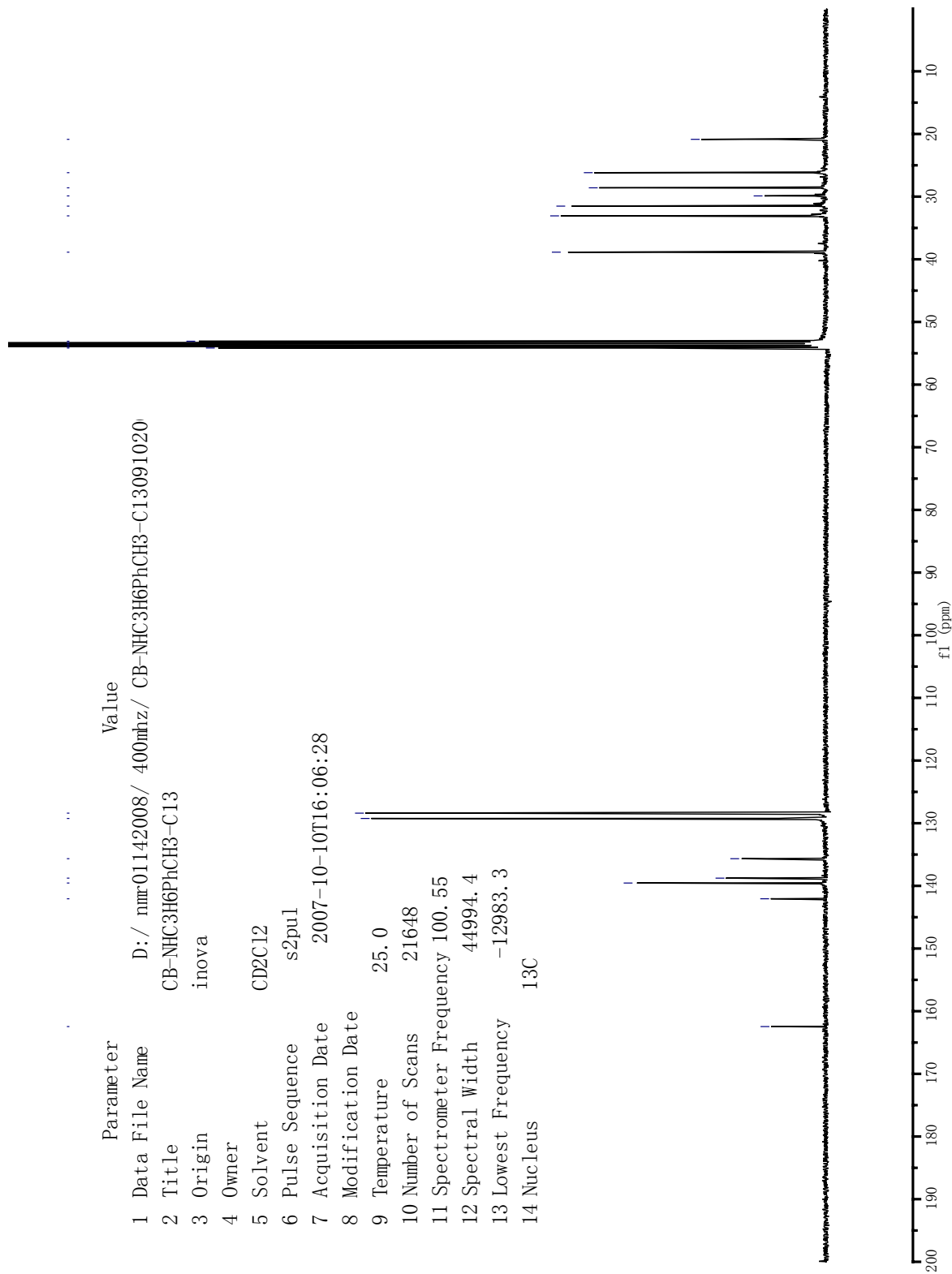
A-14: ¹³C-NMR spectrum of 6d

Parameter	Value
1 Data File Name	D:/nmr01142008/400mhz/CB-NHC3H6PhCH3062020C
2 Title	CB-NHC3H6PhCH306202007
3 Origin	inova
4 Owner	
5 Solvent	CD2Cl2
6 Pulse Sequence	s2pul
7 Acquisition Date	2007-07-20T12:38:57
8 Modification Date	
9 Temperature	25.0
10 Number of Scans	320
11 Spectrometer Frequency	399.84
12 Spectral Width	6000.6
13 Lowest Frequency	-1000.8
14 Nucleus	¹ H

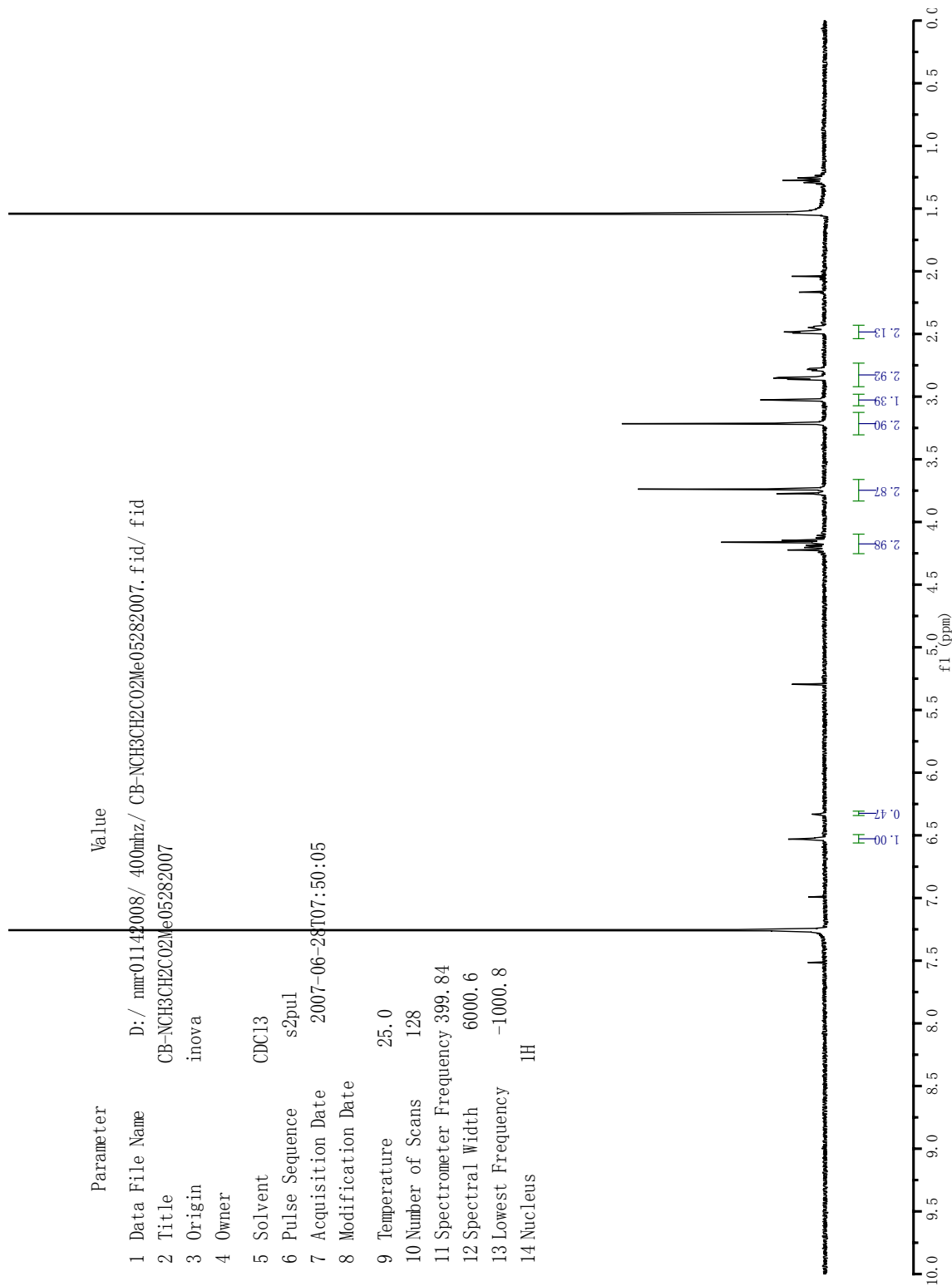


A-15: ¹H-NMR spectrum of 6e

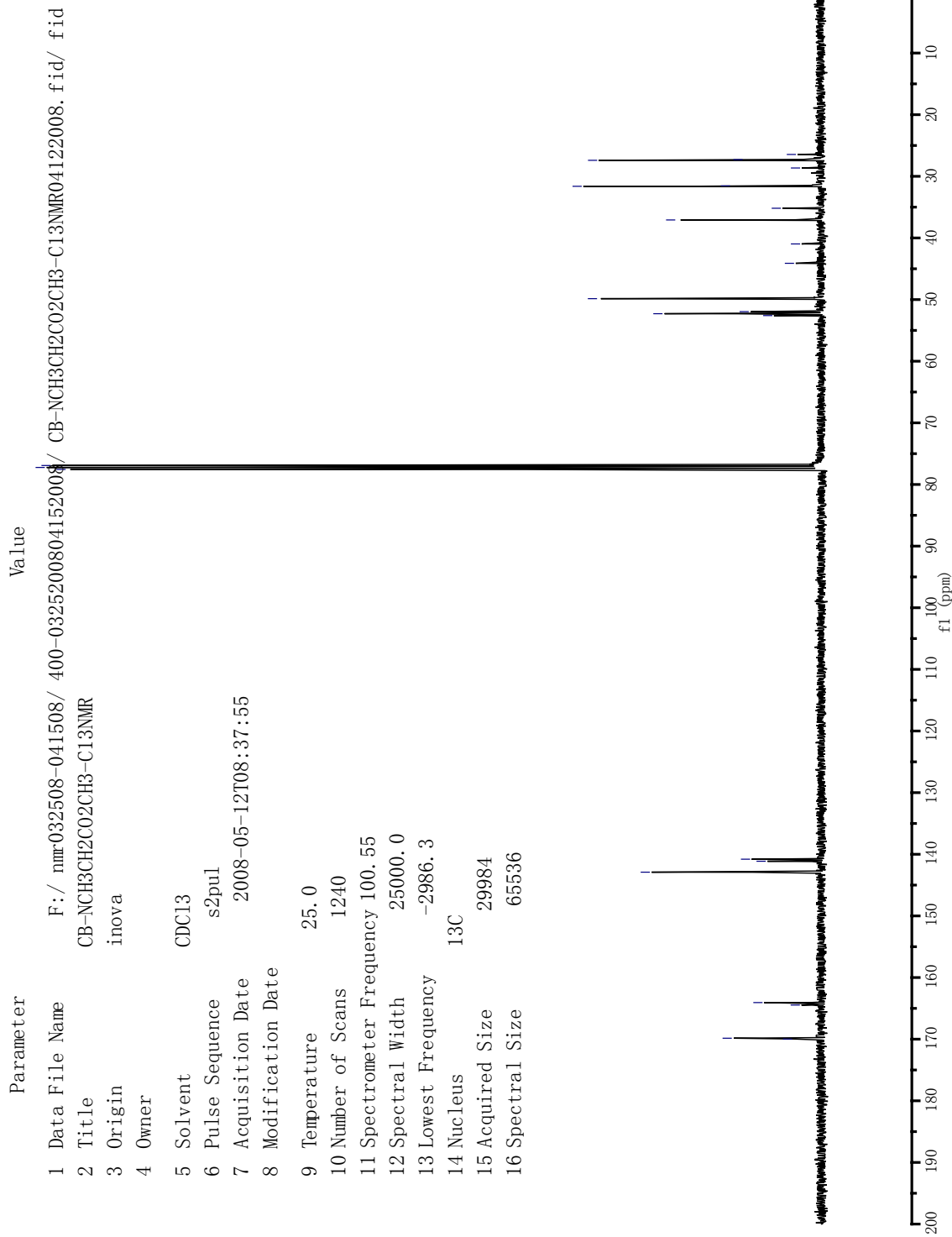
Parameter Value
1 Data File Name D:/ nmr-01142008/ 400mhz/ CB-NHC3H6PhCH3-C13091020
2 Title CB-NHC3H6PhCH3-C13
3 Origin inova
4 Owner
5 Solvent CD2Cl2
6 Pulse Sequence s2pu1
7 Acquisition Date 2007-10-10T16:06:28
8 Modification Date
9 Temperature 25.0
10 Number of Scans 21648
11 Spectrometer Frequency 100.55
12 Spectral Width 44994.4
13 Lowest Frequency -12983.3
14 Nucleus ¹³C



A-16: ¹³C-NMR spectrum of 6e

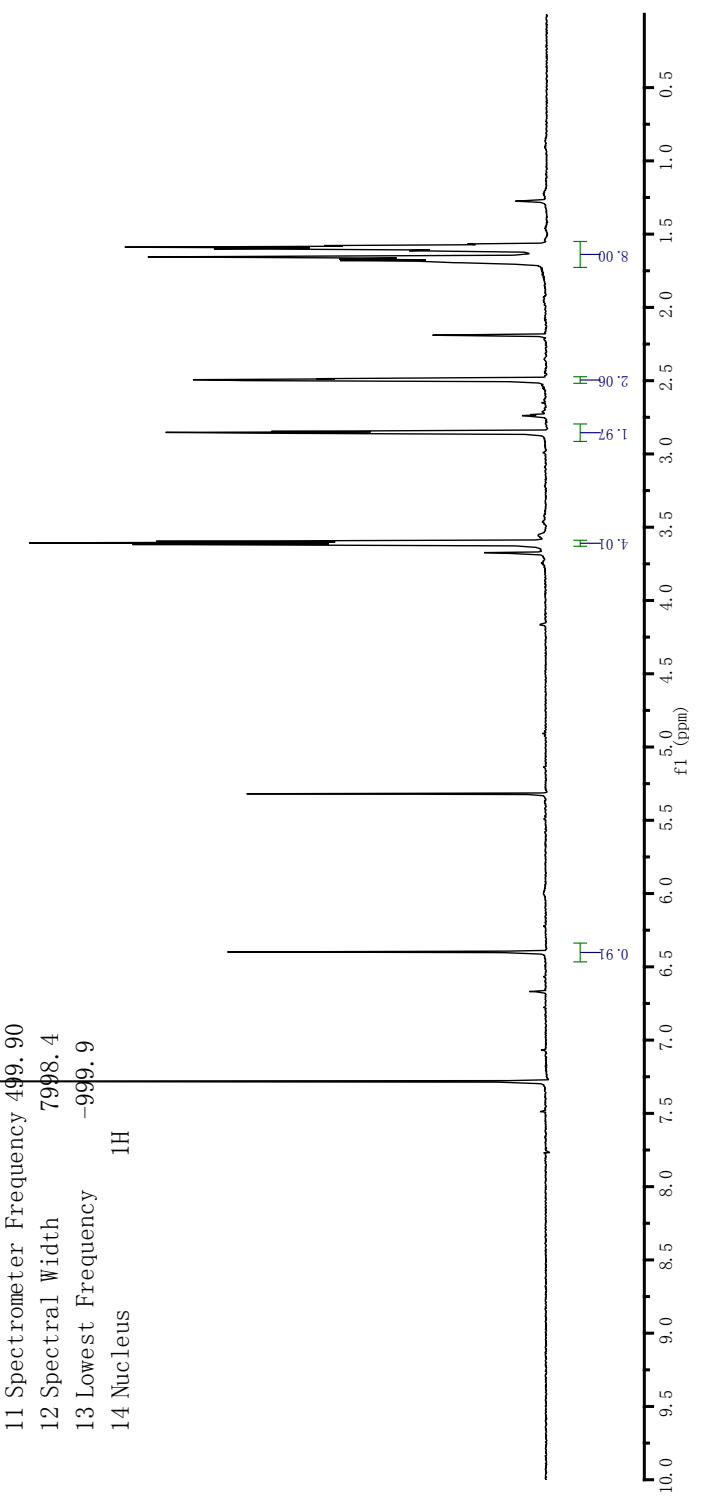


A-17: ¹H-NMR spectrum of 7a



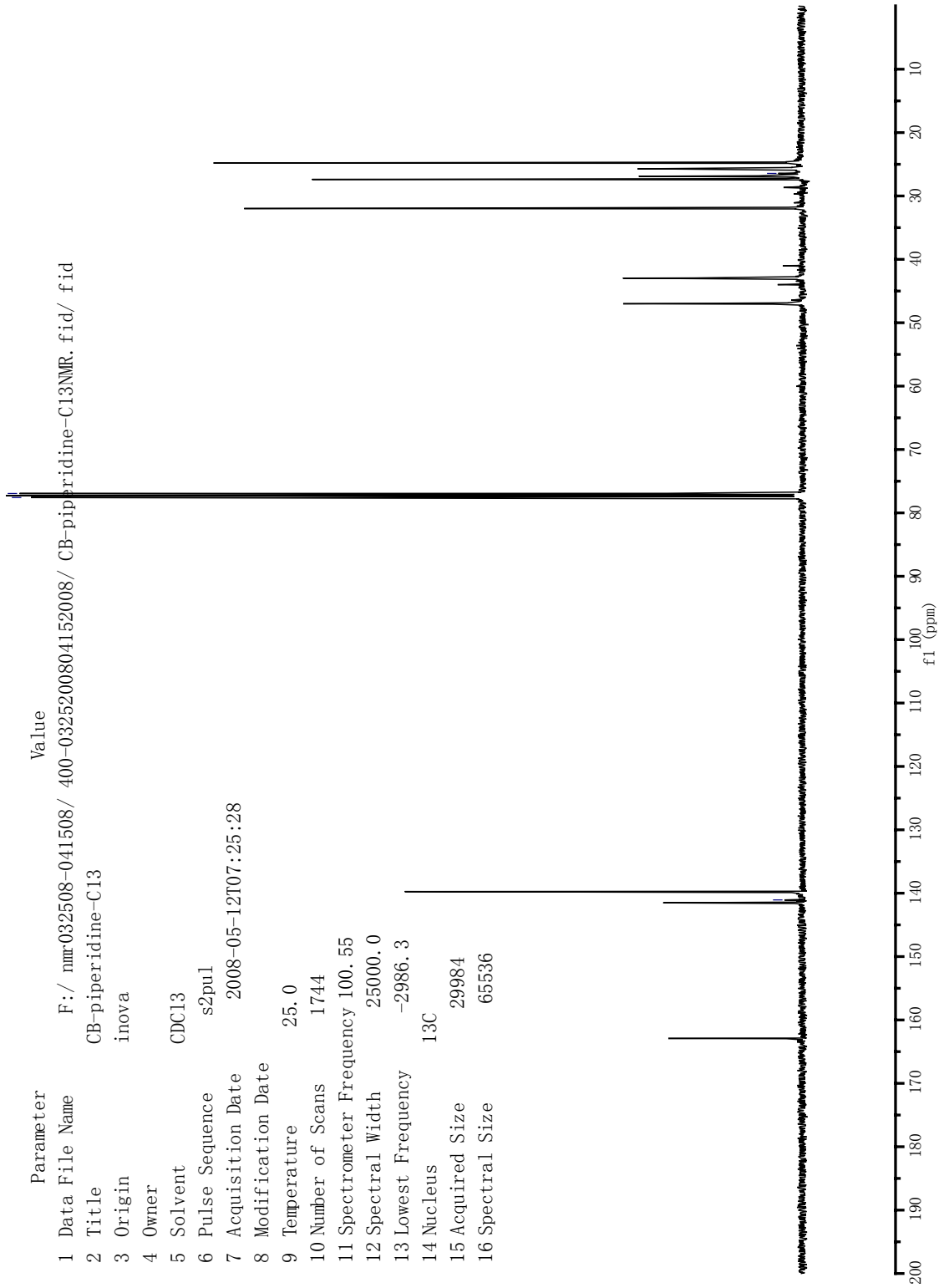
A-18: ¹³C-NMR spectrum of 7a

Parameter	Value
1 Data File Name	D:/nmr01142008/ 500mhz/ CB-piperidine10112007.fid/ fid
2 Title	CB-piperidine
3 Origin	inova
4 Owner	
5 Solvent	CDCl3
6 Pulse Sequence	s2ppl
7 Acquisition Date	2007-11-11T10:43:38
8 Modification Date	
9 Temperature	25.0
10 Number of Scans	56
11 Spectrometer Frequency	499.90
12 Spectral Width	7998.4
13 Lowest Frequency	-999.9
14 Nucleus	¹ H



A-19: ¹H-NMR spectrum of 7b

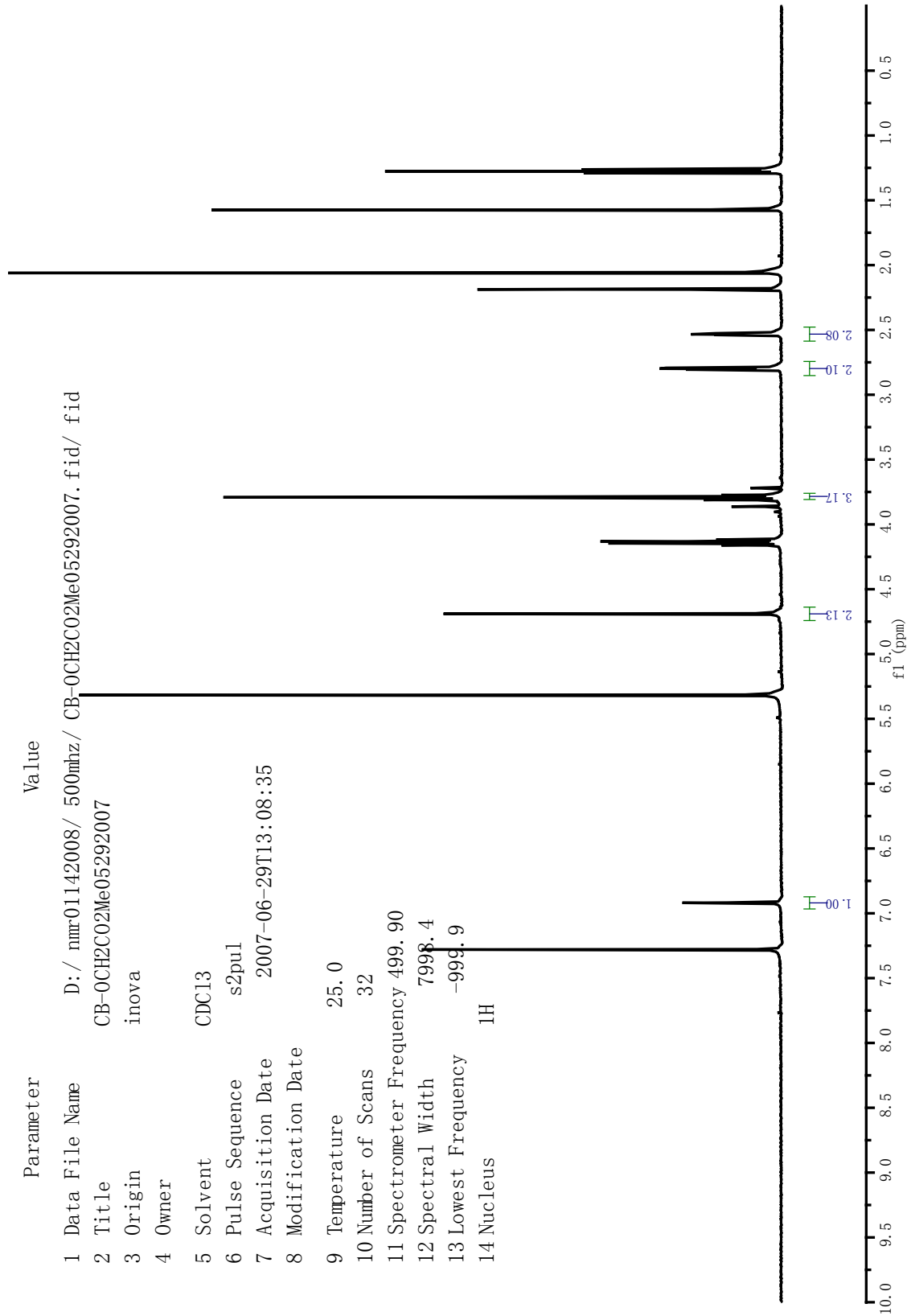
Parameter	Value
1 Data File Name	F:/ nmr032508-041508/ 400-0325200804152008/ CB-piperidine-C13NMR. fid/ fid
2 Title	CB-piperidine-C13
3 Origin	inova
4 Owner	
5 Solvent	CDCl3
6 Pulse Sequence	s2pu1
7 Acquisition Date	2008-05-12T07:25:28
8 Modification Date	
9 Temperature	25.0
10 Number of Scans	1744
11 Spectrometer Frequency	100.55
12 Spectral Width	25000.0
13 Lowest Frequency	-2986.3
14 Nucleus	¹³ C
15 Acquired Size	29984
16 Spectral Size	65536



A-20: ¹³C-NMR spectrum of 7b

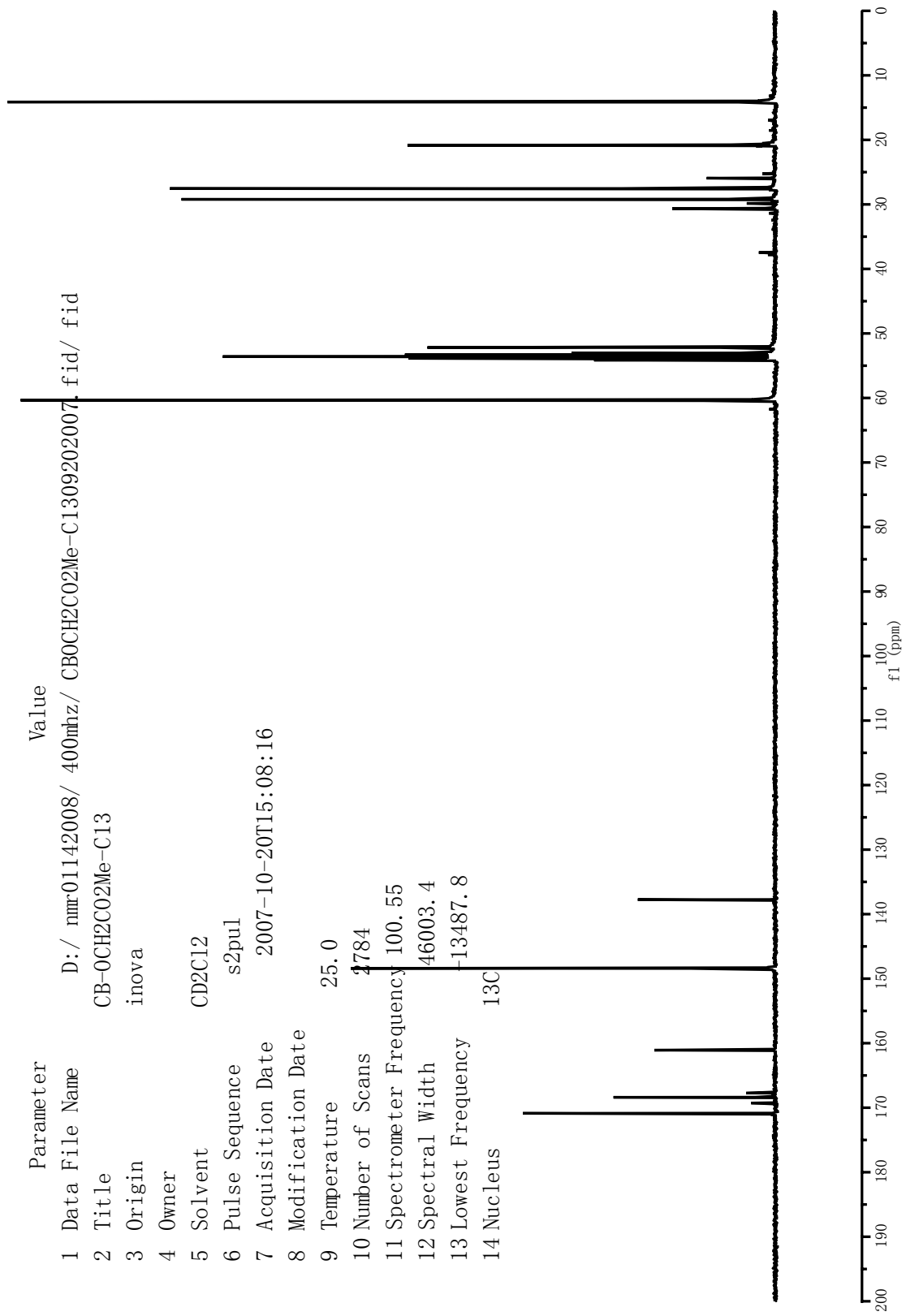
Parameter Value

1 Data File Name D:/nmr01142008/ 500mhz/ CB-OCH2CO2Me05292007.fid/ fid
2 Title CB-OCH2CO2Me05292007
3 Origin inova
4 Owner
5 Solvent CDC13
6 Pulse Sequence s2pul
7 Acquisition Date 2007-06-29T13:08:35
8 Modification Date
9 Temperature 25.0
10 Number of Scans 32
11 Spectrometer Frequency 499.90
12 Spectral Width 7996.4
13 Lowest Frequency -999.9
14 Nucleus ¹H



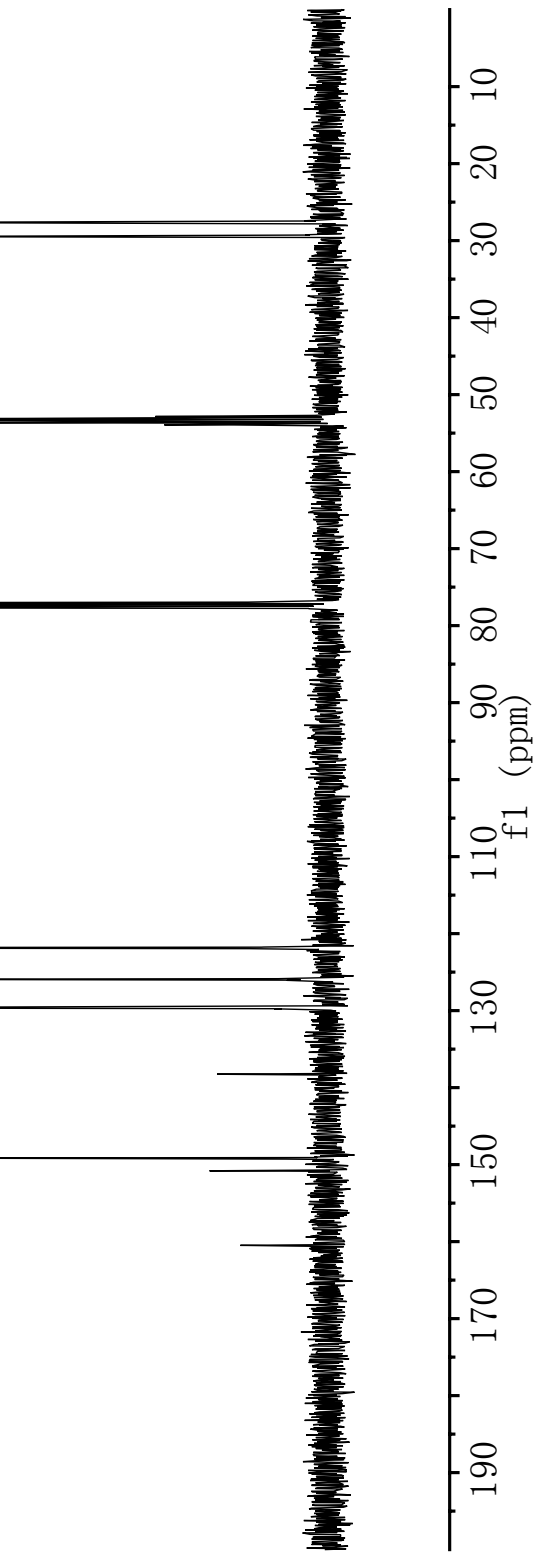
A-21: ¹H-NMR spectrum of 8b

Parameter Value
 1 Data File Name D:/ nmr01142008/ 400mhz/ CBOCH2C02Me-C1309202007. fid/ fid
 2 Title CB-OCH2C02Me-C13
 3 Origin inova
 4 Owner
 5 Solvent CD2C12
 6 Pulse Sequence s2pul
 7 Acquisition Date 2007-10-20T15:08:16
 8 Modification Date
 9 Temperature 25.0
 10 Number of Scans 4784
 11 Spectrometer Frequency 100.55
 12 Spectral Width 46003.4
 13 Lowest Frequency -13487.8
 14 Nucleus ¹³C



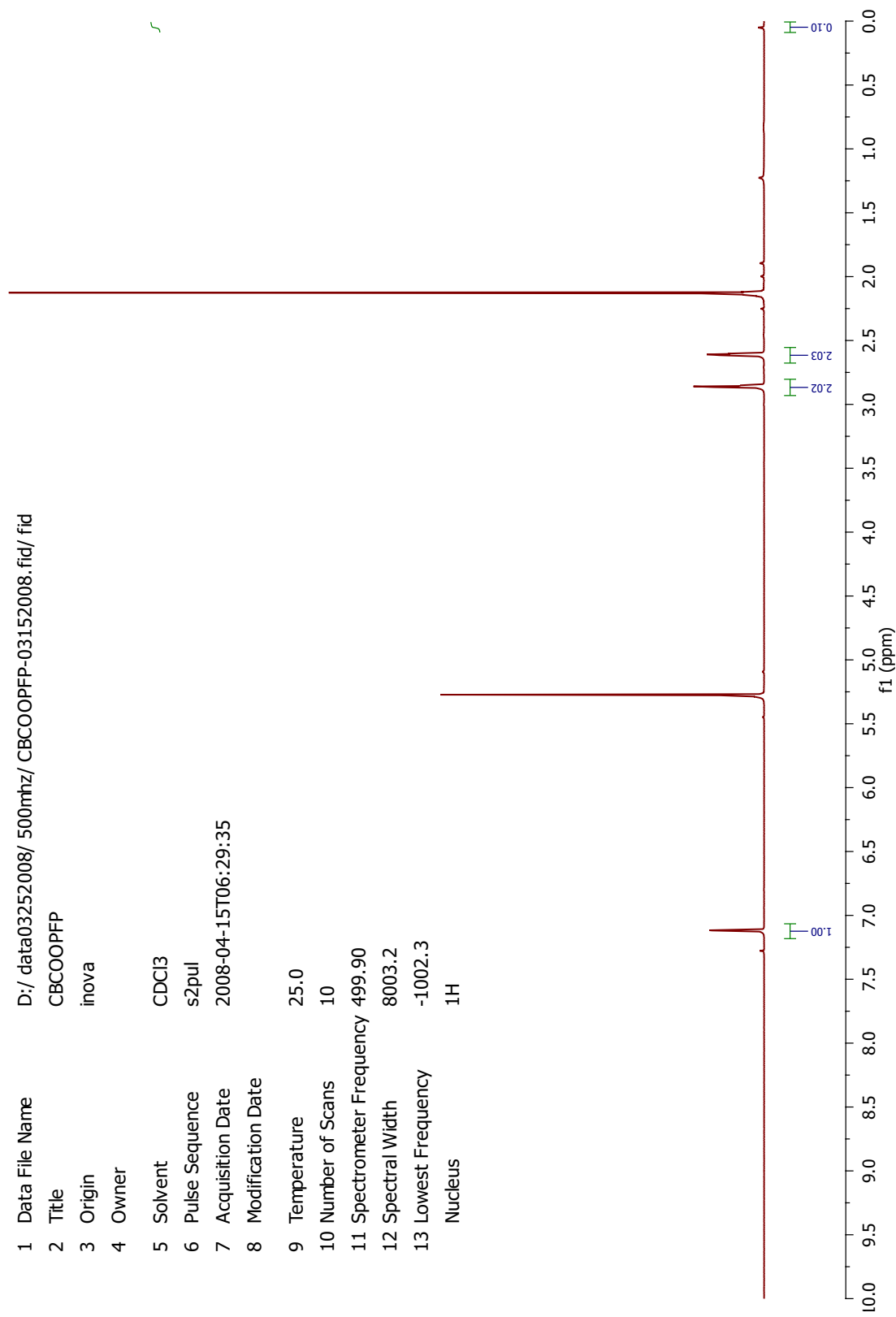
A-22: ¹³C-NMR spectrum of 8b

Parameter	Value
1 Data File Name	L:/ 07012008-07112008/ CBC00Ph-C13-07012008.fid/ fid
2 Title	CBC00Ph-C13-07012008
3 Origin	inova
4 Owner	
5 Solvent	CD2C12
6 Pulse Sequence	s2pul
7 Acquisition Date	2008-08-01T11:14:09
8 Modification Date	
9 Temperature	25.0
10 Number of Scans	1048
11 Spectrometer Frequency	100.55
12 Spectral Width	25000.0
13 Lowest Frequency	-2986.2
14 Nucleus	¹³ C
15 Acquired Size	29984
16 Spectral Size	65536



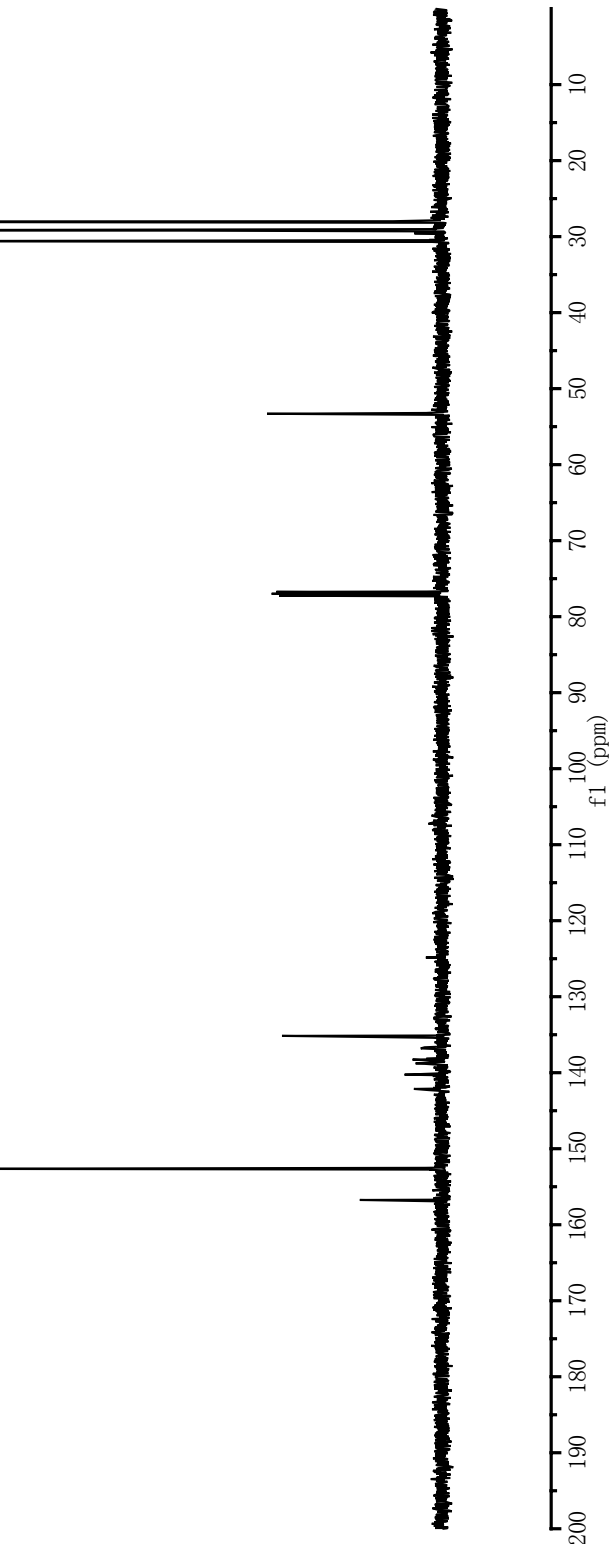
A-24: ¹³C-NMR spectrum of 8c

Parameter	Value
1 Data File Name	D:/ data03252008/ 500mhz/ CBCOOPFP-03152008.fid/ fid
2 Title	CBCOOPFP
3 Origin	inova
4 Owner	
5 Solvent	CDCl3
6 Pulse Sequence	s2pul
7 Acquisition Date	2008-04-15T06:29:35
8 Modification Date	
9 Temperature	25.0
10 Number of Scans	10
11 Spectrometer Frequency	499.90
12 Spectral Width	8003.2
13 Lowest Frequency	-1002.3
Nucleus	1H



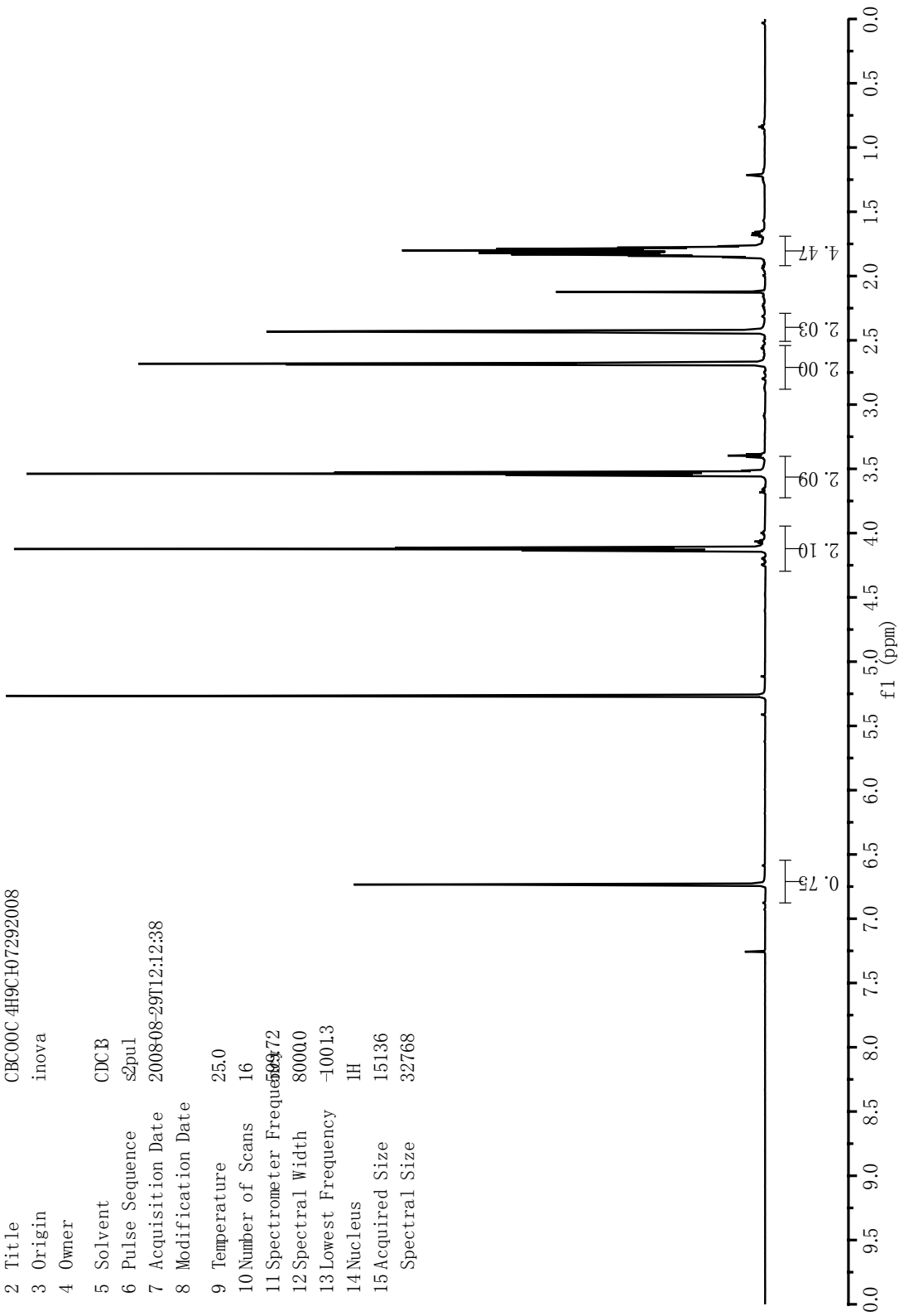
A-25: ¹H-NMR spectrum of 8d

Parameter	Value
1 Data File Name	D:/data/3252008/500mhz/CBC00PFP-1-C13-03152008fidfid
2 Title	CBC00PFP-C13
3 Origin	inova
4 Owner	sar
5 Solvent	CDCl ₃
6 Pulse Sequence	s2pul
7 Acquisition Date	200804-15T07:59:40
8 Modification Date	
9 Temperature	25.0
10 Number of Scans	512
11 Spectrometer Frequency	125.71
12 Spectral Width	314465
13 Lowest Frequency	-22389
14 Nucleus	¹³ C

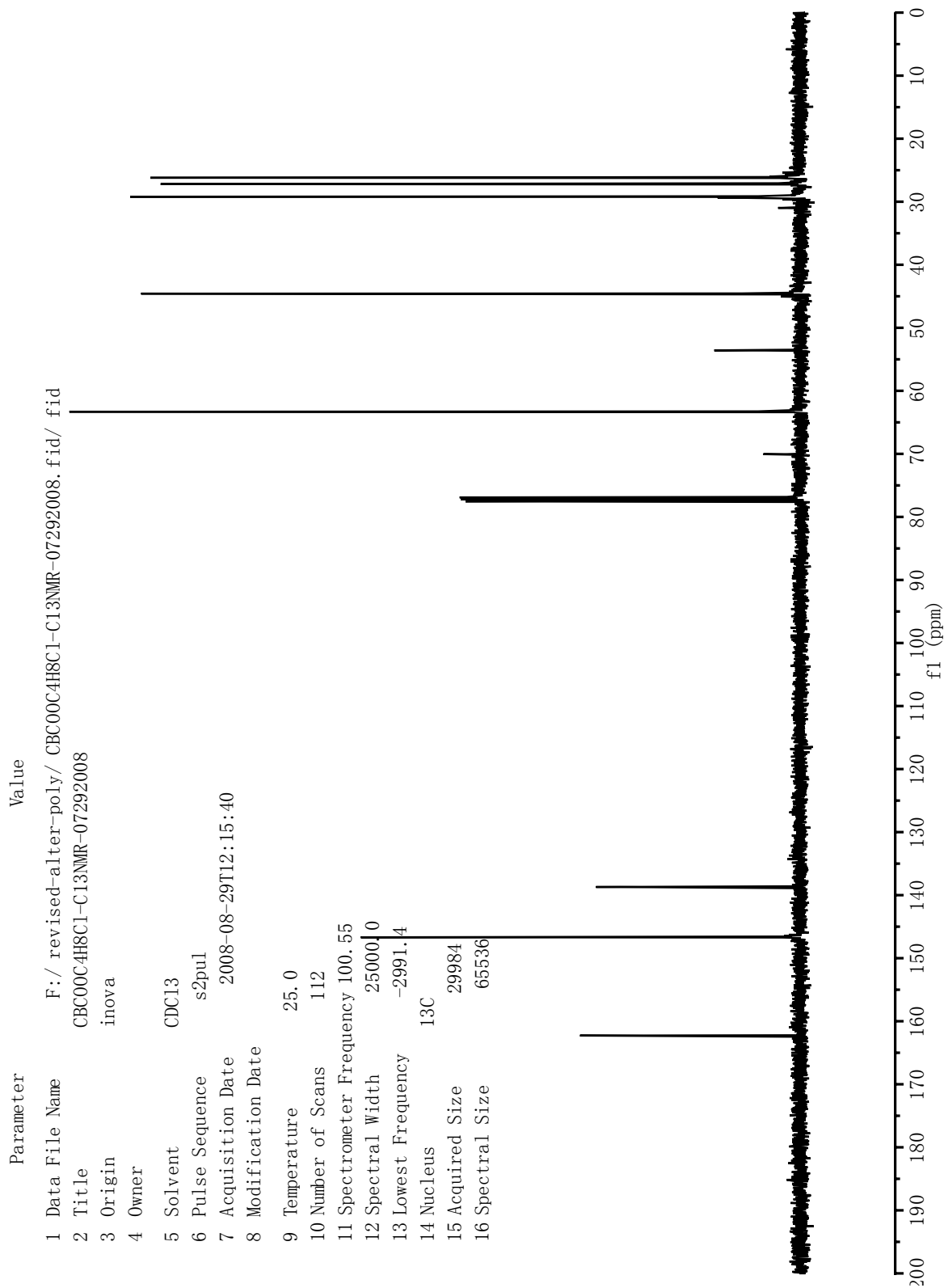


A-26: ¹³C-NMR spectrum of 8d

Parameter	Value
1 Data File Name	F:\revised\tempoly\CBC00C 4H8C107292008fid/fid
2 Title	CBC00C 4H9C107292008
3 Origin	inova
4 Owner	
5 Solvent	CDC13
6 Pulse Sequence	s2pul
7 Acquisition Date	2008-08-29T12:12:38
8 Modification Date	
9 Temperature	25.0
10 Number of Scans	16
11 Spectrometer Frequency	500.1372
12 Spectral Width	8000.0
13 Lowest Frequency	-1001.3
14 Nucleus	1H
15 Acquired Size	15136
Spectral Size	32768

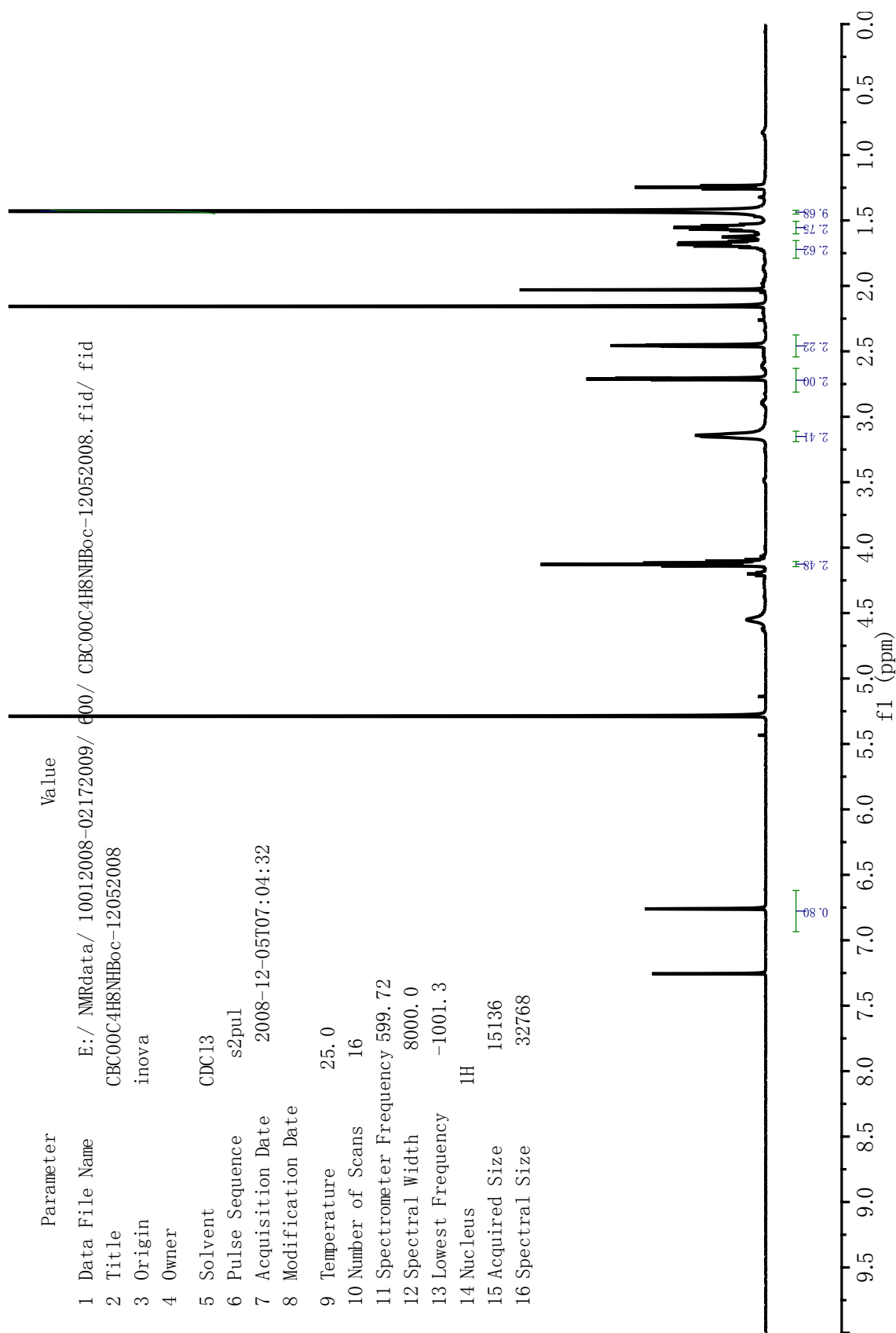


A-27: ¹H-NMR spectrum of 8e



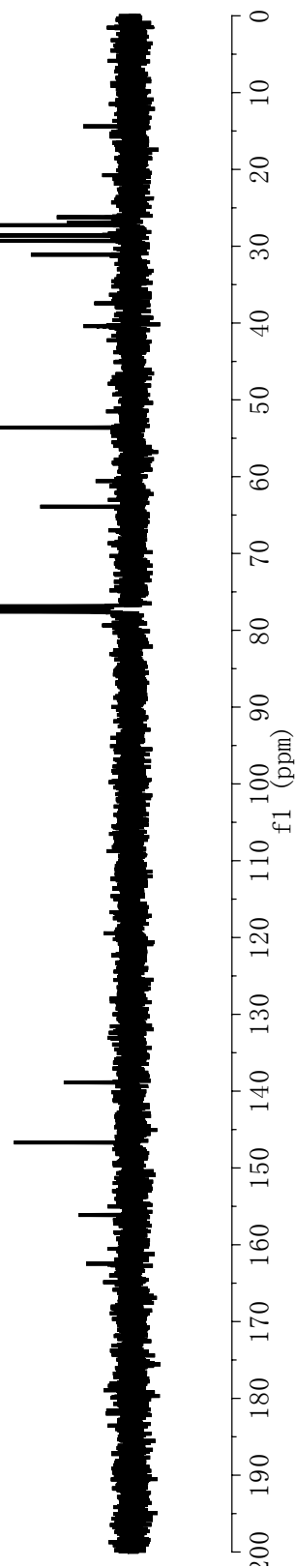
A-28: ¹³C-NMR spectrum of 8e

Parameter	Value
1 Data File Name	E:\NMRdata\10012008-02172009\600\CBC00C4HSNHoc-12052008.fid/ fid
2 Title	CBC00C4HSNHoc-12052008
3 Origin	inova
4 Owner	
5 Solvent	CDC13
6 Pulse Sequence	s2pul
7 Acquisition Date	2008-12-05T07:04:32
8 Modification Date	
9 Temperature	25.0
10 Number of Scans	16
11 Spectrometer Frequency	599.72
12 Spectral Width	8000.0
13 Lowest Frequency	-1001.3
14 Nucleus	¹ H
15 Acquired Size	15136
16 Spectral Size	32768



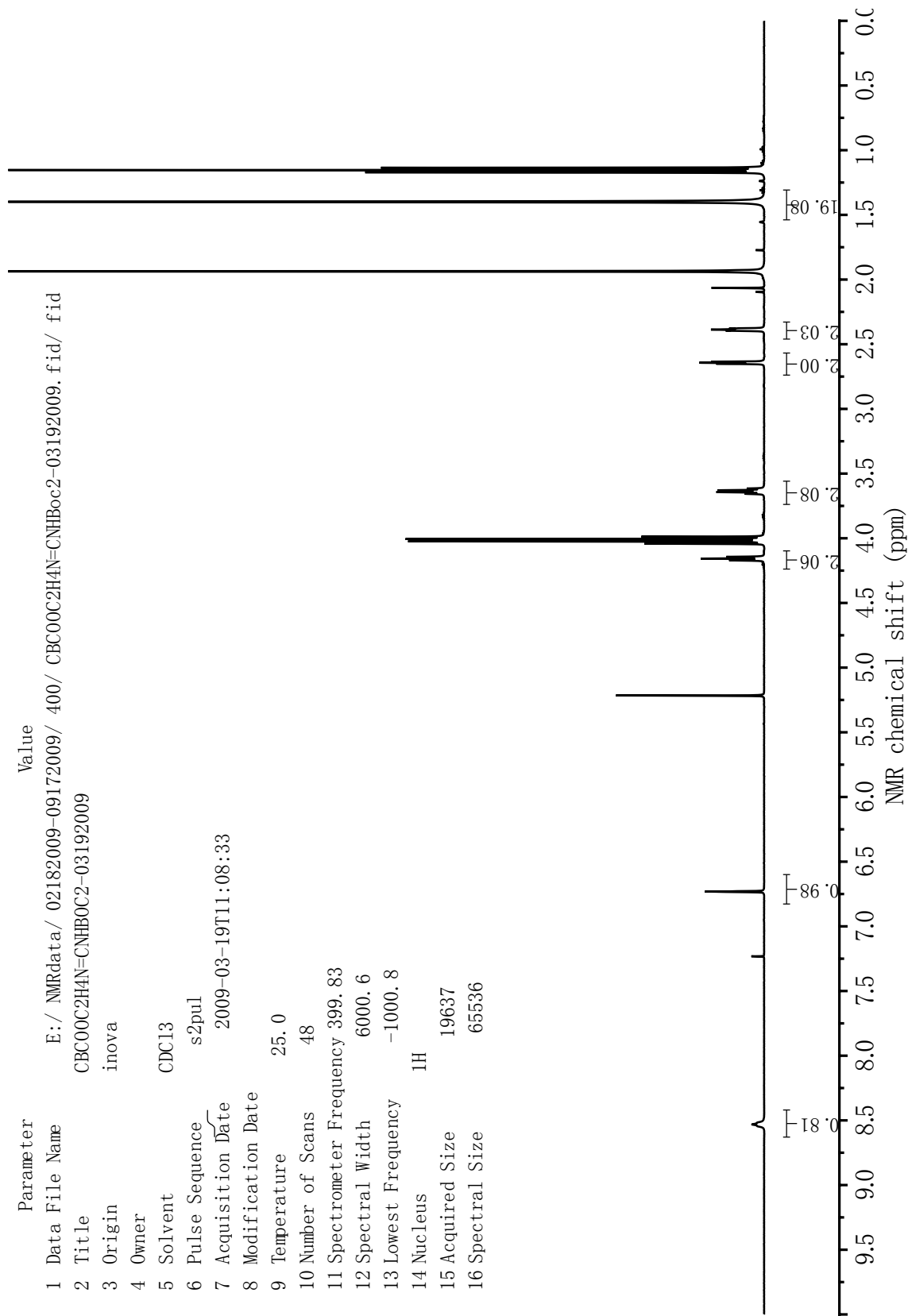
A-29: ¹H-NMR spectrum of 8f

Parameter	Value
1 Data File Name	E:/ NMRdata/ 10012008-02172009/ 400/ CBC00C4H8NH-boc-C13-2052008.fid/ fid
2 Title	CBC00C4H8NHboc-C13-
3 Origin	inova
4 Owner	
5 Solvent	CDCl3
6 Pulse Sequence	s2pul
7 Acquisition Date	2008-12-05T08:18:01
8 Modification Date	
9 Temperature	25.0
10 Number of Scans	320
11 Spectrometer Frequency	100.55
12 Spectral Width	25000.0
13 Lowest Frequency	-2986.3
14 Nucleus	¹³ C
15 Acquired Size	29984
16 Spectral Size	65536



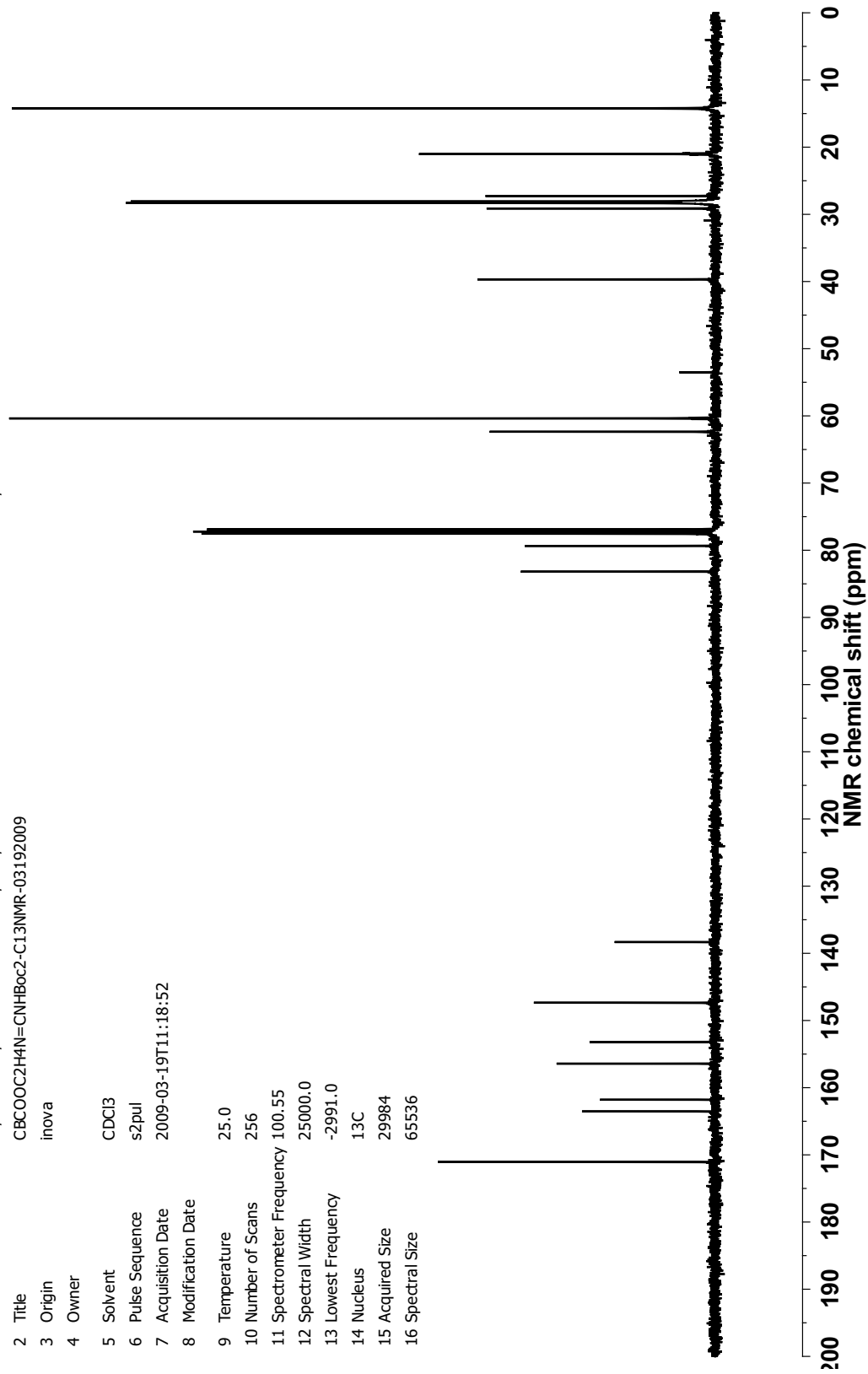
A-30: ¹³C-NMR spectrum of 8f

Parameter	Value
1 Data File Name	E:/ NMRdata/ 02182009-09172009/ 400/ CBC00C2H4N=CNHBoc2-03192009. fid/ fid
2 Title	CBC00C2H4N=CNHBoc2-03192009
3 Origin	inova
4 Owner	
5 Solvent	CDCl3
6 Pulse Sequence	s2pul
7 Acquisition Date	2009-03-19T11:08:33
8 Modification Date	
9 Temperature	25.0
10 Number of Scans	48
11 Spectrometer Frequency	399.83
12 Spectral Width	6000.6
13 Lowest Frequency	-1000.8
14 Nucleus	¹ H
15 Acquired Size	19637
16 Spectral Size	65536



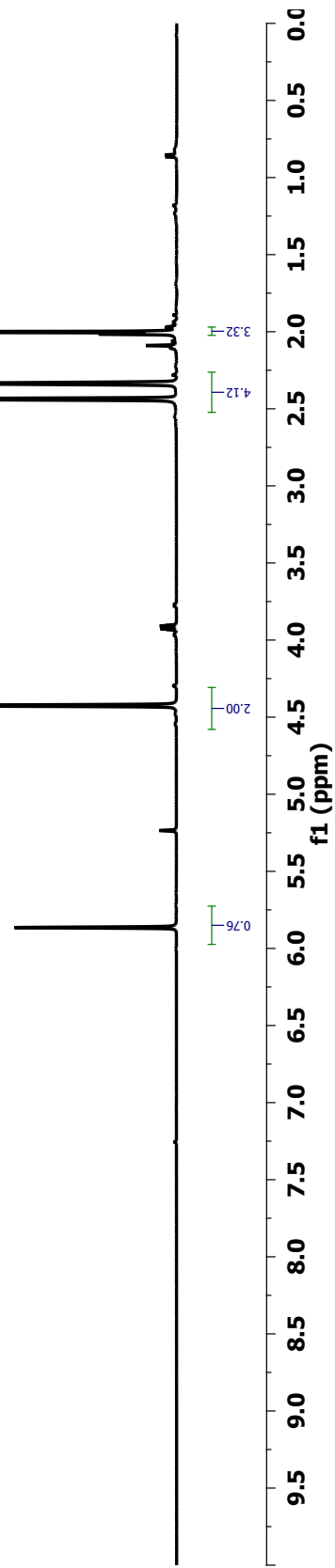
A-31: ¹H-NMR spectrum of 8g

Parameter	Value
1 Data File Name	E:/ NMRdata/ 02182009-09172009/ 400/ CBCOOC2H4N=CNHoc2-C13NMR-03192009.fid/ fid
2 Title	CBCOOC2H4N=CNHoc2-C13NMR-03192009
3 Origin	inova
4 Owner	
5 Solvent	CDCl3
6 Pulse Sequence	s2pul
7 Acquisition Date	2009-03-19T11:18:52
8 Modification Date	
9 Temperature	25.0
10 Number of Scans	256
11 Spectrometer Frequency	100.55
12 Spectral Width	25000.0
13 Lowest Frequency	-2991.0
14 Nucleus	13C
15 Acquired Size	29984
16 Spectral Size	65536



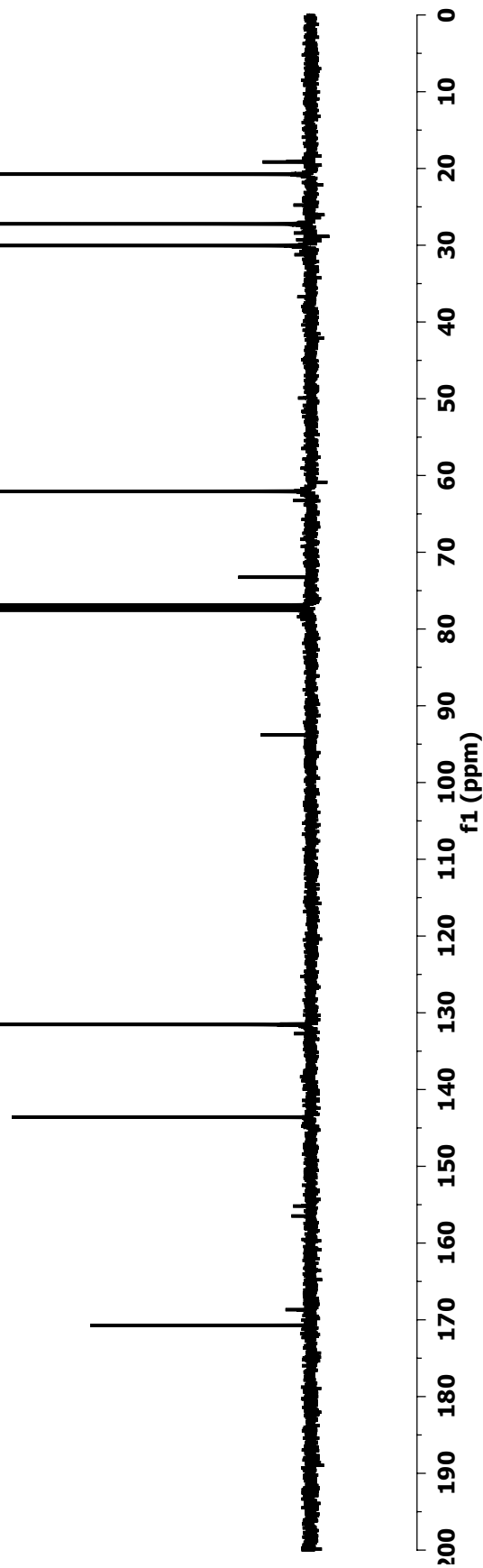
A-32: ¹³C-NMR spectrum of 8g

Parameter	Value
1 Data File Name	E:/ NMRdata/ 09182009-10132009/ 600/ CBCH2OCCOCH3-09302009.fid/ fid
2 Title	CBCH2OCCOCH3-09302009
3 Origin	Varian
4 Spectrometer	inova
5 Solvent	CDCl3
6 Temperature	25.0
7 Pulse Sequence	s2pul
8 Number of Scans	16
9 Receiver Gain	16
10 Relaxation Delay	1.0000
11 Pulse Width	0.0000
12 Acquisition Time	1.8920
13 Acquisition Date	2009-09-30T20:35:05
14 Modification Date	2009-09-30T19:37:30
15 Spectrometer Frequency	599.72
16 Nucleus	¹ H



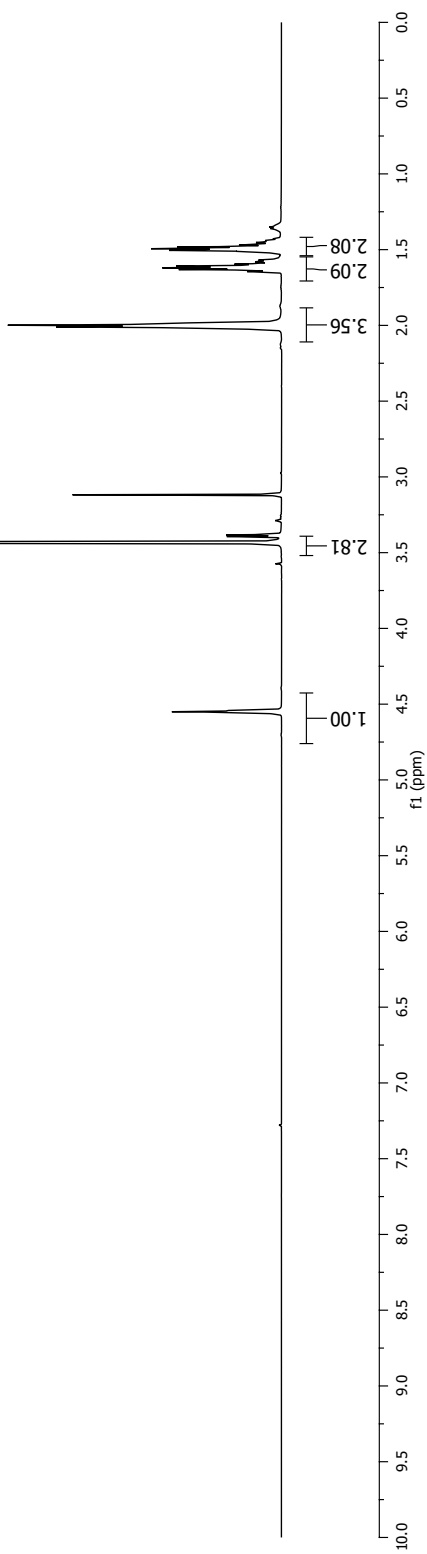
A-33: ¹H-NMR spectrum of 9a

Parameter	Value
1 Data File Name	E:/NMRdata/09182009-10132009/400/CBCH2OCOCCH3-C13NMR09302009.fid/ fid
2 Title	CBCH2OCOCCH3-C13NMR09302009
3 Origin	Varian
4 Spectrometer	inova
5 Solvent	CDCl3
6 Temperature	25.0
7 Pulse Sequence	s2pul
8 Number of Scans	56
9 Receiver Gain	60
10 Relaxation Delay	1.0000
11 Pulse Width	0.0000
12 Acquisition Time	1.1994
13 Acquisition Date	2009-09-30T21:41:29
14 Modification Date	2009-09-30T20:44:00
15 Spectrometer Frequency	100.55
16 Nucleus	¹³ C



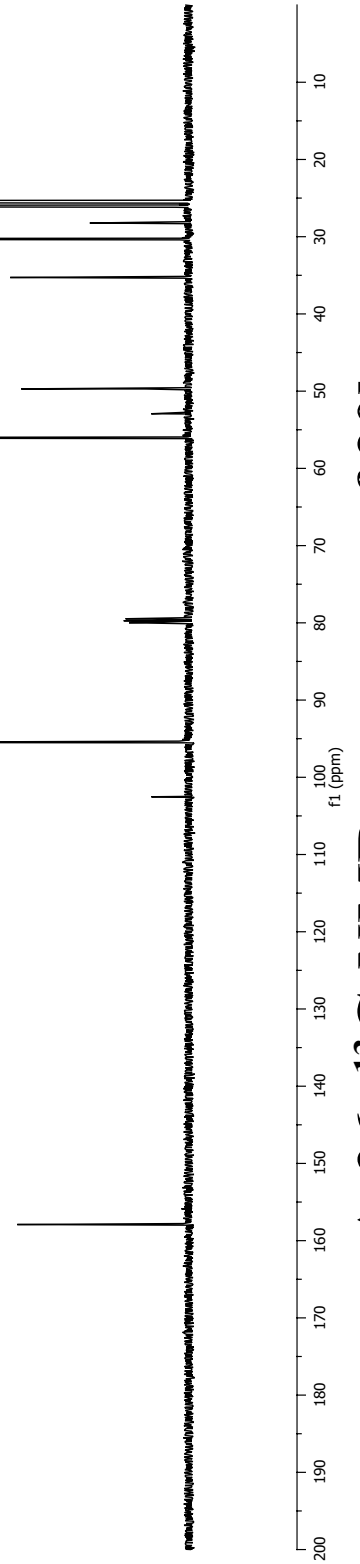
A-34: ¹³C-NMR spectrum of 9a

Parameter	Value
1 Data File Name	L:/ data03252008/ 500mhz/ Cyclohexene-enoether-02222008.fid/ fid
2 Title	STANDARD PROTON PARAMETERS
3 Origin	inova
4 Owner	
5 Solvent	CDCl3
6 Pulse Sequence	s2pul
7 Acquisition Date	2008-03-22T11:52:43
8 Modification Date	
9 Temperature	25.0
10 Number of Scans	40
11 Spectrometer Frequency	499.90
12 Spectral Width	8003.2
13 Lowest Frequency	-1002.3
14 Nucleus	1H
15 Acquired Size	15136
16 Spectral Size	32768



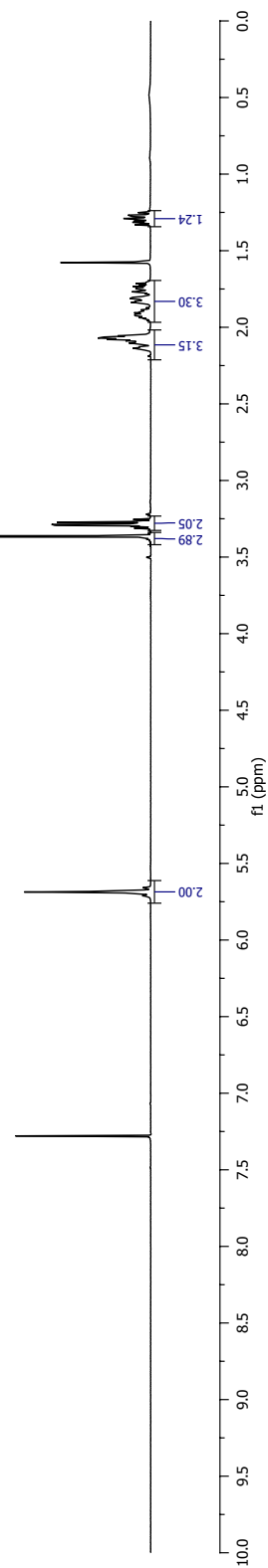
A-35: ¹H-NMR spectrum of 20b

Parameter	Value
1 Data File Name	L:/ data03252008/ 500mhz/ Cyclohexene-enoetherC13-02222008.fid/ fid
2 Title	cyclohexene-enoether
3 Origin	inova
4 Owner	
5 Solvent	CDCI3
6 Pulse Sequence	s2pul
7 Acquisition Date	2008-03-22T12:23:55
8 Modification Date	
9 Temperature	25.0
10 Number of Scans	192
11 Spectrometer Frequency	125.71
12 Spectral Width	31446.5
13 Lowest Frequency	-1896.5
14 Nucleus	13C
15 Acquired Size	40896
16 Spectral Size	131072



A-36: ¹³C-NMR spectrum of 20b

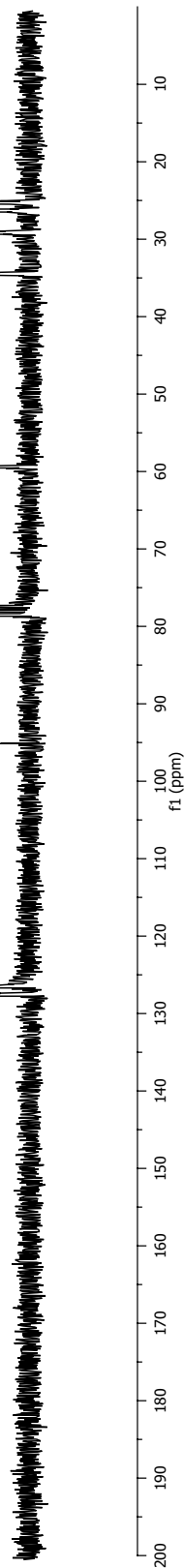
Parameter	Value
1 Data File Name	L:/nmr04162008-07012008/cyclohexene-4-methylether06172008.fid/fid
2 Title	cyclohexene-4-methylether
3 Origin	inova
4 Owner	
5 Solvent	CDCl3
6 Pulse Sequence	s2pul
7 Acquisition Date	2008-07-17T09:31:41
8 Modification Date	
9 Temperature	25.0
10 Number of Scans	32
11 Spectrometer Frequency	499.90
12 Spectral Width	8003.2
13 Lowest Frequency	-1002.3
14 Nucleus	1H
15 Acquired Size	15136
16 Spectral Size	32768



A-37: ¹H-NMR spectrum of 20d

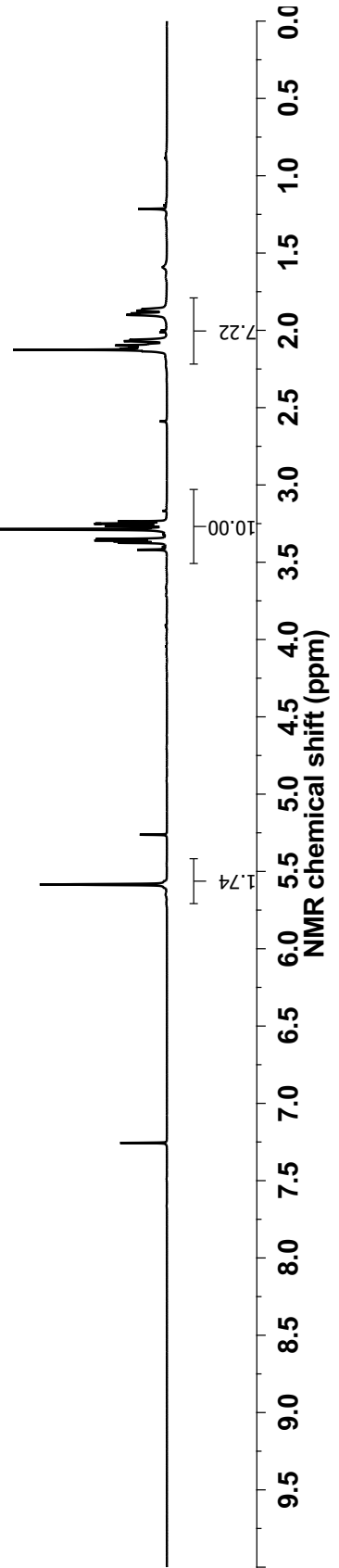
Parameter Value

1 Data File Name L:/07012008-07112008/4-Methoxymethylcyclohexene-C13.fid/ fid
2 Title 4-methoxymethylcyclohexene-C13
3 Origin inova
4 Owner
5 Solvent CDCl3
6 Pulse Sequence s2pul
7 Acquisition Date 2008-08-10T06:23:53
8 Modification Date
9 Temperature 25.0
10 Number of Scans 160
11 Spectrometer Frequency 100.55
12 Spectral Width 25000.0
13 Lowest Frequency -2986.3
14 Nucleus 13C
15 Acquired Size 29984
16 Spectral Size 65536



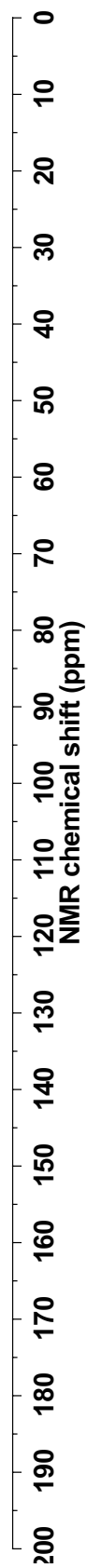
A-38: ¹³C-NMR spectrum of 20d

Parameter	Value
1 Data File Name	E:/NMRdata/nmr04162008-07012008/cyclohexenedimethylene-dimethylether-04152008.fid/fid
2 Title	cyclohexenedimethylene-dimethylether-04152008
3 Origin	inova
4 Owner	
5 Solvent	CDCB3
6 Pulse Sequence	s2pul
7 Acquisition Date	2008-04-15T10:57:57
8 Modification Date	
9 Temperature	25.0
10 Number of Scans	16
11 Spectrometer Frequency	599.72
12 Spectral Width	8000.0
13 Lowest Frequency	-1001.3
14 Nucleus	¹ H
15 Acquired Size	15136
16 Spectral Size	32768



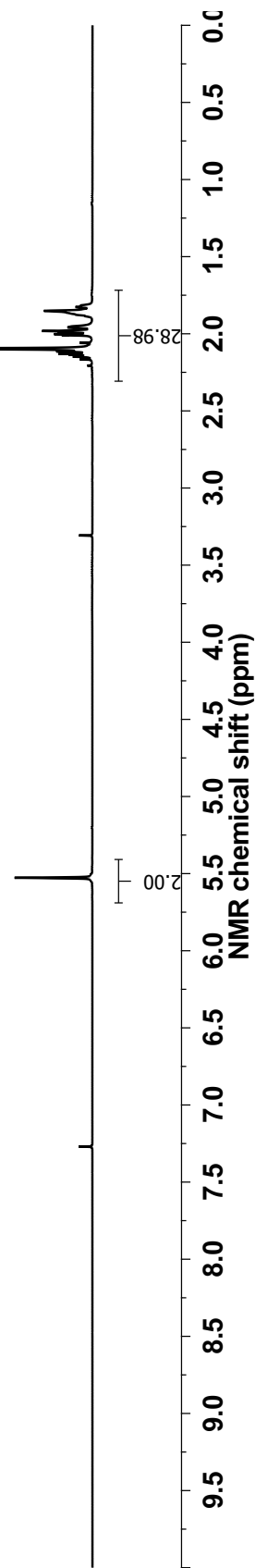
A-39: ¹H-NMR spectrum of 20e

Parameter	Value
1 Data File Name	E:/NMRdata/nmr04162008-07012008/cyclohexenedimethylether-C13NMR04232008.fid/ fid
2 Title	cyclohexenedimethylether-C13NMR
3 Origin	inova
4 Owner	
5 Solvent	CDCB3
6 Pulse Sequence	s2pul
7 Acquisition Date	2008-04-23T06:29:07
8 Modification Date	
9 Temperature	25.0
10 Number of Scans	112
11 Spectrometer Frequency	100.55
12 Spectral Width	25000.0
13 Lowest Frequency	-2986.3
14 Nucleus	¹³ C
15 Acquired Size	29984
16 Spectral Size	65536



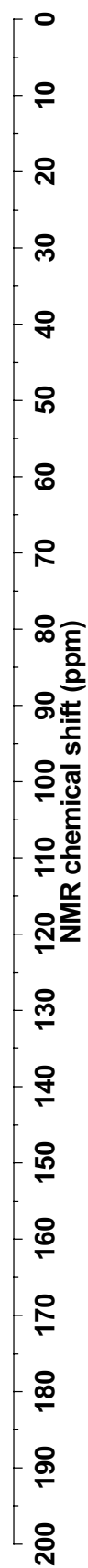
A-40: ¹³C-NMR spectrum of 20e

Parameter	Value
1 Data File Name	E:/ NMRdata/ nmr04162008-07012008/ cyclohexenetetramethylamide05142008.fid/ fid
2 Title	Cyclohexenetetramethylamide05142008
3 Origin	inova
4 Owner	
5 Solvent	CDCI3
6 Pulse Sequence	s2pul
7 Acquisition Date	2008-05-14T05:27:12
8 Modification Date	
9 Temperature	25.0
10 Number of Scans	32
11 Spectrometer Frequency	599.72
12 Spectral Width	8000.0
13 Lowest Frequency	-994.4
14 Nucleus	¹ H
15 Acquired Size	15136
16 Spectral Size	32768



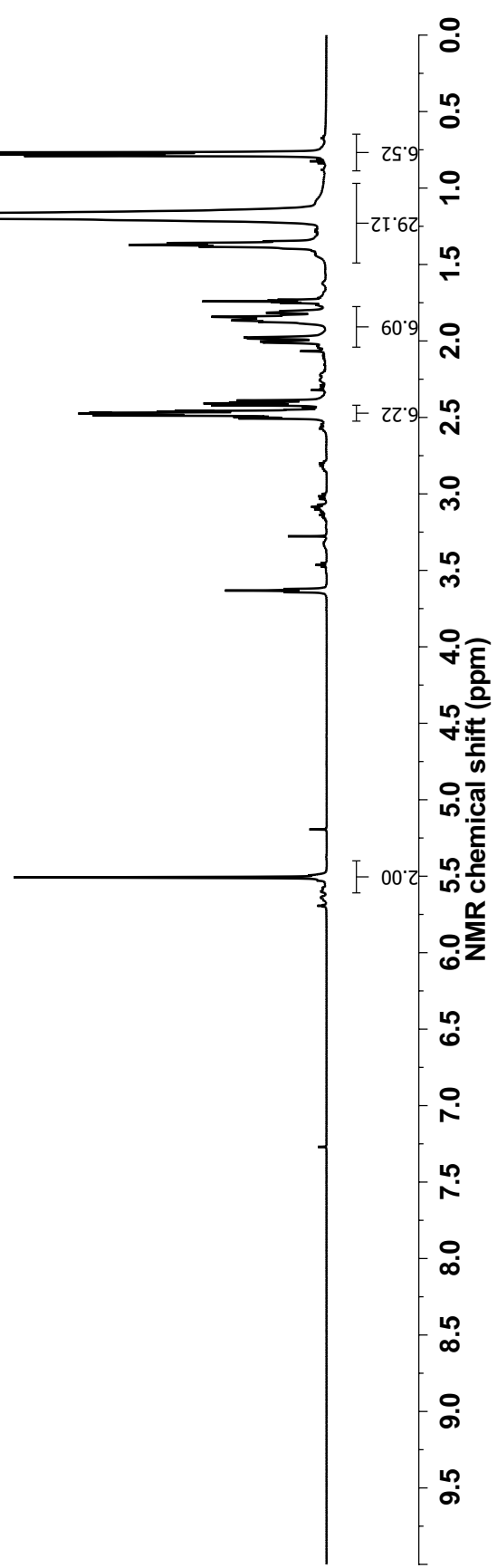
A-41: ¹H-NMR spectrum of 20f

Parameter	Value
1 Data File Name	E:/ NMRdata/ nmr04162008-07012008/ cyclohexenetetramethyldiamide-C13-05142008.fid/ fid
2 Title	cyclohexenetetramethyldiamide-C13
3 Origin	inova
4 Owner	
5 Solvent	CDCl3
6 Pulse Sequence	s2pul
7 Acquisition Date	2008-05-14T05:26:31
8 Modification Date	
9 Temperature	25.0
10 Number of Scans	24
11 Spectrometer Frequency	100.55
12 Spectral Width	25000.0
13 Lowest Frequency	-2994.0
14 Nucleus	¹³ C
15 Acquired Size	29984
16 Spectral Size	65536



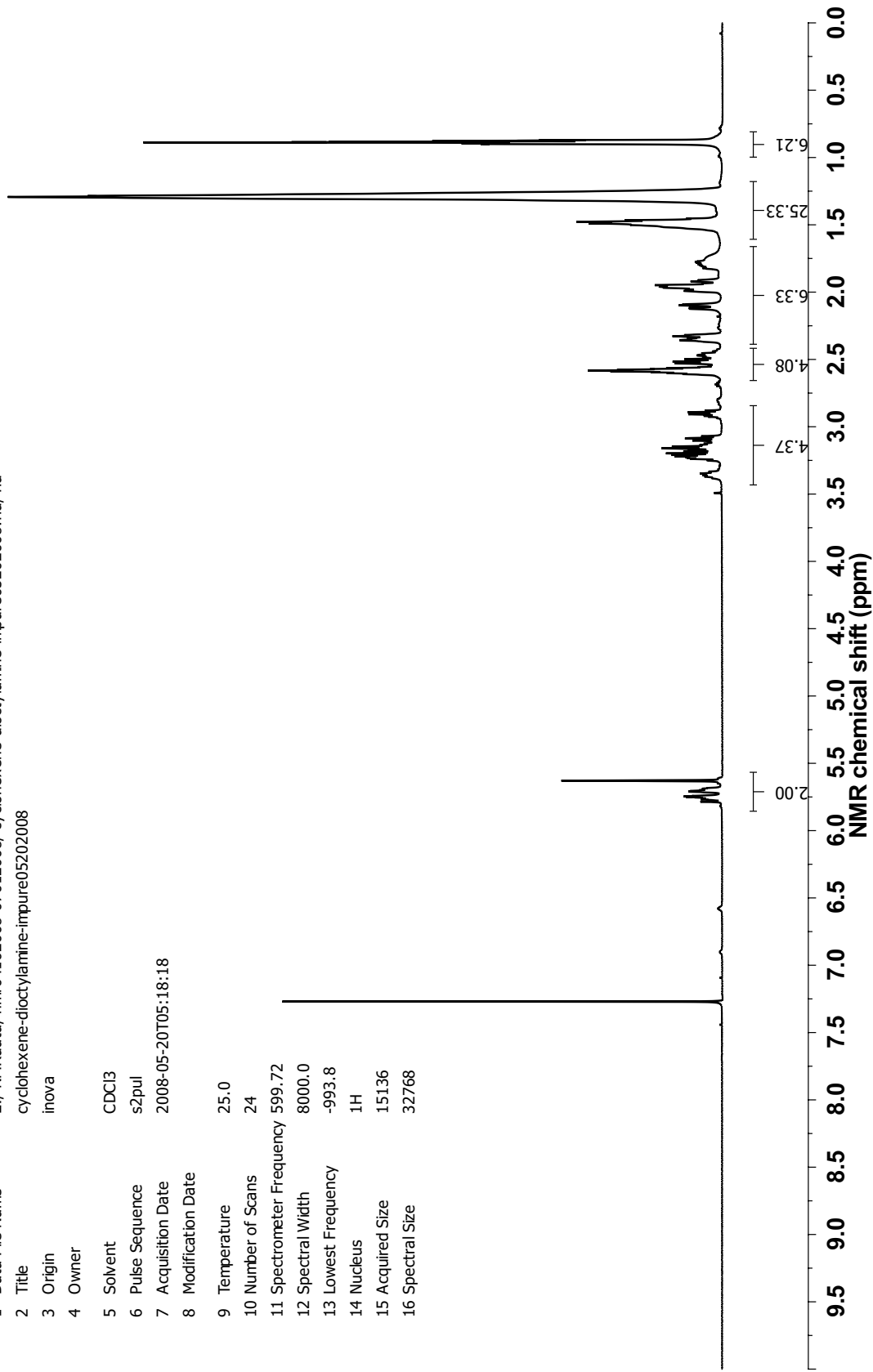
A-42: ¹³C-NMR spectrum of 20f

Parameter	Value
1 Data File Name	E:/ NMR\data/ nmr04162008-07012008/ cyclohexenedioctylidamide-impure05202008.fid/ fid
2 Title	clohexenedioctylidamide-impure
3 Origin	inova
4 Owner	
5 Solvent	CDCl3
6 Pulse Sequence	s2pul
7 Acquisition Date	2008-05-20T11:04:52
8 Modification Date	
9 Temperature	25.0
10 Number of Scans	24
11 Spectrometer Frequency	599.72
12 Spectral Width	8000.0
13 Lowest Frequency	-995.3
14 Nucleus	1H
15 Acquired Size	15136
16 Spectral Size	32768



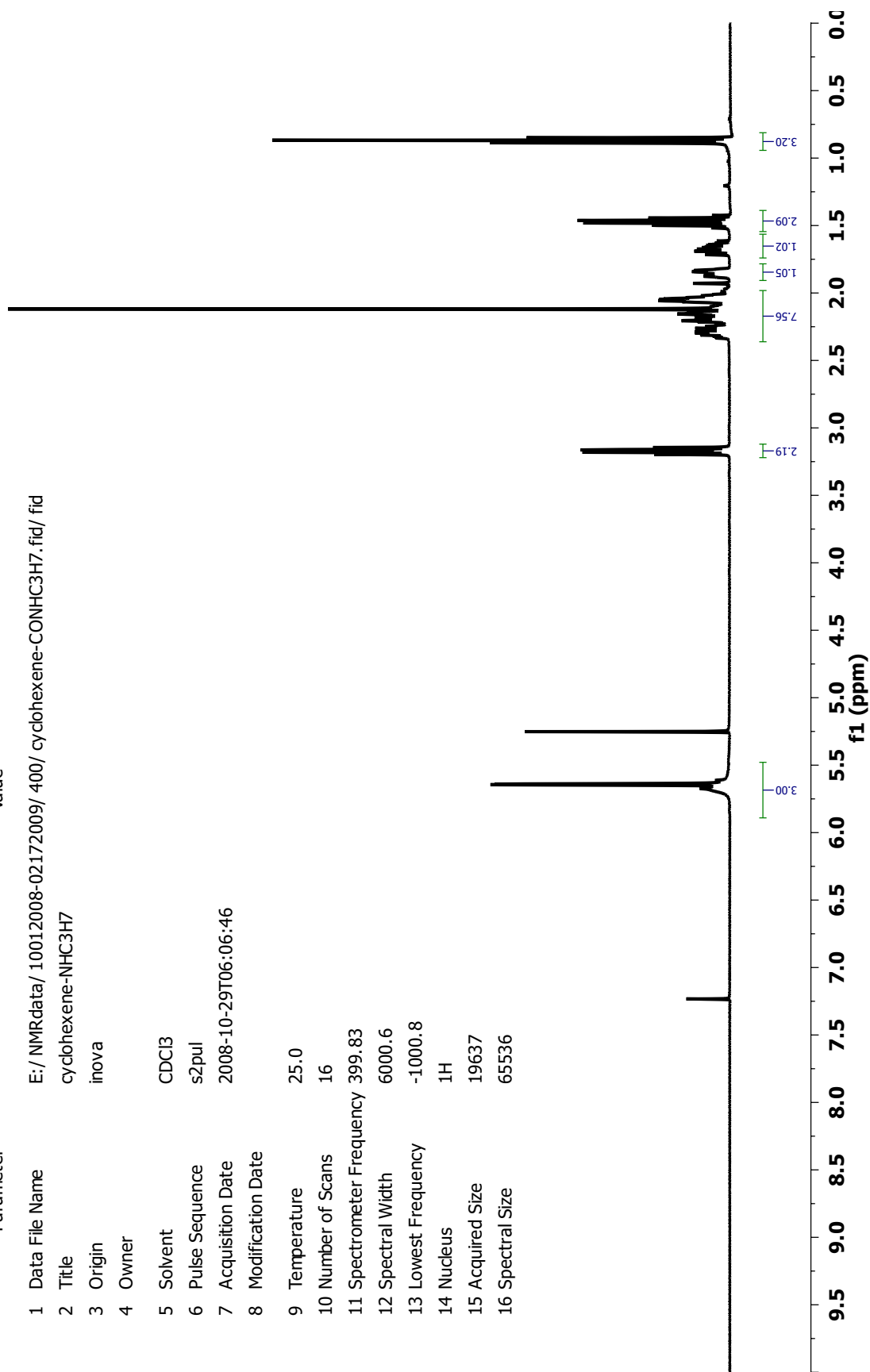
A-43: ¹H-NMR spectrum of 20g

Parameter	Value
1 Data File Name	E:/NMRdata/nmr04162008-07012008/cyclohexene-dioctylamine-impure05202008.fid/ fid
2 Title	cyclohexene-dioctylamine-impure05202008
3 Origin	inova
4 Owner	
5 Solvent	CDCl3
6 Pulse Sequence	s2pul
7 Acquisition Date	2008-05-20T05:18:18
8 Modification Date	
9 Temperature	25.0
10 Number of Scans	24
11 Spectrometer Frequency	599.72
12 Spectral Width	8000.0
13 Lowest Frequency	-993.8
14 Nucleus	1H
15 Acquired Size	15136
16 Spectral Size	32768

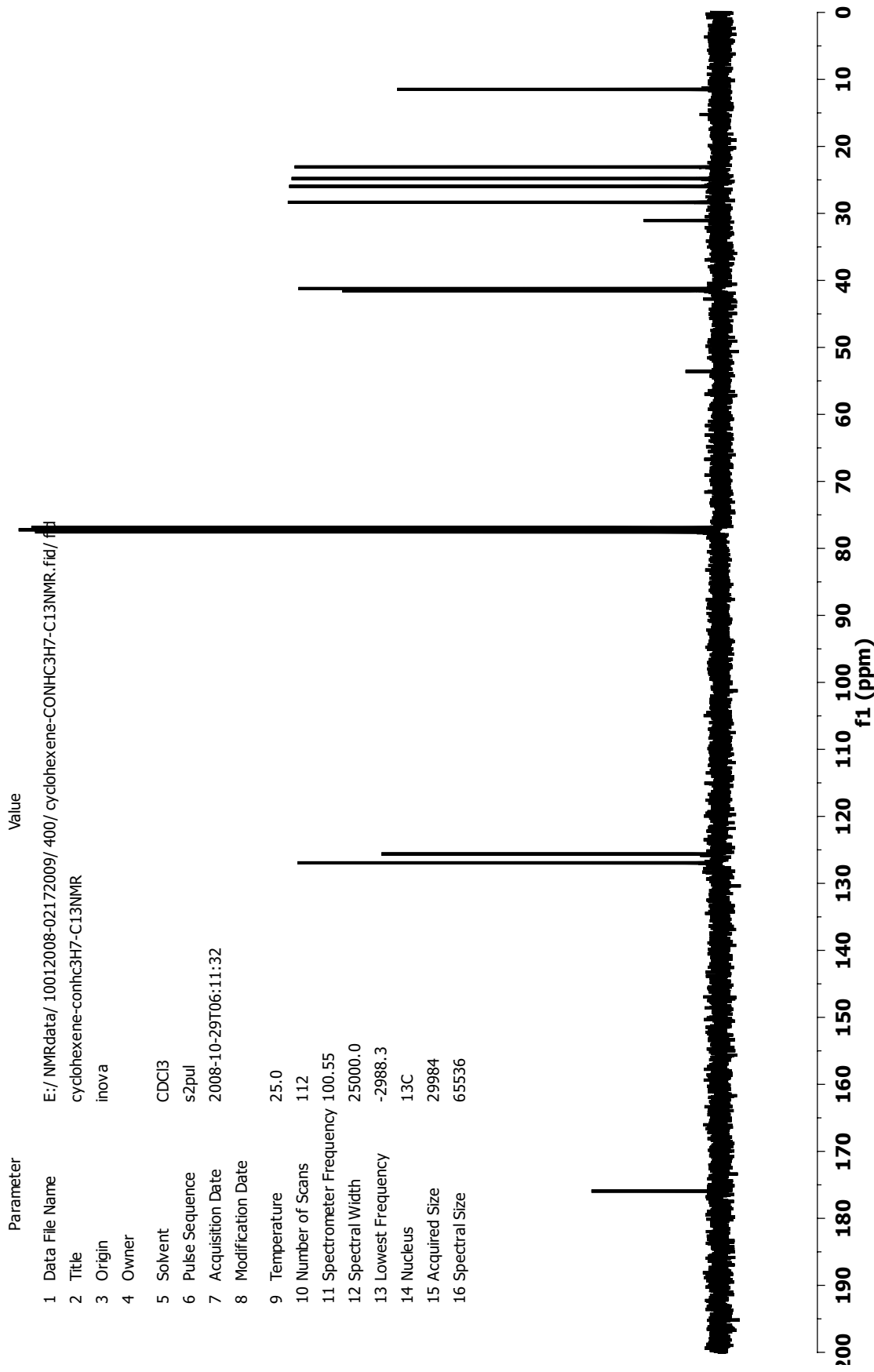


A-44: ¹H-NMR spectrum of 20h

Parameter	Value
1 Data File Name	E:/ NMRdata/ 10012008-02172009/ 400/ cyclohexene-CONHC3H7.fid/ fid
2 Title	cyclohexene-NHC3H7
3 Origin	inova
4 Owner	
5 Solvent	CDCl3
6 Pulse Sequence	s2pul
7 Acquisition Date	2008-10-29T06:06:46
8 Modification Date	
9 Temperature	25.0
10 Number of Scans	16
11 Spectrometer Frequency	399.83
12 Spectral Width	6000.6
13 Lowest Frequency	-1000.8
14 Nucleus	1H
15 Acquired Size	19637
16 Spectral Size	65536

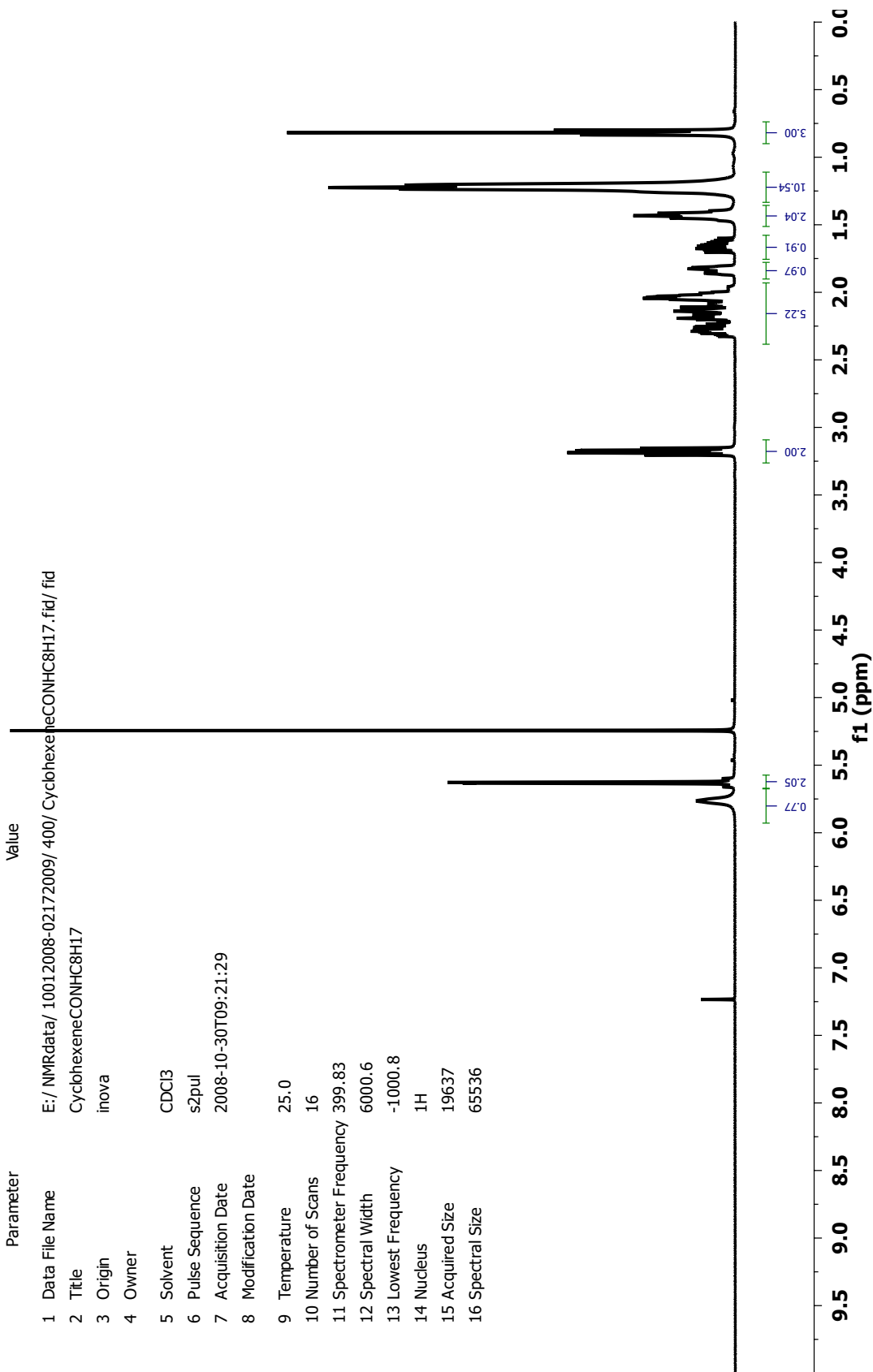


A-45: ¹H-NMR spectrum of 20k

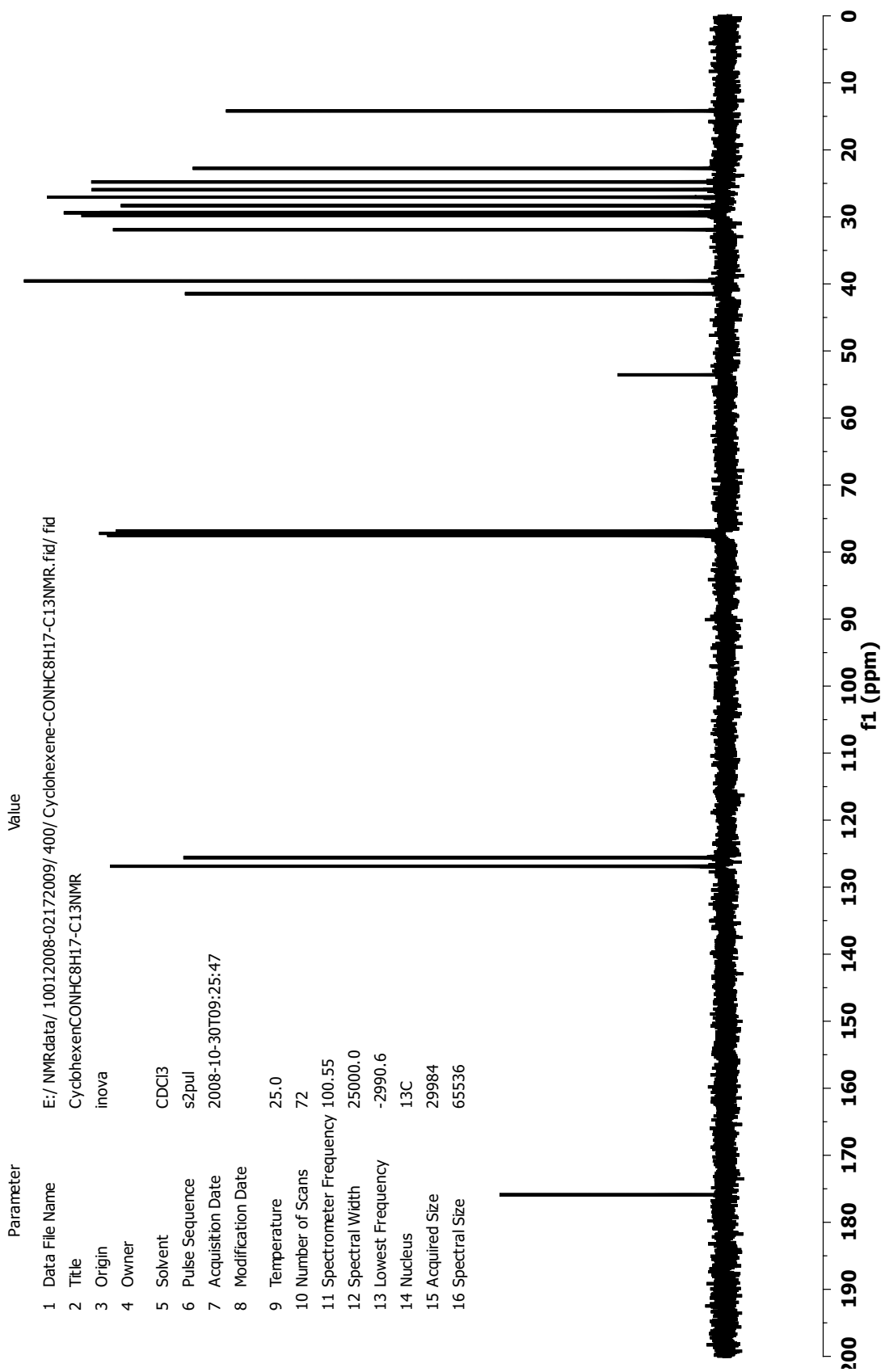


A-46: ¹³C-NMR spectrum of 20k

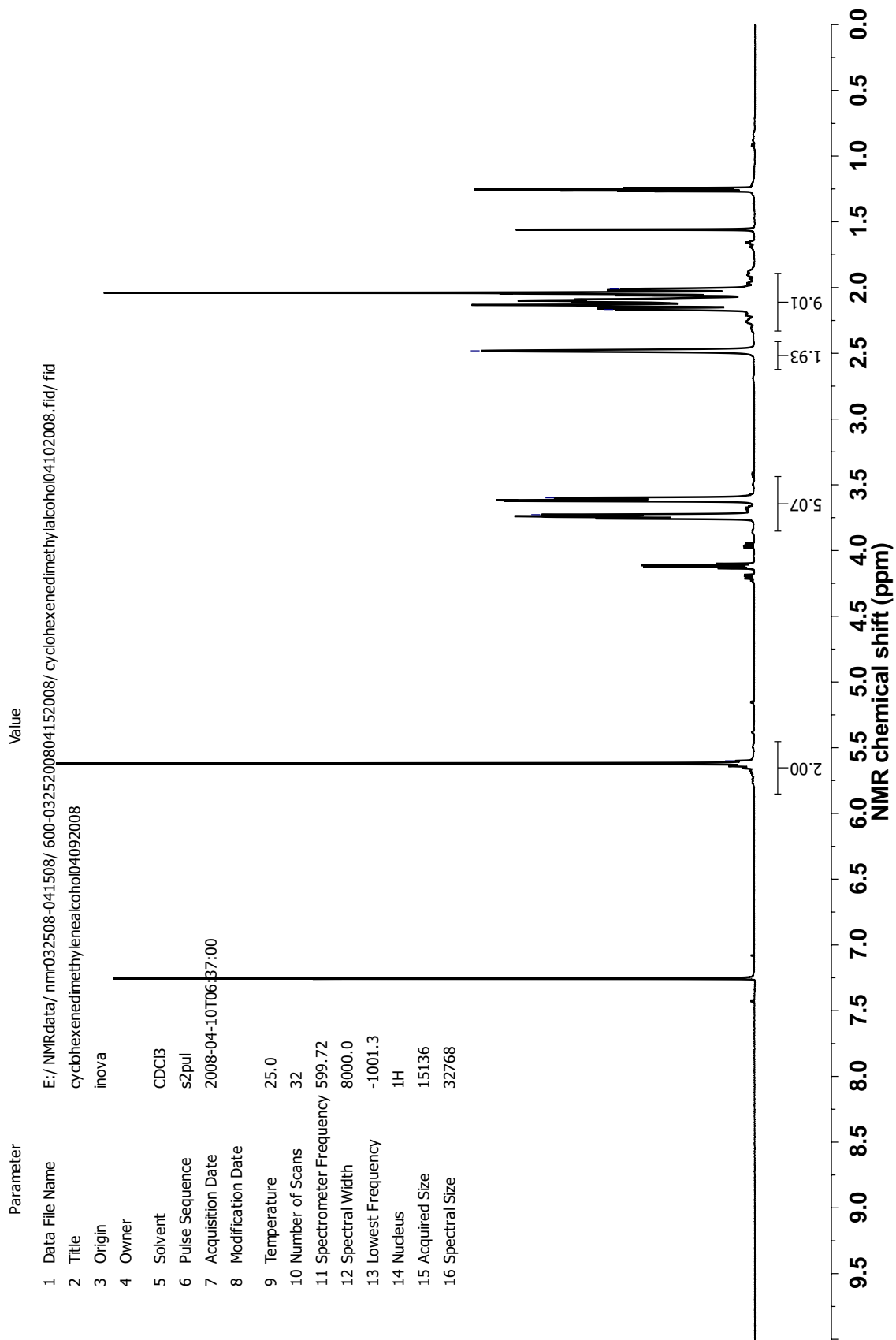
Parameter	Value
1 Data File Name	E:/NMRdata/10012008-02172009/400/CyclohexeneCONHC8H17.fid/ fid
2 Title	CyclohexeneCONHC8H17
3 Origin	inova
4 Owner	
5 Solvent	CDCl3
6 Pulse Sequence	s2pul
7 Acquisition Date	2008-10-30T09:21:29
8 Modification Date	
9 Temperature	25.0
10 Number of Scans	16
11 Spectrometer Frequency	399.83
12 Spectral Width	6000.6
13 Lowest Frequency	-1000.8
14 Nucleus	1H
15 Acquired Size	19637
16 Spectral Size	65536



A-47: ¹H-NMR spectrum of 20m

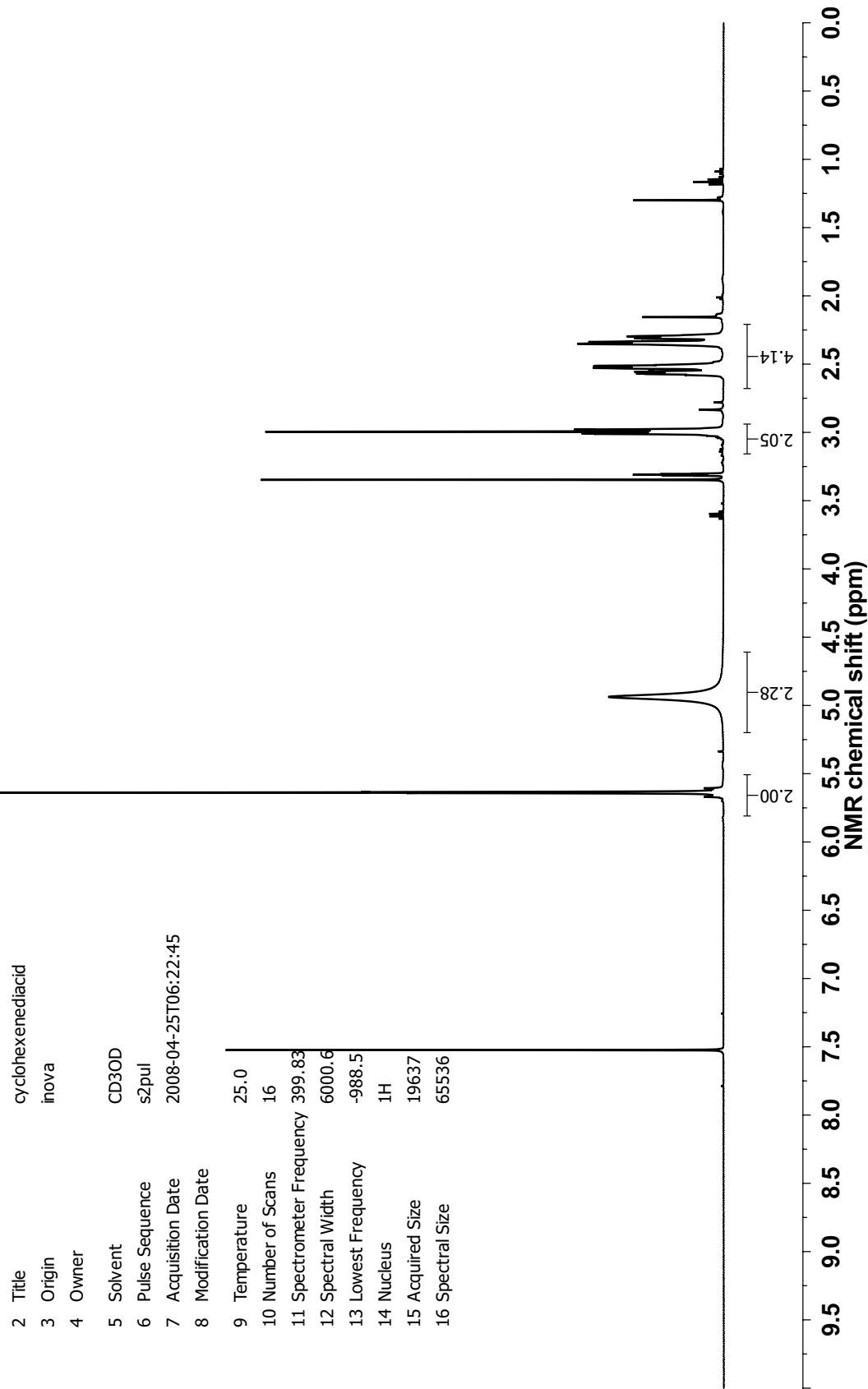


A-48: ¹³C-NMR spectrum of 20m

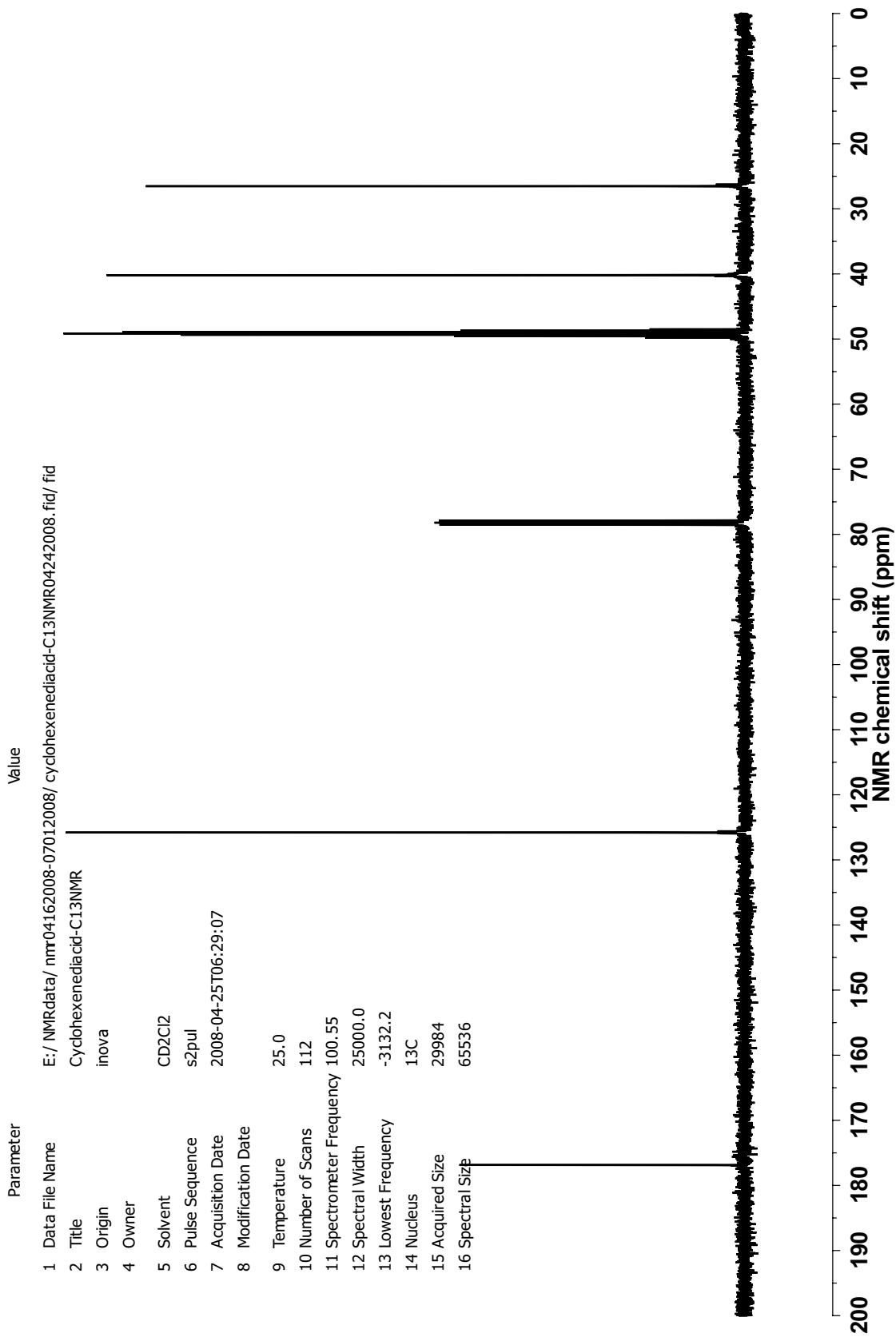


A-49: ¹H-NMR spectrum of 22

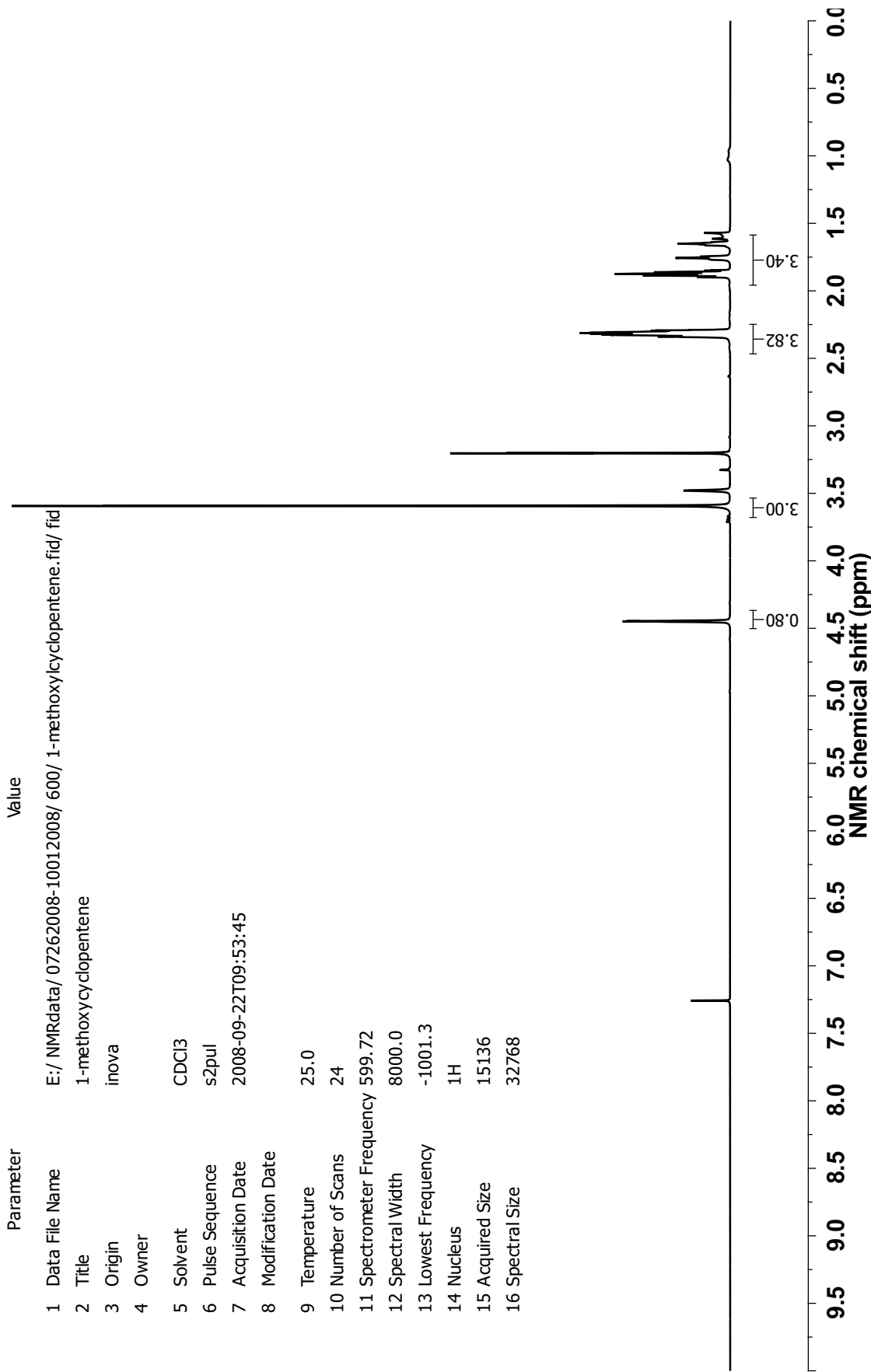
Parameter Value
 1 Data File Name E:/NMRdata/nmr04162008-07012008/cyclohexenediacid04242008.fid/ fid
 2 Title cyclohexenediacid
 3 Origin inova
 4 Owner
 5 Solvent CD3OD
 6 Pulse Sequence s2pul
 7 Acquisition Date 2008-04-25T06:22:45
 8 Modification Date
 9 Temperature 25.0
 10 Number of Scans 16
 11 Spectrometer Frequency 399.83
 12 Spectral Width 6000.6
 13 Lowest Frequency -988.5
 14 Nucleus ¹H
 15 Acquired Size 19637
 16 Spectral Size 65536



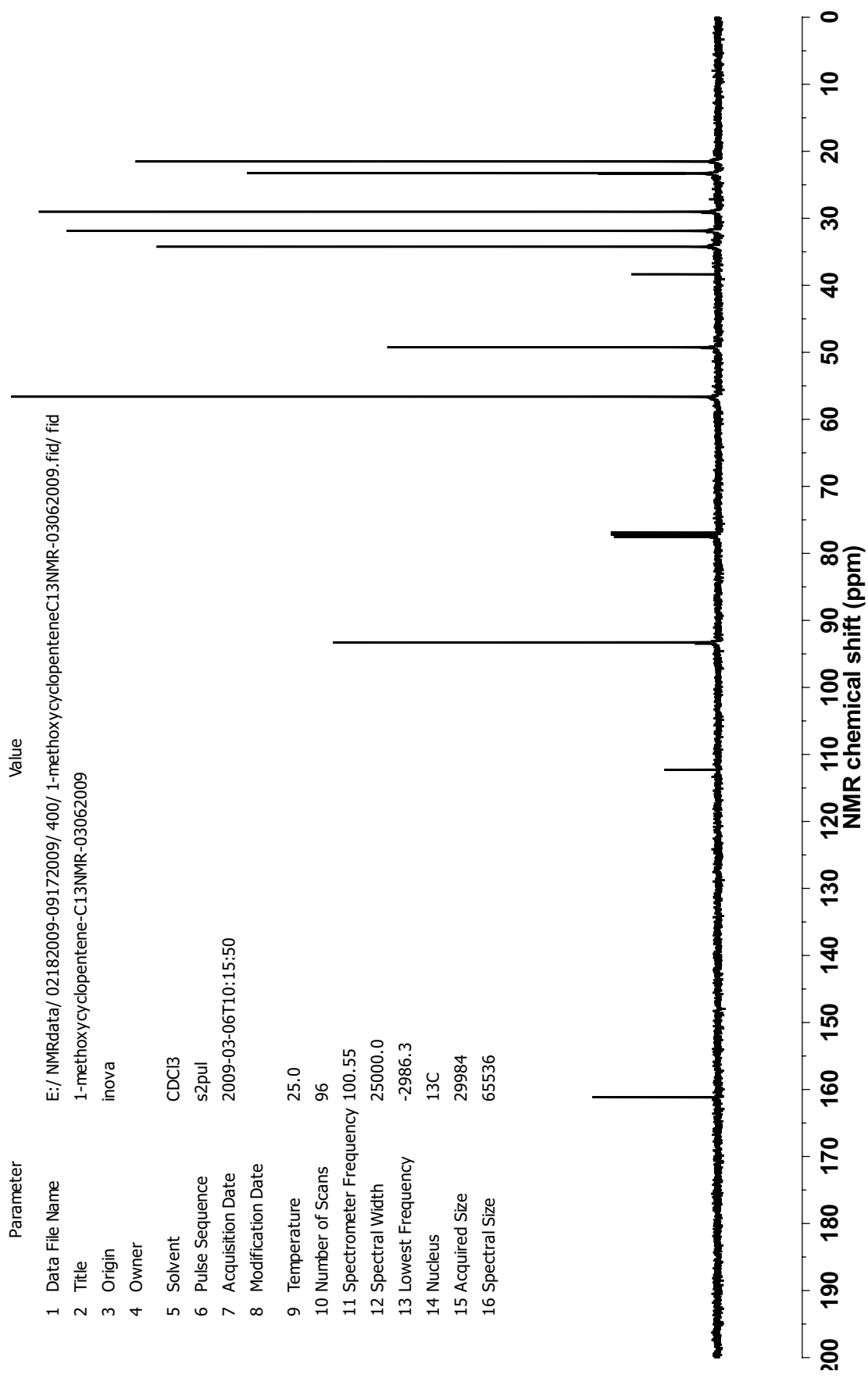
A-50: ¹H-NMR spectrum of 23



A-51: ¹³C-NMR spectrum of 23

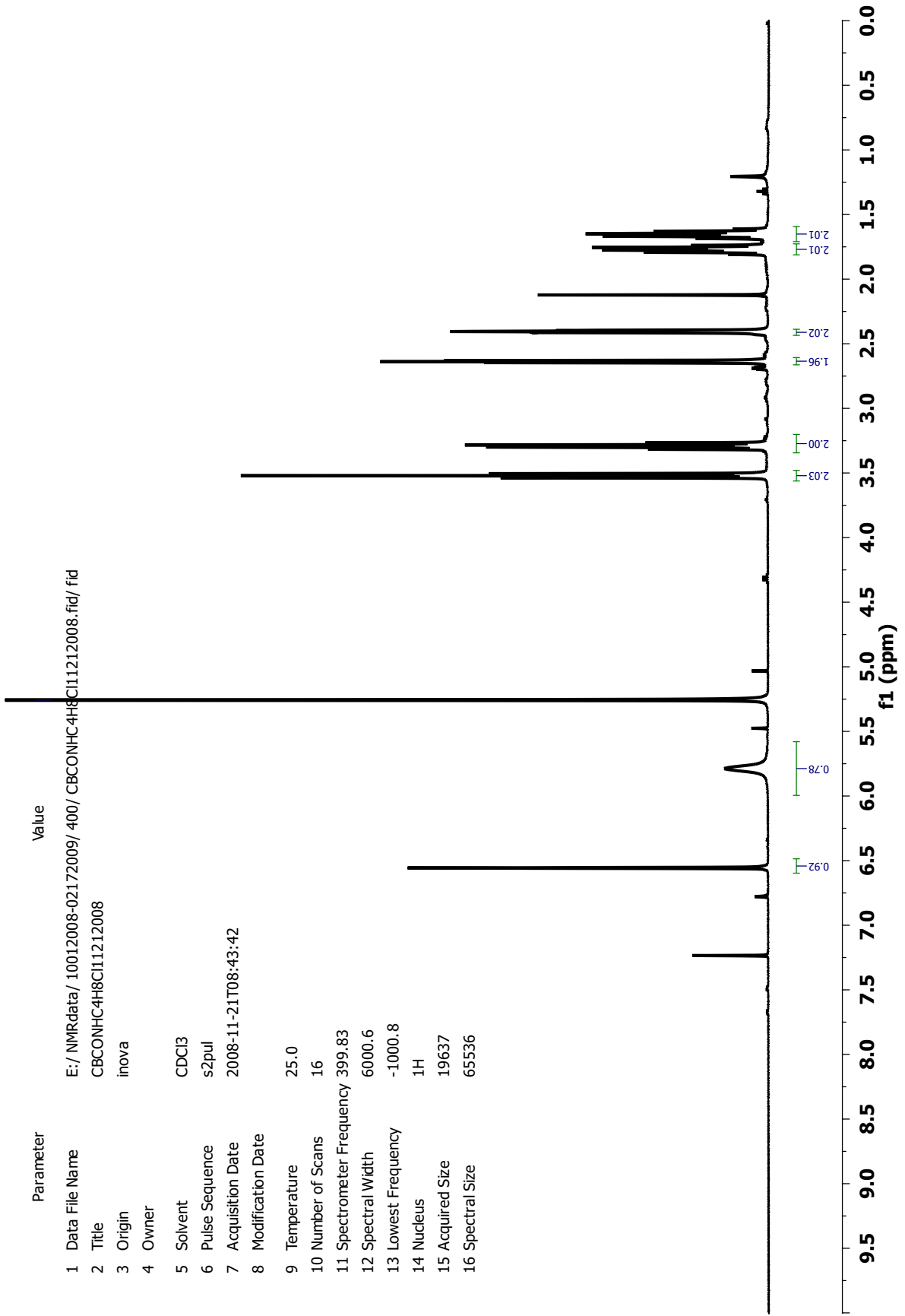


A-52: ¹H-NMR spectrum of 29b



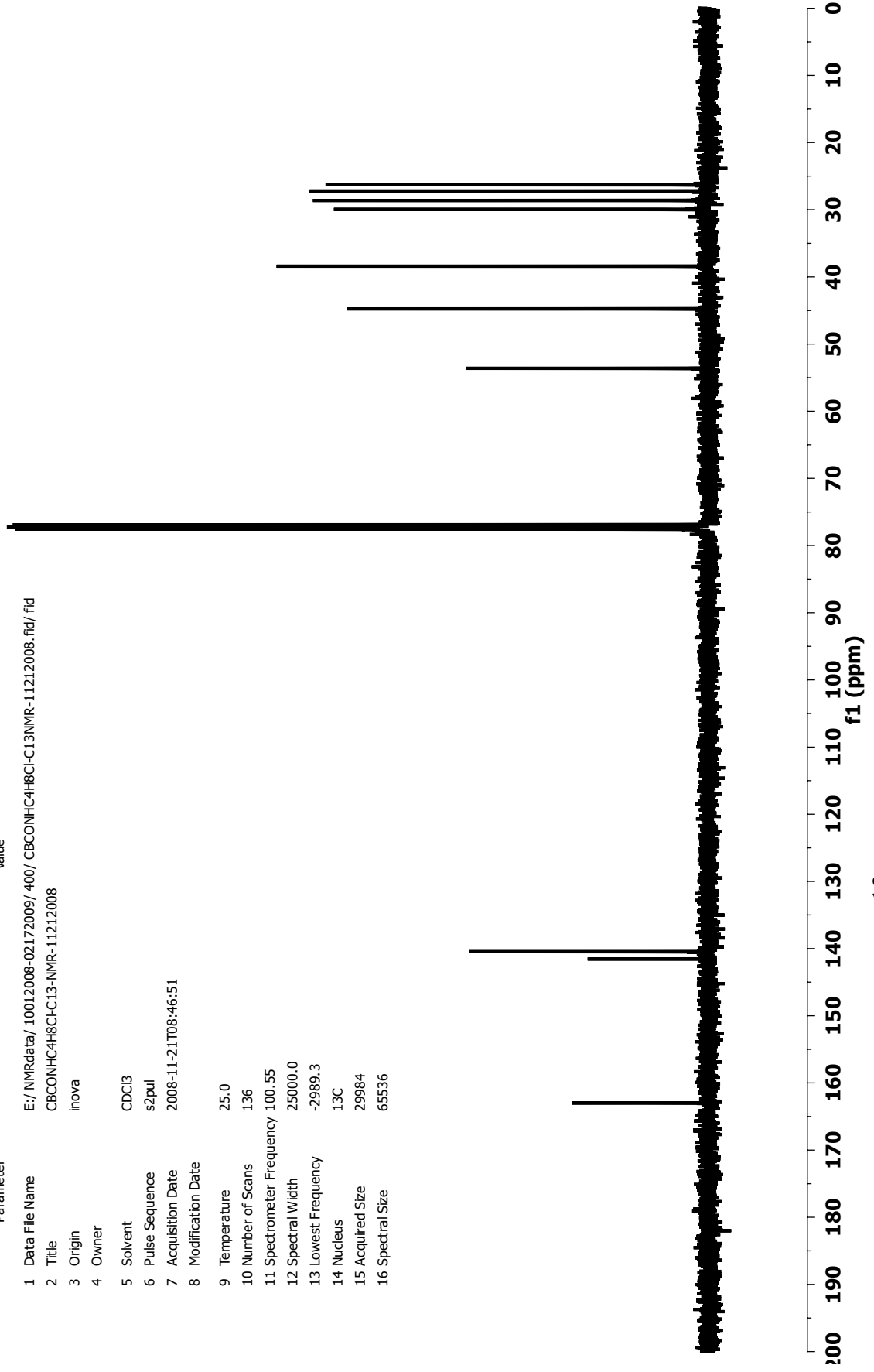
A-53: ¹³C-NMR spectrum of 29b

Parameter	Value
1 Data File Name	E:/NMRdata/10012008-02172009/400/CBCONHC4H8CI11212008.fid/ fid
2 Title	CBCONHC4H8CI11212008
3 Origin	inova
4 Owner	
5 Solvent	CDCI3
6 Pulse Sequence	s2pul
7 Acquisition Date	2008-11-21T08:43:42
8 Modification Date	
9 Temperature	25.0
10 Number of Scans	16
11 Spectrometer Frequency	399.83
12 Spectral Width	6000.6
13 Lowest Frequency	-1000.8
14 Nucleus	¹ H
15 Acquired Size	19637
16 Spectral Size	65536

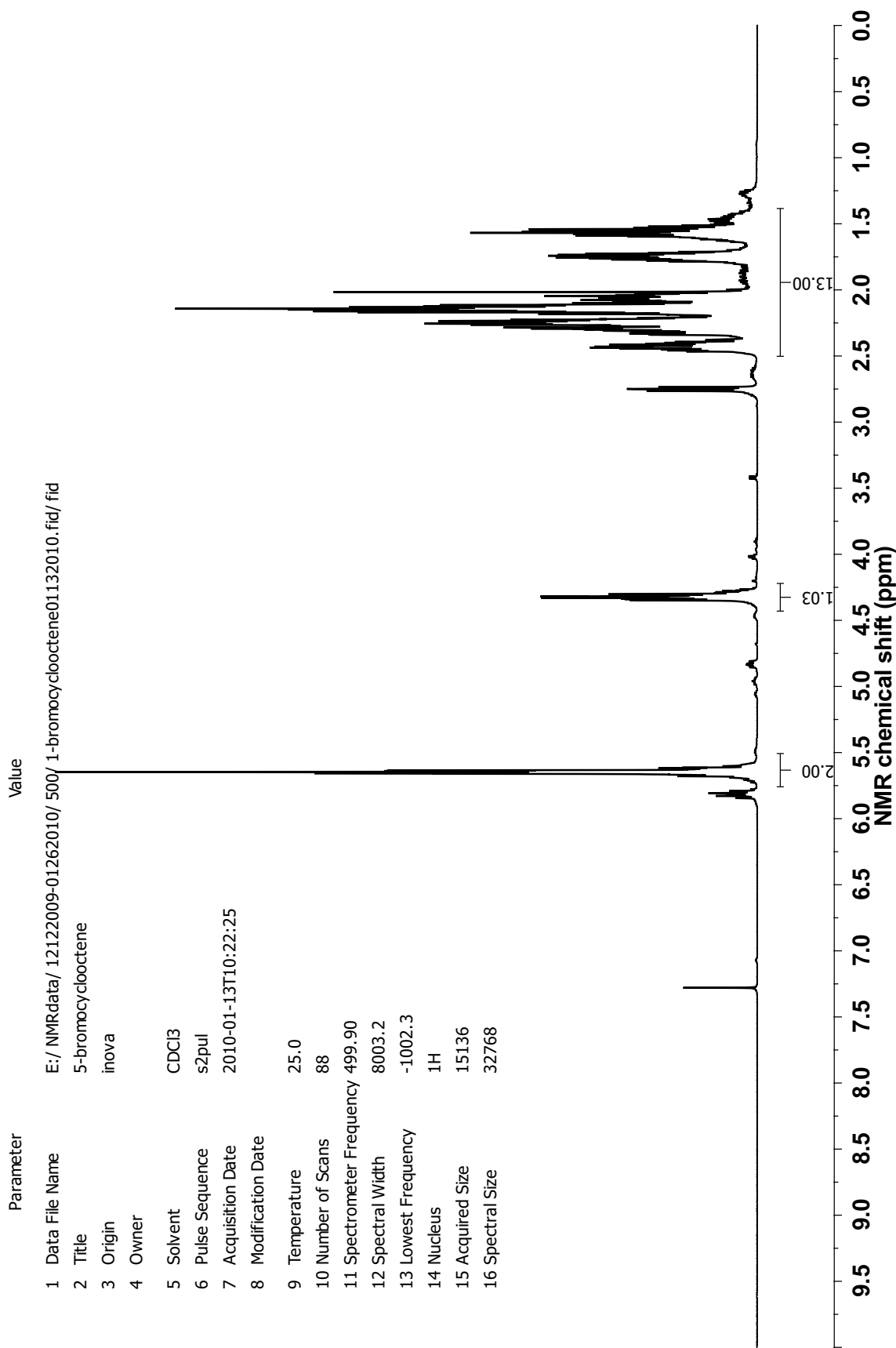


A-54: ¹H-NMR spectrum of 30

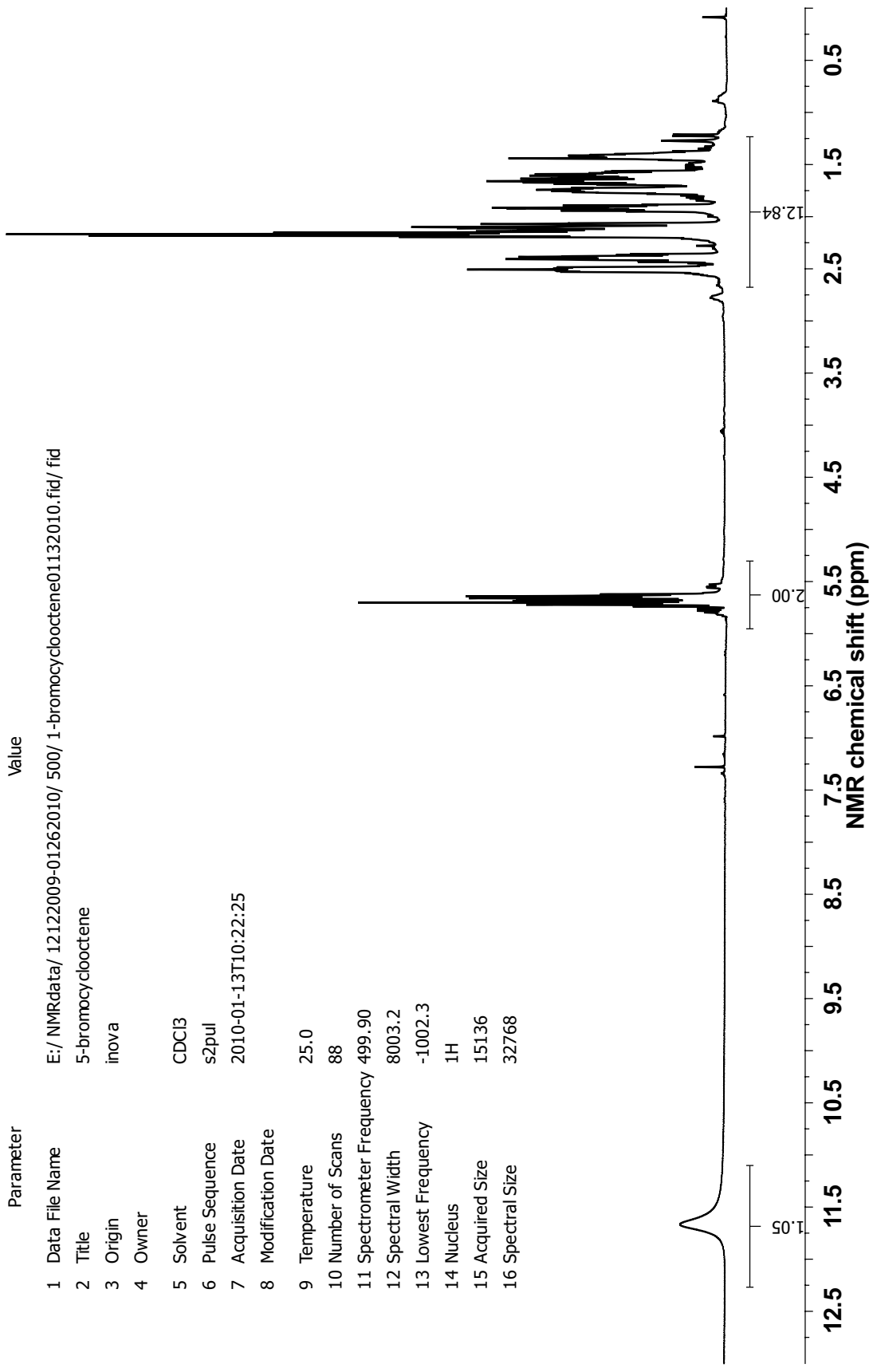
Parameter	Value
1. Data File Name	E:/ NMRdata/ 10012008-02172009/ 400/ CBCONHC4H8Cl-C13NMR-11212008.fid/ fid
2. Title	CBCONHC4H8Cl-C13-NMR-11212008
3. Origin	inova
4. Owner	
5. Solvent	CDCl3
6. Pulse Sequence	s2pul
7. Acquisition Date	2008-11-21T08:46:51
8. Modification Date	
9. Temperature	25.0
10. Number of Scans	136
11. Spectrometer Frequency	100.55
12. Spectral Width	25000.0
13. Lowest Frequency	-2989.3
14. Nucleus	13C
15. Acquired Size	29984
16. Spectral Size	65536



A-55: ¹³C-NMR spectrum of 30

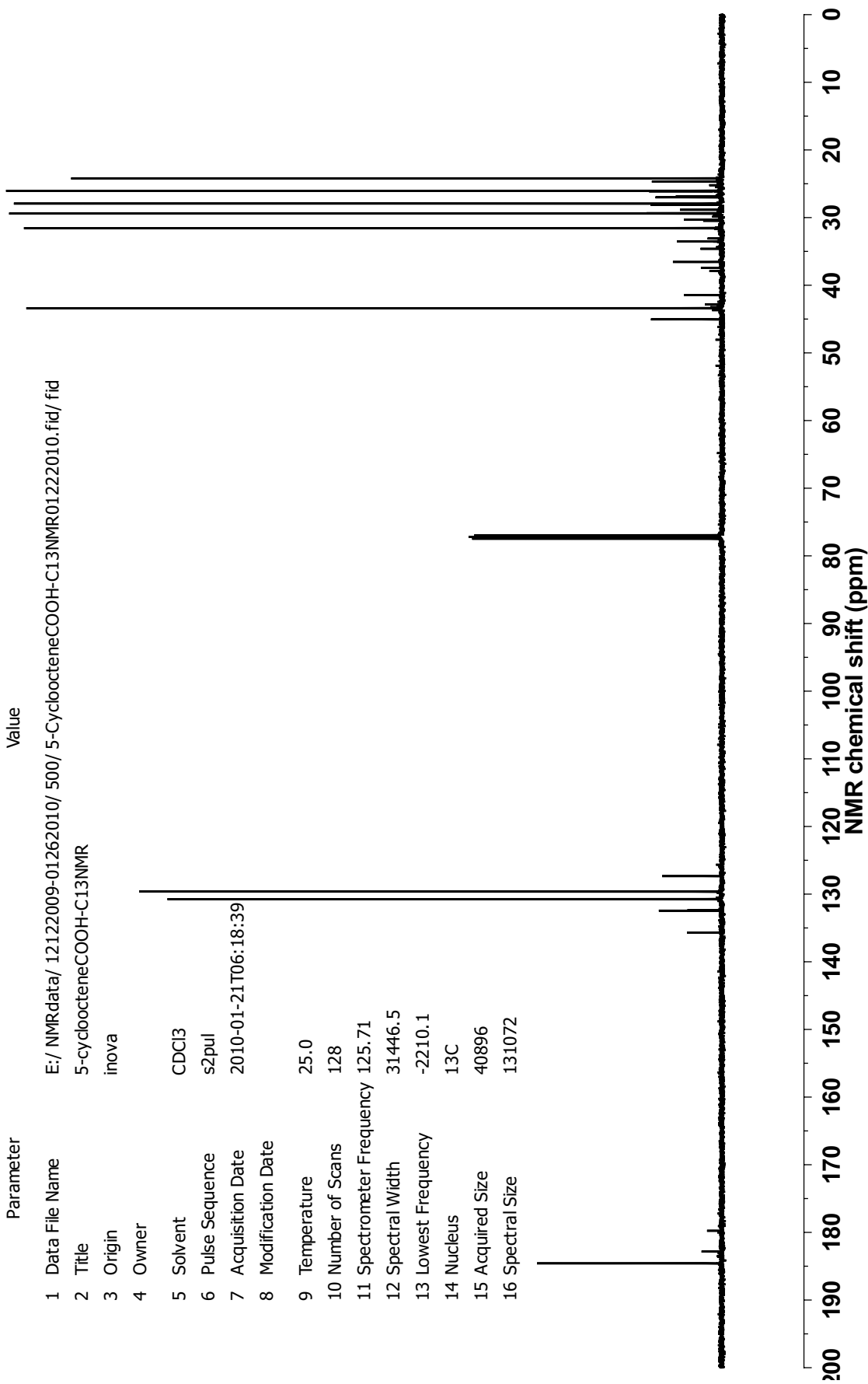


A-56: ¹H-NMR spectrum of 31



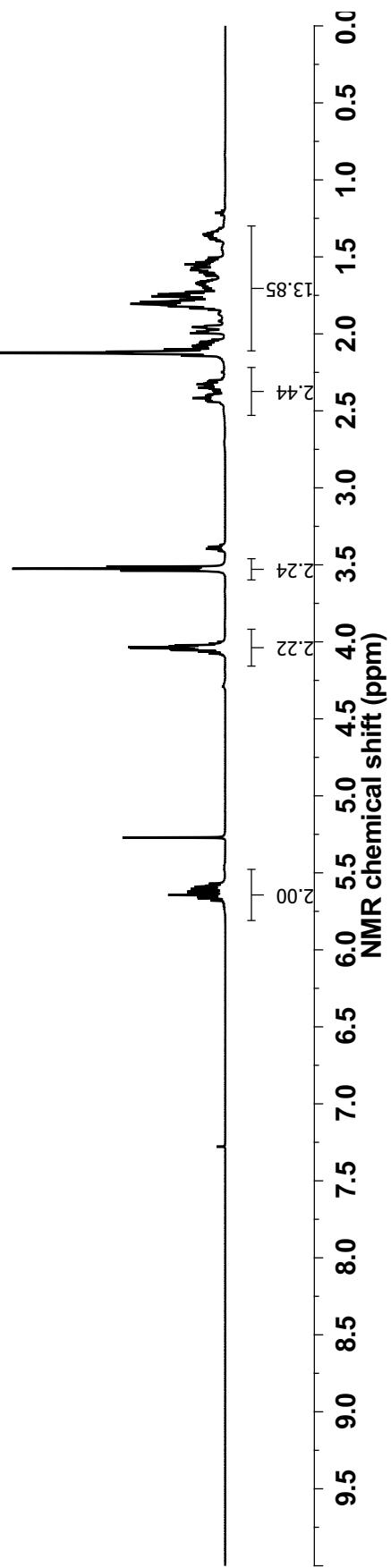
A-57: ¹H-NMR spectrum of 33

Parameter	Value
1 Data File Name	E:/ NMRdata/ 12122009-01262010/ 500/ 5-CycloocteneCOOH-C13NMR01222010.fid/ fid
2 Title	5-cycloocteneCOOH-C13NMR
3 Origin	inova
4 Owner	
5 Solvent	CDCI3
6 Pulse Sequence	s2pul
7 Acquisition Date	2010-01-21T06:18:39
8 Modification Date	
9 Temperature	25.0
10 Number of Scans	128
11 Spectrometer Frequency	125.71
12 Spectral Width	31446.5
13 Lowest Frequency	-2210.1
14 Nucleus	13C
15 Acquired Size	40896
16 Spectral Size	131072



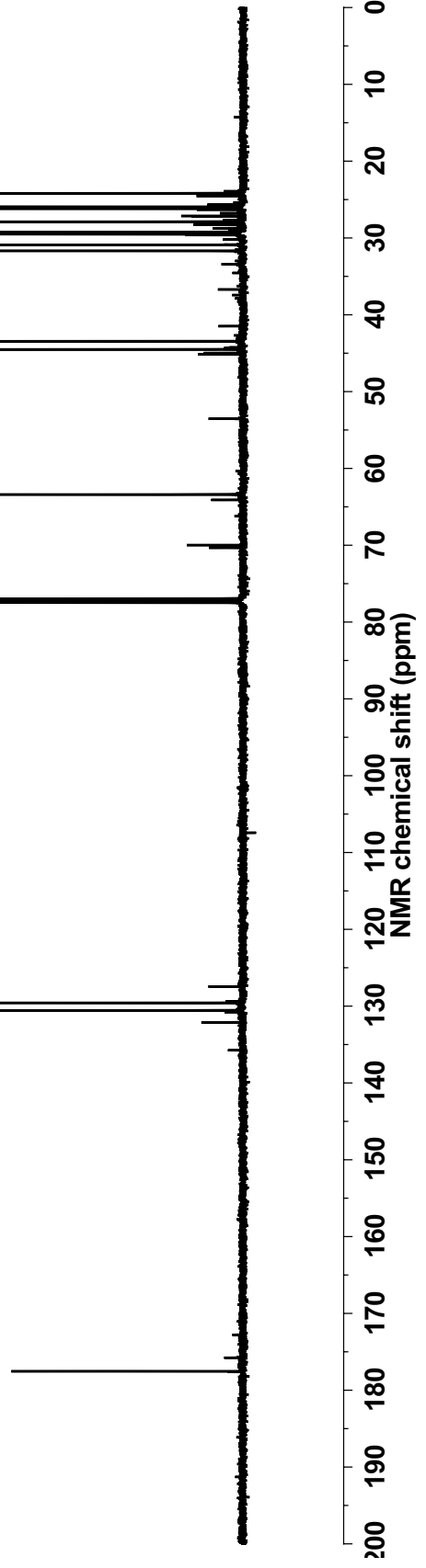
A-58: ¹³C-NMR spectrum of 33

Parameter	Value
1 Data File Name	E:/ NMRdata/ 12122009-01262010/ 500/ 5-cycloocteneCOOC4H8Cl-01232010.fid/ fid
2 Title	STANDARD PROTON PARAMETERS
3 Origin	inova
4 Owner	
5 Solvent	CDCI3
6 Pulse Sequence	s2pul
7 Acquisition Date	2010-01-22T06:29:42
8 Modification Date	
9 Temperature	25.0
10 Number of Scans	40
11 Spectrometer Frequency	499.90
12 Spectral Width	8003.2
13 Lowest Frequency	-1002.3
14 Nucleus	¹ H
15 Acquired Size	15136
16 Spectral Size	32768



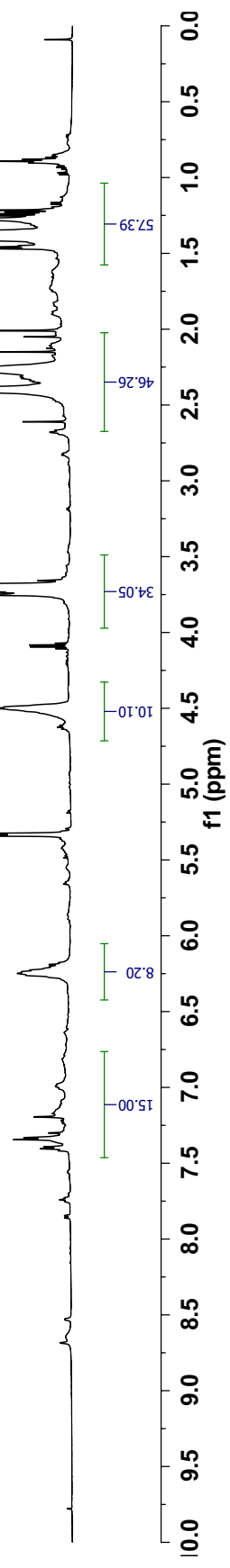
A-59: ¹H-NMR spectrum of 34

Parameter	Value
1 Data File Name	E:/NMRdata/12122009-01262010/500/5-cycloocteneCOOC4H8Cl-C13NMR01232010.fid/ fid
2 Title	5-cycloocteneCOOC4H8Cl-C13NMR
3 Origin	inova
4 Owner	
5 Solvent	CDCI3
6 Pulse Sequence	s2pul
7 Acquisition Date	2010-01-22T06:34:13
8 Modification Date	
9 Temperature	25.0
10 Number of Scans	184
11 Spectrometer Frequency	125.71
12 Spectral Width	31446.5
13 Lowest Frequency	-2218.6
14 Nucleus	13C
15 Acquired Size	40896
16 Spectral Size	131072

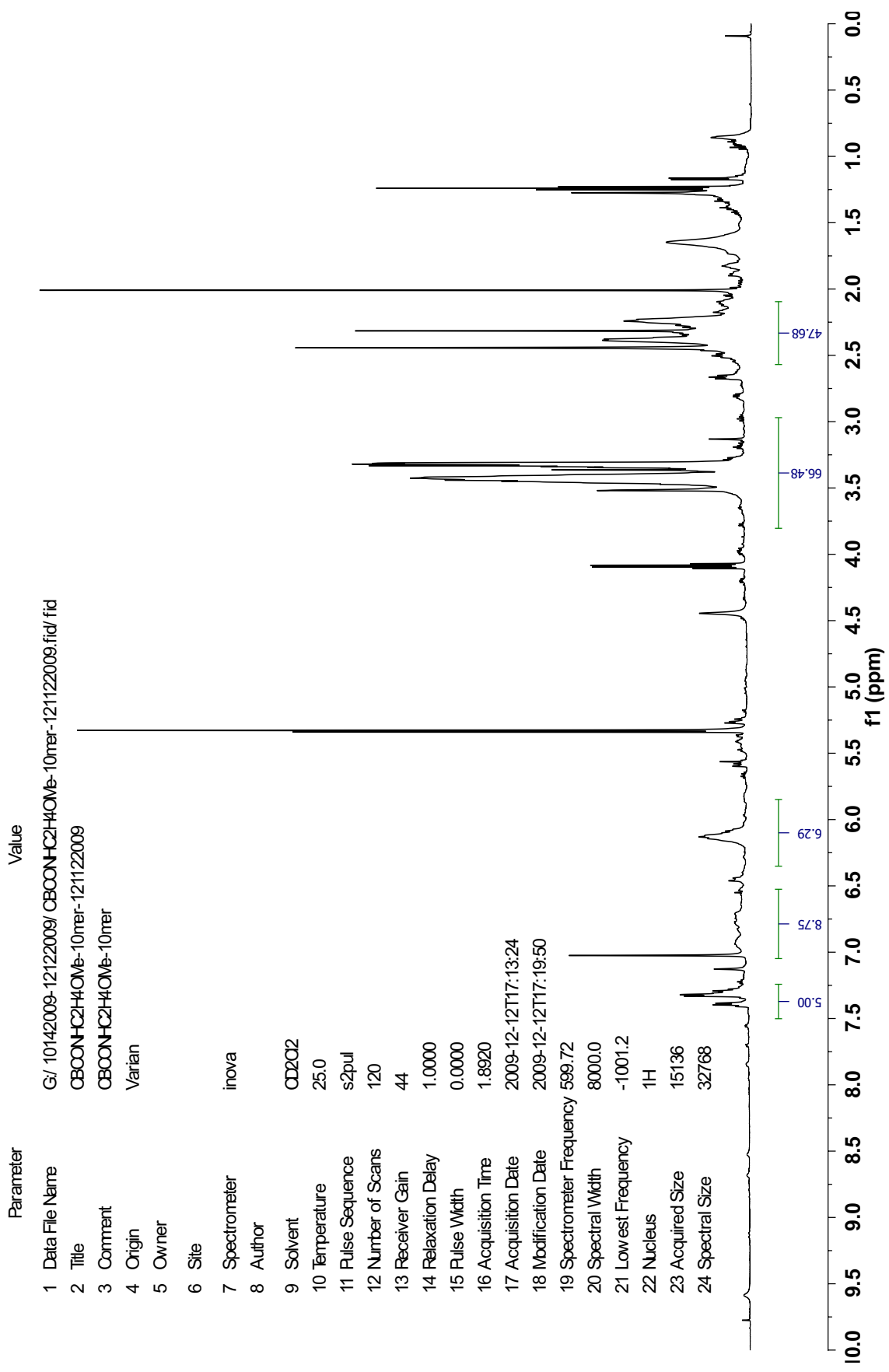


A-60: ¹³C-NMR spectrum of 34

Parameter	Value
1 Data File Name	G:/10142009-12122009/CBAlaOMe-10mer12122009-2.fid/fid
2 Title	CBAlaOMe-10mer12122009-2
3 Comment	CBAlaOMe-10mer
4 Origin	Varian
5 Owner	
6 Site	
7 Spectrometer	inova
8 Author	
9 Solvent	CDCl ₂
10 Temperature	25.0
11 Pulse Sequence	s2pul
12 Number of Scans	64
13 Receiver Gain	40
14 Relaxation Delay	1.0000
15 Pulse Width	0.0000
16 Acquisition Time	1.8920
17 Acquisition Date	2009-12-12T12:46:50
18 Modification Date	2009-12-12T12:50:34
19 Spectrometer Frequency	599.72
20 Spectral Width	8000.0
21 Lowest Frequency	-1001.2
22 Nucleus	¹ H
23 Acquired Size	15136
24 Spectral Size	32768

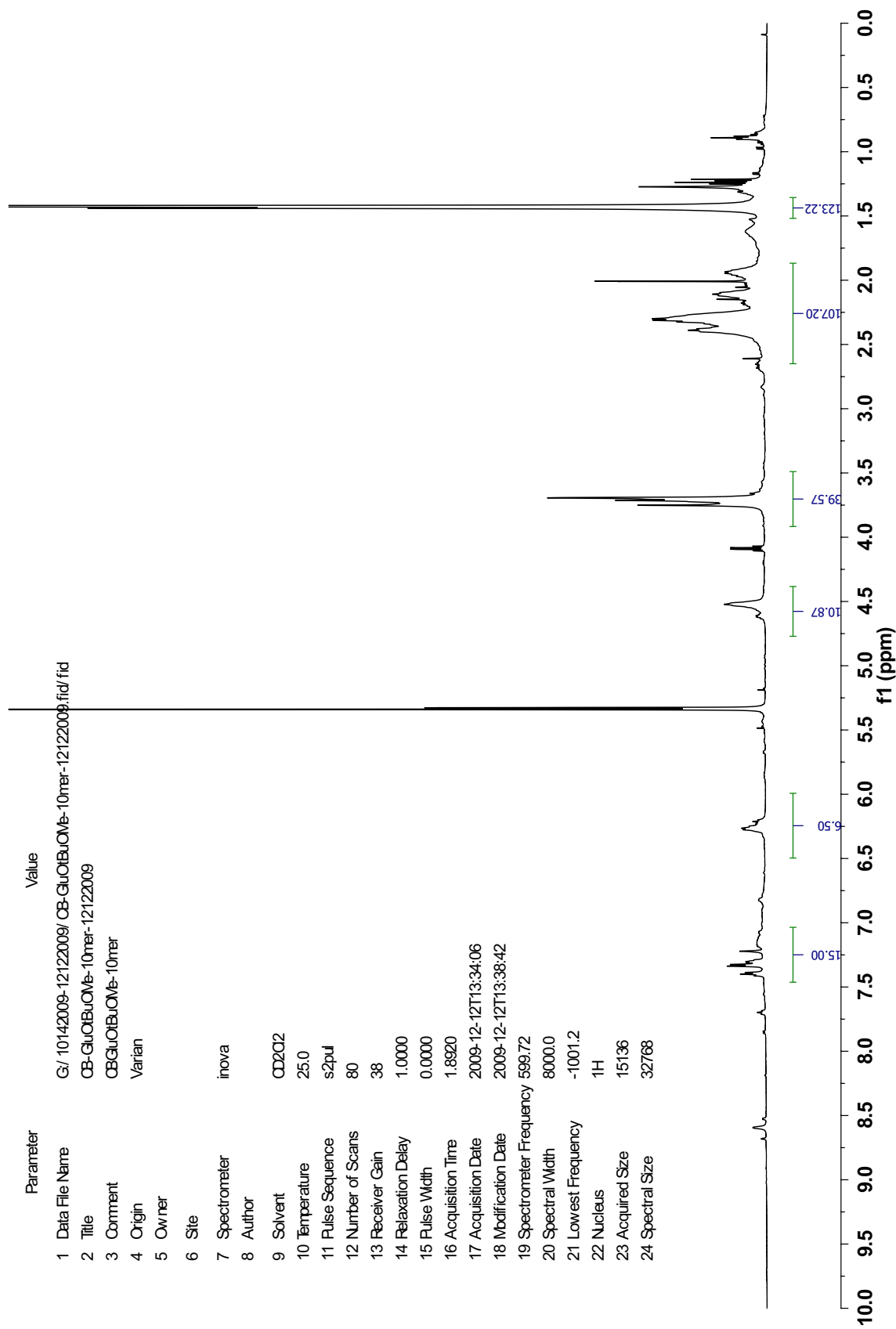


A-61: ¹H-NMR spectrum of (6b)₁₀



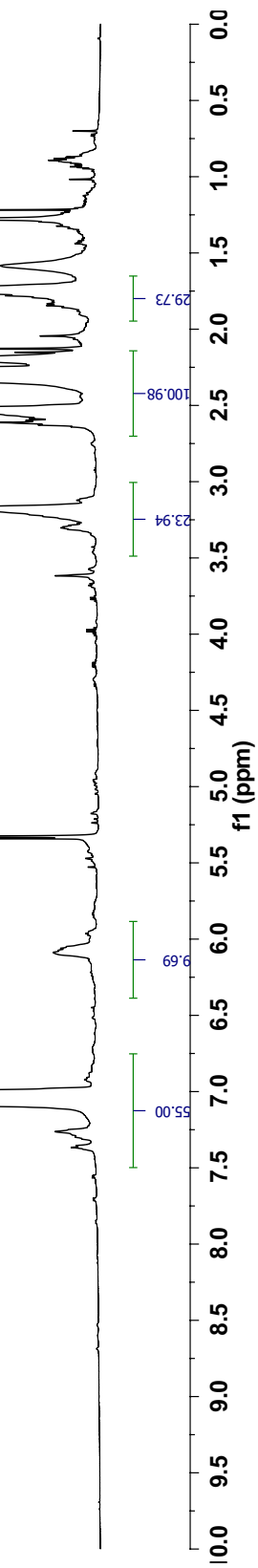
A-62: ¹H-NMR spectrum of (6c)₁₀

Parameter	Value
1 Data File Name	G:/10142009-12122009/CB-GluOtBuOMe-10mer-12122009.fid/fid
2 Title	CB-GluOtBuOMe-10mer-12122009
3 Comment	CBGluOtBuOMe-10mer
4 Origin	Varian
5 Owner	
6 Site	
7 Spectrometer	inova
8 Author	
9 Solvent	CDCl ₂
10 Temperature	25.0
11 Pulse Sequence	s2pul
12 Number of Scans	80
13 Receiver Gain	38
14 Relaxation Delay	1.0000
15 Pulse Width	0.0000
16 Acquisition Time	1.8920
17 Acquisition Date	2009-12-12T13:34:06
18 Modification Date	2009-12-12T13:38:42
19 Spectrometer Frequency	599.72
20 Spectral Width	8000.0
21 Lowest Frequency	-1001.2
22 Nucleus	¹ H
23 Acquired Size	15136
24 Spectral Size	32768



A-63: ¹H-NMR spectrum of (6d)₁₀

Parameter	Value
1 Data File Name	G:/10142009-12122009/CB-CONHC3H6FhVb-10mer12122009-2.fid/fid
2 Title	CB-CONHC3H6FhVb-10mer12122009-2
3 Comment	CB-CONHC3H6FhVb-10mer
4 Origin	Varian
5 Owner	
6 Site	
7 Spectrometer	inova
8 Author	
9 Solvent	CDCl ₂
10 Temperature	25.0
11 Pulse Sequence	s2pul
12 Number of Scans	72
13 Receiver Gain	44
14 Relaxation Delay	1.0000
15 Pulse Width	0.0000
16 Acquisition Time	1.8920
17 Acquisition Date	2009-12-12T13:44:10
18 Modification Date	2009-12-12T13:48:10
19 Spectrometer Frequency	599.72
20 Spectral Width	8000.0
21 Lowest Frequency	-1001.2
22 Nucleus	¹ H
23 Acquired Size	15136
24 Spectral Size	32768



A-64: ¹H-NMR spectrum of (6e)₁₀

Parameter Value
1 Data File Name G:/10142009-12122009/CBQ+2OAc-10mer12122009.fid/fid

2 Title CBQ+2OAc-10mer12122009

3 Comment CBQ+2OAc-10mer12122009

4 Origin Varian

5 Owner

6 Site inova

7 Spectrometer

8 Author

9 Solvent CD2O2

10 Temperature 25.0

11 Pulse Sequence s2pul

12 Number of Scans 48

13 Receiver Gain 44

14 Relaxation Delay 1.0000

15 Pulse Width 0.0000

16 Acquisition Time 1.8920

17 Acquisition Date 2009-12-12T11:57:18

18 Modification Date 2009-12-12T12:01:28

19 Spectrometer Frequency 599.72

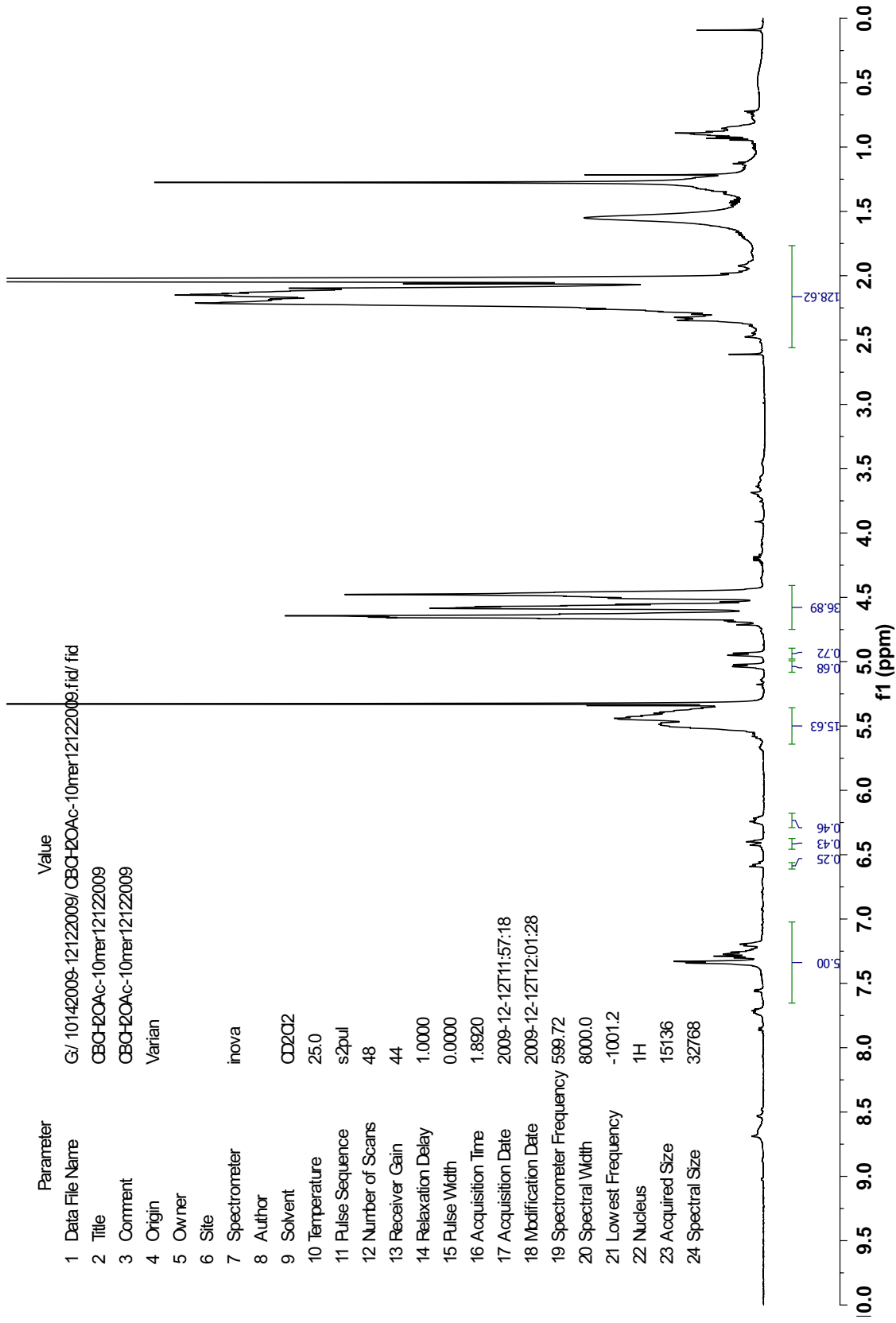
20 Spectral Width 8000.0

21 Lowest Frequency -1001.2

22 Nucleus 1H

23 Acquired Size 15136

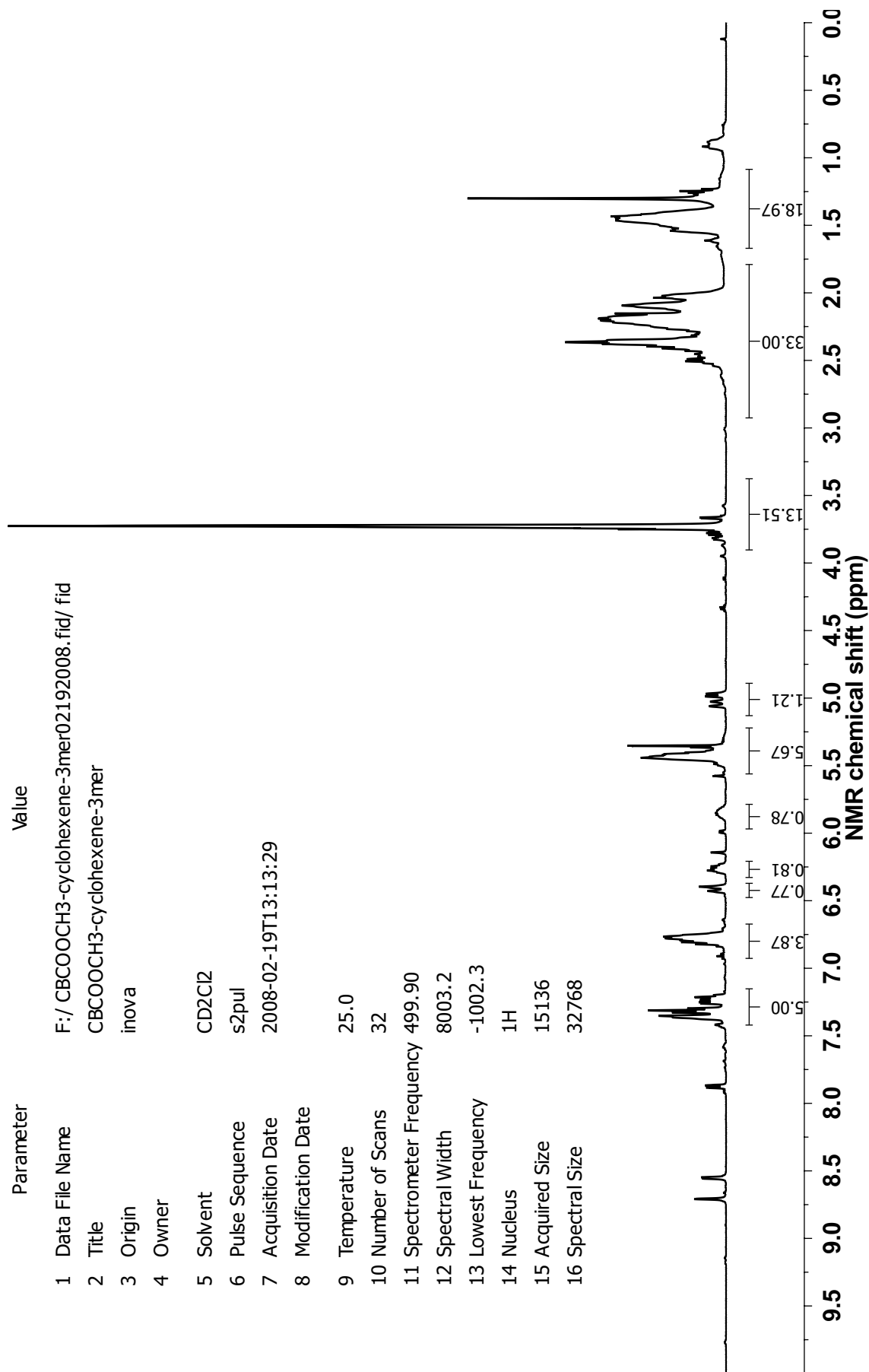
24 Spectral Size 32768



A-65: ¹H-NMR spectrum of (9a)₁₀

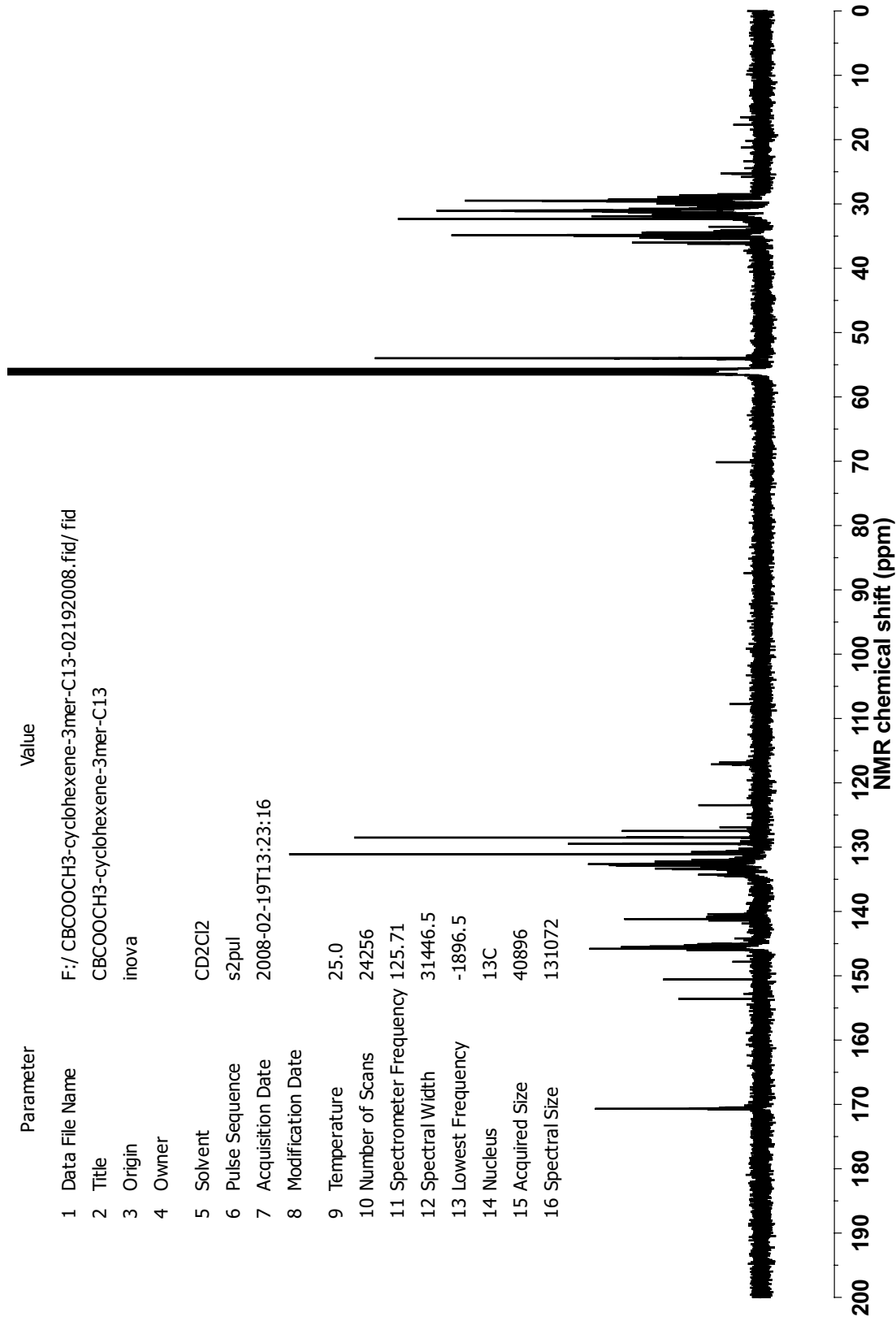
Parameter Value

1 Data File Name F:/ CBCOOCH3-cyclohexene-3mer02192008.fid/ fid
2 Title CBCOOCH3-cyclohexene-3mer
3 Origin inova
4 Owner
5 Solvent CD2Cl2
6 Pulse Sequence s2pul
7 Acquisition Date 2008-02-19T13:13:29
8 Modification Date
9 Temperature 25.0
10 Number of Scans 32
11 Spectrometer Frequency 499.90
12 Spectral Width 8003.2
13 Lowest Frequency -1002.3
14 Nucleus ¹H
15 Acquired Size 15136
16 Spectral Size 32768



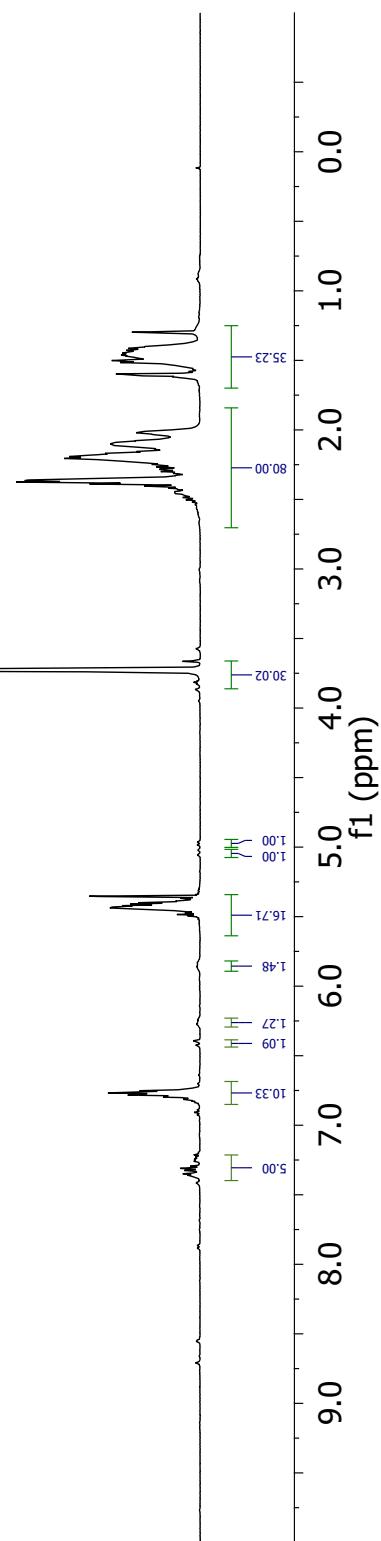
A-66: ¹H-NMR spectrum of (8a-20a)₃

Parameter	Value
1 Data File Name	F:/ CBCOOCH3-cyclohexene-3mer-C13-02192008.fid/ fid
2 Title	CBCOOCH3-cyclohexene-3mer-C13
3 Origin	inova
4 Owner	
5 Solvent	CD2Cl2
6 Pulse Sequence	s2pul
7 Acquisition Date	2008-02-19T13:23:16
8 Modification Date	
9 Temperature	25.0
10 Number of Scans	24256
11 Spectrometer Frequency	125.71
12 Spectral Width	31446.5
13 Lowest Frequency	-1896.5
14 Nucleus	13C
15 Acquired Size	40896
16 Spectral Size	131072



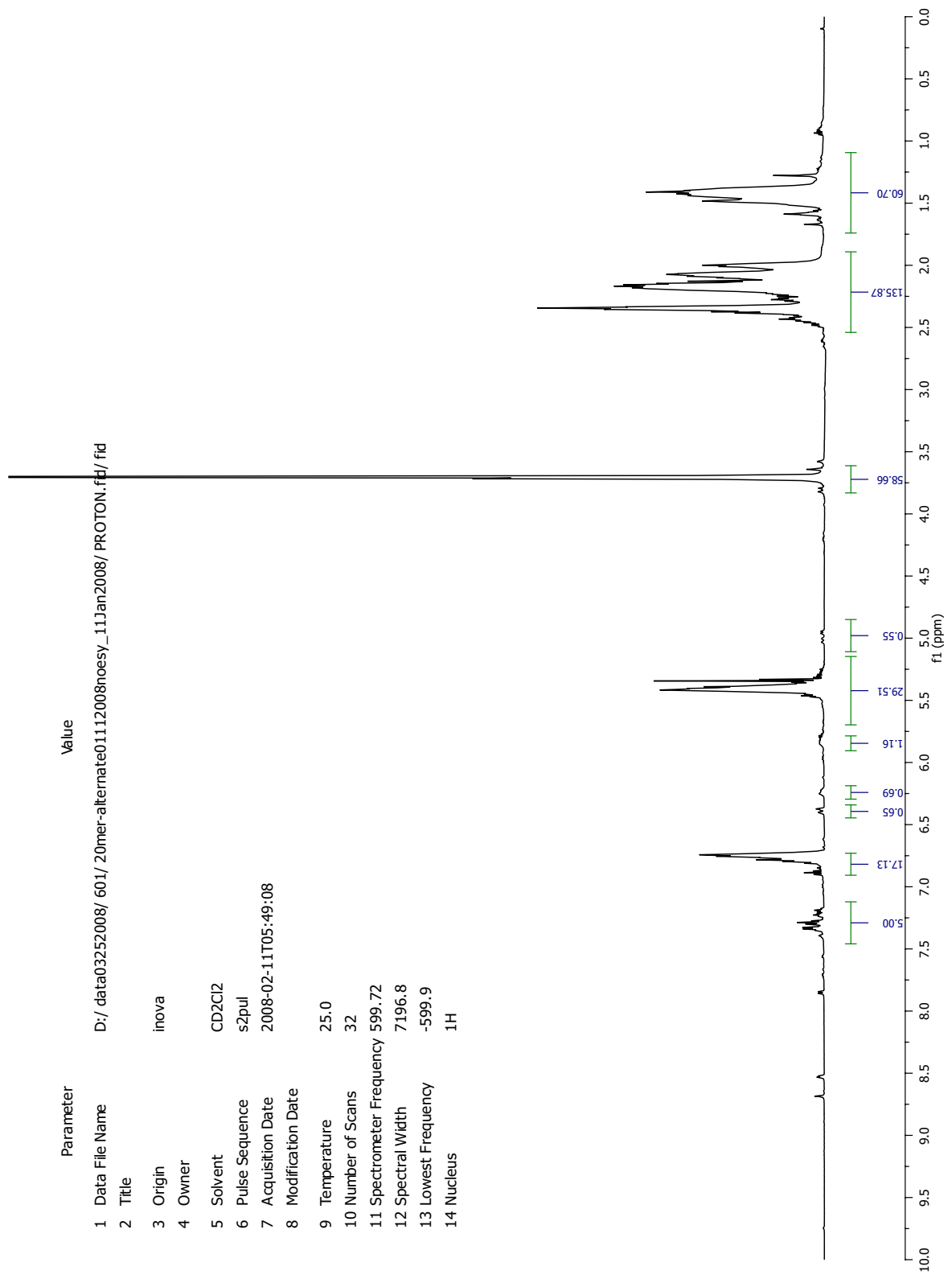
A-67: ¹³C-NMR spectrum of (8a-20a)₃

Parameter	Value
1 Data File Name	L:/ data03252008/ 500mhz/ 20mer-alternate01172008_a/ 10mer.fid/ fid
2 Title	10mer in CD2Cl21D DPFGE NOESY01/ 17/ 2008
3 Origin	inova
4 Owner	
5 Solvent	CD2Cl2
6 Pulse Sequence	s2pul
7 Acquisition Date	2008-02-17T10:46:44
8 Modification Date	
9 Temperature	25.0
10 Number of Scans	16
11 Spectrometer Frequency	499.90
12 Spectral Width	5497.5
13 Lowest Frequency	-499.2
14 Nucleus	¹ H
15 Acquired Size	16384
16 Spectral Size	32768



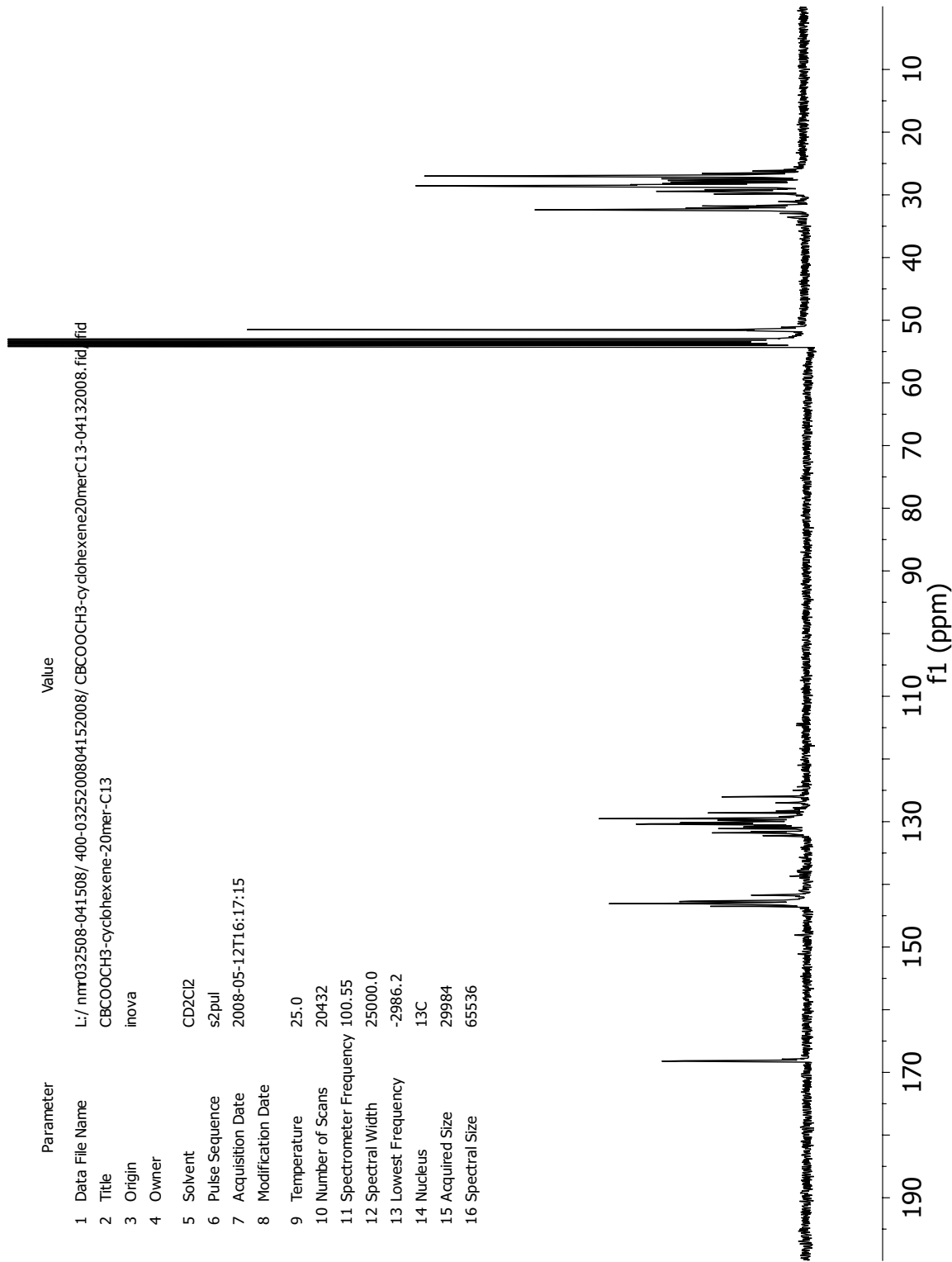
A-68: ¹H-NMR spectrum of (8a-20a)₁₀

Parameter	Value
1 Data File Name	D:/ data03252008/ 601/ 20mer-alternate01112008noesy_11Jan2008/ PROTON.fid/ fid
2 Title	
3 Origin	inova
4 Owner	
5 Solvent	CD2Cl2
6 Pulse Sequence	s2pul
7 Acquisition Date	2008-02-11T05:49:08
8 Modification Date	
9 Temperature	25.0
10 Number of Scans	32
11 Spectrometer Frequency	599.72
12 Spectral Width	7196.8
13 Lowest Frequency	-599.9
14 Nucleus	¹ H

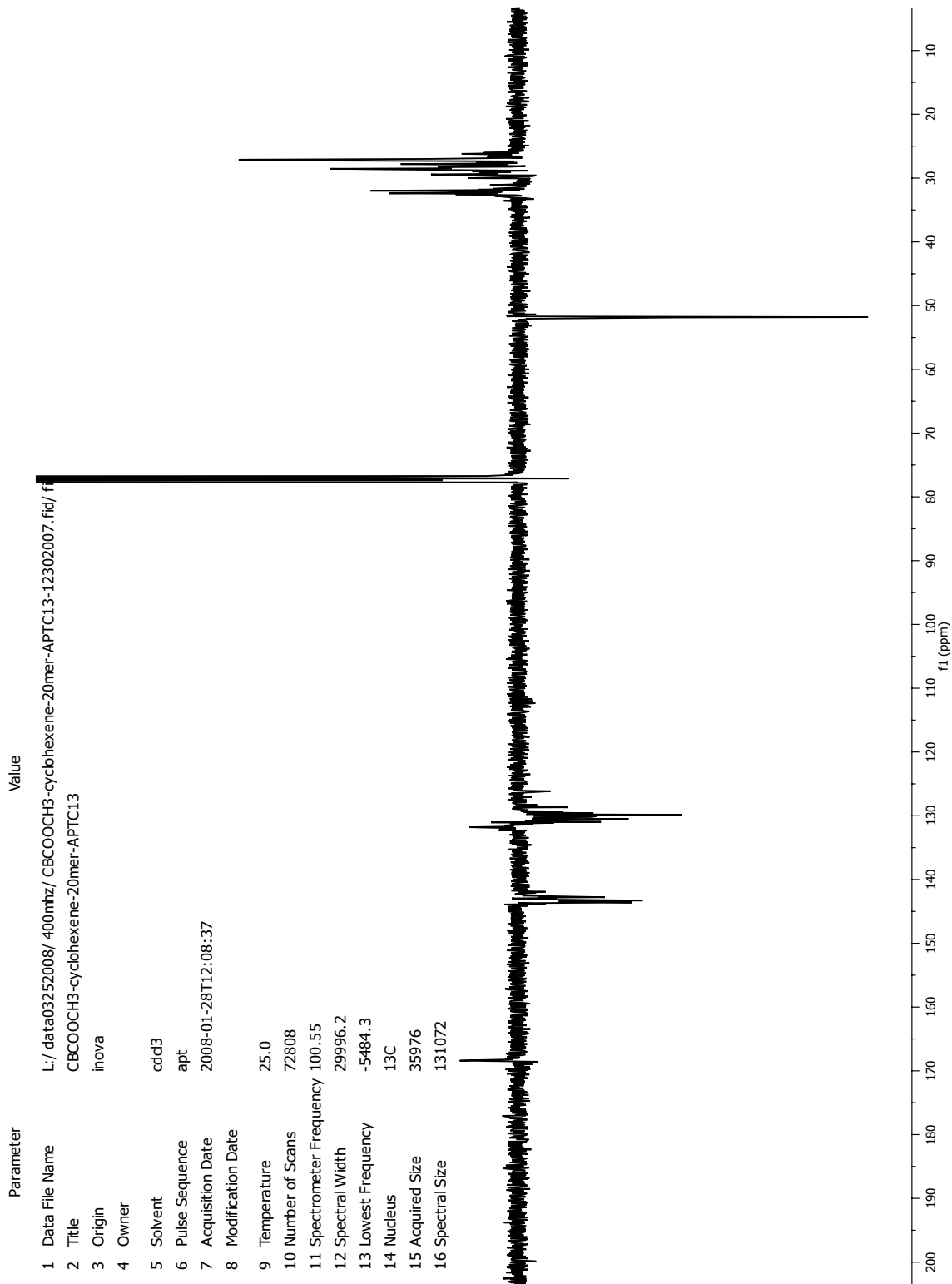


A-69: ¹H-NMR spectrum of (8a-20a)₂₀

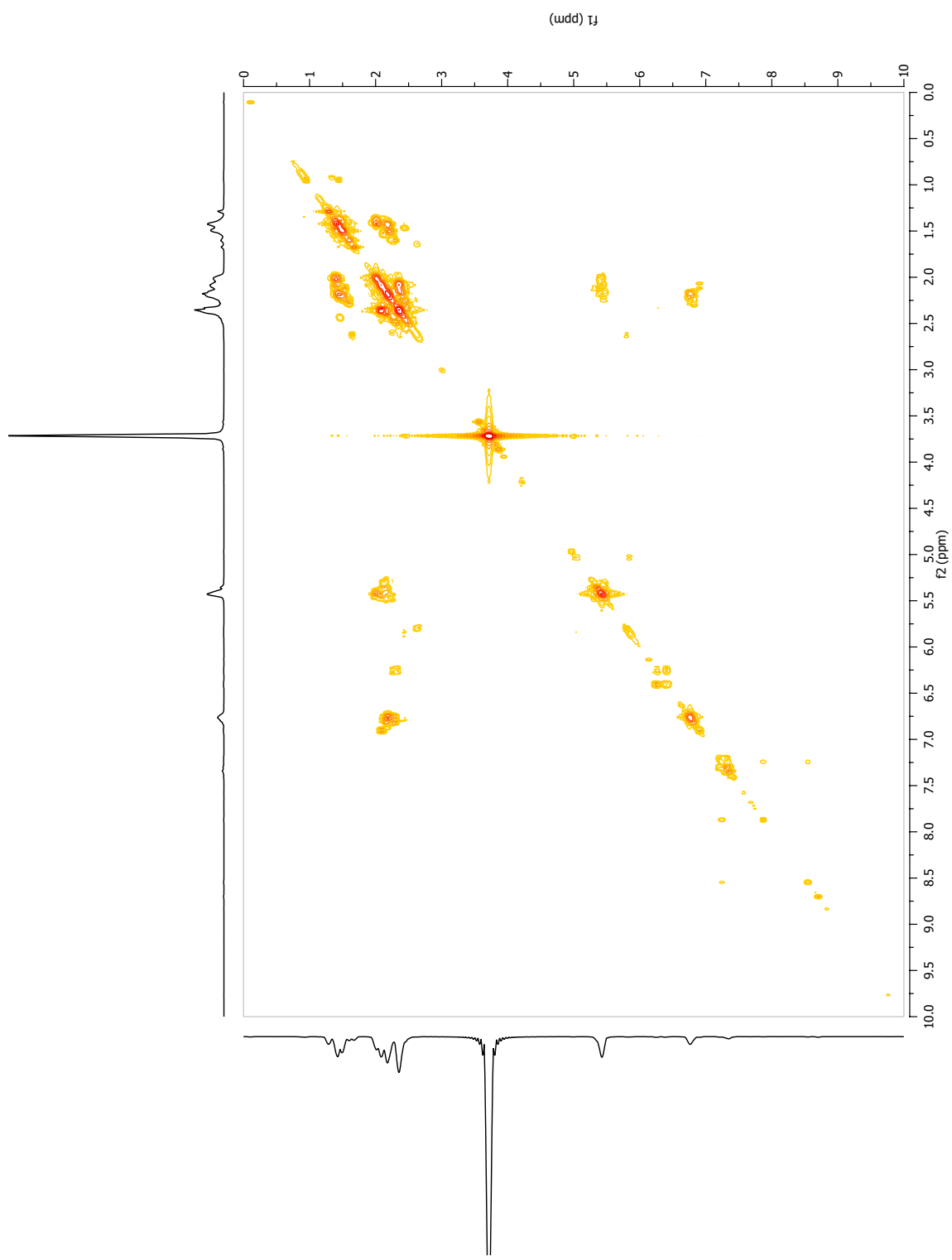
Parameter	Value
1 Data File Name	L:/nmr032508-041508/400-0325200804152008/CBCOOCH3-cyclohexene20merC13-04132008.fid
2 Title	CBCOOCH3-cyclohexene-20mer-C13
3 Origin	inova
4 Owner	
5 Solvent	CD2Cl2
6 Pulse Sequence	s2pul
7 Acquisition Date	2008-05-12T16:17:15
8 Modification Date	
9 Temperature	25.0
10 Number of Scans	20432
11 Spectrometer Frequency	100.55
12 Spectral Width	25000.0
13 Lowest Frequency	-2986.2
14 Nucleus	¹³ C
15 Acquired Size	29984
16 Spectral Size	65536



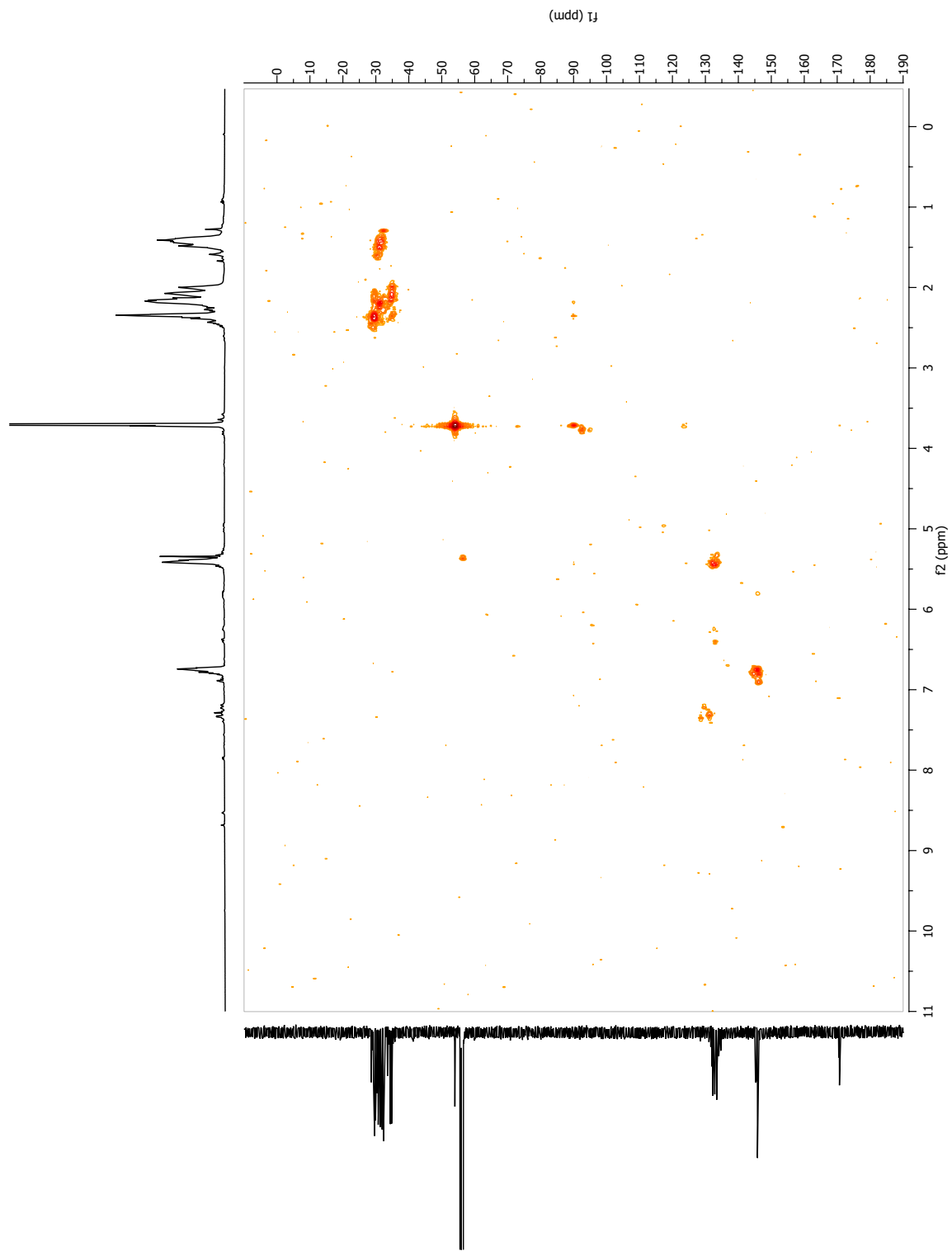
A-70: ¹³C-NMR spectrum of (8a-20a)₂₀



A-71: ¹³C-APT-NMR spectrum of (8a-20a)₂₀

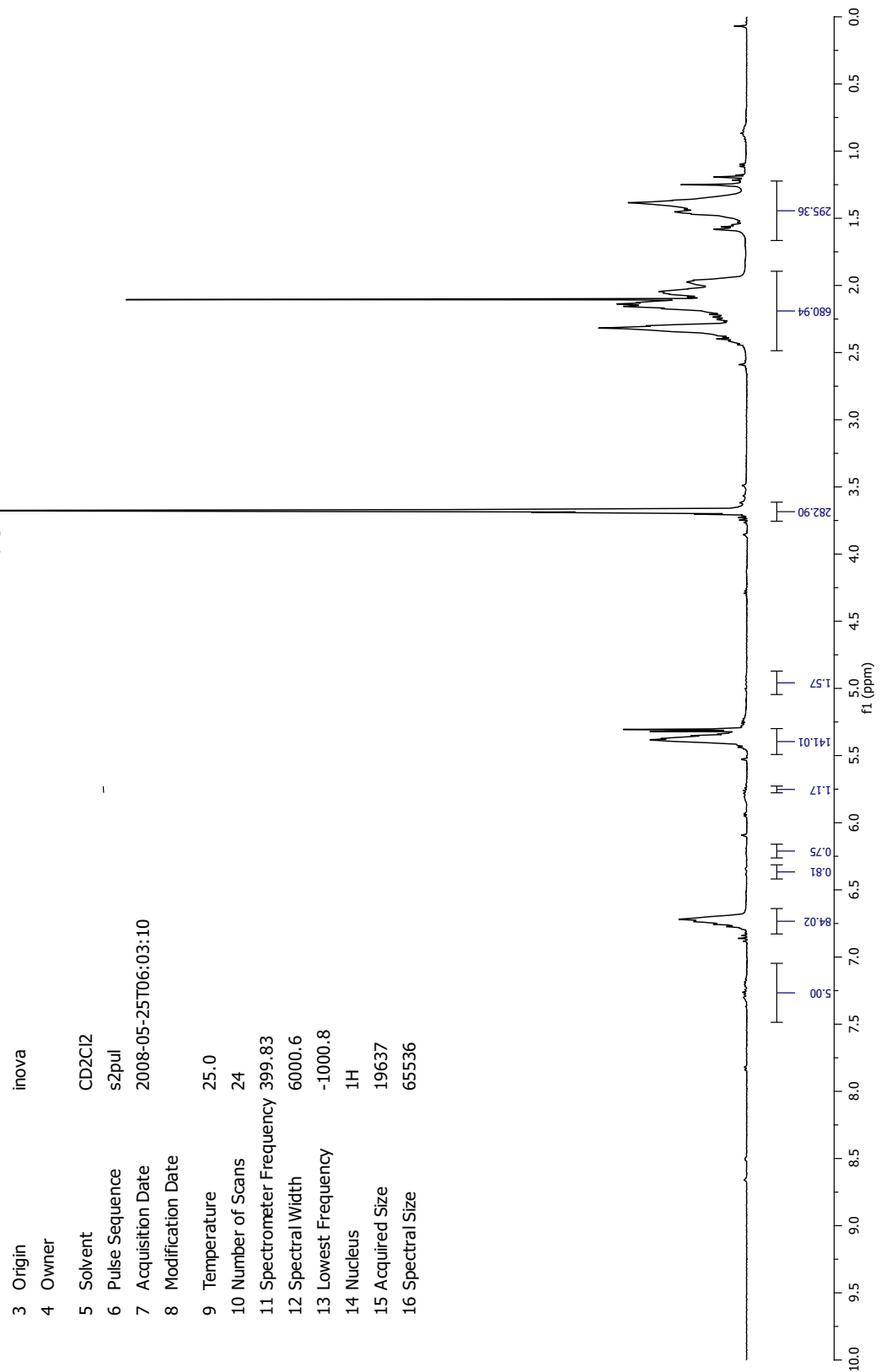


A72: ¹H-gCOSY NMR spectrum of (8a-20a)₂₀



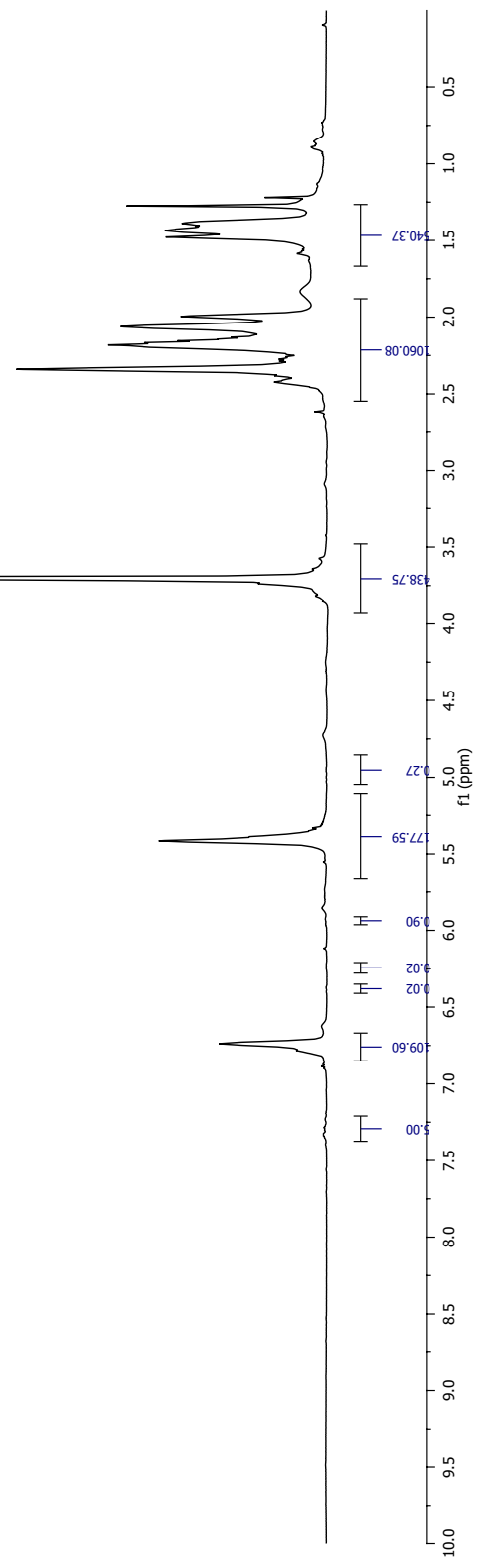
A73: ^1H - ^{13}C -HMQC-NMR spectrum of (8a-20a)₂₀

Parameter	Value
1 Data File Name	L:/nmr04162008-07012008/CBCOCH3-cyclohexene-50mer04242008.fid/ fid
2 Title	STATE UNIVERSITY OF NEW YORKKINOVA 400 Mhz SN# S011617ASWpfg PROBE SN# P0051331H SENSITIVITY0.1% ETHYLBENZENE
3 Origin	inova
4 Owner	
5 Solvent	CD2Cl2
6 Pulse Sequence	s2pul
7 Acquisition Date	2008-05-25T06:03:10
8 Modification Date	
9 Temperature	25.0
10 Number of Scans	24
11 Spectrometer Frequency	399.83
12 Spectral Width	6000.6
13 Lowest Frequency	-1000.8
14 Nucleus	¹ H
15 Acquired Size	19637
16 Spectral Size	65536



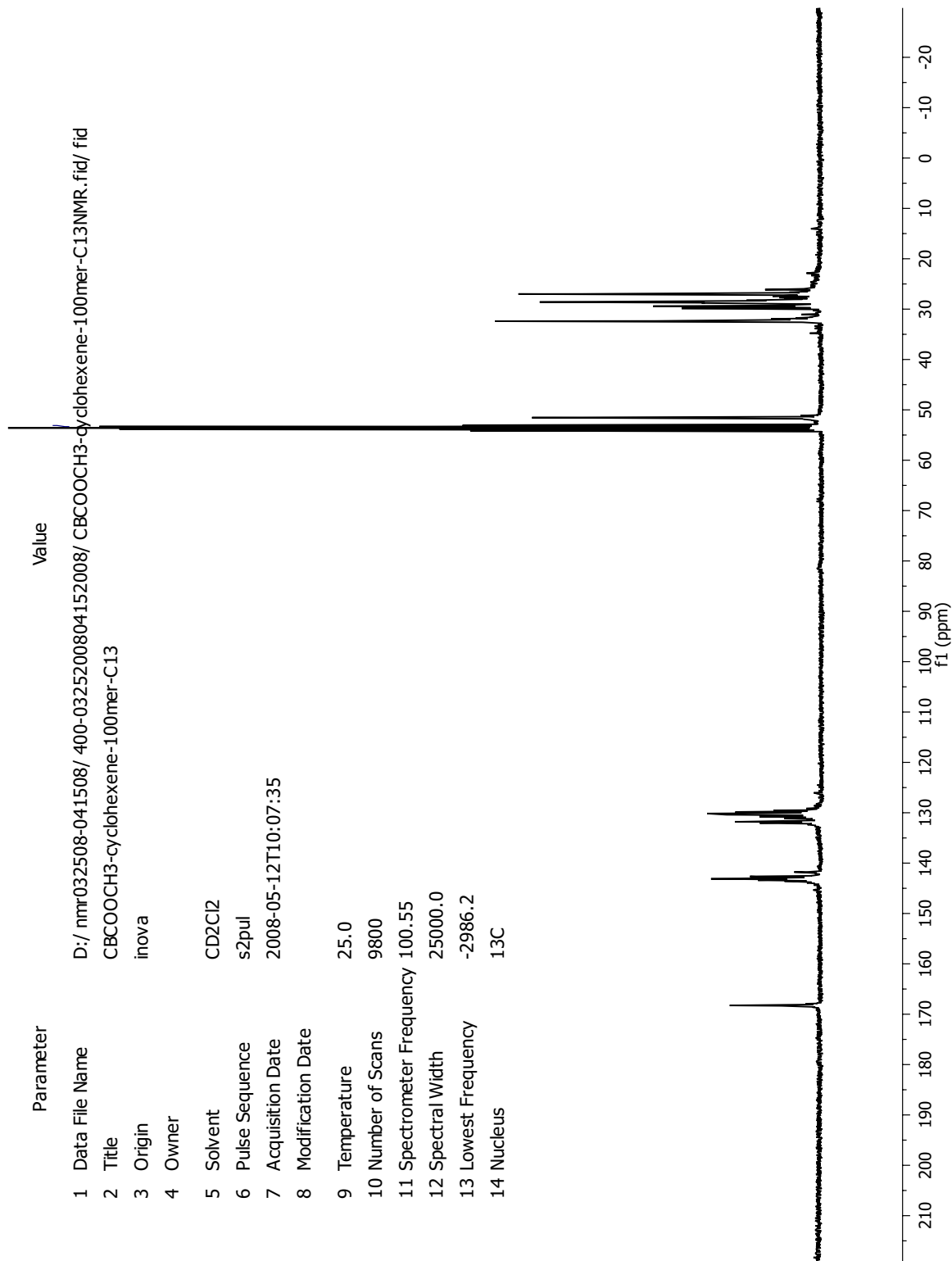
A-74: ¹H-NMR spectrum of (8a-20a)₅₀

Parameter	Value
1 Data File Name	J:/ flash-backup/ nmr032508-041508/ 600-0325200804152008/ CBCOOCCH3-cyclohexene-100mer04122008.fid/ fid
2 Title	STANDARD PROTON PARAMETERS
3 Origin	inova
4 Owner	
5 Solvent	CD2Cl2
6 Pulse Sequence	s2pul
7 Acquisition Date	2008-05-12T11:07:10
8 Modification Date	
9 Temperature	25.0
10 Number of Scans	16
11 Spectrometer Frequency	599.72
12 Spectral Width	8000.0
13 Lowest Frequency	-1001.2
14 Nucleus	¹ H
15 Acquired Size	15136
16 Spectral Size	32768



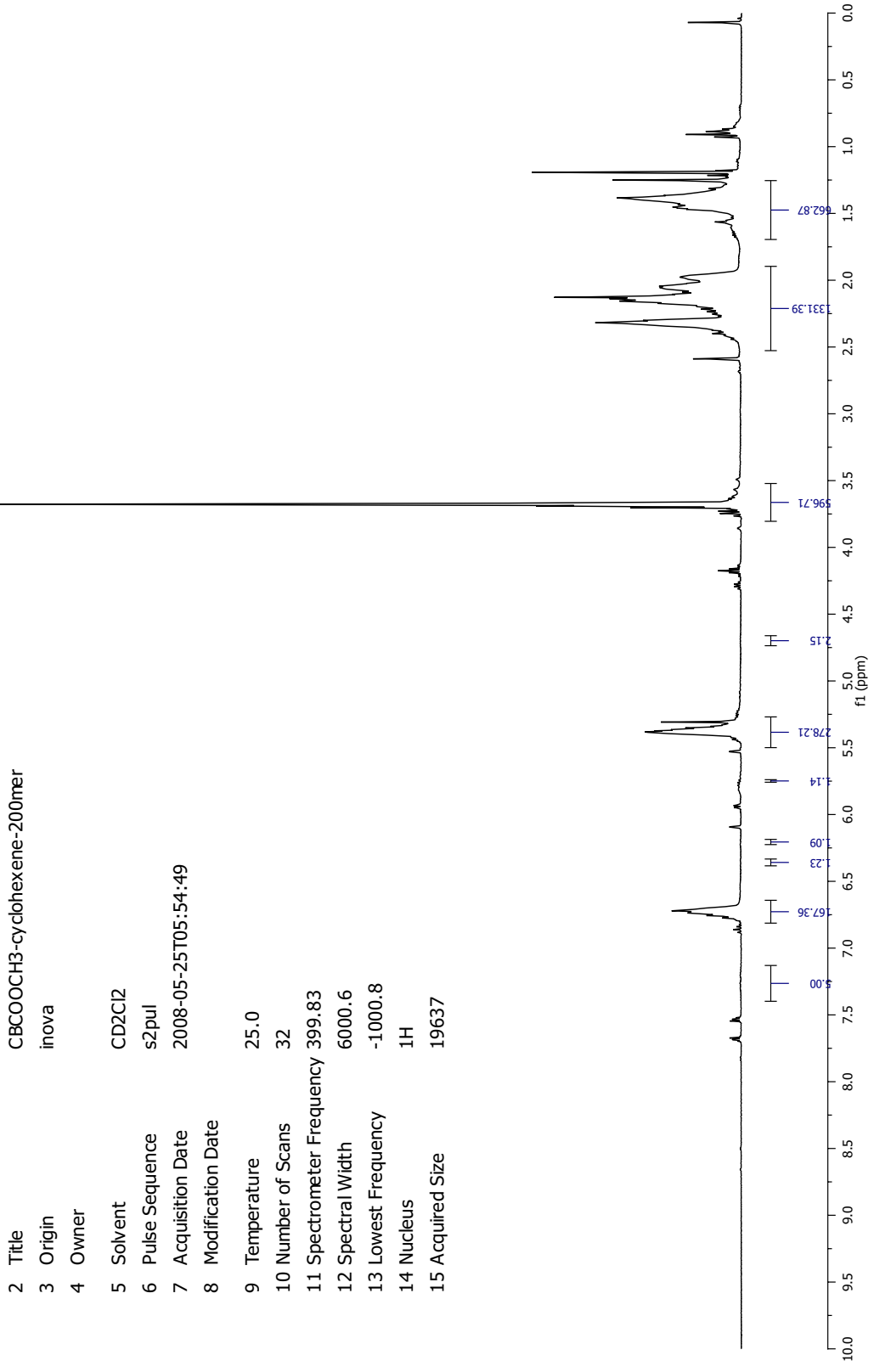
A-75: ¹H-NMR spectrum of (8a-20a)₁₀₀

Parameter	Value
1 Data File Name	D:/nmr032508-041508/400-0325200804152008/CBCOOCH3-cyclohexene-100mer-C13NMR.fid/ fid
2 Title	CBCOOCH3-cyclohexene-100mer-C13
3 Origin	inova
4 Owner	
5 Solvent	CD2Cl2
6 Pulse Sequence	s2pul
7 Acquisition Date	2008-05-12T10:07:35
8 Modification Date	
9 Temperature	25.0
10 Number of Scans	9800
11 Spectrometer Frequency	100.55
12 Spectral Width	25000.0
13 Lowest Frequency	-2986.2
14 Nucleus	¹³ C



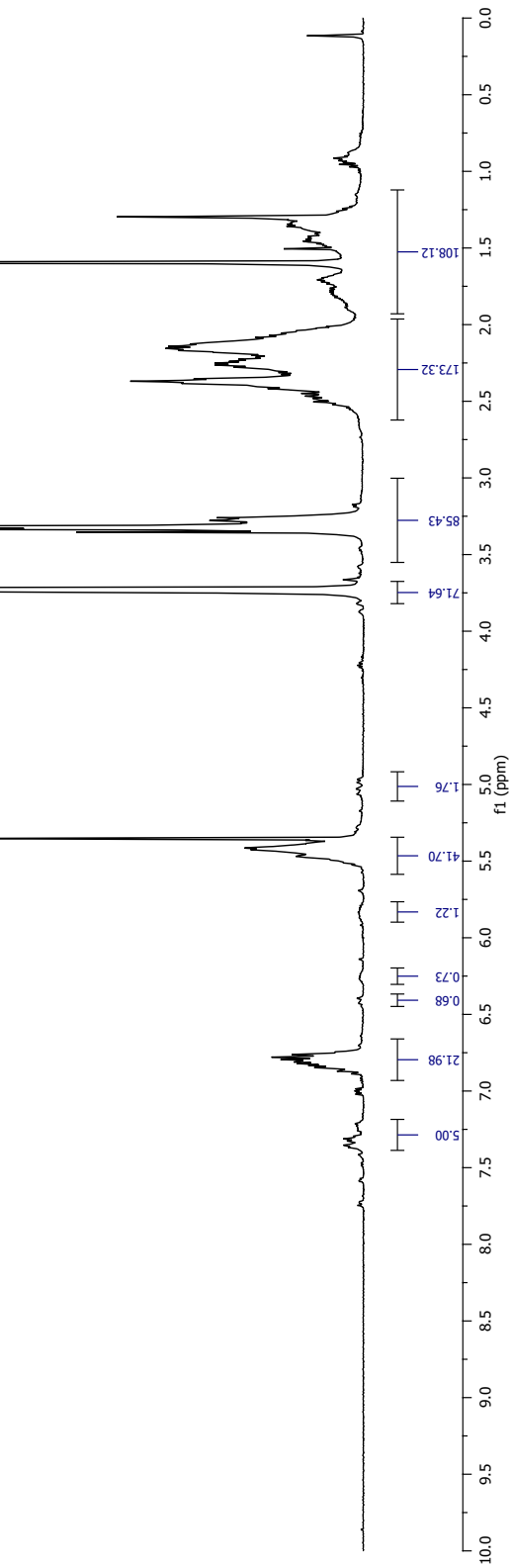
A-76: ¹³C-NMR spectrum of (8a-20a)₁₀₀

Parameter	Value
1 Data File Name	L:/nmr04162008-07012008/CBCOOCH3-cyclohexene-200mer.fid/
2 Title	CBCOOCH3-cyclohexene-200mer
3 Origin	inova
4 Owner	
5 Solvent	CD2Cl2
6 Pulse Sequence	s2pul
7 Acquisition Date	2008-05-25T05:54:49
8 Modification Date	
9 Temperature	25.0
10 Number of Scans	32
11 Spectrometer Frequency	399.83
12 Spectral Width	6000.6
13 Lowest Frequency	-1000.8
14 Nucleus	1H
15 Acquired Size	19637



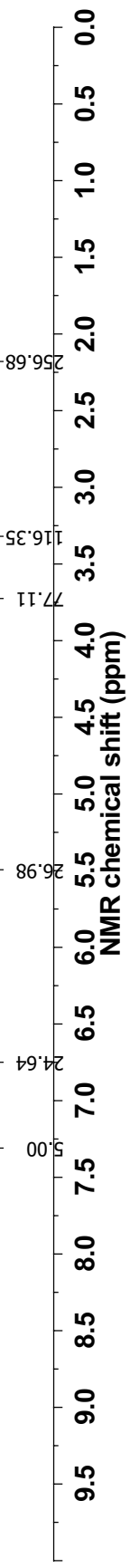
A-77: ¹H-NMR spectrum of (8a-20a)₂₀₀

Parameter	Value
1 Data File Name	L:/ nmr04162008-07012008/ CBCOOCH3-4-cyclohexenemethyl ether20mer06222008.fid/ fid
2 Title	CBCOOCH3-4-cyclohexenemethyl ether20mer
3 Origin	inova
4 Owner	
5 Solvent	CD2Cl2
6 Pulse Sequence	s2pul
7 Acquisition Date	2008-07-23T11:26:02
8 Modification Date	
9 Temperature	25.0
10 Number of Scans	56
11 Spectrometer Frequency	499.90
12 Spectral Width	8003.2
13 Lowest Frequency	-1002.3
14 Nucleus	¹ H
15 Acquired Size	15136
16 Spectral Size	32768

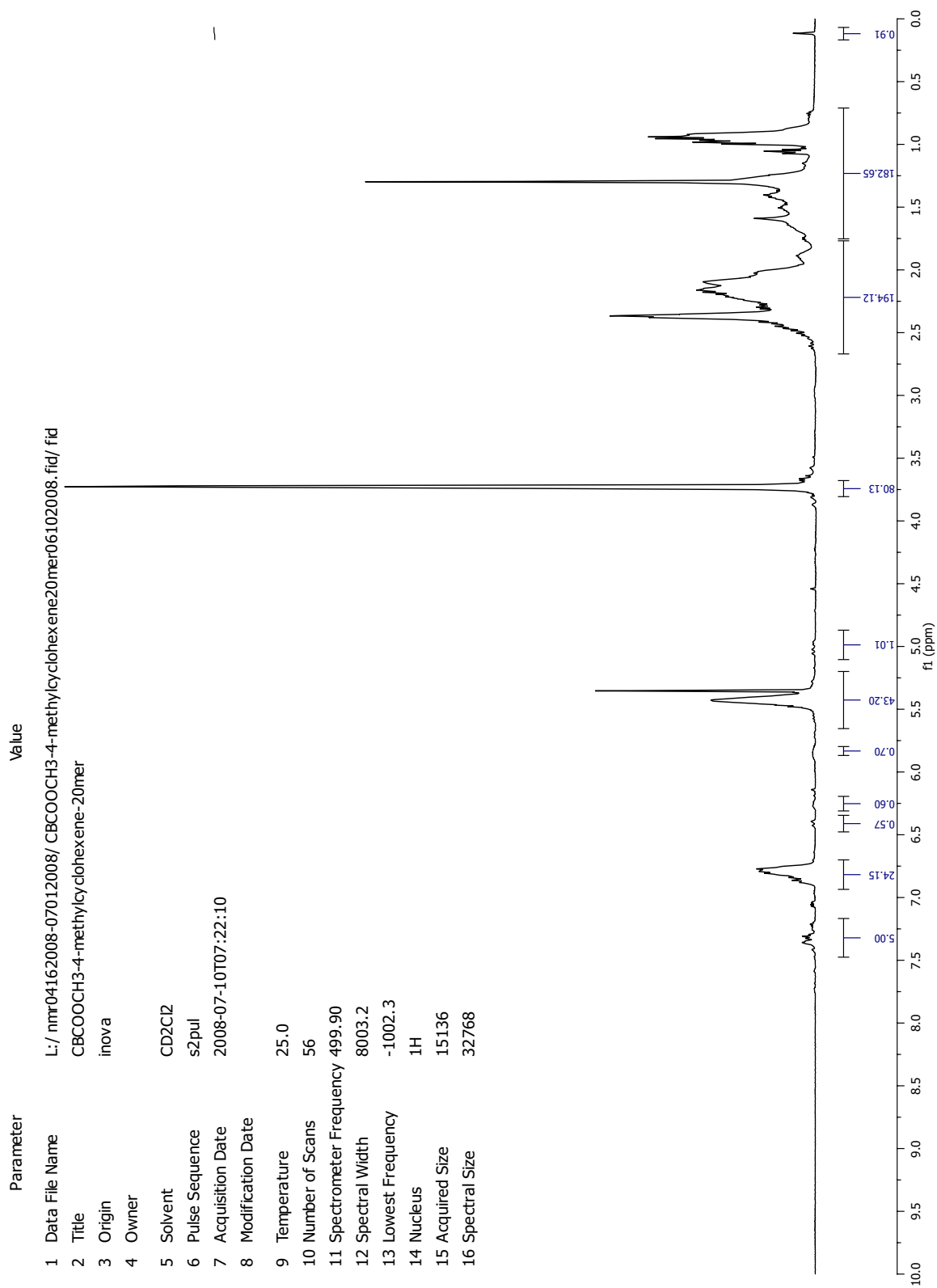


A-78: ¹H-NMR spectrum of (8a-20d)₂₀

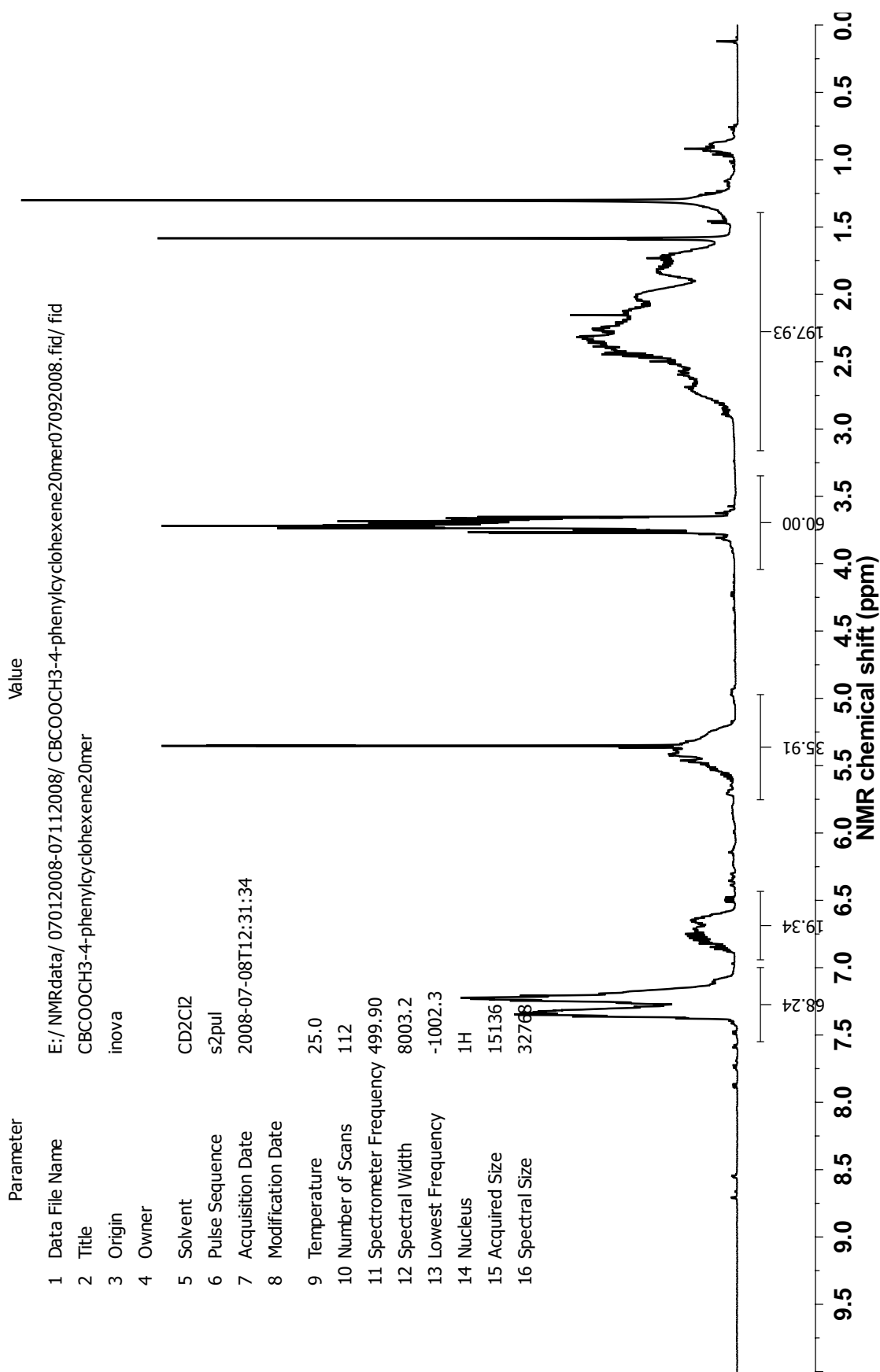
Parameter	Value
1 Data File Name	E:/ NMRdata/ nmr04162008-07012008/ CBCOOCH3-cyclohexenedimethylether20mer-2-05072008.fid/ fid
2 Title	CBCOOCH3-cyclohexenedimethylether20mer
3 Origin	inova
4 Owner	
5 Solvent	CD2Cl2
6 Pulse Sequence	s2pul
7 Acquisition Date	2008-05-07T11:25:18
8 Modification Date	
9 Temperature	25.0
10 Number of Scans	80
11 Spectrometer Frequency	499.90
12 Spectral Width	8003.2
13 Lowest Frequency	-1002.3
14 Nucleus	¹ H
15 Acquired Size	15136
16 Spectral Size	32768



A-79: ¹H-NMR spectrum of (8a-20e)₂₀



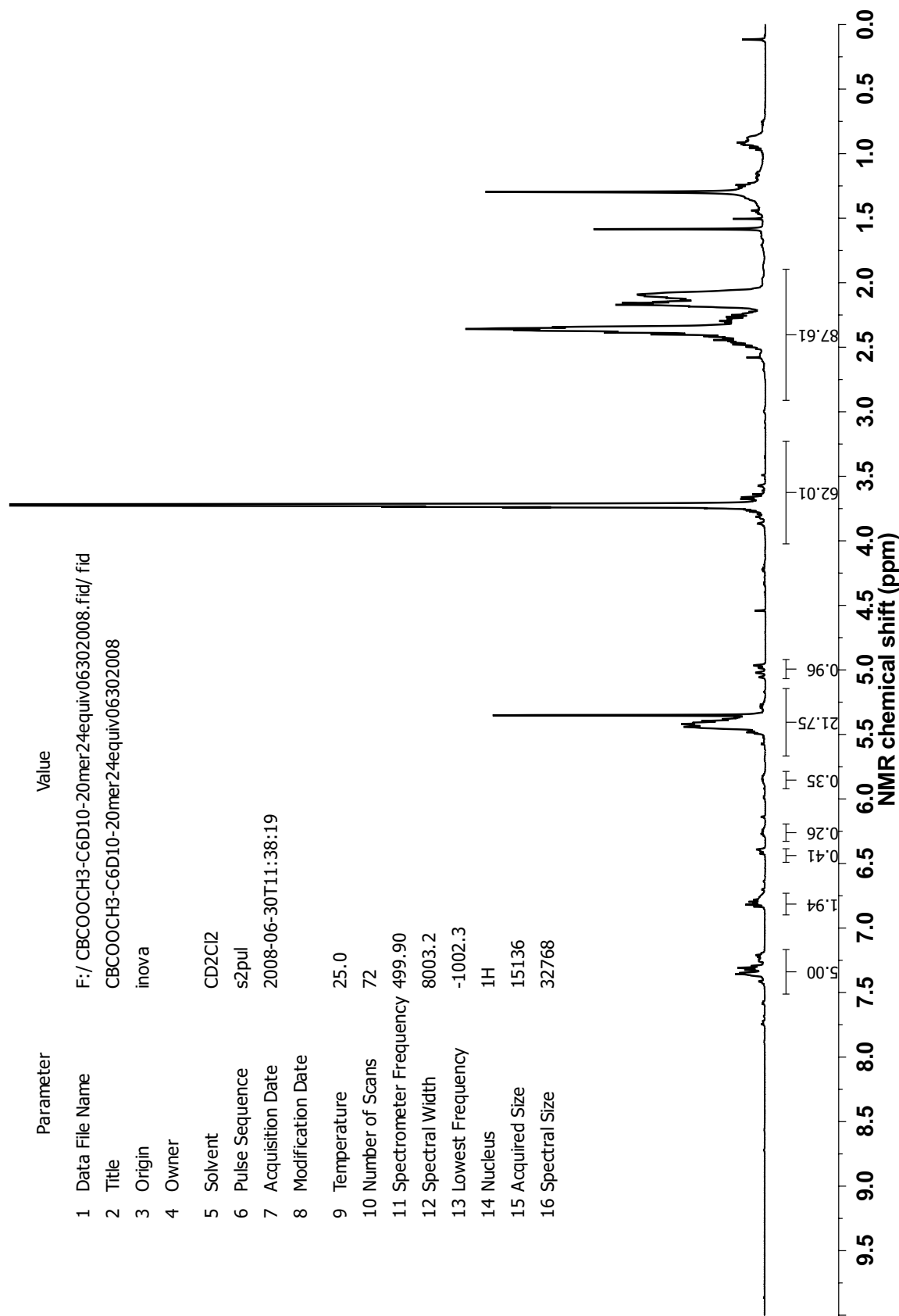
A-80: ¹H-NMR spectrum of (8a-20i)₂₀



A-81: ¹H-NMR spectrum of (8a-20j)₂₀

Parameter Value

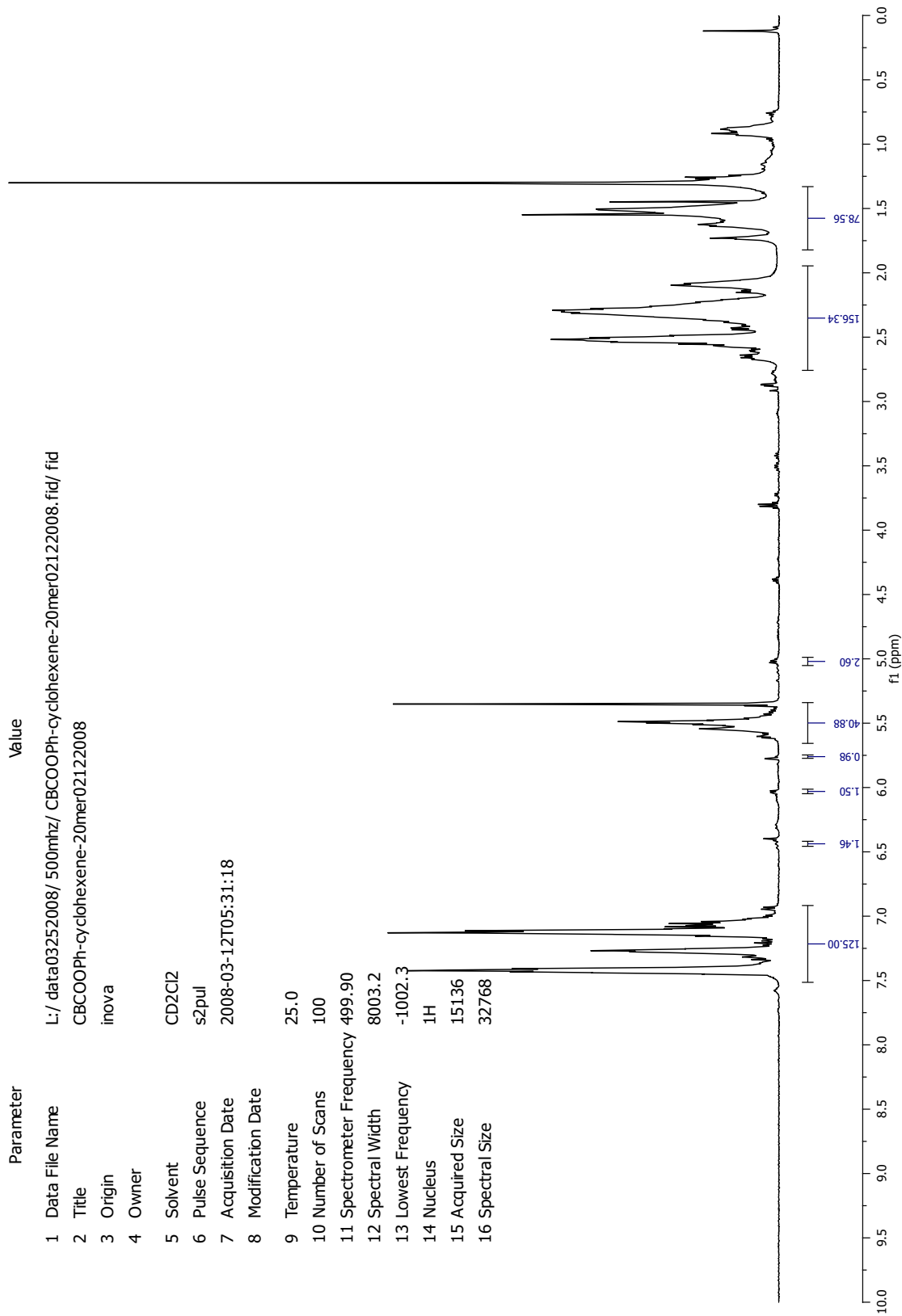
1 Data File Name F:/ CBCOOCH3-C6D10-20mer24equiv06302008.fid/ fid
2 Title CBCOOCH3-C6D10-20mer24equiv06302008
3 Origin inova
4 Owner
5 Solvent CD2Cl2
6 Pulse Sequence s2pul
7 Acquisition Date 2008-06-30T11:38:19
8 Modification Date
9 Temperature 25.0
10 Number of Scans 72
11 Spectrometer Frequency 499.90
12 Spectral Width 8003.2
13 Lowest Frequency -1002.3
14 Nucleus ¹H
15 Acquired Size 15136
16 Spectral Size 32768



A-82: ¹H-NMR spectrum of (8a-20a-D10)₂₀

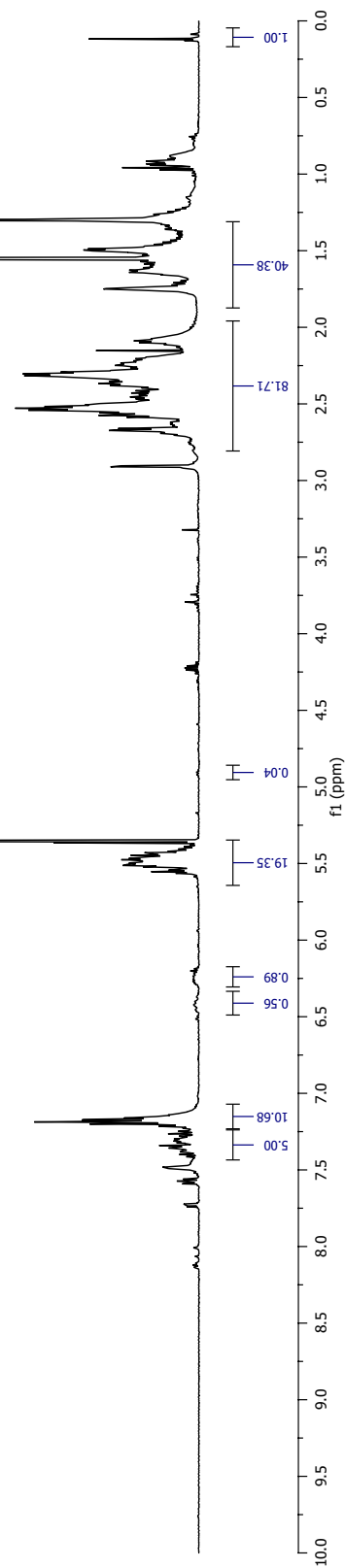
Parameter Value

1 Data File Name L:/ data03252008/ 500mhz/ CBCOOPh-cyclohexene-20mer02122008.fid/ fid
2 Title CBCOOPh-cyclohexene-20mer02122008
3 Origin inova
4 Owner
5 Solvent CD2Cl2
6 Pulse Sequence s2pul
7 Acquisition Date 2008-03-12T05:31:18
8 Modification Date
9 Temperature 25.0
10 Number of Scans 100
11 Spectrometer Frequency 499.90
12 Spectral Width 8003.2
13 Lowest Frequency -1002.3
14 Nucleus ¹H
15 Acquired Size 15136
16 Spectral Size 32768



A-83: ¹H-NMR spectrum of (8c-20a)₂₀

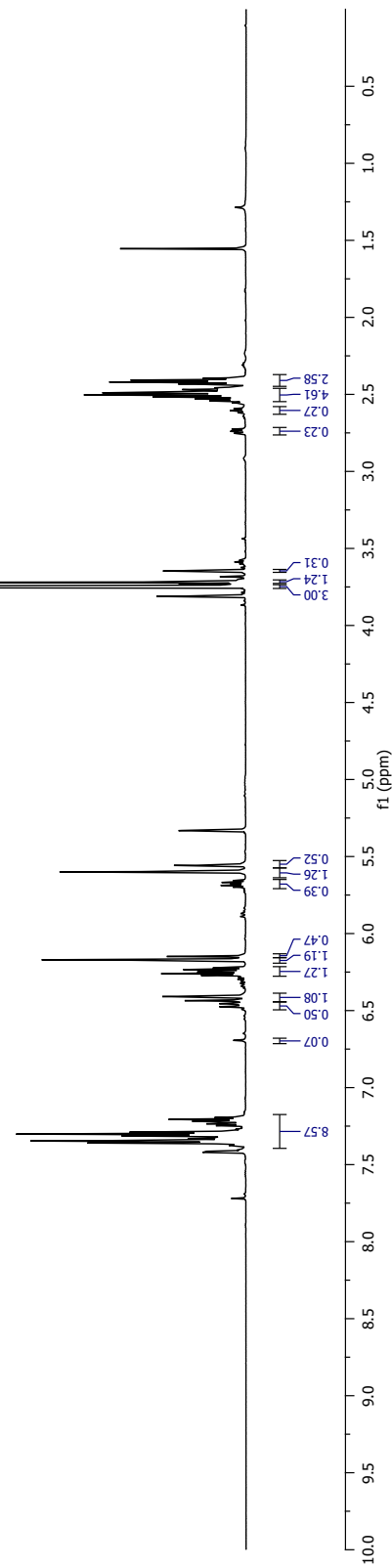
Parameter	Value
1 Data File Name	L:/ nmr04162008-07012008/ CBCOOPFP-cyclohexene10mer05062008.fid/ fid
2 Title	CBCOOPFP-cyclohexene10mer
3 Origin	inova
4 Owner	
5 Solvent	CD2Cl2
6 Pulse Sequence	s2pul
7 Acquisition Date	2008-06-06T12:43:51
8 Modification Date	
9 Temperature	25.0
10 Number of Scans	88
11 Spectrometer Frequency	499.90
12 Spectral Width	8003.2
13 Lowest Frequency	-1002.3
14 Nucleus	¹ H
15 Acquired Size	15136
16 Spectral Size	32768



A84: ¹H-NMR spectrum of (8d-20a)₁₀

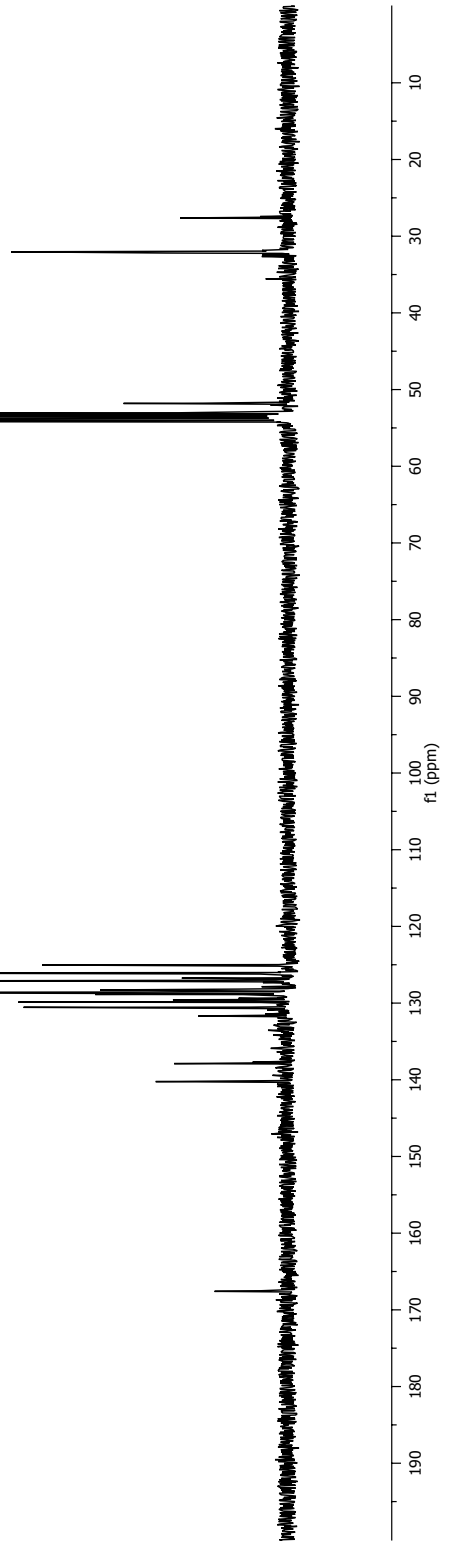
Parameter Value

1 Data File Name L:/07012008-07112008/CBCOOCH3-1mer07112008.fid/ fid
2 Title CBCOOCH3-1mer07112008
3 Origin inova
4 Owner
5 Solvent CD2Cl2
6 Pulse Sequence s2pul
7 Acquisition Date 2008-08-11T07:20:11
8 Modification Date
9 Temperature 25.0
10 Number of Scans 24
11 Spectrometer Frequency 599.72
12 Spectral Width 8000.0
13 Lowest Frequency -1001.2
14 Nucleus ¹H
15 Acquired Size 15136
16 Spectral Size 32768



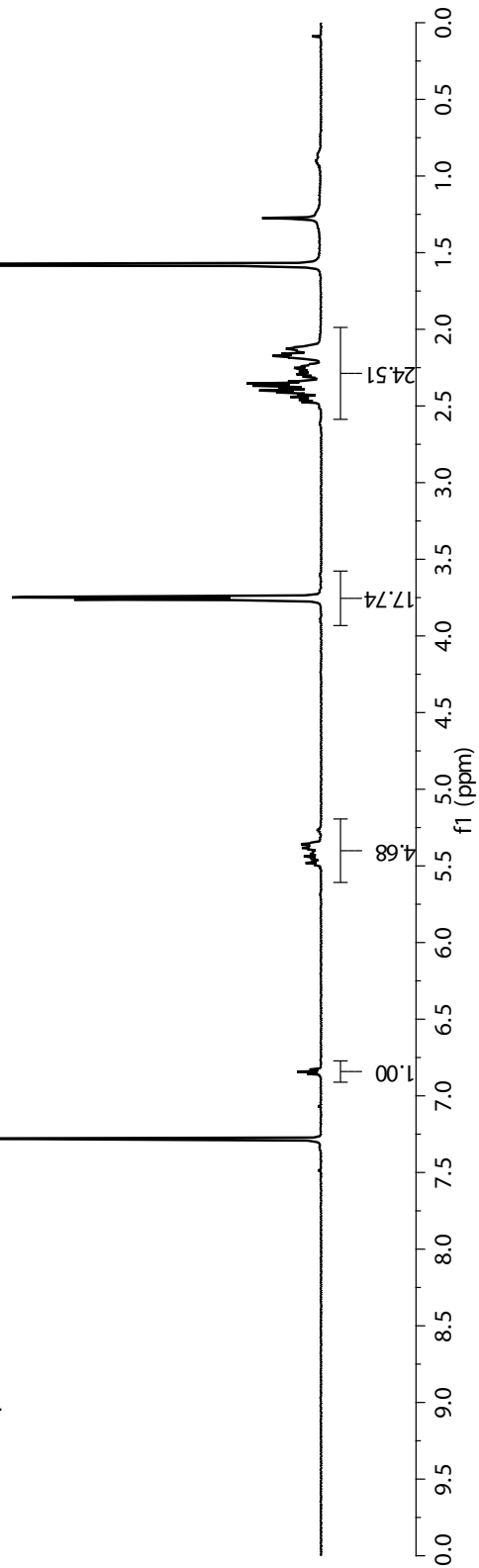
A-85: ¹H-NMR spectrum of (8a)₁

Parameter	Value
1 Data File Name	F:/ 07012008-07112008/ CBCOOCH3-1merC13-07112008.fid/ fid
2 Title	CBCOOCH3-1merC13-07112008
3 Origin	inova
4 Owner	
5 Solvent	CD2Cl2
6 Pulse Sequence	s2pul
7 Acquisition Date	2008-08-11T07:22:49
8 Modification Date	
9 Temperature	25.0
10 Number of Scans	1760
11 Spectrometer Frequency	100.55
12 Spectral Width	25000.0
13 Lowest Frequency	-2986.2
14 Nucleus	¹³ C
15 Acquired Size	29984
16 Spectral Size	65536

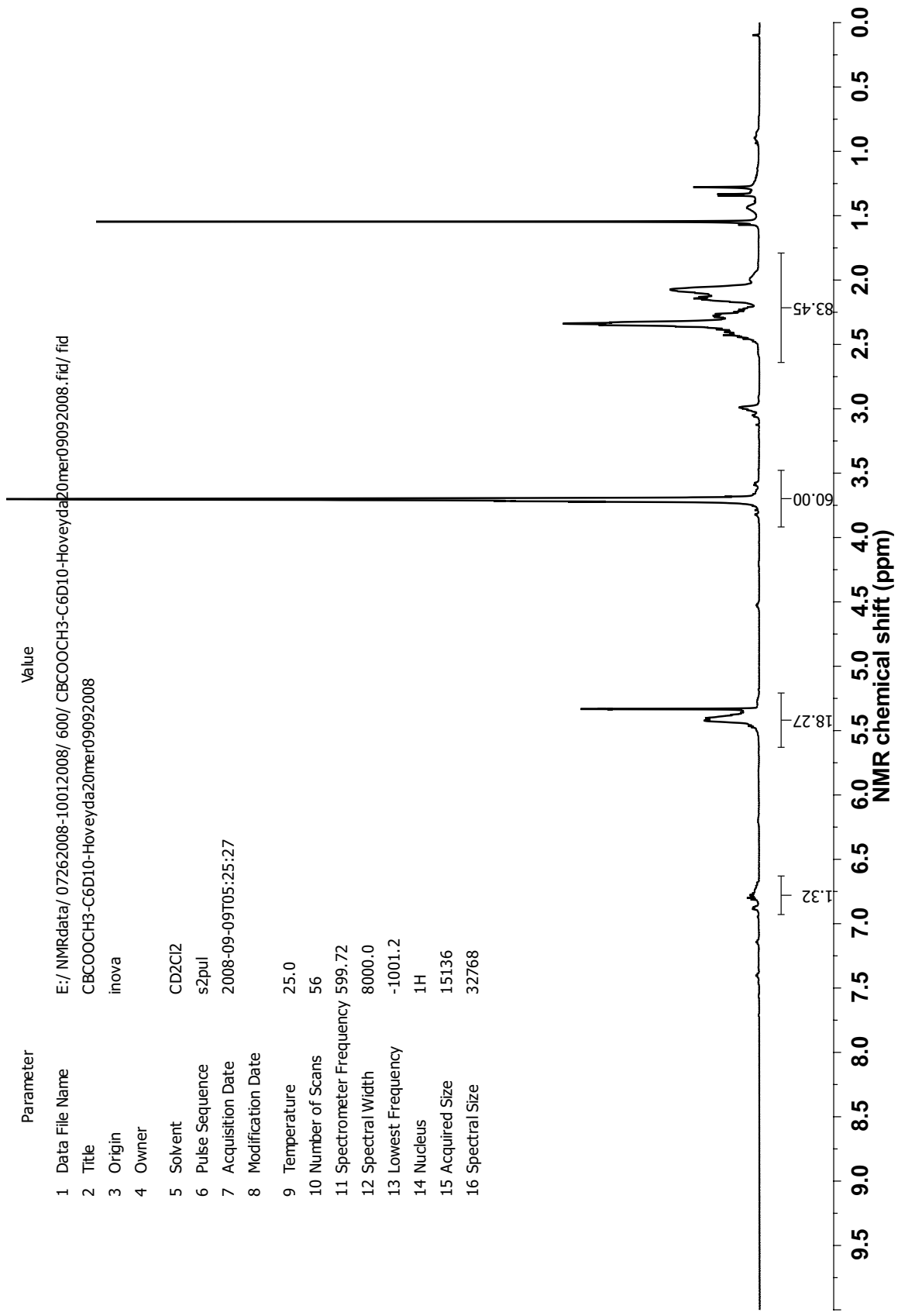


A-86: ¹³C-NMR spectrum of (8a)₁

Parameter	Value
1 Data File Name	F:/07262008-10012008/500/CBCOCH3-C6D10-benzoquinone20merA1-09032008.fid/ fid
2 Title	STANDARD PROTON PARAMETERS
3 Origin	inova
4 Owner	
5 Solvent	CDCl3
6 Pulse Sequence	s2pul
7 Acquisition Date	2008-10-03T05:39:42
8 Modification Date	
9 Temperature	25.0
10 Number of Scans	136
11 Spectrometer Frequency	499.90
12 Spectral Width	8003.2
13 Lowest Frequency	-1002.3
14 Nucleus	1H
15 Acquired Size	1536
16 SpectralSize	32768

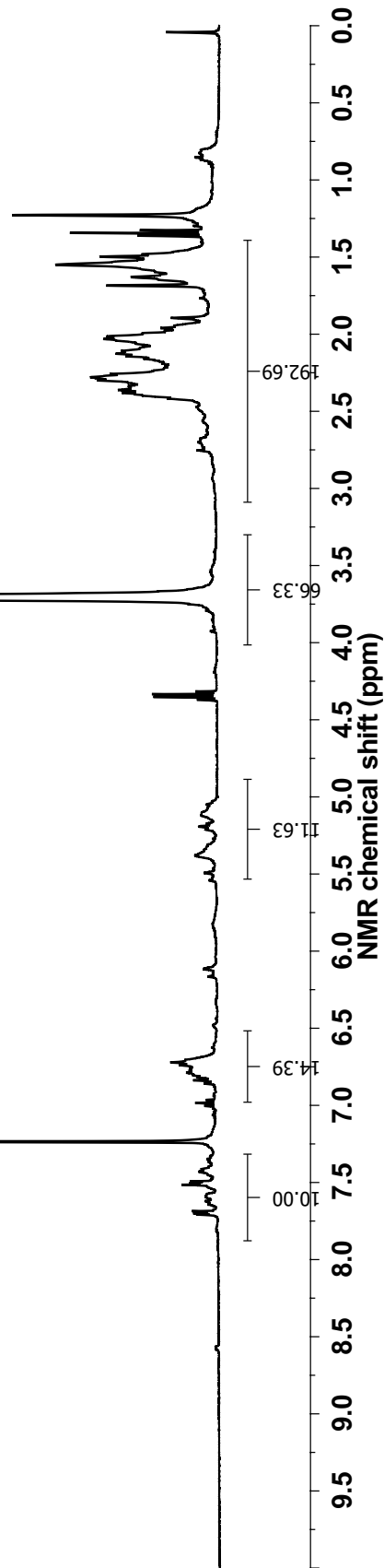


A-87: ¹H-NMR spectrum of cyc-(8a-20a-D10)₂₀



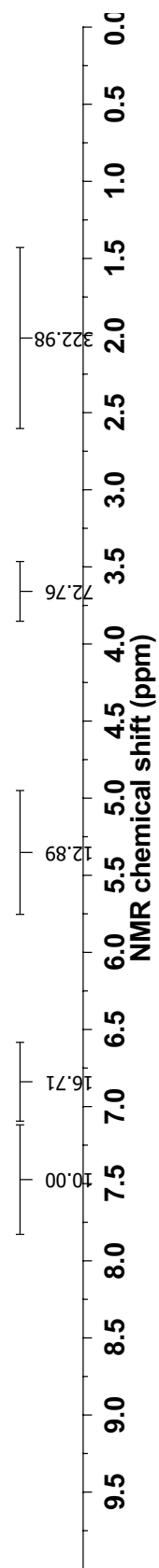
A-88: ¹H-NMR spectrum of (8a-20a-D10)₂₀-[25]

Parameter	Value
1 Data File Name	E:/NMRdata/10012008-02172009/400/CBCOCH3-1-methylcyclopentene20mer11182008.fid/ fid
2 Title	CBCOCH3-1-methylcyclopentene20mer11182008
3 Origin	inova
4 Owner	
5 Solvent	CDCl3
6 Pulse Sequence	s2pul
7 Acquisition Date	2008-11-18T06:04:22
8 Modification Date	
9 Temperature	25.0
10 Number of Scans	192
11 Spectrometer Frequency	399.83
12 Spectral Width	6000.6
13 Lowest Frequency	-1000.8
14 Nucleus	¹ H
15 Acquired Size	19637
16 Spectral Size	65536



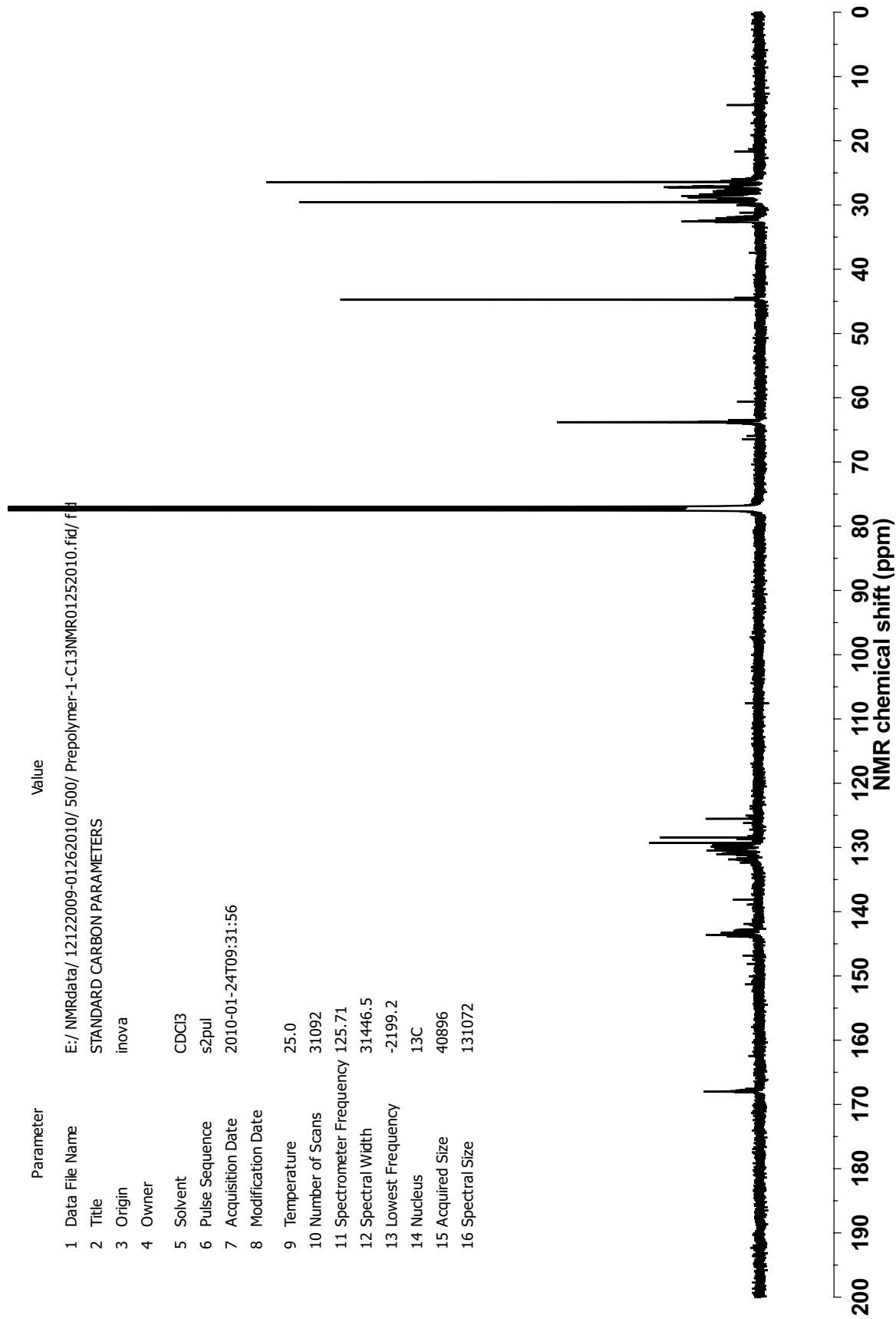
A-89: ¹H-NMR spectrum of (8a-29a)₂₀-[28](AROMP in CDCl₃)

Parameter	Value
1 Data File Name	E:/ NMRdata/ 10012008-02:172009/ 600/ CBCOCH3-1-methylcyclopentene20mer-toluene3rdNolan01082009.fid/ fid
2 Title	CBCOCH3-1-methylcyclopentene20mer-Toluene3rdNolan01072009
3 Origin	inova
4 Owner	
5 Solvent	Acetone
6 Pulse Sequence	s2pul
7 Acquisition Date	2009-01-08T05:30:52
8 Modification Date	
9 Temperature	25.0
10 Number of Scans	96
11 Spectrometer Frequency	599.72
12 Spectral Width	8000.0
13 Lowest Frequency	-1001.2
14 Nucleus	¹ H
15 Acquired Size	15136
16 Spectral Size	32768



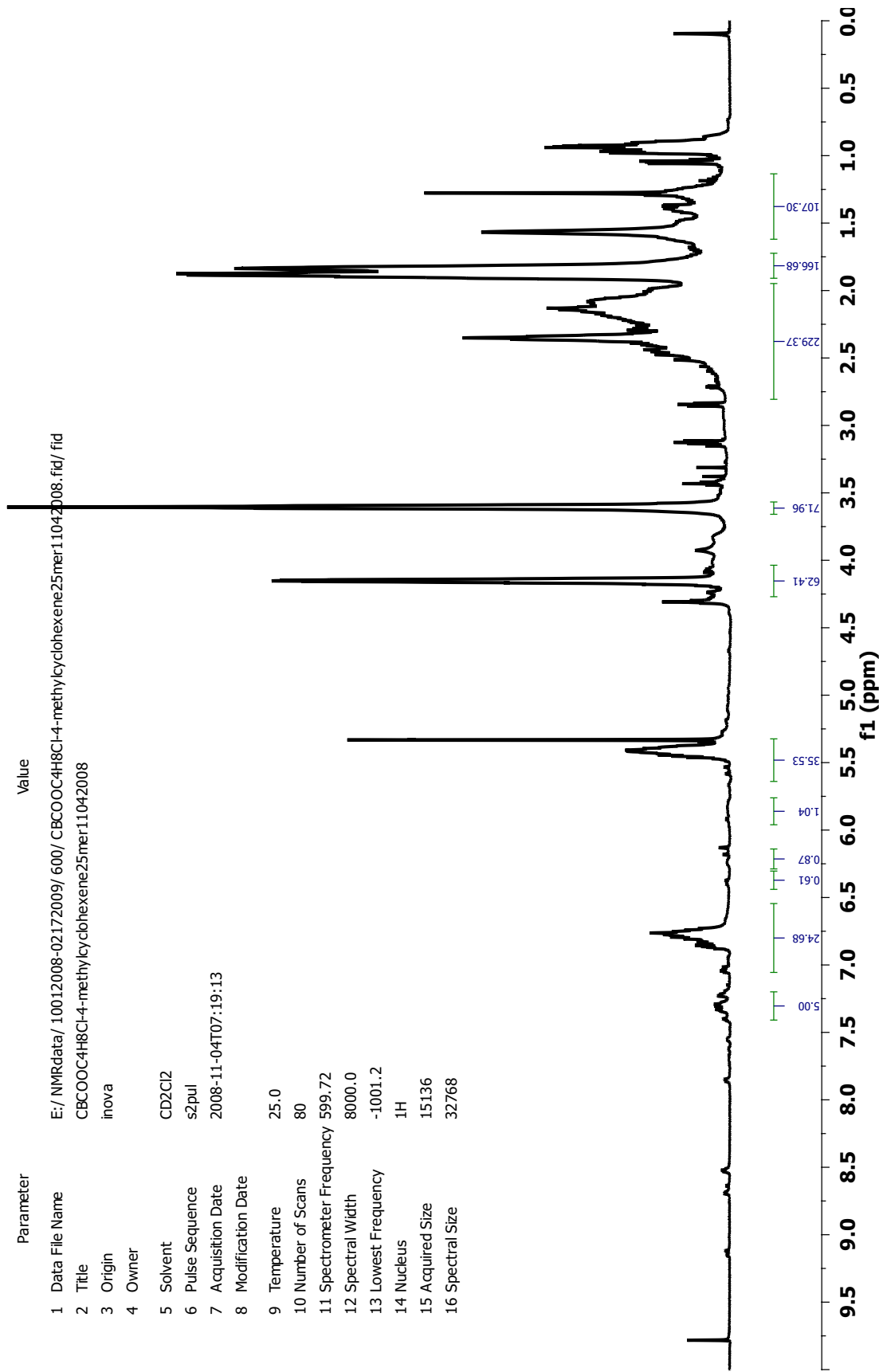
A-90: ¹H-NMR spectrum of (8a-29a)₂₀-[28](AROMP in toluene-D₉)

Parameter	Value
1 Data File Name	E:/ NMRdata/ 12122009-01262010/ 500/ Prepolymer-1-C13NMR01252010.fid/ fid
2 Title	STANDARD CARBON PARAMETERS
3 Origin	inova
4 Owner	
5 Solvent	CDCl3
6 Pulse Sequence	s2pul
7 Acquisition Date	2010-01-24T09:31:56
8 Modification Date	
9 Temperature	25.0
10 Number of Scans	31092
11 Spectrometer Frequency	125.71
12 Spectral Width	31446.5
13 Lowest Frequency	-2199.2
14 Nucleus	13C
15 Acquired Size	40896
16 Spectral Size	131072



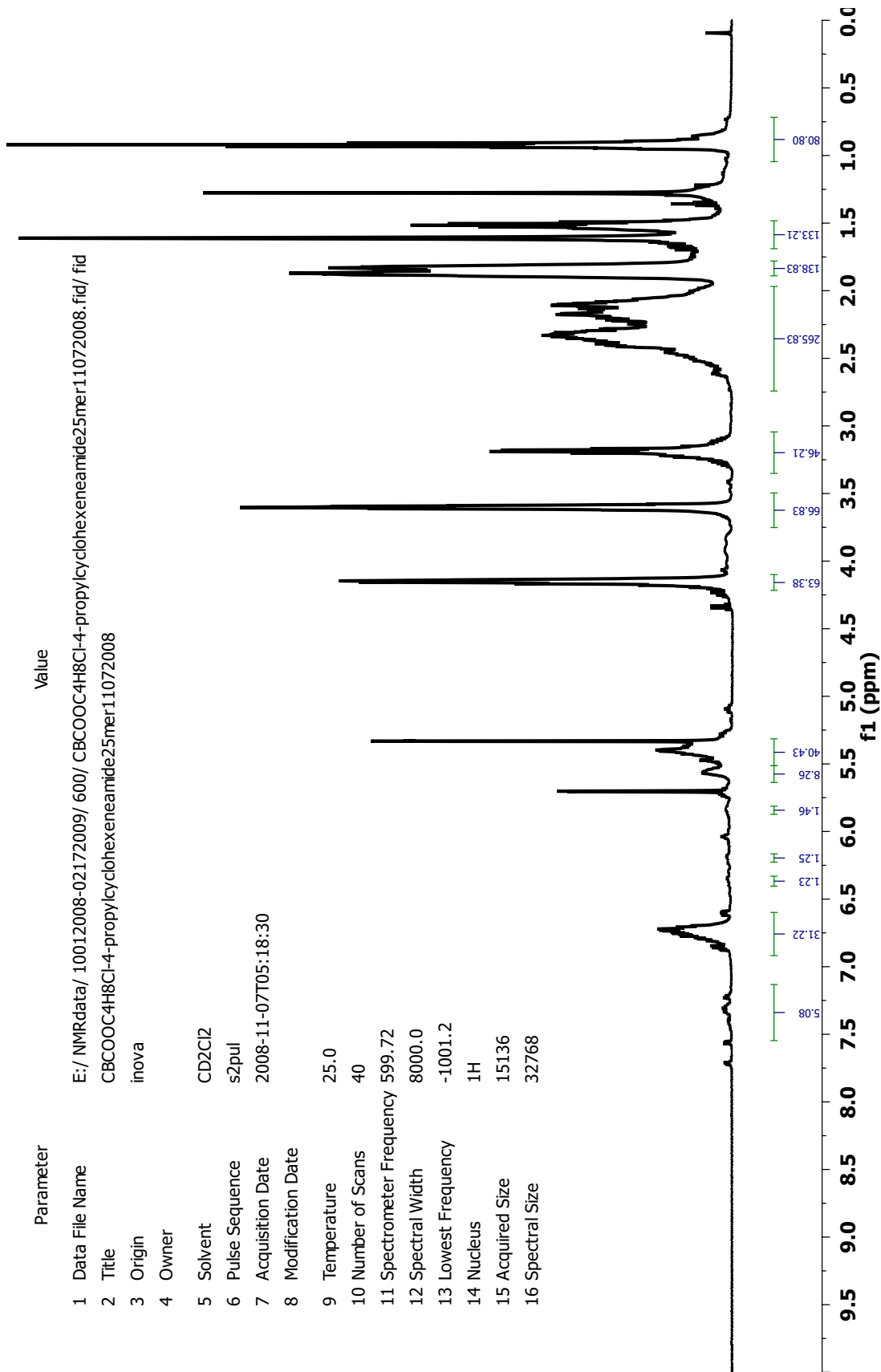
A-92: ¹³C-NMR spectrum of Intermediate-1

Parameter	Value
1 Data File Name	E:/NMRdata/10012008-02172009/600/CBOOC4H8Cl-4-methylcyclohexene25mer11042008.fid/ fid
2 Title	CBOOC4H8Cl-4-methylcyclohexene25mer11042008
3 Origin	inova
4 Owner	
5 Solvent	CD2Cl2
6 Pulse Sequence	s2pul
7 Acquisition Date	2008-11-04T07:19:13
8 Modification Date	
9 Temperature	25.0
10 Number of Scans	80
11 Spectrometer Frequency	599.72
12 Spectral Width	8000.0
13 Lowest Frequency	-1001.2
14 Nucleus	1H
15 Acquired Size	15136
16 Spectral Size	32768



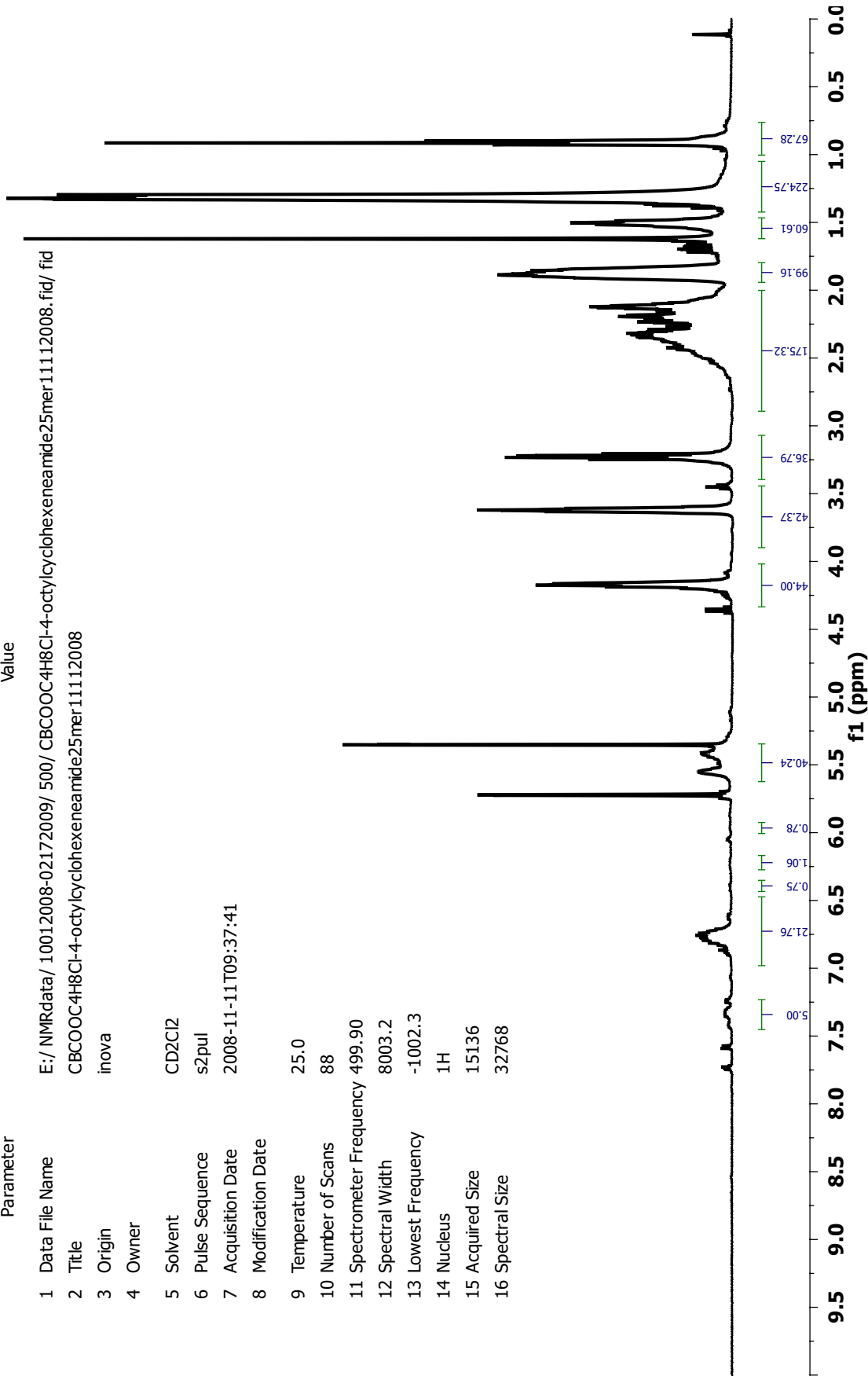
A-93: ¹H-NMR spectrum of Intermediate-2

Parameter	Value
1 Data File Name	E:/NMRdata/10012008-02172009/600/CBCOOC4H8Cl-4-propylcyclohexeneamide25mer11072008.fid/ fid
2 Title	CBCOOC4H8Cl-4-propylcyclohexeneamide25mer11072008
3 Origin	inova
4 Owner	
5 Solvent	CD2Cl2
6 Pulse Sequence	s2pul
7 Acquisition Date	2008-11-07T05:18:30
8 Modification Date	
9 Temperature	25.0
10 Number of Scans	40
11 Spectrometer Frequency	599.72
12 Spectral Width	8000.0
13 Lowest Frequency	-1001.2
14 Nucleus	1H
15 Acquired Size	15136
16 Spectral Size	32768



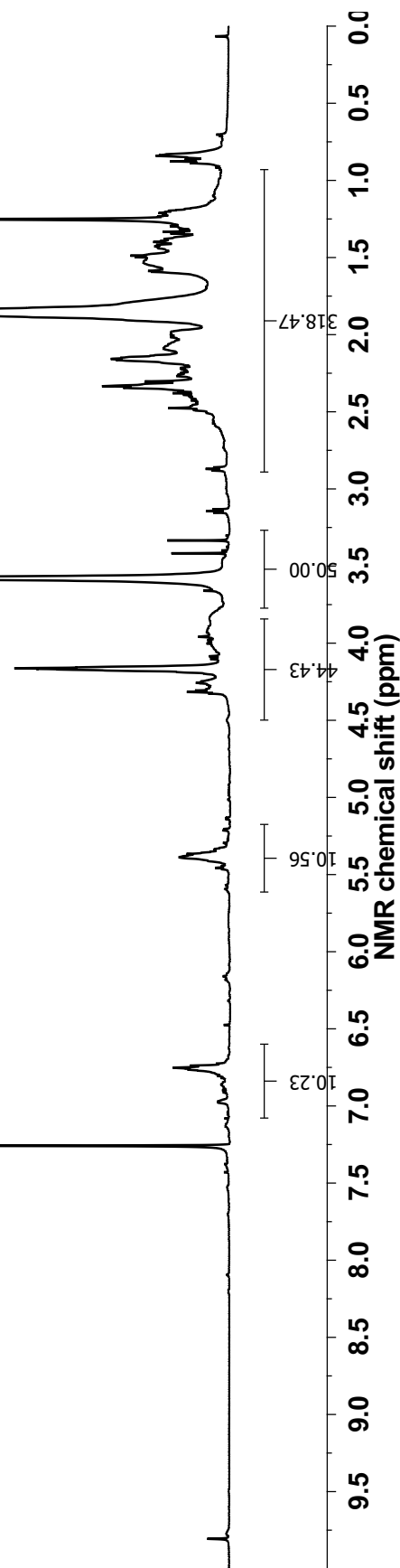
A-94: ¹H-NMR spectrum of Intermediate-3

Parameter Value
 1 Data File Name E:/NMRdata/10012008-02172009/500/CBCOOC4H8Cl-4-octylcyclohexeneamide25mer11112008.fid/ fid
 2 Title CBCOOC4H8Cl-4-octylcyclohexeneamide25mer11112008
 3 Origin inova
 4 Owner
 5 Solvent CD2Cl2
 6 Pulse Sequence s2pul
 7 Acquisition Date 2008-11-11T09:37:41
 8 Modification Date
 9 Temperature 25.0
 10 Number of Scans 88
 11 Spectrometer Frequency 499.90
 12 Spectral Width 8003.2
 13 Lowest Frequency -1002.3
 14 Nucleus ¹H
 15 Acquired Size 15136
 16 Spectral Size 32768



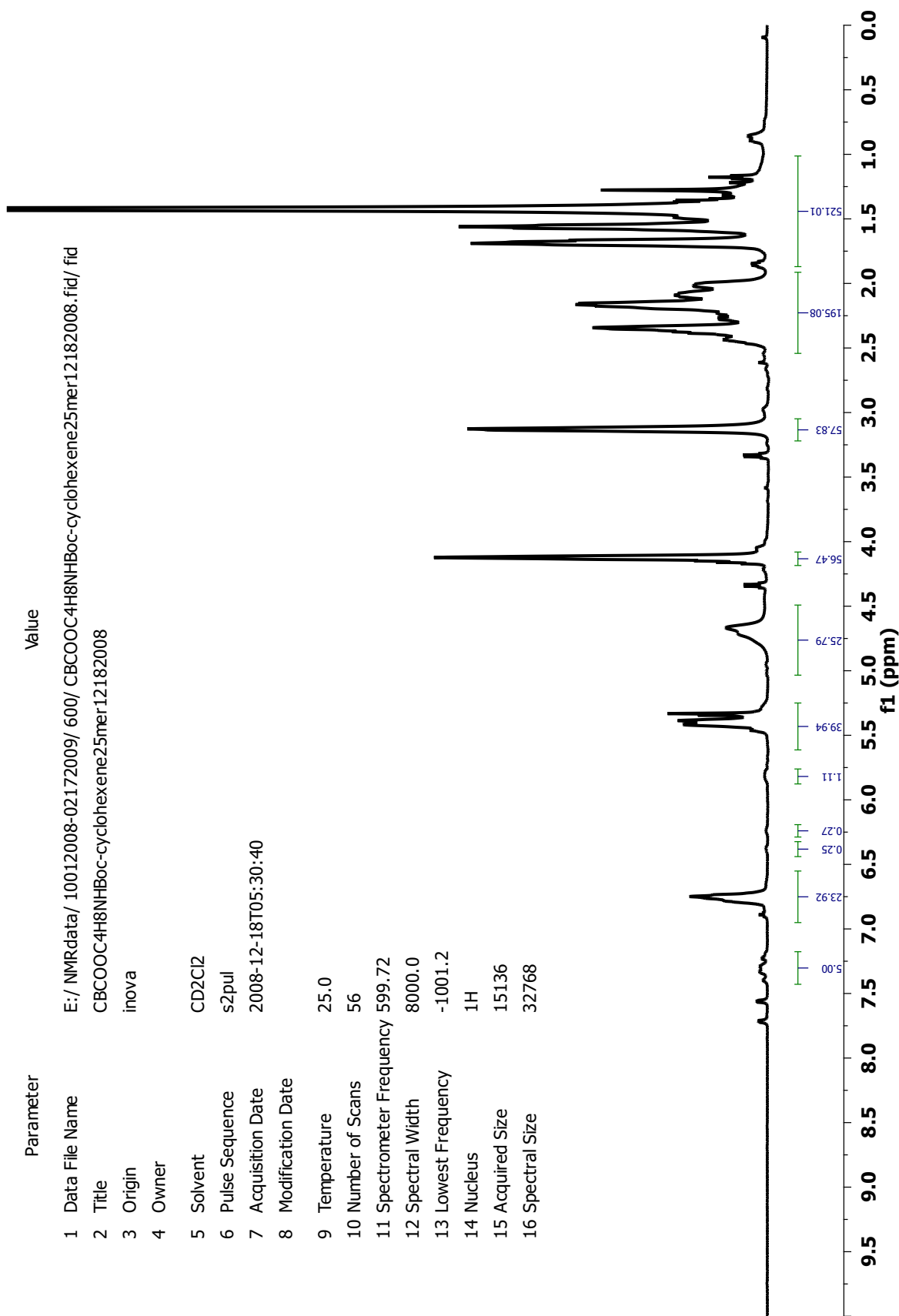
A-95: ¹H-NMR spectrum of Intermediate-4

Parameter	Value
1 Data File Name	E:/ NMRdata/ 10012008-021172009/ 600/ CBCOOC4H8Cl-cyclohexene25mer-Hoveyda10192008.fid/ fid
2 Title	CBCOOC4H8Cl-cyclohexene25mer-Hoveyda10192008
3 Origin	inova
4 Owner	
5 Solvent	CDCl3
6 Pulse Sequence	s2pul
7 Acquisition Date	2008-10-20T08:54:30
8 Modification Date	
9 Temperature	25.0
10 Number of Scans	88
11 Spectrometer Frequency	599.72
12 Spectral Width	8000.0
13 Lowest Frequency	-1001.3
14 Nucleus	1H
15 Acquired Size	15136
16 Spectral Size	32768



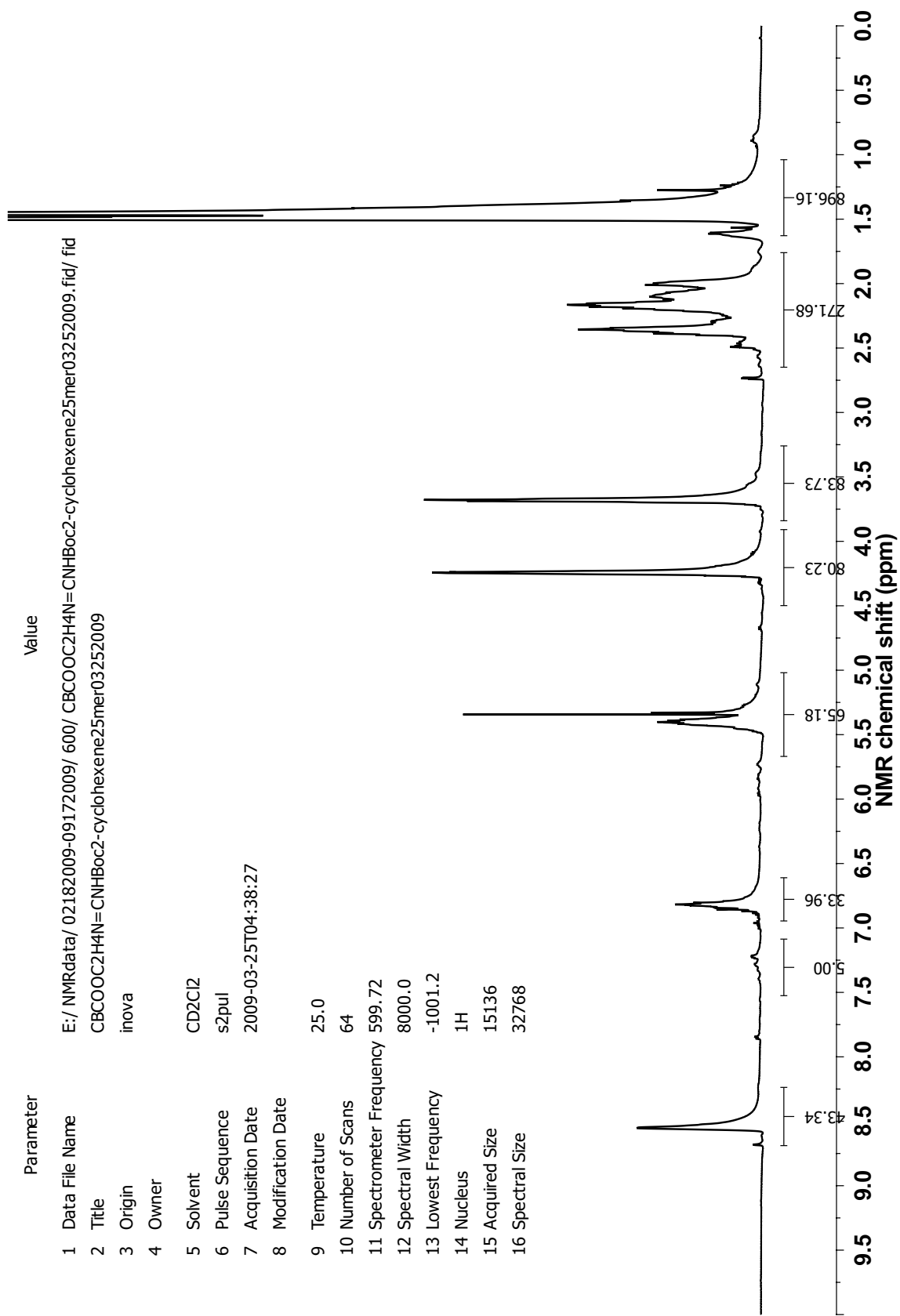
A-96: ¹H-NMR spectrum of Intermediate-5

Parameter	Value
1 Data File Name	E:/ NMRdata/ 10012008-02172009/ 600/ CBCOOC4H8NHBOC-cyclohexene25mer12182008.fid/ fid
2 Title	CBCOOC4H8NHBOC-cyclohexene25mer12182008
3 Origin	inova
4 Owner	
5 Solvent	CD2Cl2
6 Pulse Sequence	s2pul
7 Acquisition Date	2008-12-18T05:30:40
8 Modification Date	
9 Temperature	25.0
10 Number of Scans	56
11 Spectrometer Frequency	599.72
12 Spectral Width	8000.0
13 Lowest Frequency	-1001.2
14 Nucleus	¹ H
15 Acquired Size	15136
16 Spectral Size	32768



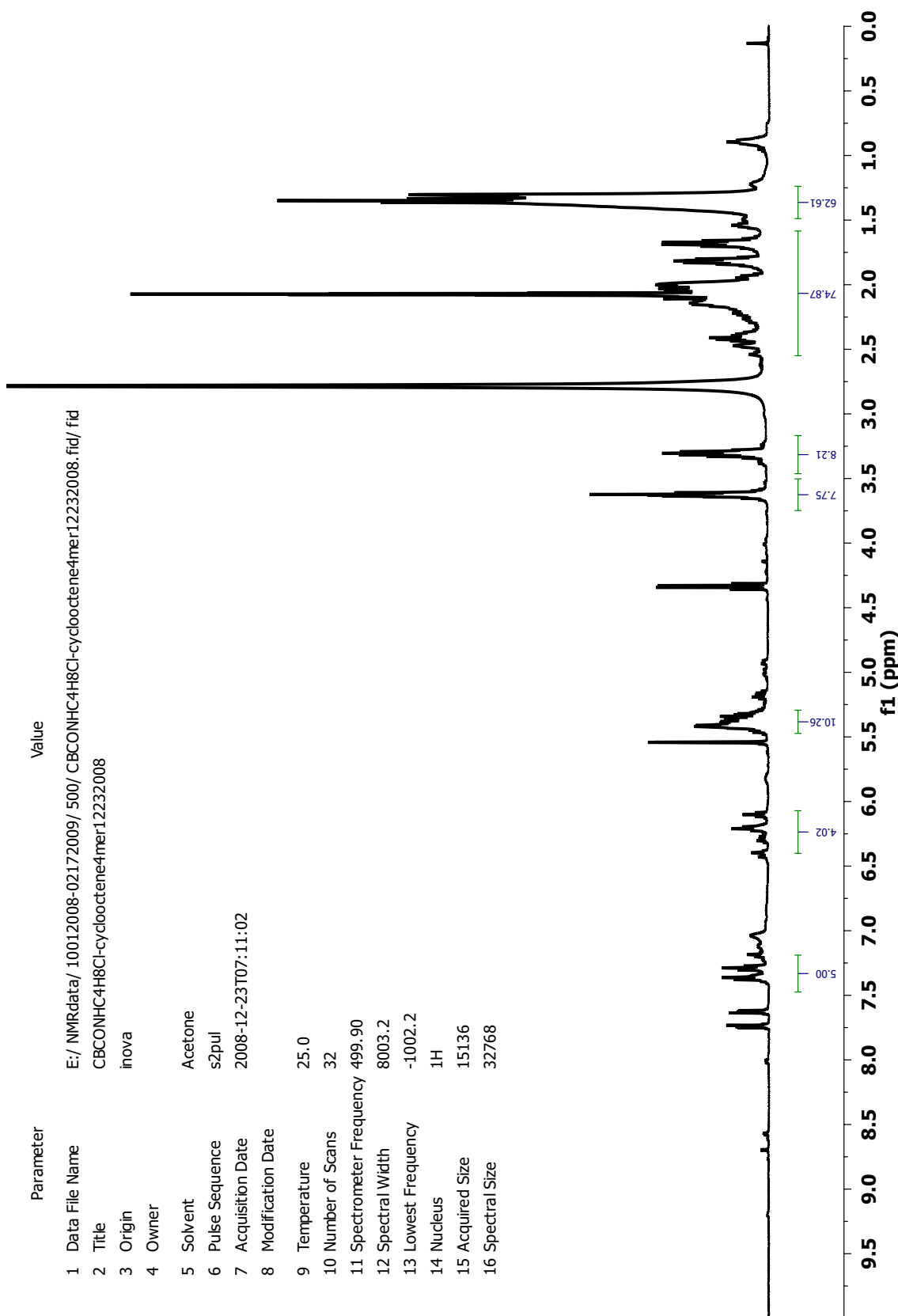
A-97: ¹H-NMR spectrum of Intermediate-6

Parameter	Value
1 Data File Name	E:/ NMRdata/ 02182009-09172009/ 600/ CBCOOC2H4N=CNHBoc2-cyclohexene25mer03252009.fid/ fid
2 Title	CBCOOC2H4N=CNHBoc2-cyclohexene25mer03252009
3 Origin	inova
4 Owner	
5 Solvent	CD2Cl2
6 Pulse Sequence	s2pul
7 Acquisition Date	2009-03-25T04:38:27
8 Modification Date	
9 Temperature	25.0
10 Number of Scans	64
11 Spectrometer Frequency	599.72
12 Spectral Width	8000.0
13 Lowest Frequency	-1001.2
14 Nucleus	1H
15 Acquired Size	15136
16 Spectral Size	32768



A-98: ¹H-NMR spectrum of Intermediate-7

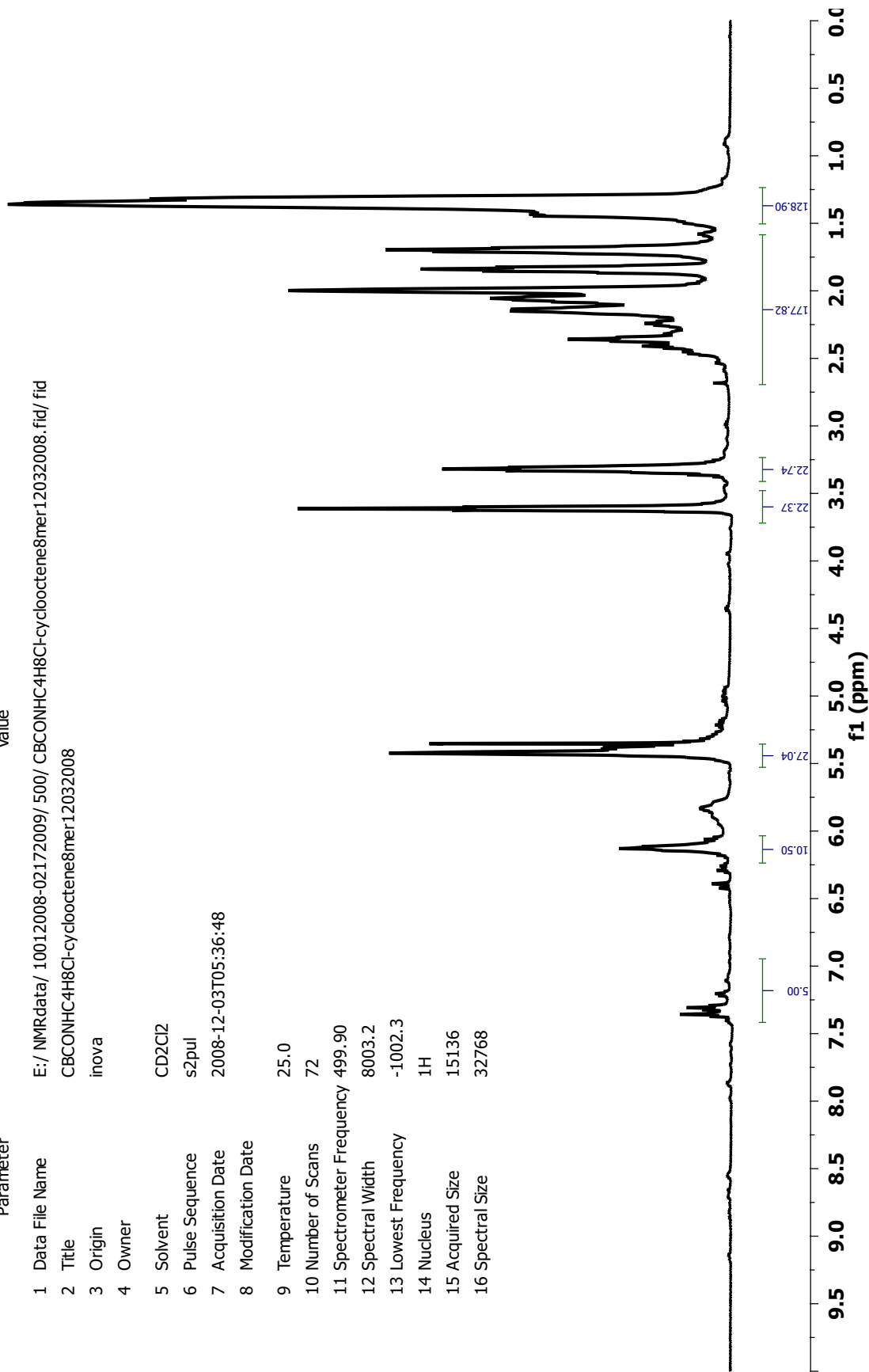
Parameter	Value
1 Data File Name	E:/ NMRdata/ 10012008-02172009/ 500/ CBCONHC4H8Cl-cyclooctene4mer12232008.fid/ fid
2 Title	CBCONHC4H8Cl-cyclooctene4mer12232008
3 Origin	inova
4 Owner	
5 Solvent	Acetone
6 Pulse Sequence	s2pul
7 Acquisition Date	2008-12-23T07:11:02
8 Modification Date	
9 Temperature	25.0
10 Number of Scans	32
11 Spectrometer Frequency	499.90
12 Spectral Width	8003.2
13 Lowest Frequency	-1002.2
14 Nucleus	¹ H
15 Acquired Size	15136
16 Spectral Size	32768



A-99: ¹H-NMR spectrum of Intermediate-8

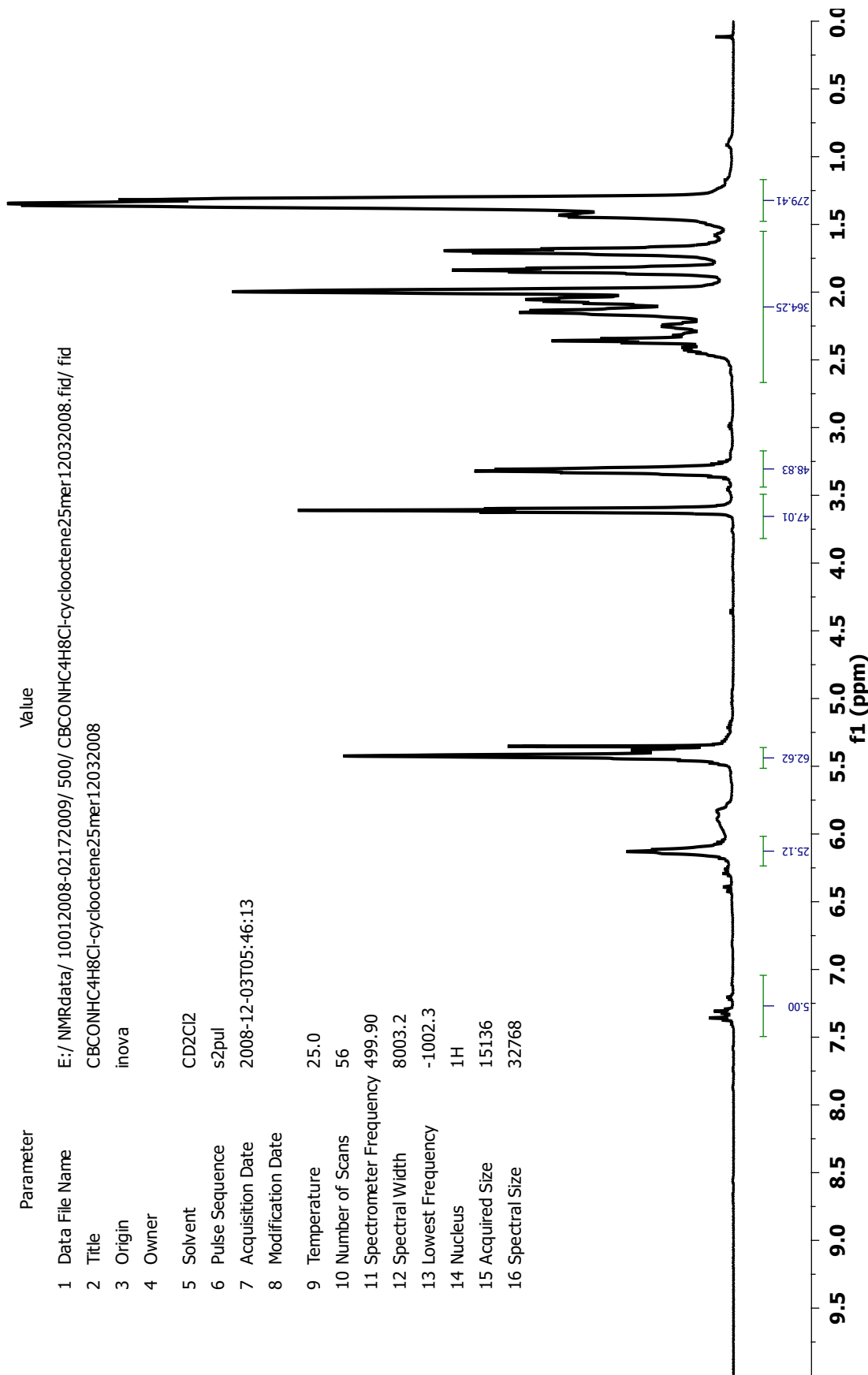
Parameter Value

1 Data File Name E:/NMRdata/10012008-02172009/500/CBCONHC4H8C-cyclooctene8mer12032008.fid/ fid
2 Title CBCONHC4H8C-cyclooctene8mer12032008
3 Origin inova
4 Owner
5 Solvent CD2Cl2
6 Pulse Sequence s2pul
7 Acquisition Date 2008-12-03T05:36:48
8 Modification Date
9 Temperature 25.0
10 Number of Scans 72
11 Spectrometer Frequency 499.90
12 Spectral Width 8003.2
13 Lowest Frequency -1002.3
14 Nucleus ¹H
15 Acquired Size 15136
16 Spectral Size 32768

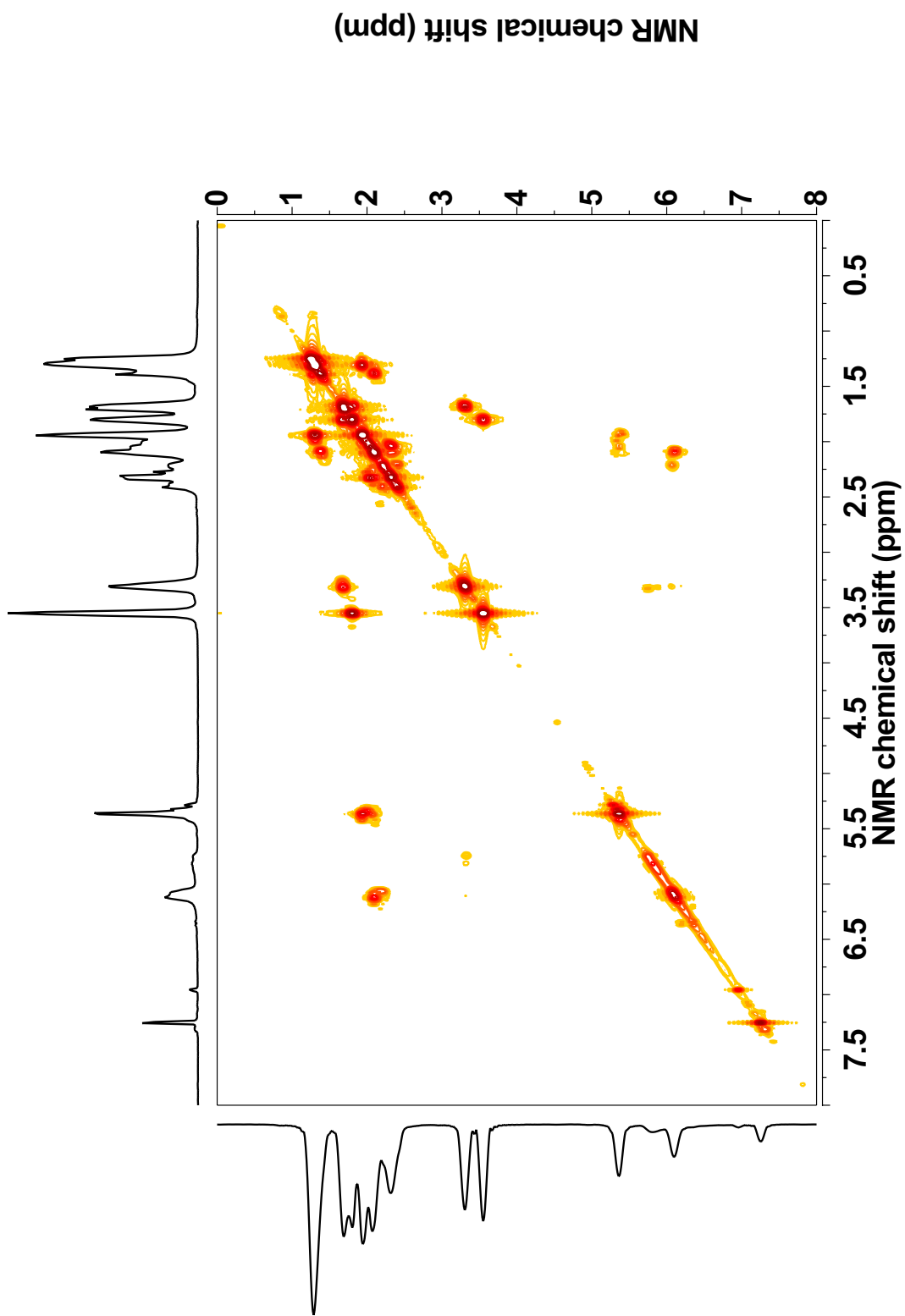


A-100: ¹H-NMR spectrum of Intermediate-9

Parameter	Value
1 Data File Name	E:/ NMRdata/ 10012008-02172009/ 500/ CBCONHC4H8Cl-cyclooctene25mer.12032008.fid/ fid
2 Title	CBCONHC4H8Cl-cyclooctene25mer.12032008
3 Origin	inova
4 Owner	
5 Solvent	CD2Cl2
6 Pulse Sequence	s2pul
7 Acquisition Date	2008-12-03T05:46:13
8 Modification Date	
9 Temperature	25.0
10 Number of Scans	56
11 Spectrometer Frequency	499.90
12 Spectral Width	8003.2
13 Lowest Frequency	-1002.3
14 Nucleus	¹ H
15 Acquired Size	15136
16 Spectral Size	32768

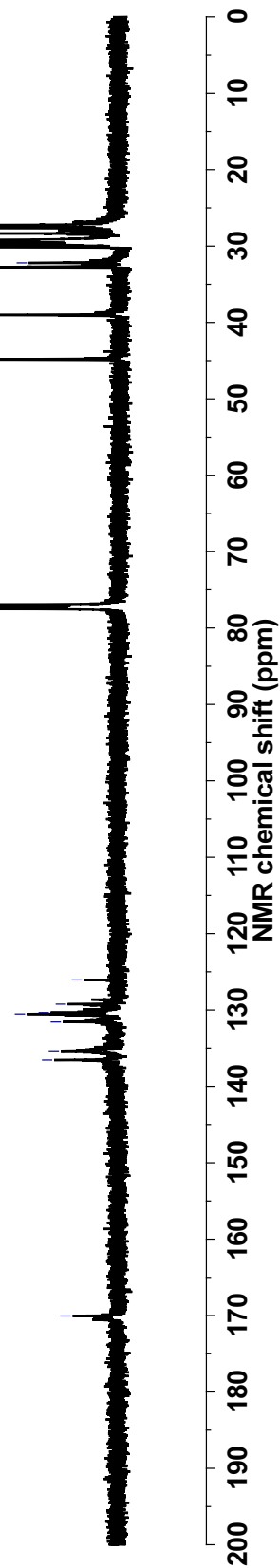


A-101: ¹H-NMR spectrum of Intermediate-10

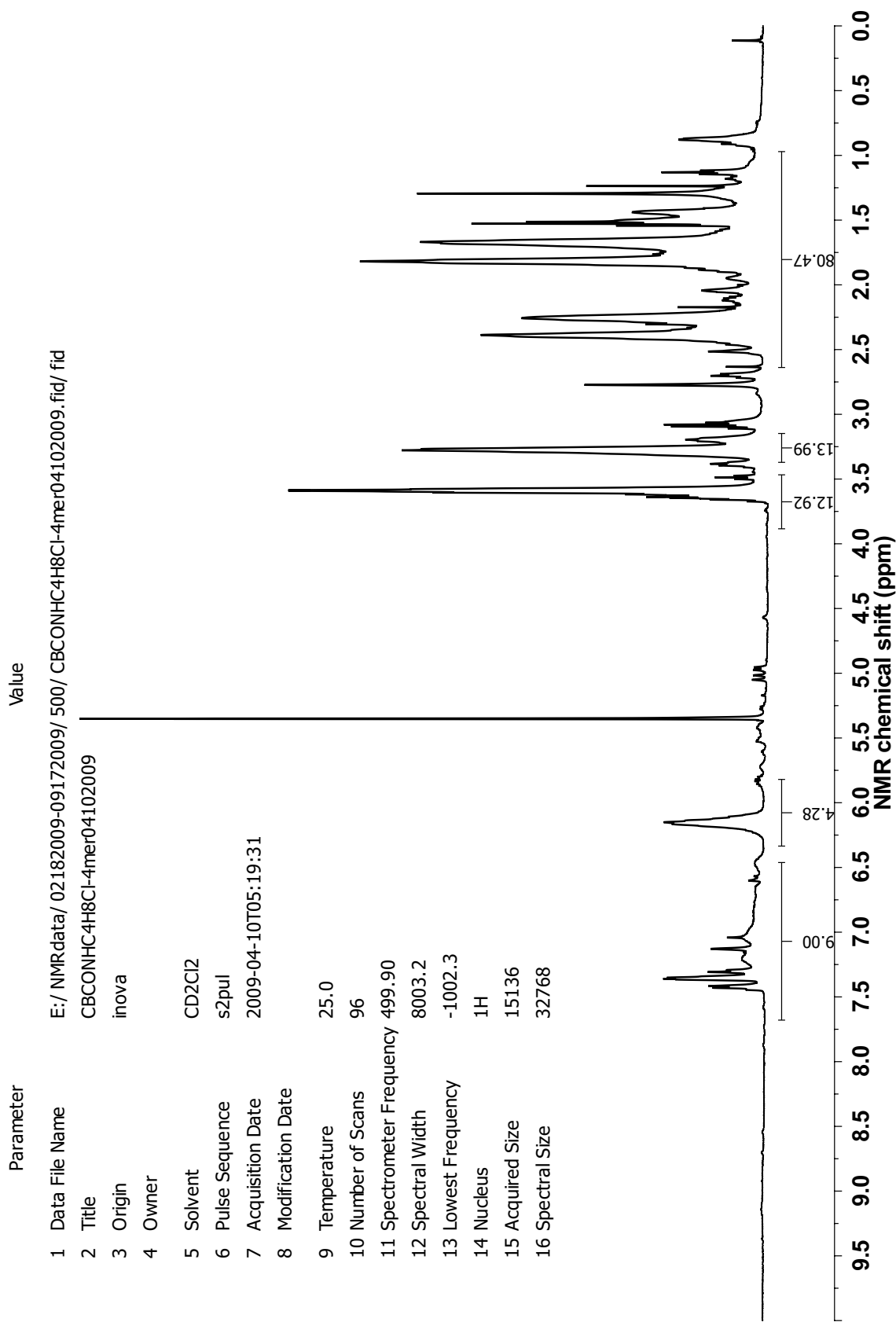


A-102: ^1H - ^1H -gCOSY-NMR spectrum of Intermediate-10

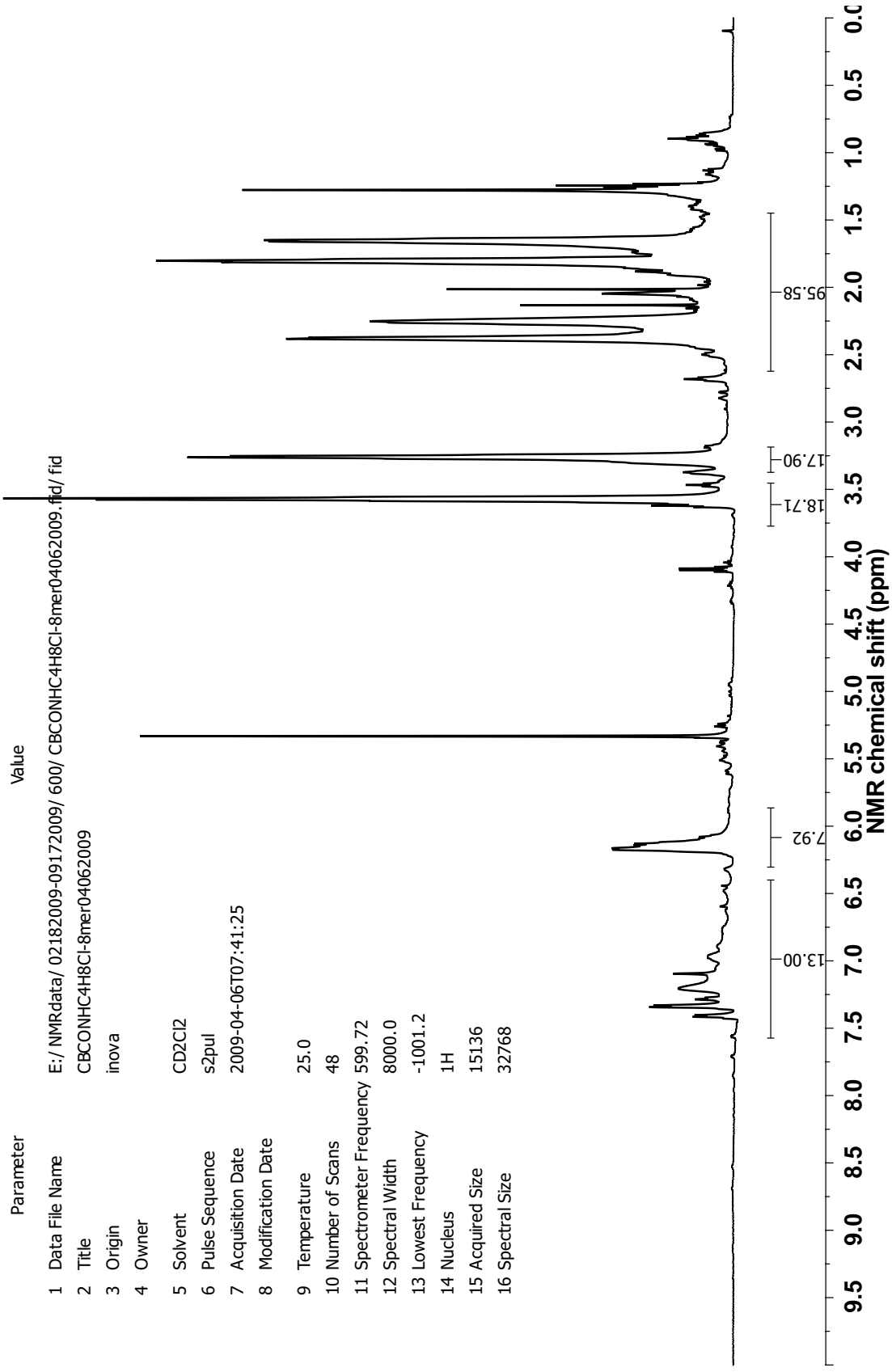
Parameter	Value
1 Data File Name	E:/NMRdata/12122009-01262010/500/Pre-Polymer-10-C13NMR/01252010.fid/ fid
2 Title	CBCONHC4H8Cl-cyclooctene25mer-C13NMR
3 Origin	inova
4 Owner	
5 Solvent	CDCl3
6 Pulse Sequence	s2pul
7 Acquisition Date	2010-01-25T13:12:42
8 Modification Date	
9 Temperature	25.0
10 Number of Scans	5944
11 Spectrometer Frequency	125.71
12 Spectral Width	31446.5
13 Lowest Frequency	-2206.6
14 Nucleus	13C
15 Acquired Size	40896
16 Spectral Size	131072



A-103: ¹³C-NMR spectrum of Intermediate-10

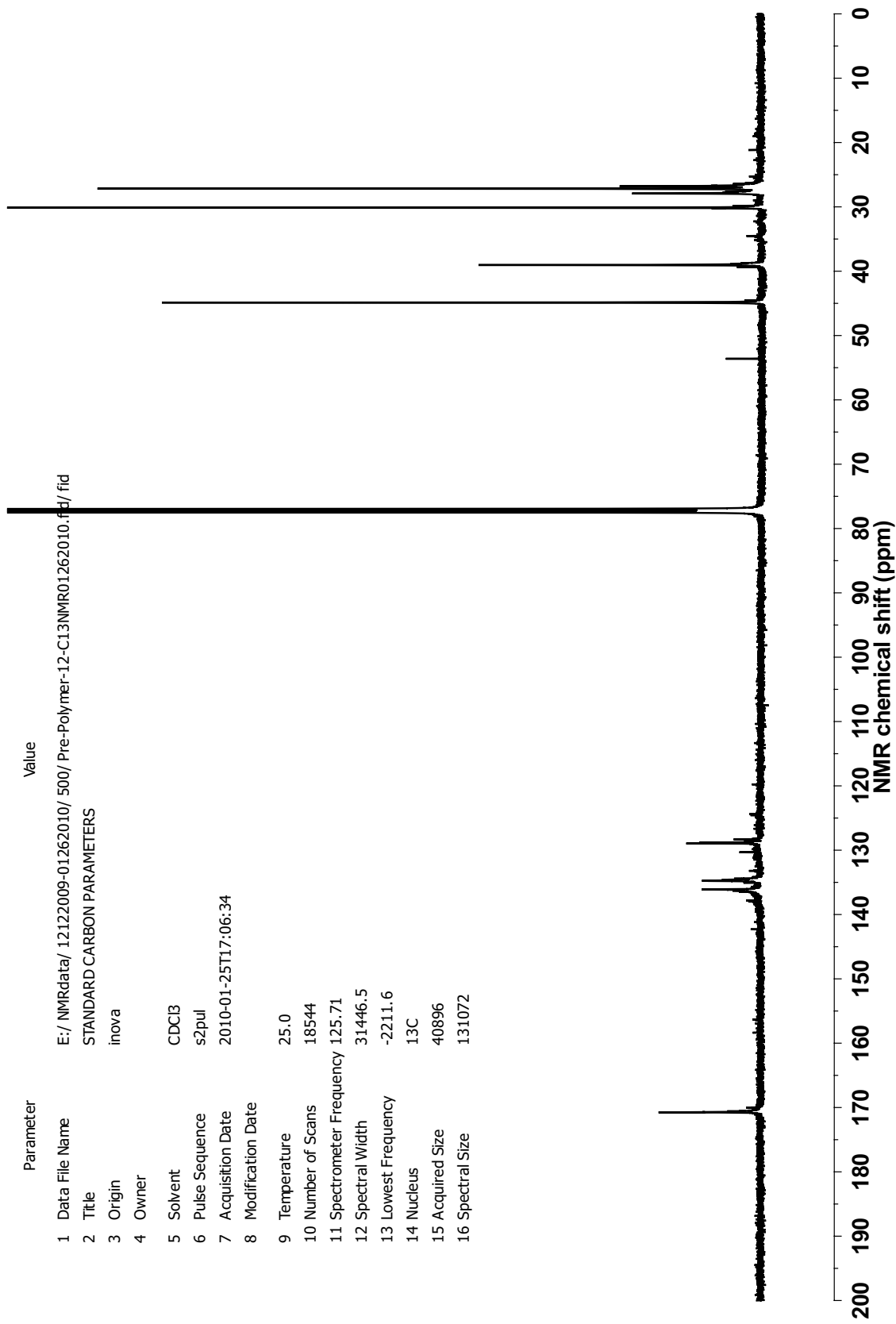


A-104: ¹H-NMR spectrum of Intermediate-11



A-105: ¹H-NMR spectrum of Intermediate-12

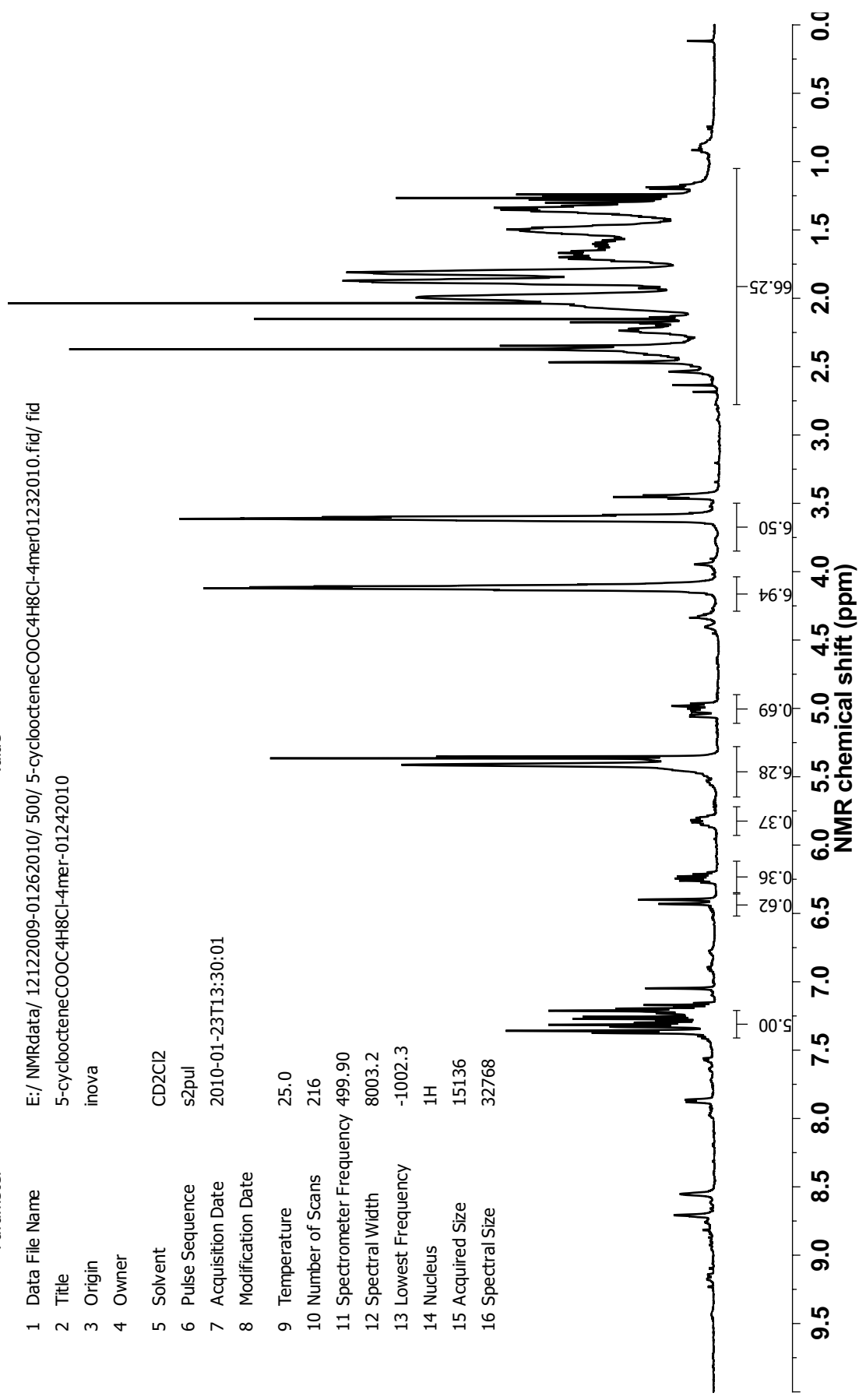
Parameter	Value
1 Data File Name	E:/ NMRdata/ 12122009-01262010/ 500/ Pre-Polymer-12-C13NMR01262010.fid/ fid
2 Title	STANDARD CARBON PARAMETERS
3 Origin	inova
4 Owner	
5 Solvent	CDCl3
6 Pulse Sequence	s2pul
7 Acquisition Date	2010-01-25T17:06:34
8 Modification Date	
9 Temperature	25.0
10 Number of Scans	18544
11 Spectrometer Frequency	125.71
12 Spectral Width	31446.5
13 Lowest Frequency	-2211.6
14 Nucleus	13C
15 Acquired Size	40896
16 Spectral Size	131072



A-106: ¹³C-NMR spectrum of Intermediate-12

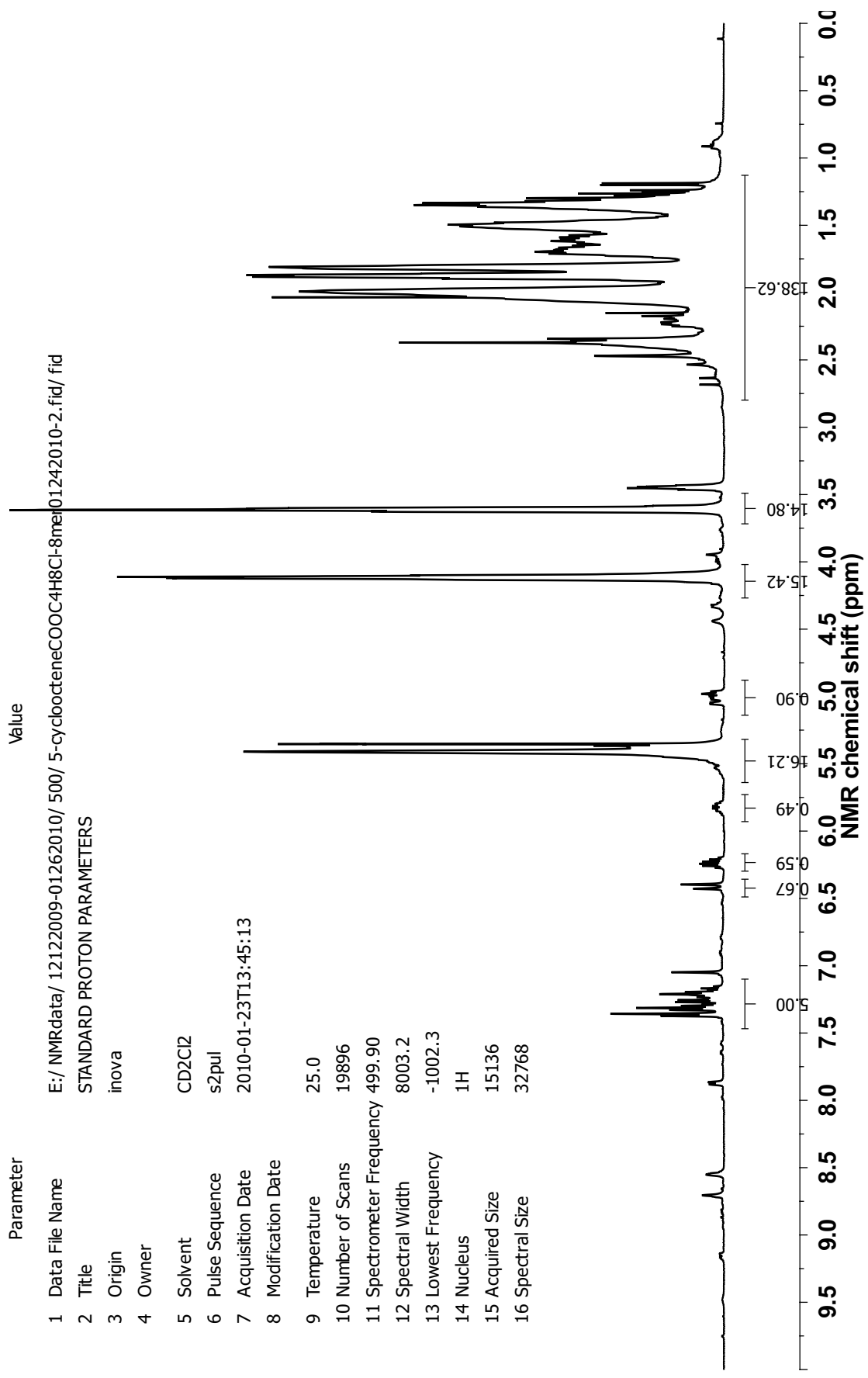
Parameter Value

1 Data File Name E:/ NMRdata/ 12122009-01262010/ 500/ 5-cycloocteneCOOC4H8Cl-4mer01232010.fid/ fid
2 Title 5-cycloocteneCOOC4H8Cl-4mer-01242010
3 Origin inova
4 Owner
5 Solvent CD2Cl2
6 Pulse Sequence s2pul
7 Acquisition Date 2010-01-23T13:30:01
8 Modification Date
9 Temperature 25.0
10 Number of Scans 216
11 Spectrometer Frequency 499.90
12 Spectral Width 8003.2
13 Lowest Frequency -1002.3
14 Nucleus ¹H
15 Acquired Size 15136
16 Spectral Size 32768



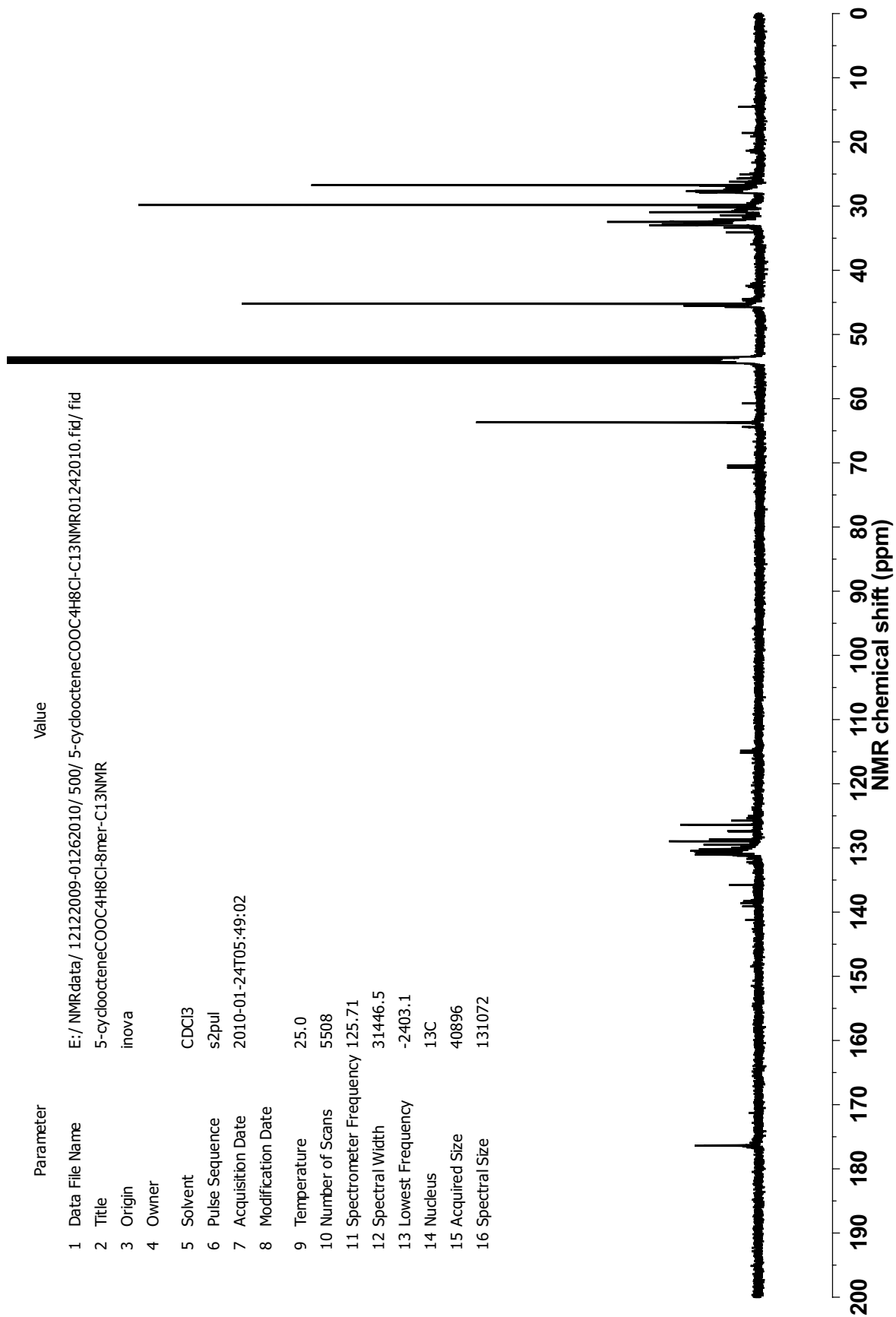
A-107: ¹H-NMR spectrum of Intermediate-13

Parameter Value
 1 Data File Name E:/ NMRdata/ 12122009-01262010/ 500/ 5-cycloocteneCOOC4H8Cl-8mer01242010-2.fid/ fid
 2 Title STANDARD PROTON PARAMETERS
 3 Origin inova
 4 Owner
 5 Solvent CD2Cl2
 6 Pulse Sequence s2pul
 7 Acquisition Date 2010-01-23T13:45:13
 8 Modification Date
 9 Temperature 25.0
 10 Number of Scans 19896
 11 Spectrometer Frequency 499.90
 12 Spectral Width 8003.2
 13 Lowest Frequency -1002.3
 14 Nucleus 1H
 15 Acquired Size 15136
 16 Spectral Size 32768



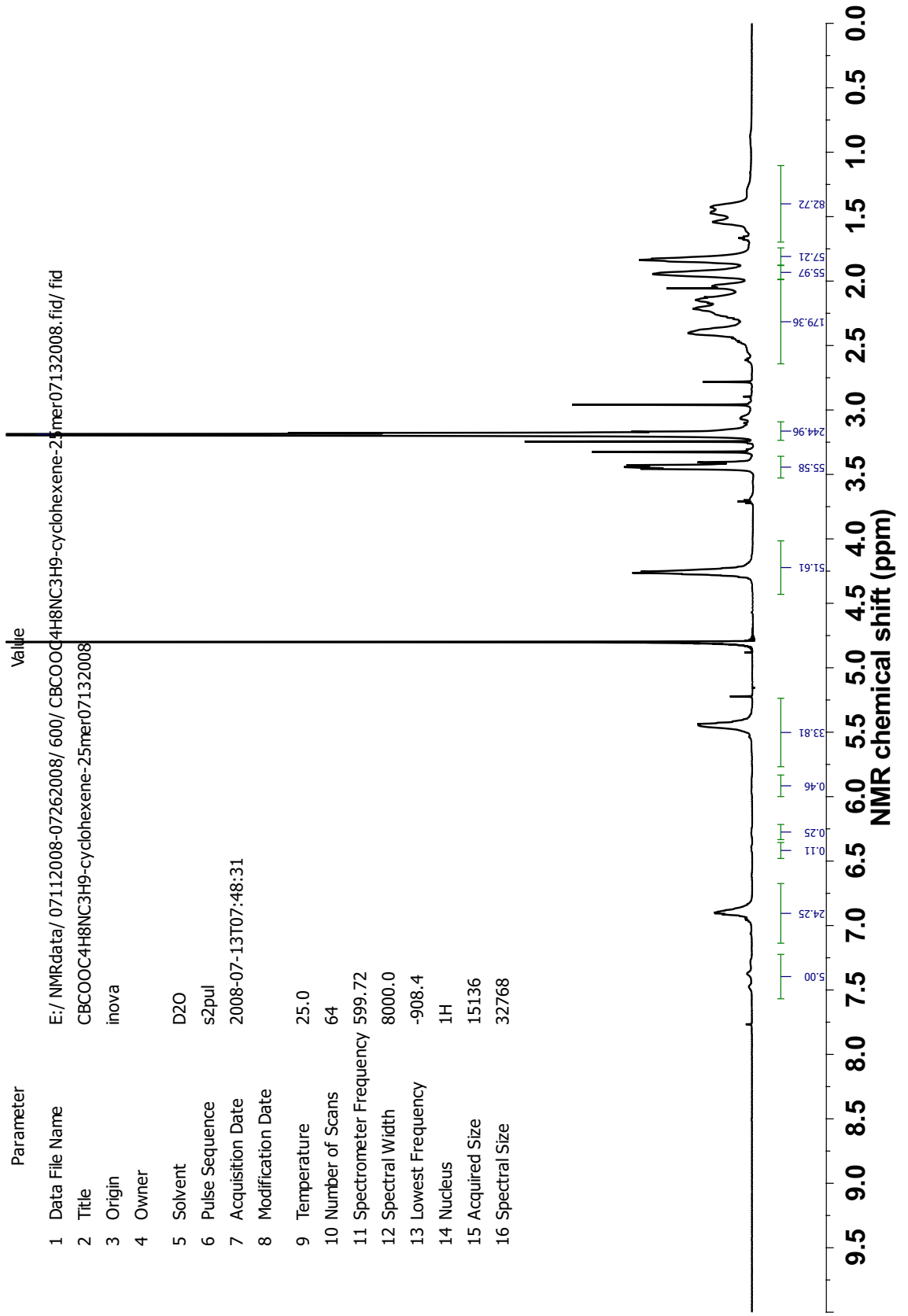
A-108: ¹H-NMR spectrum of Intermediate-14

Parameter	Value
1 Data File Name	E:/ NMRdata/ 12122009-01262010/ 500/ 5-cycloocteneCOOC4H8Cl-C13NMR01242010.fid/ fid
2 Title	5-cycloocteneCOOC4H8Cl-8mer-C13NMR
3 Origin	inova
4 Owner	
5 Solvent	CDCl3
6 Pulse Sequence	s2pul
7 Acquisition Date	2010-01-24T05:49:02
8 Modification Date	
9 Temperature	25.0
10 Number of Scans	5508
11 Spectrometer Frequency	125.71
12 Spectral Width	31446.5
13 Lowest Frequency	-2403.1
14 Nucleus	¹³ C
15 Acquired Size	40896
16 Spectral Size	131072



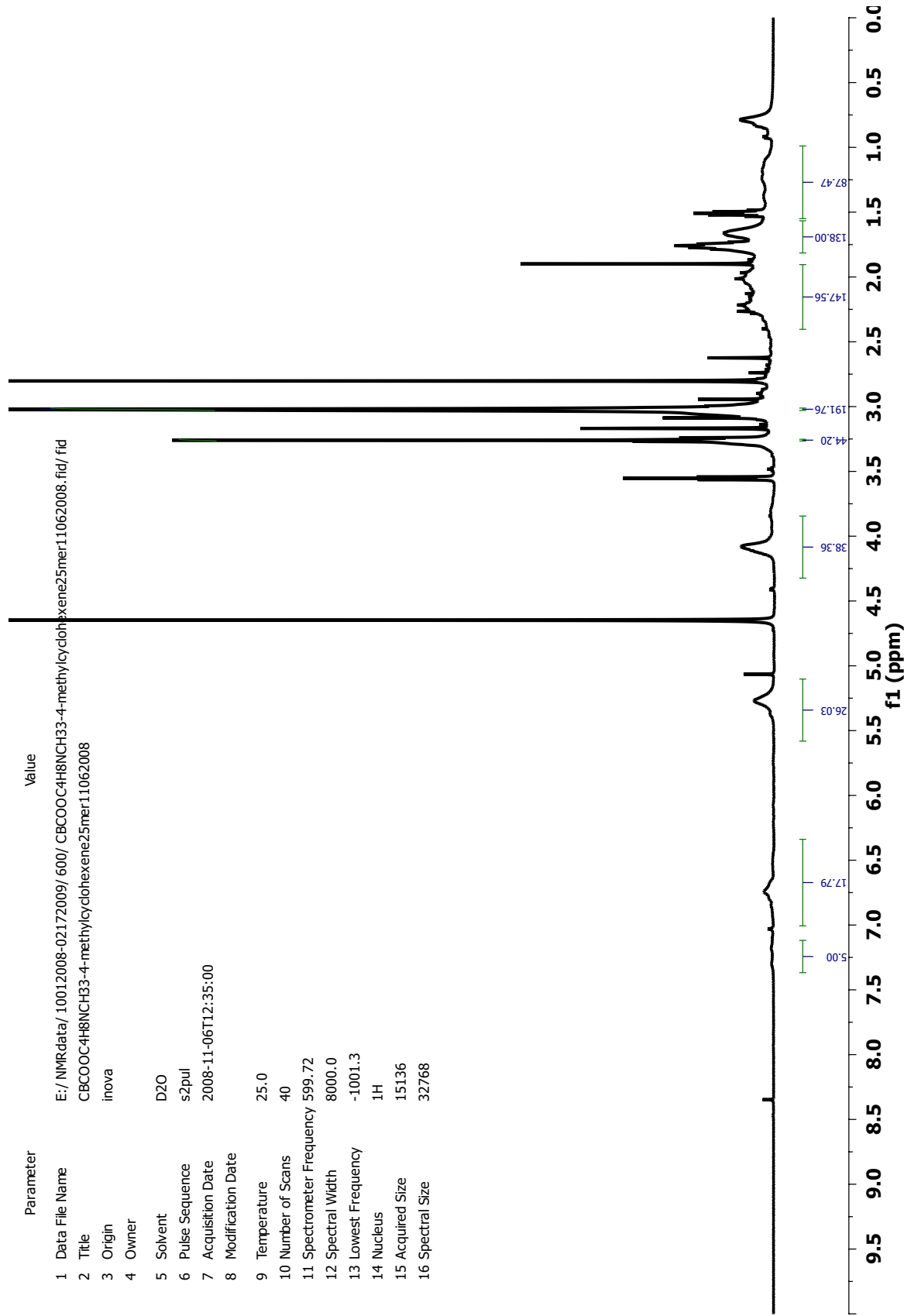
A-109: ¹³C-NMR spectrum of Intermediate-14

Parameter	Value
1 Data File Name	E:/ NMRdata/ 07112008-07262008/ 600/ CBCOOC4H8NC3H9-cyclohexene-25mer07132008.fid/ fid
2 Title	CBCOOC4H8NC3H9-cyclohexene-25mer07132008
3 Origin	inova
4 Owner	
5 Solvent	D2O
6 Pulse Sequence	s2pul
7 Acquisition Date	2008-07-13T07:48:31
8 Modification Date	
9 Temperature	25.0
10 Number of Scans	64
11 Spectrometer Frequency	599.72
12 Spectral Width	8000.0
13 Lowest Frequency	-908.4
14 Nucleus	¹ H
15 Acquired Size	15136
16 Spectral Size	32768



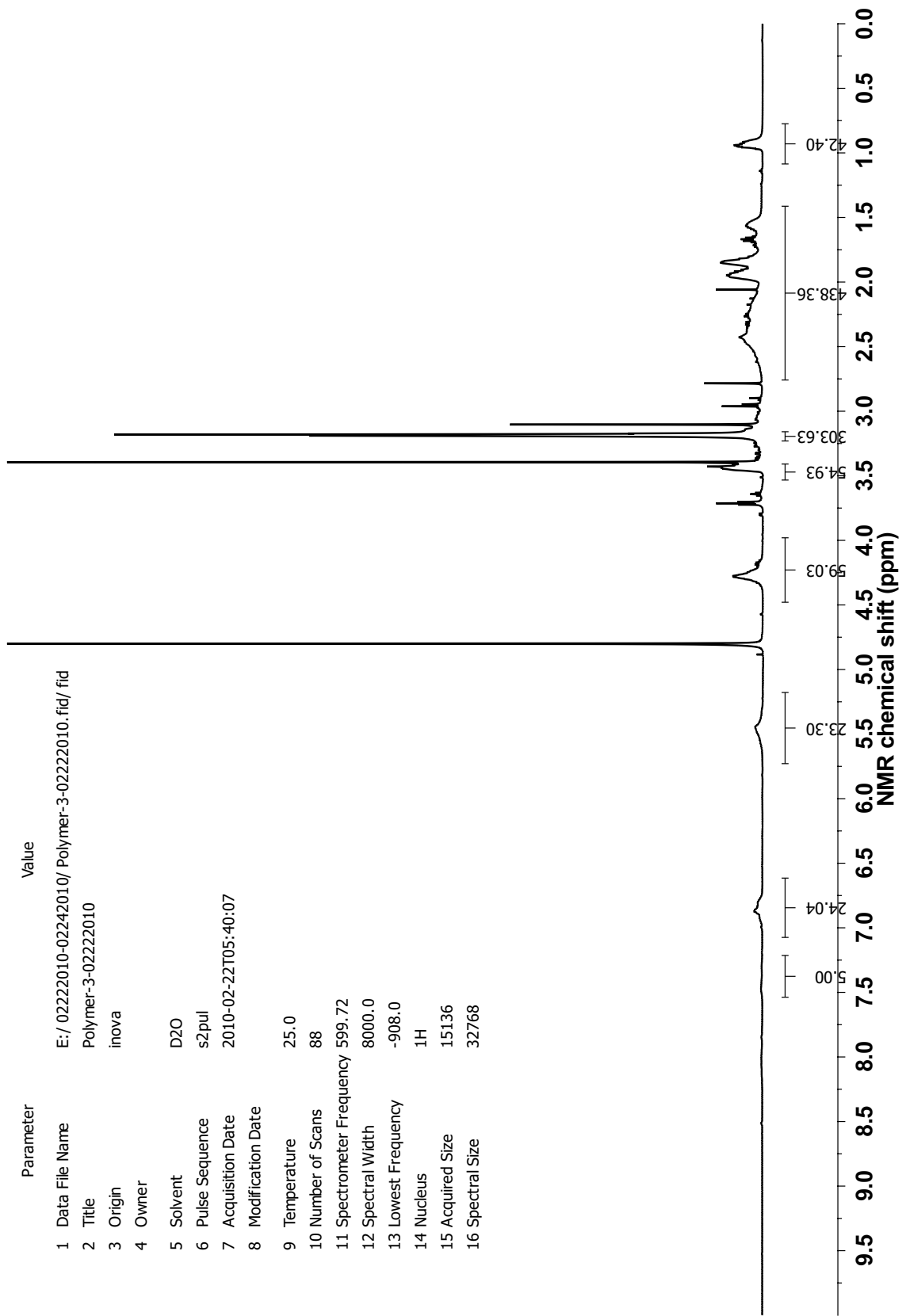
A-110: ¹H-NMR spectrum of Acopolymer-1

Parameter	Value
1 Data File Name	E:/NMRdata/10012008-02172009/600/CBCOOC4H8NCH33-4-methylcyclohexene25mer11062008.fid/ fid
2 Title	CBCOOC4H8NCH33-4-methylcyclohexene25mer11062008
3 Origin	inova
4 Owner	
5 Solvent	D2O
6 Pulse Sequence	s2pul
7 Acquisition Date	2008-11-06T12:35:00
8 Modification Date	
9 Temperature	25.0
10 Number of Scans	40
11 Spectrometer Frequency	599.72
12 Spectral Width	8000.0
13 Lowest Frequency	-1001.3
14 Nucleus	¹ H
15 Acquired Size	15136
16 Spectral Size	32768



A-111: ¹H-NMR spectrum of Acopolymer-2

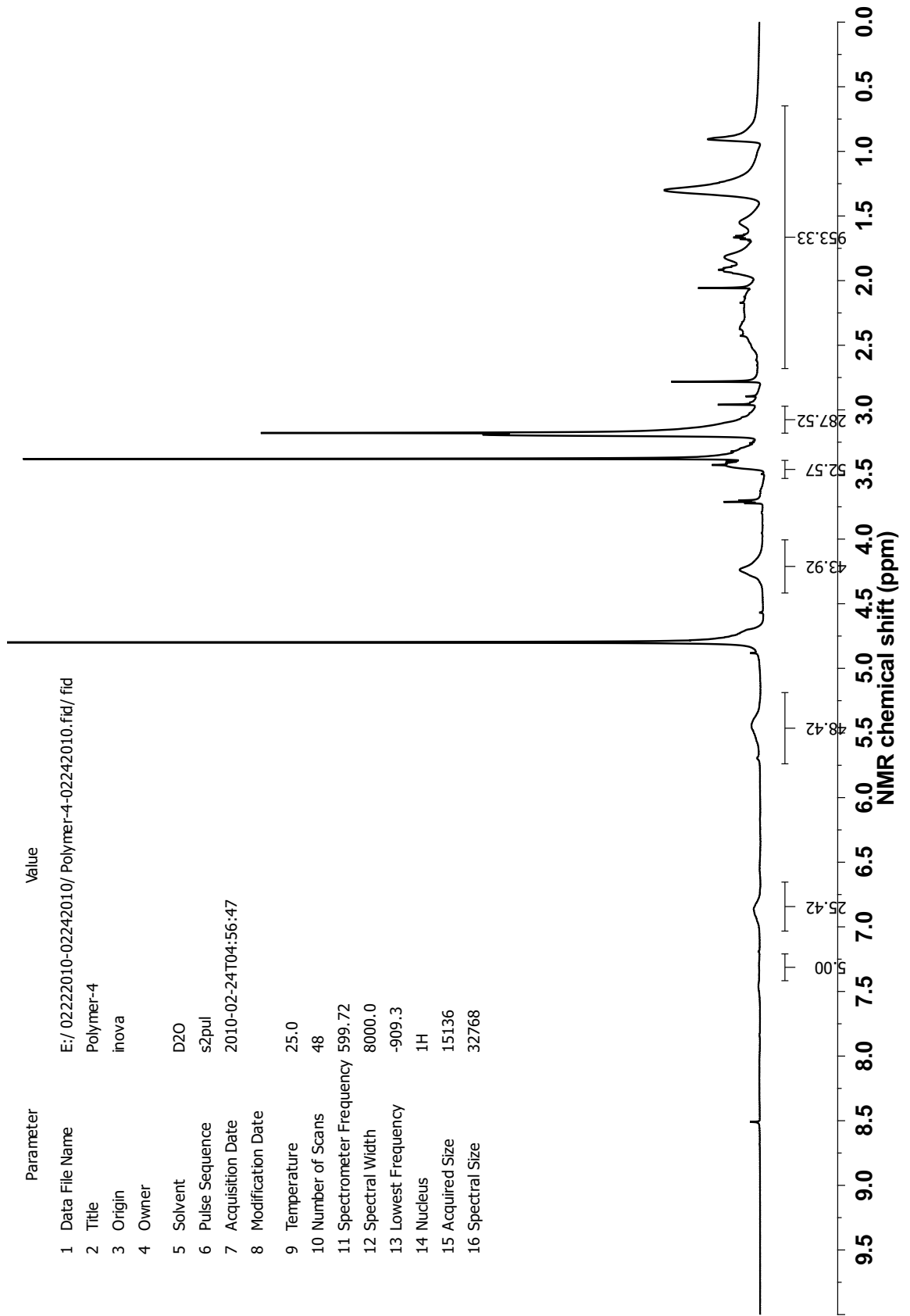
Parameter	Value
1 Data File Name	E:/02222010-02242010/Polymer-3-02222010.fid/ fid
2 Title	Polymer-3-02222010
3 Origin	inova
4 Owner	
5 Solvent	D2O
6 Pulse Sequence	s2pul
7 Acquisition Date	2010-02-22T05:40:07
8 Modification Date	
9 Temperature	25.0
10 Number of Scans	88
11 Spectrometer Frequency	599.72
12 Spectral Width	8000.0
13 Lowest Frequency	-908.0
14 Nucleus	¹ H
15 Acquired Size	15136
16 Spectral Size	32768



A-112: ¹H-NMR spectrum of Acopolymer-3

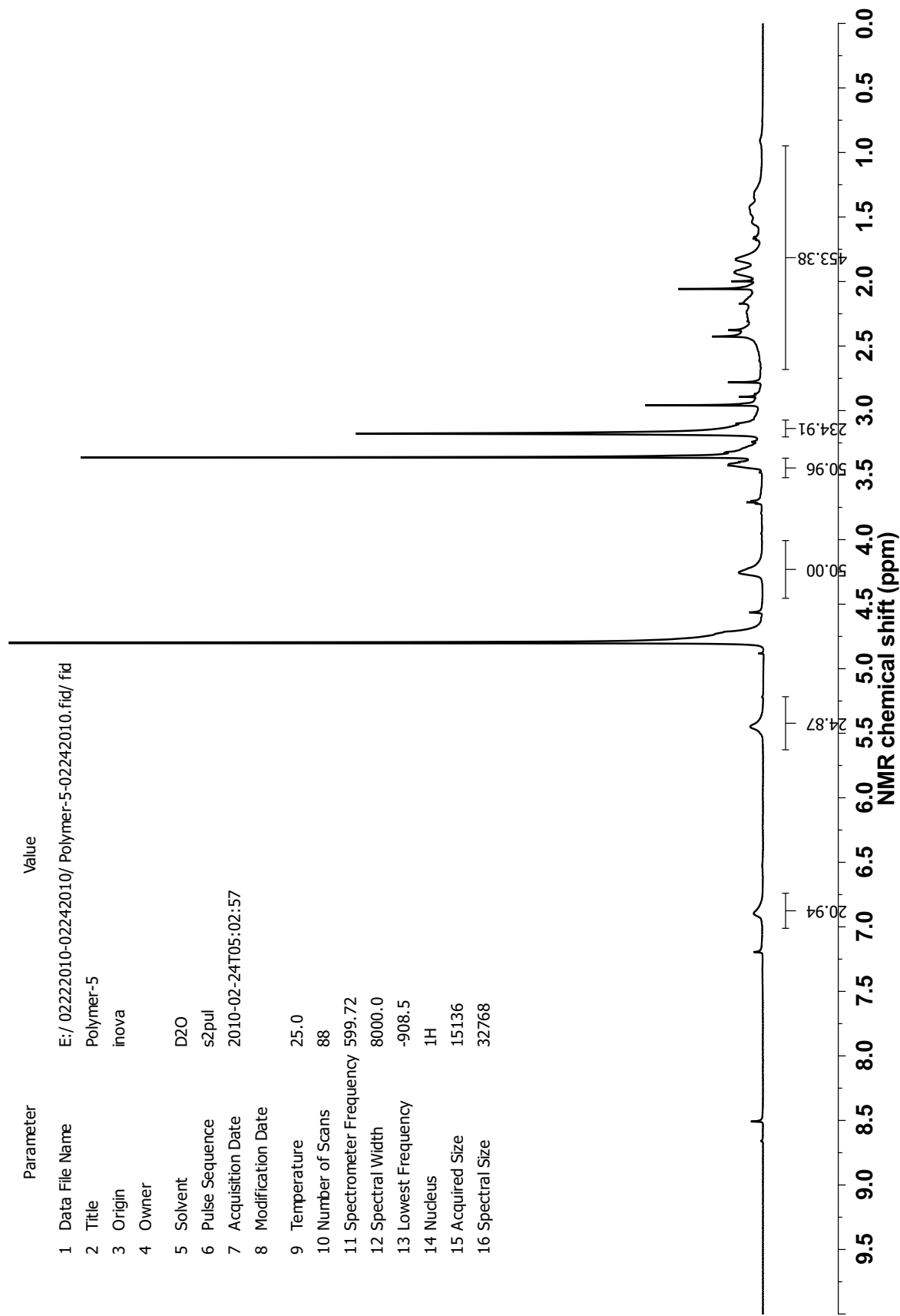
Parameter Value

1 Data File Name E:/ 02222010-02242010/ Polymer-4-02242010.fid/ fid
2 Title Polymer-4
3 Origin inova
4 Owner
5 Solvent D2O
6 Pulse Sequence s2pul
7 Acquisition Date 2010-02-24T04:56:47
8 Modification Date
9 Temperature 25.0
10 Number of Scans 48
11 Spectrometer Frequency 599.72
12 Spectral Width 8000.0
13 Lowest Frequency -909.3
14 Nucleus ¹H
15 Acquired Size 15136
16 Spectral Size 32768



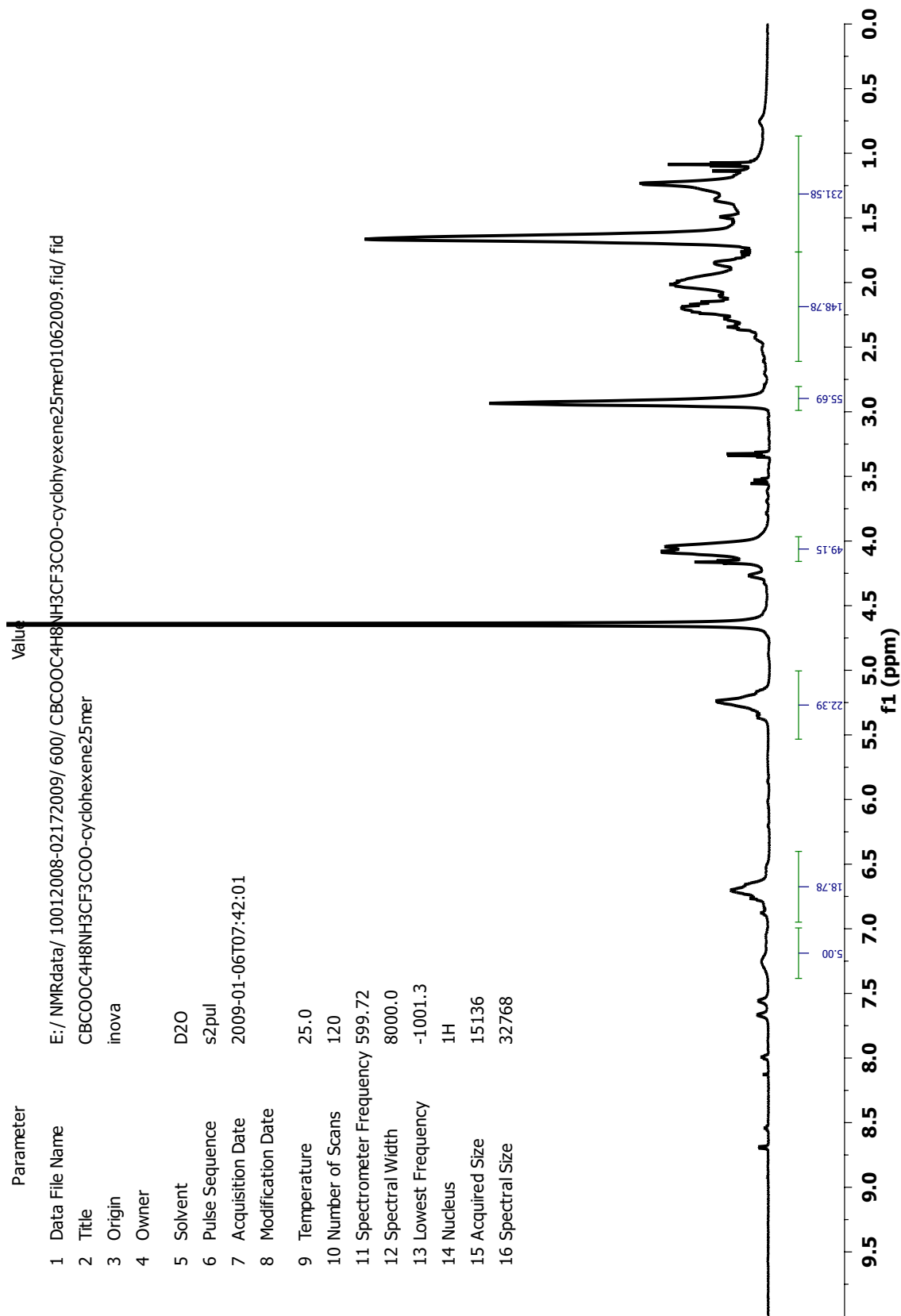
A-113: ¹H-NMR spectrum of Acopolymer-4

Parameter	Value
1 Data File Name	E:/ 02222010-02242010/ Polymer-5-02242010.fid/ fid
2 Title	Polymer-5
3 Origin	inova
4 Owner	
5 Solvent	D2O
6 Pulse Sequence	s2pul
7 Acquisition Date	2010-02-24T05:02:57
8 Modification Date	
9 Temperature	25.0
10 Number of Scans	88
11 Spectrometer Frequency	599.72
12 Spectral Width	8000.0
13 Lowest Frequency	-908.5
14 Nucleus	¹ H
15 Acquired Size	15136
16 Spectral Size	32768

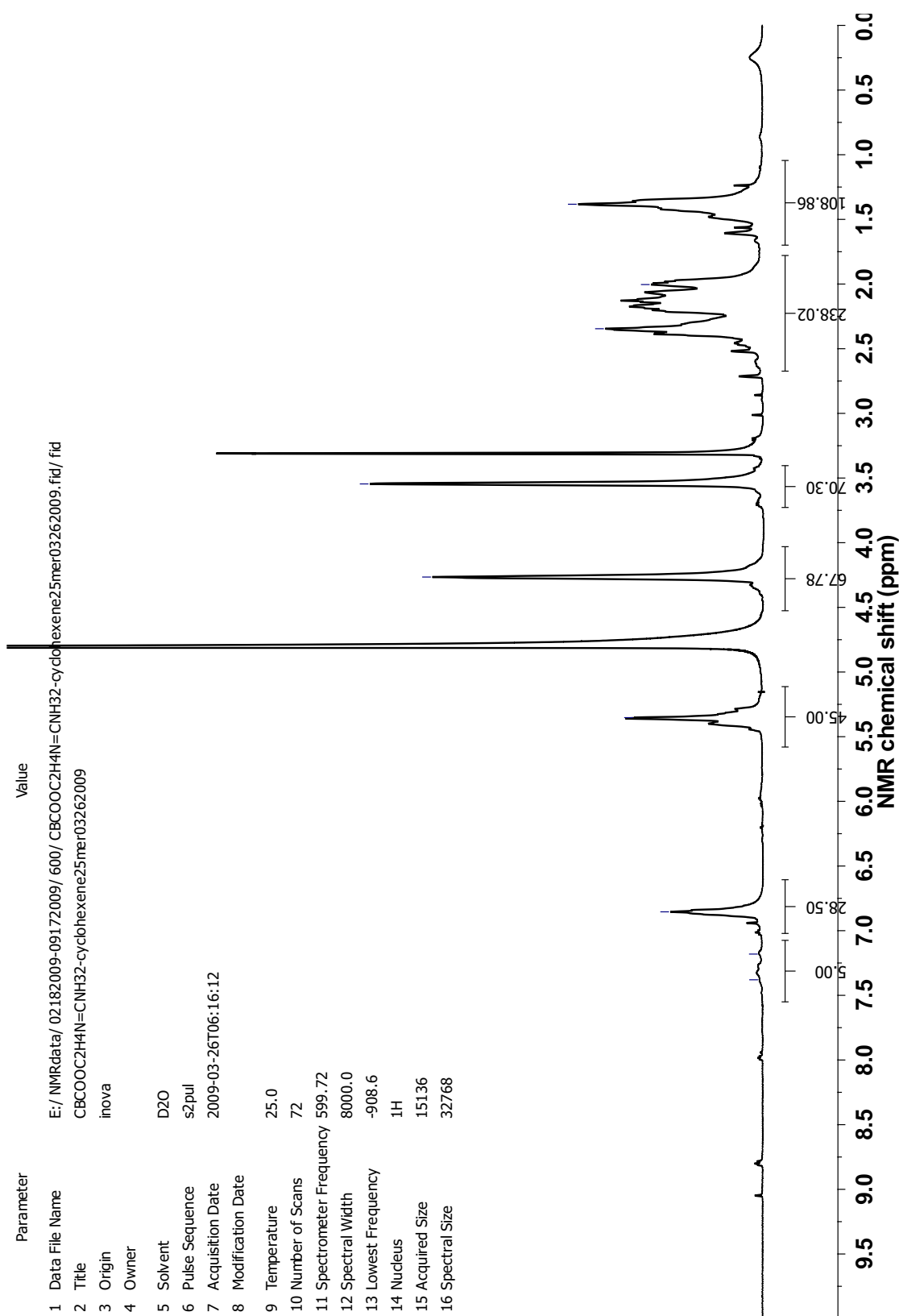


A-114: ¹H-NMR spectrum of Acopolymer-5

Parameter	Value
1 Data File Name	E:/ NMRdata/ 10012008-02172009/ 600/ CBCOOC4H8NH3CF3COO-cyclohexene25mer01062009.fid/ fid
2 Title	CBCOOC4H8NH3CF3COO-cyclohexene25mer
3 Origin	inova
4 Owner	
5 Solvent	D2O
6 Pulse Sequence	s2pul
7 Acquisition Date	2009-01-06T07:42:01
8 Modification Date	
9 Temperature	25.0
10 Number of Scans	120
11 Spectrometer Frequency	599.72
12 Spectral Width	8000.0
13 Lowest Frequency	-1001.3
14 Nucleus	¹ H
15 Acquired Size	15136
16 Spectral Size	32768

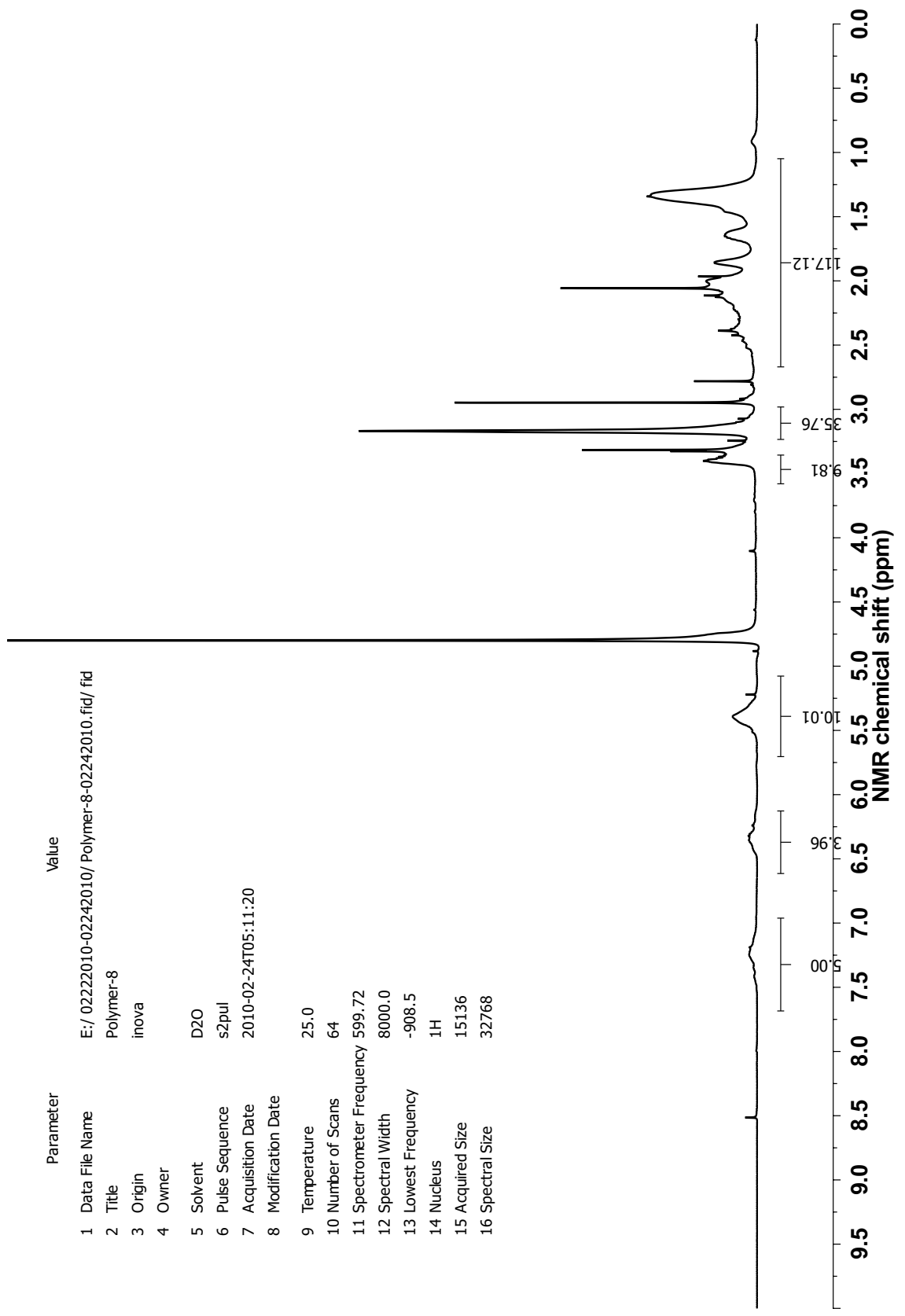


A-115: ¹H-NMR spectrum of Acopolymer-6



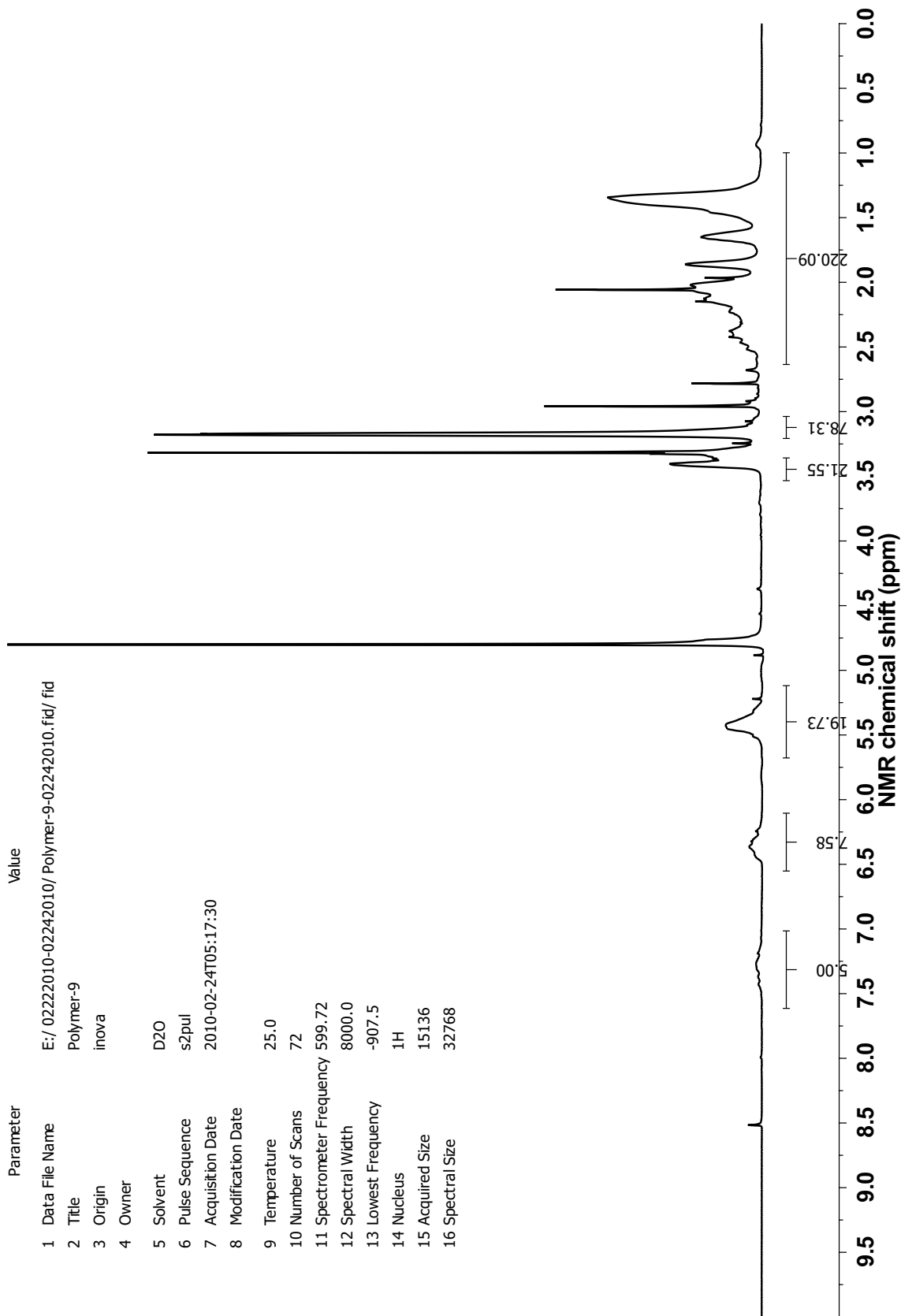
A-116: ¹H-NMR spectrum of Acopolymer-7

Parameter	Value
1 Data File Name	E:/ 02222010-02242010/ Polymer-8-02242010.fid/ fid
2 Title	Polymer-8
3 Origin	inova
4 Owner	
5 Solvent	D2O
6 Pulse Sequence	s2pul
7 Acquisition Date	2010-02-24T05:11:20
8 Modification Date	
9 Temperature	25.0
10 Number of Scans	64
11 Spectrometer Frequency	599.72
12 Spectral Width	8000.0
13 Lowest Frequency	-908.5
14 Nucleus	¹ H
15 Acquired Size	15136
16 Spectral Size	32768



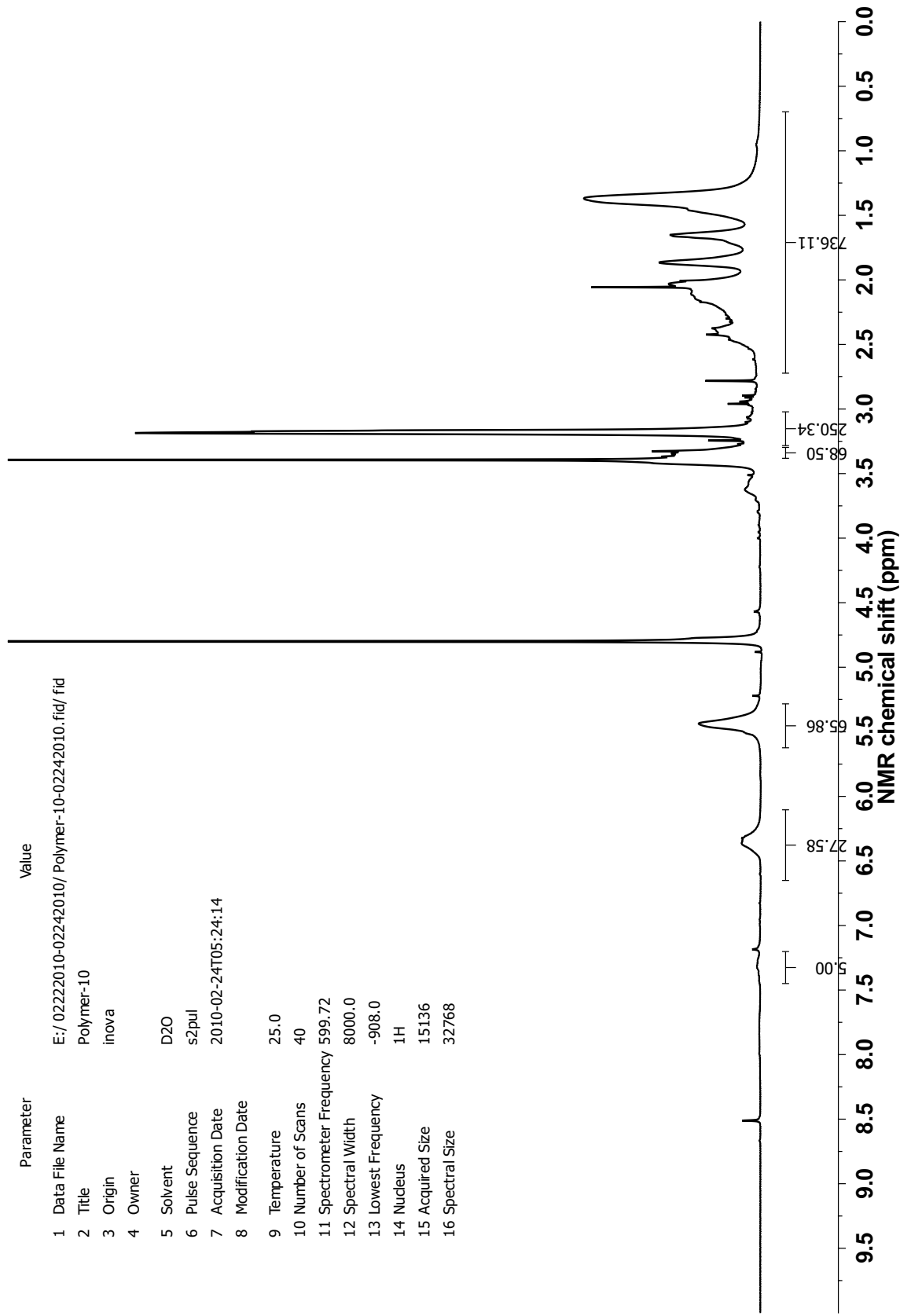
A-117: ¹H-NMR spectrum of Rcopolymer-8

Parameter	Value
1 Data File Name	E:/02222010-02242010/Polymer-9-02242010.fid/ fid
2 Title	Polymer-9
3 Origin	inova
4 Owner	
5 Solvent	D2O
6 Pulse Sequence	s2pul
7 Acquisition Date	2010-02-24T05:17:30
8 Modification Date	
9 Temperature	25.0
10 Number of Scans	72
11 Spectrometer Frequency	599.72
12 Spectral Width	8000.0
13 Lowest Frequency	-907.5
14 Nucleus	¹ H
15 Acquired Size	15136
16 Spectral Size	32768



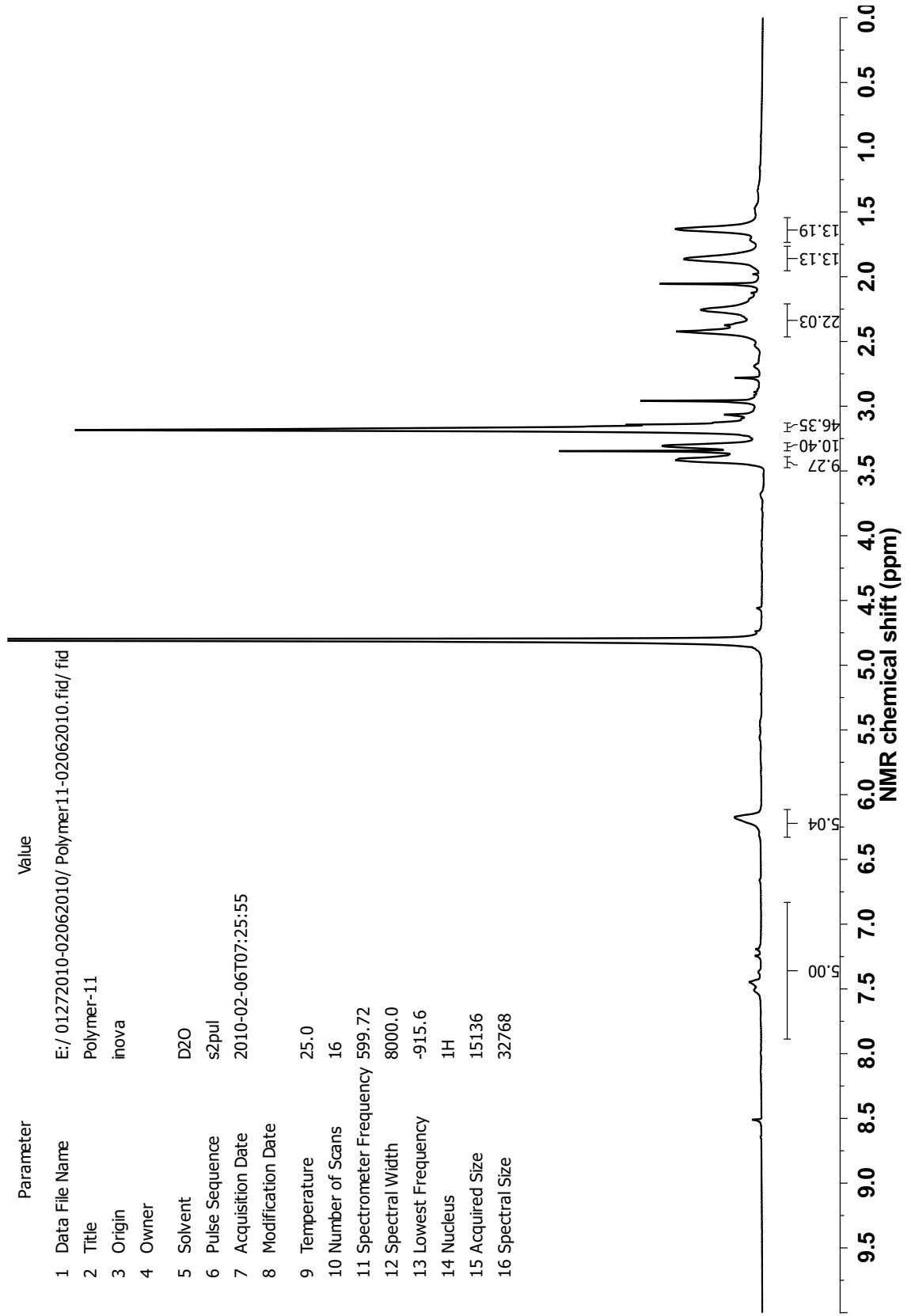
A-118: ¹H-NMR spectrum of Rcopolymer-9

Parameter	Value
1 Data File Name	E:/02222010-02242010/ Polymer-10-02242010.fid/ fid
2 Title	Polymer-10
3 Origin	inova
4 Owner	
5 Solvent	D2O
6 Pulse Sequence	s2pul
7 Acquisition Date	2010-02-24T05:24:14
8 Modification Date	
9 Temperature	25.0
10 Number of Scans	40
11 Spectrometer Frequency	599.72
12 Spectral Width	8000.0
13 Lowest Frequency	-908.0
14 Nucleus	¹ H
15 Acquired Size	15136
16 Spectral Size	32768



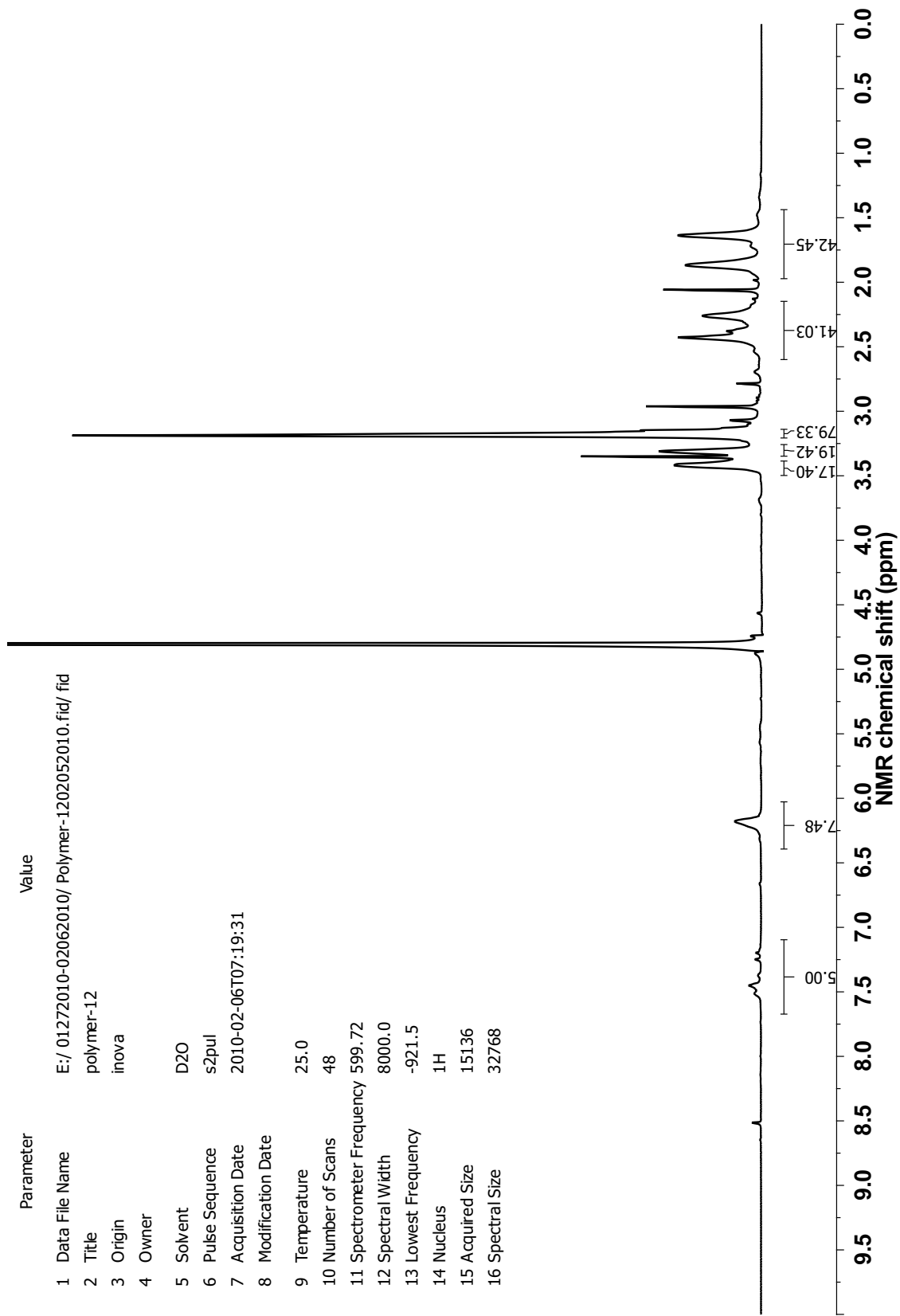
A-119: ¹H-NMR spectrum of Rcopolymer-10

Parameter	Value
1 Data File Name	E:/ 01272010-02062010/ Polymer11-02062010.fid/ fid
2 Title	Polymer-11
3 Origin	inova
4 Owner	
5 Solvent	D2O
6 Pulse Sequence	s2pul
7 Acquisition Date	2010-02-06T07:25:55
8 Modification Date	
9 Temperature	25.0
10 Number of Scans	16
11 Spectrometer Frequency	599.72
12 Spectral Width	8000.0
13 Lowest Frequency	-915.6
14 Nucleus	¹ H
15 Acquired Size	15136
16 Spectral Size	32768

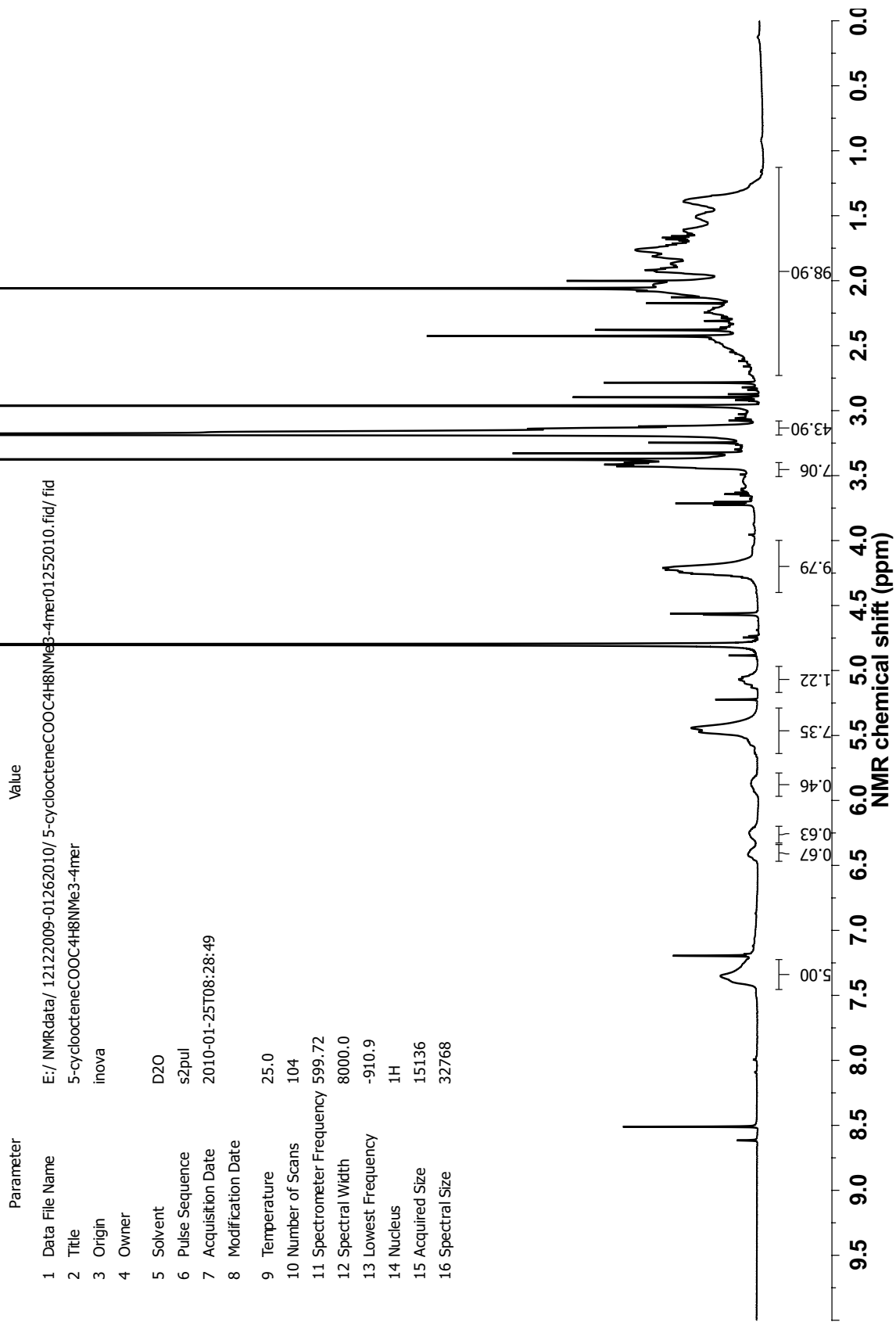


A-120: ¹H-NMR spectrum of Homopolymer-11

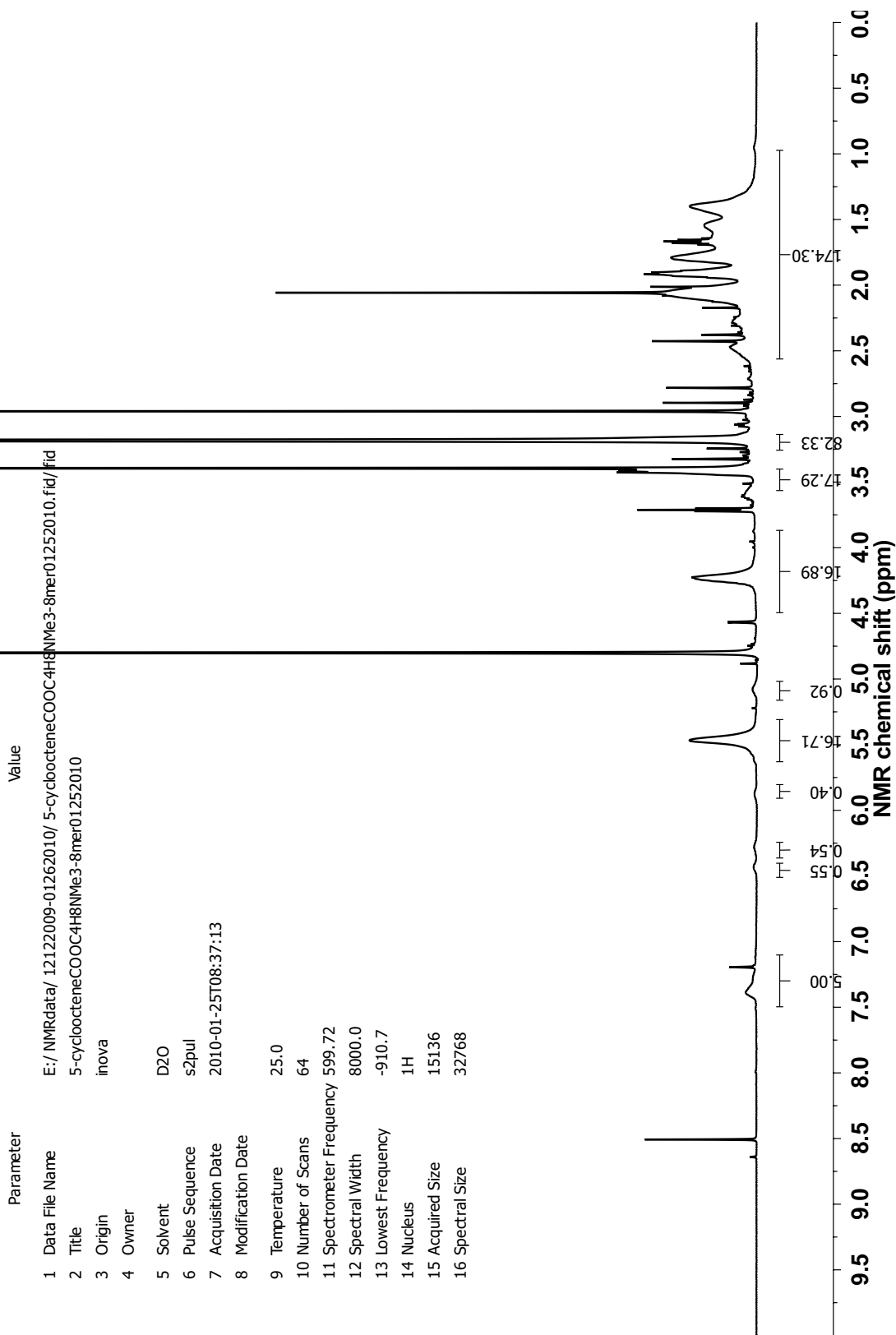
Parameter	Value
1 Data File Name	E:/01272010-02062010/ Polymer-1202052010.fid/ fid
2 Title	polymer-12
3 Origin	inova
4 Owner	
5 Solvent	D2O
6 Pulse Sequence	s2pul
7 Acquisition Date	2010-02-06T07:19:31
8 Modification Date	
9 Temperature	25.0
10 Number of Scans	48
11 Spectrometer Frequency	599.72
12 Spectral Width	8000.0
13 Lowest Frequency	-921.5
14 Nucleus	¹ H
15 Acquired Size	15136
16 Spectral Size	32768



A-121: ¹H-NMR spectrum of Homopolymer-12



A-122: ¹H-NMR spectrum of Homopolymer-13



A-123: ¹H-NMR spectrum of Homopolymer-14